frontiers | Research Topics

# Targeted alpha particle therapy in oncology

**Edited by**
Asta Juzeniene, Richard P. Baum, Øyvind Bruland and Roy Larsen

**Published in**
Frontiers in Medicine

ISSN 1664-8714
ISBN 978-2-83251-983-7
DOI 10.3389/978-2-83251-983-7

## About Frontiers

Frontiers is more than just an open access publisher of scholarly articles: it is a pioneering approach to the world of academia, radically improving the way scholarly research is managed. The grand vision of Frontiers is a world where all people have an equal opportunity to seek, share and generate knowledge. Frontiers provides immediate and permanent online open access to all its publications, but this alone is not enough to realize our grand goals.

## Frontiers journal series

The Frontiers journal series is a multi-tier and interdisciplinary set of open-access, online journals, promising a paradigm shift from the current review, selection and dissemination processes in academic publishing. All Frontiers journals are driven by researchers for researchers; therefore, they constitute a service to the scholarly community. At the same time, the *Frontiers journal series* operates on a revolutionary invention, the tiered publishing system, initially addressing specific communities of scholars, and gradually climbing up to broader public understanding, thus serving the interests of the lay society, too.

## Dedication to quality

Each Frontiers article is a landmark of the highest quality, thanks to genuinely collaborative interactions between authors and review editors, who include some of the world's best academicians. Research must be certified by peers before entering a stream of knowledge that may eventually reach the public - and shape society; therefore, Frontiers only applies the most rigorous and unbiased reviews. Frontiers revolutionizes research publishing by freely delivering the most outstanding research, evaluated with no bias from both the academic and social point of view. By applying the most advanced information technologies, Frontiers is catapulting scholarly publishing into a new generation.

## What are Frontiers Research Topics?

Frontiers Research Topics are very popular trademarks of the *Frontiers journals series*: they are collections of at least ten articles, all centered on a particular subject. With their unique mix of varied contributions from Original Research to Review Articles, Frontiers Research Topics unify the most influential researchers, the latest key findings and historical advances in a hot research area.

Find out more on how to host your own Frontiers Research Topic or contribute to one as an author by contacting the Frontiers editorial office: frontiersin.org/about/contact

# Targeted alpha particle therapy in oncology

**Topic editors**

Asta Juzeniene — Oslo University Hospital, Norway
Richard P. Baum — Deutsche Klinik für Diagnostik, Germany
Øyvind Bruland — Oslo University Hospital, Norway
Roy Larsen — Sciencons AS, Oslo Norway, Norway

**Citation**

Juzeniene, A., Baum, R. P., Bruland, Ø., Larsen, R., eds. (2023). *Targeted alpha particle therapy in oncology*. Lausanne: Frontiers Media SA.
doi: 10.3389/978-2-83251-983-7

# Table of contents

frontiers | Frontiers in Medicine

TYPE Editorial
PUBLISHED 07 March 2023
DOI 10.3389/fmed.2023.1165747



OPEN ACCESS

EDITED AND REVIEWED BY
Giorgio Treglia,
Ente Ospedaliero Cantonale (EOC), Switzerland

*CORRESPONDENCE
Asta Juzeniene
✉ astaj@rr-research.no

SPECIALTY SECTION
This article was submitted to Nuclear Medicine, a section of the journal Frontiers in Medicine

RECEIVED 14 February 2023
ACCEPTED 16 February 2023
PUBLISHED 07 March 2023

CITATION
Bruland ØS, Larsen RH, Baum RP and Juzeniene A (2023) Editorial: Targeted alpha particle therapy in oncology.
*Front. Med.* 10:1165747.
doi: 10.3389/fmed.2023.1165747



# Editorial: Targeted alpha particle therapy in oncology

Øyvind Sverre Bruland[1,2], Roy Hartvig Larsen[3], Richard Paul Baum[4] and Asta Juzeniene[5,6]*

[1]Department of Oncology, The Norwegian Radium Hospital, Oslo University Hospital, Oslo, Norway, [2]Institute for Clinical Medicine, University of Oslo, Oslo, Norway, [3]Sciencons AS, Oslo, Norway, [4]Curanosticum Wiesbaden-Frankfurt, Center for Advanced Radiomolecular Precision Oncology, Wiesbaden, Germany, [5]Department of Radiation Biology, Institute for Cancer Research, The Norwegian Radium Hospital, Oslo University Hospital, Oslo, Norway, [6]Department of Physics, University of Oslo, Oslo, Norway

KEYWORDS

**actinium-225, astatine-211, lead-212, radium-223, radium-224, thorium-227, targeted alpha therapy (TAT), targeted radionuclide therapy (TRT)**

Editorial on the Research Topic
Targeted alpha particle therapy in oncology

Targeted radionuclide therapy (TRT), also known as molecular radiotherapy, targeted radiotherapy, or radiotheranostics, is a rapidly developing area with important recent breakthroughs (1–3). It aims to treat disseminated cancer, the main clinical challenge in oncology (4, 5). TRT is based on personalized patient selection using molecular imaging to verify the presence of a biologic target either on the cancer cell surface or in vascular and/or stromal elements of metastases. The only approved alpha-emitting radiopharmaceutical is Xofigo ($^{223}RaCl_2$, approved in 2013). The recent approval of beta-emitting $^{177}$Lu-PSMA-617 (Pluctivo, approved in 2022) for the treatment of metastatic castration-resistant prostate cancer (mCRPC) expressing prostate-specific membrane antigen (PSMA), and of $^{177}$Lu-DOTATATE (Lutathera, approved by EMA in 2018) for therapy of somatostatin receptor positive neuroendocrine tumors (NETs) will clearly shift TRT into the mainstream of cancer treatment. Nevertheless, some patients either do not respond, or, following initially good response, develop resistance to $^{177}$Lu-based therapies, in spite of sufficient expression of target proteins on cancer cell surfaces (6, 7). Many preclinical and clinical trials have demonstrated that alpha-particle-emitting radiopharmaceuticals, due to their physical properties, high linear energy transfer, and short range in tissue relative to beta-emissions, are emerging as a promising approach for cancer treatment (8–11); they can also directly kill hypoxic or radio- and chemo-resistant cancer cells.

The goal of this Research Topic is to describe the development of novel alpha-emitting radiopharmaceuticals for different cancers, recent preclinical, completed, and ongoing clinical trials of targeted alpha-particle therapy (TAT) alone or in combination, dosimetry, safety, challenges related to supply and availability of suitable alpha-emitting radionuclides, as well as some future perspectives. This Research Topic includes 16 articles focusing on original research (four articles), reviews on different aspects of TAT (9 articles), ongoing clinical trials (one article), study protocols (one article), and hypotheses and theories (one article). Key opinion leaders, medical doctors, and scientists from Australia, Belgium, France, Germany, Poland, Norway, Singapore, Sweden, Switzerland, the United Kingdom, and the United States have contributed to this Research Topic.

Only a few radionuclides, namely, $^{225}$Ac, $^{211}$At, $^{212}$Bi, $^{212}$Pb/$^{213}$Bi, $^{224}$Ra, $^{223}$Ra, and $^{227}$Th, are of interest for TAT. In this Research Topic, the challenges and benefits of these radionuclides are reviewed.

Bone-seeking $^{223}RaCl_2$ is approved for patients with mCRPC and dominant osteoblastic skeletal metastases. Attempts to complex $^{223}$Ra to cancer cell–targeting moieties have been unsuccessful. Some researchers and medical doctors speculate that $^{223}RaCl_2$ will be less used after the approval of cancer cell–targeting $^{177}$Lu-PSMA-617. In this Research Topic, O'Sullivan et al., Sartor and Baghian, and Kostos et al. discuss the potential of $^{223}$Ra and why it seems underutilized. Despite the survival rate benefit of cancer cell–targeting $^{177}$Lu-PSMA-617, responses for many patients with mCRPC are not long-term, and almost all patients will subsequently develop progressive disease. Sartor and Baghian reviewed the rapidly developing, most promising radiopharmaceuticals, including $^{225}$Ac-, $^{212}$Pb-, and $^{227}$Th-labeled PSMA-binding ligands and their future. Tandem therapies combining beta and alpha radiopharmaceuticals are also presented. Kostos et al. present a protocol for the clinical study of AlphaBet, combining a bone-specific alpha-emitter $^{223}$Ra with the beta-emitter $^{177}$Lu-PSMA-I&T, for the eradication of micrometastatic osseous disease, since the bone marrow is the most common site of cancer progression. Micrometastases in the skeleton likely receive an inadequate dose of radiation as the emitted beta-particles from $^{177}$Lu travel an average distance of 0.7 mm in soft tissue, well-beyond the diameter of micrometastases. Bone-seeking $^{223}RaCl_2$ can be used alone or in combination with gemcitabine or denosumab for osteoblastic osteosarcoma treatment, as described by Anderson et al.. Unfortunately, not all areas of osteosarcoma lesions are osteoblastic. In such cases, TAT with $^{225}$Ac or $^{227}$Th targeting IGF1R or Her-2 overexpressed in osteosarcoma may become efficient treatment for osteosarcoma (NCT03746431 and NCT04147819).

In TAT, radionuclides are delivered to cancer cells through a wide variety of formulations such as radiolabeled antibodies, peptides, or small molecules. A recent strategy incorporates $^{224}$Ra into $CaCO_3$ microparticles (Radspherin®), designed as a treatment of the remaining peritoneal micrometastasis in ovarian and colorectal cancer after complete cytroreductive surgery, as a means to decrease $^{224}$Ra and its daughters' redistribution from the peritoneal cavity (12). The goal of the product is to generate an alpha particle radiation field on the surfaces and liquid volumes of the peritoneal cavity. Wouters et al. have shown the therapeutic efficacy of $^{224}$Ra-$CaCO_3$ in a mouse model of ovarian cancer, and the possibility for safe sequential administration using several chemotherapy regimens commonly employed in patients. Larsen et al. report the first study on Radspherin for peritoneal metastasis of colorectal cancer in 23 patients. Biodistribution studies demonstrated that Radspherin was distributed peritoneally. Dose-limiting toxicity was not reached. The safety issues of Radspherin and the level of radiation exposure from the patients to surrounding people were described by Grønningsæter et al.. It was concluded that there was no need for any restrictions or precautions due to external exposure.

The dosimetry and radiation risk–related aspects of $^{224}$Ra and $^{223}$Ra have been discussed by Lassmann and Eberlein.

A novel dual alpha technology with potentially broad therapeutic applications (new generator and radiopharmaceuticals), comprising $^{224}$Ra for targeting the osteoblastic stroma of bone metastases and the chelated-conjugate daughter $^{212}$Pb for selective binding to tumor cells, has been proposed by Juzeniene et al. and Tornes et al. in this Research Topic.

Shi et al. reviewed the strengths, weakness, and the present and future of $^{225}$Ac-labeled somatostatin receptor agonists and antagonists in preclinical and clinical applications for NETs.

Karlsson et al. summarized preclinical and clinical studies on $^{227}$Th-conjugates for various cancer types. The authors also discussed the feasibility of using $^{227}$Th-conjugates in combination with other therapies. The potential of the combination of $^{227}$Th-conjugates and PD-1 check-point inhibitors in preclinical models was demonstrated by Berg-Larsen et al..

In a comprehensive review, Albertsson et al. discussed completed and ongoing clinical trials of different $^{211}$At-conjugates.

Kunikowska et al. provide an overview of strategies for the local treatment of primary and secondary glioblastomas using $^{213}$Bi, $^{225}$Ac, and $^{211}$At. Antibodies targeting the extracellular matrix protein tenascin and substance P targeting the neurokinin type-1 receptor overexpressed in glioblastomas were discussed as targeting moieties for TAT.

It is crucial to select novel target molecules that are expressed in various types of cancers, and preferentially develop radiopharmaceuticals both for imaging and therapy, allowing a theranostic approach. However, not all targets are suitable for TAT; some are useful only for imaging. The biological effect of TAT depends on the absorbed dose, which is related to the "area under the curve"; the biological half-life at tumor sites and normal tissues, matched with the physical half-life of the given alpha emitter. Additionally, dosimetry calculations of TAT are challenging, since alpha particles have short ranges ($<100\,\mu m$) that may provide heterogeneous irradiation and their daughters may have different pharmacokinetic profiles and chemical properties.

TAT is one of the most rapidly growing fields in the management of different types of cancer, and many radiopharmaceuticals are already in clinical trials. Commercial and business aspects of alpha radioligands have been discussed by Ostuni and Taylor.

We hope that this Research Topic on TAT will stimulate more research and clinical trials in this field.

## Author contributions

All authors listed have made a substantial, direct, and intellectual contribution to the work and approved it for publication.

## Funding

This research was funded by the South-Eastern Norway Regional Health Authority (project number 2020028, Oslo, Norway).

## Conflict of interest

ØB and RL hold ownership interest in Oncoinvent AS and ArtBio AS . RL is the owner of company Sciencons AS.

The remaining authors declare that the research was conducted in the absence of any commercial or financial relationships that could be construed as a potential conflict of interest.

## Publisher's note

All claims expressed in this article are solely those of the authors and do not necessarily represent those of their affiliated organizations, or those of the publisher, the editors and the reviewers. Any product that may be evaluated in this article, or claim that may be made by its manufacturer, is not guaranteed or endorsed by the publisher.

## References

1. Herrmann K, Schwaiger M, Lewis JS, Solomon SB, McNeil BJ, Baumann M, et al. Radiotheranostics: a roadmap for future development. *Lancet Oncol.* (2020) 21:e146–e56. doi: 10.1016/S1470-2045(19)30821-6

2. Dolgin E. Radioactive drugs emerge from the shadows to storm the market. *Nat Biotechnol.* (2018) 36:1125–7. doi: 10.1038/nbt1218-1125

3. Dolgin E. Drugmakers go nuclear, continuing push into radiopharmaceuticals. *Nat Biotechnol.* (2021) 39:647–9. doi: 10.1038/s41587-021-00954-z

4. Dillekås H, Rogers MS, Straume O. Are 90% of deaths from cancer caused by metastases? *Cancer Med.* (2019) 8:5574–6. doi: 10.1002/cam4.2474

5. Coleman R, Hadji P, Body JJ, Santini D, Chow E, Terpos E, et al. Bone health in cancer: ESMO clinical practice guidelines. *Ann Oncol.* (2020) 31:1650–63. doi: 10.1016/j.annonc.2020.07.019

6. Kratochwil C, Bruchertseifer F, Giesel FL, Weis M, Verburg FA, Mottaghy F, et al. $^{225}$Ac-PSMA-617 for PSMA-targeted α-radiation therapy of metastatic castration-resistant prostate cancer. *J Nucl Med.* (2016) 57:1941–4. doi: 10.2967/jnumed.116.178673

7. Ballal S, Yadav MP, Tripathi M, Sahoo RK, Bal C. Survival outcomes in metastatic gastroenteropancreatic neuroendocrine tumor patients receiving concomitant (225)Ac-DOTATATE targeted alpha therapy and capecitabine: a real-world scenario management based long-term outcome study. *J Nucl Med.* (2022). doi: 10.2967/jnumed.122.264043

8. Pouget JP, Constanzo J. Revisiting the radiobiology of targeted alpha therapy. *Front Med.* (2021) 8:692436. doi: 10.3389/fmed.2021.692436

9. Makvandi M, Dupis E, Engle JW, Nortier FM, Fassbender ME, Simon S, et al. Alpha-emitters and targeted alpha therapy in oncology: from basic science to clinical investigations. *Target Oncol.* (2018) 13:189–203. doi: 10.1007/s11523-018-0550-9

10. Nelson BJB, Andersson JD, Wuest F. Targeted alpha therapy: progress in radionuclide production, radiochemistry, and applications. *Pharmaceutics.* (2020) 13:49. doi: 10.3390/pharmaceutics13010049

11. Eychenne R, Chérel M, Haddad F, Guérard F, Gestin JF. Overview of the most promising radionuclides for targeted alpha therapy: the "hopeful eight". *Pharmaceutics.* (2021) 13:906. doi: 10.3390/pharmaceutics13060906

12. Li RG, Lindland K, Tonstad SK, Bønsdorff TB, Juzeniene A, Westrøm S, et al. Improved formulation of (224)Ra-labeled calcium carbonate microparticles by surface layer encapsulation and addition of EDTMP. *Pharmaceutics.* (2021) 13:634. doi: 10.3390/pharmaceutics13050634

frontiers | Frontiers in Medicine

TYPE Original Research
PUBLISHED 10 October 2022
DOI 10.3389/fmed.2022.995325



OPEN ACCESS

EDITED BY
Giorgio Treglia,
Ente Ospedaliero Cantonale (EOC), Switzerland

REVIEWED BY
Weijun Wei,
Shanghai Jiao Tong University, China
Ronghua Liu,
Huazhong University of Science and Technology, China

*CORRESPONDENCE
Roxanne Wouters
roxanne.wouters@kuleuven.be

SPECIALTY SECTION
This article was submitted to Nuclear Medicine, a section of the journal Frontiers in Medicine

RECEIVED 15 July 2022
ACCEPTED 21 September 2022
PUBLISHED 10 October 2022

CITATION
Wouters R, Westrøm S, Berckmans Y, Riva M, Ceusters J, Bønsdorff TB, Vergote I and Coosemans A (2022) Intraperitoneal alpha therapy with $^{224}$Ra-labeled microparticles combined with chemotherapy in an ovarian cancer mouse model. *Front. Med.* 9:995325. doi: 10.3389/fmed.2022.995325



# Intraperitoneal alpha therapy with $^{224}$Ra-labeled microparticles combined with chemotherapy in an ovarian cancer mouse model

Roxanne Wouters[1,2]*, Sara Westrøm[2], Yani Berckmans[1], Matteo Riva[1,3], Jolien Ceusters[2], Tina B. Bønsdorff[2], Ignace Vergote[4,5] and An Coosemans[1]

[1]Laboratory of Tumor Immunology and Immunotherapy, Department of Oncology, Leuven Cancer Institute, KU Leuven, Leuven, Belgium, [2]Oncoinvent AS, Oslo, Norway, [3]Department of Neurosurgery, Mont-Godinne Hospital, UCL Namur, Yvoir, Belgium, [4]Division of Gynecological Oncology, Department of Obstetrics and Gynecology, Leuven Cancer Institute, University Hospitals Leuven, Leuven, Belgium, [5]Department of Oncology, Gynecological Oncology, KU Leuven, Leuven, Belgium

A novel alpha-therapy consisting of $^{224}$Ra-labeled calcium carbonate microparticles ($^{224}$Ra-$CaCO_3$-MP) has been designed to treat micrometastatic peritoneal disease via intraperitoneal (IP) administration. This preclinical study aimed to evaluate its efficacy and tolerability when given as a single treatment or in combination with standard of care chemotherapy regimens, in a syngeneic model of ovarian cancer in immune competent mice. Female C57BL/6 mice bearing ID8-fLuc ovarian cancer were treated with $^{224}$Ra-$CaCO_3$-MP 1 day after IP tumor cell inoculation. The activity dosages of $^{224}$Ra ranged from 14 to 39 kBq/mouse. Additionally, $^{224}$Ra-$CaCO_3$-MP treatment was followed by either carboplatin (80 mg/kg)-pegylated liposomal doxorubicin (PLD, 1.6 mg/kg) or carboplatin (60 mg/kg)-paclitaxel (10 mg/kg) on day 14 post tumor cell inoculation. All treatments were administered via IP injections. Readouts included survival, clinical signs, and body weight development over time. There was a slight therapeutic benefit after single treatment with $^{224}$Ra-$CaCO_3$-MP compared to the vehicle control, with median survival ratios (MSRs) ranging between 1.1 and 1.3. The sequential administration of $^{224}$Ra-$CaCO_3$-MP with either carboplatin-paclitaxel or carboplatin-PLD indicated a synergistic effect on overall survival at certain $^{224}$Ra activities. Moreover, the combinations tested appeared well tolerated in terms of weight assessment in the first 4 weeks after treatment. Overall, this research supports the further evaluation of $^{224}$Ra-$CaCO_3$-MP in patients with ovarian cancer. However, the most optimal chemotherapy regimen to combine with $^{224}$Ra-$CaCO_3$-MP should be identified to fully exploit its therapeutic potential.

KEYWORDS

**ovarian cancer, alpha therapy, radium-224, chemotherapy, carboplatin, paclitaxel, pegylated liposomal doxorubicin**

# Introduction

Ovarian cancer is the eight leading cause of cancer related deaths within the female population worldwide (1, 2). The most dominant subtype is high-grade serous ovarian cancer (HGSOC), which has an epithelial origin (3, 4). Due to the absence of symptoms at earlier stages of the disease, patients are often diagnosed at an advanced disease stage (International Federation of Gynecology and Obstetrics (FIGO) stage III and IV). In first line, the current standard of care of advanced ovarian cancer consists of a cytoreductive debulking surgery combined with platinum-based chemotherapy and eventually bevacizumab and/or poly (ADP-ribose) polymerase (PARP) inhibitors (5). The carboplatin-paclitaxel chemotherapy combination is the preferred regimen in a first-line treatment setting. However, the choice of chemotherapy at recurrence depends on tumor characteristics and whether platinum is again an option or not. At the time of recurrence, both platinum and non-platinum agents such as paclitaxel, gemcitabine, pegylated liposomal doxorubicin (PLD) and topotecan, as well as targeted therapies such as PARP inhibitors and bevacizumab can be used as single agents or in combination schedules (6). Nevertheless, HGSOC patients who get diagnosed in an advanced disease stage have a poor 5 year survival of only 20%-41% (7).

In most patients, recurrence of the disease involves the presence of metastases confined to the peritoneal cavity. In the ongoing search for more effective treatment strategies to locally target this peritoneal disease, the rapidly evolving research field of radionuclide therapy is of interest. Historically, the main focus in the context of ovarian cancer was on the investigation of β-particle emitters, with various success rates. In the past, radiocolloids containing $^{32}$P or $^{198}$Au have been used for IP treatment of patients with ovarian cancer (8–11). However, its use was limited in time due to the increased incidence of adverse effects, and replacement with chemotherapy treatment was recommended (9). Additionally, antibody guided $^{90}$Y has been explored in the context of ovarian cancer, but it did not proceed from phase III clinical trials (12, 13). Alternative types of radiotherapy options that have been explored for ovarian cancer include proton beam therapy and carbon ion therapy with successful outcomes in two case reports of patients with recurrent ovarian cancer (14, 15).

The use of $\alpha$-particle emitters is assumed to have advantages over the prior $\beta$-therapies. They are particularly of interest for the treatment of micrometastatic cancer dissemination in body cavities, one of the characteristics of peritoneal carcinomatosis in patients with ovarian cancer (16). Alpha-emitters are highly cytotoxic for the cancer cells residing in the abdominal cavity, while sparing surrounding radiosensitive organs because of their short penetration depth, thus limiting toxicities compared to $\beta$-emitters. To date, Xofigo® ($^{223}RaCl_2$) remains the only $\alpha$-emitting radiopharmaceutical approved by the European Medicines Agency and the Food and Drug Administration, and is currently used for the treatment of skeletal metastases of castration-resistant prostate cancer (17). However, $\alpha$-emitters, such as $^{212}$Pb and $^{211}$At have been investigated for ovarian cancer in phase I clinical trials, where feasibility of this type of treatment was confirmed without apparent signs of dose-limiting toxicities (18, 19).

The $\alpha$-emitter $^{224}$Ra, when adsorbed onto the microparticle drug carrier $CaCO_3$, has shown therapeutic potential in immunodeficient ovarian cancer xenograft mouse models, when administered as an IP treatment (20, 21). Based on these promising data, the $^{224}$Ra-$CaCO_3$-MP are currently being assessed in phase I clinical trials for both ovarian cancer (22) and colorectal carcinoma (23), two cancer types characterized by the presence of a widespread metastatic disease within the peritoneal cavity.

The current paper focusses on the evaluation of $^{224}$Ra-$CaCO_3$-MP in terms of its potential to treat peritoneally disseminated ovarian cancer in an immune competent mouse model. The aim was to examine the tolerability and efficacy of combinations with chemotherapy regimens commonly used in patients with ovarian cancer.

# Materials and methods

## Ovarian cancer tumor model

The ID8-fLuc cell line was transduced with a lentiviral vector (pCHMWS_CMV-fluc-I-PuroR) by the Laboratory of Molecular Virology and Gene Therapy and Leuven Viral Vector Core in our institute (KU Leuven, Belgium) (24). Female C57BL/6 mice (Envigo, Horst, The Netherlands) of seven to 9 weeks of age were inoculated IP with 5 x $10^6$ ID8-fLuc ovarian cancer cells on day 0 of the experiment, in the lower right quadrant of the abdomen. All animal experiments were approved by the ethical committee of the KU Leuven (P123/2017) and followed the most recent ethical standards (NIH guidelines for the Care and Use of Laboratory Animals and EU Directive 2010/63/EU as amended by Regulation (EU) 2019/1010) and the ARRIVE (Animal Research: Reporting of In Vivo Experiments) guidelines (25, 26). All mice in experiment were monitored at least three times per week in terms of body weight and clinical signs of disease, and drained from ascites when mice reached 32 grams. When pre-defined humane endpoints were reached [previously published (24)], mice were euthanized by cervical dislocation.

## $^{224}$Ra-$CaCO_3$-MP preparation and treatment in mice

Two product formulations of $^{224}$Ra-$CaCO_3$-MP have been used: $^{224}$Ra-$CaCO_3$-MP-1 from the early-phase of development and the optimized $^{224}$Ra-$CaCO_3$-MP-2, developed for clinical use in humans. The preparation of the $^{224}$Ra-$CaCO_3$-MP-1 product formulation is described as second generation microparticles (27), whereas the preparation of the $^{224}$Ra-$CaCO_3$-MP-2 formulation can be found in a separate publication where they are described as layer-encapsulated microparticles (28). In brief, $CaCO_3$ microparticles were prepared by a spontaneous precipitation method which yielded particles with a mainly spherical geometry with a volume-based median diameter of approximately 6 μm when measured by laser diffraction (Mastersizer 3000, Malvern Instruments Ltd, Worcestershire, UK). For radiolabeling, $^{224}RaCl_2$ solution was added to a suspension of $CaCO_3$ microparticles in the presence of $Ba^{2+}$ and $SO_4^{2-}$ (0.004% and 0.6% (*w*/*w*) relative to $CaCO_3$ respectively) for the coprecipitation of $^{224}$Ra. After the radiolabeling process, the $^{224}$Ra-$CaCO_3$-MP-1 were dispersed to a concentration of approximately 12.5 mg/ml in 0.9% NaCl. To fulfill the requirements for the clinical use of the radiopharmaceutical, it was necessary to control the size of microparticles in suspension over time and introduce a sterilization process. Hence, for the $^{224}$Ra-$CaCO_3$-MP-2, an additional layer of $CaCO_3$ was precipitated on the microparticles before they were dispersed to 25 mg/ml in 0.9% NaCl and 2.4% (*w*/*w*) EDTMPA [ethylenediamine tetra(methylenephosphonic acid)] and sterilized in an autoclave at 121 °C for 20 min. The $^{224}$Ra-$CaCO_3$-MP-2 product was diluted to a final concentration of 12.5 mg/ml with Plasmalyte (Baxter, Deerfield, IL, USA) prior to treatment administration in mice. Radium-224 labeled microparticles were administered *via* an IP injection at a volume of 0.4 ml on day 1 post tumor cell inoculation at a mass dose of 5 mg $CaCO_3$ and an activity dose ranging between 14 and 39 kBq/mouse $^{224}$Ra (805 and 2118 kBq/kg, respectively).

## Chemotherapy preparation and treatment in mice

Carboplatin and paclitaxel (Hospira, ONCO-TAIN, Pfizer, New York, NY, USA) were dissolved in Dulbecco's phosphate-buffered saline (DPBS, Thermo Fisher Scientific, Waltham, MA, USA) and administered IP at a dose of 60 or 80 mg/kg and 10 mg/kg, respectively, calculated for an average body weight of 20 g per mouse. Pegylated liposomal doxorubicin (Caelyx/Doxil®, Janssens Cilag International NV, Beerse, Belgium) was administered IP at a dose of 1.6 mg/kg. All chemotherapy doses used in this manuscript were determined previously via *in vivo* dosage experiments for each of the combination schedules in the ID8-fLuc mouse model for ovarian cancer (unpublished results).

## Experimental design

All $^{224}$Ra-$CaCO_3$-MP treatments were administered on day 1 post tumor cell inoculation (Figures 1A, 2A, 3A). This time point was chosen to mimic minimal residual disease after a cytoreductive debulking surgery in patients, a situation highly relevant to target micro-metastatic disseminations in the peritoneal cavity. Chemotherapy administration in all experiments was performed at day 14 post tumor cell inoculation (Figures 2A, 3A), to mimic the adjuvant chemotherapy initiation in patients. All treatments were administered *via* IP injections. For all injection time points, control mice received either DPBS, 0.9% NaCl or Plasmalyte without additives as the appropriate vehicle control solution for their respective experimental treatment.

## Data analysis

A statistical power analysis was performed to determine sample sizes for all experiments. A power of at least 0.80 was reached with 6 to 10 mice per treatment group, depending on the type of experiment. Survival curves were compared using the log-rank (Mantel-Cox) test. Adjustment for multiple comparisons was performed with the Benjamini-Hochberg procedure (with Q = 5%). The comparisons made for the different experiments can be found in Supplementary Tables S1, S2. Median survival ratios (MSR) were calculated as the median survival of the experimental group divided by the median survival of the respective control group and served as an additional measure for efficacy. A linear mixed model was fitted to assess the effects of the $^{224}$Ra-$CaCO_3$-MP on the weight changes of the mice in the first 4 weeks after treatment administration, with data points taken at 1 week intervals. An (adjusted) $p < 0.05$ was considered significant. Synergy between chemotherapy treatment and $^{224}$Ra-$CaCO_3$-MP was assessed using the Bliss analysis method (29). For this, a Cox proportional-hazards model was fitted to the survival data. Synergy is evaluated based on the hazard ratios (HRs) of the interaction of groups treated with both chemotherapy and $^{224}$Ra-$CaCO_3$-MP and the monotherapy treatment groups. Interaction values lower than 1 are considered synergistic, with statistical significance defined by a $p < 0.05$ and by the confidence interval not including 1.

The HR in case of synergy ($HR_{combination}$) is calculated by multiplying the HRs of both single treatment and the HR of the interaction, and the HR in case of an additive effect

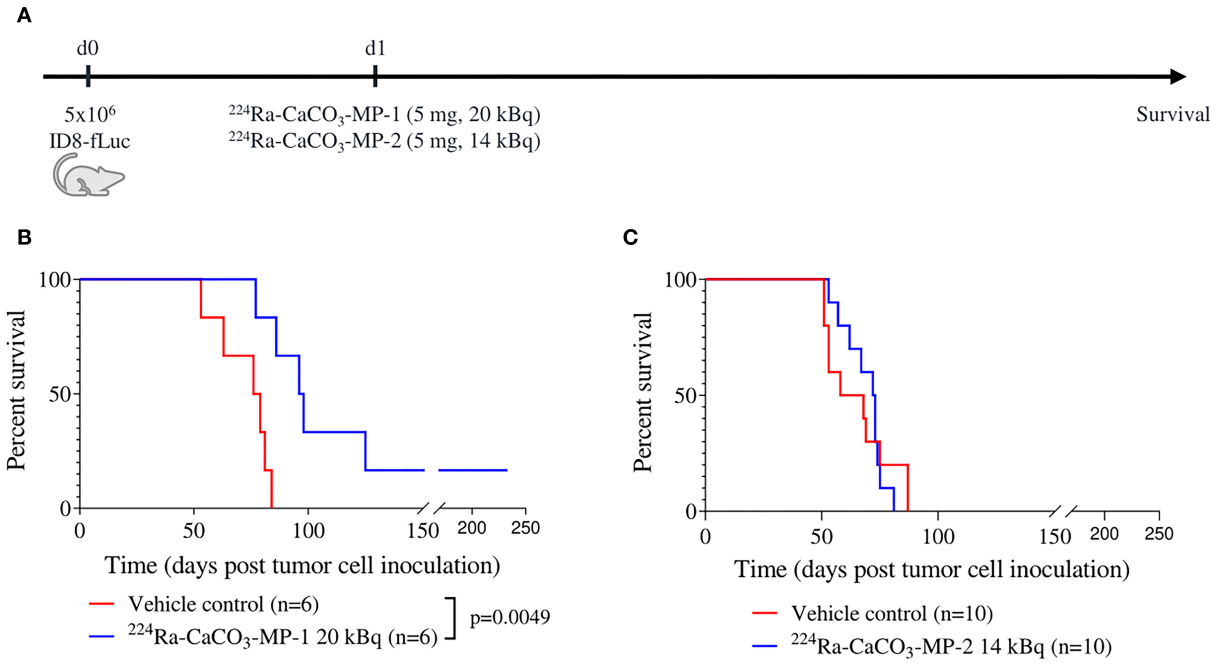


FIGURE 1
Experimental set-up **(A)** with corresponding Kaplan-Meier curves **(B,C)** for survival of mice injected IP with vehicle control and $^{224}$Ra-CaCO$_3$-MP-1 (5 mg, 20 kBq) or $^{224}$Ra-CaCO$_3$-MP-2 (5 mg, 14 kBq) on day 1 post tumor cell inoculation.

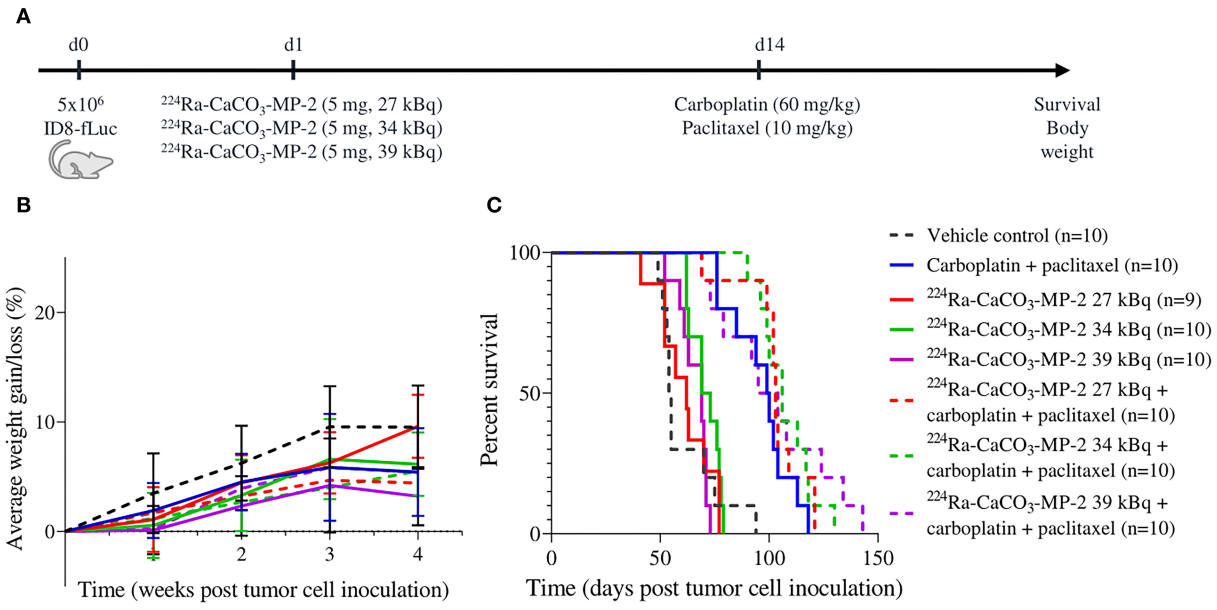


FIGURE 2
Experimental set-up **(A)** with corresponding body weight evolution as a percentage of starting weight **(B)** and Kaplan-Meier curve for survival **(C)** of mice injected IP with vehicle control, $^{224}$Ra-CaCO$_3$-MP-2 (5 mg, 27/34/39 kBq) on day 1 post tumor cell inoculation and/or carboplatin (60 mg/kg) and paclitaxel (10 mg/kg) on day 14 post tumor cell inoculation. Due to procedural complications during tumor cell inoculation (injection in visceral peritoneum instead of peritoneal cavity), one animal allocated to the $^{224}$Ra-CaCO$_3$-MP-2 27 kBq single treatment group was excluded from all further data analysis.

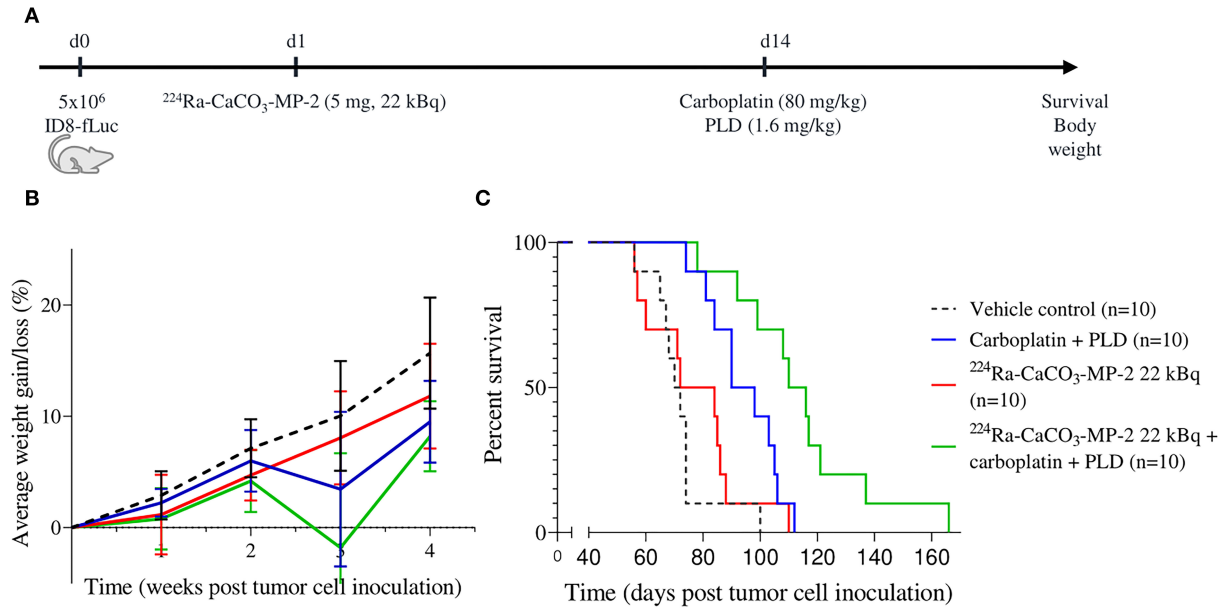


FIGURE 3
Experimental set-up **(A)** with corresponding body weight evolution as a percentage of starting weight **(B)** and Kaplan-Meier curve for survival **(C)** of mice injected IP with vehicle control, $^{224}$Ra-CaCO$_3$-MP-2 (5 mg, 22 kBq) on day 1 post tumor cell inoculation and/or carboplatin (80 mg/kg) and PLD (1.6 mg/kg) on day 14 post tumor cell inoculation.

($HR_{additive}$) is calculated by multiplying only the HRs of the single treatments.

The power analysis, Bliss analysis and linear mixed model fitting were performed using R version 4.1.0 (R Foundation for Statistical Computing, Vienna, Austria, https://www.R-project.org/), all other statistical analyses were performed using GraphPad Prism version 8.2.1 (GraphPad Software, San Diego, CA, USA).

# Results

## Therapeutic potential of $^{224}$Ra-CaCO$_3$-MP as an IP treatment in the immune competent ID8-fLuc mouse model for ovarian cancer

Two product formulations of $^{224}$Ra-CaCO$_3$-MP were evaluated in the immune competent ID8-fLuc mouse model for ovarian cancer. Treatment with the early-phase development product formulation $^{224}$Ra-CaCO$_3$-MP-1 was able to significantly prolong survival compared to vehicle control mice (median survival of 97 and 77.5 days, respectively, $p = 0.0049$) and cured 17% of the mice at an activity dose of 20 kBq/mouse with an average of 1,004 kBq/kg body weight (Figure 1B). In a follow-up experiment with the $^{224}$Ra-CaCO$_3$-MP-2 formulation developed for clinical use, where control of microparticle size over time was achieved and a sterilization procedure was introduced [20], there was no effect on overall survival at an activity dose of 14 kBq/mouse with an average of 805 kBq/kg body weight (Figure 1C). Even though the activity dose in this experiment was lower (14 compared to 20 kBq/mouse), higher activity doses that were used in the combination studies discussed below (ranging between 22 and 39 kBq/mouse) had a similar outcome (Figures 2C, 3C). The MSRs of all single treatments with $^{224}$Ra-CaCO$_3$-MPs, were higher than 1 in all investigated conditions (Table 1).

## Therapeutic synergistic effect of $^{224}$Ra-CaCO$_3$-MP combined with chemotherapy

$^{224}$Ra-CaCO$_3$-MPs were combined with two different chemotherapy regimens commonly used in clinical practice. In these studies, our first readout included therapeutic efficacy in terms of survival. In a first experiment we combined the first-line chemotherapy regimen carboplatin-paclitaxel with different activity doses of $^{224}$Ra-CaCO$_3$-MP: 27, 34 and 39 kBq/mouse with an average of 1,466, 1,847 and 2,118 kBq/kg body weight. None of the activity dose levels of $^{224}$Ra-CaCO$_3$-MP-2 in combination with carboplatin-paclitaxel were able to significantly improve survival compared to mice treated with carboplatin-paclitaxel alone (Figure 2C). No statistically significant synergistic effects were observed for any of the

TABLE 1 Median survival ratios (MSRs) for $^{224}$Ra-$CaCO_3$-MP as a single treatment compared to vehicle control.

| Treatment (dose) | Median survival experimental group (days) | Median survival vehicle control group (days) | MSR |
|---|---|---|---|
| *$^{224}$Ra-$CaCO_3$-MP-1 (5 mg, 20 kBq)* | 97.0 | 77.5 | 1.3 |
| *$^{224}$Ra-$CaCO_3$-MP-2 (5 mg, 14 kBq)* | 72.5 | 63.0 | 1.2 |
| *$^{224}$Ra-$CaCO_3$-MP-2 (5 mg, 22 kBq)* | 78.0 | 71.0 | 1.1 |
| *$^{224}$Ra-$CaCO_3$-MP-2 (5 mg, 27 kBq)* | 62.5 | 54.5 | 1.1 |
| *$^{224}$Ra-$CaCO_3$-MP-2 (5 mg, 34 kBq)* | 71.0 | 54.5 | 1.3 |
| *$^{224}$Ra-$CaCO_3$-MP-2 (5 mg, 39 kBq)* | 69.0 | 54.5 | 1.3 |

TABLE 2 Assessment of synergistic effect between $^{224}$Ra-$CaCO_3$-MP-2 and carboplatin-paclitaxel or carboplatin-PLD.

| Treatment | Hazard ratio | 95% CI | *p-value* |
|---|---|---|---|
| **$^{224}$Ra-$CaCO_3$-MP-2 (5 mg, 27 kBq) with carboplatin (60 mg/kg)-paclitaxel (10 mg/kg)** | | | |
| Carboplatin-paclitaxel | 0.0823 | (0.0251–0.2691) | < 0.001 |
| $^{224}$Ra-$CaCO_3$-MP-2 | 0.9125 | (0.3617–2.3020) | 0.846 |
| Carboplatin-paclitaxel and $^{224}$Ra- $CaCO_3$-MP-2 | 0.6020 | (0.1609–2.2523) | 0.451 |
| $HR_{combination}$ | 0.0452 | na | na |
| $HR_{additive}$ | 0.0751 | na | na |
| **$^{224}$Ra-$CaCO_3$-MP-2 (5 mg, 34 kBq) with carboplatin (60 mg/kg)-paclitaxel (10 mg/kg)** | | | |
| Carboplatin-paclitaxel | 0.0645 | (0.0200–0.2080) | < 0.001 |
| $^{224}$Ra-$CaCO_3$-MP-2 | 0.6153 | (0.2444–1.5493) | 0.303 |
| Carboplatin-paclitaxel and $^{224}$Ra- $CaCO_3$-MP-2 | 0.8600 | (0.2339–3.1623) | 0.820 |
| $HR_{combination}$ | 0.0341 | na | na |
| $HR_{additive}$ | 0.0397 | na | na |
| **$^{224}$Ra-$CaCO_3$-MP-2 (5 mg, 39 kBq) with carboplatin (60 mg/kg)-paclitaxel (10 mg/kg)** | | | |
| Carboplatin-paclitaxel | 0.1117 | (0.0399–0.3132) | < 0.001 |
| $^{224}$Ra-$CaCO_3$-MP-2 | 1.0801 | (0.4141–2.8174) | 0.875 |
| Carboplatin-paclitaxel and $^{224}$Ra- $CaCO_3$-MP-2 | 0.5525 | (0.1404–2.1745) | 0.396 |
| $HR_{combination}$ | 0.0667 | na | na |
| $HR_{additive}$ | 0.1206 | na | na |
| **$^{224}$Ra-$CaCO_3$-MP-2 (5 mg, 22 kBq) with carboplatin (80 mg/kg) -PLD (1.6 mg/kg)** | | | |
| Carboplatin-PLD | 0.2421 | (0.0944–0.6208) | 0.0032 |
| $^{224}$Ra-$CaCO_3$-MP-2 | 0.5262 | (0.2086–1.3273) | 0.1738 |
| Carboplatin-PLD and $^{224}$Ra- $CaCO_3$-MP-2 | 0.5023 | (0.1221–2.0658) | 0.3399 |
| $HR_{combination}$ | 0.0640 | na | na |
| $HR_{additive}$ | 0.1274 | na | na |

PLD, pegylated liposomal doxorubicin; CI, confidence interval; na, not applicable.

activity doses and the carboplatin-paclitaxel chemotherapy regimen. However, there is a tendency toward synergism for the highest activity dose level of $^{224}$Ra-$CaCO_3$-MP-2 (39 kBq) when comparing the $HR_{combination}$ (0.0667) with the $HR_{additive}$ (0.1206). An overview of all HRs can be found in Table 2.

Subsequently, we assessed a combination with carboplatin-PLD as an example of a second-line chemotherapy regimen. Only one activity dose of $^{224}$Ra-$CaCO_3$-MP was included: 22 kBq/mouse with an average of 1,300 kBq/kg body weight. While $^{224}$Ra-$CaCO_3$-MP-2 as a single treatment was not able to prolong survival, the combination of $^{224}$Ra-$CaCO_3$-MP-2 combined with the carboplatin-PLD resulted in a prolonged survival compared to mice that received chemotherapy alone (median survival of 114 and 94.5 days, respectively, $p_{adj} = 0.0102$) (Figure 3C). However, the biologically observed synergistic effect between carboplatin-PLD and $^{224}$Ra-$CaCO_3$-MP-2 treatment is not supported by a statistically significant effect ($p = 0.3399$), although there is a tendency toward synergism when comparing the $HR_{combination}$ (0.0640) and the

TABLE 3 Median survival ratios (MSRs) for $^{224}$Ra-$CaCO_3$-MP combined with chemotherapy compared to chemotherapy as a single treatment.

| Treatment (dose) | Median survival combination group (days) | Median survival chemotherapy only group (days) | MSR |
|---|---|---|---|
| Carboplatin (60 mg/kg)-paclitaxel (10 mg/kg) and $^{224}$Ra-$CaCO_3$-MP-2 (5 mg, 27 kBq) | 103 | 99.5 | 1.0 |
| Carboplatin (60 mg/kg)-paclitaxel (10 mg/kg) and $^{224}$Ra-$CaCO_3$-MP-2 (5 mg, 34 kBq) | 106 | 99.5 | 1.1 |
| Carboplatin (60 mg/kg)-paclitaxel (10 mg/kg) and $^{224}$Ra-$CaCO_3$-MP-2 (5 mg, 39 kBq) | 99.5 | 99.5 | 1.0 |
| Carboplatin (80 mg/kg)-PLD (1.6 mg/kg) and $^{224}$Ra-$CaCO_3$-MP-2 (5 mg, 22 kBq) | 113 | 94 | 1.2 |

PLD, pegylated liposomal doxorubicin.

TABLE 4 Overview of weight change assessment in mice that received $^{224}$Ra-$CaCO_3$-MPs as a single treatment and in combination with both carboplatin-paclitaxel and carboplatin-PLD chemotherapy regimens.

| | | $^{224}$Ra-$CaCO_3$-MP-2 (5 mg, 22 kBq) vs. vehicle control | | | |
|---|---|---|---|---|---|
| | | **Estimate** | **SE** | **95% CI** | **p-value** |
| **Intercept** | | −0.7547 | 0.3625 | [−1.465; −0.044] | 0.041 |
| **Time** | | 2.9845 | 0.3951 | [2.210; 3.759] | <0.001 |
| **Time*treatment** | | 0.9329 | 0.5319 | [−0.110; 1.975] | 0.097 |
| | | **$^{224}$Ra-$CaCO_3$-MP-2 (5 mg, 27/34/39 kBq) vs. vehicle control** | | | |
| **Intercept** | | −0.0792 | 0.2810 | [−0.632; 0.473] | 0.779 |
| **Time** | | 2.5870 | 0.2699 | [2.086; 3.102] | <0.001 |
| **Time*treatment** | 27 kBq | −0.1453 | 0.3904 | [−0.890; 0.577] | 0.712 |
| | 34 kBq | −0.7783 | 0.3800 | [−1.501; −0.073] | 0.047 |
| | 39 kBq | −1.5413 | 0.3800 | [−2.262; −0.835] | <0.001 |
| | | **$^{224}$Ra-$CaCO_3$-MP-2 (5 mg, 22 kBq) with carboplatin (80 mg/kg)-PLD (1.6 mg/kg) vs. carboplatin-PLD** | | | |
| **Intercept** | | −0.1514 | 0.7267 | [−1.576; 1.273] | 0.836 |
| **Time** | | 1.2681 | 0.4324 | [0.421; 2.116] | 0.006 |
| **Time*treatment** | | 0.8688 | 0.5065 | [−0.124; 1.862] | 0.103 |
| | | **$^{224}$Ra-$CaCO_3$-MP-2 (5 mg, 27/34/39 kBq) with carboplatin (60 mg/kg)-paclitaxel (10 mg/kg) vs. carboplatin-paclitaxel** | | | |
| **Intercept** | | 0.1806 | 0.2556 | [−0.322; 0.683] | 0.481 |
| **Time** | | 1.5512 | 0.3093 | [0.974; 2.133] | <0.001 |
| **Time*treatment** | 27 kBq | −0.3239 | 0.4323 | [−1.133; 0.484] | 0.458 |
| | 34 kBq | −0.2156 | 0.4323 | [−1.027; 0.590] | 0.621 |
| | 39 kBq | 0.0202 | 0.4323 | [−0.792; 0.825] | 0.963 |
| | | **$^{224}$Ra-$CaCO_3$-MP-2 (5 mg, 22 kBq) vs. carboplatin (80 mg/kg)-PLD (1.6 mg/kg)** | | | |
| **Intercept** | | −0.3848 | 0.4784 | [−1.322; 0.553] | 0.424 |
| **Time** | | 2.2147 | 0.3974 | [1.436; 2.994] | <0.001 |
| **Time*treatment** | | 0.6465 | 0.5148 | [−0.363; 1.656] | 0.225 |
| | | **$^{224}$Ra-$CaCO_3$-MP-2 (5 mg, 27/34/39 kBq) vs. carboplatin (60 mg/kg)-paclitaxel (10 mg/kg)** | | | |
| **Intercept** | | −0.1183 | 0.2762 | [−0.665; 0.428] | 0.670 |
| **Time** | | 1.5848 | 0.2781 | [1.049; 2.129] | <0.001 |
| **Time*treatment** | 27 kBq | 0.8301 | 0.3994 | [0.046; 1.606] | 0.045 |
| | 34 kBq | 0.2130 | 0.3887 | [−0.543; 0.963] | 0.587 |
| | 39 kBq | −0.5364 | 0.3887 | [−1.287; 0.210] | 0.176 |

Statistical analysis was performed by fitting a linear mixed model.
PLD, pegylated liposomal doxorubicin; SE, standard error; CI, confidence interval.

$HR_{additive}$ (0.1274). An overview of the different HRs can be found in Table 2.

The MSRs were also determined for the combinations of $^{224}$Ra-$CaCO_3$-MP-2 with the two different chemotherapy regimens, when compared to mice treated with chemotherapy alone. All MSRs ranged between 1 and 1.2 (Table 3).

## Combination of $^{224}$Ra-$CaCO_3$-MPs with standard of care chemotherapy regimens is feasible in terms of tolerability

Changes in body weight over time was assessed as a measure of tolerability. From the body weight curves (Supplementary Figures S1, S2), there were no indications of persistent treatment related effects. A transient loss in body weight was observed in the days following both treatment with $^{224}$Ra-$CaCO_3$-MP-2 and chemotherapy, with longest time to recovery (approximately 1 week) for the carboplatin and PLD regime. When body weight development over time was analyzed by fitting a linear mixed model, a statistically significant delay in body weight gain was found for the mice treated with the highest activity doses of 34 and 39 kBq/mouse compared to vehicle control mice ($p = 0.047$ and $p < 0.001$, respectively). However, $^{224}$Ra-$CaCO_3$-MP-2 treatment was not inferior to chemotherapy treatment in terms of body weight development over time. If anything, treatment with carboplatin-paclitaxel resulted in a delayed weight progression compared to mice that received $^{224}$Ra-$CaCO_3$-MP-2 at a dose of 27 kBq/mouse (p=0.045). More importantly, none of the groups receiving a combination of chemotherapy with the $^{224}$Ra-$CaCO_3$-MP-2 treatment presented with delayed weight progression compared to mice that received chemotherapy alone, irrespective of the chemotherapy regimen (Figures 2B, 3B, Table 4). In addition, no apparent clinical signs of toxicity were observed in any of the mice in the duration of the studies.

# Discussion

In the search for more effective treatment strategies for ovarian cancer, $\alpha$-emitting radionuclide therapies are emerging. The high energy deposition in combination with limited penetration depth can be exploited to target residual microscopic disease without affecting the surrounding radiosensitive organs. These micrometastases remain present within the peritoneal cavity after cytoreductive debulking surgery and are often related to the high recurrence rate of the disease. In this study, we specifically investigated the therapeutic potential of a newly developed $\alpha$-emitting radiopharmaceutical which consists of $^{224}$Ra adsorbed onto $CaCO_3$ microparticles, and the safety to use this in combination with chemotherapy regimens commonly used in clinical practice. We provide proof-of-principle of the therapeutic potential of $^{224}$Ra-$CaCO_3$-MPs in a syngeneic model of ovarian cancer in immune competent mice. Furthermore, the sequential administration of $^{224}$Ra-$CaCO_3$-MPs with two different standard of care chemotherapy regimens indicated that a synergistic effect can be obtained, however, the synergism was more pronounced with carboplatin-PLD compared to carboplatin-paclitaxel. In general, the various treatment combinations appeared well-tolerated in the mice.

The therapeutic potential of $^{224}$Ra-$CaCO_3$-MPs in the immune compromised ES-2 and SKOV3 mouse model for ovarian cancer have previously been demonstrated. Different product formulations of $^{224}$Ra-$CaCO_3$-MPs were able to prolong survival with MSRs ranging between 1.5 and 2.8 (20, 21, 28), while the MSRs observed in the current study ranged between 1.1 and 1.3. An important factor that might negatively influence the therapeutic efficacy in the immune competent ID8-fLuc mouse model for ovarian cancer is the reaction of the tumor immune microenvironment to the particle drug carrier ($CaCO_3$ microparticles). It has been shown that IP injections of microparticle drug carriers, including but not limited to $CaCO_3$ microparticles, elicit an immune suppressive and tumor promoting effect in the ID8-fLuc model, mediated by innate immune suppressive cells such as myeloid-derived suppressor cells and M2-like macrophages (30). Both cell types are known to be involved in ovarian cancer development and progression [recently reviewed (31)]. We believe that the slight survival benefit in the ID8-fLuc model can be explained by the fact that the immune-related tumor promoting mechanisms in response to the $CaCO_3$ microparticles partially counteract the therapeutic effect of the $^{224}$Ra. In another syngeneic mouse model of disseminated peritoneal disease, albeit of colorectal origin (CT26.WT), treatment with the $^{224}$Ra-$CaCO_3$-MPs was able to significantly prolong survival (MSR of 1.8) (28), indicating that the tumor-promoting mechanisms are not universal among different disease models.

One novelty with the current study is the use of the fully immune competent ID8-fLuc mouse model for ovarian cancer. Previously published work on the $^{224}$Ra-$CaCO_3$-MPs in ovarian cancer models was performed in immune compromised mouse models (ES-2 and SKOV3). Since the strong immune suppressive tumor microenvironment in patients with ovarian cancer is an important factor in the disease progression (31), we provide additional proof of the therapeutic potential of the $^{224}$Ra-$CaCO_3$-MPs in a mouse model that closely resembles this clinical situation. The study design was aimed to mimic the clinically relevant standard of care chemotherapy regimens, although, it should be noted that the IP administration route of the different chemotherapeutics differs from the standard administration route in patients with ovarian cancer (intravenous administration).

However, we recognize that our study encounters some limitations. With the current data, we are not able to provide

a mechanistic explanation as to why two chemotherapy chemotherapy regimens result in a different outcome when combined with $^{224}$Ra-$CaCO_3$-MPs. Several mechanisms can be responsible for creating synergistic or additive effects between chemotherapy and radiation therapy. The mechanism of action for the specific chemotherapeutic drug may radiosensitize tumor cells to α-radiation to a varying degree. In addition, it is known that different chemotherapy regimens have different effects on the ovarian cancer immune microenvironment in mice (32, 33). Hence, the immune response caused by the $^{224}$Ra-$CaCO_3$-MPs and the chemotherapeutics may favor some but not all combinations and dosages. A future characterization of both the cytotoxic mechanisms and immunological responses of the combined $^{224}$Ra-$CaCO_3$-MPs and chemotherapy treatment might therefore aid with identifying the most optimal combination regimens.

In the past, other applications with $\alpha$-particle emitters have been evaluated for the treatment for ovarian cancer. Preclinical evaluation of IP treatment with $^{211}$At-labeled monoclonal antibodies showed a high therapeutic efficacy in treating micrometastatic growth in the OVCAR-3 ovarian cancer mouse model (34, 35). Additionally, the $\alpha$-emitter $^{212}$Pb has been evaluated as an IP treatment in the immunodeficient ES-2 and A2780cp20 mouse models for ovarian cancer showing a therapeutic potential when labeled to a monoclonal antibody or $CaCO_3$ microparticles (36, 37). Additionally, $^{212}$Pb and $^{211}$At colloids have also been investigated previously in a preclinical setting for IP ovarian cancer dissemination, where they have proven their therapeutic potential (38, 39). No immediate and/or late signs of local radiation-induced toxicities were observed in the phase I clinical evaluation of $^{211}$At- or $^{212}$Pb-labeled antibody treatments in patients with ovarian cancer (18, 19, 40, 41). These results are as expected with the limited range of tissue penetration of $\alpha$-emitters, preventing irradiation of other radiosensitive organs within the peritoneal cavity.

Furthermore, the combined effects of $\alpha$-therapies and chemotherapeutics on weight development in mice as a measure for toxicity have been evaluated previously. Milenic and colleagues reported a modest weight loss in mice treated sequentially with $^{212}$Pb-trastuzumab and gemcitabine compared to mice that received gemcitabine alone in a model for colon carcinoma (LS-174T) (42), which is in contrast to what we observed in our study. However, the same group reported no difference in weight development between mice that received paclitaxel and $^{213}$Bi-trastuzumab or paclitaxel alone in the same tumor model (43), indicating a differential response to combinations of different types and dosages of chemotherapy and radionuclides. Both combination regimens described above also produced synergistic therapeutic effects that could not be reached by these therapeutics separately (42, 43).

We provide proof-of-principle for the therapeutic efficacy $^{224}$Ra-$CaCO_3$-MPs in an immune competent mouse model for ovarian cancer, both alone and in combination with chemotherapy. Furthermore, the results indicate a safe sequential administration with two different chemotherapy regimens often used in clinical practice. The results support further evaluation of $^{224}$Ra-$CaCO_3$-MPs in patients with ovarian cancer. However, further investigations remain to identify the most optimal chemotherapy regimen to combine with $^{224}$Ra-$CaCO_3$-MPs and the sequence of therapies to fully exploit a potential synergistic effect.

## Data availability statement

The raw data supporting the conclusions of this article will be made available by the authors, without undue reservation.

## Ethics statement

The animal study was reviewed and approved by Katholieke Universiteit Leuven.

## Author contributions

Conceptualization and interpretation of results: RW, SW, AC, and TB. Design of experiments: RW and SW. *In vivo* experiments: RW, YB, and MR. Analysis of results: RW and MR. Statistics: RW and JC. Manuscript writing: RW. Manuscript proof-reading: JC, YB, MR, SW, TB, IV, and AC. Supervision: SW, TB, IV, and AC. Funding acquisition: TB and AC. All authors have read and agreed to the published version of the manuscript.

## Funding

This research was funded by the Norwegian Research Council (with project number 304591) and Oncoinvent AS.

## Acknowledgments

The authors would like to thank Ann Vankerckhoven, Gitte Thirion, and Katja Vandenbrande for their support in the execution and follow-up of the animal experiments described in this manuscript. Additionally, the R&D department of Oncoinvent AS is acknowledged for the production, shipping, and activity measurements of the $^{224}$Ra-labeled $CaCO_3$ microparticles used in these experiments.

## Conflict of interest

RW was employed by Oncoinvent AS. AC was a contracted researcher for Oncoinvent AS and Novocure and a consultant

for Sotio a.s. SW was employed by and a shareholder of Oncoinvent AS. TB was employed by and a shareholder of Oncoinvent AS. IV is a consultant for Agenus, Akesobio, AstraZeneca, Bristol Myers Squibb, Deciphera Pharmaceuticals, Eisai, Elevar Therapeutics, F. Hoffmann-La Roche, Genmab, GSK, Immunogen, Jazzpharma, Karyopharm, Mersana, MSD, Novocure, Novartis, Oncoinvent, OncXerna, Sanofi, Seagen, Sotio, Verastem Oncology and Zentalis, was a contracted researcher for Oncoinvent AS, performs corporate sponsored research for Amgen and Roche, and receives accommodation and travel expenses from Karyopharm, Genmab and Novocure. The funders (The Norwegian Research Council (project 304591) and Oncoinvent AS) provided support in the form of salaries for authors RW, SW, and TB but did not have any additional role in the study design, data collection, analysis or interpretation, preparation of the manuscript, or decision to publish.

The remaining authors declare that the research was conducted in the absence of any commercial or financial relationships that could be construed as a potential conflict of interest.

## Publisher's note

All claims expressed in this article are solely those of the authors and do not necessarily represent those of their affiliated organizations, or those of the publisher, the editors and the reviewers. Any product that may be evaluated in this article, or claim that may be made by its manufacturer, is not guaranteed or endorsed by the publisher.

## Supplementary material

The Supplementary Material for this article can be found online at: https://www.frontiersin.org/articles/10.3389/fmed.2022.995325/full#supplementary-material

## References


1. Bray F, Ferlay J, Soerjomataram I, Siegel RL, Torre LA, Jemal A. Global cancer statistics 2018: GLOBOCAN estimates of incidence and mortality worldwide for 36 cancers in 185 countries. CA Cancer J Clin. (2018) 68:394–424. doi: 10.3322/caac.21492

2. Cabasag CJ, Fagan PJ, Ferlay J, Jerome V, Mathieu L, Lihua L, et al. Ovarian cancer today and tomorrow: A global assessment by world region and Human Development Index using GLOBOCAN 2020. *Int J Cancer*. (2022) 151:1535–41. doi: 10.1002/ijc.34002

3. Siegel RL, Miller KD, Jemal A. Cancer statistics 2016. *CA Cancer J Clin*. (2016) 66:7–30. doi: 10.3322/caac.21332

4. Prat J. Staging classification for cancer of the ovary, fallopian tube, and peritoneum. *Int J Gynecol Obstet*. (2014) 124:1–5. doi: 10.1016/j.ijgo.2013.10.001

5. Vergote I, Gonzalez-Martin A, Lorusso D, Gourley C, Mirza MR, Kurtz J-E, et al. Clinical research in ovarian cancer: consensus recommendations from the Gynecologic Cancer InterGroup. *Lancet Oncol*. (2022) 23:e374–84. doi: 10.1016/S1470-2045(22)00139-5

6. Baert T, Ferrero A, Sehouli J, O'donnell DM, González-Martín A, Joly F, et al. The systemic treatment of recurrent ovarian cancer revisited. (2021) 32:710–25. doi: 10.1016/j.annonc.2021.02.015

7. Torre LA, Trabert B, DeSantis CE, Miller KD, Samimi G, Runowicz CD, et al. Ovarian cancer statistics, 2018. *CA Cancer J Clin*. (2018) 68:284–96. doi: 10.3322/caac.21456

8. Bakri YN, Given FT, Peeples WJ, Frazier AB. Complications from intraperitoneal radioactive phosphorus in ovarian malignancies. *Gynecol Oncol*. (1985) 21:294–9. doi: 10.1016/0090-8258(85)90266-5

9. Vergote IB, Vergote-De Vos LN, Abeler VM, Aas M, Lindegaard MW, Kjmstad KE, et al. Randomized trial comparing cisplatin with radioactive phosphorus or whole-abdomen irradiation as adjuvant treatment of ovarian cancer. *Cancer*. (1992) 69:741–9.3.0.CO;2-G" target="_blank">https://doi.org/10.1002/1097-0142(19920201)69:3<741::AID-CNCR2820690322>3.0.CO;2-G

10. Rosenshein NB, Leichner PK, Vogelsang G. Radiocolloids in the treatment of ovarian cancer. Obstet Gynecol Surv. (1979) 34:708–20. doi: 10.1097/00006254-197909000-00028

11. Aure J, Høeg K, Kolstad P. Radioactive colloidal gold in the treatment of ovarian carcinoma. *Acta Radiol Ther Phys Biol*. (1971) 10:399–407. doi: 10.3109/02841867109130785

12. Verheijen RH, Massuger LF, Benigno BB, Epenetos AA, Lopes A, Soper JT, et al. Phase iii trial of intraperitoneal therapy with yttrium-90-labeled hmfg1 murine monoclonal antibody in patients with epithelial ovarian cancer after a surgically defined complete remission. *J Clin Oncol*. (2006) 24:571–8. doi: 10.1200/JCO.2005.02.5973

13. Epenetos AA, Hird V, Lambert H, Mason P, Coulter C. Long term survival of patients with advanced ovarian cancer treated with intraperitoneal radioimmunotherapy. *Int J Gynecol Cancer*. (2000) 10 (Suppl. 1):44–6. doi: 10.1046/j.1525-1438.2000.99510.x

14. Kino T, Ando N, Ogawara Y, Shigeta H. Proton beam therapy for recurrent ovarian carcinoma: A case report. *J Obstet Gynaecol Res*. (2019) 45:1952–6. doi: 10.1111/jog.14036

15. Nawa A, Suzuki K, Kato S, Fujiwara S, Kajiyama H, Shibata K, et al. Carbon beam therapy in recurrent ovarian cancer. *Ann Oncol*. (2008) 19:192–4. doi: 10.1093/annonc/mdm553

16. Vergote I, Larsen RH, De Vos L, Nesland JM, Bruland Ø, Bjørgum J, et al. Therapeutic efficacy of the α-emitter 211At bound on microspheres compared with 90Y and 32P colloids in a murine intraperitoneal tumor model. *Gynecol Oncol*. (1992) 47:366–72. doi: 10.1016/0090-8258(92)90141-5

17. Parker C, Nilsson S, Heinrich D, Helle SI, O'Sullivan JM, Fosså SD, et al. Alpha emitter radium-223 and survival in metastatic prostate cancer. *N Engl J Med*. (2013) 369:213–23. doi: 10.1056/NEJMoa1213755

18. Hallqvist A, Bergmark K, Bäck T, Andersson H, Dahm-Kähler P, Johansson M, et al. Intraperitoneal α-emitting radioimmunotherapy with 211At in relapsed ovarian cancer: long-term follow-up with individual absorbed dose estimations. *J Nucl Med*. (2019) 60:1073–9. doi: 10.2967/jnumed.118.220384

19. Meredith RF, Torgue JJ, Rozgaja TA, Banaga EP, Bunch PW, Alvarez RD, et al. Safety and outcome measures of first-in-human intraperitoneal α radioimmunotherapy with 212Pb-TCMC-trastuzumab. *Am J Clin Oncol*. (2018) 41:716. doi: 10.1097/COC.0000000000000353

20. Westrøm S, Bønsdorff TB, Bruland ØS, Larsen RH. Therapeutic effect of α-emitting 224 ra-labeled calcium carbonate microparticles in mice with intraperitoneal ovarian cancer. *Transl Oncol*. (2018) 11:259–67. doi: 10.1016/j.tranon.2017.12.011

21. Li RG, Napoli E, Jorstad IS, Bønsdorff TB, Juzeniene A, Bruland ØS, et al. Calcium carbonate microparticles as carriers of 224ra: impact of specific activity in mice with intraperitoneal ovarian cancer. *Curr Radiopharm*. (2020) 13. doi: 10.2174/18744710MTEx5OTYyy

22. National Library of Medicine (US). *Identifier NCT03732768. Study of Radspherin® in Recurrent Ovarian Cancer Subjects With Peritoneal Carcinomatosis*. ClinicalTrials.gov.

23. National Library of Medicine (US). Identifier NCT03732781. *Study of Radspherin® in Colorectal Carcinoma Subjects With Peritoneal Carcinomatosis Treated With HIPEC*. ClinicalTrials.gov.

24. Baert T, Verschuere T, Van Hoylandt A, Gijsbers R, Vergote I, Coosemans A. The dark side of ID8-Luc2: pitfalls for luciferase tagged murine models for ovarian cancer. *J Immunother Cancer*. (2015) 3:57. doi: 10.1186/s40425-015-0102-0

25. Kilkenny C, Browne WJ, Cuthill IC, Emerson M, Altman DG. Improving bioscience research reporting: The arrive guidelines for reporting animal research. *PLoS Biol*. (2010) 8:e1000412. doi: 10.1371/journal.pbio.1000412

26. Council NR. *Guide for the Care and Use of Laboratory Animals. Guide for the Care and Use of Laboratory Animals*. Washington, DC: National Academies Press. (2011).

27. Westrøm S, Malenge M, Jorstad IS, Napoli E, Bruland ØS, Bønsdorff TB, et al. Ra-224 labeling of calcium carbonate microparticles for internal α-therapy: Preparation, stability, and biodistribution in mice. *J Labelled Comp Radiopharm*. (2018) 61:472–86. doi: 10.1002/jlcr.3610

28. Li RG, Lindland K, Tonstad SK, Bønsdorff TB, Juzeniene A, Westrøm S, et al. Improved formulation of 224Ra-labeled calcium carbonate microparticles by surface layer encapsulation and addition of EDTMP. *Pharmaceutics*. (2021) 13:5. doi: 10.3390/pharmaceutics13050634

29. Demidenko E, Miller TW. Statistical determination of synergy based on Bliss definition of drugs independence. *PLoS ONE*. (2019) 14:e0224137. doi: 10.1371/journal.pone.0224137

30. Wouters R, Westrøm S, Vankerckhoven A, Thirion G, Ceusters J, Claes S, et al. Effect of particle carriers for intraperitoneal drug delivery on the course of ovarian cancer and its immune microenvironment in a mouse model. *Pharm*. (2022) 14:687. doi: 10.3390/pharmaceutics14040687

31. Fucikova J, Coosemans A, Orsulic S, Cibula D, Vergote I, Galluzzi L, et al. Immunological configuration of ovarian carcinoma: features and impact on disease outcome. *J Immunother Cancer*. (2021) 9:2873. doi: 10.1136/jitc-2021-002873

32. Vankerckhoven A, Baert T, Riva M, De Bruyn C, Thirion G, Vandenbrande K, et al. Type of chemotherapy has substantial effects on the immune system in ovarian cancer. *Transl Oncol*. (2021) 14:101076. doi: 10.1016/j.tranon.2021.101076

33. Zitvogel L, Apetoh L, Ghiringhelli F, Kroemer G. Immunological aspects of cancer chemotherapy. *Nat Rev Immunol*. (2008) 8:59–73. doi: 10.1038/nri2216

34. Elgqvist J, Andersson H, Bäck T, Hultborn R, Jensen H, Karlsson B, et al. Therapeutic efficacy and tumor dose estimations in radioimmunotherapy of intraperitoneally growing OVCAR-3 cells in nude mice with 211At-labeled monoclonal antibody MX35. *J Nucl Med*. (2005) 46.

35. Elgqvist J, Andersson H, Jensen H, Kahu H, Lindegren S, Warnhammar E, et al. Repeated intraperitoneal alpha-radioimmunotherapy of ovarian cancer in mice. *J Oncol*. (2010) 2010:394913. doi: 10.1155/2010/394913

36. Kasten BB, Arend RC, Katre AA, Kim H, Fan J, Ferrone S, et al. B7-H3-targeted 212Pb radioimmunotherapy of ovarian cancer in preclinical models. *Nucl Med Biol*. (2017) 47:23–30. doi: 10.1016/j.nucmedbio.2017.01.003

37. Li RG, Lindland K, Bønsdorff TB, Westrøm S, Larsen RH. A novel single-step-labeled 212Pb-CaCO3 microparticle for internal alpha therapy: preparation, stability, and preclinical data from mice. *Materials (Basel)*. (2021) 14:7130. doi: 10.3390/ma14237130

38. Bloomer WD, McLaughlin WH, Neirinckx RD, Adelstein SJ, Gordon PR, Ruth TJ, et al. Astatine-211—tellurium radiocolloid cures experimental malignant ascites. *Science*. (1981) 212:340–1. doi: 10.1126/science.7209534

39. Rotmensch J, Atcher RW, Schlenker R, Hines J, Grdina D, Block BS, et al. The effect of the α-emitting radionuclide lead-212 on human ovarian carcinoma: A potential new form of therapy. *Gynecol Oncol*. (1989) 32:236–9. doi: 10.1016/S0090-8258(89)80040-X

40. Meredith R, Torgue J, Shen S, Fisher DR, Banaga E, Bunch P, et al. Dose escalation and dosimetry of first-in-human α radioimmunotherapy with 212Pb-TCMC-trastuzumab. *J Nucl Med*. (2014) 55:1636–42. doi: 10.2967/jnumed.114.143842

41. Meredith RF, Torgue J, Azure MT, Shen S, Saddekni S, Banaga E, et al. Pharmacokinetics and imaging of 212Pb-TCMC-trastuzumab after intraperitoneal administration in ovarian cancer patients. *Cancer Biother Radiopharm*. (2014) 29:12. doi: 10.1089/cbr.2013.1531

42. Milenic DE, Garmestani K, Brady ED, Albert PS, Abdulla A, Flynn J, et al. Potentiation of high-LET radiation by gemcitabine: targeting HER2 with trastuzumab to treat disseminated peritoneal disease. *Clin Cancer Res*. (2007) 13:1926–35. doi: 10.1158/1078-0432.CCR-06-2300

43. Milenic DE, Garmestani K, Brady ED, Baidoo KE, Albert PS, Wong KJ, et al. Multimodality therapy: potentiation of high-LET radiation with paclitaxel for the treatment of disseminated peritoneal disease. *Clin Cancer Res*. (2008) 14:5108. doi: 10.1158/1078-0432.CCR-08-0256

frontiers | Frontiers in Medicine

TYPE Original Research
PUBLISHED 15 November 2022
DOI 10.3389/fmed.2022.1033303



OPEN ACCESS

EDITED BY
Roy Larsen,
Sciencons AS, Norway

REVIEWED BY
Jostein Dahle,
Nordic Nanovector, Norway
Calogero D'Alessandria,
Technical University of Munich,
Germany

*CORRESPONDENCE
Axel Berg-Larsen
axel.berg-larsen@bayer.com
Alan Cuthbertson
alan.cuthbertson@bayer.com

SPECIALTY SECTION
This article was submitted to Nuclear Medicine, a section of the journal Frontiers in Medicine

RECEIVED 31 August 2022
ACCEPTED 18 October 2022
PUBLISHED 15 November 2022

CITATION
Berg-Larsen A, Mobergslien A, Moen I, Petros G, Kristian A, Gunvaldsen KS, Cruciani V, Wickstroem K, Bjerke RM, Karlsson J and Cuthbertson A (2022) Tumor growth inhibition and immune system activation following treatment with thorium-227 conjugates and PD-1 check-point inhibition in the MC-38 murine model. *Front. Med.* 9:1033303. doi: 10.3389/fmed.2022.1033303



# Tumor growth inhibition and immune system activation following treatment with thorium-227 conjugates and PD-1 check-point inhibition in the MC-38 murine model

Axel Berg-Larsen*, Anne Mobergslien, Ingrid Moen, Gebregziabher Petros, Alexander Kristian, Kristine Sponheim Gunvaldsen, Véronique Cruciani, Katrine Wickstroem, Roger Malerbakken Bjerke, Jenny Karlsson and Alan Cuthbertson*

Bayer AS, Oslo, Norway

Targeted thorium-227 conjugates comprise the combination of a monoclonal antibody with specificity for a tumor cell antigen and a 3,2-HOPO chelator enabling complexation of thorium-227 (Th-227). The radiolabeled conjugate functions as an effective delivery system of alpha-particle radiation to the surface of the tumor cell inducing difficult to repair complex DNA damage and cell death. In addition, the mechanism of action of targeted alpha therapy (TAT) appears to involve a significant component linked to stimulation of the immune system. We report herein evidence of immune activation and long-lasting immune protection of a TAT in a syngeneic model using the MC-38 murine cell line. Firstly, MC-38 cells were irradiated *ex vivo* with the thorium labeled antibody before subcutaneous implantation into mice. These mice were then rechallenged with MC-38 cells contra-laterally. In the group receiving irradiated cells, 9 out of 10 animals had no measurable tumor growth compared to aggressive tumor growth in the control group. Secondly, in an efficacy study, 500 kBq/kg of thorium labeled antibody alone or in combination with PD-1 checkpoint inhibitor gave statistically significant tumor growth inhibition compared to vehicle control. Animals with no measurable tumors were once again rechallenged contra-laterally with MC-38 cells. The re-growth of tumors was significantly delayed (approx. 60 days) in the treatment group compared to age-matched controls (approx. 30 days) in the monotherapy group. Interestingly, in the TAT/ PD-1 combination group no re-growth was observed demonstrating the potential of combining a TAT with checkpoint inhibition therapy. Finally, tumors were excised from treated mice and analyzed by flow cytometry and immunohistochemistry

(IHC). Analysis revealed significant infiltration of CD8+ T-cells and mature dendritic cells compared to vehicle controls. Together these results indicated that an ongoing immune response from treatment with alpha radiation could be enhanced by check-point inhibition.

KEYWORDS

**thorium, alpha-therapy, PD-1/L1, radiotherapy, immune activation, immune checkpoint inhibitors, conjugate**

## Introduction

Targeted alpha therapy (TAT) is an emerging modality in the field of anti-cancer therapy and is dependent on the targeted delivery of alpha-particle emitting radionuclides to the tumor tissue (1). Targeted thorium-227 conjugates (TTCs) represent one such therapeutic approach comprising the combination of an antibody, with specificity for a tumor cell antigen, conjugated to a 3,2-HOPO chelator enabling complexation of Th-227 (2, 3). The resulting radiolabeled conjugate functions as an effective delivery system of alpha radiation inducing double strand DNA breaks and tumor cell death (4). In addition, due to the short range of the alpha-particle track there is limited damage to the surrounding healthy tissue (5).

The half-life of Th-227 (18.7 days) is compatible with the blood half-life of antibodies in humans, a key factor which allows for significant accumulation of the TTC in the tumor. Th-227 decay results in the generation of a total of five high-energy alpha and two beta particles ending with the stable element lead-207 (Pb-207) (6). The first daughter of thorium-227 is radium-223 (Ra-223), which also has a long decay half-life of 10.4 days. Radium-223 dichloride, the only TAT product currently approved by the FDA, is a calcium mimetic which deposits at the sites of abnormal re-modeling in bone metastases in patients with mCRPC. Adjacent tumor cells are therefore destroyed by crossfire of alpha particles (7). TTCs target the surface of the tumor cell and are not dependent on internalization as the path length of an alpha particle is between 2 and 10 cell diameters, extending the breadth of tumor specific antigens to non-internalizing targets. The high and localized energy deposited by the alpha-particle induces difficult to repair DNA double strand breaks in the target cell and TATs may therefore effectively evade many of the pathways by which cancer cells acquire resistance (8).

We have previously published TTCs with potential for the treatment of acute myeloid leukemia, renal-, breast-, lung cancer as well as mesothelioma and prostate cancer (9–14). We have also demonstrated their efficacy in *in vitro* and *in vivo* models as monotherapies as well as strong synergistic effects observed in combination with inhibitors of DNA damage repair (9, 11, 12). However, the influence TAT has on the immune system seems also to make an important contribution to the mechanism of action (15). The evaluation of synergies with immunotherapies have not been exhaustively studied and still need to be better understood (16).

The immune system plays a key role in inhibiting tumor growth through a process often referred to as immunoediting (17). Immune activation works in concert with selected anti-cancer treatments through the induction of immunogenic cell death further enhancing the therapeutic effect, the nature and potency of which, is dependent on the mechanism of action and tumor biology (18). This concept has been explored thoroughly in mice and has also been shown to be transferable to the human setting. The type and location of immune cell infiltrates in the tumor determines the outcome of immunoediting and is influenced both by the tumor environment and the choice of therapy (19). Immune cells can either infiltrate the core of the tumor or remain confined to the tumor margins and adjacent lymphatic vessels. Notably, infiltration post therapy can often be highly heterogeneous across specific tumor-types in a given population as well as in the metastatic setting within individual patients (20).

Depending on the type of immune response that is prevalent in the tumor, different outcomes are expected. In particular, the nature of the infiltrating T-lymphocytes (CD3+ T-cells) is critical for a positive outcome. An immune response dominated by $T_H1$ helper T-cells and CD8+ cytotoxic T-cells is often correlated with inhibition of tumor growth and complete tumor regression both in mice and humans (21), while a response dominated by T-regulatory cells (FOXP3+) is often neutral or even negatively correlated with patient overall survival (22). Likewise, the nature and type of the innate immune cells in the tumor may have a profound role to play. A tumor with a large macrophage population is correlated with poorer outcomes than one where a large mature dendritic cell population is present (23).

The success of check-point inhibitors has led to a greater understanding of the nature of the immune response even in advanced tumors (24). Programmed death-ligand 1 (PD-L1) and its receptor PD-1 on immune cells have been the most frequent targets of such therapy (25). PD-L1 is normally

not expressed at high levels in tissue that is not immune-privileged in some manner, but is upregulated in response to certain inflammatory cytokines such as interferon-γ (IFN-γ) (26). The PD-L1/PD-1 interaction deactivates T-cells and prevents target cell killing, and this mechanism is used by tumor cells to avoid immunoediting. As such, there is often a latent immune response against even advanced cancers already present at the tumor site, being suppressed by such check-points as well as other immune system avoidance strategies (27). By introducing check-point inhibitors it is possible to reactivate the immune response and induce regression of tumor growth, but it is still the case that only a minority of patients respond to a significant degree. Check-point inhibition can therefore be administered in combination with other therapies to further enhance efficacy and patient outcomes (28).

We describe herein the effect of a combination of TAT and a check-point inhibitor in murine models of CRC utilizing the tumor cell line MC-38 in an attempt to explore potential synergies with TAT (29). The principle aim of this study was to investigate if such an effect can be observed using a PD-L1 TTC in combination with PD-1 targeted therapy.

# Materials and methods

## Preparation of thorium conjugated antibodies

Conjugates were prepared as described in Hagemann et al. (9), using a recombinant murine anti-PD-L1 antibody based on the sequence of atezolizumab to make murine IgG1 (Anti-PD-L1 mIgG1 Kappa, RG7446 chimera, PPB-6390), produced in-house by Bayer AG (Wuppertal, Germany). For isotype antibody conjugate, mouse isotype BAY 2862727 (SSB-Isotype-mIgG1Lambda) was used. HOPO-chelator-to-antibody ratio was measured using SE-HPLC at 280 nm (antibody) and 335 nm (HOPO). Briefly, the conjugates were prepared by coupling an *N*-hydroxysuccinimide-activated 3,2-hydroxypyridinone (HOPO) chelator covalently to the $\epsilon$-amino groups of the lysine residues. The chelator-to-antibody ratio (CAR) for the prepared batch was 0.6. Radiolabeling with thorium-227 was done in 30 mmol/L citrate, 70 mmol/L NaCl, 0.5 mg/mL PABA, 2 mmol/L EDTA, pH 5.5 at room temperature for 1 h.

## Media and cell lines

As a target cell for TTC treatment we used the colon cell line MC-38 (NMI) cultured in RPMI (Biowest) + 10%FBS (Hyclone) 1%P/S (Corning) + 1xMEM-NEAA (Gibco) + 1xNaPyr (Gibco) + 0.5 μg/ml Blasticidin (Life Technologies). As a control cell line, we used the skin cell line B16-F10 (ATCC) cultured in DMEM/Ham's F12 (Biochrom.) + 10% FBS (HyClone) + 1% P/S (Corning).

Cell viability was measured using CellTiter Glo (# G924C, Nerliens Meszansky) read of on an EndoSafe platereader after 6 days of TTC or control treatment.

## *In vivo* procedures

The *in vivo* procedures described in this manuscript have all been approved by the National Animal Research Authority and were carried out in compliance with the European Convention for the Protection of Vertebrates Used for Scientific Purposes. Female C57BL/6JRj C57B/k (H-2b) aged 4, 5, or 16 weeks, weighing 15–18 or 18–25 g, acquired from Janvier Labs, France were used as host animals. 200.000 MC-38 cells were inoculated subcutaneously (s.c.) in the right flank for efficacy and distribution studies, 100.000 MC-38 or B16-F10 cells were inoculated (s.c.) in the left flank for rechallenge experiments.

For distribution experiments, PD-L1-TTC or an untargeted isotype Th-227 conjugate) was administered at 0.14 mg/kg and 500 kBq/kg via the tail vein. Organs were harvested at predefined timepoints, and the distribution was investigated by measuring thorium-227 in selected organs by high purity geranium detector detector (HPGe). Pre-treatment with 0.2 mg/animal anti-PD-L1 antibody was given to separate groups by intraperitoneal (i.p.) injection the day before TTC treatment. In the efficacy and rechallenge experiments, animals were treated with PD-L1-TTC or isotype conjugate at 0.14 mg/kg and 500 kBq/kg, with or without 0.2 mg/animal anti-PD-L1 or anti-PD-1 antibody pretreatment. Anti-PD-L1 was identical to non-conjugated PD-L1 as described above. Anti-PD-1 antibody was supplied by BioXCell (RMP1-14). For each rechallenge with MC-38 or B16-F10 cells, five age-matched control animals received the same inoculation of cells.

When pre-inoculation irradiation with thorium-227 was required, cells were exposed to 40 kBq/ml thorium-227 for 48 h. Excess thorium-227 was removed by wash cycle and cells were harvested and inoculated as described above.

## Isolation of immune cells from mice tumor and spleen

Tumors were cut into small pieces and dissociated using a tumor dissociation kit (Miltenyi Biotec) with the gentleMACS tumor dissociator according to manufactures protocol. CD45+ cells were isolated from the resulting cell suspension using magnetic microbeads (Miltenyi Biotec) on a MACS separator column (Miltenyi Biotec) mounted on a magnetic scaffold.

Spleens were mashed through a 70 μm nylon cell strainer using a sterile plunger. The resulting spleenocytes were washed

in PBS and then resuspended in 5X RCB lysis buffer (Milenyi Biotec). Once erythrocytes were removed, the cells were strained through a 40 μm nylon filter and washed in PBS three times in succession for a final suspension of spleenocytes.

## Cell toxicity assay

MC-38 cells were seeded in 384 wells plates and incubated over night at 37°C, 5% $CO_2$. Next day, added 0.03% tween to the PD-L1 TTCs and isotype Th-227 conjugate before they were added to the cells, by using the D300e digital dispenser with concentrations as indicated. The plates were normalized to highest fluidic volume.

After 7 days incubation was 30 μl CellTiter-Glo added to each well. Read-out was luminescence on Wallace Envision Platereader.

## γH2AX and DAMP measurement

MC-38 cells were seeded in six wells plates, 250,000 cells per well in 5 ml medium. Next day, added the compounds; 2, 10, and 25 kBq/ml was used for the PD-L1-TTCs and 10 and 25 kBq/ml for isotype Th-227 conjugate. After 48 and 72 h exposure the cells were harvested, permeabilized and stained with yH2AX or DAMPS markers as described below.

## Flow cytometry

Cells were stained for flow cytometry using CD3, CD4, and CD8 antibodies as well as dead cell marker for T-cells, and CD86, CD64, and CD11c for dendritic cells and macrophages. T-regulatory cells were fixed and stained using the T reg detection kit Miltenyi Biotec) according to manufacturer's specification.

Antibodies used for flow were as follows: α-CD4 PE (Miltenyi Biotec), α-CD8 Vivobright FITC (Miltenyi Biotec), α-CD3 APC (MIltenyi Biotec), α-CD11c FITC (MiItenyi Biotec), α-CD86-PE (Miltenyi Biotec), and α-CD64-APC (Miltenyi Biotec).

Danger-Associated Molecular Patterns were analyzed by staining targeted cells with anti-human Calreticulin (CRT)-A647 (Bioss), anti-human HSP70-A647 (Bioss), anti-human GRP94-A647 (Bioss), and anti-human HMGB1-A647 (Bioss). yH2AX was analyzed by staining the cells using anti-human yH2AX (Biolegend). All antibodies were cross-reactive with mice.

To measure immunomarkers, the cells were stained with APC anti-mouse IFNAR-1 (Biolegend), APC anti-mouse CD252 (Biolegend), APC anti-mouse CD54 (Biolegend), APC anti-mouse CD152 (Biolegend), APC anti-mouse CD274 (Biolegend), APC anti-mouse CD137 (Biolegend), APC anti-mouse CEACAM-1/CD66a (R&D), Alexa Fluor 647 anti-mouse B7-H2 (R&D) Alexa Fluor 647 anti-mouse TRAILR1/TNFRSF10A (Novus), Alexa Fluor 647 anti-mouse CD27 ligand/TNFSF7/CD70 (Novus).

All cells were analyzed on a Guava Easycyte 8HT flow cytometer.

## Immunohistochemistry

Immunostaining of tumor sections was performed on 3 μm-thick FFPE (formalin fixed paraffin embedded) sections. Sections incubated in 60°C for 30 min in a heating cabinet before deparaffinization in xylene and then hydrated in graded alcohol solutions. Target retrieval performed in a preheated steamer for 25 min in Target Retrieval solution pH9, 10x (Dako). Thereafter cooled on ice until temperature reached 50°C. Slides were placed in a humidifying chamber and incubated with primary Ab for 60 min. Sections were stained with primary Ab against PD-L1 (Nordic Biosite, 1:100 dilution), CD4 (AbCam, 1:1,000 dilution) and CD8 (AbCam, 1:2,000 dilution). Slides then blocked with 3% peroxidase blocking solution, $H_2O_2$ (Nordic Biosite), before incubation with Envision labeled polymer anti Rabbit (Dako) for 30 min. Antibody-antigen complex was visualized with DAB substrate system for 10 min (Dako) followed by counterstaining with Hematoxilin (Sigma) for 60 s. Slides were dehydrated in increasing alcohol-containing solutions, ending in xylene, before mounting. Positive control tissue added to all staining set-ups (sections of spleen and lymph with a known expression of the target).

## Statistical analysis

Performed as indicated in figure legends. Differences between groups were considered statistical significant when $p < 0.05$.

# Results

## *In-vitro* targeted thorium-227 conjugates treatment induces danger associate molecular patterns upregulation and immunogenic cell death

To determine the effectiveness of the radiolabeled conjugate we first measured the response of our target cells *in vitro*. PD-L1 TTC was cytotoxic to MC-38 cells (**Figure 1A**), and DNA damage measured by detecting γH2Ax levels by flowcytometry (**Figure 1B**). In culture, a dose dependent increase in the danger associate molecular patterns (DAMPS) calreticulin,

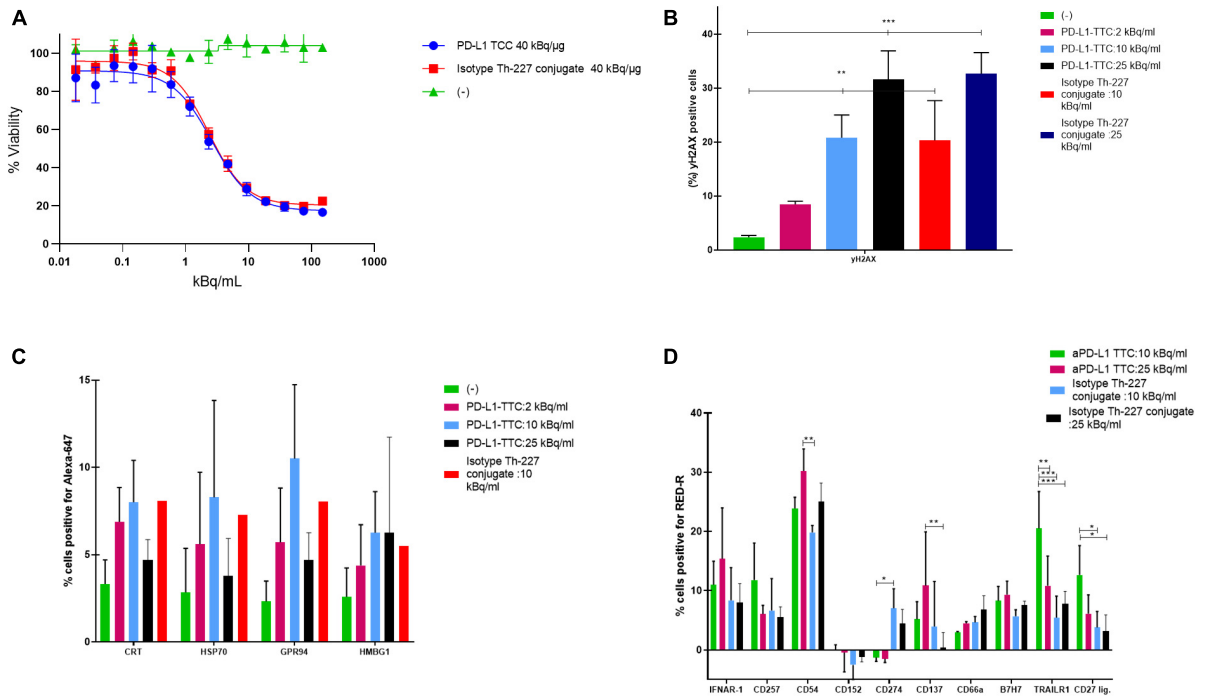


FIGURE 1
**(A)** Cell viability of MC-38 treated for 7 days with indicated targeted thorium-227 conjugates (TTC) or cold conjugate. **(B)** MC-38 cells (%) positive for γH2AX by flow cytometry staining after 7 days of treatment with indicated TTC or cold conjugate. **(C)** MC-38 cells (%) positive for four common DAMPs by flow cytometry after 7 days of treatment with indicated TTC or cold conjugate. **(D)** MC-38 cells (%) positive for 10 additional DAMPs by flow cytometry after 7 days of treatment with indicated TTC or cold conjugate. Tukey's multiple comparison test, $*p < 0.05$, $**p < 0.01$, $***p < 0.001$.

HSP70, GPR94, and HMBG1, expressed on the cell surface, was observed (Figure 1C) indicating the potential for induction of immunogenic cell death (ICD) by alpha radiation (30). This effect was also significant for the isotype Th-227 conjugate. We also observed a strong dose dependent expression of immune marker ICAM-1 (CD54) and cytokine receptors IFNAR-1 and CD137 (Figure 1D).

To investigate whether such an immune response could induce immunity *in vivo*, we performed a study similar to Gorin et al. (31) whereby we firstly irradiated MC-38 cells with thorium conjugated antibodies *in vitro* 48 h prior to subcutaneous implantation of the irradiated cells in mice. After 7 days mice were challenged with living, non-irradiated cells (Figure 2A).

In the group initially receiving irradiated MC-38 cells, 9 out of 10 mice rejected the non-irradiated MC-38 tumor at challenge (day 7), while growth was observed in all mice in the age-matched control group (Figure 2A). The specificity for MC-38 cells was evaluated by rechallenge of the immunized mice, with either B16-F10 or MC-38 cells 90 days after the initial cell inoculation (Figure 2B). Tumor growth was observed in 5 out of 5 mice rechallenged with B16-F10 cells, while the mice rechallenged with MC-38 showed no tumor growth, indicating that the immunization effect was specific for MC-38 cells.

## Programmed death-ligand 1 targeted thorium-227 conjugates monotherapy and combination with anti-PD-1 check-point inhibition

Based on the initial results, we then explored whether the PD-L1 TTC would be efficacious *in vivo*, inducing a similar immunization effect following systemic administration. A biodistribution study in the MC-38 model initially demonstrated rapid blood PK (Figure 3A) for the PD-L1 TTC due to the rapid accumulation in the spleen with an observed uptake of >50% ID/g after 24 h (Figure 3C).

As a result, tumor accumulation was low at around 5–8% ID/g at 24 h, decreasing to 2–3% ID/g at the 168 h timepoint (Figure 3B). The high splenic uptake was reduced by blocking with a pre-dose of PD-L1 (i.p. 0.2 mg/kg) resulting in an increased tumor uptake of the PD-L1 TTC to 20% ID/g at 168 h.

The high level of PD-L1 expression in both liver and spleen was confirmed by IHC staining (Figures 3F,G) with significantly less staining observed in the tumor (Figure 3E). As such, pre-dosing of the check-point inhibitor appeared to prevent excessive binding of the PD-L1 TTC in liver and spleen allowing for improved delivery to the tumor.

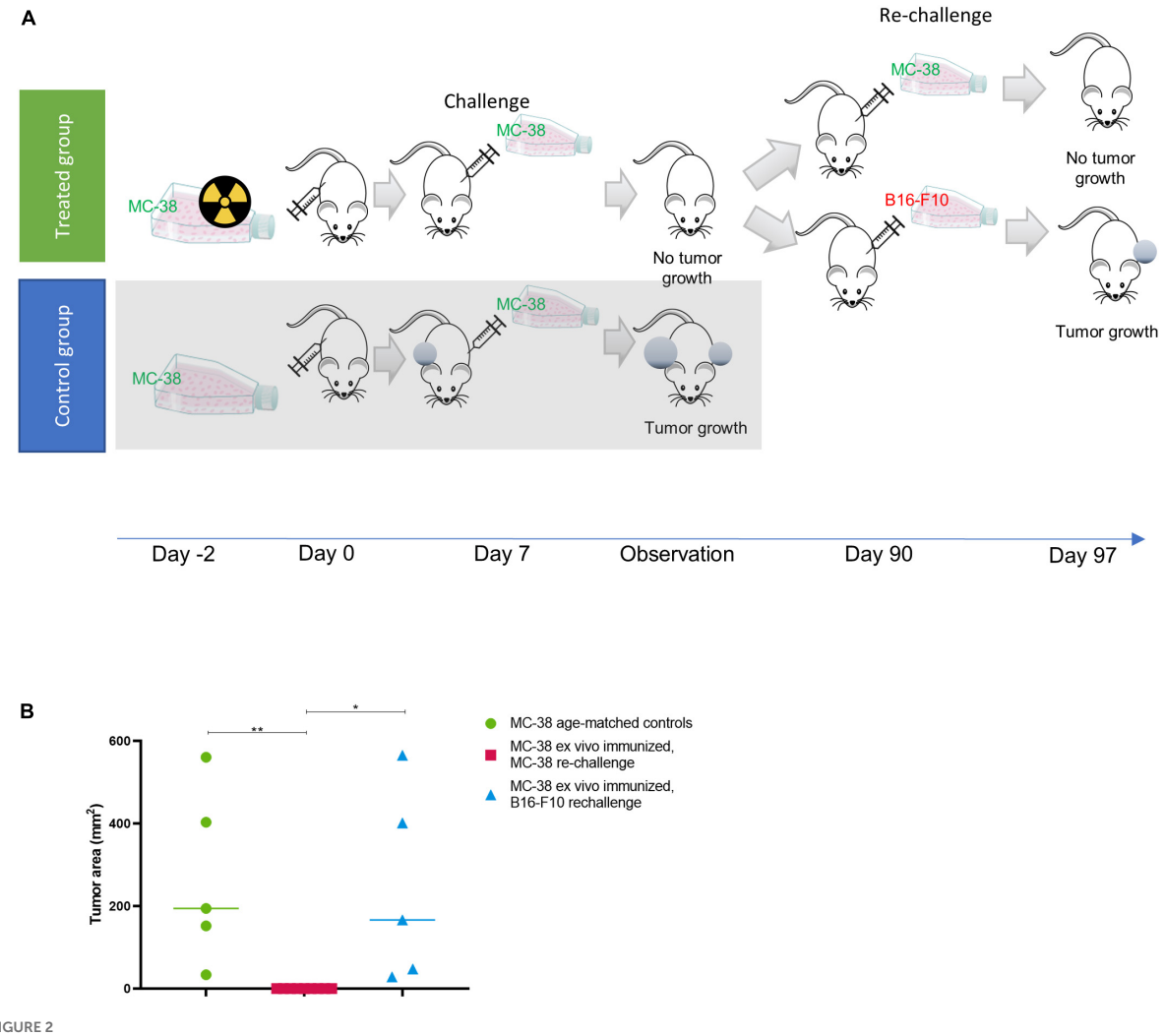


FIGURE 2
*Ex vivo* immunization with irradiated MC-38 cells. **(A)** Scheme detailing *ex-vivo* immunization using targeted thorium-227 conjugates (TTC) irradiated MC-38 cells. In brief, mice were implanted with MC-38 cells pretreated with alpha radiation ($n = 10$), or with healthy MC-38 cells to serve as control ($n = 5$). The mice were then challenged with a new MC-38 implantation after 7 days, and the mice that did not develop tumor were rechallenged once again after 90 days using MC-38 or the unrelated B16-F10 cell line ($n = 5$). **(B)** Size of tumors at day of sacrifice in each treatment group. 0 indicates no measurable tumor observed at sacrifice. Student's *T*-test, $*p < 0.05$ and $**p < 0.01$.

An efficacy study was then performed with an anti-PD-1 check point inhibitor alone or in combination with isotype Th-277 conjugate or PD-L1 TTC. While no effect on tumor growth was observed for the anti-PD-1 group alone, statistically significant inhibition of tumor growth was observed for all other treatment groups including the isotype Th-227 conjugate dosed at 500 kBq/kg with no apparent synergy for either PD-L1 TTC or isotype Th-227 conjugate with addition of the check point inhibitor (Figure 4). On day 23 after treatment, there were six mice with no measurable tumor, all treated with TTC. Interestingly, two of these mice were treated with isotype conjugate, 1 with isotype conjugate + anti-PD-1, 1 with PD-L1 TTC and 2 with PD-L1 TTC + anti-PD-1, showing no clear bias between treatment groups.

## Mice rechallenged after treatment with combination therapy show no tumor re-growth

To understand if efficacy was related to the induction of an effective and specific immune response these animals were further challenged with a second inoculation of MC-38 and B16-F10 cells. The six responding mice were randomized into two treatment groups ($n = 3$) along with a third age-matched control group ($n = 5$). To allow for full immune recovery, the mice were left until day 129 before rechallenge.

In the age-matched control group the tumors grew rapidly over the first 30 days post implantation while in the TTC monotherapy group the growth was significantly delayed out

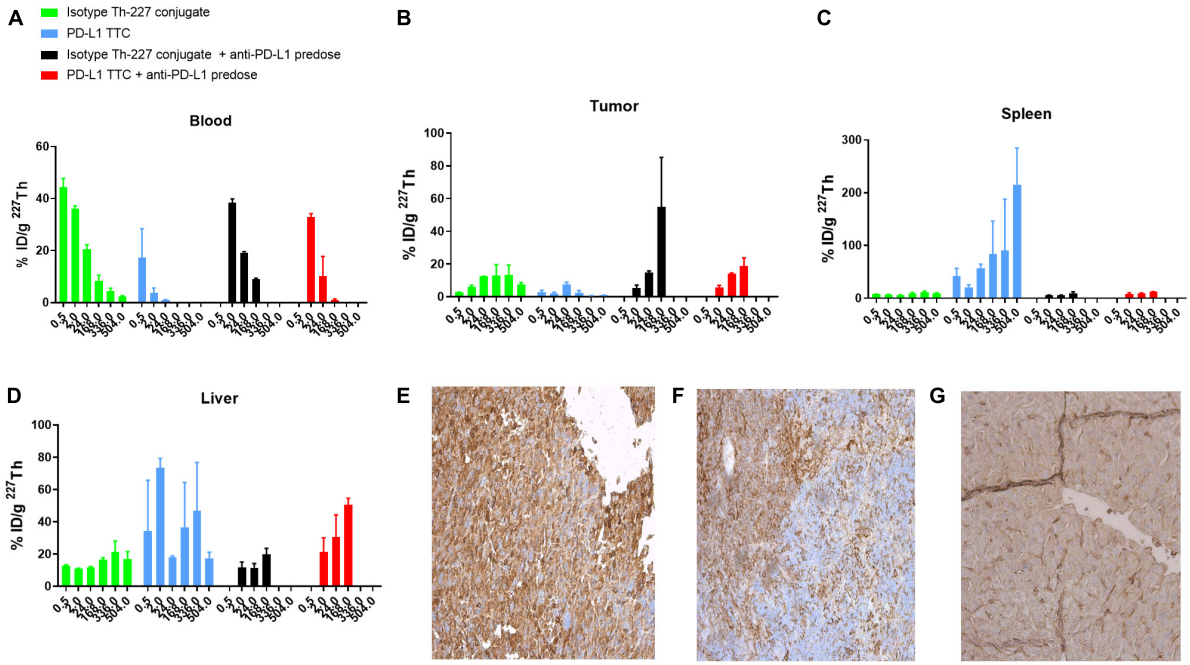


FIGURE 3
**(A–D)** Biodistribution of 500 kBq/kg isotype Th-227 conjugate or PD-L1-TTC in MC-38_EGFP mice without and with 0.2 mg anti-PD-L1 predosing before dosing. $n = 3$/group/timepoint. **(E)** PD-L1 expression in MC-38 tumor. **(F)** PD-L1 expression in C57BL/6 spleen. **(G)** PD-L1 expression in C57BL/6 liver. For blanks of IHC staining, see **Supplementary Figure 4**.

to 60 days. Surprisingly, mice from the combination group showed no re-growth of MC-38 tumors (**Figure 5A**). To evaluate the specificity of the response all treated mice ($n = 6$) were inoculated with B16-F10 cells contralaterally 42 days after MC-38 cell rechallenge and compared once again to a new age-matched control group ($n = 5$). B16-F10 cells tumor growth was observed in all mice (**Figure 5B**) including the anti-PD1 combination groups.

The tumors which had regrown in the TTC monotherapy groups were excised and immunohistochemistry performed to investigate the extent of T-cell infiltration (**Figure 5C**). Both CD8+ and CD4+ T-cells were present in large numbers in the MC-38 tumors but not in the B16-F10 tumors. Based on these data, we wished to further investigate the infiltration of immune cells into treated tumors in a new study.

## Cytotoxic T-cells infiltrate the tumors and contribute to cancer treatment

In this follow-up study all mice were pre-dosed with anti-PD-L1 antibody prior to PD-L1 TTC monotherapy and combination treatments. Tumors and spleens were isolated from all mice and immune cells extracted. Flow cytometry (**Supplementary Figure 1**) performed 6 days after treatment revealed CD3+ T-cell infiltration in all tumors (**Figure 6**). Over time we observed a change in the sub-population of T-cells from day 6 to day 14. There was a reduction of CD4+ cells (**Figure 6A**) in the TTC-treated group in comparison to the other groups, with a corresponding increase in CD8+ T-cells (**Figure 6B**). Identifying T-regulatory cells (Tregs) in the tumors as FOXP3+ CD4+, we also observed that Tregs are reduced significantly in PD-L1 TTC treated tumors, and slightly reduced in other treatment groups outside of vehicle control (**Figure 6C**). The ratio of Tregs to $CD8^+$ cells (**Figure 6D**) was also significantly increased in the TTC+PD-L1 treatment group, indicating an ongoing cytotoxic immune response, correlating with the shrinking tumor size (**Figure 3**).

## Mature dendritic cells supporting immune responses in targeted thorium-227 conjugates treated tumors

In addition to T-cells we also isolated dendritic cells and macrophages from the tumors to investigate the innate immune response to the TTC treatment. We found that mature DCs (CD45+, CD11+, CD86+, and CD64-) were increased after 14 days in PD-L1 TTC treated tumors, but not in any other group (**Figure 7A**). Macrophages (CD45+, CD64+, and CD11-) were high after 6 days but decreased in all treatment groups after 14

10.3389/fmed.2022.1033303

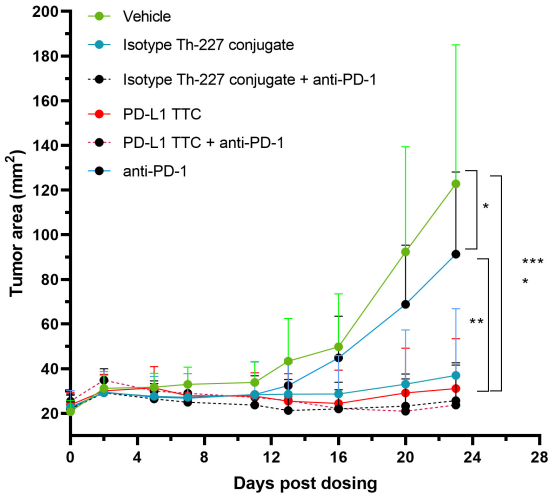


FIGURE 4
MC-38 tumor bearing mice were treated with vehicle, 500 kBq/kg isotype Th-227 conjugate, 500 kBq/kg PD-L1-TTC, anti-PD-1 (10 mg/kg, 2× weekly) or a combination of 500 kBq/kg PD-L1-TTC and anti-PD-1 (10 mg/kg, 2× weekly). All mice were pre-dosed with 0.2 mg of anti-PD-L1 prior to TTC dosing. After 23 days all TTC treatment groups demonstrated statistically significant tumor growth inhibition compared to the vehicle control group, ($n = 8$) as analyzed by 2-way ANOVA with Tukey's post hoc test *=0.05, **=0.01, ****=0,0001.

days (**Figure 7B**). Together, these results indicate that dendritic cells are driving the innate immune response in the tumors in contrast to macrophages.

## Discussion

The cytotoxic effect of radiotherapy in general is well documented (32). However, it appears that direct cell death inducing apoptosis and necrosis is only partially responsible for the observed efficacy and that the immune response triggered by the radiation also plays a role to a significant degree (33–35). Radiation therefore functions as an immunological adjuvant, triggering an immune response that overcomes the tumors inherit acquired immune evasive state (36, 37). The combination of check-point inhibitors and high dose radiation in some indications has demonstrated synergy in several studies (38–41). The immunogenicity of cells targeted by radiation therapy varies from tumor to tumor depending on both type of radiation and the cell lines inherit immunogenicity (31). In the current study, we show that alpha radiation in combination with check-point inhibition not only induces tumor regression but also appears to lead to the increased infiltration of CD8+ T-cells into tumors and the development of long-lasting immunity against tumor cells.

Our initial goal was to show that TAT treatment alone could induce a sufficient immune response to allow for long lasting immunity, as has been previously published (15, 31). MC-38 is an immunogenic cell line that also expresses PD-L1 and as such is a good target for both check-point inhibition and TAT treatment (**Figures 1A,B**). The *in vitro* treatment with both PD-L1 TTC and isotype Th-227 conjugate induced equivalent amounts of cell death (**Figure 1A**) and upregulation of markers of immunologic cell death including the DAMPs HMGB1, CRT and HSPs (**Figures 1C,D**), known to have immunostimulatory effects in tumors (42–45). Although there is no known antigen for the isotype antibody expressed on the tumor cells, it appears there is some non-specific binding to the MC-38 cell line, indicating that the antibody is not a true negative control. It is also of note that MC-38 cells do not express much PD-L1 *in vitro* (data not shown) but upregulate PD-L1 *in vivo* due to the changing microenvironment (**Figure 3**). Thus the observed *in vitro* effects are due to the damage induced by alpha particles and not dependent on antibody specificity.

By irradiating target cells in vitro followed by inoculation into immune competent mice, an immune response was triggered that resulted in long lasting immunity against MC-38 cells (**Figure 2A**). Rechallenged with fresh MC-38 cells, tumor growth was completely inhibited in 9 out of 10 animals in the group of immune stimulated mice, but not in the age-matched control mice or in mice inoculated with the B16-F10 cell line (**Figure 2B**). This demonstrated that some degree of specific immune protection had been achieved comparable to the previously published work of Gorin et al. (31).

Having demonstrated that we could induce immunity in this manner, we then went on to explore the potential of the TAT inducing immune responses directly *in vivo*. MC-38 tumors express PD-L1 *in vivo* (**Figure 3E**), however, as PD-L1 is also expressed in normal tissues such as spleen and liver (**Figures 3F,G**) a PD-L1 pre-dose was required to reduce non-target organ uptake and increase tumor targeting (**Figures 3C,D**). Interestingly, the non-targeting isotype antibody also displayed relatively high tumor uptake, similar to PD-L1 TTC (**Figure 3B**), likely due to a combination of non-specific binding (**Figure 1**), and a significantly enhanced permeability and retention effect in this tumor model (46). The high tumor uptake of both TTCs may also explain why statistically significant tumor growth inhibition was achieved for both PD-L1 TTC and isotype Th-227 conjugate as a monotherapy and in combination with PD-1 check-point inhibition (**Figure 4**). Anti-PD-1 alone had only a modest effect in this tumor model (**Figure 4**). Alpha radiation treatment appears therefore to induce an immune response through immunogenic cell death, with enhanced efficacy in combination with check-point inhibition. This has been previously reported with other methods of irradiation in combination with check point inhibition (47).

A common response to immune activation within a tumor is the upregulation of checkpoint ligands including PD-L1 resulting in the loss of significant immune response (41, 48).

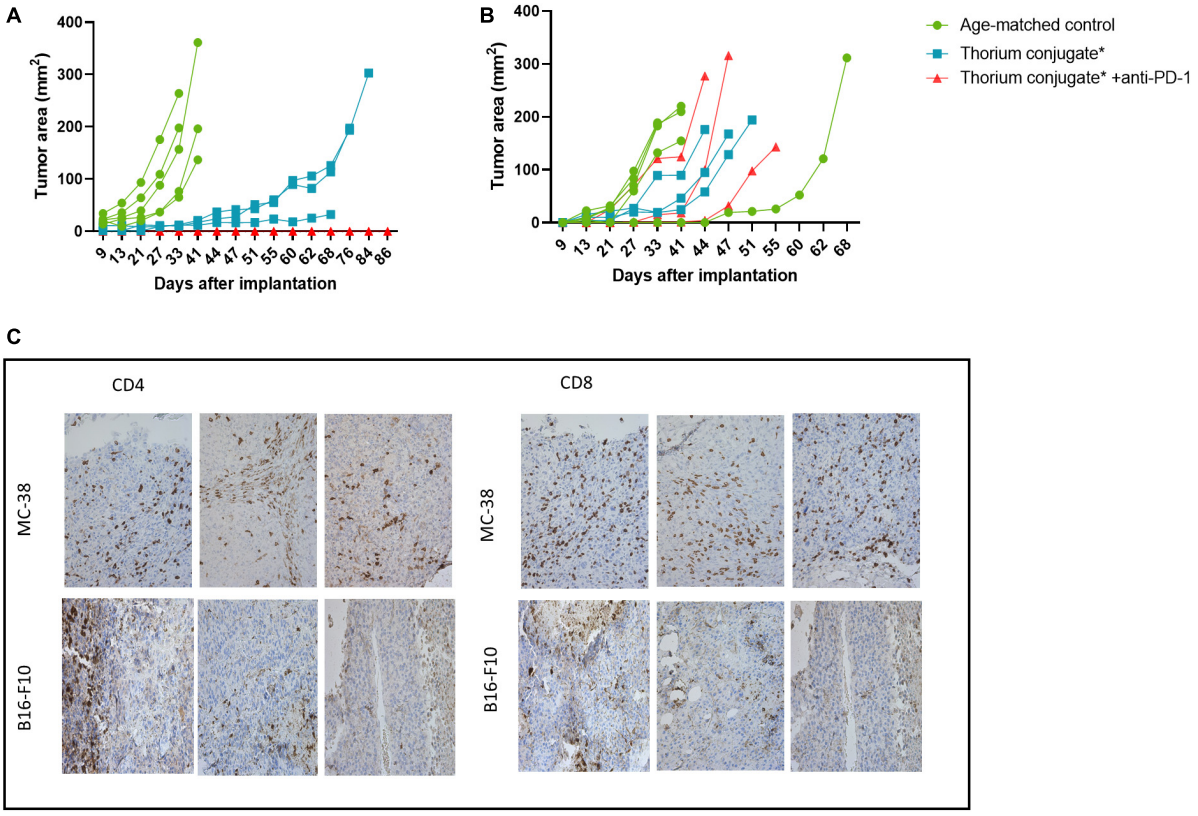


FIGURE 5
**(A)** Growth curve for rechallenge with MC-38 cells after treatment as indicated, $n = 5$ in control groups, three in treatment groups. **(B)** Growth curve for rechallenge with B16-F10 cells after treatment as indicated, $n = 5$ in control groups, three in treatment groups. **(C)** IHC slides from MC-38 and B16-F10 tumors stained for CD4+ and CD8+ T-cells. Slides are from regrowing tumors of monotherapy treated mice. *Animals previously treated with either PD-L1 TTC or isotype Th-227 conjugate.

Any increase in expression would be expected to increase the radiation dose delivered to the tumor by the PD-L1 TTC as more radionuclide is delivered to the target. Furthermore, the addition of an anti-PD-1 antibody seemed to complement alpha radiation treatment, likely due to the presence of PD-1 expressing CD8+ T-cells in the tumors (Figure 6B). The addition of anti-PD-1 would counteract increasing PD-L1 levels and work by inducing T-cell activation even as more cells express PD-L1. PD-1 is also known to be expressed at increasing levels during persistent encounters with antigens, as is likely in a tumor environment. The effect of the combination therapy should increase over time, as the immune response continues, and immune memory is generated. As immune memory is also known to be modulated through the PD-1 pathway, the effect of the combination therapy should also be persistent in rechallenge experiments (49), as we indeed observed (Figure 5).

In order to investigate further the key components of immune activation and protection, mice with no detectable tumor from the combination and monotherapy groups (Figure 4) were pooled and after 90 days rechallenged with MC-38 cells. Interestingly, Figure 5 shows that the age-matched control group all grew tumors of $>100$ mm$^2$ in 30–40 days while in the TTC monotherapy group regrowth was significantly delayed with tumors $>100$ mm$^2$ measured after 60 days. Surprisingly there were no measurable tumors in the group treated with the combination of TTC and PD-1. This was a clear indication that the combination therapy had triggered a stronger, more robust immune response leading to long term protection. To further characterize the immune response, tumors from the monotherapy group were excised on regrowth ($>200$ mm$^2$) and cells extracted for analysis and IHC. IHC (Figure 5C) revealed the presence of infiltrating T-cells in the TTC treated group but not in the age-matched control tumors. This response was enough to delay tumor growth but not enough to result in long term protection potentially due to the development of tumor immune evasion or resistance (50, 51).

We postulated that the observed longer-term protection of the anti-PD-1/TTC combination therapy reflected the nature of the immune response. The combination group was less susceptible to escaping immune surveillance, allowing the development of a robust intra-tumoral memory effector T-cell response (52) which eliminated the nascent tumor. The

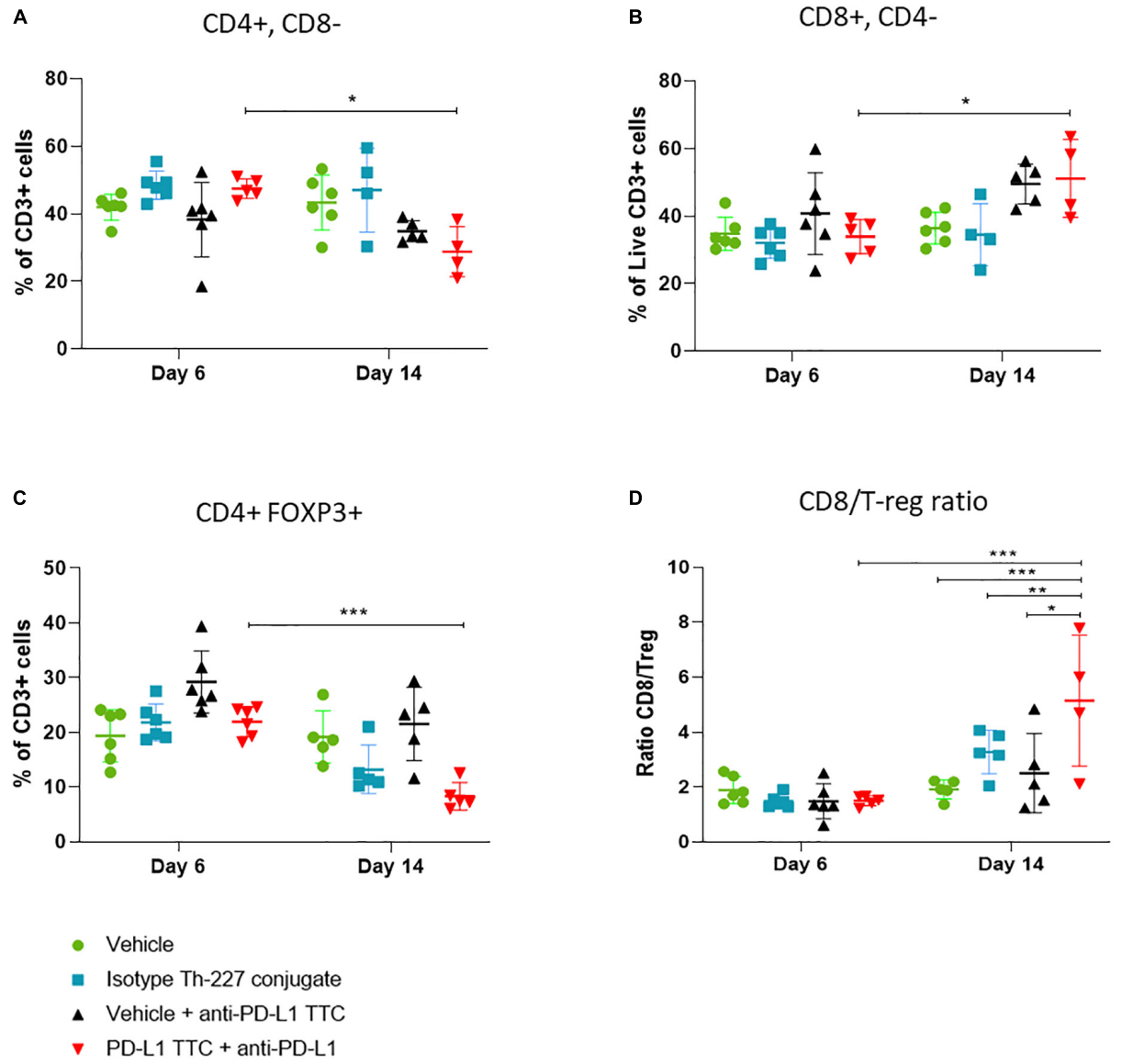


FIGURE 6
Lymphocytes (%) that are CD3+ in tumors, in each treatment group, $n = 5$/group. **(A)** CD3+ cells (%) that are CD4+ CD8- in tumors, representing T-helper cells, $n = 5$/group. **(B)** CD3+ cells (%) that are CD8+ CD4-, representing cytotoxic T-cells, $n = 5$. **(C)** CD3+ cells (%) that are CD4+ FOXP3+ CD25+ in tumors, representing T-regulatory cells, $n = 5$/group. **(D)** Ratio of CD8+ cells to T regulator cells in tumor, $n = 5$. Student's *t*-test $^{*}p < 0.05$, $^{**}p < 0.01$, $^{***}p < 0.001$.

specificity of the immune response was also confirmed by inoculation of the mice with B16-F10 (Figure 5B). B16-F10 tumors grew in both control animals and animals with complete tumor regression indicating that the immune response was specific for MC-38 cells.

In addition to IHC, we extracted infiltrating immune cells from TTC treated tumors. As expected, we found both CD4+ and CD8+ T-cells as well as Tregs (Figure 6) infiltrating the tumors to varying degrees, depending on time and treatment. In many tumor environments regulatory cells and CD4+ T-cells would dominate the response and produce an immune tolerant microenvironment (53). In addition, check point inhibition alone has the potential to increase immune evasion through proliferation of Tregs in the tumor when no additional immune stimulation is present (54). However, the combination of alpha therapy induced ICD and check-point inhibition appeared to allow for an increase in active infiltrating CD8+ T-cells (Figure 6B), the alpha radiation promoting an immune stimulatory environment that supports CD8+ T-cell activation and the anti-PD-L1 breaking tolerance from PD-L1 expressed on the tumor cells (55, 56). The result is a cytotoxic immune response dominated by CD8+ cells over Tregs as expressed in

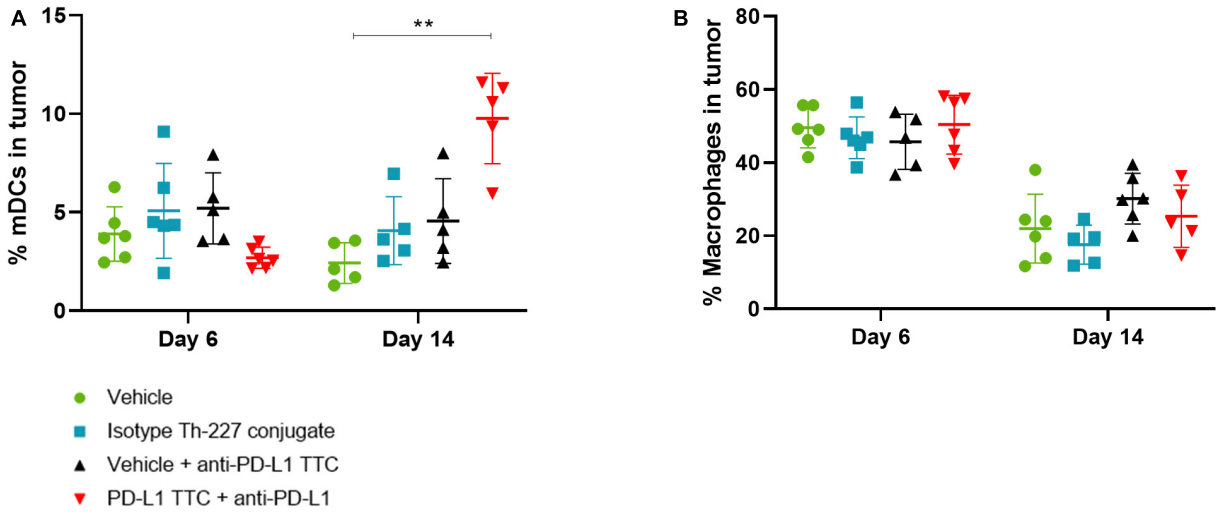


FIGURE 7
**(A)** Mature DCs [CD11c+, CD86+, CD64- (%)] in tumors in each treatment group, $n = 6$/group. A significant increase is seen after 14 days in the combination therapy group. **(B)** Macrophages [CD11c+, CD64+ (%)] in tumors in each treatment group, $n = 6$/group. Student's $t$-test $^{**}p < 0.01$.

the high ratio of CD8+ to Tregs in the tumor (Figure 6C). This ratio has been linked to breaking Treg dependent resistance in tumors (51), preventing metastasis (57) as well as better prognosis for patients in ICI treatment (50, 58, 59). The increase in CD8+/Treg ratio in the combination group seems to confirm the previous findings and support the observations.

The presence of mature dendritic cells and macrophages in the tumor microenvironment has a large effect on the developing immune response and even the prognosis of tumor growth and metastasis (60–62). The presence of large amounts of mature dendritic cells is helpful for the immune response (62), while macrophages, especially M2 macrophages, are often immunosuppressive (61). In tumors treated with combination therapy, we see an increase in mature dendritic cells over time (Figure 7A), while we see a drop in macrophages in all treatment groups (Figure 7B). This supports our T-cell data, and the hypothesis of a developing immune response initially dominated by infiltrating macrophages and immature DCs, which over time shifts to mature DCs supporting CD8+ T-cells as effector cells leading to tumor elimination.

In conclusion, the persistent immune effect we observed is exemplified by the complete rejection of tumors implanted in mice with complete tumor regression from previous treatment. It is clear from the *ex vivo* immunization data (Figure 2) that this effect is mainly from the radiation induced killing of the target cells, but the presence of the check-point inhibitor also plays a crucial role for the treatment to work optimally *in vivo* (Figure 5). Intriguingly we observe a clear effect even in the mice where complete tumor regression was achieved initially but rechallenge with tumor resulted in new tumor growth. The original combination of TTC and ICI appears to have induced a more lasting immunity due to the nature of the initial response they produced together with a strong cytotoxic T-cell component being critical (63, 64). Although the conclusions from this study are based on modest sample size, it appears to provide promising evidence of immune stimulatory effects of TAT in combination with check-point inhibitors. MC-38 is already known to be an immunogenic cell line (15) shown to respond to immune check point inhibition (65). Based on these preclinical findings, combinations of TAT and ICI may be of interest in treatment of cancers with high mutational load in a similar manner. It remains to be seen if such combinations can be used to make nonimmunogenic tumors respond to check-point inhibition. In addition, these combinations may also have clinical relevance in indications were check-point inhibition is already approved by the FDA, such as melanoma and non-small cell lung cancer, in patient populations that become non-responsive to ICI.

## Data availability statement

The raw data supporting the conclusions of this article will be made available by the authors, without undue reservation.

## Ethics statement

The animal study was reviewed and approved by Norwegian Food and Safety Authority.

## Author contributions

AB-L, AC, RB, and JK conceived and designed the project. AB-L, AM, IM, VC, KW, KG, GP, and AK contributed data and performed the experiments. AB-L, AM, IM, JK, GP, and AC performed the analysis. AB-L and AC wrote the manuscript, with significant support from IM and JK. All authors contributed to the article and approved the submitted version.

## Acknowledgments

We thank Lars Linden and the team at Bayer Biologics Research, Wuppertal, Germany, for supplying antibodies used for conjugation.

## Conflict of interest

The authors declare that the research was conducted in the absence of any commercial or financial relationships that could be construed as a potential conflict of interest.

## Publisher's note

All claims expressed in this article are solely those of the authors and do not necessarily represent those of their affiliated organizations, or those of the publisher, the editors and the reviewers. Any product that may be evaluated in this article, or claim that may be made by its manufacturer, is not guaranteed or endorsed by the publisher.

## Supplementary material

The Supplementary Material for this article can be found online at: https://www.frontiersin.org/articles/10.3389/fmed.2022.1033303/full#supplementary-material

SUPPLEMENTARY FIGURE 1
Gating scheme for all cells. **(A)** Gating scheme for T-cells in tumor. CD45+ cells from tumor were gated on FSC/SSC, then live vs. dead, then CD3+. CD3+ T-cells were gated as CD4+. CD8+ or CD4+ FOXP3+ as shown. **(B)** Gating scheme for dendritic cells and macrophages in tumor. CD45+ cells from tumor were gated on FSC/SSC, then live vs. dead, then CD11c+. Macrophages were gated as CD64+, mDCs as CD64- CD86. **(C)** Gating scheme for T-cells in spleen. CD45+ cells spleen was gated on FSC/SSC, then live vs. dead, then CD3+. CD3+ T-cells were gated as CD4+. CD8+ or CD4+ as shown. **(D)** Gating scheme for dendritic cells and macrophages in spleen. CD45+ cells from spleen were gated on FSC/SSC, then live vs. dead, then CD11c+. Macrophages were gated as CD64+, mDCs as CD64- CD86.

SUPPLEMENTARY FIGURE 2
**(A)** Lymphocytes (%) that are CD3+ in spleen, in each treatment group, $n = 5$/group. **(B)** CD3+ cells (%) that are CD4+ CD8- in spleen, $n = 5$/group. **(C)** CD3+ cells (%) that are CD8+ CD4- in spleen, $n = 5$/group. **(D)** Ratio of CD8+ cells to CD4+ in spleen, $n = 5$/group. Student's $t$-test $^{*}p < 0.05$, $^{**}p < 0.01$, $^{***}p < 0.001$.

SUPPLEMENTARY FIGURE 3
**(A)** Mature DCs [CD11c+, CD86+, CD64-(%)] in spleen, in each treatment group, $n = 5$/group. **(B)** Macrophages [CD11c+, CD64+ (%)] in spleens, in each treatment group, $n = 5$/group. Student's $t$-test $^{*}p < 0.05$.

SUPPLEMENTARY FIGURE 4
Blank IHC samples **(A)** Blank MC-38 tumor. **(B)** Blank C57BL/6 spleen. **(C)** Blank C57BL/6 liver.

## References

1. Targeted Alpha Therapy Working Group, Parker C, Lewington V, Shore N, Kratochwil C, Levy M, et al. Targeted alpha therapy, an emerging class of cancer agents: a review. *JAMA Oncol.* (2018) 4:1765–72. doi: 10.1001/jamaoncol.2018.4044

2. Ramdahl T, Bonge-Hansen HT, Ryan OB, Larsen S, Herstad G, Sandberg M, et al. An efficient chelator for complexation of thorium-227. *Bioorg Med Chem Lett.* (2016) 26:4318–21. doi: 10.1016/j.bmcl.2016.07.034

3. Deblonde GJ-P, Lohrey TD, Booth CH, Carter KP, Parker BF, Larsen Å, et al. Solution thermodynamics and kinetics of metal complexation with a hydroxypyridinone chelator designed for thorium-227 targeted alpha therapy. *Inorg Chem.* (2018) 57:14337–46. doi: 10.1021/acs.inorgchem.8b02430

4. Graf F, Fahrer J, Maus S, Morgenstern A, Bruchertseifer F, Venkatachalam S, et al. DNA double strand breaks as predictor of efficacy of the alpha-particle emitter ac-225 and the electron emitter lu-177 for somatostatin receptor targeted radiotherapy. *PLoS One.* (2014) 9:e88239. doi: 10.1371/journal.pone.0088239

5. Dekempeneer Y, Keyaerts M, Krasniqi A, Puttemans J, Muyldermans S, Lahoutte T, et al. Targeted alpha therapy using short-lived alpha-particles and the promise of nanobodies as targeting vehicle. *Expert Opin Biol Ther.* (2016) 16:1035–47. doi: 10.1080/14712598.2016.1185412

6. Dahle J, Borrebæk J, Jonasdottir TJ, Hjelmerud AK, Melhus KB, Bruland ØS, et al. Targeted cancer therapy with a novel low-dose rate A-emitting radioimmunoconjugate. *Blood.* (2007) 110:2049–56. doi: 10.1182/blood-2007-01-066803

7. Bruland ØS, Nilsson S, Fisher DR, Larsen RH. High-linear energy transfer irradiation targeted to skeletal metastases by the A-emitter 223ra: adjuvant or alternative to conventional modalities? *Clin Cancer Res.* (2006) 12:6250S–7S.

8. Hammer S, Hagemann UB, Zitzmann-Kolbe S, Larsen A, Ellingsen C, Geraudie S, et al. Preclinical efficacy of a Psma-targeted thorium-227 conjugate (Psma-Ttc), a targeted alpha therapy for prostate cancerpreclinical efficacy of Psma-Ttc in prostate cancer. *Clin Cancer Res.* (2020) 26:1985–96. doi: 10.1158/1078-0432.CCR-19-2268

9. Hagemann UB, Ellingsen C, Schuhmacher J, Kristian A, Mobergslien A, Cruciani V, et al. Mesothelin-targeted thorium-227 conjugate (Msln-Ttc): preclinical evaluation of a new targeted alpha therapy for mesothelin-positive cancers. *Clin Cancer Res.* (2019) 25:4723–34. doi: 10.1158/1078-0432.ccr-18-3476

10. Wickstroem K, Hagemann UB, Kristian A, Ellingsen C, Sommer A, Ellinger-Ziegelbauer H, et al. Preclinical combination studies of an Fgfr2 targeted thorium-227 conjugate and the Atr inhibitor Bay 1895344. *Int J Radiat Oncol Biol Phys.* (2019) 105:410–22. doi: 10.1016/j.ijrobp.2019.06.2508

11. Hagemann UB, Mihaylova D, Uran SR, Borrebaek J, Grant D, Bjerke RM, et al. Targeted alpha therapy using a novel Cd70 targeted thorium-227 conjugate in in vitro and in vivo models of renal cell carcinoma. *Oncotarget.* (2017) 8:56311–26. doi: 10.18632/oncotarget.16910

12. Hagemann UB, Wickstroem K, Wang E, Shea AO, Sponheim K, Karlsson J, et al. In vitro and in vivo efficacy of a novel Cd33-targeted thorium-227 conjugate

for the treatment of acute myeloid leukemia. *Mol Cancer Ther.* (2016) 15:2422–31. doi: 10.1158/1535-7163.mct-16-0251

13. Wickstroem K, Karlsson J, Ellingsen C, Cruciani V, Kristian A, Hagemann UB, et al. Synergistic effect of a Her2 targeted thorium-227 conjugate in combination with olaparib in a Brca2 deficient xenograft model. *Pharmaceuticals.* (2019) 12:155. doi: 10.3390/ph12040155

14. Wickstroem K, Hagemann UB, Cruciani V, Wengner AM, Kristian A, Ellingsen C, et al. Synergistic effect of a mesothelin-targeted (227)Th conjugate in combination with DNA damage response inhibitors in ovarian cancer xenograft models. *J Nucl Med.* (2019) 60:1293–300. doi: 10.2967/jnumed.118.223701

15. Lejeune P, Cruciani V, Berg-Larsen A, Schlicker A, Mobergslien A, Bartnitzky L, et al. Immunostimulatory effects of targeted thorium-227 conjugates as single agent and in combination with anti-Pd-L1 therapy. *J Immunother Cancer.* (2021) 9:e002387. doi: 10.1136/jitc-2021-002387

16. Ferrara TA, Hodge JW, Gulley JL. Combining radiation and immunotherapy for synergistic antitumor therapy. *Curr Opin Mol Therapeut.* (2009) 11:37–42.

17. Vesely MD, Kershaw MH, Schreiber RD, Smyth MJ. Natural innate and adaptive immunity to cancer. *Annu Rev Immunol.* (2011) 29:235–71. doi: 10.1146/annurev-immunol-031210-101324

18. Kroemer G, Galluzzi L, Kepp O, Zitvogel L. Immunogenic cell death in cancer therapy. *Annu Rev Immunol.* (2013) 31:51–72. doi: 10.1146/annurev-immunol-032712-100008

19. Garnett CT, Palena C, Chakraborty M, Tsang KY, Schlom J, Hodge JW. Sublethal irradiation of human tumor cells modulates phenotype resulting in enhanced killing by cytotoxic T lymphocytes. *Cancer Res.* (2004) 64:7985–94. doi: 10.1158/0008-5472.can-04-1525

20. Fridman WH, Pagès F, Sautès-Fridman C, Galon J. The immune contexture in human tumours: impact on clinical outcome. *Nat Rev Cancer.* (2012) 12:298–306. doi: 10.1038/nrc3245

21. Bindea G, Mlecnik B, Tosolini M, Kirilovsky A, Waldner M, Obenauf AC, et al. Spatiotemporal dynamics of intratumoral immune cells reveal the immune landscape in human cancer. *Immunity.* (2013) 39:782–95. doi: 10.1016/j.immuni.2013.10.003

22. Preston CC, Maurer MJ, Oberg AL, Visscher DW, Kalli KR, Hartmann LC, et al. The ratios of Cd8+ T cells to Cd4+Cd25+ Foxp3+ and Foxp3- T cells correlate with poor clinical outcome in human serous ovarian cancer. *PLoS One.* (2013) 8:e80063. doi: 10.1371/journal.pone.0080063

23. Lewis CE, Pollard JW. Distinct role of macrophages in different tumor microenvironments. *Cancer Res.* (2006) 66:605–12. doi: 10.1158/0008-5472.can-05-4005

24. Pardoll DM. The blockade of immune checkpoints in cancer immunotherapy. *Nat Rev Cancer.* (2012) 12:252–64. doi: 10.1038/nrc3239

25. Topalian SL, Hodi FS, Brahmer JR, Gettinger SN, Smith DC, McDermott DF, et al. Safety, activity, and immune correlates of Anti-Pd-1 antibody in cancer. *N Engl J Med.* (2012) 366:2443–54. doi: 10.1056/NEJMoa1200690

26. Castro F, Cardoso AP, Gonçalves RM, Serre K, Oliveira MJ. Interferon-gamma at the crossroads of tumor immune surveillance or evasion. *Front Immunol.* (2018) 9:847. doi: 10.3389/fimmu.2018.00847

27. Sun C, Mezzadra R, Schumacher TN. Regulation and function of the Pd-L1 checkpoint. *Immunity.* (2018) 48:434–52. doi: 10.1016/j.immuni.2018.03.014

28. Patel SA, Minn AJ. Combination cancer therapy with immune checkpoint blockade: mechanisms and strategies. *Immunity.* (2018) 48:417–33. doi: 10.1016/j.immuni.2018.03.007

29. Vatner RE, Cooper BT, Vanpouille-Box C, Demaria S, Formenti SC. Combinations of immunotherapy and radiation in cancer therapy. *Front Oncol.* (2014) 4:325. doi: 10.3389/fonc.2014.00325

30. Vénéreau E, Ceriotti C, Bianchi ME. Damps from cell death to new life. *Front Immunol.* (2015) 6:422. doi: 10.3389/fimmu.2015.00422

31. Gorin J-B, Ménager J, Gouard S, Maurel C, Guilloux Y, Faivre-Chauvet A, et al. Antitumor immunity induced after α irradiation. *Neoplasia.* (2014) 16:319–28. doi: 10.1016/j.neo.2014.04.002

32. Sia J, Szmyd R, Hau E, Gee HE. Molecular mechanisms of radiation-induced cancer cell death: a primer. *Front Cell Dev Biol.* (2020) 8:41. doi: 10.3389/fcell.2020.00041

33. Formenti SC, Demaria S. Combining radiotherapy and cancer immunotherapy: a paradigm shift. *JNCI.* (2013) 105:256–65. doi: 10.1093/jnci/djs629

34. Gorin JB, Gouard S, Ménager J, Morgenstern A, Bruchertseifer F, Faivre-Chauvet A, et al. Alpha particles induce autophagy in multiple myeloma cells. *Front Med.* (2015) 2:74. doi: 10.3389/fmed.2015.00074

35. Barker HE, Paget JTE, Khan AA, Harrington KJ. The tumour microenvironment after radiotherapy: mechanisms of resistance and recurrence. *Nat Rev Cancer.* (2015) 15:409–25. doi: 10.1038/nrc3958

36. Chajon E, Castelli J, Marsiglia H, De Crevoisier R. The synergistic effect of radiotherapy and immunotherapy: a promising but not simple partnership. *Crit Rev Oncol.* (2017) 111:124–32. doi: 10.1016/j.critrevonc.2017.01.017

37. Gorin JB, Guilloux Y, Morgenstern A, Chérel M, Davodeau F, Gaschet J. Using α radiation to boost cancer immunity? *Oncoimmunology.* (2014) 3:e954925. doi: 10.4161/21624011.2014.954925

38. Deng L, Liang H, Burnette B, Beckett M, Darga T, Weichselbaum RR, et al. Irradiation and anti–Pd-L1 treatment synergistically promote antitumor immunity in mice. *J Clin Investig.* (2014) 124:687–95. doi: 10.1172/JCI67313

39. Dovedi SJ, Cheadle EJ, Popple AL, Poon E, Morrow M, Stewart R, et al. Fractionated radiation therapy stimulates antitumor immunity mediated by both resident and infiltrating polyclonal T-cell populations when combined with Pd-1 blockade. *Clin Cancer Res.* (2017) 23:5514–26. doi: 10.1158/1078-0432.ccr-16-1673

40. Gong J, Le TQ, Massarelli E, Hendifar AE, Tuli R. Radiation therapy and Pd-1/Pd-L1 blockade: the clinical development of an evolving anticancer combination. *J ImmunoTher Cancer.* (2018) 6:46. doi: 10.1186/s40425-018-0361-7

41. Twyman-Saint Victor C, Rech AJ, Maity A, Rengan R, Pauken KE, Stelekati E, et al. Radiation and dual checkpoint blockade activate non-redundant immune mechanisms in cancer. *Nature.* (2015) 520:373–7. doi: 10.1038/nature14292

42. Basu S, Binder RJ, Ramalingam T, Srivastava PK. Cd91 is a common receptor for heat shock proteins Gp96, Hsp90, Hsp70, and Calreticulin. *Immunity.* (2001) 14:303–13. doi: 10.1016/S1074-7613(01)00111-X

43. Andersson U, Tracey KJ. Hmgb1 is a therapeutic target for sterile inflammation and infection. *Annu Rev Immunol.* (2011) 29:139–62. doi: 10.1146/annurev-immunol-030409-101323

44. Birmpilis AI, Paschalis A, Mourkakis A, Christodoulou P, Kostopoulos IV, Antimissari E, et al. Immunogenic cell death, damps and prothymosin α as a putative anticancer immune response biomarker. *Cells.* (2022) 11:1415. doi: 10.3390/cells11091415

45. Kepp O, Galluzzi L, Martins I, Schlemmer F, Adjemian S, Michaud M, et al. Molecular determinants of immunogenic cell death elicited by anticancer chemotherapy. *Cancer Metastasis Rev.* (2011) 30:61–9. doi: 10.1007/s10555-011-9273-4

46. Matsumura Y, Maeda HA. New concept for macromolecular therapeutics in cancer chemotherapy: mechanism of tumoritropic accumulation of proteins and the antitumor agent smancs. *Cancer Res.* (1986) 46(12 Pt 1):6387–92.

47. Yamamoto J, Takahashi Y, Minami K. High dose local photon irradiation is crucial in anti-Ctla-4 antibody therapy to enhance the abscopal response in a murine pancreatic carcinoma model. *Cancers.* (2022) 14:2087. doi: 10.3390/cancers14092087

48. Alsaab HO, Sau S, Alzhrani R, Tatiparti K, Bhise K, Kashaw SK, et al. Pd-1 and Pd-L1 checkpoint signaling inhibition for cancer immunotherapy: mechanism, combinations, and clinical outcome. *Front Pharmacol.* (2017) 8:561. doi: 10.3389/fphar.2017.00561

49. Sharpe AH, Pauken KE. The diverse functions of the Pd1 inhibitory pathway. *Nat Rev Immunol.* (2018) 18:153–67. doi: 10.1038/nri.2017.108

50. Shabaneh TB, Molodtsov AK, Steinberg SM, Zhang P, Torres GM, Mohamed GA, et al. Oncogenic $BRAF^{V600E}$ governs regulatory T-cell recruitment during melanoma tumorigenesis. *Cancer Res.* (2018) 78:5038–49. doi: 10.1158/0008-5472.can-18-0365

51. Saleh R, Elkord E. Treg-mediated acquired resistance to immune checkpoint inhibitors. *Cancer Lett.* (2019) 457:168–79. doi: 10.1016/j.canlet.2019.05.003

52. Ribas A, Shin DS, Zaretsky J, Frederiksen J, Cornish A, Avramis E, et al. Pd-1 blockade expands intratumoral memory T cells. *Cancer Immunol Res.* (2016) 4:194–203. doi: 10.1158/2326-6066.cir-15-0210

53. Yang K. Regulation of treg cell metabolism and function in non-lymphoid tissues. *Front Immunol.* (2022) 13:909705. doi: 10.3389/fimmu.2022.909705

54. Kamada T, Togashi Y, Tay C, Ha D, Sasaki A, Nakamura Y, et al. Pd-1(+) regulatory T cells amplified by Pd-1 blockade promote hyperprogression of cancer. *Proc Natl Acad Sci USA.* (2019) 116:9999–10008. doi: 10.1073/pnas.1822001116

55. Lee Y, Auh SL, Wang Y, Burnette B, Wang Y, Meng Y, et al. Therapeutic effects of ablative radiation on local tumor require Cd8+ T cells: changing strategies for cancer treatment. *Blood.* (2009) 114:589–95. doi: 10.1182/blood-2009-02-206870

56. Garnett CT, Palena C, Chakarborty M, Tsang K-Y, Schlom J, Hodge JW. Sublethal irradiation of human tumor cells modulates phenotype resulting in enhanced killing by cytotoxic T lymphocytes. *Cancer Res.* (2004) 64:7985–94.

57. Solis-Castillo LA, Garcia-Romo GS, Diaz-Rodriguez A, Reyes-Hernandez D, Tellez-Rivera E, Rosales-Garcia VH, et al. Tumor-infiltrating regulatory T Cells, Cd8/Treg ratio, and cancer stem cells are correlated with lymph node metastasis in patients with early breast cancer. *Breast Cancer*. (2020) 27:837–49. doi: 10.1007/s12282-020-01079-y

58. Takeuchi Y, Nishikawa H. Roles of regulatory T cells in cancer immunity. *Int Immunol*. (2016) 28:401–9. doi: 10.1093/intimm/dxw025

59. Farhood B, Najafi M, Mortezaee K. Cd8(+) cytotoxic T lymphocytes in cancer immunotherapy: a review. *J Cell Physiol*. (2019) 234:8509–21. doi: 10.1002/jcp.27782

60. Roberts EW, Broz ML, Binnewies M, Headley MB, Nelson AE, Wolf DM, et al. Critical role for Cd103(+)/Cd141(+) dendritic cells bearing Ccr7 for tumor antigen trafficking and priming of T cell immunity in melanoma. *Cancer Cell*. (2016) 30:324–36. doi: 10.1016/j.ccell.2016.06.003

61. Li Z, Wang YJ, Zhou J, Umakoshi M, Goto A. The prognostic role of M2 tumor-associated macrophages in non-small-cell lung cancer. *Histol Histopathol*. (2022) [Online ahead of print]. doi: 10.14670/hh-18-474.

62. Kim CW, Kim KD, Lee HK. The role of dendritic cells in tumor microenvironments and their uses as therapeutic targets. *BMB Rep*. (2021) 54:31–43. doi: 10.5483/BMBRep.2021.54.1.224

63. Pilones KA, Charpentier M, Garcia-Martinez E, Daviaud C, Kraynak J, Aryankalayil J, et al. Radiotherapy cooperates with Il15 to induce antitumor immune responses. *Cancer Immunol Res*. (2020) 12:2020. doi: 10.1158/2326-6066.cir-19-0338

64. Newton JM, Hanoteau A, Liu H-C, Gaspero A, Parikh F, Gartrell-Corrado RD, et al. Immune microenvironment modulation unmasks therapeutic benefit of radiotherapy and checkpoint inhibition. *J Immunother Cancer*. (2019) 7:216. doi: 10.1186/s40425-019-0698-6

65. Woo SR, Turnis ME, Goldberg MV, Bankoti J, Selby M, Nirschl CJ, et al. Immune inhibitory molecules Lag-3 and Pd-1 synergistically regulate T-cell function to promote tumoral immune escape. *Cancer Res*. (2012) 72:917–27. doi: 10.1158/0008-5472.can-11-1620

frontiers | Frontiers in Medicine

TYPE Review
PUBLISHED 15 November 2022
DOI 10.3389/fmed.2022.1030094



OPEN ACCESS

EDITED BY
Asta Juzeniene,
Oslo University Hospital, Norway

REVIEWED BY
Jacek Capala,
National Cancer Institute (NIH), United States
Ivar Hompland,
Oslo University Hospital, Norway

*CORRESPONDENCE
Peter M. Anderson
andersp@ccf.org

SPECIALTY SECTION
This article was submitted to Nuclear Medicine, a section of the journal Frontiers in Medicine

RECEIVED 28 August 2022
ACCEPTED 07 October 2022
PUBLISHED 15 November 2022

CITATION
Anderson PM, Subbiah V and Trucco MM (2022) Current and future targeted alpha particle therapies for osteosarcoma: Radium-223, actinium-225, and thorium-227. *Front. Med.* 9:1030094. doi: 10.3389/fmed.2022.1030094



# Current and future targeted alpha particle therapies for osteosarcoma: Radium-223, actinium-225, and thorium-227

Peter M. Anderson[1]*, Vivek Subbiah[2,3] and Matteo M. Trucco[1]

[1]Department of Pediatric Hematology, Oncology and Bone Marrow Transplant, Cleveland Clinic Children's Hospital, Pediatric Institute, Cleveland Clinic, Cleveland, OH, United States, [2]Investigational Cancer Therapeutics, Cancer Medicine, Clinical Center for Targeted Therapy, The University of Texas MD Anderson Cancer Center, Houston, TX, United States, [3]Division of Pediatrics, The University of Texas MD Anderson Cancer Center, Houston, TX, United States

Osteosarcoma is a high-grade sarcoma characterized by osteoid formation, nearly universal expression of IGF1R and with a subset expressing HER-2. These qualities provide opportunities for the use of the alpha particle-emitting isotopes to provide targeted radiation therapy *via* alpha particles precisely to bone-forming tumors in addition to IFG1R or Her-2 expressing metastases. This review will detail experience using the alpha emitter radium-223 ($^{223}$Ra, tradename Xofigo), that targets bone formation, in osteosarcoma, specifically related to patient selection, use of gemcitabine for radio-sensitization, and using denosumab to increasing the osteoblastic phenotype of these cancers. A case of an inoperable left upper lobe vertebral-paraspinal-mediastinal osteoblastic lesion treated successfully with $^{223}$Ra combined with gemcitabine is described. Because not all areas of osteosarcoma lesions are osteoblastic, but nearly all osteosarcoma cells overexpress IGF1R, and some subsets expressing Her-2, the anti-IGF1R antibody FPI-1434 linked to actinium-225 ($^{225}$Ac) or the Her-2 antibody linked to thorium-227 ($^{227}$Th) may become other means to provide targeted alpha particle therapy against osteosarcoma (NCT03746431 and NCT04147819).

KEYWORDS

**osteosarcoma, osteoblastic metastases, bone metastases, lung metastases, radiosensitization, denosumab, IGF1R antibody FPI-1434-225Ac**

## Biologic characteristics of osteosarcoma, a bone forming cancer

Pathologic diagnosis of osteosarcoma requires the demonstration of bone formation in the form of osteoid production (1). Despite accurate pathologic diagnosis, genomic instability has resulted in osteosarcomas having heterogeneous molecular signatures, with a relative paucity of actionable molecular targets. Many osteosarcoma tumors and metastases harbor p53 mutations or other mechanisms (e.g., MDM2 amplification) that

interfere with apoptosis after damage from standard chemotherapy, newer agents such as tyrosine kinase inhibitors (TKI) of vascular endothelial growth factor (VEGF) (2, 3), and/or radiation therapy (4, 5).

Although osteosarcoma has long been considered relatively radio-resistant (6), this assessment was in the pre-chemotherapy era; radiotherapy has been shown to be more effective against osteosarcoma when given in combination with chemotherapy (5, 7–10) or using proton radiotherapy (11). Another approach that is more biologically effective for bone metastases than conventional low dose fractionated radiation to enhance radiation effectiveness is stereotactic body radiotherapy (SBRT) which delivers precise high dose fractions (12–17). The high Linear Energy Transfer (LET) of alpha particles emitted by $^{223}$Ra, $^{225}$Ac, or $^{227}$Th causes hard to repair double strand breaks, providing another way to potentially overcome the intrinsic biologic resistance of osteosarcoma to radiotherapy (18–20).

## Current therapy of osteosarcoma

The importance of local control measures, especially surgery was shown in a series by Jaffe (21). Current osteosarcoma protocols use variations of the 3-drug (Methotrexate Adriamycin, Platinum, MAP) or 5-drug (MAP + Ifosfamide/etoposide, MAPIE) chemotherapy similar to that reported by the Euramos-1 study (22, 23). The addition of Mifamurtide may also improve outcomes (24–27). Metastatic disease, age > 18 (28) and poor response to neoadjuvant chemotherapy are associated with worse prognosis that to date we have not been able to effectively overcome (29, 30).

Ifosfamide is clearly an active drug in osteosarcoma as shown by its effectiveness against bone metastases and responses in patients not responding to MAP (31). Ifosfamide/mesna can be given with reduced toxicity and improved quality of life when given as an outpatient (32–37). If surgery is not possible or would have an unacceptable effect on the quality of life after response to ifosfamide/mesna, then use of not only radiotherapy with radio-sensitizers (10), but also alpha emitting radiopharmaceuticals such as $^{223}$Ra can provide options for local and systemic control (12, 17).

## Alpha emitter radium-223 for osteosarcoma

### Osteoblastic phenotype is necessary for bone-seeking radiopharmaceutical targeting against osteosarcoma

An osteoblastic phenotype is often suspected when calcified osteosarcoma metastases are seen on scans. However, active bone formation for the metastases >1 cm should be demonstrated using $^{99m}$TcMDP bone scan or $^{18}$FNa bone PET-CT before contemplating use of $^{223}$Ra in osteosarcoma (12, 17). Better images are obtained when planar images are combined with CT (SPECT-CT). $^{18}$FNa bone PET-CT has increased sensitivity toward osteoblastic metastases and, because a standard uptake value can be obtained on individual metastases, $^{18}$FNa bone PET-CT also provides a semi-quantitative assessment of disease burden that can be followed to measure the treatment response (38–46). Radiation is excellent if delivered precisely to tumors avoiding normal tissue. Thus, if there is avid $^{99m}$Tc-MDP (47) and/or $^{18}$FNa uptake in osteosarcoma metastases or a local recurrence, then the patient is excellent candidate for the use of $^{223}$Ra to deliver alpha particle radiation to osteoblastic osteosarcoma tumors and minimal radiation to the surrounding normal tissues, be it adjacent lung, spine, or limb salvage hardware from prior surgeries. If little or no bone formation is seen on these imaging modalities, then the patient is not a good candidate for $^{223}$Ra.

We have given $^{223}$Ra in osteosarcoma using the standard dose and monthly infusion schedule of 1.49 microCi/kg intravenously monthly (12) and at 50, 75, and 100 kBq/kg in a dose escalation study (48). From the perspective of the patient, getting $^{223}$Ra is relatively simple: there is a discussion of the minimal radiation safety requirements (wash hands, flush toilet 2 × because unbound $^{223}$Ra comes out in the stool), and in our Nuclear Medicine Departments getting $^{223}$Ra is similar to getting a bone scan injection and takes approximately 10 min. Our current practice is to use the standard $^{223}$Ra dose on a Wednesday or Thursday to allow gemcitabine to be given as a radio-sensitizer the following day. We also use $^{223}$Ra in combination with other agents such as denosumab and local control measures in an attempt to both improve the efficacy of $^{223}$Ra and also to treat areas of metastases that do not have $^{223}$Ra deposition as illustrated in **Figure 1**.

## Improving therapeutic index of radium-223 in osteosarcoma

### Denosumab

Denosumab is a fully humanized anti-RANKL antibody that improves bone density. It is used to treat osteoporosis, reduce skeletal complications of bone metastases, and treat giant cell tumor of bone (49–53). We have made the observation that some osteosarcomas increase the amount of bone formation after denosumab. Thus, monthly denosumab injections during $^{223}$Ra therapy can increase the amount of $^{223}$Ra deposited in osteoblastic metastases in osteosarcoma (12).

### Gemcitabine

Gemcitabine is an excellent radio-sensitizer (10, 54–59). The toxicity of gemcitabine is dependent on not only schedule

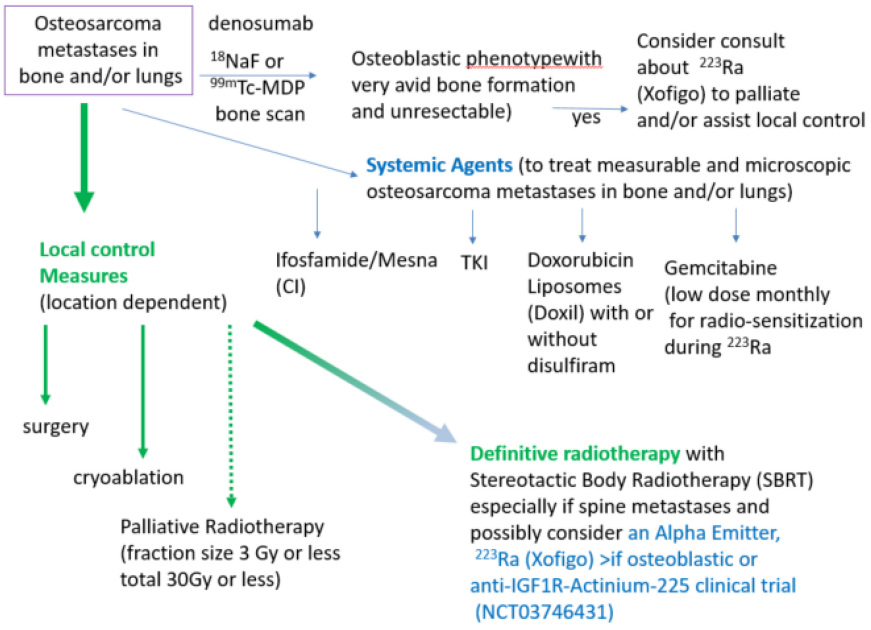


FIGURE 1
Algorithm of treatment of metastatic, recurrent osteosarcoma with systemic agents, local control measures, and with alpha-emitters $^{223}$Ra or Anti-IGF1R-Actinium-225. Note if unresectable, referral to a center with expertise in administration of alpha emitters in combination with radiotherapy will be needed.

and dose, but also infusion duration. Shorter infusions (30 min) are associated with less hematologic toxicity than 90 min infusions. Gemcitabine is given daily 5 × had unacceptable mucosal toxicity. Weekly or day 1 and 8 of 3-week cycles are better tolerated. Since gemcitabine must be taken up and phosphorylated to act on the cancer cell, longer infusion times are associated with more hematologic toxicity (60, 61). Giving gemcitabine 600 mg/m$^2$ intravenously (iv) once over 30 min 1 day after $^{223}$Ra is deposited in osteoblastic tumors is a convenient monthly strategy that allows gemcitabine to increase effects within osteoblastic metastases with minimal hematologic toxicity.

### Case report

The following case (Figure 2) illustrates the successful use of $^{223}$Ra and gemcitabine (62). A 27-year-old patient presented with a large osteosarcoma tumor involving T2-4 extending into both the spinal canal and the left upper lobe. Because of giant cell features, he was initially given denosumab, but when molecular testing revealed FGFR mutation and pathology was reviewed, the diagnosis of osteosarcoma was made. He received 2 cycles of MAP chemotherapy and then because of minimal response was switched to ifosfamide + etoposide. Because the tumor was deemed unresectable, 50.4 Gy over 28 fractions with concurrent ifosfamide + etoposide was given during cycles 5 and 6. He received 2 more cycles of ifosfamide + etoposide then had radiographic progression and clinical worsening (weakness of both lower extremities, some tingling, and need to use a cane). Cardiothoracic, orthopedic, and spine surgeons reviewed his case at the sarcoma conference at the Cleveland Clinic and also deemed the tumor to be unresectable because of the combination of vertebral, spinal canal, and mediastinal involvement. Bone scan with Spect-CT showed avid $^{99m}$Tc-MDP uptake and he was given 6 monthly cycles of Denosumab, $^{223}$Ra, followed by gemcitabine. Cytopenias were modest, no transfusions were needed. The patient experienced a clinical response as characterized by increased strength in his legs, no longer requiring a cane to ambulate and resolution of paresthesia. Uptake of $^{18}$FDG as well and $^{99m}$Tc-MDP was decreased on repeat imaging. After the response to $^{223}$Ra monthly 6 ×, he was given oral cyclophosphamide for 6 months (Figure 2). He is now over 9 months off therapy without evidence of recurrence. His activity level has increased and he is able to skateboard (even able to do tricks such as a "treflip," insert top on Figure 2; Supplementary Video 1), rock climbs often, and has gone skydiving six times.

## Other chemotherapy agents worth determining suitability in combination with radium-223 in osteosarcoma

Local and systemic therapy is often needed before the logistics of evaluating osteoblastic phenotype and obtaining $^{223}$Ra for osteosarcoma treatment can be solved. Some active agents in the relapsed metastatic osteosarcoma setting are illustrated in Figure 1 (ifosfamide, TKI, and doxorubicin liposomes). Since many patients have had MAP initially without

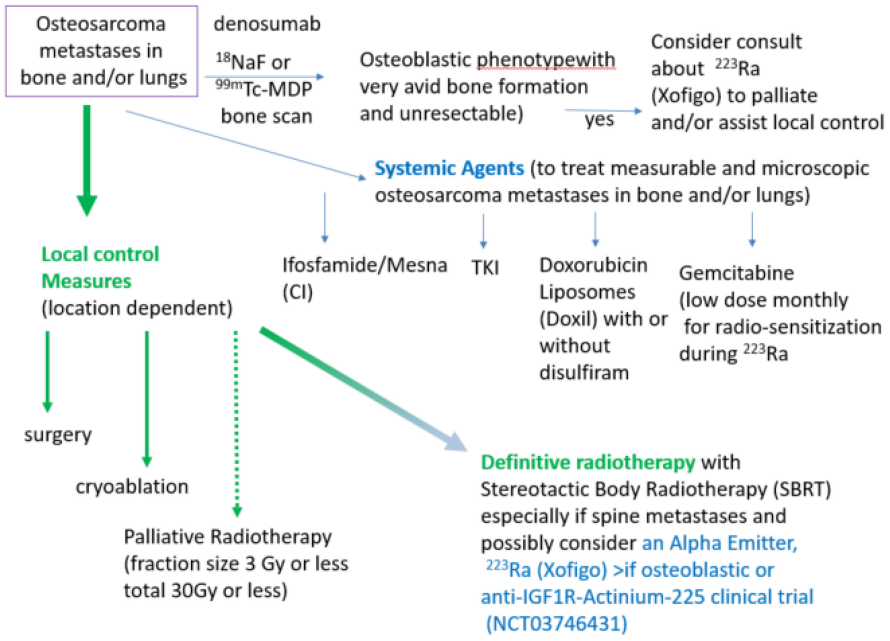


FIGURE 2
Top shows $^{99m}$Tc-MDP screening bone scan with avid uptake indicating suitability for alpha particle therapy with the bone-seeking radiopharmaceutical, $^{223}RaCl_2$ (Xofigo). $^{223}$Ra (blue), then gemcitabine (green) next day + monthly denosumab 6 × monthly cycles resulted in improvement, then resolution of symptoms of the unresectable mediastinal and vertebral body osteosarcoma. Currently, the patient is on no therapy and enjoys active lifestyles, such as skateboarding, rock climbing, and skydiving (62).

ifosfamide, ifosfamide with or without etoposide is often the $2^{nd}$ line therapy of choice (31–34). When ifosfamide is given with mesna as a continuous infusion, thrombocytopenia, encephalopathy, and renal toxicity are seen less often (33–37, 63). We have also demonstrated that outpatient continuous infusion of ifosfamide + mesna was associated with fewer transfusions and episodes of fever and neutropenia (63). If continuous infusion of ifosfamide + mesna is to be used with $^{223}$Ra, we would recommend starting 1 day after $^{223}$Ra administration using a dose of 1 gm/m$^2$/d × 1 week. Administration of PEG–GCSF after completion of the ifosfamide infusion is also recommended. This regimen can be repeated every 4 weeks to allow for the combination of the cytotoxic effects when the bone-seeking radiopharmaceutical is most active in bone-forming lesions and to allow for hematologic recovery as $^{223}$Ra decays.

Tyrosine kinase inhibitors including regorafenib (2, 64) and cabozantinib (3) have efficacy against osteosarcoma. Although a dose adjustment of TKI is sometimes needed to limit skin or GI toxicity, we have found the use of glutamine-disaccharide (Healios) can be helpful in ameliorating GI side effects and helping in eating and nutrition while on these agents (35).

Liposomal doxorubicin (tradenames Doxil or Caelyx) has very low heart toxicity (65, 66). This preparation can be given monthly and has modest hematologic toxicity and is not associated with alopecia when given at 40 mg/m$^2$. Thus liposomal doxorubicin has high patient acceptance among relapsed osteosarcoma patients. Cold packs on hands, feet, and the use of glutamine + disaccharide (Healios) can be used to limit hand/foot erythroderma and mucositis/esophagitis, respectively (35). Liposomal doxorubicin is probably most suitable in relapsed osteosarcoma patients who had an initial excellent response to MAP chemotherapy. There is also a clinical trial using liposomal doxorubicin in combination with disulfiram to try to target slowly repopulating cancer stem cells high in aldehyde dehydrogenase (67, 68) (NCT05210374 M. Trucco, PI).

## Use of local control measures including stereotactic body radiotherapy before or in combination with radium-223

As illustrated in Figure 1, surgery, cryoablation, and/or radiation can provide local control of osteosarcoma metastases. Location and number of metastases ("oligometastatic" is <10) may determine whether to do surgery, cryoablation, or to definitively treat with radiation (e.g., 3 Gy × 20 fractions RT or SBRT 8 Gy × 5 fractions = 40 Gy) or whether palliative radiation (e.g., 3 Gy × 10 fractions) is most appropriate. Reasons to use local control include treatment or prevention of pain as well as reduction of tumor burden, particularly where tumor growth may cause complications (e.g., spine or sacral metastases, and hilar or mediastinal metastases. Unfortunately, for the most common pattern of end-stage metastases (numerous lung

TABLE 1 Alpha emitters for osteosarcoma.

| Radiopharmaceutical | $^{223}$RaCl2 | $^{225}$Ac-anti-IGF1R | $^{227}$Th-Anti Her2 |
|---|---|---|---|
| Half-life of radio-metal | 11.4 days | 10 days | 18.7 days |
| Alpha Particles emitted | 4 | 4 | 5 |
| Blood clearance | Rapid (<1% at 24 h) | Antibody clearance | Antibody clearance |
| Radon daughter half-life | 4 s | no radon daughter | 4 s |
| Penetration of radioisotope | 0.1 mm | 0.1 mm | 0.1 mm |
| Imaging with gamma camera | Possible | Not done | Possible |
| Decays to stable isotope | 207-Pb | 209-Bi | 207-Pb |

metastases) neither whole lung radiation nor $^{223}$Ra will provide effective doses. Clinical trials such as anti-IGF1R–Actinium 225 (NCT03746431) or Doxil + disulfiram (NCT05210374) would be appropriate in these situations.

## IGF-1R expression in osteosarcoma: An opportunity for anti-IGF-1R antibody-actinium-225 alpha particle therapy

Sarcomas, particularly Ewing sarcoma and osteosarcoma have overexpression of IGF1R (69). Although cold antibody was only modestly effective in Ewing sarcoma and not in osteosarcoma (69), chelation of the alpha emitter $^{225}$Ac can arm the anti-IGF1R antibody to become a potent alpha emitter (70, 71). **Table 1** compares $^{223}$Ra, which targets areas of bone turnover, with anti-IGF1R-Actinium-225. Currently, the clinical trial NCT0374631 is open at MD Anderson Cancer Center, City of Hope, Memorial Sloan Kettering, University of Minnesota, Dana Farber Cancer Institute, University of Pennsylvania, Juravinski/Hamilton Health, CHU-Montreal, Princess Margaret (Toronto), and CHU Quebec. We expect patients <18 years old to be able to be enrolled when the recommended phase 2 dose is achieved. Thus, the anti-IGF1R-Actinium-225 strategy may be another way to treat osteosarcoma metastases that are not osteoblastic and with alpha-particle radiation that effectively acts at short distances in a powerful manner. Nevertheless, the expression of IGF-1R in normal tissue and/or non-specific binding of antibodies may limit the effectiveness of this approach.

## Her-2 expression in osteosarcoma: An opportunity for targeted thorium conjugates

Her-2 is expressed in a subset of osteosarcomas. Earlier attempts to target this Her2 expression using trastuzumab were unsuccessful. However, clinical trials using Her2-targeted CAR T-cells suggest that Her2-targeted therapy could be active in osteosarcoma (72). Moreover, better-designed novel antibody drug conjugates like Trastuzumab-Deruxtecan (T-DXd) is showing activity in low Her-2 expressing breast cancers, are also being explored in osteosarcoma. HER2-thorium-227 targeted conjugate (TTC) has recently entered clinical trials in Europe and the USA. "A First in Human Study of BAY2701439 to Look at Safety, How the Body Absorbs, Distributes, and Excretes the Drug, and How Well the Drug Works in Participants With Advanced Cancer Expressing the HER2 Protein" (NCT04147819) is a combination of the alpha-emitting radionuclide thorium-227, an antibody targeting HER2, and a chelator molecule that strongly attaches the thorium-227 to the antibody. This technology harnesses the antibody's ability to target HER2 by using it to transport the alpha particle emitting thorium-227 to the tumor. Both radium-223 and thorium-227 decay produce alpha particle radiation (**Table 1**) that causes highly lethal double strand DNA damage in tumor cells, but also useful emission for gamma scintigraphy (73). Although the first in human trial is open for breast and gastric only, the expansion part of the study will include patients with a range of tumor indications with HER2 expression which occurs on osteosarcoma. Only in the context of a clinical trial will it be possible to determine whether benefits for the binding to HER-2 on osteosarcoma outweigh potential toxicity from expression on normal cells and/or non-specific binding of the alpha emitter.

## Summary and conclusion

Alpha emitters have some potent biological advantages that may eventually prove useful for the treatment of osteosarcoma. However, the rarity of this sarcoma and specific situations to test efficacy in randomized clinical trials will be very difficult. Perhaps the use of patients as their own controls with benefit as improved quality of life and/or clinical course better than expected—especially compared to historical controls (74) is possibly the best we can do currently.

## Author contributions

PA: writing of the manuscript and experience with $^{223}$Ra combination therapy. VS: editing of manuscript and experience with $^{223}$Ra, anti-IGF1R-Ac225 antibody, and Her-2 TTC. MT: editing of manuscript and current treatment of relapsed osteosarcoma including doxorubicin liposomes with or without disulfiram. All authors contributed to the article and approved the submitted version.

## Funding

This work was funded by the Cleveland Clinic Sarcoma program. VS was an Andrew Sabin Family Foundation Fellow at The University of Texas MD Anderson Cancer Center. VS acknowledged the support of the Jacquelyn A. Brady Fund. VS was supported by the US National Institutes of Health (NIH) (Grant nos. R01CA242845 and R01CA273168), the MD Anderson Cancer Center Department of Investigational Cancer Therapeutics is supported by the Cancer Prevention and Research Institute of Texas (Grant no. RP1100584), the Sheikh Khalifa Bin Zayed Al Nahyan Institute for Personalized Cancer Therapy (Grant no. 1U01 CA180964), the NCATS (Center for Clinical and Translational Sciences) (Grant no. UL1 TR000371), and the MD Anderson Cancer Center Support (Grant no. P30 CA016672).

## Acknowledgments

The efforts of physicians and physicists in the Departments of Nuclear Medicine at MD Anderson and Cleveland Clinic area acknowledged. The efforts of the C level and Clinic Pediatric Hematology/Oncology infusion nurses and care coordination by Shauna Sartoski, RN for $^{223}RaCl_2$ (Xofigo) and chemotherapy infusions have been much appreciated.

## Conflict of interest

The authors declare that the research was conducted in the absence of any commercial or financial relationships that could be construed as a potential conflict of interest.

## Publisher's note

All claims expressed in this article are solely those of the authors and do not necessarily represent those of their affiliated organizations, or those of the publisher, the editors and the reviewers. Any product that may be evaluated in this article, or claim that may be made by its manufacturer, is not guaranteed or endorsed by the publisher.

## Supplementary material

The Supplementary Material for this article can be found online at: https://www.frontiersin.org/articles/10.3389/fmed.2022.1030094/full#supplementary-material

SUPPLEMENTARY VIDEO 1
Excellent return of lower extremity function after 223-Ra treatment of thoracic paraspinal osteosarcoma as demonstrated by skateboarding.

## References

1. Rivera-Valentin RK, Zhu L, Hughes DP. Bone sarcomas in pediatrics: progress in our understanding of tumor biology and implications for therapy. *Paediatr Drugs.* (2015) 17:257–71. doi: 10.1007/s40272-015-0134-4

2. Duffaud F, Mir O, Boudou-Rouquette P, Piperno-Neumann S, Penel N, Bompas E, et al. Efficacy and safety of regorafenib in adult patients with metastatic osteosarcoma: a non-comparative, randomised, double-blind, placebo-controlled, phase 2 study. *Lancet Oncol.* (2019) 20:120–33. doi: 10.1016/S1470-2045(18)30742-3

3. Italiano A, Mir O, Mathoulin-Pelissier S, Penel N, Piperno-Neumann S, Bompas E, et al. Cabozantinib in patients with advanced Ewing sarcoma or osteosarcoma (CABONE): a multicentre, single-arm, phase 2 trial. *Lancet Oncol.* (2020) 21:446–55. doi: 10.1016/S1470-2045(19)30825-3

4. Prudowsky ZD, Yustein JT. Recent insights into therapy resistance in osteosarcoma. *Cancers.* (2020) 13:83. doi: 10.3390/cancers13010083

5. Hernberg MM, Kivioja AH, Böhling TO, Janes RJ, Wiklund TA. Chemoradiotherapy in the treatment of inoperable high-grade osteosarcoma. *Med Oncol.* (2011) 28:1475–80. doi: 10.1007/s12032-010-9592-2

6. Dahlin DC. Prognostic factors in osteosarcoma. *Int J Radiat Oncol Biol Phys.* (1980) 6:1755. doi: 10.1016/0360-3016(80)90266-7

7. Machak GN, Tkachev SI, Solovyev YN, Sinyukov PA, Ivanov SM, Kochergina NV, et al. Neoadjuvant chemotherapy and local radiotherapy for high-grade osteosarcoma of the extremities. *Mayo Clin Proc.* (2003) 78:147–55. doi: 10.4065/78.2.147

8. Anderson PM. Effectiveness of radiotherapy for osteosarcoma that responds to chemotherapy. *Mayo Clin Proc.* (2003) 78:145–6. doi: 10.4065/78.2.145

9. Mahajan A, Woo SY, Kornguth DG, Hughes D, Huh W, Chang EL, et al. Multimodality treatment of osteosarcoma: radiation in a high-risk cohort. *Pediatr Blood Cancer.* (2008) 50:976–82. doi: 10.1002/pbc.21451

10. Anderson P, Aguilera D, Pearson M, Woo S. Outpatient chemotherapy plus radiotherapy in sarcomas: improving cancer control with radiosensitizing agents. *Cancer Control.* (2008) 15:38–46. doi: 10.1177/107327480801500105

11. Patel S, DeLaney TF. Advanced-technology radiation therapy for bone sarcomas. *Cancer Control.* (2008) 15:21–37. doi: 10.1177/107327480801500104

12. Anderson PM, Scott J, Parsai S, Zahler S, Worley S, Shrikanthan S, et al. 223-Radium for metastatic osteosarcoma: combination therapy with other agents and external beam radiotherapy. *ESMO Open.* (2020) 5:e000635. doi: 10.1136/esmoopen-2019-000635

13. Baumann BC, Bernstein KA, DeLaney TF, Simone CB II, Kolker JD, Choy E, et al. Multi-institutional analysis of stereotactic body radiotherapy for sarcoma pulmonary metastases: High rates of local control with favorable toxicity. *J Surg Oncol.* (2020) 122:877–83. doi: 10.1002/jso.26078

14. Baumann BC, Nagda SN, Kolker JD, Levin WP, Weber KL, Berman AT, et al. Efficacy and safety of stereotactic body radiation therapy for the treatment of pulmonary metastases from sarcoma: A potential alternative to resection. *J Surg Oncol.* (2016) 114:65–9. doi: 10.1002/jso.24268

15. Park C, Papiez L, Zhang S, Story M, Timmerman RD. Universal survival curve and single fraction equivalent dose: useful tools in understanding potency of ablative radiotherapy. *Int J Radiat Oncol Biol Phys.* (2008) 70:847–52. doi: 10.1016/j.ijrobp.2007.10.059

16. Anderson PM, Subbiah V, Rohren E. Bone-seeking radiopharmaceuticals as targeted agents of osteosarcoma: samarium-153-EDTMP and radium-223. *Adv Exp Med Biol.* (2014) 804:291–304. doi: 10.1007/978-3-319-04843-7_16

17. Anderson PM. Radiopharmaceuticals for Treatment of Osteosarcoma. *Adv Exp Med Biol.* (2020) 1257:45–53. doi: 10.1007/978-3-030-43032-0_4

18. Bruland OS, Nilsson S, Fisher DR, Larsen RH. High-linear energy transfer irradiation targeted to skeletal metastases by the alpha-emitter 223Ra: adjuvant or alternative to conventional modalities? *Clin Cancer Res.* (2006) 12(20 Pt. 2):6250s–7s. doi: 10.1158/1078-0432.CCR-06-0841

19. Haro KJ, Scott AC, Scheinberg DA. Mechanisms of resistance to high and low linear energy transfer radiation in myeloid leukemia cells. *Blood.* (2012) 120:2087–97. doi: 10.1182/blood-2012-01-404509

20. Melville G, Melville P. A theoretical model for the production of Ac-225 for cancer therapy by neutron capture transmutation of Ra-226. *Appl Radiat Isot.* (2013) 72:152–7. doi: 10.1016/j.apradiso.2012.09.019

21. Jaffe N, Carrasco H, Raymond K, Ayala A, Eftekhari F. Can cure in patients with osteosarcoma be achieved exclusively with chemotherapy and abrogation of surgery? *Cancer.* (2002) 95:2202–10. doi: 10.1002/cncr.10944

22. Bielack SS, Carrasco H, Raymond K, Ayala A, Eftekhari F. Methotrexate, Doxorubicin, and Cisplatin (MAP) Plus Maintenance Pegylated Interferon Alfa-2b Versus MAP alone in patients with resectable high-grade osteosarcoma and good histologic response to preoperative MAP: first results of the EURAMOS-1 good response randomized controlled trial. *J Clin Oncol.* (2015) 33:2279–87.

23. Marina NM, Smeland S, Bielack SS, Bernstein M, Jovic G, Krailo MD, et al. Comparison of MAPIE versus MAP in patients with a poor response to preoperative chemotherapy for newly diagnosed high-grade osteosarcoma (EURAMOS-1): an open-label, international, randomised controlled trial. *Lancet Oncol.* (2016) 17:1396–408. doi: 10.1016/S1470-2045(16)30214-5

24. Meyers PA, Schwartz CL, Krailo MD, Healey JH, Bernstein ML, Betcher D, et al. Osteosarcoma: the addition of muramyl tripeptide to chemotherapy improves overall survival–a report from the Children's Oncology Group. *J Clin Oncol.* (2008) 26:633–8. doi: 10.1200/JCO.2008.14.0095

25. Chou AJ, Kleinerman ES, Krailo MD, Chen Z, Betcher DL, Healey JH, et al. Addition of muramyl tripeptide to chemotherapy for patients with newly diagnosed metastatic osteosarcoma: a report from the Children's Oncology Group. *Cancer.* (2009) 115:5339–48. doi: 10.1002/cncr.24566

26. Anderson PM, Meyers P, Kleinerman E, Venkatakrishnan K, Hughes DP, Herzog C, et al. Mifamurtide in metastatic and recurrent osteosarcoma: a patient access study with pharmacokinetic, pharmacodynamic, and safety assessments. *Pediatr Blood Cancer.* (2014) 61:238–44. doi: 10.1002/pbc.24686

27. Anderson PM, Tomaras M, McConnell K. Mifamurtide in osteosarcoma–a practical review. *Drugs Today.* (2010) 46:327–37. doi: 10.1358/dot.2010.46.5.1500076

28. Janeway KA, Barkauskas DA, Krailo MD, Meyers PA, Schwartz CL, Ebb DH, et al. Outcome for adolescent and young adult patients with osteosarcoma: a report from the Children's Oncology Group. *Cancer.* (2012) 118:4597–605. doi: 10.1002/cncr.27414

29. Bacci G, Mercuri M, Longhi A, Ferrari S, Bertoni F, Versari M, et al. Grade of chemotherapy-induced necrosis as a predictor of local and systemic control in 881 patients with non-metastatic osteosarcoma of the extremities treated with neoadjuvant chemotherapy in a single institution. *Eur J Cancer.* (2005) 41:2079–85. doi: 10.1016/j.ejca.2005.03.036

30. Musta E, van Geloven N, Anninga J, Gelderblom H, Fiocco M. Short-term and long-term prognostic value of histological response and intensified chemotherapy in osteosarcoma: a retrospective reanalysis of the BO06 trial. *BMJ Open.* (2022) 12:e052941. doi: 10.1136/bmjopen-2021-052941

31. Goorin AM, Harris MB, Bernstein M, Ferguson W, Devidas M, Siegal GP, et al. Phase II/III trial of etoposide and high-dose ifosfamide in newly diagnosed metastatic osteosarcoma: a pediatric oncology group trial. *J Clin Oncol.* (2002) 20:426–33. doi: 10.1200/JCO.2002.20.2.426

32. Meazza C, Bisogno G, Casanova M, Zanetti I, Carli M, Ferrari A. Full-dose ifosfamide can be safely administered to outpatients. *Pediatr Blood Cancer.* (2008) 50:375–8. doi: 10.1002/pbc.20958

33. Meazza C, Casanova M, Luksch R, Podda M, Favini F, Cefalo G, et al. Prolonged 14-day continuous infusion of high-dose ifosfamide with an external portable pump: feasibility and efficacy in refractory pediatric sarcoma. *Pediatr Blood Cancer.* (2010) 55:617–20. doi: 10.1002/pbc.22596

34. Anderson P. Continuously improving ifosfamide/mesna: a winning combination. *Pediatr Blood Cancer.* (2010) 55:599–600. doi: 10.1002/pbc.22652

35. Anderson PM, Thomas SM, Sartoski S, Scott JG, Sobilo K, Bewley S, et al. Strategies to mitigate chemotherapy and radiation toxicities that affect eating. *Nutrients.* (2021) 13:4397. doi: 10.3390/nu13124397

36. Martin-Liberal J, Alam S, Constantinidou A, Fisher C, Khabra K, Messiou C, et al. Clinical activity and tolerability of a 14-day infusional Ifosfamide schedule in soft-tissue sarcoma. *Sarcoma.* (2013) 2013:868973. doi: 10.1155/2013/868973

37. Zhang Y, Kawedia JD, Myers AL, McIntyre CM, Anderson PM, Kramer MA, et al. Physical and chemical stability of high-dose ifosfamide and mesna for prolonged 14-day continuous infusion. *J Oncol Pharm Pract.* (2014) 20:51–7. doi: 10.1177/1078155213478284

38. Etchebehere E, Brito AE, Kairemo K, Rohren E, Araujo J, Macapinlac H. Is interim (18)F-fluoride PET/CT a predictor of outcomes after radium-223 therapy? *Radiol Bras.* (2019) 52:33–40. doi: 10.1590/0100-3984.2017.0178

39. Etchebehere EC, Araujo JC, Fox PS, Swanston NM, Macapinlac HA, Rohren EM. Prognostic Factors in Patients Treated with 223Ra: the role of skeletal tumor burden on baseline 18F-fluoride PET/CT in predicting overall survival. *J Nucl Med.* (2015) 56:1177–84. doi: 10.2967/jnumed.115.158626

40. Etchebehere EC, Araujo JC, Milton DR, Erwin WD, Wendt RE III, Swanston NM, et al. Skeletal tumor burden on baseline 18F-Fluoride PET/CT predicts bone marrow failure after 223Ra therapy. *Clin Nucl Med.* (2016) 41:268–73. doi: 10.1097/RLU.0000000000001118

41. Harmon SA, Bergvall E, Mena E, Shih JH, Adler S, McKinney Y, et al. A Prospective Comparison of (18)F-Sodium Fluoride PET/CT and PSMA-Targeted (18)F-DCFBC PET/CT in Metastatic Prostate Cancer. *J Nucl Med.* (2018) 59:1665–71. doi: 10.2967/jnumed.117.207373

42. Harmon SA, Mena E, Shih JH, Adler S, McKinney Y, Bergvall E, et al. A comparison of prostate cancer bone metastases on (18)F-sodium fluoride and prostate specific membrane antigen ((18)F-PSMA) PET/CT: discordant uptake in the same lesion. *Oncotarget.* (2018) 9:37676–88. doi: 10.18632/oncotarget.26481

43. Harmon SA, Perk T, Lin C, Eickhoff J, Choyke PL, Dahut WL, et al. Quantitative assessment of early [(18)F]Sodium Fluoride positron emission tomography/computed tomography response to treatment in men with metastatic prostate cancer to bone. *J Clin Oncol.* (2017) 35:2829–37. doi: 10.1200/JCO.2017.72.2348

44. Kairemo K, Milton DR, Etchebehere E, Rohren EM, Macapinlac HA. Final Outcome of 223Ra-therapy and the Role of 18F-fluoride-PET in response evaluation in metastatic castration-resistant prostate cancer-A single institution experience. *Curr Radiopharm.* (2018) 11:147–52. doi: 10.2174/1874471011666180629145030

45. Kairemo K, Rohren EM, Anderson PM, Ravizzini G, Rao A, Macapinlac HA, et al. Development of sodium fluoride PET response criteria for solid tumours (NAFCIST) in a clincal trial of radium-223 in osteosarcoma: from RECIST to PERCIST to NAFCIST. *EMSO Open.* (2019) 4:e000439. doi: 10.1136/esmoopen-2018-000439

46. Rohren EM, Etchebehere EC, Araujo JC, Hobbs BP, Swanston NM, Everding M, et al. Determination of skeletal tumor burden on 18F-Fluoride PET/CT. *J Nucl Med.* (2015) 56:1507–12. doi: 10.2967/jnumed.115.156026

47. Nilsson S, Larsen RH, Fosså SD, Balteskard L, Borch KW, Westlin JE, et al. First clinical experience with alpha-emitting radium-223 in the treatment of skeletal metastases. *Clin Cancer Res.* (2005) 11:4451–9. doi: 10.1158/1078-0432.CCR-04-2244

48. Subbiah V, Anderson PM, Kairemo K, Hess K, Huh WW, Ravi V, et al. Alpha particle Radium 223 dichloride in high-risk osteosarcoma: a phase I dose escalation trial. *Clin Cancer Res.* (2019) 25:3802–10. doi: 10.1158/1078-0432.CCR-18-3964

49. Branstetter DG, Nelson SD, Manivel JC, Blay JY, Chawla S, Thomas DM, et al. Denosumab induces tumor reduction and bone formation in patients with giant-cell tumor of bone. *Clin Cancer Res.* (2012) 18:4415–24. doi: 10.1158/1078-0432.CCR-12-0578

50. Chawla S, Henshaw R, Seeger L, Choy E, Blay JY, Ferrari S, et al. Safety and efficacy of denosumab for adults and skeletally mature adolescents with giant cell tumour of bone: interim analysis of an open-label, parallel-group, phase 2 study. *Lancet Oncol.* (2013) 14:901–8. doi: 10.1016/S1470-2045(13)70277-8

51. Seeman E, Delmas PD, Hanley DA, Sellmeyer D, Cheung AM, Shane E, et al. Microarchitectural deterioration of cortical and trabecular bone: differing effects of denosumab and alendronate. *J Bone Miner Res.* (2010) 25:1886–94. doi: 10.1002/jbmr.81

52. Thomas D, Henshaw R, Skubitz K, Chawla S, Staddon A, Blay JY, et al. Denosumab in patients with giant-cell tumour of bone: an open-label, phase 2 study. *Lancet Oncol.* (2010) 11:275–80. doi: 10.1016/S1470-2045(10)70010-3

53. Zebaze RM, Libanati C, Austin M, Ghasem-Zadeh A, Hanley DA, Zanchetta JR, et al. Differing effects of denosumab and alendronate on cortical and trabecular bone. *Bone.* (2014) 59:173–9. doi: 10.1016/j.bone.2013.11.016

54. Shewach DS, Lawrence TS. Radiosensitization of human tumor cells by gemcitabine in vitro. *Semin Oncol.* (1995) 22(4 Suppl. 11):68–71.

55. Shewach DS, Lawrence TS. Radiosensitization of human solid tumor cell lines with gemcitabine. *Semin Oncol.* (1996) 23(5 Suppl. 10):65–71.

56. Shewach DS, Lawrence TS. Gemcitabine and radiosensitization in human tumor cells. *Invest New Drugs.* (1996) 14:257–63. doi: 10.1007/BF00194528

57. Lawrence TS, Chang EY, Hahn TM, Shewach DS. Delayed radiosensitization of human colon carcinoma cells after a brief exposure to 2',2'-difluoro-2'-deoxycytidine (Gemcitabine). *Clin Cancer Res.* (1997) 3:777–82.

58. Lawrence TS, Eisbruch A, McGinn CJ, Fields MT, Shewach DS. Radiosensitization by gemcitabine. *Oncology.* (1999) 13(10 Suppl 5):55–60.

59. Lawrence TS, Eisbruch A, Shewach DS. Gemcitabine-mediated radiosensitization. *Semin Oncol.* (1997) 24(2 Suppl 7):S7–24.

60. Brand R, Capadano M, Tempero M. A phase I trial of weekly gemcitabine administered as a prolonged infusion in patients with pancreatic cancer and other solid tumors. *Invest New Drugs.* (1997) 15:331–41. doi: 10.1023/A:1005981317532

61. Tempero M, Plunkett W, Ruiz Van Haperen V, Hainsworth J, Hochster H, Lenzi R. Randomized phase II comparison of dose-intense gemcitabine: thirty-minute infusion and fixed dose rate infusion in patients with pancreatic adenocarcinoma. *J Clin Oncol.* (2003) 21:3402–8. doi: 10.1200/JCO.2003.09.140

62. Anderson PM. *Radium Knocks out Tumor cells in Case of Unresectable Paraspinalosteosarcoma.* New York, NY: Consult QD (2022).

63. Plutt AA, Stanton MP, Zembillas AS, Pierson CE, Zahler S, Anderson PM, et al. Excellent Tolerability of Ifosfamide and Mesna Via Continuous Infusion in a Pediatric Patient Population. *J Pediatr Hematol Oncol.* (2021) [Epub ahead of print]. doi: 10.1097/MPH.0000000000002361

64. Daudigeos-Dubus E, Le Dret L, Lanvers-Kaminsky C, Bawa O, Opolon P, Vievard A, et al. Regorafenib: antitumor activity upon mono and combination therapy in preclinical pediatric malignancy models. *PLoS One.* (2015) 10:e0142612. doi: 10.1371/journal.pone.0142612

65. Blank N, Laskov I, Kessous R, Kogan L, Lau S, Sebag IA, et al. Absence of cardiotoxicity with prolonged treatment and large accumulating doses of pegylated liposomal doxorubicin. *Cancer Chemother Pharmacol.* (2017) 80:737–43. doi: 10.1007/s00280-017-3412-8

66. Skubitz KM, Blaes AH, Konety SH, Francis GS. Cardiac safety profile of patients receiving high cumulative doses of pegylated-liposomal doxorubicin: use of left ventricular ejection fraction is of unproven value. *Cancer Chemother Pharmacol.* (2017) 80:787–98. doi: 10.1007/s00280-017-3420-8

67. Tomita H, Tanaka K, Tanaka T, Hara A. Aldehyde dehydrogenase 1A1 in stem cells and cancer. *Oncotarget.* (2016) 7:11018–32. doi: 10.18632/oncotarget.6920

68. Kang JH, Lee SH, Hong D, Lee JS, Ahn HS, Ahn JH, et al. Aldehyde dehydrogenase is used by cancer cells for energy metabolism. *Exp Mol Med.* (2016) 48:e272. doi: 10.1038/emm.2016.103

69. Anderson PM, Bielack SS, Gorlick RG, Skubitz K, Daw NC, Herzog CE, et al. A phase II study of clinical activity of SCH 717454 (robatumumab) in patients with relapsed osteosarcoma and Ewing sarcoma. *Pediatr Blood Cancer.* (2016) 63:1761–70. doi: 10.1002/pbc.26087

70. Thiele NA, Wilson JJ. Actinium-225 for targeted alpha therapy: coordination chemistry and current chelation approaches. *Cancer Biother Radiopharm.* (2018) 33:336–48. doi: 10.1089/cbr.2018.2494

71. Muller C, van der Meulen NP, Benešová M, Schibli R. Therapeutic Radiometals Beyond (177)Lu and (90)Y: production and application of promising alpha-particle, beta(-)-particle, and auger electron emitters. *J Nucl Med.* (2017) 58(Suppl 2):91S–6S. doi: 10.2967/jnumed.116.186825

72. Ahmed N, Brawley VS, Hegde M, Robertson C, Ghazi A, Gerken C, et al. Human Epidermal Growth Factor Receptor 2 (HER2) -Specific Chimeric Antigen Receptor-Modified T Cells for the Immunotherapy of HER2-Positive Sarcoma. *J Clin Oncol.* (2015) 33:1688–96. doi: 10.1200/JCO.2014.58.0225

73. Murray I, Rojas B, Gear J, Callister R, Cleton A, Flux GD. Quantitative dual-isotope planar imaging of thorium-227 and Radium-223 using defined energy windows. *Cancer Biother Radiopharm.* (2020) 35:530–9. doi: 10.1089/cbr.2019.3554

74. Lagmay JP, Krailo MD, Dang H, Kim A, Hawkins DS, Beaty O III, et al. Outcome of patients with recurrent osteosarcoma enrolled in seven phase II Trials through children's cancer group, pediatric oncology group, and children's oncology group: learning from the past to move forward. *J Clin Oncol.* (2016) 34:3031–8. doi: 10.1200/JCO.2015.65.5381

frontiers | Frontiers in Medicine

TYPE Study Protocol
PUBLISHED 18 November 2022
DOI 10.3389/fmed.2022.1059122



OPEN ACCESS

EDITED BY
Roy Larsen,
Sciencons AS, Norway

REVIEWED BY
Laura Evangelista,
University of Padua, Italy
Caroline Stokke,
Oslo University Hospital, Norway

*CORRESPONDENCE
Michael S. Hofman
Michael.Hofman@petermac.org
Arun A. Azad
Arun.Azad@petermac.org

†These authors share senior authorship

SPECIALTY SECTION
This article was submitted to Nuclear Medicine, a section of the journal Frontiers in Medicine

RECEIVED 30 September 2022
ACCEPTED 03 November 2022
PUBLISHED 18 November 2022

CITATION
Kostos L, Buteau JP, Yeung T, Iulio JD, Xie J, Cardin A, Chin KY, Emmerson B, Owen KL, Parker BS, Fettke H, Furic L, Azad AA and Hofman MS (2022) AlphaBet: Combination of Radium-223 and [$^{177}$Lu]Lu-PSMA-I&T in men with metastatic castration-resistant prostate cancer (clinical trial protocol). *Front. Med.* 9:1059122. doi: 10.3389/fmed.2022.1059122



# AlphaBet: Combination of Radium-223 and [$^{177}$Lu]Lu-PSMA-I&T in men with metastatic castration-resistant prostate cancer (clinical trial protocol)

Louise Kostos[1,2], James P. Buteau[2,3,4], Theresa Yeung[5], Juliana Di Iulio[5], Jing Xie[5], Anthony Cardin[2,3,6], Kwang Y. Chin[2,6], Brittany Emmerson[3,4], Katie L. Owen[2,7], Belinda S. Parker[2,7], Heidi Fettke[2,8], Luc Furic[2,8], Arun A. Azad[1,2*†] and Michael S. Hofman[2,3,4*†]

[1]Department of Medical Oncology, Peter MacCallum Cancer Centre, Melbourne, VIC, Australia, [2]Sir Peter MacCallum Department of Oncology, University of Melbourne, Melbourne, VIC, Australia, [3]Molecular Imaging and Therapeutic Nuclear Medicine, Peter MacCallum Cancer Centre, Melbourne, VIC, Australia, [4]Prostate Cancer Theranostics and Imaging Centre of Excellence, Peter MacCallum Cancer Centre, Melbourne, VIC, Australia, [5]Centre for Biostatistics and Clinical Trials (BaCT), Peter MacCallum Cancer Centre, Melbourne, VIC, Australia, [6]Department of Cancer Imaging, Peter MacCallum Cancer Centre, Melbourne, VIC, Australia, [7]Cancer Evolution and Metastasis Program, Peter MacCallum Cancer Centre, Melbourne, VIC, Australia, [8]Cancer Research Division, Peter MacCallum Cancer Centre, Melbourne, VIC, Australia

**Background:** [$^{177}$Lu]Lu-PSMA is a radioligand therapy used in metastatic castration-resistant prostate cancer (mCRPC). Despite a survival benefit, the responses for many patients receiving [$^{177}$Lu]Lu-PSMA are not durable, and all patients eventually develop progressive disease. The bone marrow is the most common site of progression. Micrometastases in this area likely receive an inadequate dose of radiation, as the emitted beta-particles from $^{177}$Lu travel an average range of 0.7 mm in soft tissue, well beyond the diameter of micrometastases. Radium-223 ($^{223}$Ra) is a calcium-mimetic and alpha-emitting radionuclide approved for use in men with mCRPC with bone metastases. The range of emitted alpha particles in soft tissue is much shorter ($\leq$100 $\mu$m) with high linear energy transfer, likely more lethal for osseous micrometastases. We anticipate that combining a bone-specific alpha-emitter with [$^{177}$Lu]Lu-PSMA will improve eradication of micrometastatic osseous disease, and thereby lead to higher and longer responses.

**Methods:** This is a single-center, single-arm phase I/II trial evaluating the combination of $^{223}$Ra and [$^{177}$Lu]Lu-PSMA-I&T in men with mCRPC. Thirty-six patients will receive 7.4 GBq of [$^{177}$Lu]Lu-PSMA-I&T, concurrently with $^{223}$Ra in escalating doses (28 kBq/kg – 55kBq/kg), both given intravenously every six weeks for up to six cycles. Eligible patients will have at least two untreated bone metastases visible on bone scintigraphy, and PSMA-positive disease on PSMA PET scan. Patients must have adequate bone marrow and organ function and be willing to undergo tumor biopsies. Patients with discordant disease visible

on FDG PET scan (defined as FDG positive disease with minimal or no PSMA expression and no uptake on bone scan) will be excluded. Other key exclusion criteria include the presence of diffuse marrow disease, prior treatment with $^{223}$Ra or [$^{177}$Lu]Lu-PSMA, or more than one prior line of chemotherapy for prostate cancer. The co-primary objectives of this study are to determine the maximum tolerated dose of $^{223}$Ra when combined with [$^{177}$Lu]Lu-PSMA-I&T and the 50% PSA response rate.

**Conclusion:** The AlphaBet trial is a phase I/II study combining $^{223}$Ra with [$^{177}$Lu]Lu-PSMA-I&T in patients with mCRPC. We aim to enroll the first patient in Q3 2022, and recruitment is anticipated to continue for 24 months.

**Study registration:** NCT05383079.

KEYWORDS

**metastatic castration-resistant prostate cancer, alpha therapy, micrometastatic disease, $^{177}$Lu-PSMA, radium-223, PSMA**

## Background

One of the recent practice changes for mCRPC, a leading cause of cancer-related death worldwide (1), has been the integration of [$^{177}$Lu]Lu-PSMA into the post-taxane and androgen receptor inhibitor (ARI) treatment paradigm. [$^{177}$Lu]Lu-PSMA is a form of radionuclide therapy whereby the isotope lutetium-177 ($^{177}$Lu) is attached to a prostate-specific membrane antigen (PSMA) radioligand to enable targeted delivery of radiation to prostate cancer cells *via* beta-particle emission. The landmark TheraP trial compared the use of [$^{177}$Lu]Lu-PSMA-617 with cabazitaxel in patients with mCRPC and found greater PSA responses (66 vs. 37% by intention to treat), a reduction in pain scores, and fewer grade 3 or higher adverse events (AEs) in the [$^{177}$Lu]Lu-PSMA-617 arm (2). [$^{177}$Lu]Lu-PSMA-617 was proven to extend overall survival (OS) as well as progression-free survival (PFS) in the VISION trial, where it was compared to protocol-defined best standard care alone (3). Both the TheraP and VISION trials utilized [$^{68}$Ga]Ga-PSMA-11 PET/CT for patient selection, with TheraP requiring a higher intensity of uptake of SUVmax greater than or equal to 20, compared to greater than liver in VISION. TheraP additionally used 2-[18F]fluoro-2-deoxy-D-glucose (FDG) PET/CT to identify sites of PSMA-negative disease whereas VISION used contrast-enhanced CT alone. Following publication of the VISION results, [$^{177}$Lu]Lu-PSMA-617 has been approved by the Food and Drug Administration (FDA) for use in the post-taxane, post-ARI mCRPC setting.

Several forms of PSMA-directed therapy exist in addition to PSMA-617, including the radioligand PSMA-I&T and monoclonal antibody J591. Comparing PSMA-I&T and PSMA-617, they are almost identical peptides with the main difference being the chemical chelator that binds the radioactive element and PSMA receptor binding structure. Dosimetry data demonstrates comparable absorbed doses and retrospective analyses suggest similar toxicities and clinical responses (4, 5). The European Association of Nuclear Medicine (EANM) radionuclide therapy guidelines apply to both [$^{177}$Lu]Lu-PSMA-617 and [$^{177}$Lu]Lu-PSMA-I&T (5).

Long-term follow-up of the 50 patients enrolled in the LuPSMA trial (6), the first phase II trial evaluating [$^{177}$Lu]Lu-PSMA-617 in men with mCRPC, found that all patients eventually developed PSA progression, even if they had an initial complete or exceptional response on post-therapy SPECT/CT. The majority of patients (56%) developed progressive bone marrow disease (7). The inability to deliver lethal doses of radiation to micrometastatic sites such as in the bone marrow may be a contributing reason for the lack of durable response for many patients. $^{177}$Lu releases relatively low linear energy transfer (LET) (0.2 keV/μm) beta radiation, which usually results in single-stranded DNA (ssDNA) breaks. Single metastatic cells or small cell clusters may not receive adequate radiation to result in cell death, owing to the lack of cross-fire effect which normally occurs in macro-tumors where there are abundant neighboring cells.

Alternative radionuclides with a higher LET may overcome this by inducing cytotoxic double-stranded DNA (dsDNA) breaks, leading to more robust treatment of micrometastatic disease. Alpha-emitters are one such example, which generally have a short path-length and high LET compared to beta-emitters, making them ideal for treating micrometastases. Usually only a few alpha particles through a cell nucleus are sufficient to induce cell death, and due to the short path length, bystander radiation is minimal. Examples of clinically available alpha-emitters include bismuth-213 ($^{213}$Bi), astatine-221 ($^{221}$At) and lead-212 ($^{212}$Pb). Limitations of these alpha-emitters, however, are the short half-life ($t_{1/2}$, 7.2 h for $^{221}$At, 10.6 hours for $^{212}$Pb, and 45.6 min for $^{213}$Bi), making treatment

of cancer cells in solid tumors where deep penetration is required or less accessible sites a challenge. To overcome this, several other alpha-emitters were introduced to the clinic with longer half-lives, including radium-223 ($^{223}$Ra, $t_{1/2}$ = 11.4 days) and actinium-225 ($^{225}$Ac, $t_{1/2}$ = 10.0 days) (8). There are several studies ongoing evaluating the combination of alpha-emitters with a PSMA-based radioligand (NCT04597411, NCT05219500) or monoclonal antibody (NCT04886986). Preliminary data from an $^{225}$Ac radionuclide compounded with J591 looks promising in terms of safety and efficacy (9). Unfortunately, several factors limit mass distribution of some targeted alpha therapies including complex radiochemistry and production leading to limited supply.

$^{223}$Ra is a calcium-mimetic alpha-emitter, with targeted activity against bone metastases. It has been studied extensively in mCRPC and is FDA approved for use in patients with bone-metastases and no visceral disease. Consequently, it is readily available and delivered in a pre-formulated vial (unlike other alpha-emitters). The short path length of <100 μm and high LET of 80 KeV/μm make $^{223}$Ra ideal for treating osseous micrometastases. In a phase II dose-finding study of $^{223}$Ra, patients received one of three differing doses of $^{223}$Ra—25 kBq/kg, 50 kBq/kg, and 80 kBq/kg. There was no difference in hematological toxicity amongst the three cohorts, with a low frequency of grade 2 or higher adverse events overall. The dose of 50 kBq/kg was selected for future studies. In the practice-changing phase III ALSYMPCA trial, $^{223}$Ra was delivered at a dose of 50 kBq/kg intravenously every 4 weeks for up to 6 doses (10). Compared to placebo, treatment with $^{223}$Ra was associated with an improvement in median OS (14.9 months vs. 11.3 months, HR 0.70) (10). $^{223}$Ra was well tolerated with fewer AEs compared to placebo and improved quality of life (QoL) scores. For $^{223}$Ra, the incidence of grade 3 or higher anemia, neutropaenia and thrombocytopaenia was 13, 3 and 6%, respectively (vs. 13, 3 and 1% in the placebo arm). Pathologic fractures occurred in 4% of patients receiving $^{223}$Ra compared to 5% in the placebo arm.

A reassessment of the primary standardization of $^{223}$Ra radioactivity measurement was initiated by the US National Institute of Standards and Technology (NIST) in 2015 (11). A discrepancy of approximately 10% between the initial published NIST primary standardization (12) and this assessment was identified, and as a result the recommended dose of $^{223}$Ra was adjusted from 50 kBq/kg to 55 kBq/kg every 4 weeks (11).

$^{223}$Ra has been studied in combination with a variety of other anti-cancer therapies including chemotherapy, anti-androgen therapy, immunotherapy, and PARP inhibitors for the treatment of advanced prostate cancer (see Table 1). In the pivotal studies evaluating $^{223}$Ra in combination with second-generation anti-androgens, a significantly increased fracture risk was an unexpected finding. In the phase III ERA-223 trial, patients with mCRPC received abiraterone acetate plus prednisolone in combination with $^{223}$Ra, vs. abiraterone acetate alone (13). OS did not differ significantly between groups, but the combination arm was associated with increased fracture risk (28.6 vs. 11.4%) leading to premature unblinding of the trial. The EORTC 1333/PEACEIII trial evaluates the addition of $^{223}$Ra to enzalutamide in mCRPC patients (14). On safety analysis, it was noted that, similarly to the ERA-223 trial, the fracture risk was significantly increased in the group who received enzalutamide in combination with $^{223}$Ra, without concomitant bone protective treatment. Following the results of the ERA-223 study, however, the EORTC 1333 study was amended, and bisphosphonate treatment was then mandated for all patients. Following this, the fracture rate significantly decreased in both arms of the study. Recruitment continues and efficacy outcomes are awaited.

Similarly, $^{223}$Ra has been combined with docetaxel chemotherapy (15). In a phase I trial, 20 patients were enrolled and received up to 5 doses of $^{223}$Ra given every 6 weeks, and docetaxel every 3 weeks. The starting dose of $^{223}$Ra was 27.5 kBq/kg and was then escalated to 55 kBq/kg if tolerated. Docetaxel was given at a dose of 75 mg/m$^2$ which is the standard therapeutic dose, with a plan to reduce to 60 mg/m$^2$ in the event of a dose-limiting toxicity (DLT). Febrile neutropaenia was dose limiting and therefore the recommended phase II dose (RP2D) for the combination was $^{223}$Ra 55 kBq/kg every 6 weeks × 5 doses, plus docetaxel 60 mg/m$^2$ every 3 weeks × 10 doses. In the phase II study, which compared this combination to docetaxel alone, the combination arm had more durable suppression of PSA (median time to PSA progression, 6.6 vs. 4.8 months, respectively) and alkaline phosphatase (ALP) (median time to ALP progression 9 vs. 7 months).

Though $^{223}$Ra has not previously been combined with [$^{177}$Lu]Lu-PSMA, sequential alpha/beta-emitting therapy using $^{177}$Lu and $^{223}$Ra has previously been studied in both prospective and retrospective analyses (16–18). Sartor et al. analyzed safety data from patients who were administered [$^{177}$Lu]Lu-PSMA following treatment with $^{223}$Ra (19). Twenty-six patients from a real-world patient registry (REASSURE study) were included in this analysis. The median time between the two treatments was 8 months (range 1–31). Five patients had Grade 3 or higher haematologic AEs during or after treatment with [$^{177}$Lu]Lu-PSMA, most commonly anemia. Overall, though this was a small patient sample, there were no apparent new safety signals.

Similarly, Baumgarten et al. explored the safety of [$^{177}$Lu]Lu-PSMA when given immediately after $^{223}$Ra in a retrospective analysis. Twenty-nine patients were studied who received [$^{177}$Lu]Lu-PSMA within 5 weeks (±3 weeks) of $^{223}$Ra injection. Grade 3-4 anemia necessitating a blood transfusion was seen in 5 patients, 2 patients required a dose-reduction and 7 patients discontinued treatment due to significant cytopaenias. Following this analysis, the authors concluded that treatment with [$^{177}$Lu]Lu-PSMA within 12 weeks of $^{223}$Ra had an acceptable risk profile (20). The retrospective WARMTH and RALU studies corroborated

TABLE 1 Combination studies with $^{223}$Ra in patients with mCRPC.

| Clinical trial registration number | Intervention | Phase | Primary outcome | Results |
|---|---|---|---|---|
| **Chemotherapy** | | | | |
| NCT03737370 | Radium-223 55 kBq/kg Q4W + Docetaxel Q2W (escalating doses) | I | Incidence of DLTs | NA, recruitment ongoing |
| NCT03574571 | Radium-223 55 kBq/kg Q6W + Docetaxel 60 mg/m$^2$ Q3W X 10 vs. Docetaxel 75 mg/m$^2$ Q3W alone | III | OS | NA, recruitment ongoing |
| NCT01106352 | Radium-223 50 kBq/kg Q6W + Docetaxel 60 mg/m$^2$ Q3W X 10 vs. Docetaxel 75 mg/m$^2$ Q3W alone | I/II | Incidence of DLTs and AEs | The RP2D for the combination was radium-223 55 kBq/kg Q6W × 5 doses, + docetaxel 60 mg/m$^2$ Q3W × 10 doses. Median time to PSA progression favored the combination (6.6 vs. 4.8 m) |
| **Immunotherapy** | | | | |
| NCT03093428 | Radium-223 55 kBq/kg Q4W + Pembrolizumab 200 mg Q3W vs. Radium-223 55 kBq/kg Q4W alone | II | Number of Participants with Increased Immune Cell Infiltration Across Arms | No difference between Arm A and B in rPFS (6.7 m vs. 5.7 m) or OS (16.9 vs. 16.0 m)<br>No evidence of increased CD4+ or CD8+ T-cell infiltration in Arm A |
| NCT04109729 | Radium-223 55 kBq/kg Q4W + Nivolumab 480 mg Q4W | I/II | Safety, ctDNA reduction after 6 weeks of nivolumab treatment | NA, recruitment ongoing |
| NCT02814669 | Radium-223 55 kBq/kg Q4W + Atezolizumab 480 mg Q2W | I | Incidence of DLTs and AEs, ORR | ORR 6.3%, Median rPFS 3.0 m, Median OS 16.3 m<br>No clear evidence of benefit with increased toxicity in combination than either drug alone |
| NCT04071236 | Radium-223 Q4W x 6 + Peposertib +/- Avelumab Q2W vs. Radium-223 Q4W x 6 alone | I/II | Incidence of DLTs, rPFS | NA, recruitment ongoing |
| NCT02463799 | Radium-223 50 kBq/kg Q4W + Sipuleucel-T Q2W vs. Sipuleucel-T Q2W alone | II | Immune responses to treatment with Sipuleucel-T measured by peripheral PA2024 T-cell proliferation | Higher 50% PSA response rate (31 vs. 0%) and longer PFS (39 vs. 12 w) and OS (NR vs. 2.6 y) seen in combination arm |
| **Anti-androgen therapy** | | | | |
| NCT02199197 | Radium-223 55 kBq/kg Q4W + Enzalutamide 160 mg daily vs. Enzalutamide alone | II | Incidence of AEs, change in serum N-telopeptides from baseline | No statistically significant difference in OS, rPFS, PSA PFS<br>PSA PFS2 improved with combination (18.7 vs. 8.4 m) |
| NCT02194842 | Radium-223 55 kBq/kg Q4W + Enzalutamide 160 mg daily vs. Enzalutamide alone | III | rPFS | NA, recruitment ongoing |
| NCT02043678 (ERA-223) | Radium-223 55 kBq/kg Q4W + Abiraterone Acetate 1000 mg daily and Prednisolone vs. Abiraterone alone | III | Symptomatic skeletal event free survival | No improvement in OS or median symptomatic skeletal event-free survival |
| **PARP inhibitors** | | | | |
| NCT03317392 | Radium-223 Q4W + Olaparib | I/II | MTD of Radium-223 and Olaparib, rPFS | NA, recruitment ongoing |
| NCT03076203 | Radium-223 Q4W + Niraparib | I | MTD | The MTD of Niraparib was 100 mg in the chemo-exposed arm and 200 mg in the chemo-naïve arm |

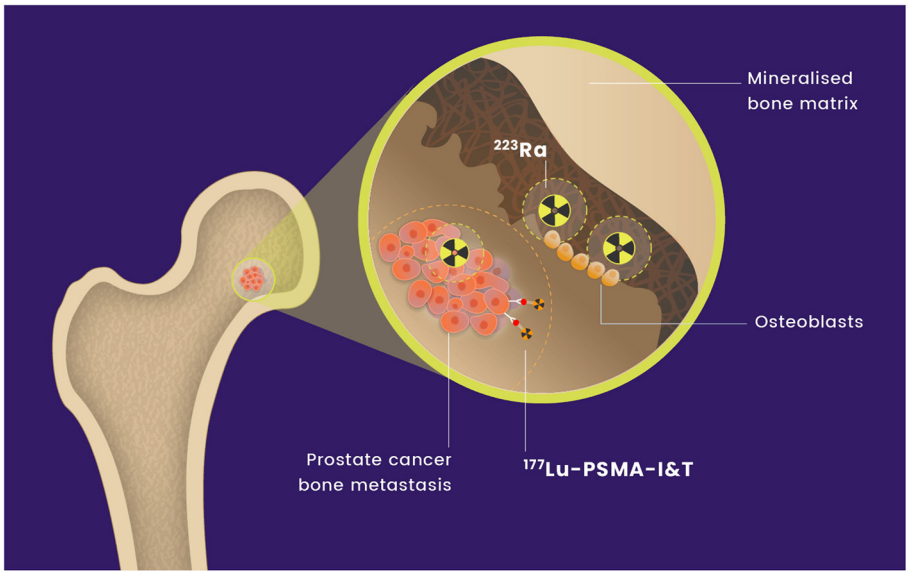


FIGURE 1
Mechanism of action of [$^{177}$Lu]Lu-PSMA-I&T and $^{223}$Ra on osseous metastases.

prior data and found that sequential therapy was feasible and well-tolerated (21).

[$^{177}$Lu]Lu-PSMA-I&T is currently being evaluated in combination with $^{255}$Ac-J591, a PSMA-directed monoclonal antibody radiolabelled with an alpha-emitter (NCT04886986). [$^{177}$Lu]Lu-PSMA-I&T has not previously been combined with $^{223}$Ra. We hypothesize that the combination of [$^{177}$Lu]Lu-PSMA-I&T and $^{223}$Ra will deliver effective radiation to sites of metastatic prostate cancer with an acceptable safety profile (see Figure 1). We anticipate that this combination will be synergistic and lead to higher and more durable responses through more effective treatment of micrometastatic marrow disease.

The physiologic bio-distribution of $^{223}$Ra and [$^{177}$Lu]Lu-PSMA-I&T is non-overlapping, further supporting our rationale for combining these radionuclides. $^{223}$Ra and [$^{177}$Lu]Lu-PSMA-I&T have different methods of clearance (fecal and renal, respectively). Bowel uptake by both tracers is a potential overlapping toxicity, although the binding sites are different with specific small bowel uptake with [$^{177}$Lu]Lu-PSMA compared to fecal excretion with $^{223}$Ra (22). It is possible, however, that overlapping toxicities will occur with this combination, with myeloid toxicity being of greatest concern. For [$^{177}$Lu]Lu-PSMA, the incidence of grade 3 or higher anemia, neutropaenia and thrombocytopaenia is in the range of 8–13, 2.5–7, and 8–13%, respectively, based on pooled data from the LuPSMA (6), TheraP (2) and VISION (3) trials. Given this, the frequency of anemia and thrombocytopaenia in particular may be higher when combined with $^{223}$Ra. Due to this, a traditional 3+3 dose escalation model will be utilized initially, as described below.

## AlphaBet study design

The AlphaBet study is a single-center, single-arm, phase I/II clinical trial evaluating the combination of $^{223}$Ra with [$^{177}$Lu]Lu-PSMA-I&T in men with mCRPC who have progressed on a prior ARI. We aim to recruit approximately thirty-six patients over the course of 24 months. The chosen sample size was pragmatic, and sufficient to determine the maximum tolerated dose (MTD). The dose of [$^{177}$Lu]Lu-PSMA-I&T will be fixed at 7.4 GBq every six weeks, whereas the dose of $^{223}$Ra will be escalated in a two-step process in the first phase of this trial (range 28 kBq/kg−55 kBq/kg every six weeks). The study schema is demonstrated in Figure 2.

This investigator-initiated study is sponsored by the Peter MacCallum Cancer Centre (PMCC), and ethics approval has been obtained from the PMCC Human Research Ethics Committee (HREC) in July 2022. This study was financially supported by Bayer and the Peter MacCallum Cancer Foundation, in addition to a Prostate Cancer Foundation (PCF) grant. The funders had no input into the trial design. The trial is registered at clinicaltrials.gov (NCT05383079).

The co-primary aims of the study are to determine the MTD and RP2D of $^{223}$Ra when combined with [$^{177}$Lu]Lu-PSMA-I&T, as well as the 50% PSA response rate (PSA-RR) for all

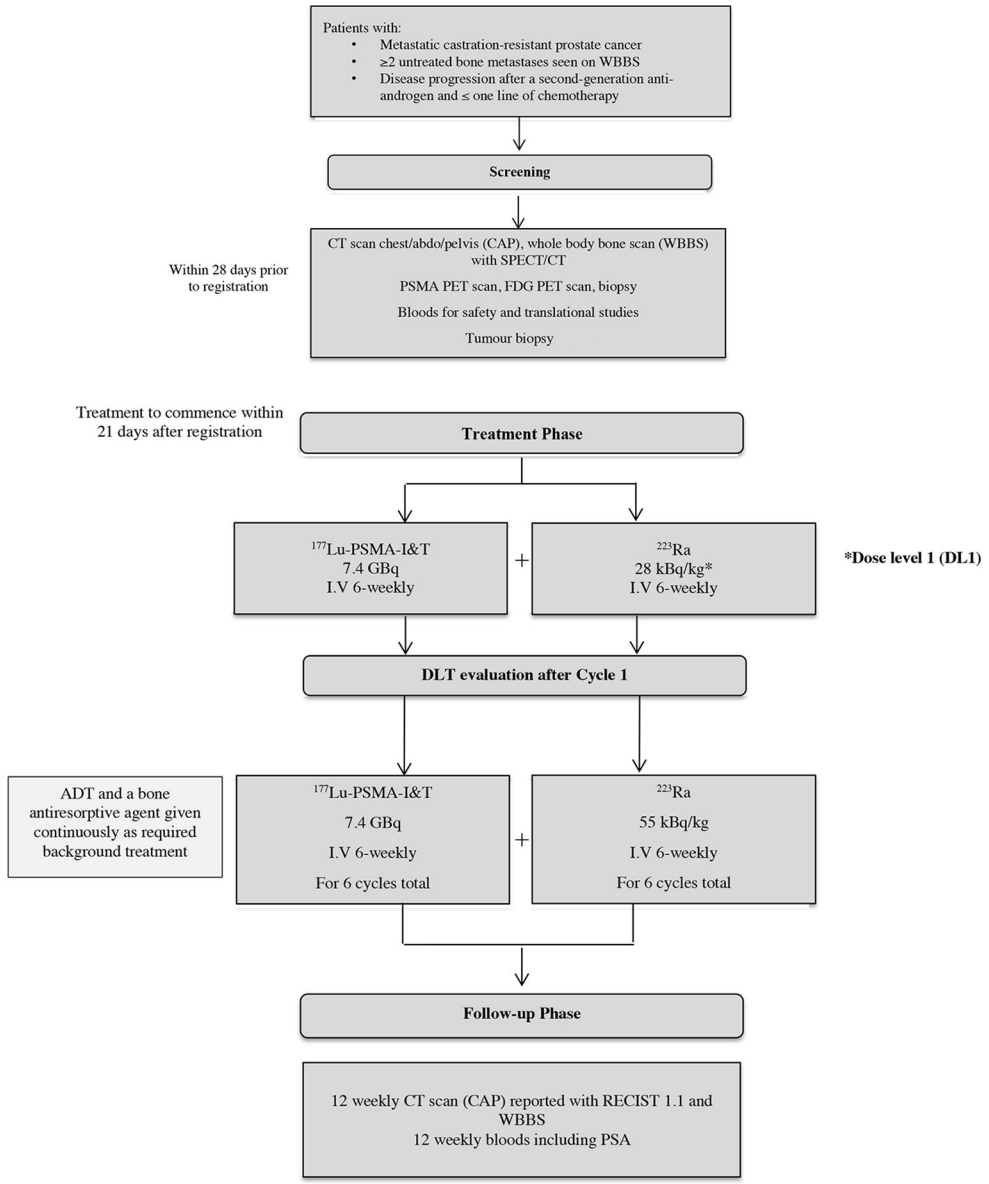


FIGURE 2
Study schema.

patients treated at the MTD. See Table 2 for secondary and exploratory objectives.

## Study population

Patients eligible for this study have mCRPC which has progressed after prior treatment with an ARI. Patients must have at least two untreated bone metastases visible on bone scintigraphy, PSMA-avid disease (SUVmax ≥20), and no discordant disease on FDG PET imaging (unless discordant lesions have increased uptake on bone scintigraphy). The full inclusion and exclusion criteria are detailed in Table 3.

## Treatment

In the dose-escalation phase of this study, patients will receive 7.4 GBq of [$^{177}$Lu]Lu-PSMA-I&T in combination with escalating doses of $^{223}$Ra, both given intravenously every six weeks. The [$^{177}$Lu]Lu-PSMA-I&T will be given on day 1 of a six-week cycle, and $^{223}$Ra administered after the

TABLE 2 Secondary and exploratory objectives.

| | |
|---|---|
| **Secondary objectives** | • To evaluate the safety of $^{223}$Ra in combination with [$^{177}$Lu]Lu-PSMA-I&T in patients with mCRPC through assessing the frequency and severity of AEs as per Common Terminology Criteria for Adverse Events version 5.0 (CTCAE v 5.0).<br>• Radiographic PFS (rPFS).<br>• PSA-PFS.<br>• PFS.<br>• OS.<br>• Objective Response Rate (ORR).<br>• To evaluate changes in health-related quality of life (HR-QoL) using FACT-P and pain using BPI-SF within 12 months of treatment commencement. |
| **Exploratory objectives** | • Time to ALP response.<br>• Time to ALP progression.<br>• Associations between imaging (PSMA PET/CT, FDG PET/CT, bone scan SPECT/CT, and post therapy SPECT-CT) and baseline characteristics and outcomes.<br>• Dynamic changes in circulating tumor DNA (ctDNA) fraction and utility of ctDNA genomic aberrations as a predictive biomarker of response.<br>• Changes to circulating and tumor infiltrating immune cells post therapy and their association with clinical outcome. |

[$^{177}$Lu]Lu-PSMA-I&T between days 1–5. A maximum of six cycles will be administered in total, in line with previous clinical trials evaluating [$^{177}$Lu]Lu-PSMA (2, 3). The total number of cycles administered for each patient will be determined by the treating investigators, and take into account PSA response, post-treatment SPECT/CT imaging, and any toxicities experienced. Treatment may be paused early in the setting of an exceptional response (see below–Treatment Discontinuation). All patients will receive concomitant bone protective therapy whilst on this trial, either with denosumab or zoledronic acid, in addition to ongoing androgen deprivation therapy (ADT). Patients will receive ondansetron (or equivalent) on days 1–3 of each cycle and additional antiemetics as required.

Dose escalation will employ a traditional 3 + 3 design to assess the safety and MTD of $^{223}$Ra in combination with [$^{177}$Lu]Lu-PSMA-I&T. There are 2 planned dose levels of $^{223}$Ra (Table 4) that will be evaluated in conjunction with 7.4 GBq of [$^{177}$Lu]Lu-PSMA-I&T.

In the dose expansion phase, up to 27 patients will be treated at the determined MTD or maximum administered dose (MAD), to provide further characterization of the safety and efficacy of $^{223}$Ra and [$^{177}$Lu]Lu-PSMA-I&T in combination. It is possible with this treatment combination that delayed or cumulative myeloid toxicity may occur. The RP2D will be defined by all available safety data and may be less than the MTD or MAD depending on the type and severity of AEs that occur during and after the first cycle.

## Dose limiting toxicities

Hematological recovery following administration of $^{223}$Ra is expected within 21–28 days, and the nadir following [$^{177}$Lu]Lu-PSMA is within 30 days. Therefore, we expect that any hematological toxicities will be resolved or improving by the end of the six-week cycle. This provides our justification for the DLT assessment period being the first six-weeks (or first cycle) of treatment.

Any of the following AEs will be considered a DLT if it occurs within 6 weeks of Cycle 1 Day 1 and is considered related to [$^{177}$Lu]Lu-PSMA-I&T and/or $^{223}$Ra:

- Grade 4 neutropaenia lasting > 7 days.
  - Granulocyte colony-stimulating factor (G-CSF) is permitted only for use in the management of febrile neutropaenia in this study.
- Grade 4 febrile neutropaenia of any duration.
- Grade ≥3 anemia lasting > 7 days, or necessitating administration of a blood transfusion for a Hb <70g/L or symptoms directly related to anemia.
- Grade 4 thrombocytopaenia lasting > 7 days, or necessitating administration of a platelet transfusion.
- Any grade ≥ 3 non-hematological AE with the following exceptions:
  - Grade 3 tumor flare (local pain) that resolves to ≤ Grade 2 in ≤ 7 days.
  - Grade 3 nausea, vomiting, or diarrhea that is optimally treated and resolves to Grade ≤ 2 in ≤ 5 days.
  - Grade 3 fatigue.
- Any grade 3 or higher hematological AE resulting in an inability to deliver the second cycle of treatment.

Treatment with [$^{177}$Lu]Lu-PSMA-I&T should be withheld during treatment-related Grade 3 or higher AEs (with the exception of fatigue or lymphocytopaenia) and not restarted until the AE has resolved to Grade 0–2 or baseline. $^{223}$Ra is to be delayed in conjunction with [$^{177}$Lu]Lu-PSMA-I&T, otherwise the dose is to be omitted if required due to attributable toxicity. Dose reductions to either [$^{177}$Lu]Lu-PSMA-I&T (20% reduction) or $^{223}$Ra (20–25% reduction) will be considered for treatment-related AEs of grade 3 or higher, with the exception of grade 2 xerostomia and dry eyes also warranting a dose reduction to [$^{177}$Lu]Lu-PSMA-I&T. Up to two dose reductions of $^{223}$Ra and [$^{177}$Lu]Lu-PSMA-I&T respectively are allowed. No dose re-escalations for either drug is allowed in this trial. If [$^{177}$Lu]Lu-PSMA-I&T is discontinued due to toxicity, patients can proceed with treatment with $^{223}$Ra alone.

TABLE 3 Inclusion and exclusion criteria.

| | |
|---|---|
| **Inclusion criteria** | 1. Patient has provided written informed consent.<br>2. Male patients must be 18 years of age or older at the time of written informed consent.<br>3. Histologically or cytologically confirmed adenocarcinoma of the prostate OR unequivocal diagnosis of metastatic prostate cancer (i.e., involving bone or pelvic lymph nodes or para-aortic lymph nodes) with an elevated serum prostate specific antigen (PSA).<br>4. Eastern Cooperative Oncology Group (ECOG) performance status of $\leq 2$.<br>5. Patients must have progressed on a $\geq$1 second-generation androgen receptor (AR)-targeted agent (e.g., enzalutamide, abiraterone, darolutamide, or apalutamide).<br>6. Patients must have progressive disease for study entry defined as any one of the following:<br>• PSA progression: minimum of two rising PSA values from a baseline measurement with an interval of $\geq$ 1 week between each measurement.<br>• Soft tissue progression as per Response Evaluation Criteria in Solid Tumors version 1.1 (RECIST 1.1) criteria.<br>• Bone progression: $\geq$ 2 new lesions on bone scan.<br>• Symptomatic progression e.g., bone pain.<br>7. At least 3 weeks since the completion of systemic therapy, surgery, or radiotherapy prior to registration.<br>8. Prior surgical orchiectomy or chemical castration maintained on luteinizing hormone-releasing hormone (LHRH) analog (agonist or antagonist).<br>9. Serum testosterone levels $\leq$ 1.75nmol/L within 28 days prior to registration.<br>10. Significant PSMA avidity on PSMA PET/CT, defined as a minimum uptake of maximum standardized uptake value (SUVmax) of 20 at a site of disease, and SUVmax $\geq$10 at sites of measurable disease $\geq$10 mm (unless subject to factors explaining a lower uptake, e.g., respiratory motion, reconstruction artifact).<br>11. The presence of $\geq$ 2 bone metastases on bone scintigraphy, which have not been previously treated with radiotherapy.<br>12. No contraindication to treatment with a bone antiresorptive agent such as denosumab or zoledronic acid.<br>13. Patients must have adequate bone marrow, hepatic and renal function documented within 28 days prior to registration, defined as:<br>• Hemoglobin $\geq$ 90 g/L independent of transfusions (no red blood cell transfusion in last four weeks)<br>• Absolute neutrophil count (ANC) $\geq$ 1.5 x $10^9$/L<br>• Platelets $\geq$ 150 x $10^9$/L<br>• Total bilirubin $\leq$ 1.5 x upper limit of normal (ULN) except for patients with known Gilbert's syndrome, where this applies for the unconjugated bilirubin component<br>• Aspartate transaminase (AST) and alanine transaminase (ALT) $\leq$ 2.5 x ULN if there is no evidence of liver metastasis or $\leq$ 5 x ULN in the presence of liver metastases<br>• Albumin $\geq$ 25 g/L<br>• Adequate renal function: patients must have a creatinine clearance estimated of $\geq$ 40 mL/min using the Cockcroft Gault equation.<br>14. Sexually active patients are willing to use medically acceptable forms of barrier contraception.<br>15. Willing to undergo biopsies if disease is considered accessible and biopsy is feasible.<br>16. Willing and able to comply with all study requirements, including all treatments and the timing and nature of all required assessments. |
| **Exclusion criteria** | 1. Superscan on whole body bone scan (WBBS) or diffuse marrow disease on PSMA PET.<br>2. Prior treatment with $^{223}$Ra or [$^{177}$Lu]Lu-PSMA.<br>3. Has received more than one previous line of chemotherapy for the treatment of metastatic prostate cancer.<br>4. Site(s) of discordant FDG positive disease defined by minimal PSMA expression and no uptake on whole body bone scan ([WBBS] for bone metastases).<br>5. Other malignancies (in addition to the prostate cancer being treated in this study) within the previous 2-years prior to registration other than basal cell or squamous cell carcinomas of skin or other cancers that are unlikely to recur within 24 months.<br>6. Symptomatic brain metastases or leptomeningeal metastases.<br>7. Patients with symptomatic or impending cord compression unless appropriately treated beforehand and clinically stable for $\geq$ 4 weeks.<br>8. Concurrent illness, including severe infection that may jeopardize the ability of the patient to undergo the procedures outlined in this protocol with reasonable safety. |

## Study assessments

### Dosimetry

For all cycles, a post-treatment SPECT/CT will occur on Day 2, approximately 24 h after administration of [$^{177}$Lu]Lu-PSMA-I&T. Additional SPECT/CT imaging may occur at 4, 48 and 96 hours at the discretion of the study investigators. The purpose of post-treatment SPECT/CT imaging is to estimate tumor radiation doses.

TABLE 4 $^{223}$Ra planned dose levels.

| Dose level | $^{223}$Ra |
|---|---|
| Dose level 1 | 28 kBq/kg |
| Dose level 2 | 55 kBq/kg |

## Patient reported outcomes

Patient Reported Outcomes (PROs) will be completed immediately prior to Cycle 1 Day 1, at six and twelve weeks, and then 12-weekly thereafter up to 48 weeks. For this study, the Functional Assessment of Cancer Therapy for Prostate Cancer (FACT-P) questionnaire will be used to describe health-related QoL, and the Brief Pain Inventory–Short Form (BPI-SF) will be used to assess pain.

## Imaging

Patients will undergo a baseline CT chest/abdomen/pelvis and WBBS with SPECT/CT, and have both scans repeated every 12 weeks until radiographic progression, a new anti-cancer treatment is commenced, or death. After each imaging timepoint, a response assessment will be performed. RECIST1.1 will be used to assess soft tissue lesions seen on CT, and Prostate Cancer Working Group 3 (PCWG3) criteria will be used to evaluate bone lesions visible on bone scintigraphy. A repeat PSMA PET and FDG PET scan will be performed prior to Cycle 3 Day 1 for exploratory analyses only.

## PSA

PSA will be measured every 3 weeks during treatment, and every 6 weeks from the day 21 safety visit for 48 weeks. PSA response and progression are defined according to PCWG3 recommendations (23).

## Translational blood samples

Blood samples will be taken at baseline, prior to Cycle 2, Cycle 4 and on progression for the purposes of genomic analysis.

## Biopsies

For patients considered to have a lesion that is safe to biopsy, a radiologically guided biopsy will occur at baseline, after 2–4 weeks from Cycle 1 Day 1, and again on progression. Biopsies will ideally be taken from the same site each time. These will be matched with serum samples taken at the same timepoints and will be used to analyse the immune response to radiotherapy.

# Follow up

After completion or discontinuation of study treatment, a 21-day safety visit will be performed. Patients will then enter the follow-up phase and continue clinical reviews and blood tests every 6 weeks for 48 weeks, at which point the reviews will then change to 12-weekly. Clinical reviews will continue until unequivocal disease progression, commencement of a new anti-cancer treatment, death, or until it has been 12 months after the last patient has completed treatment (end of trial follow-up). Additionally, PSA testing will continue until the criteria for PSA progression has been met.

# Treatment discontinuation

Reasons for study treatment discontinuation include unequivocal disease progression, unacceptable toxicity, withdrawal of consent by the patient, inter-current illness preventing further treatment, the need to start a prohibited therapy, and significant protocol non-compliance. For the purposes of this study, unequivocal progression is defined as radiographic progression (based on RECIST1.1 for soft tissue lesions and PCWG3 for bone lesions) or clinical progression (symptomatic progression and/or a need to start a new anti-cancer therapy). PSA progression alone is not considered to be unequivocal progression.

Of note, patients may also suspend treatment (both [$^{177}$Lu]Lu-PSMA-I&T and $^{223}$Ra) if they demonstrate an marked reduction in uptake at all sites of disease on the 24-h post-treatment SPECT/CT scan (PSMA-uptake intensity less than liver at all sites). On progression, patients can then recommence study treatment provided they have received < six cycles in total.

# Development of biomarkers that predict patient response

The translational research arm of AlphaBet proposes to develop tumor and immune biomarkers to predict improved patient survival following combination therapy with [$^{177}$Lu]Lu-PSMA and $^{223}$Ra.

Through pre-clinical work using single-cell transcriptomics and *ex-vivo* profiling, Owen et al. established that proliferating prostate cancer cells in the bone display dampened tumor cell-inherent type I interferon signaling, which renders bone metastases poorly immunogenic and treatment-resistant (24). Additionally, tumor interferon status predicts intratumoural and systemic immune reactivity, as well as radiotherapy and Immune checkpoint inhibitor (ICI) responses (25–28). We aim to measure the expression of interferon biomarkers in

tumor cells pre- and post- [$^{177}$Lu]Lu-PSMA-I&T and $^{223}$Ra, along with markers of immunogenicity and infiltrating immune cells. This could potentially uncover new strategies through which to predict patient response and response durability. Importantly, given that interferon signals mediate DNA damage responses upon radiotherapy, such biomarkers may be readouts of the likely benefit of [$^{177}$Lu]Lu-PSMA-I&T and $^{223}$Ra before treatment commences.

Using the peripheral blood samples, the baseline, on-treatment, and progression ctDNA fractions will be analyzed and correlated with baseline patient and disease characteristics and treatment outcomes. Similarly, the genomic profile of each patient, including how this evolves throughout the trial will be analyzed. Potential biomarkers to predict for both response and resistance to treatment will be interrogated.

## Analysis plan

For the dose-escalation phase, the analysis will be focused primarily on adverse events, particularly DLTs reported in the DLT observation period. From this data, the MTD or MAD will be decided. There are 2 analyses planned for the dose-expansion phase of this study: safety analysis and final analysis. The final analysis will be performed at the completion of the study, which will be 12 months after the last patient has completed treatment, assessing all endpoints including treatment efficacy.

Descriptive statistics of baseline characteristics of all patients will be summarized overall and by trial phase. Continuous variables will be described as mean, standard deviation, interquartile range, median, minimum, and maximum, and qualitative variables will be described as counts and percentages. PSA-response rate and objective response rate will be described as percentages with 95% confidence intervals using exact methods. Survival outcomes will be described using Kaplan-Meier methods.

Pain and health related-QoL will be analyzed using linear mixed models (LMM) with time (as factor) included as a fixed effect and patient included as a random effect. The area under the curve (AUC) of relevant pain and QoL domains will be calculated using appropriate linear contrast from the LMM.

# Discussion

Given progression following [$^{177}$Lu]Lu-PSMA-I&T is linked in many cases to micro-metastatic osseous disease, the shorter path length and high LET of $^{223}$Ra against bone disease provides a rationale for combining it with [$^{177}$Lu]Lu-PSMA-I&T. These qualities, which are specific to alpha-emitters, result in a higher chance of cell death due to inducing dsDNA breaks, rather than a reliance on crossfire radiation from neighboring cells to accumulate enough cytotoxic radiation.

Due to the potential for overlapping toxicities, particularly myeloid, we opted to follow a traditional 3+3 escalation model to ensure that safety could be monitored carefully. As discussed above, we plan to dose-escalate the $^{223}$Ra and keep the dose of [$^{177}$Lu]Lu-PSMA-I&T fixed as per the VISION trial (3). We have pre-specified only two dose levels for $^{223}$Ra (28 kBq/kg and 55 kBq/kg) given that it is well-tolerated as monotherapy. Reassuringly, a phase 2 randomized study comparing the combination of $^{223}$Ra with docetaxel to docetaxel alone found that the safety profile of the two groups were similar (15). In fact, febrile neutropaenia occurred more frequently in the docetaxel alone group (0% in the combination vs. 15% for docetaxel monotherapy). Any potential fracture risk from $^{223}$Ra, which has been observed only when combined with an ARI, will be mitigated by concurrent use of a bone-antiresorptive agent.

In terms of eligibility criteria, a minimum number of two bone lesions with increased uptake on bone scintigraphy was chosen based on the inclusion criteria from prior trials evaluating $^{223}$Ra (10). Patients with extensive bone metastases or diffuse marrow disease, however, were excluded as these were considered to be at increased risk of myeloid toxicity. This was defined as having a "superscan" on bone scintigraphy, which is an imaging appearance that occurs due to a high ratio of bone to soft tissue tracer accumulation, thereby diminishing renal and background soft tissue uptake. Diffuse marrow disease seen on PET scan, determined by central Nuclear Medicine review, was also excluded. This study will allow patients with discordant bone lesions (PSMA-, FDG+ on PET imaging) as defined in Table 3, as long as they have increased uptake on bone scintigraphy. Outcomes from this cohort of patients specifically will be analyzed as an exploratory endpoint.

The primary endpoint of the phase II portion of this study is PSA-RR, with survival outcomes such as OS and PFS listed as secondary endpoints. We chose this primary endpoint to enable an early assessment of disease activity, with longer follow-up required to evaluate the secondary survival outcomes. Predictive markers of response are needed to assist with future patient selection for this therapy. Similar to PSMA PET SUVmean $\geq$10 being a predictive imaging biomarker for response to [$^{177}$Lu]Lu-PSMA (29, 30), exploratory analyses from the ALSYMPCA study suggest that a decline in total ALP level at 12 weeks after initiation of $^{223}$Ra treatment correlates with improved survival (31). This finding was corroborated in the REASSURE study (32) and therefore time to ALP response and ALP progression will also be exploratory biomarkers in our study.

With this novel combination, osseous micrometastatic disease will hopefully receive robust treatment, though an obvious limitation is that soft tissue micrometastases may remain suboptimally treated. We chose to prioritize treatment of bone lesions based on the knowledge that the bone marrow is the most common site of disease progression following [$^{177}$Lu]Lu-PSMA therapy. Combining a PSMA radioligand with alternative alpha-emitters that are not specific to bone may overcome this limitation (eg., $^{225}$Ac or $^{212}$Pb), however this is fraught with other challenges involving manufacture and mass distribution. As previously discussed, several studies are

ongoing evaluating different combinations of alpha-emitters and PSMA-based radioligands (NCT04597411, NCT05219500).

In terms of the ideal radionuclide to combine with a PSMA ligand, theoretically this would involve an isotope with high LET and a half-life matched to that of the PSMA ligand, a straightforward and reliable manufacturing process and limited toxicity of daughter isotopes. Of the potential aforementioned alpha-emitters ($^{212}$Pb, $^{223}$Ra, $^{225}$Ac, $^{211}$At), all have a high LET however $^{212}$Pb and $^{211}$At are the only isotopes with a half-life similar to the PSMA ligand (10.6 and 7.2 h respectively). $^{225}$Ac and $^{211}$At are restricted by a complex production process thereby limiting supply, with $^{211}$At in particular having complex radiochemistry. $^{212}$Pb and $^{211}$At produce the least toxic daughter isotopes. $^{212}$Pb can have reliable supply as production is generator-based, so potentially this will emerge as the ideal alpha-emitter to combine with a PSMA ligand. Currently there are no studies evaluating this combination to our knowledge.

In conclusion, we hope that the AlphaBet study will be a step forward in improving outcomes for patients with mCRPC and bone metastases, and potentially inform the design of subsequent later-phase randomized studies. In particular, the exploratory translational data from tissue, blood and novel imaging will lead to a deeper understanding of the reasons and predictors for treatment response and resistance and the immune response to radiotherapy.

## Ethics statement

This study involving human participants was reviewed and approved by Peter MacCallum Cancer Centre. The patients provided their written informed consent to participate in this study.

## Author contributions

LK wrote the first draft of the manuscript. JI, TY, JX, AC, KC, KO, BP, HF, LF, JB, and MH assisted with editing and revising the manuscript. AA, JB, and MH provided oversight of the protocol and edited the manuscript. All authors contributed to the article and approved the submitted version.

## Funding

This trial is made possible through a grant from the Prostate Cancer Foundation (PCF) funded by CANICA Oslo Norway, Peter MacCallum Foundation, and support from Bayer who are providing supply of $^{223}$Ra and financial support. $^{177}$Lu, no carrier added, was supplied from the Australian Nuclear Science and Technology Organization (ANSTO). LK was supported by a Vincent Fairfax Family Foundation Research Entry Scholarship from the RACP Foundation, and LK and JB are both supported by a University of Melbourne Australian Government Research Training Program Scholarship. MH and AA are supported by NHMRC Investigator Grants.

## Acknowledgments

We are grateful for the help and support of Ms. Annette Van Der Heyden, Prostate Cancer Theranostics and Imaging Centre of Excellence (ProsTIC) Programme Manager.

## Conflict of interest

Author LK has the following disclosures: Honoraria for speaker duties from Bayer. Author AA has the following disclosures (lifetime): Consultant—Astellas, Janssen, Novartis, Aculeus Therapeutics; Speakers Bureau—Astellas, Janssen, Novartis, Amgen, Ipsen, Bristol Myers Squibb; Merck Serono, Bayer; Honoraria—Astellas, Novartis, Sanofi, AstraZeneca, Tolmar, Telix, Merck Serono, Janssen, Bristol Myers Squibb, Ipsen, Bayer, Pfizer, Amgen, Noxopharm, Merck Sharpe Dome, Aculeus Therapeutics; Scientific Advisory Board—Astellas, Novartis, Sanofi, AstraZeneca, Tolmar, Pfizer, Telix, Merck Serono, Janssen, Bristol Myers Squibb, Ipsen, Bayer, Merck Sharpe Dome, Amgen, Noxopharm; Travel + Accommodation—Astellas, Merck Serono, Amgen, Novartis, Janssen, Tolmar, Pfizer; Research Funding—Astellas (investigator), Merck Serono (investigator), Astra Zeneca (investigator), Bristol Myers Squibb (institutional), Astra Zeneca (institutional), Aptevo Therapeutics (institutional), Glaxo Smith Kline (institutional), Pfizer (institutional), MedImmune (institutional), Astellas (institutional), SYNthorx (institutional), Bionomics (institutional), Sanofi Aventis (institutional), Novartis (institutional), Ipsen (institutional), Exelixis (institutional), Merck Sharpe Dome (institutional), Janssen (institutional), Eli Lilly (institutional), Gilead Sciences (institutional), Merck Serono (institutional), Hinova (institutional). MH acknowledged philanthropic/government grant support from the Prostate Cancer Foundation (PCF) funded by CANICA Oslo Norway, Peter MacCallum Foundation, Medical Research Future Fund, NHMRC Investigator Grant, Movember, U.S. Department of Defense and the Prostate Cancer Foundation of Australia (PCFA). Author MH acknowledges grant support from AAA/Novartis, ANSTO, Bayer, Isotopia. Consulting fees for lectures or advisory boards from Astellas, AstraZeneca, Janssen, Merck/MSD, Mundipharma and Point Biopharma.

The remaining authors declare that the research was conducted in the absence of any commercial or financial relationships that could be construed as a potential conflict of interest.

The authors declare that this study received funding from Bayer. The funder was not involved in the study design, the writing of this article or the decision to submit it for publication.

## Publisher's note



## References

1. Sung H, Ferlay J, Siegel RL, Laversanne M, Soerjomataram I, Jemal A, et al. Global cancer statistics 2020: GLOBOCAN estimates of incidence and mortality worldwide for 36 cancers in 185 countries. *CA Cancer J Clin.* (2021) 71:209–49. doi: 10.3322/caac.21660

2. Hofman MS, Emmett L, Sandhu S, Iravani A, Joshua AM, Goh JC, et al. [$^{177}$Lu]Lu-PSMA-617 versus cabazitaxel in patients with metastatic castration-resistant prostate cancer (TheraP): a randomised, open-label, phase 2 trial. *Lancet.* (2021) 397:797–804. doi: 10.1016/S0140-6736(21)00237-3

3. Sartor O, de Bono J, Chi KN, Fizazi K, Herrmann K, Rahbar K, et al. Lutetium-177-PSMA-617 for metastatic castration-resistant prostate cancer. *N Engl J Med.* (2021) 385:1091–103. doi: 10.1056/NEJMoa2107322

4. Schuchardt C, Zhang J, Kulkarni HR, Chen X, Mueller D, Baum RP. Prostate-specific membrane antigen radioligand therapy using $^{177}$Lu-PSMA I&T and $^{177}$Lu-PSMA-617 in patients with metastatic castration-resistant prostate cancer: comparison of safety, biodistribution and dosimetry. *J Nucl Med.* (2021). doi: 10.2967/jnumed.121.262713

5. Kratochwil C, Fendler WP, Eiber M, Baum R, Bozkurt MF, Czernin J, et al. EANM procedure guidelines for radionuclide therapy with $^{177}$Lu-labelled PSMA-ligands ($^{177}$Lu-PSMA-RLT). *Eur J Nucl Med Mol Imaging.* (2019) 46:2536–44. doi: 10.1007/s00259-019-04485-3

6. Hofman MS, Violet J, Hicks RJ, Ferdinandus J, Thang SP, Akhurst T, et al. [$^{177}$Lu]-PSMA-617 radionuclide treatment in patients with metastatic castration-resistant prostate cancer (LuPSMA trial): a single-centre, single-arm, phase 2 study. *Lancet Oncol.* (2018) 19:825–33. doi: 10.1016/S1470-2045(18)30198-0

7. Violet J, Sandhu S, Iravani A, Ferdinandus J, Thang SP, Kong G, et al. Long-term follow-up and outcomes of retreatment in an expanded 50-patient single-center phase ii prospective trial of $^{177}$Lu-PSMA-617 theranostics in metastatic castration-resistant prostate cancer. *J Nucl Med.* (2020) 61:857–65. doi: 10.2967/jnumed.119.236414

8. de Kruijff RM, Wolterbeek HT, Denkova AG, A. Critical review of alpha radionuclide therapy-how to deal with recoiling daughters? *Pharmaceuticals (Basel).* (2015) 8:321–36. doi: 10.3390/ph8020321

9. Tagawa ST, Sun M, Sartor AO, Thomas C, Singh S, Bissassar M, et al. Phase I study of 225Ac-J591 for men with metastatic castration-resistant prostate cancer (mCRPC). *J Clin Oncol.* (2021) 39(Suppl. 15):5015. doi: 10.1200/JCO.2021.39.15_suppl.5015

10. Hoskin P, Sartor O, O'Sullivan JM, Johannessen DC, Helle SI, Logue J, et al. Efficacy and safety of radium-223 dichloride in patients with castration-resistant prostate cancer and symptomatic bone metastases, with or without previous docetaxel use: a prespecified subgroup analysis from the randomised, double-blind, phase 3 ALSYMPCA trial. *Lancet Oncol.* (2014) 15:1397–406. doi: 10.1016/S1470-2045(14)70474-7

11. Zimmerman BE, Bergeron DE, Cessna JT, Fitzgerald R, Pibida L. Revision of the NIST standard for (223)Ra: new measurements and review of 2008 data. *J Res Natl Inst Stand Technol.* (2015) 120:37–57. doi: 10.6028/jres.120.004

12. Cessna JT, Zimmerman BE. Standardization of radium-223 by liquid scintillation counting. *Appl Radiat Isot.* (2010) 68:1523–8. doi: 10.1016/j.apradiso.2009.11.068

13. Smith M, Parker C, Saad F, Miller K, Tombal B, Ng QS, et al. Addition of radium-223 to abiraterone acetate and prednisone or prednisolone in patients with castration-resistant prostate cancer and bone metastases (ERA 223): a randomised, double-blind, placebo-controlled, phase 3 trial. *Lancet Oncol.* (2019) 20:408–19. doi: 10.1016/S1470-2045(18)30860-X

14. Gillessen S, Choudhury A, Rodriguez-Vida A, Nole F, Diaz EG, Roumeguere TA, et al. Decreased fracture rate by mandating bone protecting agents in the EORTC 1333/PEACEIII trial combining Ra223 with enzalutamide versus enzalutamide alone: an updated safety analysis. *J Clin Oncol.* (2021) 39(Suppl. 15):5002. doi: 10.1200/JCO.2021.39.15_suppl.5002

15. Morris MJ, Loriot Y, Sweeney CJ, Fizazi K, Ryan CJ, Shevrin DH, et al. Radium-223 in combination with docetaxel in patients with castration-resistant prostate cancer and bone metastases: a phase 1 dose escalation/randomised phase 2a trial. *Eur J Cancer.* (2019) 114:107–16. doi: 10.1016/j.ejca.2019.04.007

16. Ahmadzadehfar H, Zimbelmann S, Yordanova A, Fimmers R, Kürpig S, Eppard E, et al. Radioligand therapy of metastatic prostate cancer using $^{177}$Lu-PSMA-617 after radiation exposure to (223)Ra-dichloride. *Oncotarget.* (2017) 8:55567–74. doi: 10.18632/oncotarget.15698

17. Ferdinandus J, Eppard E, Gaertner FC, Kürpig S, Fimmers R, Yordanova A, et al. Predictors of response to radioligand therapy of metastatic castrate-resistant prostate cancer with $^{177}$Lu-PSMA-617. *J Nucl Med.* (2017) 58:312–9. doi: 10.2967/jnumed.116.178228

18. Ahmadzadehfar H, Rahbar K, Baum RP, Seifert R, Kessel K, Bögemann M, et al. Prior therapies as prognostic factors of overall survival in metastatic castration-resistant prostate cancer patients treated with [$^{177}$Lu]Lu-PSMA-617. A WARMTH multicenter study (the 617 trial). *Eur J Nucl Med Mol Imaging.* (2021) 48:113–22. doi: 10.1007/s00259-020-04797-9

19. Sartor AO, la Fougère C, Essler M, Ezziddin S, Kramer G, Elllinger J, et al. Lutetium-177–prostate-specific membrane antigen ligand following radium-223 treatment in men with bone-metastatic castration-resistant prostate cancer: real-world clinical experience. *J Nuclear Med.* (2021):jnumed.121.262240. doi: 10.2967/jnumed.121.262240

20. Baumgarten J, Groener D, Ngoc CN, Mader N, Chaurasia M, Davis K, et al. Safety and efficacy of $^{177}$lutetium-psma-617 radioligand therapy shortly after failing 223radium-dichloride. *Cancers (Basel).* (2022) 14:557. doi: 10.3390/cancers14030557

21. Kambiz Rahbar, Markus Essler, Matthias Eiber, Christian la Fougère, Vikas Prasad, Wolfgang P. Fendler, et al. Lutetium-177–*Prostate-Specific Membrane Antigen Therapy in Patients with Prior Radium-223: Safety and Effectiveness Outcomes*. Paris: European Society of Medical Oncology (ESMO) (2022).

22. Ogawa K, Higashi T, Mishiro K, Wakabayashi H, Shiba K, Odani A, et al. Decreasing undesirable absorbed radiation to the intestine after administration of radium-223 dichloride for treatment of bone metastases. *Sci Rep.* (2020) 10:11917. doi: 10.1038/s41598-020-68846-x

23. Scher HI, Morris MJ, Stadler WM, Higano C, Basch E, Fizazi K, et al. Trial Design and Objectives for Castration-Resistant Prostate Cancer: Updated Recommendations From the Prostate Cancer Clinical Trials Working Group 3. *J Clin Oncol.* (2016) 34:1402–18. doi: 10.1200/JCO.2015.64.2702

24. Owen KL, Gearing LJ, Zanker DJ, Brockwell NK, Khoo WH, Roden DL, et al. Prostate cancer cell-intrinsic interferon signaling regulates dormancy and metastatic outgrowth in bone. *EMBO Rep.* (2020) 21:e50162. doi: 10.15252/embr.202050162

25. Formenti SC, Rudqvist NP, Golden E, Cooper B, Wennerberg E, Lhuillier C, et al. Radiotherapy induces responses of lung cancer to CTLA-4 blockade. *Nat Med.* (2018) 24:1845–51. doi: 10.1038/s41591-018-0232-2

26. Wennerberg E, Spada S, Rudqvist NP, Lhuillier C, Gruber S, Chen Q, et al. CD73 blockade promotes dendritic cell infiltration of irradiated tumors and tumor rejection. *Cancer Immunol Res.* (2020) 8:465–78. doi: 10.1158/2326-6066.CIR-19-0449

27. Brockwell NK, Owen KL, Zanker D, Spurling A, Rautela J, Duivenvoorden HM, et al. Neoadjuvant interferons: critical for effective PD-1-based immunotherapy in TNBC. *Cancer Immunol Res.* (2017) 5:871–84. doi: 10.1158/2326-6066.CIR-17-0150

28. Demaria S, Pilones KA, Vanpouille-Box C, Golden EB, Formenti SC. The optimal partnership of radiation and immunotherapy: from preclinical studies to clinical translation. *Radiat Res.* (2014) 182:170–81. doi: 10.1667/RR13500.1

29. Buteau JP, Martin AJ, Emmett L, Iravani A, Sandhu S, Joshua AM, et al. PSMA and FDG-PET as predictive and prognostic biomarkers in patients given [$^{177}$Lu] Lu-PSMA-617 versus cabazitaxel for metastatic castration-resistant prostate cancer (TheraP): a biomarker analysis from a randomised, open-label, phase 2 trial. *Lancet Oncol.* (2022) 23:1389–97. doi: 10.1016/S1470-2045(22)00605-2

30. Kuo P, Hesterman J, Rahbar K, Kendi AT, Wei XX, Fang B, et al. [68Ga]Ga-PSMA-11 PET baseline imaging as a prognostic tool for clinical outcomes to [$^{177}$Lu]Lu-PSMA-617 in patients with mCRPC: A VISION substudy. *J Clin Oncol.* (2022) 40(Suppl. 16):5002. doi: 10.1200/JCO.2022.40.16_suppl.5002

31. Sartor O, Coleman RE, Nilsson S, Heinrich D, Helle SI, O'Sullivan JM, et al. An exploratory analysis of alkaline phosphatase, lactate dehydrogenase, and prostate-specific antigen dynamics in the phase 3 ALSYMPCA trial with radium-223. *Ann Oncol.* (2017) 28:1090–7. doi: 10.1093/annonc/mdx044

32. James ND, Heinrich D, Castro E, George S, Song DY, Dizdarevic S, et al. Alkaline phosphatase (ALP) decline and overall survival (OS) in patients (pts) with metastatic castration-resistant prostate cancer (mCRPC) treated with radium-223 (Ra-223) in the REASSURE study. *J Clin Oncol.* (2022) 40(Suppl. 16):5041. doi: 10.1200/JCO.2022.40.16_suppl.5041

frontiers | Frontiers in Medicine

TYPE Original Research
PUBLISHED 23 November 2022
DOI 10.3389/fmed.2022.1058863



OPEN ACCESS

EDITED BY
Antonio Paulo,
Universidade de Lisboa, Portugal

REVIEWED BY
Alice D'Onofrio,
Universidade de Lisboa, Portugal
Yongkang Gai,
Huazhong University of Science and Technology, China
Julie Bolcaen,
iThemba Laboratory, South Africa

*CORRESPONDENCE
Anna Julie Kjøl Tornes
anna.julie.kjol.tornes@rr-research.no

SPECIALTY SECTION
This article was submitted to Nuclear Medicine, a section of the journal Frontiers in Medicine

RECEIVED 30 September 2022
ACCEPTED 04 November 2022
PUBLISHED 23 November 2022

CITATION
Tornes AJK, Stenberg VY, Larsen RH, Bruland ØS, Revheim M-E and Juzeniene A (2022) Targeted alpha therapy with the $^{224}$Ra/$^{212}$Pb-TCMC-TP-3 dual alpha solution in a multicellular tumor spheroid model of osteosarcoma. *Front. Med.* 9:1058863. doi: 10.3389/fmed.2022.1058863



# Targeted alpha therapy with the $^{224}$Ra/$^{212}$Pb-TCMC-TP-3 dual alpha solution in a multicellular tumor spheroid model of osteosarcoma

Anna Julie Kjøl Tornes[1,2,3]*, Vilde Yuli Stenberg[1,2,3], Roy Hartvig Larsen[2], Øyvind Sverre Bruland[3,4], Mona-Elisabeth Revheim[3,5] and Asta Juzeniene[1,6]

[1]Department of Radiation Biology, Institute for Cancer Research, Oslo University Hospital, Oslo, Norway, [2]ArtBio AS, Oslo, Norway, [3]Institute of Clinical Medicine, University of Oslo, Oslo, Norway, [4]Department of Oncology, Oslo University Hospital, Oslo, Norway, [5]Division of Radiology and Nuclear Medicine, Oslo University Hospital, Oslo, Norway, [6]Department of Physics, University of Oslo, Oslo, Norway

Osteosarcoma patients with overt metastases at primary diagnosis have a 5-year survival rate of less than 20%. TP-3 is a murine IgG2b monoclonal antibody with high affinity for an epitope residing on the p80 osteosarcoma cell surface membrane antigen. The tumor-associated antigen p80 is overexpressed in osteosarcomas, and has very low normal tissue expression. We propose a novel dual alpha targeting solution containing two radionuclides from the same decay chain, including the bone-seeking $^{224}$Ra, and cancer cell-surface seeking $^{212}$Pb-TCMC-TP-3 for the treatment of osteoblastic bone cancers, circulating cancer cells and micrometastases. In this *in vitro* study, the cytotoxic effects of $^{212}$Pb-TCMC-TP-3 (single alpha solution) and $^{224}$Ra/$^{212}$Pb-TCMC-TP-3 (dual alpha solution) were investigated in a multicellular spheroid model mimicking micrometastatic disease in osteosarcoma. OHS spheroids with diameters of 253 ± 98 μm treated with 4.5, 2.7, and 3.3 kBq/ml of $^{212}$Pb-TCMC-TP-3 for 1, 4, and 24 h, respectively, were disintegrated within 3 weeks. The $^{212}$Pb-TCMC-TP-3 induced a 7-fold delay in spheroid doubling time compared to a 28-times higher dose with the non-specific $^{212}$Pb-TCMC-rituximab. The $^{224}$Ra/$^{212}$Pb-TCMC-TP-3 completely disintegrated spheroids with diameters of 218–476 μm within 3 and 2 weeks after 4 and 24 h incubation with 5 kBq/ml, respectively. Treatment with 1 kBq/ml of $^{224}$Ra/$^{212}$Pb-TCMC-TP-3 for 24 h caused an 11.4-fold reduction in spheroid viability compared with unconjugated $^{224}$Ra/$^{212}$Pb. The

single and dual alpha solutions with TP-3 showed cytotoxicity in spheroids of clinically relevant size, which warrant further testing of the dual alpha solution using *in vivo* osteosarcoma models.

KEYWORDS

**targeted alpha therapy, osteosarcoma, dual alpha therapy, radium-224, lead-212, TP-3 antibody**

## Introduction

Osteosarcoma (OS) is the second most common bone cancer after chondrosarcoma, and the most common bone malignancy in adolescents and young adults (1, 2). The 5-year survival rate is <20% for patients with metastatic OS at primary diagnosis, and the median survival after multiple recurrences is only 1 year (3–6). Few new treatment options have been developed for metastatic OS during the past three decades, underscoring the need for novel therapies.

Immunotherapy using monoclonal antibodies (mAbs) specific for overexpressed cancer-related antigens is a promising treatment strategy for micrometastases and circulating tumor cells (7–10). Clinical trials have evaluated the efficacy of mAbs in OS, including trastuzumab targeting the human epidermal growth factor receptor 2 (HER2) (11), glembatumumab targeting glycoprotein nonmetastatic B (12), cixutumumab targeting insulin-like growth factor 1 (13, 14), and pembrolizumab, nivolumab and camrelizumab targeting PD-1 (15–19). Unfortunately, sufficient antitumor response was not demonstrated for OS patients receiving these immune-based therapies, possibly due to low expression of the tumor antigens and internal resistance mechanisms (20, 21). The murine IgG2b TP-3 mAb binds to an 80 kDa sarcoma-associated cell surface membrane antigen (p80) on an alkaline phosphatase isoform (22, 23). TP-3 is directly related to osteoblastic differentiation and has previously shown to bind to the vast majority of OS metastases in patients (23, 24). Moreover, an immunomagnetic isolation procedure using the TP-3 mAb detected single OS cells in bone marrow aspirates from OS patients that was shown to have prognostic information (24, 25). Because of the nonreactive activity of TP-3 on healthy human tissues, it is well suited for targeted therapy (22, 23).

Osteosarcoma is clinically regarded as a radioresistant cancer, and external beam radiotherapy is usually not effective for OS (26–29). Unfortunately, the mechanisms of action related to the radioresistance are not well investigated and remain unresolved (30). Targeted therapies using mAbs labeled with the beta emitting $^{188}$Re or $^{177}$Lu, and the alpha emitting $^{211}$At or $^{213}$Bi have been studied for OS *in vitro* and *in vivo* (31–38). However, beta particles have low linear energy transfer (LET, ∼ 0.2 keV/μm), making them less effective for treating radioresistant tumor cells (39). In contrast, alpha particles have a high LET (∼ 100 keV/μm) and short range in tissue (50–100 μm) compared to beta particles (0.5–12 mm), resulting in high cytotoxic potency via DNA double stranded breaks (39). Therefore, alpha particles should be preferred over beta particles to overcome radiation resistance in OS.

The alpha emitting $^{223}$Ra ($t_{1/2}$ ≈ 11.4 d) is a calcium-mimetic radiopharmaceutical with naturally bone-seeking properties (40, 41). Its accumulation in osteoblastic lesions resulted in improved overall survival and approval for the treatment of castration-resistant prostate cancer patients with symptomatic bone metastases (42). Thus, $^{223}$Ra can also be efficient for OS patients due to the osteoblastic phenotype of this cancer (43–46). In 2021, a phase I escalation trial with 50, 75, and 100 kBq/kg of $^{223}$Ra was completed in 18 OS patients with progressive, locally recurrent or metastatic disease (3). The radiopharmaceutical was well tolerated and a recommended phase II dose was set to 100 kBq/kg — a twice as high dose as approved for prostate cancer, due to the high radiation tolerance (3). Unfortunately, the majority of patients developed extra-skeletal metastases (3). Since $^{223}$Ra cannot be stably chelated to a targeting moiety, it must be combined with other agents that can target extra-skeletal disease in these patient groups (45).

Similar to $^{223}$Ra, $^{224}$Ra ($t_{1/2}$ ≈ 3.6 d) has the same bone-seeking properties, four alpha emissions in the decay chain and a relevant half-life for radiopharmaceutical production and shipment (47). An important difference is that $^{224}$Ra decays into $^{212}$Pb ($t_{1/2}$ ≈ 10.6 h), which, compared to $^{211}$Pb ($t_{1/2}$ ≈ 36.1 min) in the $^{223}$Ra-series, has a convenient half-life for conjugation to targeting molecules (47–49). Lead-212 is itself a beta emitter, but serves as an *in vivo* generator of alpha particles via its decay to $^{212}$Bi ($t_{1/2}$ ≈ 60.6 min) and $^{212}$Po ($t_{1/2}$ ≈ 0.3 μs). With the bifunctional 1,4,7,10-tetraaza-1,4,7,10-tetra(2-carbamoylmethyl)cyclododecane (TCMC) chelator for $^{212}$Pb, several radioconjugates have been produced and tested in preclinical and clinical studies (49–61). The dual alpha technology utilizes the osteoblastic stroma-seeking properties of $^{224}$Ra that can treat primary bone cancer or bone metastases, while extra-skeletal and skeletal metastases can be targeted by a cancer specific moiety labeled with $^{212}$Pb (47). In a preclinical prostate cancer study employing this technology, the biodistribution data showed high uptake of $^{224}$Ra in the

femur and skull while a $^{212}$Pb-conjugate had high prostate tumor uptake (62). The technology also showed promising potential in a breast cancer study, where the $^{224}$Ra solution with bone targeting $^{212}$Pb-EDTMP [ethylenediamine tetra (methylenephosphonic acid)] prolonged survival and lowered the incidence of bone metastases in mice (63).

Representative *in vitro* models are essential to mimic tumor micrometastases. Three-dimensional (3D) multicellular spheroids have been utilized in preclinical cancer therapy studies since they exhibit physiologically relevant cell–cell and cell–matrix interactions, heterogeneity and structural complexity which better reflect cancer metastases that are found in patients (64–68). The cell–cell interactions allow contribution by the bystander and cross-fire effects to the cytotoxicity of targeted radionuclide therapy to be considered. Spheroids have a necrotic core surrounded by a viable rim of proliferating cells (69), where steep gradients can exist for cellular oxygen levels, proliferation, pH and glucose concentration (70, 71), leading to development of cell subpopulations that may be resistant to treatment, similar to tumor cells *in vivo* (72). Therefore, spheroids are advantageous *in vitro* models because overcoming these factors could not be considered in 2D monolayer models (66, 70).

In this work, the cytotoxic effect of a single alpha solution comprising $^{212}$Pb conjugated to the OS cell targeting mAb TP-3 and a dual alpha solution containing $^{224}$Ra in equilibrium with $^{212}$Pb-TCMC-TP-3 were evaluated using an *in vitro* 3D multicellular spheroid model.

# Materials and methods

## Cell line

The human OS cell line OHS (established at the Norwegian Radium Hospital) was used in this study (73). The OHS cell line used in the present study was obtained from a repository at the Norwegian Radium Hospital, Oslo University Hospital. The cell line was cultured in RPMI 1640 medium (Sigma-Aldrich Norway AS, Oslo) supplemented with 10% heat inactivated fetal bovine serum (FBS, GE Healthcare Life Sciences, Chicago, IL), 100 units/ml penicillin and 100 μg/ml streptomycin (Sigma-Aldrich) at 37°C with 5% $CO_2$.

## Antibodies

The anti-p80 IgG2b murine mAb TP-3 was produced and purified as described by Bruland et al. (22). TP-3 (PAK-732 batch), was used in all experiments (22, 25). The chimeric anti-CD20 IgG1 mAb rituximab (RTX, MabThera, Roche, Basel) and the humanized anti-HER2 IgG1 mAb trastuzumab (TRA, Herceptin, Roche) were used as antigen negative controls.

## Flow cytometry

The expression of p80 on OHS cells was verified by flow cytometry using TP-3. The primary mAbs (TP-3 or RTX) were added to $5 \times 10^5$ OHS cells in 100 μl flow buffer [Dulbecco's PBS with 0.5% bovine serum albumin (BSA) and 0.1% $NaN_3$] at a concentration of 10 μg/ml and incubated at 4°C with gentle shaking for 60 min, followed by three washes with 2 ml flow buffer. FITC-conjugated anti-mouse IgG F(ab')2 fragment (Thermo Fisher Scientific, Waltham, MA) was used as a secondary Ab and added at a concentration of 10 μg/ml, incubated at 4°C with gentle shaking for 30 min in the dark and washed as in the previous step. All wash steps were performed by centrifugation at $260 \times g$ for 5 min. Washed cell pellets were resuspended in 200 μl flow buffer and analyzed by a Cytoflex S flow cytometer (Beckman Coulter, Inc., Brea, CA) using the CytExpert 2.0 software (Beckman Coulter, Inc.) for data acquisition. The FlowJo software (FlowJo, LLC, Ashland, OR) was used for data analysis.

## Preparation of radionuclides and activity measurements

Radium-224 was extracted from a generator column containing DIPEX® actinidine resin (Eichrom Technologies, Lisle, IL) with immobilized $^{228}$Th (Eckert & Ziegler, Braunschweig) by elution with 1 M HCl. The details of the $^{224}$Ra generator setup have previously been described by Westrøm et al. and Stenberg et al. (62, 74). Lead-212 was produced and extracted from a $^{228}$Th generator, via emanation of $^{220}$Rn in a simplified single-chamber generator system, described by Li et al. (75). Lead-212 was extracted from the flask using 0.1 M HCl, with a $^{228}$Th breakthrough $\leq$0.005%. The collector flask was replaced 2–3 days prior to the experiments to prevent accumulation of $^{208}$Pb. A Capintec CRC-25R radioisotope dose calibrator (Capintec Inc., Ramsey, NJ) was used to quantify the $^{224}$Ra and $^{212}$Pb activities (76).

A Hidex automatic gamma counter (Hidex Oy, Turku) or Cobra gamma counter (Packard Instrument Company, Downer Grove, IL) with the 50–120 keV counting window was used to determine $^{212}$Pb activities. The counting window mainly measures $^{212}$Pb activity (34.9% relative to the $^{224}$Ra mother nuclide) with only small contribution from other radionuclides (1.2% relative to $^{224}$Ra) in the $^{224}$Ra series (47, 62, 74, 77). All samples were measured at least 2 h after $^{212}$Pb extraction to ensure transient equilibrium with daughters. The activity of $^{224}$Ra was determined by measurements performed 4–5 days after the experiment, when $^{212}$Pb had decayed and equilibrium between $^{224}$Ra and the newly formed $^{212}$Pb was reached.

## Radiolabeling of antibodies

The mAbs were conjugated to a TCMC chelator (Macrocyclics Inc., Dallas, TX), to allow radiolabeling with $^{212}$Pb. The original buffer of the mAbs was first exchanged with carbonate buffer (0.1 M $NaHCO_3$ and 5 mM $Na_2CO_3$ in metal free water) by washing the mAb solution through a centrifugal concentrator (30 kDa, Amicon Ultra-15 Centrifugal Filter Unit, Millipore, Sigma-Aldrich) three times at 1620 × *g* for 15–25 min. A TCMC solution in 5 mM HCl was added to the Abs in a 5:1 molar ratio, and the mixture were allowed to react for 2 h with gentle shaking (250 $min^{-1}$) at room temperature. Then, unconjugated TCMC was removed from TCMC-mAb conjugates by exchanging the carbonate buffer to 0.9% NaCl by washing the mAb solution through the centrifugal concentrator as described above. The concentration of the mAbs was quantified by Nanodrop (Nanodrop 1000 Spectrophotometer, V3.8, Thermo Fisher Scientific), using the standard absorbance value of IgG at 280 nm and 10 mm path length.

The mAbs were labeled with $^{212}$Pb using $^{224}$Ra or $^{212}$Pb solutions (pH adjusted to 5–6 by 0.5 M $C_2H_7NO_2$ or $C_2H_3NaO_2$) in equilibrium with daughters. TCMC-TP-3, TCMC-RTX, or TCMC-TRA was added to a final concentration of 0.1–1 mg/ml. The solutions were mixed on a Thermomixer (Eppendorf, Hamburg) for 45 min at 37°C and 450–750 rpm. Radiochemical purity of the samples was determined by instant thin layer chromatography (Tec-control, Biodex, Medical Systems, Shirley, NY), and only products with purities ≥95% were used in the experiments. The final solution consisting of $^{212}$Pb-TCMC-mAb is referred to as the "single alpha solution" while $^{212}$Pb-labeled mAbs in the presence of $^{224}$Ra is called the "dual alpha solution."

## Saturation binding studies

OHS cells were detached from a cell culture flask using TrypLE Express (Sigma-Aldrich). Saturation binding studies of $^{212}$Pb-TCMC-TP-3 to OHS cells were performed by collecting $10^6$ of the cells and incubating them as cell suspension in 0.2 ml of PBS including 0.5% BSA (Sigma-Aldrich) with 6 different concentrations (0.03–10 μg/ml) of the radioimmunoconjugate (in duplicates) for 1 h at 37°C and 150 $min^{-1}$. Non-specific binding was measured by pre-incubating cells with unlabeled TP-3 (5–20 μg/ml) for 15 min before addition of $^{212}$Pb-TCMC-TP-3. Activities were measured in a gamma counter before (added activity) and after incubated cells were washed 3 times with PBS containing 0.5% BSA (cell bound activity). Specific cell bound activity was estimated as percentage of added activity minus non-specific binding (activity on blocked cells). The number of specifically bound ligands per cell was plotted against ligand concentration and the equilibrium dissociation constant ($K_D$) and the number of specific binding sites (Bmax), were determined by nonlinear regression (Sigmaplot version 14.5, Systat Software, Inc., San Jose, CA, USA).

## Spheroid formation and treatment

Multicellular tumor spheroids were generated using the liquid-overlay technique (78, 79). Spheroids were formed by seeding 500 OHS cells in 100 μl of culture medium per well in a 96-well flat-bottom plate coated with 50 μl of 1.5% agarose (weight/volume, Sigma-Aldrich) solution in PBS (Sigma Aldrich). The plates were centrifuged at 470–1000 × *g* for 15 min, and maintained at 37°C with 5% $CO_2$.

For the single alpha solution studies, spheroids were treated 4–5 days after formation (day 0) with 0.3–100 kBq/ml of $^{212}$Pb-TCMC-TP-3 (specific activities of 7.3–15.4 MBq/mg) or $^{212}$Pb-TCMC-RTX (specific activities of 7.5–9.9 MBq/mg). For the dual alpha solution studies, 0.3–10 kBq/ml of $^{224}$Ra/$^{212}$Pb, $^{224}$Ra/$^{212}$Pb-TCMC-TP-3 (specific activities of 2.3–9 MBq/mg), or $^{224}$Ra/$^{212}$Pb-TCMC-RTX/TRA (specific activities of 3.7–9 MBq/mg) were added 3 or 14 days after spheroids were formed. One experiment with TP-3 alone (0.25 μg per spheroid 2.1 μg/ml) was performed in OHS spheroids to investigate the cytotoxicity of the mAb itself. The spheroids were incubated with the mAb alone or with radioconjugates at 37°C for 1, 4, or 24 h before they were carefully washed 6 times with medium and further incubated for 3 weeks. Replacement of culture medium was performed 2–3 times per week. The spheroid diameter (d) was measured weekly using an inverted Axiovert 200M microscope (Carl Zeiss AG, Jena, Germany). Volumes of each spheroid were calculated using the formula $V = \frac{4}{3}\pi r^3$, where $r$ = d/2. The spheroid volumes were normalized by dividing the volumes at different activities by the volume at 0 kBq/ml at each time point (activity vs. normalized volume), and by dividing the volumes of the treated spheroids at each week by the volume of spheroids at day 0 for each activity concentration (time vs. normalized volume).

A CellTiter-Glo®3D cell viability assay (Promega Corporation, Madison, WI, USA), was performed 48 h, 72 h and 12 days after spheroids were administered with $^{224}$Ra/$^{212}$Pb, $^{224}$Ra/$^{212}$Pb-TCMC-TP-3 and $^{224}$Ra/$^{212}$Pb-TCMC-TRA for 24 h according to the manufacture's protocol.

Live and dead cells in the spheroids were determined by a fluorescence-based staining assay using fluorescein diacetate (FDA, 5 mg/ml, Sigma-Aldrich) and propidium iodide (PI, 2 mg/ml, Sigma-Aldrich), respectively. Fluorescent images of spheroids were taken by an inverted Axiovert 200M microscope (Carl Zeiss AG) and analyzed with the AxioVision Rel. 4.8 software (Carl Zeiss AG). The experiment was performed with 3–12 spheroids per treatment condition. The relative viability was calculated by dividing the viability of the treated spheroid by the viability of the control spheroid (0 kBq/ml) at different activity concentrations.

Complete growth inhibition of a spheroid was considered when no live cells were detected in the spheroid, or when the spheroid diameter was reduced or remained unchanged, or when the spheroid was disintegrated/fell apart.

## Statistical analyses

SigmaPlot 14.5 (Systat Software) was used for the statistical analyses. Nonlinear regression with one-site saturation ligand binding was used to estimate the number of specific binding sites ($B_{max}$) and the equilibrium dissociation constant ($K_D$) for $^{212}$Pb-TCMC-TP-3 on the OHS cells:

$$B = \frac{Bmax \times [Ab]}{K_D + [Ab]}$$

where B is the number of antigens per cell and [Ab] is the Ab concentration. Exponential decay fitting was used to plot the correlation between the radioactivity and spheroid volume.

The spheroid volumes and viabilities were analyzed for significance using a one-way ANOVA with multiple comparisons and a pairwise *t*-test, respectively, using SigmaPlot 14.5 (Systat Software). A *p*-value of $< 0.05$ was considered statistically significant.

# Results

## Binding of TP-3

A high expression of p80 was confirmed by a well-defined histogram shape of TP-3, which demonstrated binding to 99.7% of the OHS cells with no overlap and clear separation from the histograms representing the control samples (**Figure 1A**). Negligible non-specific binding was detected ($< 0.06\%$) as the histogram of RTX was identical as the unstained cells and the secondary Ab control.

The OHS cells showed an average of $2.7 \pm 0.3 \times 10^5$ binding sites per cell ($B_{max}$). The $^{212}$Pb-TCMC-TP-3 demonstrated increased binding to OHS cells at 0.03–1 μg/ml after 1 h with a $K_D$ of $0.49 \pm 0.05$ μg/ml (**Figure 1B**). Similar levels of $^{212}$Pb-TCMC-TP-3 were bound to the OHS cells at 4 h (**Supplementary Figure 1**). From 1 to 10 μg/ml, the percentage of specific bound $^{212}$Pb-TCMC-TP-3 was reduced due to saturated binding sites (**Figure 1C**). Of total added radioimmunoconjugate, 5.7–12.2% was internalized to the cells after 1 h (**Supplementary Figure 1**).

## Cytotoxicity of the $^{212}$Pb-TCMC-TP-3 single alpha solution

The spheroids had a diameter of $253 \pm 98$ μm and a volume of $8.5 \pm 0.5 \times 10^6$ μm$^3$ at day 0 (treatment day). The majority of OHS cells in these spheroids were viable at this time point (**Supplementary Figure 6**). The volume of spheroids decreased with increasing $^{212}$Pb-TCMC-TP-3 activity (**Figure 2A** and **Supplementary Figure 2**). At 3 weeks, 1 and 4 h incubation with 2.7–9 kBq/ml of $^{212}$Pb-TCMC-TP-3 significantly inhibited the spheroid growth and reduced the number of live cells compared to the control ($p < 0.005$, **Figures 2B,C**, **Supplementary Figures 3, 4**, and **Supplementary Table 3**). The doubling time was 7-fold longer for the spheroids treated with 2.7 kBq/ml of $^{212}$Pb-TCMC-TP-3 for 4 h compared to the control, while 6.3-fold longer than for the spheroids treated with 75 kBq/ml of $^{212}$Pb-TCMC-RTX (**Supplementary Table 1**). After 3 weeks, no live cells or spheroid growth were detected in the spheroids treated with $\geq$ 2.7 kBq/ml of $^{212}$Pb-TCMC-TP-3 for 4 and 24 h (**Figure 2C** and **Supplementary Figures 4, 5**). The non-specific $^{212}$Pb-TCMC-RTX was only able to completely inhibit spheroid growth after 3 weeks when treated with the high activity dose of 72.8 kBq/ml for 24 h (**Supplementary Figure 5**).

## Cytotoxicity of the $^{224}$Ra/$^{212}$Pb-TCMC-TP-3 dual alpha solution

The cytotoxicity of the dual alpha solutions was investigated in small (diameter of $222 \pm 14.0$ μm and volume of $5.8 \pm 1.0 \times 10^6$ μm$^3$ at day 0) and large (diameter of $474 \pm 2$ μm and volume of $60 \pm 5.0 \times 10^6$ μm$^3$ at day 0) spheroids. The majority of OHS cells in the small spheroids were viable, while the large spheroids developed central necrosis with a 20–30 μm rim of viable cells (**Supplementary Figure 6**). All spheroid volumes were reduced at increasing activities, and the growth of spheroids treated for 4 or 24 h with $\geq$ 5 kBq/ml of $^{224}$Ra/$^{212}$Pb-TCMC-TP-3 was completely inhibited (**Figure 3** and **Supplementary Figure 7**).

Over time, the volume of spheroids treated with 1 kBq/ml of $^{224}$Ra/$^{212}$Pb or $^{224}$Ra/$^{212}$Pb-TCMC-RTX for 4 h increased, whereas this activity concentration of $^{224}$Ra/$^{212}$Pb-TCMC-TP3 inhibited spheroid growth (**Supplementary Figure 7**). The doubling time of spheroids treated with 10 kBq/ml of $^{224}$Ra/$^{212}$Pb-TCMC-TP-3 for 1 h was 101 days, while it was 15 and 22 days for spheroids treated with $^{224}$Ra/$^{212}$Pb and $^{224}$Ra/$^{212}$Pb-TCMC-RTX, respectively (**Supplementary Table 2**).

A viability assay was performed for spheroids treated with the dual alpha solutions for 24 h. At 72 h, a significant reduction in viability was seen in the spheroids treated with 5 kBq/ml of $^{224}$Ra/$^{212}$Pb-TCMC-TP-3 versus $^{224}$Ra/$^{212}$Pb or $^{224}$Ra/$^{212}$Pb-TCMC-TRA ($p < 0.05$, **Supplementary Table 4**). Twelve days after treatment, the relative viabilities of the spheroids treated with 1 kBq/ml of the $^{224}$Ra/$^{212}$Pb-TCMC-TP-3,$^{224}$Ra/$^{212}$Pb and $^{224}$Ra/$^{212}$Pb-TCMC-TRA dual alpha solutions were $11.6 \pm 2.7$, $56.2 \pm 6.6$ and $47.2 \pm 6$, respectively (**Figure 4A**).

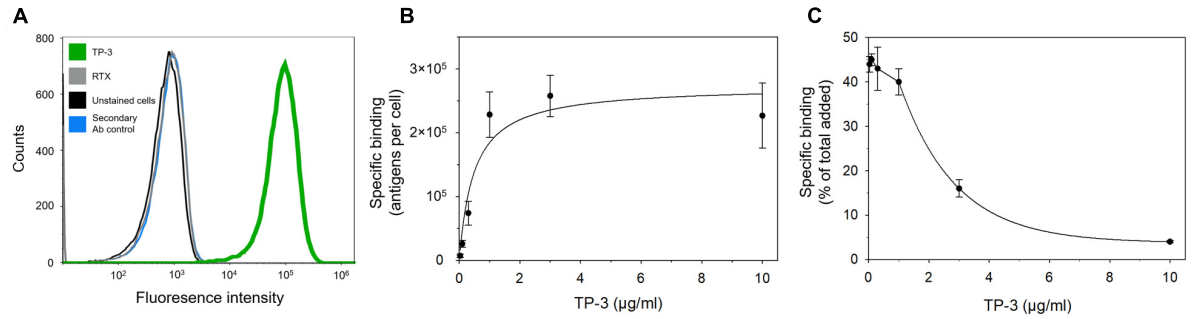


FIGURE 1
p80 expression and specific binding of TP-3 to OHS human osteosarcoma cells. **(A)** A flow cytometry histogram that demonstrates the binding of TP-3 to the p80 antigen (green curve), compared to the non-specific primary antibody rituximab (RTX; gray curve), OHS cells stained only with the secondary antibody (blue curve) or unstained control cells (black curve). **(B)** Specific binding (antigens per cell) and **(C)** percentage specific bound TP-3 (of total added) to OHS cells after 1 h incubation with 0.03–10 µg/ml of $^{212}$Pb-TCMC-TP-3.

Complete disintegration was observed for all spheroids incubated for 24 h with 10 kBq/ml of any dual alpha solution. However, only spheroids treated with the $^{224}$Ra/$^{212}$Pb-TCMC-TP-3 dual alpha solution were disintegrated 12 days after incubation with 5 kBq/ml (**Figure 4B**), while the relative viability of spheroids treated with $^{224}$Ra/$^{212}$Pb and $^{224}$Ra/$^{212}$Pb-TCMC-TRA were 8.0 ± 3.4 and 7.4 ± 2.4 at this time point, respectively.

## Discussion

The treatment options for advanced OS after standard regimen are limited due to chemotherapeutic resistance (80–82). Micrometastases are found in the majority of patients with advanced and/or recurrent OS (25, 83). Patients with micrometastases in the bone marrow or peripheral blood, also from other forms of cancer than OS, have shown statistically poorer survival compared to patients without micrometastases (25, 82, 84–88). The size of spheroids used in the present study was chosen based on a previous study by Däster et al. (89). In agreement with the study, the small spheroids herein consisted almost entirely of viable cells, while the large spheroids had a necrotic core surrounded by a rim of viable cells (**Supplementary Figure 6**). The single and dual alpha solutions containing TP-3 were able to disintegrate spheroids with diameters ranging from 210 to 480 µm, which is similar to the diameter of micrometastatic clusters found in patients (250–750 µm) (65, 90, 91). As already mentioned, TP-3 has previously shown the ability to detect single micrometastatic cells in bone marrow aspirates from OS patients, in which a strong correlation was detected between the TP-3 bound OS cells and poor therapeutic response following relapse (24, 25). In the present study, the TP-3 mAb itself did not initiate any cytotoxicity on OHS multicellular spheroids, which is in agreement with a previous study (33).

In contrast, the cytotoxic effect was significantly improved when spheroids were treated with ≥ 2.7 kBq/ml of the $^{212}$Pb-TCMC-TP-3 radioimmunoconjugate ($p < 0.005$, **Figure 2** and **Supplementary Table 3**). The therapeutic efficacy of $^{211}$At-TP-3 was extensively explored three decades ago and showed promising potential for OS *in vitro* and *in vivo*, similar to a more recent study evaluating a $^{213}$Bi radioimmunoconjugate (33–35, 38, 92). Unfortunately, challenges related to the production of $^{211}$At and the very short half-life of $^{213}$Bi limits the applicability of these radionuclides in targeted therapy. TP-3 immunotoxins have previously showed to be effective in clonogenic OS cells *in vitro*, and in a subcutaneous as well as in a soft-tissue sarcoma model *in vivo* (93–95). SCID mice xenografted with OHS cells were treated with 1.0 mg/kg of a TP-3 immunotoxin and 67 ± 19% of the mice were tumor-free at 150 days, compared to the control mice which had a median survival of 19 days (94). Despite these encouraging data, immunogenicity and nonspecific toxicity is known to limit the clinical success of immunotoxins (96). Nevertheless, TP-3 seems highly promising for targeted therapies because of the high expression levels of p80 on the OS cell surface and the limited normal-tissue distribution (22, 23).

An important advantage with the 3D spheroid model is the possibility to observe the treatment response over an extended period, and thereby observe the repopulation potential of surviving cells. After 1 week, the volume of spheroids treated with 2.7 kBq/ml of $^{212}$Pb-TCMC-TP-3 for 1 h looked similar as spheroids treated with 4.5 and 9 kBq/ml (**Figure 2B**). Yet, regrowth of the spheroids was seen from week 2. After 4 h incubation with 2.7 kBq/ml of the $^{212}$Pb-TCMC-TP-3 single alpha solution, spheroids were disintegrated and no viable cells were observed at week 3 (**Figure 2**). This cytotoxic effect is similar to a study investigating comparable activities of $^{212}$Pb in 3D prostate cancer spheroids (52). A study by

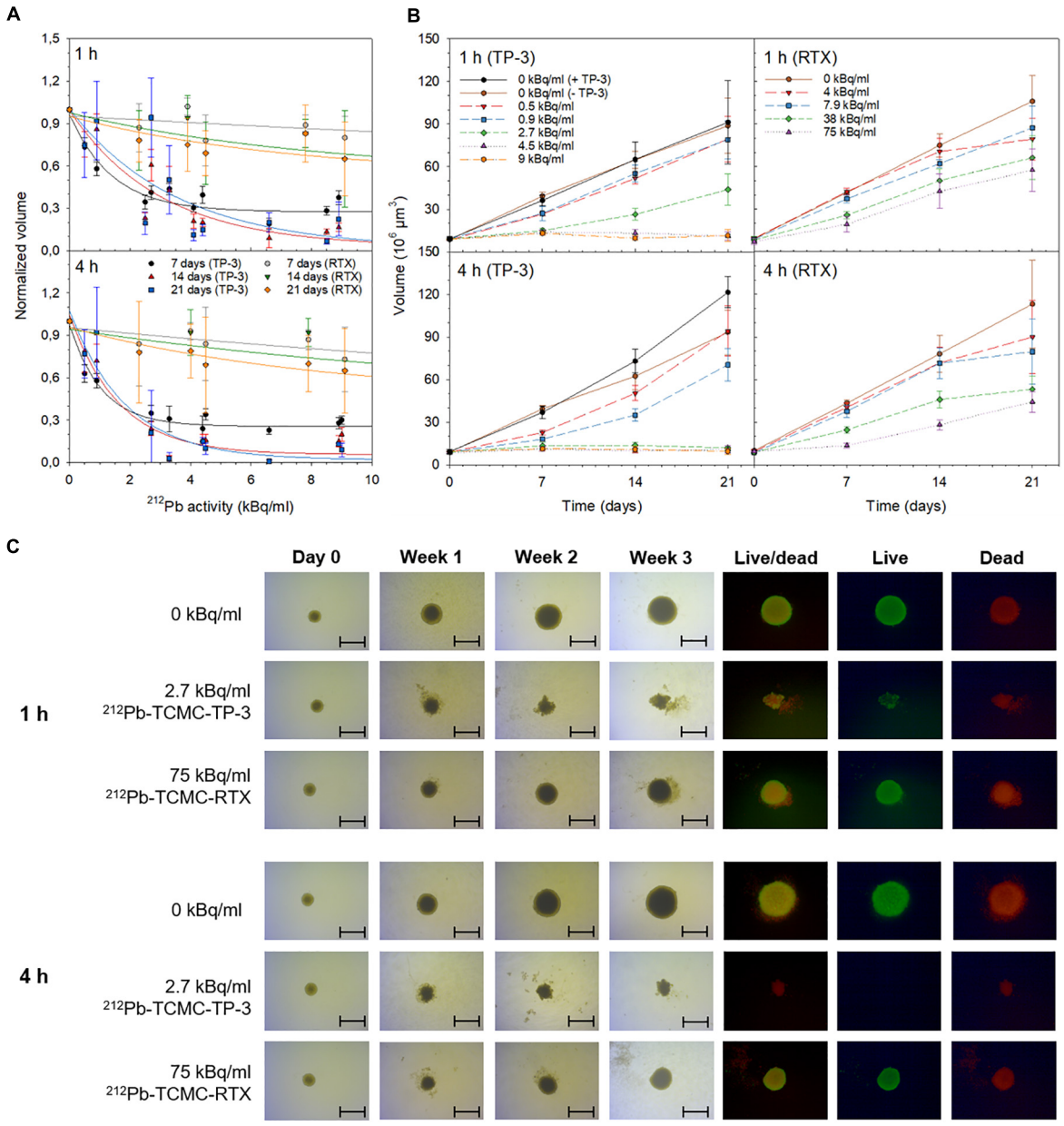


FIGURE 2
Cytotoxicity of single alpha solutions. The influence of $^{212}$Pb-TCMC-TP-3 or $^{212}$Pb-TCMC-rituximab (RTX) on OHS spheroid growth after 1 or 4 h treatment at **(A)** increasing $^{212}$Pb-activities and **(B,C)** over time. The normalized volume was calculated by dividing the volume of the treated spheroid by the volume of untreated spheroids (0 kBq/ml) at each time point. **(C)** Microscope images (4× magnification, scale bar = 500 µm) were taken from the day of treatment (day 0, 8.5 ± 0.5 × $10^6$ µm$^3$) to week 3. At the experimental end point (week 3), spheroids were stained with fluorescein diacetate and propidium iodide to observe live and dead cells, respectively. All spheroid images were taken by an inverted Axiovert 200M microscope (Carl Zeiss AG) and analyzed with the AxioVision Rel. 4.8 software (Carl Zeiss AG). Specific activities were 7.3–15.4 MBq/mg.

Ballangrud et al. investigated the therapeutic effect of a $^{213}$Bi labeled mAb in multicellular prostate cancer spheroids with a diameter of 200 µm, and showed that the penetration time of the radioimmunoconjugate was around 3 h (97). This supports the results observed herein, where a substantial increased cytotoxic effect was seen in spheroids (diameter of 253 ± 98 µm) treated with 2.7 kBq/ml of $^{212}$Pb-TCMC-TP-3 when the treatment duration increased from 1 to 4 h (Figure 2). These results are also in agreement with Hjelstuen et al. who demonstrated that 6 h was required for the $^{125}$I labeled mAb to reach the inner center of an OHS spheroid with a diameter of 400–450 µm (98). Nevertheless, because of the

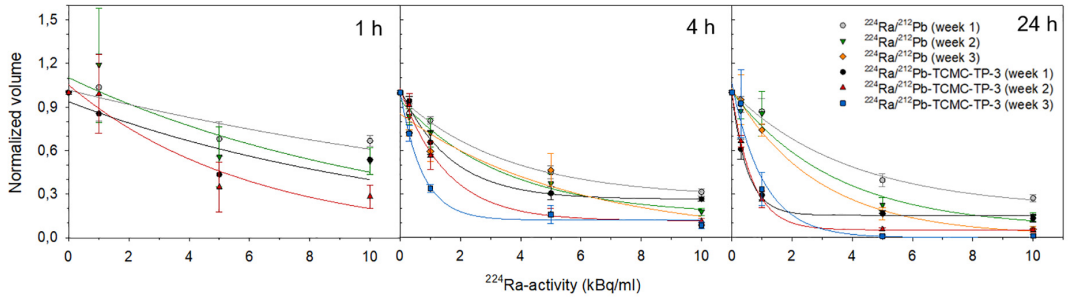


FIGURE 3
Cytotoxicity of dual alpha solutions. The influence of 1, 4, or 24 h incubation of $^{224}$Ra/$^{212}$Pb and $^{224}$Ra/$^{212}$Pb-TCMC-TP-3 on OHS spheroid growth at increasing $^{224}$Ra/$^{212}$Pb-activities. The normalized volume was calculated by dividing the volume of the treated spheroid by the volume of untreated spheroids at each week. Spheroids were 5.8–60 × $10^6$ μm$^3$ at day 0. Specific activities were 2.3–9 MBq/mg.

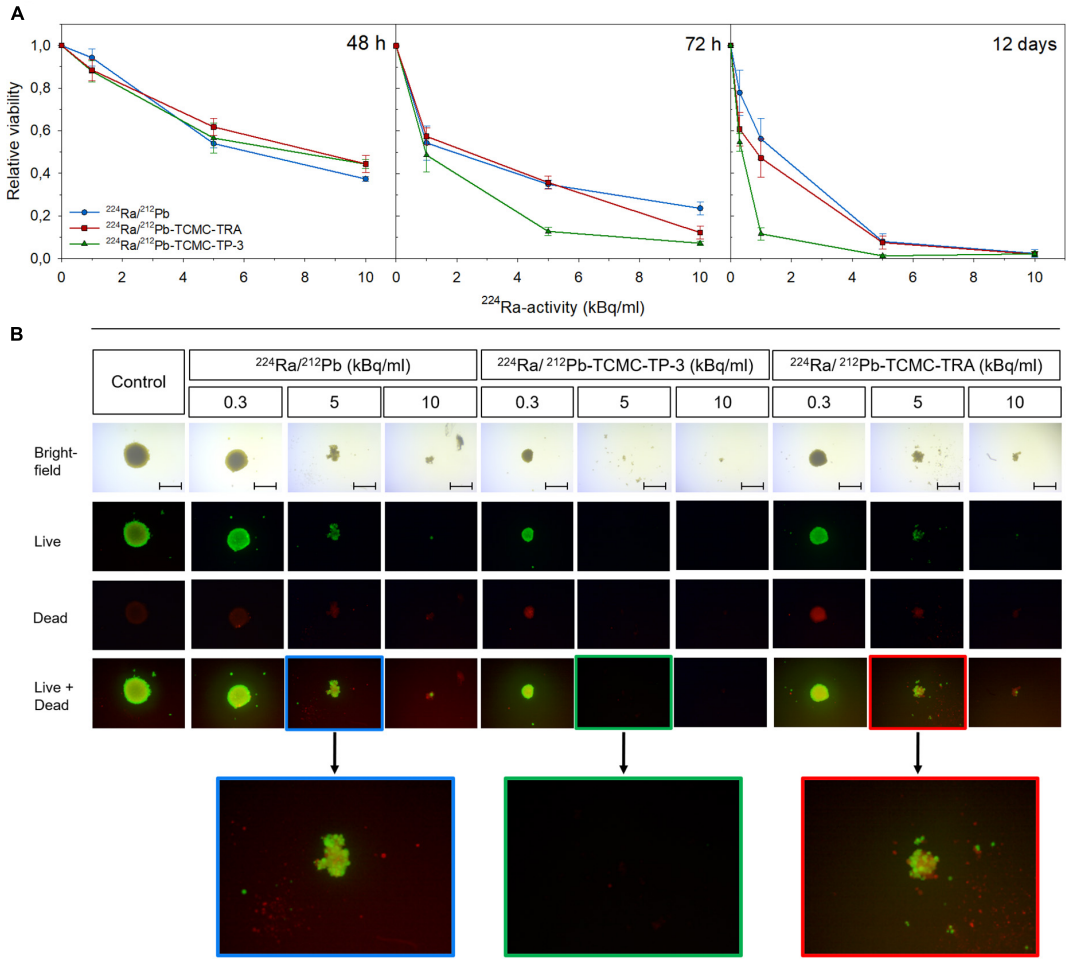


FIGURE 4
Viability of OHS spheroids treated with dual alpha solutions. **(A)** Viability of spheroids 48 h, 72 h, and 12 days after 24 h incubation with 1–10 kBq/ml of $^{224}$Ra/$^{212}$Pb, $^{224}$Ra/$^{212}$Pb-TCMC-TP-3 (specific activity of 2.3 MBq/mg) or $^{224}$Ra/$^{212}$Pb-TCMC-trastuzumab (TRA, specific activity of 3.7 MBq/mg). The relative viability was calculated by dividing the viability of the treated spheroids by the viability of untreated spheroids (0 kBq/ml) at each activity concentration. **(B)** At day 12, spheroids were stained with fluorescein diacetate and propidium iodide to observe live and dead cells, respectively, before spheroids were imaged (4× magnification) using an inverted Axiovert 200M microscope (Carl Zeiss AG, Jena, Germany), scale bar = 500 μm. All spheroids were analyzed with the AxioVision Rel. 4.8 software (Carl Zeiss AG). Spheroids were 60 ± 5.0 × $10^6$ μm$^3$ at day 0.

short half-life of $^{213}$Bi ($t_{1/2} \approx 46$ min), 76% of the decay in Ballangrud's study had already occurred by the time that the radioimmunoconjugate reached the inner core of the spheroid (97). This highlights the benefit of labeling a targeting molecule with $^{212}$Pb, as it has a long enough half-life for the majority of the deposited energy from the total decay to be emitted within the spheroid. However, it is important to mention that the OS tumor microenvironment is highly complex and the penetration time will also depend on other factors such as density and vascularity enabling diffusion of the targeting complex (70).

The growth inhibition of spheroids observed 3 weeks after 4 h treatment with 2.7–4.5 kBq/ml of the $^{212}$Pb-TCMC-TP-3 single alpha solution (**Figure 2** and **Supplementary Figure 4**) and 5 kBq/ml of the $^{224}$Ra/$^{212}$Pb-TCMC-TP-3 dual alpha solution (**Figure 3** and **Supplementary Table 2**) corresponds to 13.5–22.5 MBq of $^{212}$Pb and 25 MBq of $^{224}$Ra per patient ($\sim$ 5 L blood). Subbiah et al. recommended an activity of 100 kBq/kg of $^{223}RaCl_2$ for the phase II study in OS patients (3). Assuming similar clinical dosing of $^{224}$Ra as for $^{223}$Ra (taken the different half-lives into account), this would translate into a clinically relevant dosage of 315 kBq/kg of $^{224}$Ra. In equilibrium with daughters, the $^{212}$Pb-immunoconjugate in the dual alpha solution would then be given in a dosage of approximately 24 MBq per patient ($\sim$ 70 kg). This falls within the activity range of the $^{212}$Pb-TCMC-TRA radioimmunoconjugate (13–47 MBq) that was evaluated as safe for patients with HER2 overexpressing intraperitoneal cancer (55). This suggests that $^{224}$Ra/$^{212}$Pb-TCMC-TP-3 induces cytotoxic effects at clinically relevant activity doses, although activity conversions from mouse to human also may be based on body surface area and not only on radioactivity per gram of bodyweight or blood (99).

Limitations of this study include the use of non-osteoblastic OHS spheroids, leading to an insignificant improvement in cytotoxicity from the naturally bone-seeking $^{224}$Ra itself. Therefore, the dual alpha solution with TP-3 required similar activities to disintegrate spheroids as the single alpha solution, meaning that the antitumor effect of the multicellular spheroids was likely linked to the delivery of the radiation emitted from the specifically bound $^{212}$Pb-TCMC-TP-3. Preincubation of OS cells in a calcifying medium can force the cells into an osteoblastic-like state, which will enhance the similarity of a true OS microenvironment such as observed in patients, and thereby potentially initiate an effect of $^{224}$Ra (100). This should be evaluated in future studies using multicellular spheroid models of OS. Furthermore, following the protocol of Jacques et al., establishing a murine model with bone sarcoma would be the next step to fully explore the potential of the dual alpha *in vivo* (101). Nonetheless, previous dual alpha studies have verified that $^{224}$Ra accumulates in bone (62, 63). In fact, in a preclinical breast cancer study, a $^{224}RaCl_2$ solution with the $^{212}$Pb-daughter chelated to the bone-seeking EDTMP demonstrated similar therapeutic effect as a comparable *in vivo* study with $^{223}RaCl_2$, but with significantly fewer radium atoms (47, 63, 102). A $^{224}$Ra solution without a chelating agent for the lead-daughter, such as for the approved $^{223}RaCl_2$, will also have bone-seeking properties, but since $^{212}$Pb have a half-life that allows trans-organ redistribution if let free in physiological liquids like blood, saliva or lymphatic liquid, the toxicity impact from $^{212}$Pb is important to consider and will be minimized by the conjugation to TP-3 or EDTMP. An experimental limitation in this study includes adding activities from the single and dual alpha solutions to spheroids of different size. Ideally, the single and dual alpha experiments should be performed simultaneously with similar spheroid size at day 0. This should be considered in future studies.

## Conclusion

This study demonstrated high cytotoxicity at clinically relevant activities of the single and dual alpha solutions in spheroids mimicking micrometastatic OS disease. These results warrant further exploration in preclinical models to evaluate the therapeutic efficacy and cytotoxicity of the $^{224}$Ra/$^{212}$Pb-TCMC-TP-3 dual alpha solution in an osteoblastic OS environment.

## Data availability statement

The original contributions presented in this study are included in the article/**Supplementary material**, further inquiries can be directed to the corresponding author.

## Author contributions

AJKT, AJ, ØSB, and RHL: conceptualization. AJKT, AJ, VYS, ØSB, and RHL: designing the work. AJKT and AJ: *in vitro* experiments. AJKT, AJ, and VYS: analyzing the data. AJ, AJKT, VYS, ØSB, M-ER, and RHL: interpretation of results and drafting the manuscript and revising it critically for important intellectual content. All authors read and agreed to the published version of the manuscript.

## Funding

The research was funded by the Norwegian Research Council (Industrial Ph.D. project numbers: 260639 and 329538,

Oslo, Norway) and the South-Eastern Norway Regional Health Authority (project number: 2020028, Oslo, Norway).

## Acknowledgments

We thank Li-Wei Ma at the Department of Radiation Biology, The Norwegian Radiation Hospital, Oslo, Norway for the contribution with the spheroids experiments and Petras Juzenas at the Department of Pathology, and The Norwegian Radiation Hospital, Oslo, Norway for contribution with the flow cytometry experiment and analysis.

## Conflict of interest

Authors ØSB and RHL hold ownership interest in ArtBio AS.

The remaining authors declare that the research was conducted in the absence of any commercial or financial relationships that could be construed as a potential conflict of interest.

## Publisher's note



## Supplementary material

The Supplementary Material for this article can be found online at: https://www.frontiersin.org/articles/10.3389/fmed.2022.1058863/full#supplementary-material

## References

1. Mirabello L, Troisi RJ, Savage SA. Osteosarcoma incidence and survival rates from 1973 to 2004: data from the surveillance, epidemiology, and end results program. *Cancer.* (2009) 115:1531–43.

2. Cole S, Gianferante DM, Zhu B, Mirabello L. Osteosarcoma: a surveillance, epidemiology, and end results program-based analysis from 1975 to 2017. *Cancer.* (2022) 128:2107–18. doi: 10.1002/cncr.34163

3. Subbiah V, Anderson PM, Kairemo K, Hess K, Huh WW, Ravi V, et al. Alpha particle radium 223 dichloride in high-risk osteosarcoma: a phase i dose escalation trial. *Clin Cancer Res.* (2019) 25:3802–10.

4. Berner K, Johannesen TB, Berner A, Haugland HK, Bjerkehagen B, Bøhler PJ, et al. Time-trends on incidence and survival in a nationwide and unselected cohort of patients with skeletal osteosarcoma. *Acta Oncol.* (2015) 54:25–33. doi: 10.3109/0284186X.2014.923934

5. Berner K, Hall KS, Monge OR, Weedon-Fekjær H, Zaikova O, Bruland ØS. Prognostic factors and treatment results of high-grade osteosarcoma in Norway: a scope beyond the "classical" patient. *Sarcoma.* (2015) 2015:516843. doi: 10.1155/2015/516843

6. Anderson P, Aguilera D, Pearson M, Woo S. Outpatient chemotherapy plus radiotherapy in sarcomas: improving cancer control with radiosensitizing agents. *Cancer Control.* (2008) 15:38–46. doi: 10.1177/107327480801500105

7. Zahavi D, Weiner L. Monoclonal antibodies in cancer therapy. *Antibodies.* (2020) 9:34.

8. Jin S, Sun Y, Liang X, Gu X, Ning J, Xu Y, et al. Emerging new therapeutic antibody derivatives for cancer treatment. *Signal Transduct Target Ther.* (2022) 7:39.

9. Oldham RK, Dillman RO. Monoclonal antibodies in cancer therapy: 25 years of progress. *J Clin Oncol.* (2008) 26:1774–7.

10. Pantel K, Alix-Panabières C. Circulating tumour cells in cancer patients: challenges and perspectives. *Trends Mol Med.* (2010) 16:398–406.

11. Ebb D, Meyers P, Grier H, Bernstein M, Gorlick R, Lipshultz SE, et al. Phase II trial of trastuzumab in combination with cytotoxic chemotherapy for treatment of metastatic osteosarcoma with human epidermal growth factor receptor 2 overexpression: a report from the children's oncology group. *J Clin Oncol.* (2012) 30:2545–51. doi: 10.1200/JCO.2011.37.4546

12. Kopp LM, Malempati S, Krailo M, Gao Y, Buxton A, Weigel BJ, et al. Phase II trial of the glycoprotein non-metastatic B-targeted antibody-drug conjugate, glembatumumab vedotin (CDX-011), in recurrent osteosarcoma AOST1521: a report from the Children's oncology group. *Eur J Cancer.* (2019) 121:177–83. doi: 10.1016/j.ejca.2019.08.015

13. Weigel B, Malempati S, Reid JM, Voss SD, Cho SY, Chen HX, et al. Phase 2 trial of cixutumumab in children, adolescents, and young adults with refractory solid tumors: a report from the Children's oncology group. *Pediatr Blood Cancer.* (2014) 61:452–6. doi: 10.1002/pbc.24605

14. Malempati S, Weigel B, Ingle AM, Ahern CH, Carroll JM, Roberts CT, et al. Phase I/II trial and pharmacokinetic study of cixutumumab in pediatric patients with refractory solid tumors and Ewing sarcoma: a report from the Children's oncology group. *J Clin Oncol.* (2012) 30:256–62. doi: 10.1200/JCO.2011.37.4355

15. Le Cesne A, Marec-Berard P, Blay JY, Gaspar N, Bertucci F, Penel N, et al. Programmed cell death 1 (PD-1) targeting in patients with advanced osteosarcomas: results from the PEMBROSARC study. *Eur J Cancer.* (2019) 119:151–7. doi: 10.1016/j.ejca.2019.07.018

16. Tawbi HA, Burgess M, Bolejack V, Van Tine BA, Schuetze SM, Hu J, et al. Pembrolizumab in advanced soft-tissue sarcoma and bone sarcoma (SARC028): a multicentre, two-cohort, single-arm, open-label, phase 2 trial. *Lancet Oncol.* (2017) 18:1493–501. doi: 10.1016/S1470-2045(17)30624-1

17. Boye K, Longhi A, Guren T, Lorenz S, Næss S, Pierini M, et al. Pembrolizumab in advanced osteosarcoma: results of a single-arm, open-label, phase 2 trial. *Cancer Immunol Immunother.* (2021) 70:2617–24. doi: 10.1007/s00262-021-02876-w

18. D'Angelo SP, Mahoney MR, Van Tine BA, Atkins J, Milhem MM, Jahagirdar BN, et al. Nivolumab with or without ipilimumab treatment for metastatic sarcoma (Alliance A091401): two open-label, non-comparative, randomised, phase 2 trials. *Lancet Oncol.* (2018) 19:416–26.

19. Xie L, Xu J, Sun X, Guo W, Gu J, Liu K, et al. Apatinib plus camrelizumab (anti-PD1 therapy, SHR-1210) for advanced osteosarcoma (APFAO) progressing after chemotherapy: a single-arm, open-label, phase 2 trial. *J Immunother Cancer.* (2020) 8:e000798.

20. Wedekind MF, Wagner LM, Cripe TP. Immunotherapy for osteosarcoma: where do we go from here? *Pediatr Blood Cancer.* (2018) 65:e27227. doi: 10.1002/pbc.27227

21. Prudowsky ZD, Yustein JT. Recent insights into therapy resistance in osteosarcoma. *Cancers.* (2020) 13:83.

22. Bruland O, Fodstad O, Funderud S, Pihl A. New monoclonal antibodies specific for human sarcomas. *Int J Cancer.* (1986) 38:27–31.

23. Bruland OS, Fodstad O, Stenwig AE, Pihl A. Expression and characteristics of a novel human osteosarcoma-associated cell surface antigen. *Cancer Res.* (1988) 48:5302–9.

24. Bruland OS, Høifødt H, Saeter G, Smeland S, Fodstad O. Hematogenous micrometastases in osteosarcoma patients. *Clin Cancer Res.* (2005) 11:4666–73.

25. Bruland ØS, Høifødt H, Hall KS, Smeland S, Fodstad Ø. Bone marrow micrometastases studied by an immunomagnetic isolation procedure in extremity localized non-metastatic osteosarcoma patients. *Cancer Treat Res.* (2009) 152:509–15. doi: 10.1007/978-1-4419-0284-9_30

26. Biazzo A, De Paolis M. Multidisciplinary approach to osteosarcoma. *Acta Orthop Belg.* (2016) 82:690–8.

27. Weichselbaum R, Little JB, Nove J. Response of human osteosarcoma in vitro to irradiation: evidence for unusual cellular repair activity. *Int J Radiat Biol Relat Stud Phys Chem Med.* (1977) 31:295–9. doi: 10.1080/09553007714550351

28. Spałek MJ, Poleszczuk J, Czarnecka AM, Dudzisz-Śledź M, Napieralska A, Matysiakiewicz J, et al. Radiotherapy in the management of pediatric and adult osteosarcomas: a multi-institutional cohort analysis. *Cells.* (2021) 10:366. doi: 10.3390/cells10020366

29. Schwarz R, Bruland O, Cassoni A, Schomberg P, Bielack S. The role of radiotherapy in oseosarcoma. *Cancer Treat Res.* (2009) 152:147–64. doi: 10.1007/978-1-4419-0284-9_7

30. Koutsomplia G, Lambrou G. Resistance mechanisms in the radiation therapy of osteosarcoma: a brief review. *J Res Pract Muscoloskeletal Syst.* (2020) 4:15–9.

31. Geller DS, Morris J, Revskaya E, Kahn M, Zhang W, Piperdi S, et al. Targeted therapy of osteosarcoma with radiolabeled monoclonal antibody to an insulin-like growth factor-2 receptor (IGF2R). *Nucl Med Biol.* (2016) 43:812–7. doi: 10.1016/j.nucmedbio.2016.07.008

32. Westrøm S, Bønsdorff TB, Abbas N, Bruland ØS, Jonasdottir TJ, Mælandsmo GM, et al. Evaluation of CD146 as target for radioimmunotherapy against osteosarcoma. *PLoS One.* (2016) 11:e0165382. doi: 10.1371/journal.pone.0165382

33. Larsen RH, Bruland OS, Hoff P, Alstad J, Lindmo T, Rofstad EK. Inactivation of human osteosarcoma cells in vitro by 211At-TP-3 monoclonal antibody: comparison with astatine-211-labeled bovine serum albumin, free astatine-211 and external-beam X rays. *Radiat Res.* (1994) 139:178–84.

34. Larsen RH, Bruland OS, Hoff P, Alstad J, Rofstad EK. Analysis of the therapeutic gain in the treatment of human osteosarcoma microcolonies in vitro with 211At-labelled monoclonal antibody. *Br J Cancer.* (1994) 69:1000–5. doi: 10.1038/bjc.1994.196

35. Larsen RH, Bruland OS. Intratumour injection of immunoglobulins labelled with the alpha-particle emitter 211At: analyses of tumour retention, microdistribution and growth delay. *Br J Cancer.* (1998) 77:1115–22. doi: 10.1038/bjc.1998.185

36. Aurlien E, Larsen RH, Akabani G, Olsen DR, Zalutsky MR, Bruland OS. Exposure of human osteosarcoma and bone marrow cells to tumour-targeted alpha-particles and gamma-irradiation: analysis of cell survival and microdosimetry. *Int J Radiat Biol.* (2000) 76:1129–41. doi: 10.1080/09553000050111604

37. Li HK, Hasegawa S, Nakajima NI, Morokoshi Y, Minegishi K, Nagatsu K. Targeted cancer cell ablation in mice by an α-particle-emitting astatine-211-labeled antibody against major histocompatibility complex class I chain-related protein A and B. *Biochem Biophys Res Commun.* (2018) 506:1078–84. doi: 10.1016/j.bbrc.2018.10.157

38. Karkare S, Allen KJH, Jiao R, Malo ME, Dawicki W, Helal M, et al. Detection and targeting insulin growth factor receptor type 2 (IGF2R) in osteosarcoma PDX in mouse models and in canine osteosarcoma tumors. *Sci Rep.* (2019) 9:11476. doi: 10.1038/s41598-019-47808-y

39. Martins CD, Kramer-Marek G, Oyen WJG. Radioimmunotherapy for delivery of cytotoxic radioisotopes: current status and challenges. *Expert Opin Drug Deliv.* (2018) 15:185–96. doi: 10.1080/17425247.2018.1378180

40. Bruland O, Thora JJ, Darrell FR, Roy LH. Radium-223: from radiochemical development to clinical applications in targeted cancer therapy. *Curr Radiopharm.* (2008) 1:203–8.

41. Bruland ØS, Nilsson S, Fisher DR, Larsen RH. High-linear energy transfer irradiation targeted to skeletal metastases by the alpha-emitter 223Ra: adjuvant or alternative to conventional modalities? *Clin Cancer Res.* (2006) 12(20 Pt 2):6250s–7s.

42. Parker C, Nilsson S, Heinrich D, Helle SI, O'Sullivan JM, Fosså SD, et al. Alpha emitter radium-223 and survival in metastatic prostate cancer. *N Engl J Med.* (2013) 369:213–23.

43. Anderson PM, Subbiah V, Rohren E. Bone-seeking radiopharmaceuticals as targeted agents of osteosarcoma: samarium-153-EDTMP and radium-223. *Adv Exp Med Biol.* (2014) 804:291–304. doi: 10.1007/978-3-319-04843-7_16

44. Anderson PM. Radiopharmaceuticals for Treatment of Osteosarcoma. *Adv Exp Med Biol* (2020) 1257:45–53.

45. Anderson PM, Scott J, Parsai S, Zahler S, Worley S, Shrikanthan S, et al. 223-Radium for metastatic osteosarcoma: combination therapy with other agents and external beam radiotherapy. *ESMO Open.* (2020) 5:e000635. doi: 10.1136/esmoopen-2019-000635

46. Subbiah V, Anderson P, Rohren E. Alpha emitter radium 223 in high-risk osteosarcoma: first clinical evidence of response and blood-brain barrier penetration. *JAMA Oncol.* (2015) 1:253–5. doi: 10.1001/jamaoncol.2014.289

47. Larsen RH, Sciencons AS. *Radiopharmaceutical Solutions with Advantageous Properties*. U.S. Patent No US 9,433,690 B1. (2016). Available online at: https://patents.google.com/patent/US9433690B1/en

48. Nelson BJB, Andersson JD, Wuest F. Targeted alpha therapy: progress in radionuclide production, radiochemistry, and applications. *Pharmaceutics.* (2020) 13:49. doi: 10.3390/pharmaceutics13010049

49. Kokov KV, Egorova BV, German MN, Klabukov ID, Krasheninnikov ME, Larkin-Kondrov AA, et al. (212)Pb: production approaches and targeted therapy applications. *Pharmaceutics.* (2022) 14:189. doi: 10.3390/pharmaceutics14010189

50. Chappell LL, Dadachova E, Milenic DE, Garmestani K, Wu C, Brechbiel MW. Synthesis, characterization, and evaluation of a novel bifunctional chelating agent for the lead isotopes 203Pb and 212Pb. *Nucl Med Biol.* (2000) 27:93–100. doi: 10.1016/s0969-8051(99)00086-4

51. Maaland AF, Saidi A, Torgue J, Heyerdahl H, Stallons TAR, Kolstad A, et al. Targeted alpha therapy for chronic lymphocytic leukaemia and non-Hodgkin's lymphoma with the anti-CD37 radioimmunoconjugate 212Pb-NNV003. *PLoS One.* (2020) 15:e0230526. doi: 10.1371/journal.pone.0230526

52. Stenberg VY, Larsen RH, Ma LW, Peng Q, Juzenas P, Bruland ØS, et al. Evaluation of the PSMA-binding ligand (212)Pb-NG001 in multicellular tumour spheroid and mouse models of prostate cancer. *Int J Mol Sci.* (2021) 22:4815. doi: 10.3390/ijms22094815

53. Stenberg VY, Tornes AJK, Nilsen HR, Revheim ME, Bruland ØS, Larsen RH, et al. Factors influencing the therapeutic efficacy of the PSMA targeting radioligand (212)Pb-NG001. *Cancers.* (2022) 14:2784. doi: 10.3390/cancers14112784

54. Kasten BB, Gangrade A, Kim H, Fan J, Ferrone S, Ferrone CR, et al. (212)Pb-labeled B7-H3-targeting antibody for pancreatic cancer therapy in mouse models. *Nucl Med Biol.* (2018) 58:67–73.

55. Meredith RF, Torgue JJ, Rozgaja TA, Banaga EP, Bunch PW, Alvarez RD, et al. Safety and outcome measures of first-in-human intraperitoneal α radioimmunotherapy with 212Pb-TCMC-trastuzumab. *Am J Clin Oncol.* (2018) 41:716–21. doi: 10.1097/COC.0000000000000353

56. Milenic DE, Baidoo KE, Kim YS, Brechbiel MW. Evaluation of cetuximab as a candidate for targeted α-particle radiation therapy of HER1-positive disseminated intraperitoneal disease. *MAbs.* (2015) 7:255–64. doi: 10.4161/19420862.2014.985160

57. Tan Z, Chen P, Schneider N, Glover S, Cui L, Torgue J, et al. Significant systemic therapeutic effects of high-LET immunoradiation by 212Pb-trastuzumab against prostatic tumors of androgen-independent human prostate cancer in mice. *Int J Oncol.* (2012) 40:1881–8. doi: 10.3892/ijo.2012.1357

58. Dos Santos JC, Schäfer M, Bauder-Wüst U, Lehnert W, Leotta K, Morgenstern A, et al. Development and dosimetry of (203)Pb/(212)Pb-labelled PSMA ligands: bringing "the lead" into PSMA-targeted alpha therapy? *Eur J Nucl Med Mol Imaging.* (2019) 46:1081–91. doi: 10.1007/s00259-018-4220-z

59. Corroyer-Dulmont A, Valable S, Falzone N, Frelin-Labalme AM, Tietz O, Toutain J, et al. VCAM-1 targeted alpha-particle therapy for early brain metastases. *Neuro Oncol.* (2020) 22:357–68.

60. Quelven I, Monteil J, Sage M, Saidi A, Mounier J, Bayout A, et al. (212)Pb α-radioimmunotherapy targeting CD38 in multiple myeloma: a preclinical study. *J Nucl Med.* (2020) 61:1058–65. doi: 10.2967/jnumed.119.239491

61. Banerjee SR, Minn I, Kumar V, Josefsson A, Lisok A, Brummet M, et al. Preclinical evaluation of (203/212)Pb-labeled low-molecular-weight compounds for targeted radiopharmaceutical therapy of prostate cancer. *J Nucl Med.* (2020) 61:80–8. doi: 10.2967/jnumed.119.229393

62. Stenberg VY, Juzeniene A, Bruland ØS, Larsen RH. In situ generated 212Pb-PSMA ligand in a 224Ra-solution for dual targeting of prostate cancer sclerotic stroma and PSMA-positive cells. *Curr Radiopharm.* (2020) 13:130–41. doi: 10.2174/1874471013666200511000532

63. Juzeniene A, Bernoulli J, Suominen M, Halleen J, Larsen RH. Antitumor activity of novel bone-seeking, α-emitting (224)Ra-solution in a breast cancer skeletal metastases model. *Anticancer Res.* (2018) 38:1947–55. doi: 10.21873/anticanres.12432

64. Sutherland RM. Cell and environment interactions in tumor microregions: the multicell spheroid model. *Science.* (1988) 240:177–84.

65. Casey RC, Burleson KM, Skubitz KM, Pambuccian SE, Oegema TR Jr., Ruff LE, et al. Beta 1-integrins regulate the formation and adhesion of ovarian carcinoma multicellular spheroids. *Am J Pathol.* (2001) 159:2071–80. doi: 10.1016/s0002-9440(10)63058-1

66. Nunes AS, Barros AS, Costa EC, Moreira AF, Correia IJ. 3D tumor spheroids as in vitro models to mimic in vivo human solid tumors resistance to therapeutic drugs. *Biotechnol Bioeng.* (2019) 116:206–26.

67. Nath S, Devi GR. Three-dimensional culture systems in cancer research: focus on tumor spheroid model. *Pharmacol Ther.* (2016) 163:94–108.

68. Edmondson R, Broglie JJ, Adcock AF, Yang L. Three-dimensional cell culture systems and their applications in drug discovery and cell-based biosensors. *Assay Drug Dev Technol.* (2014) 12:207–18.

69. Boyd M, Broglie JJ, Adcock AF, Yang L. Radiation quality-dependent bystander effects elicited by targeted radionuclides. *J Pharm Pharmacol.* (2008) 60:951–8. doi: 10.1211/jpp.60.8.0002

70. Chow T, Wutami I, Lucarelli E, Choong PF, Duchi S, Di Bella C. Creating in vitro three-dimensional tumor models: a guide for the biofabrication of a primary osteosarcoma model. *Tissue Eng Part B Rev.* (2021) 27:514–29. doi: 10.1089/ten.TEB.2020.0254

71. Mueller-Klieser W, Freyer JP, Sutherland RM. Influence of glucose and oxygen supply conditions on the oxygenation of multicellular spheroids. *Br J Cancer.* (1986) 53:345–53.

72. Jiang Y, Pjesivac-Grbovic J, Cantrell C, Freyer JP. A multiscale model for avascular tumor growth. *Biophys J.* (2005) 89:3884–94.

73. Fodstad O, Brøgger A, Bruland O, Solheim OP, Nesland JM, Pihl A. Characteristics of a cell line established from a patient with multiple osteosarcoma, appearing 13 years after treatment for bilateral retinoblastoma. *Int J Cancer.* (1986) 38:33–40. doi: 10.1002/ijc.2910380107

74. Westrøm S, Generalov R, Bønsdorff TB, Larsen RH. Preparation of (212)Pb-labeled monoclonal antibody using a novel (224)Ra-based generator solution. *Nucl Med Biol.* (2017) 51:1–9. doi: 10.1016/j.nucmedbio.2017.04.005

75. Li, RG, Stenberg VY, Larsen RH. A novel experimental generator for production of high purity lead-212 for use in radiopharmaceuticals. *J Nucl Med.* (2022):jnumed.122.264009. doi: 10.2967/jnumed.122.264009

76. Napoli E, Stenberg VY, Juzeniene A, Hjellum GE, Bruland ØS, Larsen RH. Calibration of sodium iodide detectors and reentrant ionization chambers for (212)Pb activity in different geometries by HPGe activity determined samples. *Appl Radiat Isot.* (2020) 166:109362. doi: 10.1016/j.apradiso.2020.109362

77. Larsen RH, Sciencons AS. *Production of Highly Purified 212Pb*. Patent WO 2021/110950 A1. (2021). Available online at: https://publications.gc.ca/collections/collection_2022

78. Carlsson J, Yuhas JM. Liquid-overlay culture of cellular spheroids. *Recent Results Cancer Res.* (1984) 95:1–23.

79. Ivascu A, Kubbies M. Rapid generation of single-tumor spheroids for high-throughput cell function and toxicity analysis. *J Biomol Screen.* (2006) 11:922–32. doi: 10.1177/1087057106292763

80. Grignani G, Palmerini E, Ferraresi V, D'Ambrosio L, Bertulli R, Asaftei SD, et al. Sorafenib and everolimus for patients with unresectable high-grade osteosarcoma progressing after standard treatment: a non-randomised phase 2 clinical trial. *Lancet Oncol.* (2015) 16:98–107. doi: 10.1016/S1470-2045(14)71136-2

81. Marchandet L, Lallier M, Charrier C, Baud'huin M, Ory B, Lamoureux F. Mechanisms of resistance to conventional therapies for osteosarcoma. *Cancers.* (2021) 13:683.

82. Bielack S, Jürgens H, Jundt G, Kevric M, Kühne T, Reichardt P, et al. Osteosarcoma: the COSS experience. *Cancer Treat Res.* (2009) 152:289–308.

83. Khanna C, Wan X, Bose S, Cassaday R, Olomu O, Mendoza A, et al. The membrane-cytoskeleton linker ezrin is necessary for osteosarcoma metastasis. *Nat Med.* (2004) 10:182–6.

84. Mansi JL, Gogas H, Bliss JM, Gazet JC, Berger U, Coombes RC. Outcome of primary-breast-cancer patients with micrometastases: a long-term follow-up study. *Lancet.* (1999) 354:197–202.

85. Pantel K, Cote RJ, Fodstad O. Detection and clinical importance of micrometastatic disease. *J Natl Cancer Inst.* (1999) 91:1113–24.

86. Wiedswang G, Borgen E, Kåresen R, Kvalheim G, Nesland JM, Qvist H, et al. Detection of isolated tumor cells in bone marrow is an independent prognostic factor in breast cancer. *J Clin Oncol.* (2003) 21:3469–78.

87. Brunsvig PF, Flatmark K, Aamdal S, Høifødt H, Le H, Jakobsen E, et al. Bone marrow micrometastases in advanced stage non-small cell lung carcinoma patients. *Lung Cancer.* (2008) 61:170–6.

88. Braun S, Vogl FD, Naume B, Janni W, Osborne MP, Coombes RC, et al. A pooled analysis of bone marrow micrometastasis in breast cancer. *N Engl J Med.* (2005) 353:793–802.

89. Däster S, Amatruda N, Calabrese D, Ivanek R, Turrini E, Droeser RA, et al. Induction of hypoxia and necrosis in multicellular tumor spheroids is associated with resistance to chemotherapy treatment. *Oncotarget.* (2017) 8:1725–36.

90. Perche F, Torchilin VP. Cancer cell spheroids as a model to evaluate chemotherapy protocols. *Cancer Biol Ther.* (2012) 13:1205–13. doi: 10.4161/cbt.21353

91. Carretta A. Clinical value of nodal micrometastases in patients with non-small cell lung cancer: time for reconsideration? *J Thorac Dis.* (2016) 8:E1755–8. doi: 10.21037/jtd.2016.12.83

92. Larsen RH, Hoff P, Vergote IB, Bruland OS, Aas M, De Vos L, et al. Alpha-particle radiotherapy with 211At-labeled monodisperse polymer particles, 211At-labeled IgG proteins, and free 211At in a murine intraperitoneal tumor model. *Gynecol Oncol.* (1995) 57:9–15. doi: 10.1006/gyno.1995.1093

93. Anderson PM, Meyers DE, Hasz DE, Covalcuic K, Saltzman D, Khanna C, et al. In vitro and in vivo cytotoxicity of an anti-osteosarcoma immunotoxin containing pokeweed antiviral protein. *Cancer Res.* (1995) 55:1321–7.

94. Ek O, Waurzyniak B, Myers DE, Uckun FM. Antitumor activity of TP3(anti-p80)-pokeweed antiviral protein immunotoxin in hamster cheek pouch and severe combined immunodeficient mouse xenograft models of human osteosarcoma. *Clin Cancer Res.* (1998) 4:1641–7.

95. Onda M, Bruland ØS, Pastan I. TP-3 immunotoxins improve antitumor activity in mice with osteosarcoma. *Clin Orthop Relat Res.* (2005):142–8. [Epub ahead of print].

96. Kim JS, Jun SY, Kim YS. Critical issues in the development of immunotoxins for anticancer therapy. *J Pharm Sci.* (2020) 109:104–15.

97. Ballangrud AM, Yang WH, Charlton DE, McDevitt MR, Hamacher KA, Panageas KS, et al. Response of LNCaP spheroids after treatment with an alpha-particle emitter (213Bi)-labeled anti-prostate-specific membrane antigen antibody (J591). *Cancer Res.* (2001) 61:2008–14.

98. Hjelstuen MH, Rasch-Halvorsen K, Brekken C, Bruland O, de L, Davies C. Penetration and binding of monoclonal antibody in human osteosarcoma multicell spheroids. Comparison of confocal laser scanning microscopy and autoradiography. *Acta Oncol.* (1996) 35:273–9. doi: 10.3109/02841869609101641

99. Nair AB, Jacob S. A simple practice guide for dose conversion between animals and human. *J Basic Clin Pharm.* (2016) 7:27–31. doi: 10.4103/0976-0105.177703

100. Blair HC, Larrouture QC, Li Y, Lin H, Beer-Stoltz D, Liu L, et al. Osteoblast differentiation and bone matrix formation in vivo and in vitro. *Tissue Eng Part B Rev.* (2017) 23:268–80.

101. Jacques C, Renema N, Ory B, Walkley CR, Grigoriadis AE, Heymann D. Murine models of bone sarcomas. *Methods Mol Biol.* (2019) 1914:331–42.

102. Suominen MI, Rissanen JP, Käkönen R, Fagerlund KM, Alhoniemi E, Mumberg D, et al. Survival benefit with radium-223 dichloride in a mouse model of breast cancer bone metastasis. *J Natl Cancer Inst.* (2013) 105:908–16. doi: 10.1093/jnci/djt116

frontiers | Frontiers in Medicine

TYPE Review
PUBLISHED 06 December 2022
DOI 10.3389/fmed.2022.1060922



OPEN ACCESS

EDITED BY
Asta Juzeniene,
Oslo University Hospital, Norway

REVIEWED BY
Ismaheel Lawal,
Emory University, United States
Alfred Morgenstern,
European Commission, Joint Research Centre, Germany
Ashwani Sood,
Post-Graduate Institute of Medical Education and Research, India
Kgomotso Mokoala,
University of Pretoria, South Africa

*CORRESPONDENCE
Oliver Sartor
osartor@tulane.edu

SPECIALTY SECTION
This article was submitted to Nuclear Medicine, a section of the journal Frontiers in Medicine

RECEIVED 03 October 2022
ACCEPTED 17 November 2022
PUBLISHED 06 December 2022

CITATION
Sartor O and Baghian A (2022) Prostate specific membrane antigen binding radiopharmaceuticals: Current data and new concepts. *Front. Med.* 9:1060922. doi: 10.3389/fmed.2022.1060922



# Prostate specific membrane antigen binding radiopharmaceuticals: Current data and new concepts

Oliver Sartor[1,2]* and Ali Baghian[3,4]

[1]Department of Medicine, Tulane University School of Medicine, New Orleans, LA, United States, [2]Department of Urology, Tulane University School of Medicine, New Orleans, LA, United States, [3]Section of Hematology and Medical Oncology, Deming Department of Medicine, Tulane University School of Medicine, New Orleans, LA, United States, [4]Department of Population and Public Health Sciences, University of Southern California, Los Angeles, CA, United States

Prostate specific membrane antigen (PSMA) represents a validated target for prostate cancer therapeutics. The phase III VISION study with $^{177}$lutetium ($^{177}$Lu)-PSMA-617 represented a pivotal step forward and the FDA has now approved this agent in advanced metastatic castrate-resistant prostate cancer (mCRPC). A number of other PSMA targeted radiopharmaceuticals are now under development. Some of these agents are targeted to PSMA via monoclonal antibodies such as J591 and TLX591. Others are targeted to PSMA via small molecules such as PSMA-617, PSMA I&T, MIP-1095, etc. In addition to the use of various ligands, multiple isotopes are now in clinical trials. Beta emitters in development include $^{177}$Lu, $^{131}$iodide ($^{131}$I), and $^{67}$copper ($^{67}$Cu). Targeted alpha emitters potentially include $^{225}$actinium ($^{225}$Ac), $^{227}$thorium ($^{227}$Th), and $^{212}$lead ($^{212}$Pb). Phase III trials are underway with both $^{177}$Lu-PSMA-617 and $^{177}$Lu-PSMA I&T in mCRPC. Single dose phase I trials are complete with $^{225}$Ac-J591 but additional data are need to launch a phase III. Data are promising with $^{225}$Ac-PSMA-617 but concerns remain over salivary and renal toxicity. Tandem therapies are also considered combining both beta and alpha-targeted therapy. Taken together the field of PSMA targeted radiopharmaceuticals is rapidly developing. The targeted alpha therapies are particularly promising and several developmental paths forward are being considered in the near future.

KEYWORDS

**PSMA, prostate cancer, actinium-225, alpha particles, targeted alpha therapy, clinical trials**

## Introduction

Prostate cancer is a common disease with a preponderance of bone metastases when spread is apparent. As such, it has long been targeted with bone-targeted radiopharmaceuticals including the beta-emitters $^{32}$phosphorus, $^{89}$strontium, $^{153}$samarium lexidronam, and the alpha-emitter $^{223}$radium ($^{223}$Ra) (1–4). Palliative effects on bone pain have been documented for each of these isotopes in various studies. $^{223}$Ra, which was the first alpha particle to be FDA approved, after demonstrating overall survival improvements in a randomized phase III study. This finding was catalytic for interest and investment in the broad field of therapeutic radiopharmaceuticals (4).

More recently prostate specific membrane antigen (PSMA) targeted therapies have become more prominent. A small background is justified to cover this space from a conceptual perspective. All the PSMA targeted agents in therapeutic trials to date can be readily classified in terms of small molecules or antibodies. The small molecules typically have four components, a PSMA binding moiety, a linker, a chelator, and an isotope (5–7). All the antibodies in current development are targeted to bind the extracellular domain of PSMA (at a different site than the small molecules). All the antibodies also use a chelator/isotope combination. Despite the fact that chelators and linkers are key components of the targeted therapeutics, the chemistry of those components are not covered in detail here as that is beyond the scope of this manuscript.

The PSMA small molecules typically have a Glu-ureido component that serves as the PSMA binding motif. The linker is a key component that affects tumor targeting, pharmacokinetics, and cellular uptake. Interestingly, various linker/chelator moieties have quite distinct internalization ratios (5–7). Thus the combination of linkers and chelators are critical to the PSMA small molecules and must be carefully considered in design considerations. Historically MIP-1095, PSMA-617, and PSMA I&T are three key small molecules that have been studied more than others (8–10). The most commonly studied antibody has been J591 (11). A structurally modified J591 (TLX592) and another anti-PSMA monoclonal antibody have recently entered the clinic as well (see NCT04726033 and NCT03724747, respectively).

Prostate specific membrane antigen expression is a key determinant of anti-tumor efficacy though debate continues regarding optimal selection of patients (12). PSMA is expressed in the vast majority of prostate cancer patients though heterogeneity clearly exists. Upregulation of PSMA expression in cancers is typical, relative to prostate tissue. In addition to prostate cancer and prostate tissue, PSMA expression is also encountered in neovasculature, proximal renal tubules, central nervous system, salivary tissue, and in the duodenal/jejunal brush border (13–15). Some data suggest that PSMA may be upregulated by hormonal inhibition using agents such as enzalutamide or abiraterone (16, 17). The clinical consequences of this hormonally induced PSMA upregulation are unclear at this time but potential synergy has been suggested between PSMA targeted therapeutics and potent androgen signaling inhibitors.

Prostate specific membrane antigen expression in the tumors can be assessed by PSMA PET imaging which gives quantitative uptake information, especially if software support is used. Much information is now available on PSMA PET and multiple reviews are published (18). The ratio between tumor uptake and benign tissue uptake is critical information that can be assessed and used to predict (to some degree) anti-tumor efficacy. Though heterogeneity is a key hallmark of cancer, and PSMA heterogeneous expression is well documented, the use of radionuclides helps to overcome the problem of heterogeneity by radiating both the cell to which it binds, and also the surrounding tumor microenvironment. One of the more commonly utilized isotopes $^{177}$Lutetium ($^{177}$Lu), has a maximum and mean path length of the beta particle of about 1.7 and 0.23 mm (respectively) in soft tissue (19). Thus, deposition of the isotope on a PSMA expressing tumor cell can be expected to provide radiation to surrounding tissues adjacent to the area of isotopic deposition. Alpha particles have a much shorter range and though estimates vary, typical alpha particles have a path length of less than 100 microns (20). Given the mass of alphas, relative to betas, the linear energy transfer, and the degree of induced DNA damage of alpha particles, far exceed that of the beta particles (21). Regardless, the penumbra of radiation around the site of deposition is a key concept underlying the mechanism of action for this class of therapeutic.

## Phase III trials completed with $^{177}$Lu-PSMA targeted agents

The PSMA targeted beta emitter $^{177}$Lu-PSMA-617 was tested in the PHASE III VISION trial (22). No other phase III trials have been reported to date with PSMA targeted radiopharmaceuticals. The VISION study demonstrated that the PSMA targeted isotopic therapy prolonged survival in heavily pretreated patients with metastatic castrate-resistant prostate cancer (mCRPC) and this agent is now FDA approved for PSMA PET positive men with progressive disease after prior treatments with androgen deprivation therapy (ADT), newer androgen-axis pathway inhibitors (ARPIs, i.e., abiraterone, enzalutamide, darolutamide, and apalutamide) and at least one taxane-based chemotherapy (typically docetaxel).

The phase III VISION trial selected patients by $^{68}$Ga-PSMA PET scan criteria. All patients had to have a PSMA PET positive (uptake > liver parenchyma) metastatic lesion. No tumor lesion (≥1 cm) could be PSMA negative (uptake < liver) in a visceral organ or a lytic bone lesion. No PSMA negative tumor lesion could be ≥2.5 cm in a lymph node. The negative selection criteria are important (23). Data from the VISION trial demonstrated responses as measured by both PSA decreases and

reduction in tumor size. Time to radiographic progression was substantially improved as well. Interested readers are referred to the original VISION manuscript for further reading on this phase III trial (22).

It is important to understand what was not learned in the VISION trial, as well as what was learned. The optimal dose for $^{177}$Lu-PSMA-617 is still not known. There is some belief that dosing remains sub-optimal and formal phase I studies with this agent have never demonstrated a dose limiting toxicity. The optimal selection of patients is still not clear and imaging as a predictive biomarker is far from perfect (24). The role of the standard of care therapies is still not clear, but those that received a combination of ARPIs such as enzalutamide or abiraterone had a somewhat better survival as compared to those that did not (22). There was no retreatment allowed in the VISION study. Once treatment was stopped it could not be restarted for relapse at a later date. No PSMA PET imaging was used in VISION after therapy was started and the relationship between PSMA PET changes after treatment initiation are not ascertained. Clearly there is much more to learn about PSMA targeted $^{177}$Lu therapies.

## Phase III trials underway with $^{177}$Lu-PSMA targeted isotopic therapy

Several immediate strategies are evident for $^{177}$Lu-PSMA-617 and phase III trials are now ongoing with earlier stage prostate cancer patients. In the patient with mCRPC $^{177}$Lu-PSMA-617 is being tested in men with progression post-ARPI without prior taxanes. This trial (PSMAFore) (see NCT04689828) is currently in process and evaluates rPFS as the primary endpoint. For men with metastatic castrate-sensitive prostate cancer (mCSPC), $^{177}$Lu-PSMA-617 is being evaluated in a phase III trial termed PSMAddition (NCT04720157). This trial uses an ADT + ARPI ± $^{177}$Lu-PSMA-617 design and incorporates an rPFS endpoint. Both PSMAfore and PSMAddition utilize the same dose of $^{177}$Lu as that in the VISION trial (7.4 GBq per dose q 6 weeks, up to a maximum of 6 doses).

SPLASH (NCT04647526) sponsored by POINT Biopharma and ECLIPSE (NCT05204927) sponsored by Curium are both phase III trials and both use a design similar to PSMAfore. The patient population is mCRPC patients with progression post-ADT/ARPI. Patients are required to be PSMA PET positive and rPFS is the primary endpoint. Both trials are currently accruing patients. Both the SPLASH and ECLIPSE trials use an alternative PSMA targeting agent, PSMA I&T (also termed $^{177}$Lu-PNT2002 by POINT Biopharma). Dosing in the SPLASH trial is lower than for $^{177}$Lu-PSMA-617. In SPLASH the doses are 6.8 GBq every 8 weeks up to a maximum of 4 doses. For ECLIPSE, the dose of 7.4 GBq is given every 8 weeks for up to 4 doses. $^{177}$Lu-PSMA I&T on a per dose basis, may cause more renal radiation as compared to $^{177}$Lu-PSMA-617 (25).

Given regulatory concerns, renal dose limitations of 23 Gy have generally been used in dose planning for the radiopharmaceuticals, despite the fact that this dose limitation was based on external beam studies and likely is not appropriate to apply to systemic radiopharmaceuticals (26). Regardless, legitimate issues regarding late renal toxicity exist, especially regarding the use of alpha particles. Long term safety issues are a concern for regulators and clinicians alike. Long term survival is more of an issue for earlier stage patients than patients with advanced disease who are progressing after multiple lines of therapy.

## Other prostate specific membrane antigen targeted isotopes: Antibodies, small molecules, and albumin-binders

Isotopes can be targeted to PSMA via small molecules, antibodies, and more. Most of the initial work has focused on PSMA-617 and PSMA I&T but multiple other molecules are under development. Each molecules has potential merits and in the end, only careful clinical trials will distinguish those that are best. Of note, antibodies bind to a distinct aspect of the PSMA molecule as compared to small molecules which target the PSMA "binding pocket." One potential way to mitigate renal issues with small molecules is to use albumin binding as a way to diminish glomerular filtration.

The first PSMA targeting agent using in human trials was MIP-1095 using $^{131}$I as the isotope (27). The initial trials with $^{131}$I-MIP-1095 were clearly positive as measured by PSA declines and even though more trials are in process, the lack of planned phase III trials likely means that MIP-1095 will not move forward as a practice-changing therapy.

An antibody to PSMA (J591) which has been studied extensively in men with mCRPC using both beta and alpha emitters. Phase II studies with $^{177}$Lu-J591 indicate that the antibody is associated with some provocative long term survival data (28) but these data were older and collected in an era without many of the effective therapies commonly utilized today. Data with $^{177}$Lu-J591 indicate that this agent has significant marrow suppression especially thrombocytopenia (28). The PSA response rate with $^{177}$Lu-J591 is relatively low compared to small molecules and the data on radiographic responses/progression are quite limited. Though overall survival (OS) is the gold standard for activity of an agent, the relatively sparse un-randomized data sets currently available make conclusions about the activity of this agent somewhat problematic. A phase III study (PROSTACT) of $^{177}$Lu-J591 is planned in the mCRPC space post-ARPI but this trial has yet to start accrual (NCT04876651).

Various PSMA targeting agents are under investigation and these are summarized in **Table 1**. A PSMA antibody is in phase I trials with Bayer using $^{227}$Th as an isotope (NCT03724747). $^{227}$Th has half-life of 18.7 days and decays to $^{223}$Ra which in turn has a half-life of 11.4 days. It is unlikely that cellular retention will last as long as the half-lives of $^{227}$Th and the daughters. No data are yet reported on NCT03724747 but the trial is no longer accruing patients. Additional PSMA targeting antibodies (TLX592) are in development. TLX592 is a modified J591 with more rapid blood clearance as compared to J591. It is anticipated this TLX592 will be developed with $^{225}$Ac. Current studies with TLX592 are examining $^{64}$Cu based imaging (NCT04726033) to better understand the distribution and binding of this antibody. Future studies with alpha-emitters are planned with TLX592. Once imaging studies are done, the antibody-isotope conjugate can be readily adapted for therapy.

Small molecules in development include a $^{67}$Cu-PSMA binding agent by Clarity Pharmaceuticals. This agent is being developed as a theranostics pair with $^{64}$Cu as a PET imaging agent (NCT04868604). Nucligen, a small Norwegian company, is developing a $^{212}$Pb-PSMA binding molecule NG001. The NG001 strategy may involve a dual approach using both $^{224}$Ra and $^{212}$Pb (29). $^{224}$Ra will target bone similar to $^{223}$Ra. Human trials are yet to be announced. The PSMA binding small molecule "R2" has been in phase I trials using $^{177}$Lu as an isotope but accrual was terminated (NCT03490838). No results have been reported. PSMA targeting compounds binding $^{211}$At are described (30) but are yet to be used in the clinic.

Noria developed a small molecule that binds albumin as well as PSMA and this molecule, or a similar one, will likely be developed by Bayer (31). Other albumin binding PSMA targeted molecule are in development, some including ibuprofen conjugated linkers (32). Albumin binding molecules such as Evans Blue modified PSMA-617 (EB-PSMA-617) are also under development (33) and slated for additional human clinical trials (NCT04996602). Albumin binding may or may not be effective in diminishing salivary and renal uptake but some data indicate that tumor retention can be improved relative to renal/salivary uptake (31, 34). The key elements will be the ratio of binding to target and non-target tissues, the degree of isotopic retention in the tumor, and the salivary/renal dosimetry. Human therapeutic data are not yet reported for these agents.

## Prostate specific membrane antigen targeted alpha particles in current clinical trials: Monoclonals, small molecules, and multiple isotopes

The phase III ALSYMPCA trial demonstrated an OS benefit with $^{223}$Ra in bone predominate mCRPC (4) but there is only one published prospective phase I alpha emitter trial using PSMA targeting. There is no need to cover $^{223}$Ra here given multiple reviews have been done, but the promise of targeted alpha therapy in prostate cancer is large and deserves mention.

The PSMA targeted monoclonal antibody J591 conjugated to $^{225}$Ac ($^{225}$Ac-J591) has been tested in a small phase I single dose escalation trial (NCT03276572) with no PSMA PET selection criteria (35). No dose limiting toxicities (DLTs) were observed in this trial. The maximum dose tested was 93 kBq/kg as a single dose. Patients as a whole were heavily pretreated, including pretreatments with $^{177}$Lu-PSMA for a number of patients. Thrombocytopenia and nausea was somewhat problematic and some patients had excessive fatigue but as stated, no DLTs were observed. PSA declines were seen in the majority of patients. Followup was short and incomplete. Radiographic progression-free survival was not reported. Future studies are planned using more than one dose of $^{225}$Ac-J591 (NCT04506567). Clearly more work is needed before a phase III can be launched. A Phase I/II Trial of pembrolizumab and androgen-receptor pathway inhibitor with or without $^{225}$Ac-J591 is planned in mCRPC (NCT04946370). Additional phase I/II trials are planned with $^{225}$Ac-J591 + $^{177}$Lu-PSMA I&T (NCT04886986).

$^{227}$Th-PSMA TTC monoclonal antibodies are also in formal phase I trials now (NCT03724747) but the trial is no longer accruing. As noted, the half-life of $^{227}$Th (an alpha emitter) is likely too long for optimal dose delivery. $^{225}$Ac-PSMA-617 is now in a formal phase I trial in South Africa and Australia (NCT04597411). Phase I trials are eventually planned with $^{225}$Ac-TLX592 and others. Clearly the activity of targeted alphas are noteworthy. Optimal dose and schedules are not yet established.

No formal phase I study has been reported for small molecules such as PSMA-617 or PSMA I&T with an alpha emitting payload. In an important study from Heidelberg with PSMA-617 reporting on 14 total patients looking at dose escalation (36), salivary gland toxicity (xerostomia) was reported as being dose limiting however only 2 patients reported a grade 2 xerostomia. Doses above 100 kBq/kg were deemed unfeasible though a formal phase I assessment was not reported. Extreme dry eyes were also reported in a single patient treated at 200 kBq/kg. Myelosuppression and renal toxicity were not problematic in the short term but there are potential concerns in longer term followup. This experience from Heidelberg with $^{225}$Ac-PSMA-617 suggested that 100 kBq/kg every 8 weeks was a tolerable and effective dose with 2–4 doses being typically administered (36). There was no dose response noted in the small group of patients being treated with 100–200 kBq/kg. Some have endorsed the concept of decreasing the targeted alpha dose over time given the tumor/normal tissue ratio decreases with lower tumor burden.

Dose limiting toxicity can be controversial and assessed in different ways by different investigators. The definitions

TABLE 1 Synopsis of prostate specific membrane antigen (PSMA) targeted molecules in current development or consideration.

| | Sponsor | Beta | Alpha | Prospective data published | Beta trial | Alpha trial | NCT number |
|---|---|---|---|---|---|---|---|
| **Monoclonal antibodies** | | | | | | | |
| J591 | Cornell | $^{177}$Lu | | I/II | | | Multiple |
| J591 | Cornell | | $^{225}$Ac | I | | | NCT03276572 |
| TLX591 | Telix | $^{177}$Lu | | | I | | NCT04786847 |
| PSMA TTC | Bayer | | $^{227}$Th | | | I | NCT03724747 |
| **Small molecules** | | | | | | | |
| MIP-1095 | Lantheus | $^{131}$I | | | II | | NCT03939689 |
| PSMA I&T | POINT | $^{177}$Lu | | | III | | NCT04647526 |
| PSMA I&T | Curium | $^{177}$Lu | | | III | | NCT05204927 |
| PSMA-617 | Novartis | $^{177}$Lu | | II/III | III | | Multiple |
| PSMA-R2 | Novartis | $^{177}$Lu | | | I | | NCT03490838 |
| SAR-bis-PSMA | Clarity | $^{67}$Cu | | | I | | NCT0486860 |
| EB-PSMA-617 | Peking Union | $^{177}$Lu | | I | | | NCT03403595 |
| NG-001 | Nucligen | | $^{212}$Pb | | | | Planned |
| PNT-2001 | Point | | $^{225}$Ac | | | | Planned |
| PSMA-617 | Novartis | | $^{225}$Ac | | | I | NCT04597411 |
| PSMA I&T | Excel diagnostics | | $^{225}$Ac | | | I | NCT05219500 |

of intolerable treatment also depend to some extent on the underlying disease being treated and the physician's experience at handling toxic therapies. Asymptomatic men with good prognosis are quite distinct from symptomatic men near death from an aggressive underlying cancer and what is tolerable in one setting may be deemed intolerable in another. Xerostomia, dry eyes, nausea, and fatigue are areas where considerable variation in tolerability may be encountered from patient to patient and what is tolerable for one may not be tolerable for another. Salivary gland toxicity resulting in xerostomia is an area of special concern with small molecule PSMA-binders (see below).

Dosimetry with alphas studies are problematic. There are multiple assumptions regarding the relative biologic efficacy, issues related to microdosimetry, flow rates in tubular spaces, the exact range of the emitted alpha, and the potential diffusion of daughters. Recoil from alpha emissions renders $^{225}$Ac daughters free from the chelate and these "free" isotopes may cause additional off-target damage in the patient. In the $^{225}$Ac studies there is additional uncertainty regarding dosimetry because an unknown percentage of $^{213}$Bi (half-life 45.59 mins) likely leaves the targeted cell by diffusion and the ultimate whereabouts of this radionuclide is potentially problematic. Renal toxicity with $^{213}$Bi is a theoretical possibility (37). Tracing certain isotopic daughters is feasible using selective assessments of specific energies for photon emissions and novel strategies are evolving in the field of alpha dosimetry (38–40).

Three meta-analyses have been reported using $^{225}$Ac-PSMA-617 (41–43) and recent reviews with $^{225}$Ac-PSMA-617 have been presented as well (44). Thus, an exhaustive review of the literature is not warranted here. Suffice it to say that the PSMA targeted alpha therapy data to date are impressive with regard to PSA declines in heavily pre-treated patients including those pre-treated with $^{177}$Lu-PSMA targeted therapies. The durability of these responses are not yet clear.

$^{225}$Ac-PSMA-617 has been used both in monotherapy and in tandem therapy with $^{177}$Lu-PSMA-617. For monotherapy in mCRPC chemotherapy naïve patients, individual doses were reported in the 8 MBq range in South Africa, followed by escalation or de-escalation depending on response to therapy (45). In a large German monotherapy $^{225}$Ac-PSMA-617 study from Heidelberg, the doses were initially 100 kBq/kg (46). In the monotherapy series from India, men were treated with $^{225}$Ac-PSMA-617 (100 kBq/kg) at 8 week intervals (47, 48). Four of the larger reported experiences are described in **Table 2**. Cohorts from all four trials exhibited widespread disease on PSMA imaging with median PSA ranging from 57 to 222 ng/ml. The majority of subjects in one of the series from India (47) were ECOG performance status 3 thus these results are not broadly representative of what might be expected in future prospective trials. The majority of patients in the South African series (45) were not pretreated with abiraterone/enzalutamide/taxanes. Results from the South African series are impressive but these data clearly represent patients with a better prognosis. Many of the patients in these four trials had previously been treated with radiopharmaceuticals including $^{177}$Lu-PSMA-617 as shown in **Table 2**.

There is additional experience with $^{225}$Ac-PSMA I&T from retrospective German series. One experience with PSMA I&T used 6.0−8.5 MBq $^{225}$Ac-PSMA I&T in 14 patients for 1-5 cycles every (q) 8 weeks in mCRPC patients (mostly pretreated with $^{177}$Lu-PSMA targeting agents) (49). Half the patients had a PSA

TABLE 2 Synopsis of selected experiences with 225Ac-PSMA-617 treated prostate cancer patients.

| | | | Percentage of patients pre-treated | | | | | | |
|---|---|---|---|---|---|---|---|---|---|
| $^{225}$Ac-PSMA-617 study | Number of patients | $^{225}$Ac dose | Novel hormones (Abi/Enza)% | Docetaxel/ Cabazitaxel % | $^{177}$Lu-PSMA-617/$^{223}$Ra % | Median PSA at time of trial entry | ECOG > 2 (%) | PSA > 50% decline | Median OS months |
| Sathekge et al. (45) | 73 | 8 MBq every 8 weeks† | 2/0 | 51/0 | 14/0 | 57 | 2 | 70% (51/73) | 18 |
| Kratochwil et al. (46) | 40 | 100 kBq/kg every 8 weeks | 85/60 | 70/17.5 | 0/22.5 | 169 | 20 | 60% (24/38) | > 12 |
| Sen et al. (48) | 38 | 100 kBq/kg every 8 weeks | 63/34 | 100/11 | 24/5 | 147 | 0 | 66% (25/38) | 12 |
| Yadav et al. (47) | 28 | 100 kBq/kg every 8 weeks | 79/36 | 79/4 | 54/0 | 222 | 72 | 39% (11/28) | 17 |

†Subjects were treated with 8 MBq then 7, 6, or 4 Mbq very 8 weeks on basis of response to treatment.
Abi, abiraterone; ECOG, Eastern Cooperative Oncology Group; Enza, enzalutamide; PSA, prostate specific antigen; OS, overall survival.

decline ≥50%, 5/11 of the patients pretreated with $^{177}$Lu-PSMA had a PSA decline of ≥50%. New onset grade I/II xerostomia was noted in 5/14 and this concern is addressed below in more detail A phase II with $^{225}$Ac-PSMA I&T q 8 weeks is now underway (NCT05219500) using 100 kBq/kg for dose 1, followed by dose de-escalation in responding patients (using investigator discretion). A phase I using $^{177}$Lu-PSMA I&T in combination with $^{225}$Ac-J591 is also planned (NCT 04886986). A single case report has been reported with treatment consisting of two cycles of $^{213}$Bi-PSMA-617 with a cumulative activity of 592 MBq (50).

Though formal phase 1 studies are not performed, several investigative groups are planning to perform initial studies using $^{212}$Pb-based PSMA ligands. The shorter half-life and single alpha emission is of interest.

## Late renal toxicity concerns and salivary concerns: Areas of special interest

Xerostomia from salivary toxicity and bone marrow suppression are issues that have received considerable attention but the issue of late renal toxicity is a potential special concern following targeted alpha therapy. Data from neuroendocrine tumors indicate that late renal toxicity following treatment with $^{225}$Ac-labeled small molecules (DOTATOC) can be a problematic issue for some patients (51). The renal toxicity rarely manifested in less than a year and could be delayed 2−4 years. This cautionary note is worthwhile to consider and the short term issue surrounding alpha success needs to be tempered with a concern over late effects that may be deleterious. Those with a short term poor prognosis and those with longer life expectancies are distinct and clearly the risk of the underlying uncurable disease typically outweighs longer term concerns. For those with better prognosis, the concerns related to renal toxicity may be magnified.

Several strategies might be considered to overcome renal toxicity issues and salivary toxicity issues (52). Such issues include the use of larger molecules (such as antibodies) which do not reach the renal tubule or penetrate the salivary gland. In general the glomerulus filters molecules below the 30−50 kilodalton range. Interestingly the salivary binding seen with small PSMA binding molecules is not seen with antibodies. Thus, intact antibodies would not be expected to enter the renal tubule via the glomerulus or the salivary glands. Albumin-binding PSMA targeted molecules are postulated to have diminished renal excretion and less salivary uptake and several are in development as noted above. Renal dosimetry considerations are of significant concern to regulatory bodies such as the FDA. Salivary concerns have been raised by investigators and patients alike.

A potential issue with $^{225}$Ac is that multiple daughters are anticipated after the initial decay and some of these daughters, especially $^{213}$Bi have the potential to be excreted via the kidney. Isotopes with a single alpha emission would be expected to deliver radiation more specifically to the tumor. Thus isotopes such as $^{212}$Pb, $^{149}$Tb, or $^{211}$At might be considered "more targeted" than isotopes with multiple alpha emitting daughters (like $^{225}$Ac).

Several small molecular moieties have been postulated to be capable of selectively providing shielding isotopic damage. For instance a series of "Tris-POC" molecules have been shown to be capable of diminishing renal and salivary uptake of $^{177}$Lu-PSMA without altering tumor uptake (53). Other shielding agents are also in development. Mitigating concern about salivary and renal toxicities are of special interest in the clinical development of PSMA targeted alpha therapy.

Longer term issues with secondary cancers are also a concern in those with longer life expectancies. Radiation is a known carcinogen and the effects of radiation on subsequent cancer development is well-demonstrated from many angles. In the end there may be informed consents and accepted trade-offs in risk when it comes to treating cancer patients with agents known to harbor a carcinogenic risk. That said, many of the chemotherapies commonly used in oncology have similar risks and those therapies are part of the accepted armamentarium.

## Combination therapies with alphas and betas

Tandem data using combinations of alpha and beta emitters have been reported from a number of sites in retrospective studies. Given concerns with rate-limiting xerostomia and late renal toxicities especially with small molecules, $^{225}$Ac-PSMA agents at reduced doses could be of interest. Patients resistant to $^{177}$Lu-PSMA 617 have been treated with a tandem approach with provocative results. Several studies have been reported and a complete review is not warranted herein. As an example, in a study of 20 patients 6.9 GBq of $^{177}$LuPSMA-617 and 5.3 MBq of $^{225}$Ac-PSMA-617 were tested in the initial treatment cycle (54). A total of 65% of patients had PSA decline >50%. Xerostomia was reported as being more tolerable than the use of $^{225}$Ac-PSMA-617 alone (given the lower dose of the alpha emitter).

Preclinical data indicate that monoclonal (J591) PSMA binding may result in more sustained uptake of radiolabeled PSMA small molecules ($^{177}$Lu-PSMA-617), and more cell kill (55). If true in the clinic, this would provide a strong rationale for combining a monoclonal with a radiolabeled therapeutic PSMA small molecule. The monoclonal antibody J591 chelated to $^{225}$Ac ($^{225}$Ac-J591) will soon be being tested in tandem therapy with $^{177}$Lu-PSMA-I&T (NCT04886986).

## Developmental strategies for targeted alpha therapy

Prostate specific membrane antigen targeted alpha therapy appears quite active in every prostate cancer setting tested thus far. Debate ensues over the best patient to be treated, best inclusion/exclusion selection criteria, best molecule, best dose, best isotope, and best schedule. These debates are inevitable in the context of multiple small non-comparative studies, especially when financial conflicts of interest may be present. What is clear is that this class of agent needs to be properly tested in prospective trials with a regulatory focus. Selection of patients is key.

Should targeted alphas go after beta failure, or before betas, or in combination with betas? All studies are of interest but the path to regulatory approval might be fastest in the post-$^{177}$Lu-PSMA space. What is the control group for a randomized trial? A "standard of care" control arm is typical and understanding the ethics and acceptability of the control group is a key consideration. Can the control group be an FDA approved beta emitter? That is reasonable given the degree of efficacy with alpha emitters noted in early trials. Inclusion and exclusion criteria can be debated, as can endpoints. Crossover designs are also important to consider. Though tumor shrinkage has been accepted as an endpoint in trials for accelerated approval, typical therapeutic trials in advanced prostate cancer have depended on overall survival in a controlled trial. Radiographic progression free survival using strict criteria proposed by the prostate cancer working group 3 is acceptable to the FDA (56). In addition, objective radiographic responses are of significant interest to the FDA. Definitions of radiographic progression free survival depends on traditional scans including bone scans and CT/MRI scans. PSMA-PET based endpoints and PSA declines are not acceptable at this time. Without regulatory approvals targeted alpha therapy will never reach the populations in need.

## Author contributions

OS reviewed extensively the literature and wrote the manuscript. AB involved with drafting and tables preparation for the manuscript. Both authors read and approved the final manuscript.

## Acknowledgments

We would like to thank Oyvind Bruland, Roy Larsen, Bill Goeckeler, and John Babich for their counsel, friendship, and inspiration.

## Conflict of interest

OS received consulting fees from the Advanced Accelerator Applications, Astellas, AstraZeneca, Bayer, Blue Earth Diagnostics, Inc., Bavarian Nordic, Bristol Myers Squibb, Clarity Pharmaceuticals, Clovis, Constellation, Dendreon, EMD Serono, Fusion, Isotopen Technologien München, Janssen, Merck, Myovant, Myriad, Noria Therapeutics, Inc., Novartis, Noxopharm, Progenics, POINT Biopharma, Pfizer, Sanofi, Tenebio, Telix, and Theragnostics and also received grants/contracts to his institution from the Advanced Accelerator Applications, Amgen, AstraZeneca, Bayer, Endocyte, Invitae, Janssen, Lantheus, Merck, Progenics, and Tenebio.

The remaining author declares that the research was conducted in the absence of any commercial or financial relationships that could be construed as a potential conflict of interest.

## Publisher's note

All claims expressed in this article are solely those of the authors and do not necessarily represent those of their affiliated organizations, or those of the publisher, the editors and the reviewers. Any product that may be evaluated in this article, or claim that may be made by its manufacturer, is not guaranteed or endorsed by the publisher.

## References


1. Glaser MG, Howard N, Waterfall N. Carcinoma of the prostate: the treatment of bone metastases by radiophosphorus. *Clin Radiol.* (1981) 32:695–7. doi: 10.1016/S0009-9260(81)80342-X

2. Porter AT, McEwan AJ, Powe JE, Reid R, McGowan DG, Lukka H, et al. Results of a randomized phase-III trial to evaluate the efficacy of strontium-89 adjuvant to local field external beam irradiation in the management of endocrine resistant metastatic prostate cancer. *Int J Radiat Oncol Biol Phys.* (1993) 25:805–13. doi: 10.1016/0360-3016(93)90309-J

3. Sartor O, Reid RH, Hoskin PJ, Quick DP, Ell PJ, Coleman RE, et al. Samarium-153-Lexidronam complex for treatment of painful bone metastases in hormone-refractory prostate cancer. *Urology.* (2004) 63:940–5. doi: 10.1016/j.urology.2004.01.034

4. Parker C, Nilsson S, Heinrich D, Helle SI, O'Sullivan JM, Fosså SD, et al. Alpha emitter radium-223 and survival in metastatic prostate cancer. *N Engl J Med.* (2013) 369:213–23. doi: 10.1056/NEJMoa1213755

5. Lundmark F, Olanders G, Rinne SS, Abouzayed A, Orlova A, Rosenström U. Design, synthesis, and evaluation of linker-optimised PSMA-targeting radioligands. *Pharmaceutics.* (2022) 14:1098. doi: 10.3390/pharmaceutics14051098

6. Eder AC, Schäfer M, Schmidt J, Bauder-Wüst U, Roscher M, Leotta K, et al. Rational linker design to accelerate excretion and reduce background uptake of peptidomimetic PSMA-targeting hybrid molecules. *J Nucl Med.* (2021) 62:1461–7. doi: 10.2967/jnumed.120.248443

7. Kopka K, Benešová M, Bařinka C, Haberkorn U, Babich J. Glu-ureido-based inhibitors of prostate-specific membrane antigen: lessons learned during the development of a novel class of low-molecular-weight theranostic radiotracers. *J Nucl Med.* (2017) 58(Suppl. 2):17S–26S. doi: 10.2967/jnumed.116.186775

8. Afshar-Oromieh A, Haberkorn U, Zechmann C, Armor T, Mier W, Spohn F, et al. Repeated PSMA-targeting radioligand therapy of metastatic prostate cancer with $^{131}$I-MIP-1095. *Eur J Nucl Med Mol Imaging.* (2017) 44:950–9. doi: 10.1007/s00259-017-3665-9

9. Chatalic KL, Heskamp S, Konijnenberg M, Molkenboer-Kuenen JD, Franssen GM, Clahsen-van Groningen MC, et al. Towards personalized treatment of prostate cancer: PSMA I&T, a promising prostate-specific membrane antigen-targeted theranostic agent. *Theranostics.* (2016) 6:849–61. doi: 10.7150/thno.14744

10. Afshar-Oromieh A, Hetzheim H, Kratochwil C, Benesova M, Eder M, Neels OC, et al. The theranostic PSMA Ligand PSMA-617 in the diagnosis of prostate cancer by PET/CT: biodistribution in humans, radiation dosimetry, and first evaluation of tumor lesions. *J Nucl Med.* (2015) 56:1697–705. doi: 10.2967/jnumed.115.161299

11. Ballangrud AM, Yang WH, Charlton DE, McDevitt MR, Hamacher KA, Panageas KS, et al. Response of LNCaP spheroids after treatment with an alpha-particle emitter ($^{213}$Bi)-labeled anti-prostate-specific membrane antigen antibody (J591). *Cancer Res.* (2001) 61:2008–14.

12. Fanti S, Briganti A, Emmett L, Fizazi K, Gillessen S, Goffin K, et al. EAU-EANM Consensus statements on the role of prostate-specific membrane antigen positron emission tomography/computed tomography in patients with prostate cancer and with respect to [$^{177}$Lu]Lu-PSMA radioligand therapy. *Eur Urol Oncol.* (2022) 5:530–6. doi: 10.1016/j.euo.2022.05.003

13. Silver DA, Pellicer I, Fair WR, Heston WD, Cordon-Cardo C. Prostate-specific membrane antigen expression in normal and malignant human tissues. *Clin Cancer Res.* (1997) 3:81–5.

14. Kinoshita Y, Kuratsukuri K, Landas S, Imaida K, Rovito PM Jr., Wang CY, et al. Expression of prostate-specific membrane antigen in normal and malignant human tissues. *World J Surg.* (2006) 30:628–36. doi: 10.1007/s00268-005-0544-5

15. Sokoloff RL, Norton KC, Gasior CL, Marker KM, Grauer LS. A dual-monoclonal sandwich assay for prostate-specific membrane antigen: levels in tissues, seminal fluid and urine. *Prostate.* (2000) 43:150–7. doi: 10.1002/(SICI)1097-0045(20000501)43:2<150::AID-PROS10>3.0.CO;2-B

16. Rosar F, Dewes S, Ries M, Schaefer A, Khreish F, Maus S, et al. New insights in the paradigm of upregulation of tumoral PSMA expression by androgen receptor blockade: enzalutamide induces PSMA upregulation in castration-resistant prostate cancer even in patients having previously progressed on enzalutamide. *Eur J Nucl Med Mol Imaging.* (2020) 47:687–94. doi: 10.1007/s00259-019-04674-0

17. Plouznikoff N, Artigas C, Sideris S, Martinez Chanza N, Gil T, Peltier A, et al. Evaluation of PSMA expression changes on PET/CT before and after initiation of novel antiandrogen drugs (enzalutamide or abiraterone) in metastatic castration-resistant prostate cancer patients. *Ann Nucl Med.* (2019) 33:945–54. doi: 10.1007/s12149-019-01404-2

18. Maurer T, Eiber M, Schwaiger M, Gschwend JE. Current use of PSMA–PET in prostate cancer management. *Nat Rev Urol.* (2016) 13:226–35. doi: 10.1038/nrurol.2016.26

19. Erdogan M, Sengul SS, Cetin B, Avcı M, Yagci S, Ozkoç I, et al. The role of Ga$^{68}$ PSMA PET/CT imaging in Lu$^{177}$ PSMA treatment planning in metastatic castration-resistant prostate cancer. *Ann Nucl Med.* (2022) 36:562–9. doi: 10.1007/s12149-022-01739-3

20. Graf F, Fahrer J, Maus S, Morgenstern A, Bruchertseifer F, Venkatachalam S, et al. DNA double strand breaks as predictor of efficacy of the alpha-particle emitter Ac-225 and the electron emitter Lu-177 for somatostatin receptor targeted radiotherapy. *PLoS One.* (2014) 9:e88239. doi: 10.1371/journal.pone.0088239

21. Sgouros G. Alpha-particles for targeted therapy. *Adv Drug Deliv Rev.* (2008) 60:1402–6. doi: 10.1016/j.addr.2008.04.007

22. Sartor O, De Bono J, Chi KN, Fizazi K, Herrmann K, Rahbar K, et al. Lutetium-177–PSMA-617 for metastatic castration-resistant prostate cancer. *N Engl J Med.* (2021) 385:1091–103. doi: 10.1056/NEJMoa2107322

23. Hotta M, Gafita A, Czernin J, Calais J. Outcome of patients with PSMA-PET/CT screen failure by VISION criteria and treated with $^{177}$Lu-PSMA therapy: a multicenter retrospective analysis. *J Nucl Med.* (2022) 63:1484–8. doi: 10.2967/jnumed.121.263441

24. Ferdinandus J, Violet J, Sandhu S, Hicks RJ, Ravi Kumar AS, Iravani A, et al. Prognostic biomarkers in men with metastatic castration-resistant prostate cancer

receiving [$^{177}$Lu]-PSMA-617. *Eur J Nucl Med Mol Imaging.* (2020) 47:2322–7. doi: 10.1007/s00259-020-04723-z

25. Schuchardt C, Zhang J, Kulkarni HR, Chen X, Müller D, Baum RP. Prostate-specific membrane antigen radioligand therapy using $^{177}$Lu-PSMA I&T and $^{177}$Lu-PSMA-617 in patients with metastatic castration-resistant prostate cancer: comparison of safety, biodistribution, and dosimetry. *J Nucl Med.* (2022) 63:1199–207. doi: 10.2967/jnumed.121.262713

26. Konijnenberg M, Melis M, Valkema R, Krenning E, de Jong M. Radiation dose distribution in human kidneys by octreotides in peptide receptor radionuclide therapy. *J Nucl Med.* (2007) 48:134–42.

27. Zechmann CM, Afshar-Oromieh A, Armor T, Stubbs JB, Mier W, Hadaschik B, et al. Radiation dosimetry and first therapy results with a $^{124}$I/$^{131}$I-labeled small molecule (MIP-1095) targeting PSMA for prostate cancer therapy. *Eur J Nucl Med Mol Imaging.* (2014) 41:1280–92. doi: 10.1007/s00259-014-2713-y

28. Tagawa ST, Vallabhajosula S, Christos PJ, Jhanwar YS, Batra JS, Lam L, et al. Phase 1/2 study of fractionated dose lutetium-177–labeled anti–prostate-specific membrane antigen monoclonal antibody J591 ($^{177}$Lu-J591) for metastatic castration-resistant prostate cancer. *Cancer.* (2019) 125:2561–9. doi: 10.1002/cncr.32072

29. Stenberg VY, Juzeniene A, Bruland ØS, Larsen RH. In situ Generated $^{212}$Pb-PSMA ligand in a $^{224}$Ra-Solution for dual targeting of prostate cancer sclerotic stroma and PSMA-positive cells. *Curr Radiopharm.* (2020) 13:130–41. doi: 10.2174/1874471013666200511000532

30. Mease RC, Kang CM, Kumar V, Banerjee SR, Minn I, Brummet M, et al. An improved $^{211}$At-labeled agent for PSMA-targeted α-therapy. *J Nucl Med.* (2022) 63:259–67. doi: 10.2967/jnumed.121.262098

31. Kelly JM, Amor-Coarasa A, Ponnala S, Nikolopoulou A, Williams C Jr., DiMagno SG, et al. Albumin-binding PSMA ligands: implications for expanding the therapeutic window. *J Nucl Med.* (2019) 60:656–63. doi: 10.2967/jnumed.118.221150

32. Deberle LM, Benešová M, Umbricht CA, Borgna F, Büchler M, Zhernosekov K, et al. Development of a new class of PSMA radioligands comprising ibuprofen as an albumin-binding entity. *Theranostics.* (2020) 10:1678–93. doi: 10.7150/thno.40482

33. Wang Z, Tian R, Niu G, Ma Y, Lang L, Szajek LP, et al. Single low-dose injection of Evans blue modified PSMA-617 radioligand therapy eliminates prostate-specific membrane antigen positive tumors. *Bioconjug Chem.* (2018) 29:3213–21. doi: 10.1021/acs.bioconjchem.8b00556

34. Kuo HT, Lin KS, Zhang Z, Uribe CF, Merkens H, Zhang C, et al. $^{177}$Lu-labeled albumin-binder–conjugated PSMA-targeting agents with extremely high tumor uptake and enhanced tumor-to-kidney absorbed dose ratio. *J Nucl Med.* (2021) 62:521–7. doi: 10.2967/jnumed.120.250738

35. Tagawa ST, Sun M, Sartor AO, Thomas C, Singh S, Bissassar M, et al. Phase I study of $^{225}$Ac-J591 for men with metastatic castration-resistant prostate cancer (mCRPC). *J Clin Oncol.* (2021) 39(Suppl. 15):5015–5015. doi: 10.1200/JCO.2021.39.15_suppl.5015

36. Kratochwil C, Bruchertseifer F, Rathke H, Bronzel M, Apostolidis C, Weichert W, et al. Targeted α-therapy of metastatic castration-resistant prostate cancer with $^{225}$Ac-PSMA-617: dosimetry estimate and empiric dose finding. *J Nucl Med.* (2017) 58:1624–31. doi: 10.2967/jnumed.117.191395

37. Schwartz J, Jaggi JS, O'donoghue JA, Ruan S, McDevitt M, Larson SM, et al. Renal uptake of bismuth-213 and its contribution to kidney radiation dose following administration of actinium-225-labeled antibody. *Phys Med Biol.* (2011) 56:721. doi: 10.1088/0031-9155/56/3/012

38. Sgouros G, Frey E, Du Y, Hobbs R, Bolch W. Imaging and dosimetry for alpha-particle emitter radiopharmaceutical therapy: improving radiopharmaceutical therapy by looking into the black box. *Eur J Nucl Med Mol Imaging.* (2021) 49:18–29. doi: 10.1007/s00259-021-05583-x

39. Tronchin S, Forster JC, Hickson K, Bezak E. Dosimetry in targeted alpha therapy. A systematic review: current findings and what is needed. *Phys Med Biol.* (2022) 67:09TR01. doi: 10.1088/1361-6560/ac5fe0

40. Lee CH, Lim I, Woo SK, Kim W, Kim KI, Lee KC, et al. Targeted alpha immunotherapy of CD20-positive B-cell lymphoma model: dosimetry estimate of $^{225}$Ac-DOTA-rituximab using $^{64}$Cu-DOTA-rituximab. *Ann Nucl Med.* (2021) 35:639–47. doi: 10.1007/s12149-021-01607-6

41. Satapathy S, Sood A, Das CK, Mittal BR. Evolving role of $^{225}$Ac-PSMA radioligand therapy in metastatic castration-resistant prostate cancer: a systematic review and meta-analysis. *Prostate Cancer Prostatic Dis.* (2021) 24:880–90. doi: 10.1038/s41391-021-00349-w

42. Ma J, Li L, Liao T, Gong W, Zhang C. Efficacy and safety of $^{225}$Ac-PSMA-617-targeted alpha therapy in metastatic castration-resistant prostate cancer: a systematic review and meta-analysis. *Front Oncol.* (2022) 12:796657. doi: 10.3389/fonc.2022.796657

43. Ballal S, Yadav MP, Sahoo RK, Tripathi M, Dwivedi SN, Bal C. $^{225}$Ac-PSMA-617-targeted alpha therapy for the treatment of metastatic castration-resistant prostate cancer: a systematic review and meta-analysis. *Prostate.* (2021) 81:580–91. doi: 10.1002/pros.24137

44. Sathekge MM, Bruchertseifer F, Vorster M, Morgenstern A, Lawal IO. Global experience with PSMA-based alpha therapy in prostate cancer. *Eur J Nucl Med Mol Imaging.* (2021) 49:30–46. doi: 10.1007/s00259-021-05434-9

45. Sathekge M, Bruchertseifer F, Knoesen O, Reyneke F, Lawal I, Lengana T, et al. $^{225}$Ac-PSMA-617 in chemotherapy-naive patients with advanced prostate cancer: a pilot study. *Eur J Nucl Med Mol Imaging.* (2019) 46:129–38. doi: 10.1007/s00259-018-4167-0

46. Kratochwil C, Bruchertseifer F, Rathke H, Hohenfellner M, Giesel FL, Haberkorn U, et al. Targeted α-therapy of metastatic castration-resistant prostate cancer with $^{225}$Ac-PSMA-617: swimmer-plot analysis suggests efficacy regarding duration of tumor control. *J Nucl Med.* (2018) 59:795–802. doi: 10.2967/jnumed.117.203539

47. Yadav MP, Ballal S, Sahoo RK, Tripathi M, Seth A, Bal C. Efficacy and safety of $^{225}$Ac-PSMA-617 targeted alpha therapy in metastatic castration-resistant prostate cancer patients. *Theranostics.* (2020) 10:9364–77. doi: 10.7150/thno.48107

48. Sen I, Thakral P, Tiwari P, Pant V, Das SS, Manda D, et al. Therapeutic efficacy of $^{225}$Ac-PSMA-617 targeted alpha therapy in patients of metastatic castrate resistant prostate cancer after taxane-based chemotherapy. *Ann Nucl Med.* (2021) 35:794–810. doi: 10.1007/s12149-021-01617-4

49. Zacherl MJ, Gildehaus FJ, Mittlmeier L, Böning G, Gosewisch A, Wenter V, et al. First clinical results for PSMA-targeted α-therapy using $^{225}$Ac-PSMA-I&T in advanced-mCRPC patients. *J Nucl Med.* (2021) 62:669–74. doi: 10.2967/jnumed.120.251017

50. Sathekge M, Knoesen O, Meckel M, Modiselle M, Vorster M, Marx S. $^{213}$Bi-PSMA-617 targeted alpha-radionuclide therapy in metastatic castration-resistant prostate cancer. *Eur J Nucl Med Mol Imaging.* (2017) 44:1099–100. doi: 10.1007/s00259-017-3657-9

51. Kratochwil C, Apostolidis L, Rathke H, Apostolidis C, Bicu F, Bruchertseifer F, et al. Dosing $^{225}$Ac-DOTATOC in patients with somatostatin-receptor-positive solid tumors: 5-year follow-up of hematological and renal toxicity. *Eur J Nucl Med Mol Imaging.* (2021) 49:54–63. doi: 10.1007/s00259-021-05474-1

52. Park EA, Graves SA, Menda Y. The impact of radiopharmaceutical therapy on renal function. *Semin Nucl Med.* (2022) 52:467–74. doi: 10.1053/j.semnuclmed.2022.02.004

53. Majer P, Jančařík A, Krečmerová M, Tichy T, Tenora L, Wozniak K, et al. Discovery of orally available prodrugs of the glutamate carboxypeptidase II (GCPII) inhibitor 2-phosphonomethylpentanedioic Acid (2-PMPA). *J Med Chem.* (2016) 59:2810–9. doi: 10.1021/acs.jmedchem.6b00062

54. Khreish F, Ebert N, Ries M, Maus S, Rosar F, Bohnenberger H, et al. $^{225}$Ac-PSMA-617/$^{177}$Lu-PSMA-617 tandem therapy of metastatic castration-resistant prostate cancer: pilot experience. *Eur J Nucl Med Mol Imaging.* (2020) 47:721–8. doi: 10.1007/s00259-019-04612-0

55. Tagawa ST, Fung E, Niaz MO, Bissassar M, Singh S, Patel A, et al. Results of combined targeting with prostate-specific membrane antigen (PSMA) with alpha-radiolabeled antibody$^{225}$Ac-J591 and beta-radiolabeled ligand $^{177}$Lu-PSMA I&T: preclinical and intial phase I clinical data in patients with metastatic castration-resistant prostate cancer. *Cancer Res.* (2022) 82(Suppl. 12):CT143. doi: 10.1158/1538-7445.AM2022-CT143

56. Scher HI, Morris MJ, Stadler WM, Higano C, Basch E, Fizazi K, et al. Trial design and objectives for castration-resistant prostate cancer: updated recommendations from the prostate cancer clinical trials working group 3. *J Clin Oncol.* (2016) 34:1402–18. doi: 10.1200/JCO.2015.64.2702

frontiers | Frontiers in Medicine

TYPE Review
PUBLISHED 07 December 2022
DOI 10.3389/fmed.2022.1034315



OPEN ACCESS

EDITED BY
Maria Picchio,
Vita-Salute San Raffaele University, Italy

REVIEWED BY
Marco Maccauro,
Fondazione IRCCS Istituto Nazionale Tumori, Italy
Chiara Maria Grana,
European Institute of Oncology (IEO), Italy

*CORRESPONDENCE
Jingjing Zhang
j.zhang@nus.edu.sg

SPECIALTY SECTION
This article was submitted to Nuclear Medicine, a section of the journal Frontiers in Medicine

RECEIVED 01 September 2022
ACCEPTED 21 November 2022
PUBLISHED 07 December 2022

CITATION
Shi M, Jakobsson V, Greifenstein L, Khong P-L, Chen X, Baum RP and Zhang J (2022) Alpha-peptide receptor radionuclide therapy using actinium-225 labeled somatostatin receptor agonists and antagonists. *Front. Med.* 9:1034315. doi: 10.3389/fmed.2022.1034315



# Alpha-peptide receptor radionuclide therapy using actinium-225 labeled somatostatin receptor agonists and antagonists

Mengqi Shi[1,2], Vivianne Jakobsson[1,3], Lukas Greifenstein[4], Pek-Lan Khong[1,5], Xiaoyuan Chen[1,2,5,6,7], Richard P. Baum[4] and Jingjing Zhang[1,2,5]*

[1]Department of Diagnostic Radiology, Yong Loo Lin School of Medicine, National University of Singapore, Singapore, Singapore, [2]Nanomedicine Translational Research Program, NUS Center for Nanomedicine, Yong Loo Lin School of Medicine, National University of Singapore, Singapore, Singapore, [3]Academy for Precision Oncology, International Centers for Precision Oncology (ICPO), Wiesbaden, Germany, [4]CURANOSTICUM Wiesbaden-Frankfurt, Center for Advanced Radiomolecular Precision Oncology, Wiesbaden, Germany, [5]Clinical Imaging Research Centre, Centre for Translational Medicine, Yong Loo Lin School of Medicine, National University of Singapore, Singapore, Singapore, [6]Department of Surgery, Chemical and Biomolecular Engineering, and Biomedical Engineering, Yong Loo Lin School of Medicine and College of Design and Engineering, National University of Singapore, Singapore, Singapore, [7]Agency for Science, Technology, and Research (A*STAR), Institute of Molecular and Cell Biology, Singapore, Singapore

Peptide receptor radionuclide therapy (PRRT) has over the last two decades emerged as a very promising approach to treat neuroendocrine tumors (NETs) with rapidly expanding clinical applications. By chelating a radiometal to a somatostatin receptor (SSTR) ligand, radiation can be delivered to cancer cells with high precision. Unlike conventional external beam radiotherapy, PRRT utilizes primarily β or α radiation derived from nuclear decay, which causes damage to cancer cells in the immediate proximity by irreversible direct or indirect ionization of the cells' DNA, which induces apoptosis. In addition, to avoid damage to surrounding normal cells, PRRT privileges the use of radionuclides that have little penetrating and more energetic (and thus more ionizing) radiations. To date, the most frequently radioisotopes are $\beta^-$ emitters, particularly Yttrium-90 ($^{90}$Y) and Lutetium-177 ($^{177}$Lu), labeled SSTR agonists. Current development of SSTR-targeting is triggering the shift from using SSTR agonists to antagonists for PRRT. Furthermore, targeted α-particle therapy (TAT), has attracted special attention for the treatment of tumors and offers an improved therapeutic option for patients resistant to conventional treatments or even beta-irradiation treatment. Due to its short range and high linear energy transfer (LET), α-particles significantly damage the targeted cancer cells while causing minimal cytotoxicity toward surrounding normal tissue. Actinium-225 ($^{225}$Ac) has been developed into potent targeting drug constructs including somatostatin-receptor-based radiopharmaceuticals and is in early clinical use against multiple neuroendocrine tumor types. In this article, we give a review of preclinical and clinical applications of $^{225}$Ac-PRRT

in NETs, discuss the strengths and challenges of $^{225}$Ac complexes being used in PRRT; and envision the prospect of $^{225}$Ac-PRRT as a future alternative in the treatment of NETs.

KEYWORDS

**actinium-225, neuroendocrine tumor, peptide receptor radionuclide therapy (PRRT), targeted α-particle therapy, SSTR, SSTR antagonist**

## Introduction

Neuroendocrine tumors (NETs) are well-differentiated, low proliferating neuroendocrine neoplasms (NENs) (1), most commonly arising from gastroenteropancreatic structures and the lung, although NEN have been described in almost every tissue. Accounting for only 0.5% of all malignancies, NETs are considered rare (2), however, the incidence/prevalence has been increasing in many epidemiological studies over the last decades (with GEP NETs demonstrating the highest incidence rate with 3.56 cases per 100,000) (2–7). The WHO grading system relies extensively on the proliferation rate to classify low proliferative NETs (NET-G1) with good prognosis, intermediate grade (NET-G2), and high grade (NET-G3) that show poor prognosis (8).

As a heterogeneous disease with very diverse symptomatology, NETs require multidisciplinary treatment and care, including medical control, surgery, chemotherapy, and internal or external radiation therapy (9). The cornerstone of therapy is still surgery with curative intent, whenever possible. However, in the case of metastatic disease, total excision is generally not possible due to the infiltration of other tissues and/or blood vessels or the number of metastatic sites (10, 11).

Systemic chemotherapy provides only modest benefit in rapidly proliferating tumors (grade 3) (12, 13). Therapeutic options such as somatostatin analogs (SSAs) or interferon-α may improve symptoms caused by hormonal excess or even lengthen the time to disease progression by offering hormonal and antiproliferative control over NETs, but rarely lead to partial or complete tumor response (14, 15). External beam radiotherapy (EBRT) unfortunately is not effective for the treatment of metastasized and secondary cancer sites beyond the treatment area (16, 17).

Theranostics, the concept of combining the inevitably intertwined arts of diagnostics and therapy, is a treatment option that has gained momentum over the last two and a half decades. Peptide receptor imaging and peptide receptor radionuclide therapy (PRRT) were the first successful examples of the theranostic concept, for imaging and treating cancer. PRRT has long been considered as a palliative treatment for NETs, but is now attracting more and more attention as a very effective symptomatic and well-tolerated treatment prolonging progression-free (and possibly overall) survival. As a complement to surgery, neoadjuvant therapy can make previously difficult-to-operate tumors operable by shrinking them, and as an adjuvant therapy, it may prevent tumor re-growth after surgical manipulation and growth of pre-existing micrometastases (18, 19).

Unlike chemotherapy and EBRT, PRRT targets disease at the cellular level in the systemic treatment of non-resectable and metastasized NETs (16). The overexpression of somatostatin receptors (SSTRs) of various sub-types in about 80% of NETs provides a continuously evolving way to diagnose and treat NETs (18, 20). The working principle of PRRT is using a therapeutic radionuclide chelated to a SSTR binding peptide and as the compound binds to SSTR expressing tissue, DNA-damaging radiation is delivered nearly exclusively to tumor cells and its microenvironment while sparing the surrounding healthy tissue. Somatostatin, the native peptide, is an obvious example of SSTR-binding peptide (21). However, it is susceptible to fast enzymatic degradation and is thus not suitable for *in vivo* applications (22). Instead, synthetic peptides, including those based on SSAs, have been developed with the intent to optimize metabolic stability, tumor retention time, and affinity.

## History of peptide receptor radionuclide therapy

The first PRRT was performed in the early 1990s (**Figure 1**). The Rotterdam group successfully developed [$^{111}$In-DTPA-$_{D}$-Phe$^{1}$]-octreotide ($^{111}$In-pentetreotide) somatostatin scintigraphy (Octreoscan), and subsequently examined its imaging potential in more than 1,000 patients (23–25). Based on high uptake of $^{111}$In-pentetreotide by tumors as demonstrated by imaging, Krenning's team successfully treated a patient with metastatic glucagonoma using a high dose of $^{111}$In-pentetreotide, which resulted in a decreased level of circulating glucagon as well as decreased tumor size (26).

This early work set the stage for further development of this exciting new field of radiomolecular precision medicine. For example, guided by the experience with PRRT using $^{111}$In-pentetreotide, the need for more suitable radionuclides was identified because the properties of $^{111}$In (decay by electron capture with a half-life of 2.8 days) do not provide good tissue penetration which corresponds with a modest or no tumor shrinkage. Improvement of PRRT has been made tremendously since then due to the development and availability

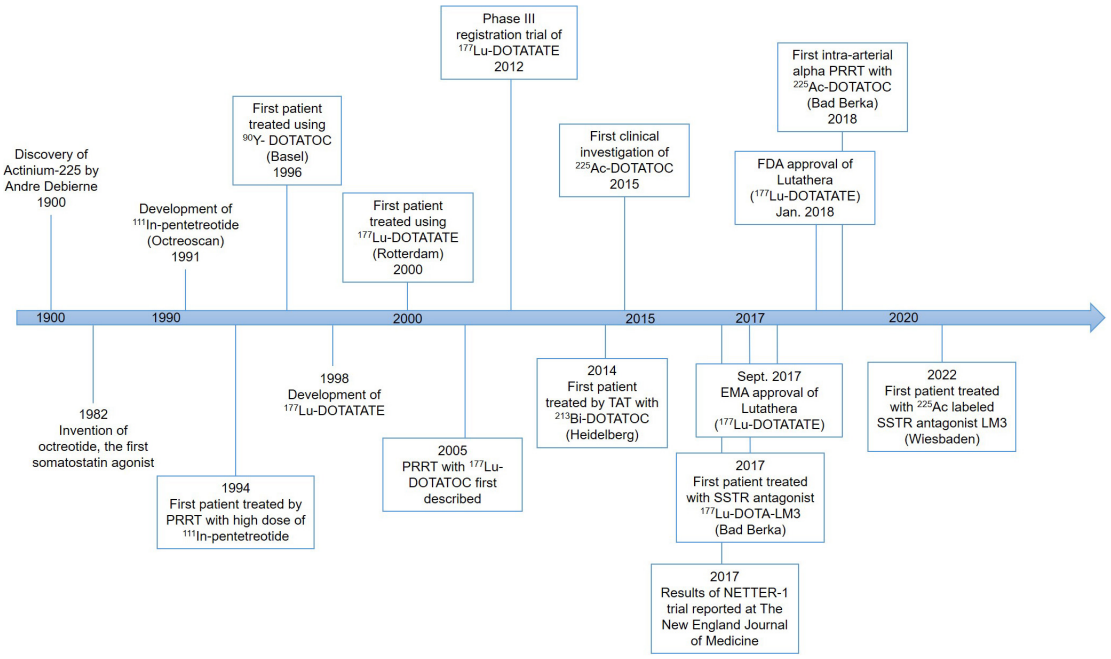


FIGURE 1
History of somatostatin-based peptide receptor radionuclide therapy (PRRT).

of novel peptides, chelators, and radionuclides in various combinations (27).

Derivatizing [Tyr$^3$]-octreotide (**Figure 2**), which has a higher binding affinity for SSTR2 than the natural somatostatin analog (SSA) octreotide, and combining it with the chelator 1,4,7,10-tetra-azacyclododecane-tetra-acetic acid (DOTA) enabled stable radiolabeling with the high-energy beta particle-emitter Yttrium-90 ($^{90}$Y-DOTATOC).

This therapeutic moiety was first applied in a pilot study for the treatment of three patients with abdominal metastases of neuroendocrine carcinoma of unknown localization (28, 29); and its therapeutic potential was evaluated subsequently with larger SSTR-positive patient numbers (30, 31). Treatment with $^{90}$Y-DOTATOC stopped rapid tumor progression, decreased the tumor marker neuron-specific enolase (NSE), and allowed disease stabilization (28, 30, 31). DOTATOC has since become a popular theranostics agent, demonstrating superior diagnostic sensitivity compared to Octreoscan, and demonstrating promising therapeutic value for treating SSTR-positive NETs when labeled with β- emitters, particularly Yttrium-90 ($^{90}$Y) and Lutetium-177 ($^{177}$Lu).

Another extensively studied SSA is DOTA-[Tyr$^3$]-octreotate (DOTATATE), where the alcohol Thr(ol) of the C-terminus of DOTATOC is replaced by the natural amino acid Thr. This somatostatin analog was developed in 1998 and was found to show an even higher affinity to SSTR2 and a higher uptake in pancreatic tumor cells compared to the previously described SSAs (32).

The first clinical trial with $^{177}$Lu-DOTATATE started in 2000 in Rotterdam, The Netherlands, and led to the multinational phase three trial named NETTER-1 (33, 34). In this randomized controlled trial, a significantly higher response rate and extended progression-free survival were demonstrated in patients with advanced progressive SSTR-positive midgut NETs, compared to the double dose of long-acting repeatable (LAR 60 mg) octreotide administrations (18, 27, 34, 35). In January 2018, $^{177}$Lu-DOTATATE under the name of Lutathera was approved by the Food and Drug Administration (FDA) for the treatment of SSTR2-positive gastroenteropancreatic NETs (GEP-NETs) in adults (36). The approval of Lutathera in Europe was granted by the European Medicines Agency (EMA) already in September 2017 (37).

Other well-known somatostatin SSAs include lanreotide and vapreotide, but as these are not approved for PRRT of NETs, possibly due to their affinity pattern to SSTR subtypes and mode of action (38–40), they will not be discussed in this review.

Despite the success of [$^{90}$Y]Y-DOTATOC and [$^{177}$Lu]Lu-DOTATATE in the treatment of NETs in terms of progression-free survival, there were problems with $^{90}$Y concerning renal toxicity and a low rate of complete remissions, suggesting an improvement in PRRT efficacy is required (27, 41) with the main aspects of (1) identification of prognostic and predictive factors; (2) α-PRRT using $^{225}$Ac labeled ligands; and (3) shift from using SSAs to somatostatin antagonists.

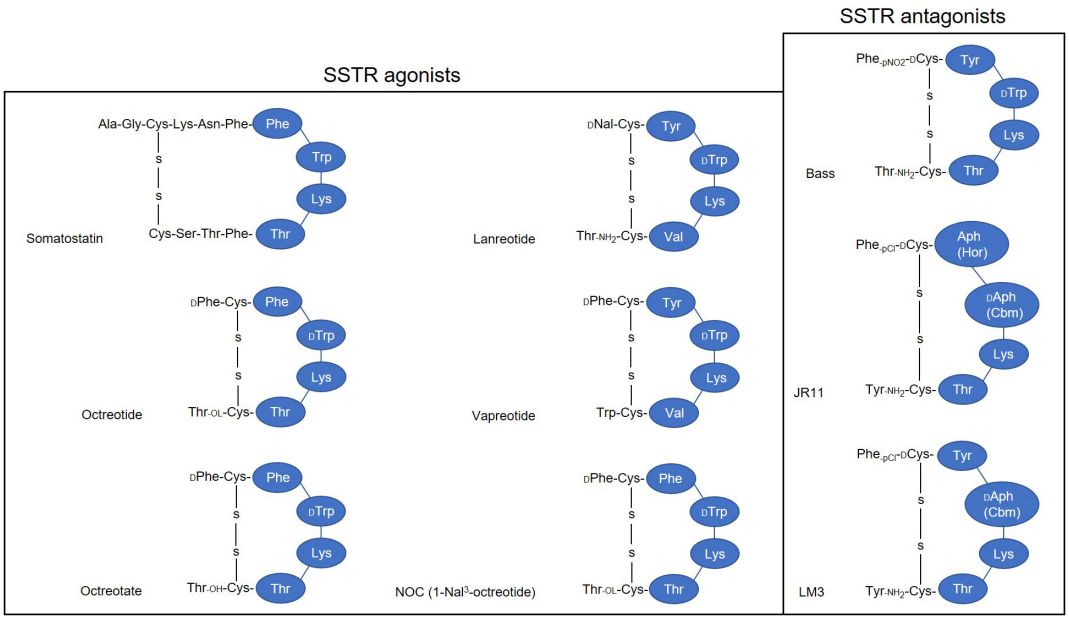


FIGURE 2
Simplified illustration of somatostatin receptor agonists and antagonists. 1-Nal, naphthyl-alanine; Aph(Hor), 4-amino-L-hydroorotyl -phenylalanine; D-Aph(Cbm), D-4-amino-carbamoyl-phenylalanine.

## $^{68}$Ga-labeled somatostatin analogs for imaging (somatostatin receptor-PET)

Even with the success of DOTATOC and DOTATATE, clinicians need to take the individual variability in the therapy response of patients with seemingly similar profiles into account. $^{68}$Ga is a positron emitter that can be chelated to DOTATOC or DOTATATE for PET/CT imaging before therapy. SSTR-PET/CT with $^{68}$Ga-labeled DOTATATE and/or DOTATOC showed very promising results (42). All studies agreed on the important role of SSTR-PET using $^{68}$Ga for NET imaging and therapy planning, supporting the potent theranostic role of a radiolabeled DOTA-peptide (43–48). As a result, $^{68}$Ga-DOTATOC was approved by the FDA in 2019 as the first $^{68}$Ga-labeled radiopharmaceutical for imaging of SSTR positive GEP-NET using PET (49).

## Choosing a radionuclide for peptide receptor radionuclide therapy

Table 1 lists the physical properties regarding the clinically most frequently used radioisotopes in PRRT of NETs.

While $^{68}$Ga is useful for imaging purposes, all other radionuclides in Table 1 are used both for therapy and for single-photon emission computed tomography (SPECT) imaging. Out of these, $^{90}$Y and $^{177}$Lu are the two favorable isotopes due to their higher particle energies compared to $^{111}$In. $^{90}$Y ($t_{1/2}$ = 64.2 h) emits $\beta^-$-particles with a maximum energy of 2.284 MeV, allowing penetration of soft tissue to a depth of around 11 mm (50, 51). Because of its longer range compared to $^{177}$Lu, $^{90}$Y-DOTATE/TOC is suggested to be more suitable for bigger lesions, while $^{177}$Lu-DOTATATE might be preferred for smaller lesions (52). It has been demonstrated that $^{90}$Y-PRRT has a small potential of causing renal toxicity when used without nephroprotection, especially in patients with compromised renal function (53, 54). For $^{177}$Lu-DOTATATE or $^{177}$Lu-DOTATOC no significant renal damage occurred even in long-term follow up studies. An increasing number of clinical studies suggest that the combination of $^{90}$Y and $^{177}$Lu could be better than either radionuclide alone for PRRT in NETs, with an improved overall survival (55, 56). In parallel to $\beta^-$-emitters, radionuclides emitting α-particles recently are gaining special interest for the treatment of NETs.

## Why alpha in peptide receptor radionuclide therapy

To date, most PRRTs rely on β-emitters, especially $^{90}$Y and $^{177}$Lu, because of the availability of these radioisotopes

TABLE 1 Physical properties of selected radioisotopes used in PRRT to treat NETs.

| Radionuclide | Decay | Half-life/h | Energy (max)/keV | Tissue penetration depth/mm | Application |
|---|---|---|---|---|---|
| $^{111}$In | EC, γ | 67.2 | 245<br>19 | 0.5 | Imaging |
| $^{90}$Y | $\beta^-$, γ | 64.2 | 2,284 | 11 | Therapy |
| $^{177}$Lu | $\beta^-$, γ | 160.8 | 498 | 1.7 | Imaging/therapy |
| $^{68}$Ga | $\beta^+$ | 1.13 | 1,920 | | Imaging |

EC, electron capture.

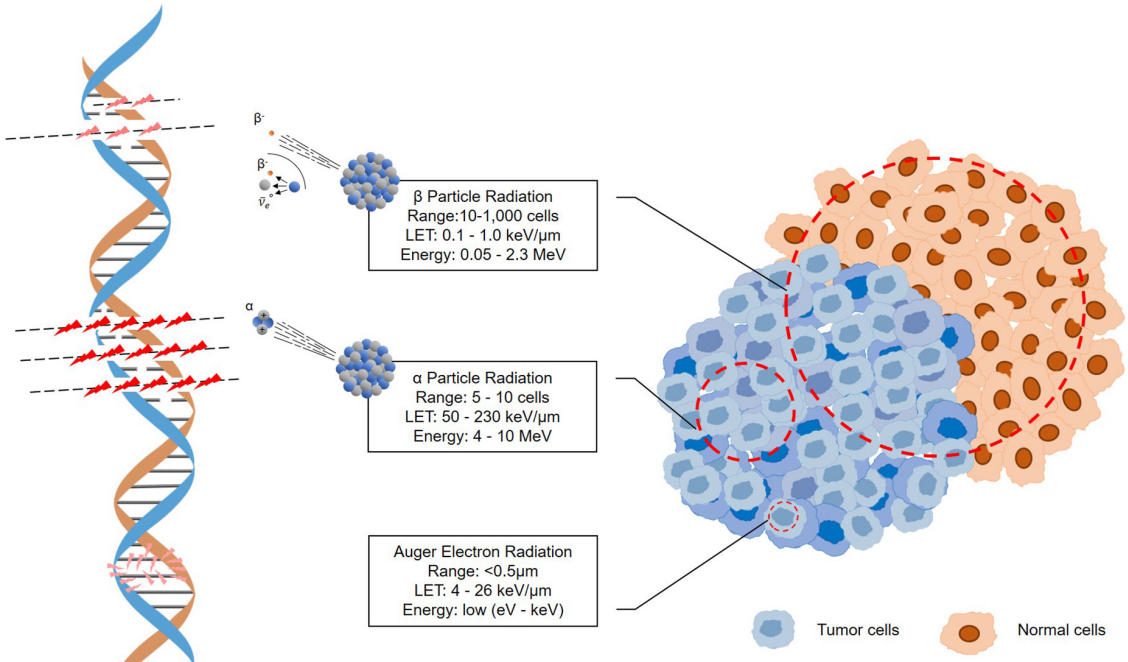


FIGURE 3
Illustration of the tracks of α-particle, β-particle, and auger election radiation.

and the proven clinical effect. However, due to the relatively large range of these radionuclides surrounding normal tissues are also exposed to radioactivity. Furthermore, hypoxic cancer tissue could be resistant to β-emitter treatment, causing radiotherapeutic failure of β-PRRT (57, 58).

Targeted α-particle therapy (TAT) offers a therapeutic option for patients resistant to β-irradiation treatments. An α-particle is a helium-4 ($^4$He) nucleus consisting of two protons and two neutrons with an overall charge of +2 (59). Because of the double-positive charge, α-particles deliver dense ionization along a linear track, often described as high linear transfer (LET), ranging from 50 to 230 keV/μm (**Figure 3**) (60). This high LET renders higher target cell toxicity originating from higher probability of DNA double strand breaks (DSB) compared to β-particles with low LET (0.1–1.0 keV/μm) (61). Moreover, the primary target of high-LET α-particle is DNA, and a low number of particles can result in irreparable DSBs and lack of oxygen effects on cytotoxicity (62–64). Thus, the cytotoxicity of α-particle may be extremely effective and may also be more dose independent than β-emissions with cell death occurring from a single or a few α-particle traversals of the cell nucleus (65, 66). On the other hand, the typical tissue range of α-particles does not exceed 100 μm, which is significantly shorter than that of β-particles (0.05–12 mm) (**Figure 3**) (16, 58). This allows for selective ablation of the targeted tumor cells whilst minimizing the damage to surrounding healthy tissues (67).

## Why actinium-225

Considering the half-life, production, availability, and ability to be stably incorporated into a suitable vector, only a handful

α-radionuclides have potential for clinical use, including actinium-225, bismuth-213, astatin-211, thorium-227, radium-223, radium-224, lead-212, bismuth-212, and terbium-149 (**Table 2**) (57, 64, 68–75).

Among all medically relevant α-particles, the generator derived radionuclide $^{225}$Ac (and its daughter radionuclide $^{213}$Bi) are considered particularly promising. $^{225}$Ac was discovered by Andre Debierne in 1899 and Friedrich Giesel in 1902 (76). As a pure α-emitter with a half-life of 9.9 days, the decay of $^{225}$Ac produces seven radionuclide daughters in the decay chain to stable $^{209}$Bi (**Figure 4**). From this decay path, a single $^{225}$Ac decay yields a total of four α, three $\beta^-$ disintegrations, and two γ emissions. As such, $^{225}$Ac is classified as nanogenerator or *in vivo* generator (77). The relatively long half-life, the multiple α-particle emissions in the decay chain, and the rapid decay to stable $^{209}$Bi makes $^{225}$Ac a candidate of great potential for application in TAT (78). Moreover, the isomeric γ emissions with energy suitable for SPECT imaging grants $^{225}$Ac the theranostic possibility (68, 69). Although the feasibility of using $^{225}$Ac for imaging is debatable because the amount administered for therapy may not produce enough gamma emission to be effectively detected by gamma camera.

The initial focus for harnessing the therapeutic potential of $^{225}$Ac was to identify a suitable chelating agent for *in vivo* delivery of $^{225}$Ac to target cells (79, 80). DOTA remains the gold standard for $^{225}$Ac labeling for all clinical work. Examples include $^{225}$Ac-PSMA-617, $^{225}$Ac-DOTATOC, $^{225}$Ac-DOTATATE, and $^{225}$Ac-DOTA-HuM195 (81). The first-in-human phase I dose escalation trial used $^{225}$Ac-DOTA-HuM195, which not only demonstrated the safety of $^{225}$Ac and its antileukemic activity, but also suggested that targeted therapy with an *in vivo* α-particle nanogenerator is a feasible approach in humans (82). With this proof of concept, $^{225}$Ac was then attached to PSMA-617 for prostate cancer therapy (83–86) and also bound to SSA-based pharmaceuticals for treating NETs.

## Preclinical studies of actinium-225-peptide receptor radionuclide therapy

Several preclinical studies tested the efficacy of α-particle emitting conjugates $^{225}$Ac-DOTATATE and $^{225}$Ac-DOTATOC in xenografted NET models and tested their toxicity as well as the biological effects of $^{225}$Ac. γH2AX was suggested as early key parameter in predicting tumor response to α-PRRT. The great reduction of growth and improved efficacy compared with $^{177}$Lu-labeled SSAs suggested that $^{225}$Ac-DOTATATE/DOTATOC has significant potential for improving PRRT in NETs and for the clinical translation in NET.

## Clinical application of actinium-225-peptide receptor radionuclide therapy

The first clinical study of $^{225}$Ac-PRRT in NET treatment was started in 2011 as a collaboration between the Joint Research Centre in Karlsruhe (Germany) and the University Hospital Heidelberg to treat patients with progressive NETs using $^{225}$Ac-DOTATOC. Based on 46 treatment cycles in 34 patients, the maximum tolerable dose was determined to be 40 MBq. The treatment was found to be safe with doses of 18.5 MBq every 2 months or 25 MBq every 4 months, and a cumulative activity of 75 MBq in regard to delayed toxicity. Despite the treatment response observed in several patients, further investigations were found to be necessary to improve patient selection and dosage regimens (87). Since then, clinical studies of $^{225}$Ac-PRRT in different NETs focused on whole-body SPECT/CT imaging possibility, efficacy and safety, therapeutic effect, as well as comparison to β-PRRT, has burgeoned (**Table 3**).

Considering the minimal/acceptable side effects, and the improved therapeutic efficacy and survival, one can conclude that $^{225}$Ac-PRRT not only provides an alternative in the treatment of β-radiation-refractory NETs, but also presents as possible frontline in treatment of NETs and can potentially usher a new era in radiopharmaceuticals even in tumors beyond NET.

## Challenges of using actinium-225 in peptide receptor radionuclide therapy

### Production of actinium-225

Limited $^{225}$Ac supply poses the most important challenge for widely implementing $^{225}$Ac-based PRRT. For more than two decades, the radiochemical extraction from $^{229}$Th, which is originated from the decay of the fissile isotope $^{233}$U (**Figure 4**), has been the most utilized strategy for the production of $^{225}$Ac and its daughter $^{213}$Bi (88, 89). Even today, $^{225}$Ac used in all clinical and virtually all preclinical studies is still obtained from the decay of $^{229}$Th. Worldwide, only three sources of $^{229}$Th are available (81). The Directorate for Nuclear Safety and Security of the Joint Research Centre (JRC) of the European Commission in Karlsruhe, Germany, the first laboratory to prepare $^{225}$Ac/$^{213}$Bi, has produced approximately 13 GBq $^{225}$Ac annually since the 1990s for their center and a wide network of clinical collaborators (89, 90). The Oak Ridge National Laboratory (ORNL), USA produces up to 33 GBq per year for extensive application of treatment (91), while the Institute of Physics and Power Engineering (IPPE) in Russia reported an estimated production of 22 GBq annually (92) with no direct clinical application reported yet to our knowledge. This amounts to a

TABLE 2 Medically relevant α-emitters with their decay properties.

| Parent | Daughter | $t_{1/2}$ | α -decay | α -energy/MeV | Emissions per decay | Radiolabeling approach |
|---|---|---|---|---|---|---|
| $^{225}$Ac | | 9.9 days | 100% | 5.94 | 4α, 3β$^-$ | Chelation by DOTA or NETA |
| | $^{213}$Bi | 46 min | 2.2% | 5.87 | 1α, 2β$^-$ | Chelation by DTPA or DOTA |
| $^{211}$At | | 7.2 h | 42% | 5.87 | 1α, 1EC | Radioastatination |
| $^{227}$Th | | 18.7 days | 100% | 6.14 | 5α, 2β$^-$ | Chelation by DOTA |
| | $^{223}$Ra | 11.4 days | 100% | 5.71 | 4α, 2β$^-$ | |
| $^{224}$Ra | | 3.6 days | 100% | 5.69 | 5α, 2β$^-$ | |
| | $^{212}$Pb | 10.6 h | | 6.09 | 1α, 2β$^-$ | Chelation by TCMC |
| | $^{212}$Bi | 1.0 h | 36% | 6.05 | 1α, 1β$^-$ | Chelation by DTPA or DOTA |
| $^{149}$Tb | | 4.1 h | 17% | 3.96 | 1α, β$^+$ | |

α-emitters that are considered not suitable for therapeutic use are not listed. EC, electron capture.

current global production of approximately 68 GBq per year. At this level of supply, $^{225}$Ac-based treatments will continue to only be available for some few 100 patients per year, which obviously is insufficient to meet the growing demand of $^{225}$Ac labeled compounds in hospitals worldwide (81, 93).

Consequently, multiple accelerator-based routes to scale up $^{225}$Ac production have been investigated, including the irradiation of $^{226}$Ra target using protons, deuterons or gamma-rays and the spallation of $^{nat}$Th or $^{nat}$U targets with highly energetic protons (**Figure 5**) (94). Among the routes described so far, the spallation of $^{nat}$Th is currently the most frequently used accelerator-based route. Even though the feasibility of the process has been demonstrated in the USA (95, 96) and Russia (97, 98), the implication of coproducing the long-lived $^{227}$Ac ($t_{1/2}$ = 21.8 years) as impurity is a serious limitation in terms of clinical translation and waste management (99). In addition, issues with licensing and clinical safe handling need to be resolved (81).

Medium-energy proton irradiation of $^{226}$Ra in a cyclotron using the reaction $^{226}$Ra(p,2n)$^{225}$Ac offers a number of advantages over the $^{nat}$Th spallation, and is currently the most promising method of large-scale and cost-effective production of $^{225}$Ac. Chemical purification of the irradiated targets generates $^{225}$Ac with high isotopic purity because there are no other long-lived actinium isotopes, such as $^{227}$Ac, co-produced (100). It is important to mention that the availability of appropriate cyclotrons worldwide [energy range 15–25 MeV (101)] makes the production of $^{225}$Ac feasible for basic and applied research (94). The downsides of this approach are related to the preparation and safe handling of targets containing milligram of radioactive $^{226}$Ra and managing its highly radiotoxic gaseous decay product $^{222}$Rn. Further research on the practical implementation of this production route is required to meet the high demand in the mid-term future (81).

The reaction $^{226}$Ra(d,3n)$^{225}$Ac has been suggested as an improved approach for producing $^{225}$Ac (102). Model calculations are predicting an increased production yield compared to the $^{226}$Ra(p,2n)$^{225}$Ac reaction. However, deuteron irradiation leads to an enhanced co-production of $^{226}$Ac *via* the $^{226}$Ra(d,2n)$^{226}$Ac reaction, resulting in an extended cooling time necessary to allow for $^{226}$Ac decay. Moreover, limited accelerators are available worldwide that can provide deuteron beams of sufficient energy and the complicated handling of $^{226}$Ra and its decay product remains an issue (81).

Other production routes being studied involve $^{226}$Ra(n, γ)$^{229}$Th(α)$^{225}$Ac, $^{226}$Ra(γ,n)$^{225}$Ra(β)$^{225}$Ac, and $^{226}$Ra(n,2n)$^{225}$Ra(β)$^{225}$Ac. It is important to point out that the main limitation of all these strategies is the handling of radium target and the generation of long-lived co-products, such as $^{227}$Ac ($t_{1/2}$ = 21.77 years) and $^{228}$Ac ($t_{1/2}$ = 1.9 years). However, preliminary results demonstrated by these above-mentioned methods are promising (94, 100, 103–105). Unfortunately, but understandably, these supply limitations bring about a high cost that is considered unaffordable by many researchers.

## Imaging

Clinical imaging using $^{225}$Ac also presents challenges. Therefore, post-therapy imaging is usually not done after $^{225}$Ac administration for tracer localization. The use of two photopeaks at 218 keV and 440 keV has long been suggested for clinical imaging of α-particles (106), until recently, Rasheed et al. focusing on gamma-ray spectrum for $^{225}$Ac showed an additional third photopeak at 78 keV, with higher counting density (107). Although imaging using the additional 78 keV photopeak was suggested to yield higher counts, better images, and more lesion delineations, the literature showing the feasibility of using the three photopeaks is limited to only few clinical case reports (108, 109).

## Dosimetry

The short mean free path of $^{225}$Ac (110), as well as the complexity and timing of $^{225}$Ac decay in relation to its radiopharmaceutical stability, uptake and clearance makes measurement of $^{225}$Ac activity very difficult. A number

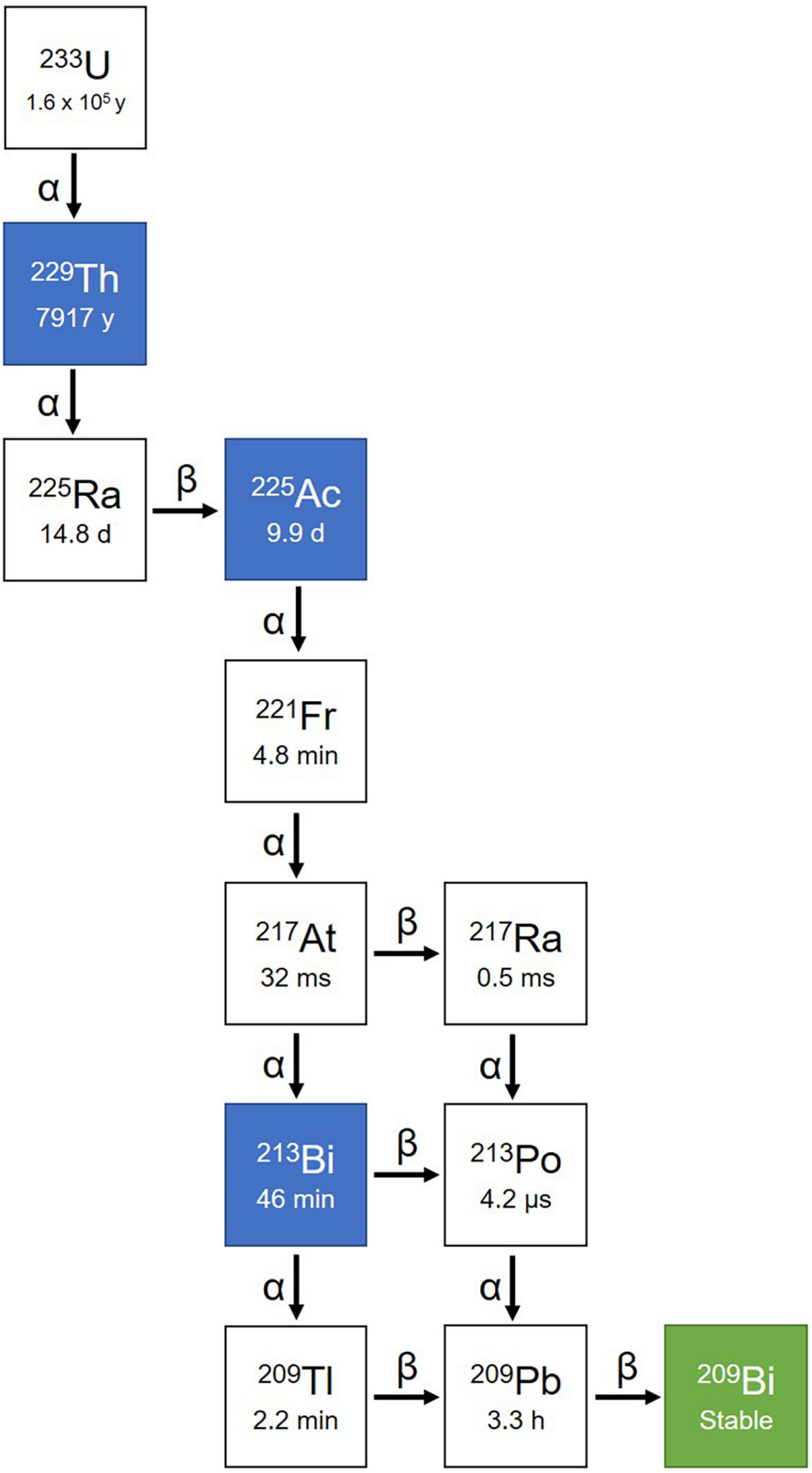


FIGURE 4
Decay chain of $^{225}$Ac. $^{225}$Ac decays to $^{209}$Bi with seven intermediate radionuclide progenies, including $^{221}$Fr, $^{217}$At, $^{213}$Bi, $^{209}$Tl, $^{217}$Ra, $^{213}$Po, and $^{209}$Pb. Among the decay chain $^{225}$Ac and $^{213}$Bi are medically relevant and intensively investigated.

TABLE 3 Actinium-225-peptide receptor radionuclide therapy in NET treatment.

| Peptide | Tumor types | Model | Key findings | Authors | References |
|---|---|---|---|---|---|
| **Pre-clinical** | | | | | |
| DOTATOC | Pancreatic NET | Xenograft | Activity up to 20 kBq had no significant toxic effect.<br>Effective accumulation in xenografted NETs<br>Reduced growth of NETs, and improved therapeutic efficacy | Miederer et al. | (117) |
| DOTATOC | Pancreatic tumor cells | *In vitro* | $^{225}$Ac and $^{177}$Lu triggered-γH2AX-foci formation is an early key parameter in predicting response to internal radiotherapy. | Graf et al. | (156) |
| DOTATATE | Lung NET | Xenograft | 1st Preclinical study for $^{225}$Ac-DOTATATE;<br>Activity up to 111 kBq had no significant toxicity<br>Significantly decreased tumor volume, increased tumor growth delay, and prolonged time to experimental endpoint for animals bearing both tumor types | Tafreshi et al. | (157) |
| **Peptide** | **Tumor types** | **Patient number** | **Key findings** | **Authors** | **References** |
| **Clinical** | | | | | |
| DOTATOC | NETs | 34 patients | Promising treatment efficacy in various patients<br>Suggesting comparative trials of α and β are needed. | Kratochwil et al. | (87) |
| DOTATOC | NETs | 10 patients | The very first intra-arterial targeted alpha peptide radionuclide therapy using $^{225}$Ac DOTATOC<br>$^{225}$Ac DOTATOC PRRT was very well-tolerated and effective. | Zhang et al. | (158) |
| DOTATATE | GEP-NET | 32 patients | First clinical experience on efficacy and safety<br>$^{225}$Ac-DOTATATE TAT as a promising treatment option for patients who are refractory to $^{177}$Lu-DOTATATE therapy | Ballal et al. | (159) |
| DOTATATE | Gastric NET | Case report | First whole-body and SPECT/CT images demonstrating high tumor uptake of $^{225}$Ac -DOTATATE. | Ocak et al. | (160) |
| DOTATATE | Rectal NET | Case report | Whole-body and SPECT/CT imaging results encourage the use of $^{225}$Ac -DOTATATE as a primary modality of treatment in advanced NET with metastases. | Kamaleshwaran et al. | (161) |
| DOTATOC | Liver NET | Case report | $^{225}$Ac-PRRT in a β-radiation-refractory NET patient was shown to be safe and effective. | Zhang et al. | (162) |
| DOTATOC | Thymus NET | Case report | No adverse effects observed after $^{225}$Ac-DOTATOC TAT in patients with metastatic neuroendocrine tumors failing β-PRRT. | Zhang et al. | (163) |
| DOTATATE | Rectal NET | Case report | Using $^{225}$Ac-DOTATATE as first-line treatment presents a novel strategy for metastatic NETs with high skeletal disease burden. | Satapathy et al. | (164) |
| DOTATATE | NET-CUP | Case report | First case report demonstrating thyroid dysfunction developed after $^{225}$Ac-DOTATATE therapy in a patient with NET with unknown primary. | Kavanal et al. | (165) |
| DOTATATE | Pancreatic NET | Case report | $^{225}$Ac-DOTATATE was well-tolerated at early stage of treatment, and patient demonstrated excellent response. | Budlewski et al. | (166) |
| DOTATATE | NET-CUP | Case report | First case who received actinium-225 first line with almost complete response at a single dosage | Alan Selçuk et al. | (167) |
| DOTATATE | GEP-NET | 91 | $^{225}$Ac-DOTATATE TAT showed improved overall survival, even in patients refractory to prior $^{177}$Lu-DOTATATE treatment with transient and acceptable adverse effects | Ballal et al. | (168) |

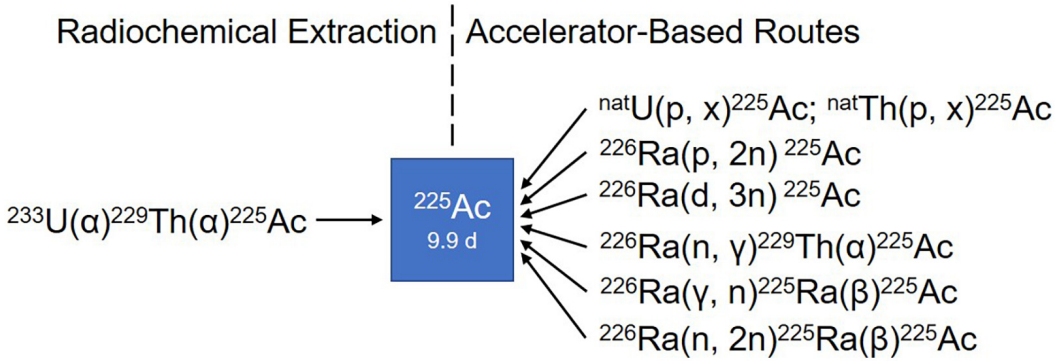


FIGURE 5
Production routes of $^{225}$Ac.

of preclinical studies have estimated $^{225}$Ac activity using measurements related to γ-emissions (111). However, a low probability of γ-emission and overlapping Bremsstrahlung due to β-emitters in the $^{225}$Ac decay chain preclude simultaneous treatment and dosimetry measurement in a clinical setting (84). Thus, current clinical TAT research relies greatly on indirect approximation by extrapolating pre-existing $^{177}$Lu-labeled pharmaceuticals (84, 112, 113). Preclinical studies focusing on $^{225}$Ac have used the standard approach described by the Medical Internal Radiation Dose (MIRD) committee. Total dosimetry was calculated from the summation of doses of $^{225}$Ac, $^{221}$Fr, $^{217}$At, $^{213}$Bi, and $^{213}$Po recorded in a biodistribution study (111). Unfortunately, collection of biodistribution data for dosimetry estimation is not possible for most α-emitters with therapeutic potential. This makes a direct and accurate preclinical dosimetry measurement for $^{225}$Ac to be extrapolated into and to guide clinical trials, as well as standardizing α-dosimetry measurement highly demanded in clinical application.

## Chelator

Finding a chelator to accommodate $^{225}$Ac and its progenies with sufficient stability was proven a great challenge given the range of different periodic properties of the daughters of $^{225}$Ac. The recoil effect associated with α-decay of $^{225}$Ac imparts an energy that is thousands of times greater than the binding energy of any chemical bond (75), resulting in an inevitable release of the daughter nuclide from the chelate moiety. Subsequently, the unbound α-emitting daughter nuclides are redistributed *in vivo* causing substantial harm to normal tissue and reducing the therapeutic effect. For example, the renal toxicity induced by $^{213}$Bi (in small animals) is considered a critical constraint to clinical use of $^{225}$Ac (114). However, recent results indicated that the release of free metals from DOTA may be not as evident as expected shown by fractioned radio-HPLC (115).

Finding a new chelator is one of the strategies to improve $^{225}$Ac-TAT. McDevitt et al. presented a comparison of $^{225}$Ac radiolabeling efficiency and *in vitro* stability of multiple chelators including DTPA, DOTA, TETA, DOTPA, TETPA, and DOTMP (116), and concluded that only DOTA and DOTMP showed chelation of $^{225}$Ac after 2 h at 37°C with radiochemical yields of >99 and 78%, respectively. Further *in vitro* serum stability testing showed that the $^{225}$Ac-DOTA complex outperformed the rest with >90% of complexes still intact after 10 days (104). Due to its outstanding stability, DOTA remains the gold standard for $^{225}$Ac-radiolabeling for all clinical research. However, DOTA has a decreased thermodynamic stability when used with larger metal ions. Moreover, chelation of $^{225}$Ac is a slow reaction demanding extensive heating and high amount of ligand for an adequate yield (77, 116, 117). Macropa, crown, and py4pa are new chelators with improved radiochemical yield and specific activity, as well as achievable labeling conditions. However, none of the new chelators was investigated enough so far to confirm *in vivo* stability, and their potential to translate into clinical application is yet to be assessed (118–122).

## Quality control of actinium-225-radiopharmaceuticals

In addition to complicated handling, standardized quality control of radiopharmaceuticals remains a problem in routine clinical production. Because of the complicated decay chain of Ac-225 (**Figure 4**), special methods must be used for both measurements of the activities and for quality control by radio-thin-layer chromatography (radio-TLC) and radio-high-performance-liquid chromatography (radio-HPLC). Since alpha emitters are difficult to detect directly, indirect measurements are usually used for all measurements by detecting the daughters

Fr-221 or Bi-213 (gamma emitters). Fr-221, with its short half-life of 4.9 min, is nearly in radioactive equilibrium after 60–120 min (123). In contrast, Bi-213, with a half-life of 45.6 min, takes hours to reach equilibrium. Thus, measurements of Fr-221 are often used for a faster quality control and release within a clinical environment. When separating free metals and labeled compounds on a TLC plate, the plate is equilibrated for an hour after development before being measured on a TLC scanner. During this period, a constant amount of Fr-221 has formed for both possible species, so comparison is possible, and a labeling yield can be determined. Afterward, an additional distinction must be made between the activity caused by the decay of Fr-221 and the activity of Bi-213. This can typically be differentiated in a gamma spectrometer by splitting the plate. Fr-221 has a line at 218 keV and Bi-213 at 440 keV (122, 124). However, the measurement with radio-TLC is not a valid method to determine the yield and purity of a radiopharmaceutical and additional radio-HPLC methods are required. Two possibilities are conceivable here. Direct detection of Ac-225 by liquid scintillation detection is relatively easy to implement, but may require large activities for injection, which is not always practical and can be very expensive. Therefore, indirect detection of the daughters can be used again by the fractionated collection of the measured sample and subsequent analysis of their components in a gamma spectrometer. In this way, the retention behavior of the compounds on the column can be investigated even when injecting small quantities, and possibly more precise statements can be made about side- or decomposition-products (115).

## Future of actinium-225-peptide receptor radionuclide therapy

### Combination with somatostatin receptor antagonist

Today, the development of novel SSTR antagonists holds promise for enhanced diagnostic accuracy and efficacy of SSTR-mediated imaging and therapy. SSTR2-selective $^{111}$In-DOTA-BASS (125) and SSTR3-selective ODN-8 (126, 127), the first generation of radiolabeled SSTR antagonists all recognized a larger number of binding sites and revealed an in general twofold higher uptake level *in vitro* than their agonist counterparts (128). Despite this, BASS labeled with $^{64}$Cu *via* the chelator 4, 11-bis(carboxymethyl)-1,4,8,11-tetraazabicyclo [6.6.2]hexadecane (CB-TE2A) ($^{64}$Cu-CB-TE2A-BASS) showed a compromised tumor uptake compared to the agonist $^{64}$Cu-CB-TE2A-octreotate in SSTR2-positive AR42J xenografts (129).

This suboptimal tumor uptake triggered the second generation of radiolabeled SSTR antagonists. In 2006, Ginj et al. presented the idea that radiolabeled SSTR antagonists may perform better than agonists despite the lack of receptor-mediated internalization (127). Despite its lack of internalization, SSTR antagonist demonstrated higher tumor uptake with a higher tumor-to-normal ratio and longer tumor retention time than that of agonist, possibly due to its capability to bind larger variety of receptor conformations, than that of SSTR agonists (130). The initial evidence that antagonists are superior to agonists guided the design and development of more potent SSTR2 antagonists with improved affinity (127, 131), with some of the potential antagonists studied as radiotracers. Among all the potential SSTR2 antagonists, LM3 and JR11 were the most interesting, having the highest hydrophilicity and best affinity. These two were evaluated in a comprehensive study, in combination with two chelators DOTA and NODAGA, and multiple radiometals (132, 133). Interestingly, $^{68}$Ga-DOTA-JR11 and -LM3, which have drastically lower affinities for SSTR2 (approximately 150-fold and 60-fold, respectively) than $^{68}$Ga-DOTATATE, showed higher tumor uptake (132). Likewise, the therapeutic counterpart $^{177}$Lu-DOTA-JR11 exhibited a higher tumor uptake, a longer tumor retention time, and an improved tumor-to-kidney ratio compared to $^{177}$Lu-DOTATATE (134), and hence led to a delayed tumor growth and an extended median survival period (135).

Lutetium-177-DOTA-JR11 was first compared in a pilot study with $^{177}$Lu-DOTATATE. In the same four patients with grade 1–3 metastatic NET, it showed a 1.7–10.6 times higher tumor dose, and at the same time a 1.1–7.2 times higher tumor-to-kidney and tumor-to-bone marrow ratio, compared with $^{177}$Lu-DOTATATE (136, 137). A phase I study with 20 grade 1–3 patients reported a best overall response of 45% (RECIST 1.1 criteria) and a median progression-free survival of 21 months (95% CI: 13.6-not reported). Unfortunately, grade 4 hematotoxicity was reported in 4 out of 7 patients after two cycles of $^{177}$Lu-DOTA-JR11, resulting in the suspension of this therapy protocol (138). The protocol was under subsequent modification to limit cumulative absorbed bone marrow dose. A phase I/II open-label study (Clinical trial identification: EudraCT: 2015-002867-41; NCT02592707) is currently ongoing to evaluate the safety and efficacy with the adjusted treatment regimen. Hitherto, only one abstract summarizing the promising efficacy and low toxicity is available. In 20 patients with adequate follow-up, no grade 3/4 renal toxicities and a 90% (95% CI: 68.3–98.8%) disease control rate was reported (139).

In parallel to $^{177}$Lu-DOTA-JR11, $^{177}$Lu-DOTA-LM3 was evaluated in 51 patients with metastatic neuroendocrine neoplasm at the Theranostics Center for Molecular Radiotherapy and Precision Oncology in Wiesbaden, Germany. $^{177}$Lu-DOTA-LM3 was reported to have a 3–5.1 times higher absorbed doses and a 22 h longer whole-body effective half-life than the agonist $^{177}$Lu-DOTATOC. All patients tolerated therapy well without any serious acute adverse effects, in particular, there was no nephrotoxicity observed (130).

Here we would like to showcase our recent therapeutic result of PRRT using $^{225}$Ac-DOTA LM3 to demonstrate the exciting

potential of $^{225}$Ac labeled SSTR antagonist in NET treatment (**Figure 6**). A 40-year-old pancreatic-NET patient suffered from bilobar liver metastases and extensive bone metastasis even after multiple cycles of PRRT with $^{177}$Lu-DOTATATE, and compromised therapeutic response after one cycle of $^{177}$Lu-DOTA-LM3 treatment, was suggested for PRRT with $^{225}$Ac-DOTA-LM3. This case with β-radiation refractory metastatic NET demonstrated incredibly auspicious therapeutic response after two cycles of $^{225}$Ac-DOTA-LM3, especially concerning the bone metastases. With this successful case reported for the first time, we would like to suggest that PRRT with $^{225}$Ac-labeled SSRT antagonist can potentially be a game changer in therapeutic nuclear medicine, and a promising cure for metastasized tumor.

Moreover, the pharmacodynamics of SSTR antagonists have been studied as the clinical interest for them is rapidly growing. The antagonist showed faster association, but slower dissociation, as well as longer cellular retention time compared to the agonist. Moreover, antagonists recognize more binding sites than agonists, providing more targeting opportunities (140). Taking the proposed mechanism, preclinical and clinical studies into consideration, it is obvious that using radiolabeled SSTR antagonists, especially LM3 and JR11, may provide more successful imaging and PRRT strategies for neuroendocrine tumors, even those with relatively low SSTR expression (130, 137, 141) compared to agonists.

## Cocktail approach

Most PRRTs using radiolabeled SSAs and antagonists has until now depended substantially on the most prominently expressed SSTR2 (142). However, NET expression of SSTR subtypes is heterogeneous, and things are made even more difficult by contradictory expression profiles due to different detection methods (20, 143–153). Also, the downregulation or loss of SSTR2 in advanced stages is inherently associated with worse disease prognosis, compromised image sensitivity, and suboptimal therapy with SSTR2-specific radiolabeled SSAs. Using SSTR agonists and antagonists with affinity to more SSTR subtypes is therefore a proposed method—a cocktail approach—of great clinical interest (154). An impressive clinical case

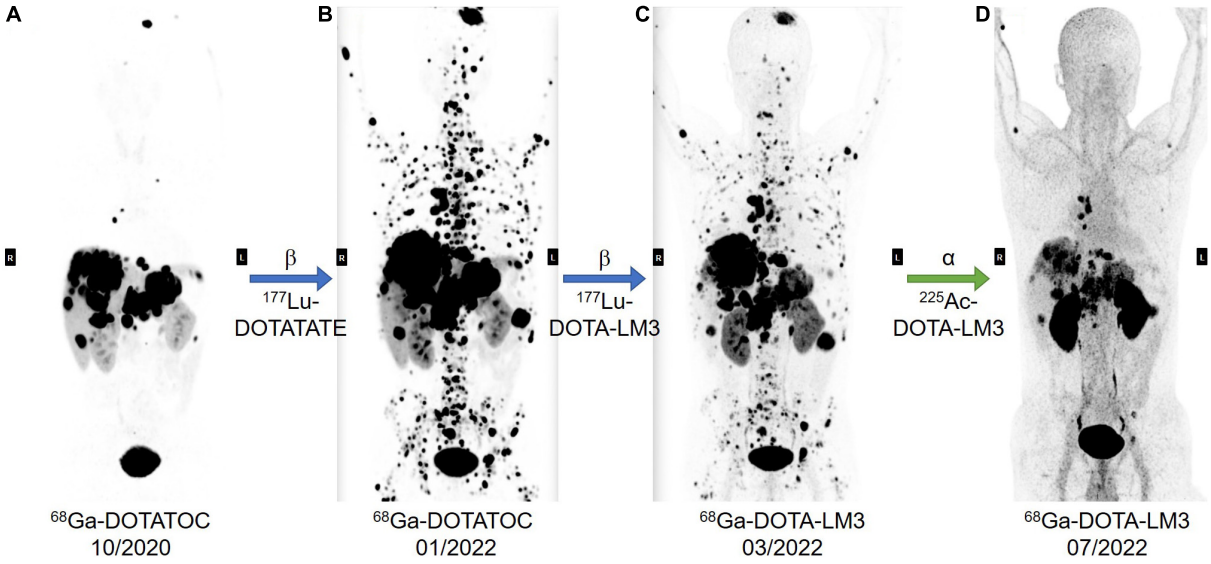


FIGURE 6
A 40-year-old patient was diagnosed with poorly differentiated non-functioning pancreatic-NET with bilobar liver and extensive bone metastases, Ki-67 index of 25% NEN-G3 without known mutations. The patients had previously undergone laparoscopic subtotal pancreatic resection and splenectomy, CAPTEM chemotherapy, transarterial chemoembolization (TACE) of right liver lobe and resection of abdominal lesion. In addition, the patient had previous ineffective treatment with Lanreotide, Everolimus, and Sunitinib. In total, the patient had received eight cycles of PRRT, and had a very poor prognosis, extensive bone metastases, even after multiple cycles treatment with $^{177}$Lu-DOTATATE (**A,B**, $^{68}$Ga-DOTATOC PET/CT before and after $^{177}$Lu-DOTATATE treatment). The 9th PRRT cycle was performed with $^{177}$Lu-DOTA-LM3 (**B,C**, PET/CT imaging before and after $^{177}$Lu-DOTA-LM3 treatment), and the last two cycles with $^{225}$Ac DOTA-LM3 (**C,D**, PET/CT imaging before and after $^{225}$Ac-DOTA-LM3 treatment), 10 MBq in March and 15 MBq in May 2022, respectively. The cumulative administered radio activities are 66.7 GBq of $^{177}$Lu and 25 MBq $^{225}$Ac. Restaging result in July 2022 showed excellent response to $^{225}$Ac-DOTA-LM3 treatment with partial remission according to the THERCIST. As shown in the most recent PET/CT, there is dramatic improvement, especially concerning the previous innumerable bone metastases in the spine, ribs, and pelvis. The primary tumor in the pancreas, and the liver and bone metastases further decreased in size and number, and no new metastatic lesions were noted. The patient felt dramatically better in comparison to the previous treatments. After the last PRRT, he only experienced mild alopecia and mild pain in the upper right abdomen over 1 week, and has been physically active and gained 3 kg body weight over the past 2 months.

showing the application of this cocktail approach, where six tracers were given to a single patient with prostate cancer, was reported at the 2016 SNMMI Highlights Lecture (155). Inspired by the cocktail approach in treating prostate cancer, using SSTR analogs and antagonists targeting various SSTR subtypes in combination with $^{225}$Ac-PRRT is worth exploring.

## Conclusion

Peptide receptor radionuclide therapy in NET patients has come a long way since Krenning's first treatments in the 1990s. Novel radionuclides are constantly being developed and tested, in a race to find the perfect theranostic pair. Modified chelators and new ligands including SSTR antagonists are gaining more and more attention, the latter in particular as they have been revealed to give great tumor uptake, retention time and tumor-to-background ratio. $^{225}$Ac in particular is very worth investigating.

The rise of the α-emitters as a compliment or replacement to β-emitters is one of the most exciting recent developments. The shorter range gives "precision" in precision medicine a new meaning: Even less damage to surrounding healthy tissue and even more powerful damage to tumor cells.

To this date, confirmed literature on PRRT using an α-emitter with a SSTR antagonist has yet to be published, and obviously, there are still many hurdles to overcome. Technical ones, such as how to best combine chemical moieties into a stable, pharmacokinetically feasible drug; economical ones, such as how to best implement a global mass production of radionuclides for research and clinical use; clinical ones, such as how to set a dosage of the existing theranostic pairs that minimizes toxicity whilst maximizing tumor uptake. Yet, to have the recent promising clinical studies on $^{177}$Lu-DOTA-LM3 and -JR11 in mind at the same time as the potentials of TAT is intriguing; hopefully a new and promising era for NET therapy will see daylight in the foreseeable future.

## Author contributions

JZ, XC, and RB: study conception and design. MS, VJ, and RB: data collection. MS and JZ: analysis and interpretation of results. MS and VJ: writing—original draft preparation. JZ, LG, P-LK, RB, and XC: writing—review and editing. All authors reviewed the results and approved the final version of the manuscript.

## Funding

This study was supported by the National University of Singapore Start-up grant (NUHSRO/2021/097/Startup/13 and NUHSRO/2020/133/Startup/08), NUS School of Medicine, Nanomedicine Translational Research Program (NUHSRO/2021/034/TRP/09/Nanomedicine), and the International Centers for Precision Oncology (ICPO) Foundation.

## Conflict of interest

The authors declare that the research was conducted in the absence of any commercial or financial relationships that could be construed as a potential conflict of interest.

## Publisher's note

All claims expressed in this article are solely those of the authors and do not necessarily represent those of their affiliated organizations, or those of the publisher, the editors and the reviewers. Any product that may be evaluated in this article, or claim that may be made by its manufacturer, is not guaranteed or endorsed by the publisher.

## References

1. Rindi G, Inzani F. Neuroendocrine neoplasm update: toward universal nomenclature. *Endocr Relat Cancer*. (2020) 27:R211–8. doi: 10.1530/ERC-20-0036

2. Taal BG, Visser O. Epidemiology of neuroendocrine tumours. *Neuroendocrinology*. (2004) 80(Suppl. 1):3–7. doi: 10.1159/000080731

3. Kulke MH, Siu LL, Tepper JE, Fisher G, Jaffe D, Haller DG, et al. Future directions in the treatment of neuroendocrine tumors: consensus report of the National Cancer Institute Neuroendocrine Tumor clinical trials planning meeting. *J Clin Oncol.* (2011) 29:934–43. doi: 10.1200/JCO.2010.33.2056

4. Dasari A, Shen C, Halperin D, Zhao B, Zhou S, Xu Y, et al. Trends in the incidence, prevalence, and survival outcomes in patients with neuroendocrine tumors in the United States. *JAMA Oncol.* (2017) 3:1335–42. doi: 10.1001/jamaoncol.2017.0589

5. Oberg K, Akerström G, Rindi G, Jelic S. Neuroendocrine gastroenteropancreatic tumours: ESMO Clinical Practice Guidelines for diagnosis, treatment and follow-up. *Ann Oncol.* (2010) 21(Suppl. 5):V223–7. doi: 10.1093/annonc/mdq192

6. Kos-Kudła B, Blicharz-Dorniak J, Handkiewicz-Junak D, Jarząb B, Jarząb M, Kunikowska J, et al. Diagnostic and therapeutic guidelines for gastro-entero-pancreatic neuroendocrine neoplasms (recommended by the Polish Network of Neuroendocrine Tumours). *Endokrynol Pol.* (2013) 64:418–43.

7. Trofimiuk-Müldner M, Lewkowicz E, Wysocka K, Pach D, Kiełtyka A, Stefańska A, et al. Epidemiology of gastroenteropancreatic neuroendocrine neoplasms in Krakow and Krakow district in 2007-2011. *Endokrynol Pol.* (2017) 68:42–6.

8. Klimstra DS, Modlin IR, Coppola D, Lloyd RV, Suster S. The pathologic classification of neuroendocrine tumors: a review of nomenclature, grading,

and staging systems. *Pancreas.* (2010) 39:707–12. doi: 10.1097/MPA.0b013e3181ec124e

9. Metz DC, Choi J, Strosberg J, Heaney AP, Howden CW, Klimstra D, et al. A rationale for multidisciplinary care in treating neuroendocrine tumours. *Curr Opin Endocrinol Diabetes Obes.* (2012) 19:306–13. doi: 10.1097/MED.0b013e32835570f1

10. Oberg K, Kvols L, Caplin M, Delle Fave G, de Herder W, Rindi G, et al. Consensus report on the use of somatostatin analogs for the management of neuroendocrine tumors of the gastroenteropancreatic system. *Ann Oncol.* (2004) 15:966–73. doi: 10.1093/annonc/mdh216

11. Sowa-Staszczak A, Hubalewska-Dydejczyk A, Tomaszuk M. PRRT as neoadjuvant treatment in NET. *Recent Results Cancer Res.* (2013) 194:479–85. doi: 10.1007/978-3-642-27994-2_27

12. Das S, Al-Toubah T, Strosberg J. Chemotherapy in neuroendocrine tumors. *Cancers.* (2021) 13:4872. doi: 10.3390/cancers13194872

13. Papamichail DG, Exadaktylou PE, Chatzipavlidou VD. [Neuroendocrine tumors: peptide receptors radionuclide therapy (PRRT)]. *Hell J Nucl Med.* (2016) 19:75–82.

14. Rinke A, Müller HH, Schade-Brittinger C, Klose KJ, Barth P, Wied M, et al. Placebo-controlled, double-blind, prospective, randomized study on the effect of octreotide LAR in the control of tumor growth in patients with metastatic neuroendocrine midgut tumors: a report from the PROMID Study Group. *J Clin Oncol.* (2009) 27:4656–63. doi: 10.1200/JCO.2009.22.8510

15. Faiss S, Pape U-F, Böhmig M, Dörffel Y, Mansmann U, Golder WA. Prospective, randomized, multicenter trial on the antiproliferative effect of lanreotide, interferon alfa, and their combination for therapy of metastatic neuroendocrine gastroenteropancreatic tumors–the International Lanreotide and Interferon Alfa Study Group. *J Clin Oncol.* (2003) 14:2689–96. doi: 10.1200/JCO.2003.12.142

16. Dash A, Knapp FF, Pillai MR. Targeted radionuclide therapy–an overview. *Curr Radiopharm.* (2013) 6:152–80. doi: 10.2174/18744710113066660023

17. Volkert WA, Hoffman TJ. Therapeutic radiopharmaceuticals. *Chem Rev.* (1999) 99:2269–92. doi: 10.1021/cr9804386

18. Hirmas N, Jadaan R, Al-Ibraheem A. Peptide receptor radionuclide therapy and the treatment of gastroentero-pancreatic neuroendocrine tumors: current findings and future perspectives. *Nucl Med Mol Imaging.* (2018) 52:190–9. doi: 10.1007/s13139-018-0517-x

19. Partelli S, Bertani E, Bartolomei M, Perali C, Muffatti F, Grana CM, et al. Peptide receptor radionuclide therapy as neoadjuvant therapy for resectable or potentially resectable pancreatic neuroendocrine neoplasms. *Surgery*. (2018) 163:761–67. doi: 10.1016/j.surg.2017.11.007

20. Reubi JC, Waser B. Concomitant expression of several peptide receptors in neuroendocrine tumours: molecular basis for in vivo multireceptor tumour targeting. *Eur J Nucl Med Mol Imaging.* (2003) 30:781–93. doi: 10.1007/s00259-003-1184-3

21. Krenning EP, Bakker WH, Breeman WA, Koper JW, Kooij PP, Ausema L, et al. Localisation of endocrine-related tumours with radioiodinated analogue of somatostatin. *Lancet.* (1989) 1:242–4. doi: 10.1016/S0140-6736(89)91258-0

22. Patel YC, Wheatley T. *In vivo* and *in vitro* plasma disappearance and metabolism of somatostatin-28 and somatostatin-14 in the rat. *Endocrinology.* (1983) 112:220–5. doi: 10.1210/endo-112-1-220

23. Bakker WH, Albert R, Bruns C, Breeman WAP, Hofland LJ, Marbach P, et al. [$^{111}$In-DTPA-D-Phe1]-octreotide, a potential radiopharmaceutical for imaging of somatostatin receptor-positive tumors: synthesis, radiolabeling and *in vitro* validation. *Life Sci.* (1991) 49:1583–91. doi: 10.1016/0024-3205(91)90052-D

24. Krenning EP, Bakker WH, Kooij PP, Breeman WA, Oei HY, de Jong M, et al. Somatostatin receptor scintigraphy with indium-111-DTPA-D-Phe-1-octreotide in man: metabolism, dosimetry and comparison with iodine-123-Tyr-3-octreotide. *J Nucl Med.* (1992) 33:652–8.

25. Krenning EP, Kwekkeboom DJ, Bakker WH, Breeman WA, Kooij PP, Oei HY, et al. Somatostatin receptor scintigraphy with [$^{111}$In-DTPA-D-Phe1]- and [$^{123}$I-Tyr3]-octreotide: the Rotterdam experience with more than 1000 patients. *Eur J Nucl Med.* (1993) 20:716–31. doi: 10.1007/BF00181765

26. Krenning EP, Kooij PP, Bakker WH, Breeman WA, Postema PT, Kwekkeboom DJ, et al. Radiotherapy with a radiolabeled somatostatin analogue, [$^{111}$In-DTPA-D-Phe1]-octreotide. A case history. *Ann N Y Acad Sci.* (1994) 733:496–506. doi: 10.1111/j.1749-6632.1994.tb17300.x

27. Feijtel D, de Jong M, Nonnekens J. Peptide receptor radionuclide therapy: looking back, looking forward. *Curr Top Med Chem.* (2020) 20:2959–69. doi: 10.2174/1568026620666200226104652

28. Otte A, Jermann E, Behe M, Goetze M, Bucher HC, Roser HW, et al. DOTATOC: a powerful new tool for receptor-mediated radionuclide therapy. *Eur J Nucl Med.* (1997) 24:792–5. doi: 10.1007/BF00879669

29. de Jong M, Bakker WH, Krenning EP, Breeman WA, van der Pluijm ME, Bernard BF, et al. Yttrium-90 and indium-111 labelling, receptor binding and biodistribution of [DOTA0, d-Phe1,Tyr3]octreotide, a promising somatostatin analogue for radionuclide therapy. *Eur J Nucl Med.* (1997) 24:368–71. doi: 10.1007/BF00881807

30. Otte A, Herrmann R, Heppeler A, Behe M, Jermann E, Powell P, et al. Yttrium-90 DOTATOC: first clinical results. *Eur J Nucl Med.* (1999) 26:1439–47. doi: 10.1007/s002590050476

31. Otte A, Mueller-Brand J, Dellas S, Nitzsche EU, Herrmann R, Maecke HR. Yttrium-90-labelled somatostatin-analogue for cancer treatment. *Lancet.* (1998) 351:417–8. doi: 10.1016/S0140-6736(05)78355-0

32. de Jong M, Breeman WA, Bakker WH, Kooij PP, Bernard BF, Hofland LJ, et al. Comparison of $^{111}$In-labeled somatostatin analogues for tumor scintigraphy and radionuclide therapy. *Cancer Res.* (1998) 58:437–41.

33. de Jong M, Breeman WA, Bernard BF, Bakker WH, Schaar M, van Gameren A, et al. [$^{177}$Lu-DOTA(0),Tyr3] octreotate for somatostatin receptor-targeted radionuclide therapy. *Int J Cancer.* (2001) 92:628–33. doi: 10.1002/1097-0215(20010601)92:5<628::AID-IJC1244>3.0.CO;2-L

34. Strosberg J, El-Haddad G, Wolin E, Hendifar A, Yao J, Chasen B, et al. Phase 3 Trial of (177)Lu-Dotatate for Midgut Neuroendocrine Tumors. *N Engl J Med.* (2017) 376:125–35. doi: 10.1056/NEJMoa1607427

35. Levine R, Krenning EP. Clinical history of the theranostic radionuclide approach to neuroendocrine tumors and other types of cancer: historical review based on an interview of eric P. krenning by rachel levine. *J Nucl Med.* (2017) 58(Suppl. 2):3S–9S. doi: 10.2967/jnumed.116.186502

36. Nelson KL, Sheetz MA. Radiation safety observations associated with 177lu dotatate patients. *Health Phys.* (2019) 117:680–7. doi: 10.1097/HP.0000000000001122

37. Hennrich U, Kopka K. Lutathera§: The First FDA- and EMA-approved radiopharmaceutical for peptide receptor radionuclide therapy. *Pharmaceuticals.* (2019) 12:114. doi: 10.3390/ph12030114

38. Fortune BE, Jackson J, Leonard J, Trotter JF. Vapreotide: a somatostatin analog for the treatment of acute variceal bleeding. *Expert Opin Pharmacother.* (2009) 10:2337–42. doi: 10.1517/14656560903207019

39. Kvols LK, Woltering EA. Role of somatostatin analogs in the clinical management of non-neuroendocrine solid tumors. *Anticancer Drugs.* (2006) 17:601–8. doi: 10.1097/01.cad.0000210335.95828.ed

40. Prasad V, Srirajaskanthan R, Toumpanakis C, Grana CM, Baldari S, Shah T, et al. Lessons from a multicentre retrospective study of peptide receptor radionuclide therapy combined with lanreotide for neuroendocrine tumours: a need for standardised practice. *Eur J Nucl Med Mol Imaging.* (2020) 47:2358–71. doi: 10.1007/s00259-020-04712-2

41. Lewington VJ. Targeted radionuclide therapy for neuroendocrine tumours. *Endocr Relat Cancer.* (2003) 10:497–501. doi: 10.1677/erc.0.0100497

42. Laudicella R, Albano D, Annunziata S, Calabrò D, Argiroffi G, Abenavoli E, et al. Theragnostic use of radiolabelled dota-peptides in meningioma: from clinical demand to future applications. *Cancers.* (2019) 11:1412. doi: 10.3390/cancers11101412

43. Sommerauer M, Burkhardt JK, Frontzek K, Rushing E, Buck A, Krayenbuehl N, et al. $^{68}$Gallium-DOTATATE PET in meningioma: a reliable predictor of tumor growth rate? *Neuro Oncol.* (2016) 18:1021–7. doi: 10.1093/neuonc/now001

44. Acker G, Kluge A, Lukas M, Conti A, Pasemann D, Meinert F, et al. Impact of 68Ga-DOTATOC PET/MRI on robotic radiosurgery treatment planning in meningioma patients: first experiences in a single institution. *Neurosurg Focus FOC.* (2019) 46:E9. doi: 10.3171/2019.3.FOCUS1925

45. Gehler B, Paulsen F, Öksüz MÖ, Hauser T-K, Eschmann SM, Bares R, et al. [$^{68}$Ga]-DOTATOC-PET/CT for meningioma IMRT treatment planning. *Radiat Oncol.* (2009) 4:56. doi: 10.1186/1748-717X-4-56

46. Henze M, Schuhmacher J, Hipp P, Kowalski J, Becker DW, Doll J, et al. PET imaging of somatostatin receptors using [$^{68}$GA]DOTA-D-Phe1-Tyr3-octreotide: first results in patients with meningiomas. *J Nucl Med.* (2001) 42:1053–6.

47. Ivanidze J, Roytman M, Lin E, Magge RS, Pisapia DJ, Liechty B, et al. Gallium-68 DOTATATE PET in the evaluation of intracranial meningiomas. *J Neuroimaging.* (2019) 29:650–6. doi: 10.1111/jon.12632

48. Rachinger W, Stoecklein VM, Terpolilli NA, Haug AR, Ertl L, Pöschl J, et al. Increased 68Ga-DOTATATE uptake in PET imaging discriminates meningioma and tumor-free tissue. *J Nucl Med.* (2015) 56:347–53. doi: 10.2967/jnumed.114.149120

49. Hennrich U, Benešová M. [$^{68}$Ga]Ga-DOTA-TOC: The First FDA-Approved $^{68}$Ga-Radiopharmaceutical for PET Imaging. *Pharmaceuticals.* (2020) 13:38. doi: 10.3390/ph13030038

50. Wu T-J, Chiu H-Y, Yu J, Cautela MP, Sarmento B, das Neves J, et al. Nanotechnologies for early diagnosis, in situ disease monitoring, and prevention. In: Uskoković V, Uskoković DP editors. *Nanotechnologies in Preventive and Regenerative Medicine*. Amsterdam: Elsevier (2018). 1–92. doi: 10.1016/B978-0-323-48063-5.00001-0

51. Chinol M, Franceschini R, Paganelli G, Pecorale A, Paiano A. Simple Production of Yttrium-90 in a Chemical form Suitable to Clinical Grade Radioconjugates. In: Bergmann H, Kroiss A, Sinzinger H editors. *Radioactive Isotopes in Clinical Medicine and Research*. Basel: Birkhäuser Basel (1997). 327–32. doi: 10.1007/978-3-0348-7772-5_49

52. Kunikowska J, Królicki L, Hubalewska-Dydejczyk A, Mikołajczak R, Sowa-Staszczak A, Pawlak D. Clinical results of radionuclide therapy of neuroendocrine tumours with 90Y-DOTATATE and tandem 90Y/177Lu-DOTATATE: which is a better therapy option? *Eur J Nucl Med Mol Imaging.* (2011) 38:1788–97. doi: 10.1007/s00259-011-1833-x

53. Bodei L, Cremonesi M, Ferrari M, Pacifici M, Grana CM, Bartolomei M, et al. Long-term evaluation of renal toxicity after peptide receptor radionuclide therapy with 90Y-DOTATOC and 177Lu-DOTATATE: the role of associated risk factors. *Eur J Nucl Med Mol Imaging.* (2008) 35:1847–56. doi: 10.1007/s00259-008-0778-1

54. Cremonesi M, Ferrari ME, Bodei L, Chiesa C, Sarnelli A, Garibaldi C, et al. Correlation of dose with toxicity and tumour response to 90Y- and 177Lu-PRRT provides the basis for optimization through individualized treatment planning. *Eur J Nucl Med Mol Imaging.* (2018) 45:2426–41. doi: 10.1007/s00259-018-4044-x

55. Todorović-Tirnanić M, Kaemmerer D, Prasad V, Hommann M, Baum RP. *Intraoperative Somatostatin Receptor Detection After Peptide Receptor Radionuclide Therapy with 177Lu- and 90Y-DOTATOC (Tandem PRRNT) in a Patient with a Metastatic Neuroendocrine Tumor. Theranostics, Gallium-68, and Other Radionuclides*. Berlin: Springer (2013). doi: 10.1007/978-3-642-27994-2_28

56. Baum RP, Kulkarni HR, Singh A, Kaemmerer D, Mueller D, Prasad V, et al. Results and adverse events of personalized peptide receptor radionuclide therapy with (90)Yttrium and (177)Lutetium in 1048 patients with neuroendocrine neoplasms. *Oncotarget.* (2018) 9:16932–50. doi: 10.18632/oncotarget.24524

57. Kunikowska J, Królicki L. Targeted α-emitter therapy of neuroendocrine tumors. *Semin Nucl Med.* (2020) 50:171–6. doi: 10.1053/j.semnuclmed.2019.11.003

58. Kassis AI, Adelstein SJ. Radiobiologic principles in radionuclide therapy. *J Nucl Med.* (2005) 46(Suppl. 1):4S–12S.

59. Sgouros G. Alpha-particles for targeted therapy. *Adv Drug Deliv Rev.* (2008) 60:1402–6. doi: 10.1016/j.addr.2008.04.007

60. Pouget JP, Constanzo J. Revisiting the radiobiology of targeted alpha therapy. *Front Med.* (2021) 8:692436. doi: 10.3389/fmed.2021.692436

61. Brechbiel MW. Targeted alpha-therapy: past, present, future? *Dalton Trans.* (2007) 43:4918–28. doi: 10.1039/b704726f

62. Zalutsky MR, Bigner DD. Radioimmunotherapy with alpha-particle emitting radioimmunoconjugates. *Acta Oncol.* (1996) 35:373–9. doi: 10.3109/02841869609101654

63. Zalutsky MR, Schuster JM, Garg PK, Archer GE Jr, Dewhirst MW, Bigner DD. Two approaches for enhancing radioimmunotherapy: alpha emitters and hyperthermia. *Recent Results Cancer Res.* (1996) 141:101–22. doi: 10.1007/978-3-642-79952-5_7

64. Poty S, Francesconi LC, McDevitt MR, Morris MJ, Lewis JS. α-Emitters for Radiotherapy: From Basic Radiochemistry to Clinical Studies-Part 1. *J Nucl Med.* (2018) 59:878–84. doi: 10.2967/jnumed.116.186338

65. Nikula TK, McDevitt MR, Finn RD, Wu C, Kozak RW, Garmestani K, et al. Alpha-emitting bismuth cyclohexylbenzyl DTPA constructs of recombinant humanized anti-CD33 antibodies: pharmacokinetics, bioactivity, toxicity and chemistry. *J Nucl Med.* (1999) 40:166–76.

66. Raju MR, Eisen Y, Carpenter S, Inkret WC. Radiobiology of alpha particles. III. Cell inactivation by alpha-particle traversals of the cell nucleus. *Radiat Res.* (1991) 128:204–9. doi: 10.2307/3578139

67. Koh TT, Bezak E, Chan D, Cehic G. Targeted alpha-particle therapy in neuroendocrine neoplasms: a systematic review. *World J Nucl Med.* (2021) 20:329–35. doi: 10.4103/wjnm.wjnm_160_20

68. Nelson BJB, Andersson JD, Wuest F. Targeted alpha therapy: progress in radionuclide production, radiochemistry, and applications. *Pharmaceutics.* (2021) 13:49. doi: 10.3390/pharmaceutics13010049

69. Tafreshi NK, Doligalski ML, Tichacek CJ, Pandya DN, Budzevich MM, El-Haddad G, et al. Development of targeted alpha particle therapy for solid tumors. *Molecules.* (2019) 24:4314. doi: 10.3390/molecules24234314

70. Wadas TJ, Pandya DN, Solingapuram Sai KK, Mintz A. Molecular targeted α-particle therapy for oncologic applications. *AJR Am J Roentgenol.* (2014) 203:253–60. doi: 10.2214/AJR.14.12554

71. Elgqvist J, Frost S, Pouget JP, Albertsson P. The potential and hurdles of targeted alpha therapy - clinical trials and beyond. *Front Oncol.* (2014) 3:324. doi: 10.3389/fonc.2013.00324

72. Kim YS, Brechbiel MW. An overview of targeted alpha therapy. *Tumour Biol.* (2012) 33:573–90. doi: 10.1007/s13277-011-0286-y

73. Jadvar H, Colletti PM. Targeted α-therapy in non-prostate malignancies. *Eur J Nucl Med Mol Imaging.* (2021) 49:47–53. doi: 10.1007/s00259-021-05405-0

74. Imam SK. Advancements in cancer therapy with alpha-emitters: a review. *Int J Radiat Oncol Biol Phys.* (2001) 51:271–8. doi: 10.1016/S0360-3016(01)01585-1

75. de Kruijff RM, Wolterbeek HT, Denkova AGA. Critical review of alpha radionuclide therapy-how to deal with recoiling daughters? *Pharmaceuticals.* (2015) 8:321–36. doi: 10.3390/ph8020321

76. Adloff JP. The centenary of a controversial discovery: actinium. *Radiochim Acta.* (2000) 88:123–8. doi: 10.1524/ract.2000.88.3-4.123

77. McDevitt MR, Ma D, Lai LT, Simon J, Borchardt P, Frank RK, et al. Tumor therapy with targeted atomic nanogenerators. *Science.* (2001) 294:1537–40. doi: 10.1126/science.1064126

78. Scheinberg DA, McDevitt MR. Actinium-225 in targeted alpha-particle therapeutic applications. *Curr Radiopharm.* (2011) 4:306–20. doi: 10.2174/1874471011104040306

79. Chen X, Ji M, Fisher DR, Wai CM. Monofunctionalization of Calix[4]arene Tetracarboxylic Acid at the Upper Rim with Isothiocyanate Group: first bifunctional chelating agent for Alpha-Emitter Ac-225. *Synlett.* (1999) 11:1784–6. doi: 10.1055/s-1999-2944

80. Deal KA, Davis IA, Mirzadeh S, Kennel SJ, Brechbiel MW. Improved in vivo stability of actinium-225 macrocyclic complexes. *J Med Chem.* (1999) 42:2988–92. doi: 10.1021/jm990141f

81. Morgenstern A, Apostolidis C, Bruchertseifer F. Supply and clinical application of Actinium-225 and Bismuth-213. *Semin Nucl Med.* (2020) 50:119–23. doi: 10.1053/j.semnuclmed.2020.02.003

82. Rosenblat TL, McDevitt MR, Pandit-Taskar N, Carrasquillo JA, Chanel S, Frattini MG, et al. Phase I trial of the targeted alpha-particle nano-generator Actinium-225 (225Ac)-HuM195 (Anti-CD33) in Acute Myeloid Leukemia (AML). *Blood.* (2007) 110:910. doi: 10.1182/blood.V110.11.910.910

83. Kratochwil C, Bruchertseifer F, Giesel FL, Weis M, Verburg FA, Mottaghy F, et al. 225Ac-PSMA-617 for PSMA-Targeted α-Radiation therapy of metastatic castration-resistant prostate cancer. *J Nucl Med.* (2016) 57:1941–4. doi: 10.2967/jnumed.116.178673

84. Kratochwil C, Bruchertseifer F, Rathke H, Bronzel M, Apostolidis C, Weichert W, et al. Targeted α-Therapy of metastatic castration-resistant prostate cancer with (225)Ac-PSMA-617: dosimetry estimate and empiric dose finding. *J Nucl Med.* (2017) 58:1624–31. doi: 10.2967/jnumed.117.191395

85. Sathekge M, Bruchertseifer F, Knoesen O, Reyneke F, Lawal I, Lengana T, et al. (225)Ac-PSMA-617 in chemotherapy-naive patients with advanced prostate cancer: a pilot study. *Eur J Nucl Med Mol Imaging.* (2019) 46:129–38. doi: 10.1007/s00259-018-4167-0

86. Sathekge M, Bruchertseifer F, Vorster M, Lawal IO, Knoesen O, Mahapane J, et al. Predictors of Overall and Disease-Free Survival in Metastatic Castration-Resistant Prostate Cancer Patients Receiving $^{225}$Ac-PSMA-617 Radioligand Therapy. *J Nucl Med.* (2020) 61:62–9. doi: 10.2967/jnumed.119.229229

87. Kratochwil C, Bruchertseifer F, Giesel F, Apostolidis C, Haberkorn U, Morgenstern A. Ac-225-DOTATOC - an empiric dose finding for alpha particle emitter based radionuclide therapy of neuroendocrine tumors. *J Nucl Med.* (2015) 56(Suppl. 3):1232.

88. Morgenstern A, Bruchertseifer F, Apostolidis C. Targeted alpha therapy with 213Bi. *Curr Radiopharm.* (2011) 4:295–305. doi: 10.2174/1874471011104040295

89. Apostolidis C, Molinet R, Rasmussen G, Morgenstern A. Production of Ac-225 from Th-229 for targeted alpha therapy. *Anal Chem.* (2005) 77:6288–91. doi: 10.1021/ac0580114

90. Zielinska B, Apostolidis C, Bruchertseifer F, Morgenstern A. An Improved Method for the Production of Ac-225/Bi-213 from Th-229 for Targeted Alpha Therapy. *Solv Extract Ion Exchang.* (2007) 25:339–49. doi: 10.1080/07366290701285108

91. Boll RA, Malkemus D, Mirzadeh S. Production of actinium-225 for alpha particle mediated radioimmunotherapy. *Appl Radiat Isot.* (2005) 62:667–79. doi: 10.1016/j.apradiso.2004.12.003

92. Samsonov M, Nerozin N, Podsoblyaev D, Prokof'ev I, Tkachev S, Khamianov S, et al. Isolation of alpha-emitting radionuclides for nuclear medicine in JSC "SSC RF–IPPE". *Proceedings of the 10th International Symposium on Targeted Alpha Therapy*. Kanazawa (2017).

93. Morgenstern A, Apostolidis C, Kratochwil C, Sathekge M, Krolicki L, Bruchertseifer F. An overview of targeted alpha therapy with $^{225}$Actinium and $^{213}$Bismuth. *Curr Radiopharm.* (2018) 11:200–8. doi: 10.2174/1874471011666180502104524

94. Ahenkorah S, Cassells I, Deroose CM, Cardinaels T, Burgoyne AR, Bormans G, et al. Bismuth-213 for targeted radionuclide therapy: from atom to bedside. *Pharmaceutics.* (2021) 13:599. doi: 10.3390/pharmaceutics13050599

95. Weidner JW, Mashnik SG, John KD, Hemez F, Ballard B, Bach H, et al. Proton-induced cross sections relevant to production of 225Ac and 223Ra in natural thorium targets below 200 MeV. *Appl Radiat Isot.* (2012) 70:2602–7. doi: 10.1016/j.apradiso.2012.07.006

96. Weidner JW, Mashnik SG, John KD, Ballard B, Birnbaum ER, Bitteker LJ, et al. $^{225}$Ac and $^{223}$Ra production via 800 MeV proton irradiation of natural thorium targets. *Appl Radiat Isot.* (2012) 70:2590–5. doi: 10.1016/j.apradiso.2012.07.003

97. Ermolaev SV, Zhuikov BL, Kokhanyuk VM, Matushko VL, Kalmykov SN, Aliev RA, et al. Production of actinium, thorium and radium isotopes from natural thorium irradiated with protons up to 141 MeV. *Radiochim Acta.* (2012) 100:223–9. doi: 10.1524/ract.2012.1909

98. Zhuikov BL, Kalmykov SN, Ermolaev SV, Aliev RA, Kokhanyuk VM, Matushko VL, et al. Production of $^{225}$Ac and $^{223}$Ra by irradiation of Th with accelerated protons. *Radiochemistry.* (2011) 53:73–80. doi: 10.1134/S1066362211010103

99. Abergel R, An D, Lakes A, Rees J, Gauny S. Actinium Biokinetics and Dosimetry: What is the Impact of Ac-227 in Accelerator-Produced Ac-225? *J Med Imaging Radiat Sci.* (2019) 50(Suppl. 1):S23. doi: 10.1016/j.jmir.2019.03.073

100. Apostolidis C, Molinet R, McGinley J, Abbas K, Möllenbeck J, Morgenstern A. Cyclotron production of Ac-225 for targeted alpha therapy. *Appl Radiat Isot.* (2005) 62:383–7. doi: 10.1016/j.apradiso.2004.06.013

101. Braccini S. Compact Medical Cyclotrons and their use for Radioisotope Production and Multi-disciplinary Research. *Proceedings of Cyclotrons 2016*. Zurich (2017).

102. Morgenstern A, Abbas K, Bruchertseifer F, Apostolidis C. Production of alpha emitters for targeted alpha therapy. *Curr Radiopharm.* (2008) 1:135–43. doi: 10.2174/1874471010801030135

103. Melville G, Meriarty H, Metcalfe P, Knittel T, Allen BJ. Production of Ac-225 for cancer therapy by photon-induced transmutation of Ra-226. *Appl Radiat Isot.* (2007) 65:1014–22. doi: 10.1016/j.apradiso.2007.03.018

104. Robertson KHA, Ramogida FC, Schaffer P, Radchenko V. Development of $^{225}$Ac Radiopharmaceuticals: TRIUMF perspectives and experiences. *Curr Radiopharm.* (2018) 11:156–72. doi: 10.2174/1874471011666180416161908

105. Sgouros G, He B, Ray N, Ludwig DL, Frey EC. Dosimetric impact of Ac-227 in accelerator-produced Ac-225 for alpha-emitter radiopharmaceutical therapy of patients with hematological malignancies: a pharmacokinetic modeling analysis. *EJNMMI Phys.* (2021) 8:60. doi: 10.1186/s40658-021-00410-6

106. Ackerman NL, Graves EE. The potential for Cerenkov luminescence imaging of alpha-emitting radionuclides. *Phys Med Biol.* (2012) 57:771–83. doi: 10.1088/0031-9155/57/3/771

107. Rasheed R, Usmani S, Naqvi SAR, Alkandari F, Marafi F. Alpha Therapy with $^{225}$Actinium Labeled Prostate Specific Membrane Antigen: Reporting New Photopeak of 78 Kilo-electron Volts for Better Image Statistics. *Indian J Nucl Med.* (2019) 34:76–7. doi: 10.4103/ijnm.IJNM_115_18

108. Usmani S, Rasheed R, Al Kandari F, Marafi F, Naqvi SAR. 225Ac Prostate-Specific Membrane Antigen Posttherapy α Imaging: Comparing 2 and 3 Photopeaks. *Clin Nucl Med.* (2019) 44:401–3. doi: 10.1097/RLU.0000000000002525

109. Vatsa R, Sood A, Vadi SK, Das CK, Kaur K, Parmar M, et al. 225Ac-PSMA-617 radioligand posttherapy imaging in metastatic castrate-resistant prostate cancer patient using 3 photopeaks. *Clin Nucl Med.* (2020) 45:437–8. doi: 10.1097/RLU.0000000000003031

110. McDevitt MR, Finn RD, Sgouros G, Ma D, Scheinberg DA. An 225Ac/213Bi generator system for therapeutic clinical applications: construction and operation. *Appl Radiat Isot.* (1999) 50:895–904. doi: 10.1016/S0969-8043(98)00151-1

111. Tafreshi NK, Tichacek CJ, Pandya DN, Doligalski ML, Budzevich MM, Kil H, et al. Melanocortin 1 Receptor-Targeted α-Particle Therapy for Metastatic Uveal Melanoma. *J Nucl Med.* (2019) 60:1124–33. doi: 10.2967/jnumed.118.217240

112. Kratochwil C, Giesel FL, Stefanova M, Benešová M, Bronzel M, Afshar-Oromieh A, et al. PSMA-targeted radionuclide therapy of metastatic castration-resistant prostate cancer with $^{177}$Lu-Labeled PSMA-617. *J Nucl Med.* (2016) 57:1170–6. doi: 10.2967/jnumed.115.171397

113. Kabasakal L, AbuQbeitah M, Aygün A, Yeyin N, Ocak M, Demirci E, et al. Pre-therapeutic dosimetry of normal organs and tissues of $^{177}$Lu-PSMA-617 prostate-specific membrane antigen (PSMA) inhibitor in patients with castration-resistant prostate cancer. *Eur J Nucl Med Mol Imaging.* (2015) 42:1976–83. doi: 10.1007/s00259-015-3125-3

114. Jaggi JS, Kappel BJ, McDevitt MR, Sgouros G, Flombaum CD, Cabassa C, et al. Efforts to control the errant products of a targeted in vivo generator. *Cancer Res.* (2005) 65:4888–95. doi: 10.1158/0008-5472.CAN-04-3096

115. Hooijman EL, Chalashkan Y, Ling SW, Kahyargil FF, Segbers M, Bruchertseifer F, et al. Development of [$^{225}$Ac]Ac-PSMA-I&T for Targeted Alpha Therapy According to GMP Guidelines for Treatment of mCRPC. *Pharmaceutics.* (2021) 13:715. doi: 10.3390/pharmaceutics13050715

116. McDevitt MR, Ma D, Simon J, Frank RK, Scheinberg DA. Design and synthesis of 225Ac radioimmunopharmaceuticals. *Appl Radiat Isot.* (2002) 57:841–7. doi: 10.1016/S0969-8043(02)00167-7

117. Miederer M, Henriksen G, Alke A, Mossbrugger I, Quintanilla-Martinez L, Senekowitsch-Schmidtke R, et al. Preclinical evaluation of the alpha-particle generator nuclide 225Ac for somatostatin receptor radiotherapy of neuroendocrine tumors. *Clin Cancer Res.* (2008) 14:3555–61. doi: 10.1158/1078-0432.CCR-07-4647

118. Yang H, Wilson JJ, Orvig C, Li Y, Wilbur DS, Ramogida CF, et al. Harnessing α-emitting radionuclides for therapy: radiolabeling method review. *J Nucl Med.* (2022) 63:5–13. doi: 10.2967/jnumed.121.262687

119. Yang H, Zhang C, Yuan Z, Rodriguez-Rodriguez C, Robertson A, Radchenko V, et al. Synthesis and evaluation of a macrocyclic Actinium-225 Chelator, Quality Control and In Vivo Evaluation of (225) Ac-crown-αMSH Peptide. *Chemistry.* (2020) 26:11435–40. doi: 10.1002/chem.202002999

120. Thiele NA, Brown V, Kelly JM, Amor-Coarasa A, Jermilova U, MacMillan SN, et al. An Eighteen-Membered Macrocyclic Ligand for Actinium-225 Targeted Alpha Therapy. *Angew Chem Int Ed Engl.* (2017) 56:14712–7. doi: 10.1002/anie.201709532

121. Li L, Rousseau J, Jaraquemada-Peláez MG, Wang X, Robertson A, Radchenko V, et al. (225)Ac-H(4)py4pa for Targeted Alpha Therapy. *Bioconjug Chem.* (2021) 32:1348–63. doi: 10.1021/acs.bioconjchem.0c00171

122. Pretze M, Kunkel F, Runge R, Freudenberg R, Braune A, Hartmann H, et al. Ac-EAZY! Towards GMP-Compliant Module Syntheses of $^{225}$Ac-Labeled Peptides for Clinical Application. *Pharmaceuticals.* (2021) 14:652. doi: 10.3390/ph14070652

123. Kelly J, Amor-Coarasa A, Sweeney E, Wilson J, Causey P, Babich J. *A Consensus Time for Performing Quality Control of 225Ac-Labeled Radiopharmaceuticals*. Durham, NC: Research Square (2021). doi: 10.21203/rs.3.rs-39342/v2

124. Thakral P, Simecek J, Marx S, Kumari J, Pant V, Sen IB. In-House Preparation and Quality Control of Ac-225 Prostate-Specific Membrane Antigen-617 for the Targeted Alpha Therapy of Castration-Resistant Prostate Carcinoma. *Ind J Nucl Med.* (2021) 36:114–9. doi: 10.4103/ijnm.ijnm_200_20

125. Bass RT, Buckwalter BL, Patel BP, Pausch MH, Price LA, Strnad J, et al. Identification and characterization of novel somatostatin antagonists. *Mol Pharmacol.* (1996) 50:709–15.

126. Reubi JC, Schaer JC, Wenger S, Hoeger C, Erchegyi J, Waser B, et al. SST3-selective potent peptidic somatostatin receptor antagonists. *Proc Natl Acad Sci U.S.A.* (2000) 97:13973–8. doi: 10.1073/pnas.250483897

127. Ginj M, Zhang H, Waser B, Cescato R, Wild D, Wang X, et al. Radiolabeled somatostatin receptor antagonists are preferable to agonists for in vivo peptide receptor targeting of tumors. *Proc Natl Acad Sci U.S.A.* (2006) 103:16436–41. doi: 10.1073/pnas.0607761103

128. Wang X, Fani M, Schulz S, Rivier J, Reubi JC, Maecke HR. Comprehensive evaluation of a somatostatin-based radiolabelled antagonist for diagnostic imaging and radionuclide therapy. *Eur J Nucl Med Mol Imaging.* (2012) 39:1876–85. doi: 10.1007/s00259-012-2231-8

129. Wadas TJ, Eiblmaier M, Zheleznyak A, Sherman CD, Ferdani R, Liang K, et al. Preparation and biological evaluation of 64Cu-CB-TE2A-sst2-ANT, a somatostatin antagonist for PET imaging of somatostatin receptor-positive tumors. *J Nucl Med.* (2008) 49:1819–27. doi: 10.2967/jnumed.108.054502

130. Baum RP, Zhang J, Schuchardt C, Müller D, Mäcke H. First-in-Humans Study of the SSTR Antagonist $^{177}$Lu-DOTA-LM3 for Peptide Receptor Radionuclide Therapy in Patients with Metastatic Neuroendocrine Neoplasms: Dosimetry, Safety, and Efficacy. *J Nucl Med.* (2021) 62:1571–81. doi: 10.2967/jnumed.120.258889

131. Cescato R, Erchegyi J, Waser B, Piccand V, Maecke HR, Rivier JE, et al. Design and in vitro characterization of highly sst2-selective somatostatin antagonists suitable for radiotargeting. *J Med Chem.* (2008) 51:4030–7. doi: 10.1021/jm701618q

132. Fani M, Braun F, Waser B, Beetschen K, Cescato R, Erchegyi J, et al. Unexpected sensitivity of sst2 antagonists to N-terminal radiometal modifications. *J Nucl Med.* (2012) 53:1481–9. doi: 10.2967/jnumed.112.102764

133. Fani M, Del Pozzo L, Abiraj K, Mansi R, Tamma ML, Cescato R, et al. PET of somatostatin receptor-positive tumors using $^{64}$Cu- and $^{68}$Ga-somatostatin antagonists: the chelate makes the difference. *J Nucl Med.* (2011) 52:1110–8. doi: 10.2967/jnumed.111.087999

134. Nicolas GP, Mansi R, McDougall L, Kaufmann J, Bouterfa H, Wild D, et al. Biodistribution, Pharmacokinetics, and Dosimetry of $^{177}$ Lu-, $^{90}$ Y-, and $^{111}$In-Labeled Somatostatin Receptor Antagonist OPS201 in Comparison to the Agonist $^{177}$Lu-DOTATATE: The Mass Effect. *J Nucl Med.* (2017) 58:1435–41. doi: 10.2967/jnumed.117.191684

135. Dalm SU, Nonnekens J, Doeswijk GN, de Blois E, van Gent DC, Konijnenberg MW, et al. Comparison of the Therapeutic Response to Treatment with a 177Lu-labeled somatostatin receptor agonist and antagonist in preclinical models. *J Nucl Med.* (2016) 57:260–5. doi: 10.2967/jnumed.115.167007

136. Wild D, Fani M, Fischer R, Del Pozzo L, Kaul F, Krebs S, et al. Comparison of somatostatin receptor agonist and antagonist for peptide receptor radionuclide therapy: a pilot study. *J Nucl Med.* (2014) 55:1248–52. doi: 10.2967/jnumed.114.138834

137. Fani M, Mansi R, Nicolas GP, Wild D. Radiolabeled somatostatin analogs-a continuously evolving class of radiopharmaceuticals. *Cancers.* (2022) 14:1172. doi: 10.3390/cancers14051172

138. Reidy-Lagunes D, Pandit-Taskar N, O'Donoghue JA, Krebs S, Staton KD, Lyashchenko SK, et al. Phase I Trial of Well-Differentiated Neuroendocrine Tumors (NETs) with Radiolabeled Somatostatin Antagonist $^{177}$Lu-Satoreotide Tetraxetan. *Clin Cancer Res.* (2019) 25:6939–47. doi: 10.1158/1078-0432.CCR-19-1026

139. Nicolas G, Ansquer C, Lenzo N, Grønbaek H, Haug A, Navalkissoor S, et al. 1160O An international open-label study on safety and efficacy of 177Lu-satoreotide tetraxetan in somatostatin receptor positive neuroendocrine tumours (NETs): An interim analysis. *Ann Oncol.* (2020) 31:S771. doi: 10.1016/j.annonc.2020.08.1373

140. Mansi R, Plas P, Vauquelin G, Fani M. Distinct In Vitro Binding Profile of the Somatostatin Receptor Subtype 2 Antagonist [$^{177}$Lu]Lu-OPS201 Compared to the Agonist [$^{177}$Lu]Lu-DOTA-TATE. *Pharmaceuticals.* (2021) 14:1265. doi: 10.3390/ph14121265

141. Fani M, Nicolas GP, Wild D. Somatostatin receptor antagonists for imaging and therapy. *J Nucl Med.* (2017) 58(Suppl. 2):61S–6S. doi: 10.2967/jnumed.116.186783

142. Klomp MJ, Dalm SU, de Jong M, Feelders RA, Hofland J, Hofland LJ. Epigenetic regulation of somatostatin and somatostatin receptors in neuroendocrine tumors and other types of cancer. *Rev Endocr Metab Disord.* (2021) 22:495–510. doi: 10.1007/s11154-020-09607-z

143. Papotti M, Bongiovanni M, Volante M, Allìa E, Landolfi S, Helboe L, et al. Expression of somatostatin receptor types 1-5 in 81 cases of gastrointestinal and pancreatic endocrine tumors. a correlative immunohistochemical and reverse-transcriptase polymerase chain reaction analysis. *Virchows Arch.* (2002) 440:461–75. doi: 10.1007/s00428-002-0609-x

144. Kulaksiz H, Eissele R, Rössler D, Schulz S, Höllt V, Cetin Y, et al. Identification of somatostatin receptor subtypes 1, 2A, 3, and 5 in neuroendocrine tumours with subtype specific antibodies. *Gut.* (2002) 50:52–60. doi: 10.1136/gut.50.1.52

145. Jaïs P, Terris B, Ruszniewski P, LeRomancer M, Reyl-Desmars F, Vissuzaine C, et al. Somatostatin receptor subtype gene expression in human endocrine gastroentero-pancreatic tumours. *Eur J Clin Invest.* (1997) 27:639–44. doi: 10.1046/j.1365-2362.1997.1740719.x

146. Hu Y, Ye Z, Wang F, Qin Y, Xu X, Yu X, et al. Role of somatostatin receptor in pancreatic neuroendocrine tumor development, diagnosis, and therapy. *Front Endocrinol.* (2021) 12:679000. doi: 10.3389/fendo.2021.679000

147. Wängberg B, Nilsson O, Johanson VV, Kölby L, Forssell-Aronsson E, Andersson P, et al. Somatostatin receptors in the diagnosis and therapy of neuroendocrine tumor. *Oncologist.* (1997) 2:50–8. doi: 10.1634/theoncologist.2-1-50

148. Remes SM, Leijon HL, Vesterinen TJ, Arola JT, Haglund CH. Immunohistochemical expression of somatostatin receptor subtypes in a panel of neuroendocrine neoplasias. *J Histochem Cytochem.* (2019) 67:735–43. doi: 10.1369/0022155419856900

149. Jonas S, John M, Boese-Landgraf J, Häring R, Prevost G, Thomas F, et al. Somatostatin receptor subtypes in neuroendocrine tumor cell lines and tumor tissues. *Langenbecks Arch Chir.* (1995) 380:90–5. doi: 10.1007/BF00186414

150. Lambertini C, Barzaghi-Rinaudo P, D'Amato L, Schulz S, Nuciforo P, Schmid HA. Evaluation of somatostatin receptor subtype expression in human neuroendocrine tumors using two sets of new monoclonal antibodies. *Regul Pept.* (2013) 187:35–41. doi: 10.1016/j.regpep.2013.10.007

151. Lou E, Gandhi N, Farrell A, Xiu J, Seeber A, Beg SS, et al. Differential expression of somatostatin receptor (SSTR) subtypes across a spectrum of neuroendocrine neoplasms (NENs). *J Clin Oncol.* (2022) 40(16_suppl):3071. doi: 10.1200/JCO.2022.40.16_suppl.3071

152. Kaemmerer D, Athelogou M, Lupp A, Lenhardt I, Schulz S, Luisa P, et al. Somatostatin receptor immunohistochemistry in neuroendocrine tumors: comparison between manual and automated evaluation. *Int J Clin Exp Pathol.* (2014) 7:4971–80.

153. Kanakis G, Grimelius L, Spathis A, Tringidou R, Rassidakis GZ, Öberg K, et al. Expression of Somatostatin Receptors 1-5 and dopamine receptor 2 in lung carcinoids: implications for a therapeutic role. *Neuroendocrinology.* (2015) 101:211–22. doi: 10.1159/000381061

154. Reubi JC, Maecke HR. Approaches to multireceptor targeting: hybrid radioligands, radioligand cocktails, and sequential radioligand applications. *J Nucl Med.* (2017) 58(Suppl. 2):10S–6S. doi: 10.2967/jnumed.116.186882

155. Weber WA. 2016 SNMMI highlights lecture: oncology, part 1. *J Nucl Med.* (2017) 58:9N–15N.

156. Graf F, Fahrer J, Maus S, Morgenstern A, Bruchertseifer F, Venkatachalam S, et al. DNA double strand breaks as predictor of efficacy of the alpha-particle emitter Ac-225 and the electron emitter Lu-177 for somatostatin receptor targeted radiotherapy. *PLoS One.* (2014) 9:e88239. doi: 10.1371/journal.pone.0088239

157. Tafreshi NK, Pandya DN, Tichacek CJ, Budzevich MM, Wang Z, Reff JN, et al. Preclinical evaluation of [$^{225}$Ac]Ac-DOTA-TATE for treatment of lung neuroendocrine neoplasms. *Eur J Nucl Med Mol Imaging.* (2021) 48:3408–21. doi: 10.1007/s00259-021-05315-1

158. Zhang J, Singh A, Kulkarni HR, Schuchardt C, Müller D, Wester HJ, et al. From bench to bedside-the bad berka experience with first-in-human studies. *Semin Nucl Med.* (2019) 49:422–37. doi: 10.1053/j.semnuclmed.2019.06.002

159. Ballal S, Yadav MP, Bal C, Sahoo RK, Tripathi M. Broadening horizons with $^{225}$Ac-DOTATATE targeted alpha therapy for gastroenteropancreatic neuroendocrine tumour patients stable or refractory to (177)Lu-DOTATATE PRRT: first clinical experience on the efficacy and safety. *Eur J Nucl Med Mol Imaging.* (2020) 47:934–46. doi: 10.1007/s00259-019-04567-2

160. Ocak M, Toklu T, Demirci E, Selçuk N, Kabasakal L. Post-therapy imaging of $^{225}$Ac-DOTATATE treatment in a patient with recurrent neuroendocrine tumor. *Eur J Nucl Med Mol Imaging.* (2020) 47:2711–2. doi: 10.1007/s00259-020-04725-x

161. Kamaleshwaran KK, Suneelkumar M, Madhusairam R, Radhakrishnan EK, Arunpandiyan S, Arnold VJ. Whole-body and Single-Photon Emission Computed Tomography/Computed Tomography Postpeptide Receptor Alpha Radionuclide Therapy Images of Actinium 225-Tetraazacyclododecanetetraacetic Acid-Octreotide as a Primary Modality of Treatment in a Patient with Advanced Rectal Neuroendocrine Tumor with Metastases. *Indian J Nucl Med.* (2020) 35:226–8. doi: 10.4103/ijnm.IJNM_58_20

162. Zhang J, Kulkarni HR, Baum RP. Peptide Receptor Radionuclide Therapy Using 225Ac-DOTATOC Achieves Partial Remission in a Patient With Progressive Neuroendocrine Liver Metastases After Repeated β-emitter peptide receptor radionuclide therapy. *Clin Nucl Med.* (2020) 45:241–3. doi: 10.1097/RLU.0000000000002915

163. Zhang J, Kulkarni HR, Baum RP. 225Ac-DOTATOC-Targeted Somatostatin Receptor α-Therapy in a Patient With Metastatic Neuroendocrine Tumor of the Thymus, Refractory to β-Radiation. *Clin Nucl Med.* (2021) 46:1030–1. doi: 10.1097/RLU.0000000000003792

164. Satapathy S, Sood A, Das CK, Kavanal AJ, Mittal BR. Alpha Before Beta: Exceptional Response to First-Line 225Ac-DOTATATE in a Patient of Metastatic Neuroendocrine Tumor With Extensive Skeletal Involvement. *Clin Nucl Med.* (2022) 47:e156–7. doi: 10.1097/RLU.0000000000003823

165. Kavanal AJ, Satapathy S, Sood A, Khosla D, Mittal BR. Subclinical Hypothyroidism After 225Ac-DOTATATE Therapy in a Case of Metastatic Neuroendocrine Tumor: Unknown Adverse Effect of PRRT. *Clin Nucl Med.* (2022) 47:e184–6. doi: 10.1097/RLU.0000000000003893

166. Budlewski T, Król ZJ, Bruchertseifer F, Majkowska-Pilip A, Morgenstern A, Wierzba W. Innovative radioisotope therapy for patients with neuroendocrine tumors using an alpha (225Ac) emitter labeled somatostatin analog: octreotate. a promising new treatment for advanced, progressive neuroendocrine neoplasms. *Pol Arch Intern Med.* (2022) 132:16275. doi: 10.20452/pamw.16275

167. Alan Selçuk N, Demirci E, Ocak M, Toklu T, Ergen S, Kabasakal L. Almost complete response with a single administration $^{225}$Ac-DOTATATE in a patient with a metastatic neuroendocrine tumor of unknown primary. *Mol Imaging Radionucl Ther.* (2022) 31:139–41. doi: 10.4274/mirt.galenos.2022.64497

168. Ballal S, Yadav MP, Tripathi M, Sahoo RK, Bal C. Survival outcomes in metastatic gastroenteropancreatic neuroendocrine tumor patients receiving concomitant $^{225}$Ac-DOTATATE targeted alpha therapy and capecitabine: a real-world scenario management based long-term outcome study. *J Nucl Med.* (2022) [Epub ahead of print]. doi: 10.2967/jnumed.122.264043

frontiers | Frontiers in Medicine

TYPE Review
PUBLISHED 16 December 2022
DOI 10.3389/fmed.2022.1085245



OPEN ACCESS

EDITED BY
Asta Juzeniene,
Oslo University Hospital, Norway

REVIEWED BY
Lurdes Gano,
Centro de Ciências e Tecnologias Nucleares (C2TN), Portugal
Ralf Bergmann,
Semmelweis University, Hungary

*CORRESPONDENCE
Jolanta Kunikowska
jolanta.kunikowska@wum.edu.pl

SPECIALTY SECTION
This article was submitted to Nuclear Medicine, a section of the journal Frontiers in Medicine

RECEIVED 31 October 2022
ACCEPTED 28 November 2022
PUBLISHED 16 December 2022

CITATION
Kunikowska J, Morgenstern A, Pełka K, Bruchertseifer F and Królicki L (2022) Targeted alpha therapy for glioblastoma.
*Front. Med.* 9:1085245.
doi: 10.3389/fmed.2022.1085245



# Targeted alpha therapy for glioblastoma

Jolanta Kunikowska [1]*, Alfred Morgenstern[2], Kacper Pełka[1,3], Frank Bruchertseifer[2] and Leszek Królicki[1]

[1]Department of Nuclear Medicine, Medical University of Warsaw, Warsaw, Poland, [2]European Commission, Joint Research Centre (JRC), Karlsruhe, Germany, [3]Laboratory of Center for Preclinical Research, Department of Methodology, Medical University of Warsaw, Warsaw, Poland

According to the 2021 World Health Organization Classification of Tumors of the Central Nervous System, glioblastoma (GB) is a primary brain tumor and presents with the worst prognosis. Due to its infiltrating characteristic, molecular heterogeneity, and only partly preserved function of the blood-brain barrier, the median overall survival time is short (9–15 months), regardless of comprehensive treatment including surgery, radiotherapy, and chemotherapy. Several novel treatment strategies are under investigation. Unfortunately, none of them produced successful results; 90% of patients have a recurrence of the disease within 6 months. Local administration of the drug could be a promising approach to delivering treatment with minimized side effects, due to the recurrence of 95% glioblastomas in a margin of 2 cm at the primary site. Several ligand-receptor systems have been evaluated, such as targeting tenascin, the extracellular matrix protein, or radiolabeled somatostatin analogs, as it is overexpressed with the SSTR-2 receptor system in around 80% of gliomas. Moreover, this study revealed that the NK-1 receptor is overexpressed in GB, suggesting that substance P (SP) may serve as a ligand. A variety of radioisotopes, beta- ($^{131}$I, $^{90}$Y, or $^{177}$Lu) and alpha emitters ($^{213}$Bi, $^{225}$Ac, or $^{211}$At), with different physical properties were tested for treatment. Alpha particles have many advantages over beta radiation such as short range with higher linear energy transfer. According to that characteristic, it is extremely dose delivered to the targeted cells, while reducing harm to nearby healthy tissue. Additionally, the biological effect of alpha radiation is independent of the cell cycle phase, cell oxygenation and O-6-methylguanine-DNA methyltransferase (*MGMT*) gene promoter methylation status. In this article, we summarize the experience with local treatment of primary and secondary GBs with locally used radioisotopes such as [$^{213}$Bi]Bi-DOTA-SP or [$^{225}$Ac]Ac-DOTA-SP.

KEYWORDS

**glioblastoma, glioma, alpha therapy, substance P, actinium, bismuth, SP, GB**

## Introduction

The most aggressive primary brain tumor with the worst prognosis is glioblastoma multiforme [called glioblastoma (GB) since 2016], according to the World Health Organization (WHO) Classification of Tumors of the Central Nervous System (CNS). At the end of Louis et al. (1) WHO in the fifth edition of CNS introduced significant changes to the tumor entities and classification.

Currently, the diagnosis of GB requires the recognition of genetic changes such as no mutation of isocitrate dehydrogenase 1 and 2 (IDH-wild type) and no mutation in histone 3 (H3-wildtype), which makes it impossible to classify the entries as not otherwise specified (NOS). In this article, based on the classification used in the discussed studies, we use the nomenclature from 2016.

Glioblastoma originates from the glial cells, which are the supportive tissue in the brain. GB grows expeditiously, and therefore, it infiltrates the surrounding healthy brain tissue. Consequently, the entire tumor is nearly impossible to excise. Moreover, a single tumor consists of different types of cells. Hence, a drug targeted at specific cells may not work on the other cells.

The survival rate in patients with GB is low, i.e., approximately 40% in the first-year post-diagnosis and 17% in the following year (2, 3). The standard treatment includes surgery, radiotherapy (RT), and chemotherapy with a median overall survival time of only up to 9–15 months (2, 3).

Therefore, it is necessary to search for new drugs and different forms of treatment. Distributing medicament to the destined area is also challenging. The blood vessels in the CNS are impenetrable to toxins and diseases from the blood. This blood-brain barrier protects the brain and spinal cord. Nonetheless, it also prevents many drugs from penetrating into GB. In that scenario, the possibility of finding local administration seems attractive.

To fulfill the concept of theragnostics, target and applied isotopes should be defined.

## Target

Several targeting vectors have been used during glioma treatment.

Their mechanism of action is a criterion of their classification:

- Targeted molecular therapies: *BRAFV600* mutation, EGFR, Exportin-1, EGFR mutations, mTOR, VEGF; the angiogenesis and its mediators such as VEGF seem to be particularly attractive targets.
- DNA-damaging agents, including RT and cytotoxic chemotherapy. A significant direction in the improvement of these methods increases their influence on cancer cells, saving the healthy ones. One of the innovative approaches is also targeting the tumor-specific DNA repair mechanism.

Targeting tumor metabolism. The data show that the regulators of GB metabolism can be used as prognostic, diagnostic, and perhaps also therapeutic tools aimed at facilitating the choice of glioblastoma treatment. Observations from several studies indicate that tumor genotype and the brain's biochemical and cellular microenvironment shape the metabolic reprogramming of glioblastoma cells, which also informs the decisions about the choice of targeted treatment.

- Immunotherapies (EGFR peptide vaccinate, anti-dendritic cell vaccinate, viral therapies, and nivolumab–checkpoint inhibitor).

Transforming growth factor-β (TGF-β) is a key molecule, which is responsible for glioblastoma-mediated immunosuppression; programmed cell death protein 1 (PD-1) is neutralizing antibodies to immune checkpoint molecules and is now leading in the field of cancer immunotherapy.

In the previous studies, some of the targets were clinically evaluated for targeting radionuclide therapy of glioma (4–8).

Zalutsky et al. (7) first evaluated the antibodies targeting tenascin as a biologically active peptide that significantly contributes to angiogenesis in glioblastoma. Tenascin activity in stem cell niches and the central nervous system was highlighted. A relationship has been demonstrated between the grade of malignancy and the expression of tenascin C. Moreover, tenascin may be one of the factors influencing the plasticity of cancer cells, i.e., the mutual conversion of transformed non-stem cells into cancer stem cells. In addition, tenascin may play the role in cancer cell plasticity, i.e., in the reciprocal conversion of transformed non-stem cells to cancer stem cells.

Thereafter, Merlo et al. and Schumacher et al. (4, 8) used the overexpression of the SSTR-2 receptor system as an approach for targeted treatment. In total, 80% of glioma tumors have been shown to express SSTR-2, which is particularly often in grades II and III and less often in grade IV (4). Human macrophages are characterized by especially the expression and upregulation of SSTR2, including tumor-associated macrophages (TAMs) and/or microglia. These components account for up to 40% of GB cells. TAMs foster the growth of malignant glioma by secreting proangiogenic factors, generation of a local immunosuppressive microenvironment, and stimulating invasion through the production of interleukin (IL)-10, TGF-β, matrix metallopeptidase-9, and vascular endothelial growth factor.

Substance P (SP), the main ligand of neurokinin type 1 receptor (NK-1) which is consistently overexpressed in all gliomas irrespective of the degree of malignancy, was

first applied by Kneifel et al. (5). NK-1 receptors were also identified on the cells of tumor-infiltrating the intertumoral and peritumoral vasculature (9). SP is an undecapeptide composed of the amino acid chain Arg-Pro-Lys-Pro-Gln-Gln-Phe-Phe-Gly-Leu-Met, with an amidation at the C-terminus. The vector has a low molecular weight of only 1.8 kDa, which is a sufficient condition and distribution between tumors after local injection. This characteristic allows for rapid diffusion in the brain and renders radiolabeled SP analogs, which makes them very promising candidates for the local treatment of glial tumors.

## Isotopes

The energy, range of radiation, and type of emission are critical in targeted radionuclide therapy. These parameters play a crucial role in the radiobiological process in which the final effect is the death of tumor cells. We could divide the radioisotopes into two types, namely, β-emitting isotopes: $^{131}$I, $^{90}$Y, and $^{177}$Lu and α-emitting isotopes: $^{225}$Ac, $^{213}$Bi, and $^{211}$At.

In the first pilot study for glioma treatment, the $\beta^-$ emitters including $^{90}$Y and $^{177}$Lu were used (the detailed physical parameters are listed in **Table 1**) (5). The range of both is millimeters (for $^{177}$Lu 3–4 mm, and for $^{90}$Y up to 10 mm), thus taking into the consideration, "cross-fire effect" and the brain as a critical organ–with tumors located near very sensitive areas and responsible for physiological process structure–the range appears to be too long. Another disadvantage of $\beta^-$ emitters is that even in high-energy emitting conditions, they are not powerful enough to induce the double-strand breaks of DNA, but rather work by the indirect effects.

In contrast to that scenario, alpha-emitting radionuclides have distinguishing features that may be useful in the targeted therapy, like a relatively small range of impact (<100 μm) and high linear energy transfer (LET ≈100 keV/μm). In human tissue, those advantages led to providing therapeutic doses to targeted cells while limiting the harm to the surrounding non-cancerous tissue. Alpha radiation has a predominantly direct effect on cell death because it induces double-strand breaks of DNA, occurring along the trajectory of densely ionizing particles, and it is largely independent of the cell oxygenation status and the cell cycle phase (10–13). Of the several alpha emitters suitable for use in anti-cancer therapy, the pair of radionuclides derived from $^{225}$Ac to $^{213}$Bi generators have proven to be particularly promising. The preferred chemical attributes of the trivalent metalions Ac(III) and Bi(III) allow obtaining a solid connection to biomolecules using the common DOTA chelate molecules (1,4,7,10-tetraazacyclododecane-1,4,7,10-tetraacetic acid).

TABLE 1 The detailed physical parameters of isotope use for local glioblastoma treatment.

| | $^{177}$Lu | $^{90}$Y | $^{213}$Bi | $^{225}$Ac |
|---|---|---|---|---|
| Half-life | 6.71 day | 64.0 h | 46 min | 9.9 day |
| Radiation | β−, γ (17%) | β− | α, β− | α |
| Mean beta energy | 133 keV | 933 keV | 435 keV | |
| Range in water | 0.25 mm | 4.3 mm | 1.45 mm | |
| Maximum beta energy | 497 keV | 2,284 keV | 1,422 KeV | |
| Range in water | 1.9 mm | 11.8 mm | 6.65 mm | |
| Maximum alpha energy | | | 8.4 MeV* | 5.9 MeV |
| Range in water | | | 85 μm* | 47 μm |

*Energy and range of alpha particle emitted by $^{213}$Po daughter nuclide.

## Clinical studies with targeted radioisotope therapy for glioma

The main indications for local targeted treatment in glial tumors are as follows:

- Critically located primary brain tumor.
- Recurrent primary brain tumor.
- Recurrent secondary brain tumor.

The first pilot study to provide the proof of principle that there is a suitable and specific distribution of the radiopharmaceutical to the tumor was performed on a group of 20 glioma patients with WHO grades II–IV. The patients had a local intratumoral injection of radiolabeled SP (5). Initially, most of the patients (18/20) were treated with the SP labeled with beta emitters $^{90}$Y and $^{177}$Lu. Only in a subset of two patients with critically located tumors, the alpha emitter $^{213}$Bi was used to reduce the "crossfire effect." Stable disease or improvement in neurological conditions was observed in the majority of the patients (13/20). The toxicity of treatment was limited only to one patient with symptomatic radiogenic edema.

Another study focused on the usage of the intertumoral injections of [$^{90}$Y]Y-DOTAGA- SP as a neoadjuvant treatment before the surgery in patients with GB. The majority of patients (15/17) had stabilization or improvement in their functional status. Neoadjuvant therapy of glioblastoma with locally injected [$^{90}$Y]Y-DOTAGA-SP is feasible and has low toxicity. Moreover, it was helpful to achieve a prognostically significant degree of resections (14).

To increase the delivery of energy and minimize the "crossfire effect," future works should be focused on the alpha emitters.

The first pilot study of local injections of [$^{213}$Bi]Bi-DOTA-[Thi8,Met(O2)11]-substance P ([$^{213}$Bi]Bi-DOTA-SP) was performed in patients with critically localized gliomas (15). Treatment was well tolerated by all patients, and the follow-up MRI suggested radiation-induced necrosis and tumor demarcation. Some of the patients underwent subsequent resection, which confirmed necrosis in histopathological

validation. Although the injection was done to critically locate gliomas, no neurologic deficit was observed. The study found that targeted local radiotherapy with [$^{213}$Bi]Bi-DOTA-SP may be an ingenious and beneficial treatment strategy for malignant gliomas that are unfavorably located, as primarily no surgical gliomas can be resected after the intertumoral radioisotope treatment.

The study for recurrent glioma tumor grades II-IV with [$^{213}$Bi]Bi-DOTA-SP has been carried out at the Medical University of Warsaw.

The analysis of 18 patients with the recurrence of primary glioma grade IV treated with [$^{213}$Bi]Bi-DOTA-SP after standard treatment demonstrated favorable survival parameters: the PFS was 3.7 months and OS was 8.5 months, measured from the start of radioisotope treatment. The median overall survival from the start of the primary diagnosis (OS-d) was 21.5 months and the median survival from the diagnosis of the recurrence (OS-r) was 9 months (16).

Secondary glioblastoma has different genetic characteristics compared to primary tumors and evolves out of the low grade or anaplastic astrocytoma precursor lesions. This has implications for the differences in clinical presentation and survival times. In secondary glioblastoma (transformation from grade II/III to grade IV), [$^{213}$Bi]Bi-DOTA-SP treatment showed that median PFS, OS-t, and OS-d was 13.6, 16.4, and 46.8 months, consecutively (17). Better results were obtained in patients with several [$^{213}$Bi]Bi-DOTA-SP doses of injections, which may be due to cumulatively a larger dose of treatment and/or finer clinical condition at the start of the treatment.

The limited supply and high cost of large $^{225}$Ac/$^{213}$Bi generators required for targeted alpha therapy with $^{213}$Bi-SP led to the investigations using SP labeled with the longer-lived mother nuclide $^{225}$Ac requiring significantly lower activities.

The first dose escalation [$^{225}$Ac]Ac-DOTA-SP treatment study with three subgroups 10, 20, and 30 MBq administered activity showed that therapy was well tolerated with only mild and transient side effects (epileptic seizures, edema, and aphasia) up to 30 MBq per cycle (18). Thrombocytopenia grade 3 was observed only in one patient treated with 30 MBq. There were no other grade 3 and 4 toxicities related to [$^{225}$Ac]Ac-DOTA-treatment in all groups. However, surprisingly, the calculated survival parameters were comparable to [$^{213}$Bi]Bi-DOTA-SP with OS-d 35.0 and OS-r/c 13.2 months. From the beginning of treatment with [$^{225}$Ac]Ac-DOTA-SP, the median PFS was 2.4 months, while OS-t was 9.0 months. No statistically significant differences have been found between the investigated dose escalation groups.

The assessment of factors influencing therapy with [$^{213}$Bi]Bi-DOTA-SP and [$^{225}$Ac]Ac-DOTA-SP is still ongoing.

The $^{212}$Pb–another alpha emitter–is currently being used in phase 1, a non-randomized, open-label, dose-escalation study of $^{212}$Pb-octreotate in adult subjects with neuroendocrine tumors (NET) overexpressing somatostatin receptors (19). Preliminary results presented during EANM, SNMMI, and ASCO congresses in 2021 and 2022 showed a high percentage of overall response rate (ORR), i.e., 83.3% per RECIST 1 (in five out of six subjects).

To our knowledge, currently, there are no other ongoing or published studies on the use of $^{212}$Pb- in the management of patients with glioma.

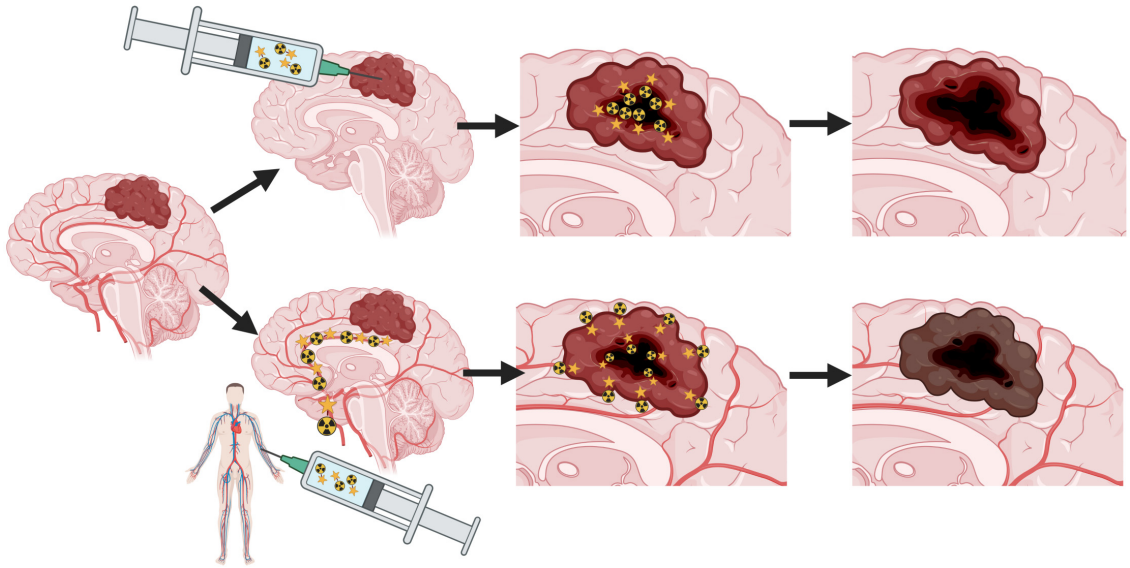

FIGURE 1
The idea of theranostic treatment of glioblastoma with local and intravenous injection of radiopharmaceutical.

## Future perspective

As the local radioisotope procedure should still be considered experimental, the place of this procedure in the treatment regimen needs to be analyzed. The following options can be evaluated:

(a) The therapy can be used as a rescue treatment option in relapsing patients.
(b) Potentially, therapy can be started right after the relapse is diagnosed.
(c) The therapy might be used as an adjuvant therapy right away after finishing the primary treatment.
(d) The therapy might be used as a neoadjuvant therapy before the surgery.

Due to the negative features of glial tumors such as diffuse and very rapid progression, new strategies should be applied. Even local injection can give satisfactory results with prolongation of survival parameters in comparison to standard treatment. Probably, the most promising will be the finding of the right target, which will allow intravenous delivery of radioisotopes to every, even peripheral, part of the tumor (**Figure 1**).

## Author contributions

JK, LK, and KP conceived and wrote the manuscript. AM and FB critically revised the manuscript for intellectual content. All authors edited and commented on the original manuscript, and read and confirmed the final manuscript.

## Conflict of interest

The authors declare that the research was conducted in the absence of any commercial or financial relationships that could be construed as a potential conflict of interest.

## Publisher's note



## References

1. Louis D, Perry A, Wesseling P, Brat D, Cree I, Figarella-Branger D, et al. The 2021 WHO classification of tumors of the central nervous system: a summary. *Neuro Oncol.* (2021) 23:1231–51. doi: 10.1093/neuonc/noab106

2. Weller M, van den Bent M, Preusser M, Le Rhun E, Tonn J, Minniti G, et al. EANO guidelines on the diagnosis and treatment of diffuse gliomas of adulthood. *Nat Rev Clin Oncol.* (2021) 18:170–86. doi: 10.1038/s41571-020-00447-z

3. Stupp R, Mason W, van den Bent M, Weller M, Fisher B, Taphoorn M, et al. European organisation for research and treatment of cancer brain tumor and radiotherapy groups, national cancer institute of Canada clinical trials group. radiotherapy plus concomitant and adjuvant temozolomide for glioblastoma. *N Engl J Med.* (2005) 352:987–96. doi: 10.1056/NEJMoa043330

4. Merlo A, Hausmann O, Wasner M, Steiner P, Otte A, Jermann E, et al. Locoregional regulatory peptide receptor targeting with the diffusible somatostatin analogue 90Y-labeled DOTA0-D-Phe1-Tyr3-octreotide (DOTATOC): a pilot study in human gliomas. *Clin Cancer Res.* (1999) 5:1025–33.

5. Kneifel S, Cordier D, Good S, Ionescu MC, Ghaffari A, Hofer S, et al. Local of malignant gliomas by the diffusible peptidic vector 1,4,7,10-tetraazacyclododecane-1-glutaric acid-4,7,10-triacetic acid-substance p. *Clin Cancer Res.* (2006) 12:3843–50. doi: 10.1158/1078-0432.CCR-05-2820

6. Bigner DD, Brown MT, Friedman AH, Coleman RE, Akabani G, Friedman HS, et al. Iodine-131-labeled antitenascin monoclonal antibody 81C6 treatment of patients with recurrent malignant gliomas: phase I trial results. *J Clin Oncol.* (1998) 16:2202–12. doi: 10.1200/JCO.1998.16.6.2202

7. Zalutsky M. Targeted radiotherapy of brain tumours. *Br J Cancer.* (2004) 90:1469–73. doi: 10.1038/sj.bjc.6601771

8. Schumacher T, Hofer S, Eichhorn K, Wasner M, Zimmerer S, Freitag P, et al. Local injection of the 90Y-labelled peptidic vector DOTATOC to control gliomas of WHO grades II and III: an extended pilot study. *Eur J Nucl Med Mol Imaging.* (2002) 29:486–93. doi: 10.1007/s00259-001-0717-x

9. Hennig I, Laissue J, Horisberger U, Reubi J. Substance-P receptors in human primary neoplasms: tumoral and vascular localization. *Int J Cancer.* (1995) 61:786–92. doi: 10.1002/ijc.2910610608

10. Sgouros G, Roeske J, McDevitt M, Palm S, Allen B, Fisher D, et al. MIRD Pamphlet No.22 (abridged): radiobiology and dosimetry of alpha-particle emitters for targeted radionuclide therapy. *J Nucl Med.* (2010) 51:311–28. doi: 10.2967/jnumed.108.058651

11. Barendsen G, Koot C, van Kerson G, Bewley D, Field S, Parnell C. The effect of oxygen on the impairment of the proliferative capacity of human cells in culture by ionizing radiations of different LET. *Int J Radiat Biol.* (1966) 10:317–27. doi: 10.1080/09553006614550421

12. Wulbrand C, Seidl C, Gaertner F, Bruchertseifer F, Morgenstern A, Essler M, et al. Alpha-particle emitting (213)Bi-anti-EGFR immunoconjugates eradicate tumor cells independent of oxygenation. *PLoS One.* (2013) 8:e64730. doi: 10.1371/journal.pone.0064730

13. Pouget J, Constanzo J. Revisiting the radiobiology of targeted alpha therapy. *Front Med.* (2021) 8:692436. doi: 10.3389/fmed.2021.692436

14. Cordier D, Forrer F, Kneifel S, Kneifel S, Sailer M, Mariani L. Neoadjuvant targeting of glioblastoma multiforme with radiolabeled DOTAGA-substance P: results from a phase I study. *J Neurooncol.* (2010) 100:129–36. doi: 10.1007/s11060-010-0153-5

15. Cordier D, Forrer F, Bruchertseifer F, Morgenstern A, Apostolidis C, Good S, et al. Targeted alpha-radionuclide therapy of functionally critically located gliomas with 213Bi-DOTA-[Thi8,Met(O2)11]-substance P: a pilot trial. *Eur J Nucl Med Mol Imaging.* (2010) 37:1335–44. doi: 10.1007/s00259-010-1385-5

16. Królicki L, Bruchertseifer F, Kunikowska J, Koziara H, Królicki B, Jakuciński M, et al. Safety and efficacy of targeted alpha therapy with 213Bi-DOTA-substance P in recurrent glioblastoma. *Eur J Nucl Med Mol Imaging.* (2019) 46:614–22. doi: 10.1007/s00259-018-4225-7

17. Krolicki L, Bruchertseifer F, Kunikowska J, Koziara H, Królicki B, Jakuciński M, et al. Prolonged survival in secondary glioblastoma following local injection of targeted alpha therapy with 213Bi-substance P analogue. *Eur J Nucl Med Mol Imaging.* (2018) 45:1636–44. doi: 10.1007/s00259-018-4015-2

18. Królicki L, Kunikowska J, Bruchertseifer F, Koziara H, Królicki B, Jakuciński M, et al. 225Ac- and 213Bi-substance P analogues for glioma therapy. *Semin Nucl Med.* (2020) 50:141–51. doi: 10.1053/j.semnuclmed.2019.11.004

19. Delpassand E, Tworowska I, Esfandiari R, Torgue J, Hurt J, Nunez R. Phase I dose-escalation study of AlphaMedix for targeted-alpha-emitter therapy of PRRT-naive neuroendocrine patients. *J Clin Oncol.* (2021) 39(15 Suppl.):4117. doi: 10.1200/JCO.2021.39.15_suppl.4117

frontiers | Frontiers in Medicine

TYPE Mini Review
PUBLISHED 22 December 2022
DOI 10.3389/fmed.2022.1070392



OPEN ACCESS

EDITED BY
Øyvind Bruland,
Oslo University Hospital, Norway

REVIEWED BY
Rob Coleman,
The University of Sheffield, United Kingdom
Oliver Sartor,
Tulane University, United States

*CORRESPONDENCE
Joe M. O'Sullivan
joe.osullivan@qub.ac.uk

SPECIALTY SECTION
This article was submitted to Nuclear Medicine, a section of the journal Frontiers in Medicine

RECEIVED 14 October 2022
ACCEPTED 07 December 2022
PUBLISHED 22 December 2022

CITATION
O'Sullivan JM, McKay RR, Rahbar K, Fizazi K, George DJ, Tombal B, Schmall A, Sandström P, Verholen F and Shore N (2022) Real-world effectiveness, long-term safety and treatment pathway integration of radium-223 therapy in patients with metastatic castration-resistant prostate cancer.
*Front. Med.* 9:fmed-09-1070392.
doi: 10.3389/fmed.2022.1070392



# Real-world effectiveness, long-term safety and treatment pathway integration of radium-223 therapy in patients with metastatic castration-resistant prostate cancer

Joe M. O'Sullivan[1]*, Rana R. McKay[2], Kambiz Rahbar[3], Karim Fizazi[4], Daniel J. George[5], Bertrand Tombal[6], Anja Schmall[7], Per Sandström[8], Frank Verholen[7] and Neal Shore[9]

[1]Patrick G. Johnston Centre for Cancer Research, Queen's University Belfast and Northern Ireland Cancer Centre, Belfast, United Kingdom, [2]Division of Hematology-Oncology, Department of Medicine, University of California, San Diego, La Jolla, CA, United States, [3]Department of Nuclear Medicine, University of Münster Medical Center, Münster, Germany, [4]Institut Gustave Roussy, University of Paris-Saclay, Villejuif, France, [5]Duke University School of Medicine, Durham, NC, United States, [6]Division of Urology, Institut de Recherche Clinique (IREC), Cliniques Universitaires Saint Luc, Brussels, Belgium, [7]Bayer Consumer Care, Basel, Switzerland, [8]Bayer HealthCare Pharmaceuticals, Whippany, NJ, United States, [9]Carolina Urologic Research Center, Myrtle Beach, SC, United States

Radium-223 dichloride ($^{223}$Ra) is an α-emitter approved for the treatment of metastatic castration-resistant prostate cancer (mCRPC) with bone metastases, but without visceral involvement. Despite being a life-prolonging therapy (LPT), $^{223}$Ra remains underutilized. A large body of real-world evidence (RWE) for $^{223}$Ra has been published in the decade since the pivotal phase 3 ALSYMPCA study, a period during which the treatment landscape has continued to evolve. How to optimize $^{223}$Ra use, including how to integrate it into the mCRPC management pathway amongst other current LPTs (i.e., with respect to timing and concurrent, layered, or sequential use), is therefore of considerable interest. RWE studies lack the conventional restraints of clinical trials and can therefore help to build an understanding of how treatments may be best used in routine practice. Here we review RWE studies investigating the efficacy and safety of $^{223}$Ra in mCRPC [including in sequence with the

recently approved 177-Lutetium conjugated to the ligand prostate-specific membrane antigen ($^{177}$Lu-PSMA)], as well as response marker development, imaging techniques, and current clinical practice recommendations.

KEYWORDS

**targeted alpha therapy, radium-223, Lutetium-177-PSMA, metastatic castration-resistant prostate cancer, real-world practice**

# 1 Introduction

The radionuclide radium-223 dichloride ($^{223}$Ra) is a life-prolonging therapy (LPT) in oncology (1), paving the way as the first approved α-emitter. $^{223}$Ra is approved for the treatment of metastatic castration-resistant prostate cancer (mCRPC) with bone metastases, but without visceral involvement (2, 3), with metastatic prostate cancer being primarily a bone-related disease (4), unlike other cancers. This approval was based on improvements in overall survival (OS) vs. placebo [14.9 vs. 11.3 months; hazard ratio (HR) 0.70; 95% confidence interval (CI) 0.58–0.83, $P < 0.001$] in patients with mCRPC (including those with low-volume lymph node metastases), with or without prior chemotherapy, in the pivotal phase 3 ALSYMPCA study (5).

In addition to investigating efficacy and safety in a real-world setting, the challenges of $^{223}$Ra being the first approved α-emitter (e.g., accessibility and understanding of mechanism of action and appropriate usage) also needed to be overcome, with implementation (logistics) and physician and patient education being key to its uptake in clinical practice. However, $^{223}$Ra remains underutilized for various reasons, including lack of prostate-specific antigen (PSA) response, intravenous administration issues and the continued use of back-to-back androgen receptor pathway inhibitor (ARPI) regimens [despite a lack of ARPI re-challenge efficacy and current guidelines (6–9) recommending multiple lines of ARPIs are avoided] (10, 11).

Since ALSYMPCA completion, the treatment landscape has evolved. Several currently approved LPTs, specifically the ARPIs abiraterone (12, 13) enzalutamide (14, 15), apalutamide (16), and darolutamide (17), the poly (adenosine diphosphate-ribose) polymerase inhibitor olaparib (18, 19), the immunotherapy sipuleucel-T (20), and 177-Lutetium conjugated to the ligand prostate-specific membrane antigen ($^{177}$Lu-PSMA-617) (21), were unavailable outside of randomized clinical trials (RCTs) during ALSYMPCA. Furthermore, although docetaxel and cabazitaxel were approved in mCRPC at the time of ALSYMPCA, their position in the treatment pathway has since changed. Consequently, ensuring the appropriate choice of patients and treatment sequence for $^{223}$Ra is key to maximizing therapeutic benefit. There is thus a need for RCTs of $^{223}$Ra regimens in the current mCRPC landscape, some of which are currently underway [RADIANT (phase 4, $^{223}$Ra vs. ARPI), PEACE III (phase 3, $^{223}$Ra plus enzalutamide vs. enzalutamide alone) and DORA (phase 3, $^{223}$Ra plus docetaxel vs. docetaxel alone)] (22–24), and for real-world evidence (RWE).

Unlike RCTs, RWE gathers data from non-interventional studies, clinical registries and other sources reflecting routine clinical practice, thus helping to refine a treatment's therapeutic index without conventional RCT constraints (25). RWE studies can complement RCTs, especially for patients ineligible for RCT inclusion and where Level 1 evidence is lacking. Despite recommended treatment algorithms, variability exists in individual treatment pathways, particularly with some mCRPC therapeutic options moving to earlier disease stages and issues around undertreatment (26, 27). Here we review RWE studies (retrospective unless otherwise specified) investigating $^{223}$Ra in mCRPC, with discussion focusing on studies with $N > 100$, except where data are limited.

# 2 Efficacy

Real-world OS in patients treated with $^{223}$Ra was 8.2–29 months (**Supplementary Table 1**), a range that encompasses the median OS of 14.9 months reported in ALSYMPCA. However, survival outcomes are influenced by patient selection as well as therapy choice, and the studies included in this review vary by patient characteristics, study designs, and prior therapies.

## 2.1 Treatment completion

OS benefits were more notable ($P < 0.01$ where reported) in patients who completed 5–6 vs. fewer cycles of $^{223}$Ra (28–34) (**Figure 1A**). Factors associated with completion of 5–6 cycles in some studies included certain patient/disease characteristics (29, 33, 35, 36) [e.g., lower PSA or alkaline phosphatase (ALP) (35) and absolute neutrophil count at least lower limit of normal (36)] and earlier $^{223}$Ra use (29) (**Figure 1B**). Indeed, there was a higher likelihood of completing all 6 cycles of $^{223}$Ra when it was given prior- vs. post-chemotherapy ($P < 0.001$) (32). However, $^{223}$Ra position in the treatment sequence (i.e., line 1 vs. 2

or ≥ 3) had no impact on treatment completion in another study (35). Moreover, there was also a greater likelihood of the mean number of $^{223}$Ra cycles being higher when $^{223}$Ra was used as combination therapy rather than monotherapy ($P = 0.003$) (32).

## 2.2 Treatment sequence

$^{223}$Ra use earlier in the mCRPC treatment pathway may improve survival outcomes, according to some studies (35, 37). Median survival was greater in patients with one vs. two prior therapies (14.7 vs. 11.2 months; $P = 0.03$) in one study (37), and another demonstrated worse OS with $^{223}$Ra used as line ≥ 3 vs. line 1 (HR 3.267; $P < 0.01$) (35). However, other studies found OS did not significantly differ by prior line of therapy (0 vs. ≥ 1 or across lines 0, 1, 2, 3, or 4) (38), and was generally similar (14.3–14.7 months) when $^{223}$Ra was given immediately after abiraterone as treatment line 2, 3, or ≥ 4 (39).

Similarly, a greater OS benefit was seen with $^{223}$Ra used pre- vs. post-chemotherapy in one study (12.3 vs. 8.1 months; $P = 0.02$), although prior enzalutamide or abiraterone plus prednisolone treatment had no significant OS impact (40). By contrast, another study found no significant OS difference with $^{223}$Ra pre- vs. post chemotherapy (including when patients receiving $^{223}$Ra in combination with enzalutamide or abiraterone were excluded; the safety of these combinations are discussed in section "3 Safety") (32). Furthermore, prior cabazitaxel use was not a predictor of OS in a prospective registry analysis (41), and prior docetaxel use had no significant impact on survival in another study (34).

# 3 Safety

In short- and long-term analyses of ALSYMPCA, $^{223}$Ra had limited myelosuppressive effects and was well tolerated, without major safety concerns (5, 42). RWE has similarly indicated that $^{223}$Ra is safe and well tolerated in patients with mCRPC (**Supplementary Table 2**), and importantly demonstrated a lack of rare treatment-emergent adverse events (TEAEs), e.g., second malignancies or cardiovascular events, which RCTs would be underpowered to detect.

When $^{223}$Ra monotherapy was compared with standard-of-care, the estimated 36-month fracture risk in the respective groups was 19% vs. 10% (HR 1.61; 95% CI: 0.96–3.02) (43). Regimens combining use of $^{223}$Ra and abiraterone (plus prednisolone) or enzalutamide have been reported in real-world studies (44–48). However, based on a significantly increased risk of fractures when $^{223}$Ra was used in combination with abiraterone plus prednisolone in the ERA 223 phase 3 RCT (49), this combination is now contraindicated in the EU (2) and is not recommended in the US (3). Of note, in the ERA 223 trial, the incidence of fractures was lower in patients who were taking bone protecting agents (bisphosphonates or denosumab) at baseline (15 and 7% in the $^{223}$Ra and placebo groups, respectively) than in patients not taking bone protective agents (37 and 15%, respectively) (49). Furthermore, an increased fracture risk was also reported with $^{223}$Ra plus enzalutamide vs. enzalutamide in the phase 3 PEACE III RCT, although fracture risk was largely eliminated in each treatment group with preventative use of bone protecting agents (denosumab and zoledronic acid) (50). Increased fracture risk due to therapy-induced bone loss has been seen for several systemic therapies for prostate cancer, and fracture risk is increased in patients with bone metastases (51). As such, the importance of regularly evaluating bone health and the use of bone protective agents in patients with prostate cancer has been highlighted in the recommendations of a working group of European experts (51).

## 3.1 Treatment sequence

RWE suggests that $^{223}$Ra is generally well tolerated, irrespective of prior chemotherapy status, although prior chemotherapy may be associated with an increased likelihood of hematological events (52, 53), possibly due to patients having more advanced disease (e.g., bone marrow involvement) and/or prior chemotherapy toxicities.

For example, in the first interim analysis of the REASSURE study, prior chemotherapy status generally did not affect the overall safety profile of $^{223}$Ra, with the incidence of drug-related TEAEs being 41 and 36% with or without prior chemotherapy (53). However, drug-related hematologic TEAEs were more than twice as frequent in patients with than without prior chemotherapy (21% vs. 9%) (53). Moreover, in a prospective Japanese study, although there was no marked difference between patients with or without prior chemotherapy with regard to the incidence of drug-related TEAEs (29% vs. 25%), including hematological TEAEs (18% vs. 17%), with $^{223}$Ra, the incidence of both events was notably numerically greater in patients who had received two lines of prior chemotherapy (36 and 24%) (52).

Furthermore, the CAPRI registry found a significant ($P \leq 0.015$) increase in the incidence of grade ≥ 2 anemia, grade ≥ 2 thrombocytopenia and blood transfusions with later-line use of $^{223}$Ra (line ≥ 3 vs. 2 vs. 1), although symptomatic skeletal event (SSE) incidence was not impacted (35). Factors associated with grade ≥ 2 hematological abnormalities include low hemoglobin (Hb) and low platelet count at baseline (52). Of note, $^{223}$Ra requires patient hematological evaluation before every dose and caution (2)/close monitoring (3) is advised for patients with evidence of compromised bone marrow reserve.

In an assessment of fracture risk by line of therapy, the estimated adjusted 36-month fracture risk with $^{223}$Ra vs. standard-of-care was 18% vs. 12% (HR 1.14; 95% CI, 0.50–2.15) when first line and 16% vs. 9% (HR 1.86; 95% CI: 0.62–10.93)

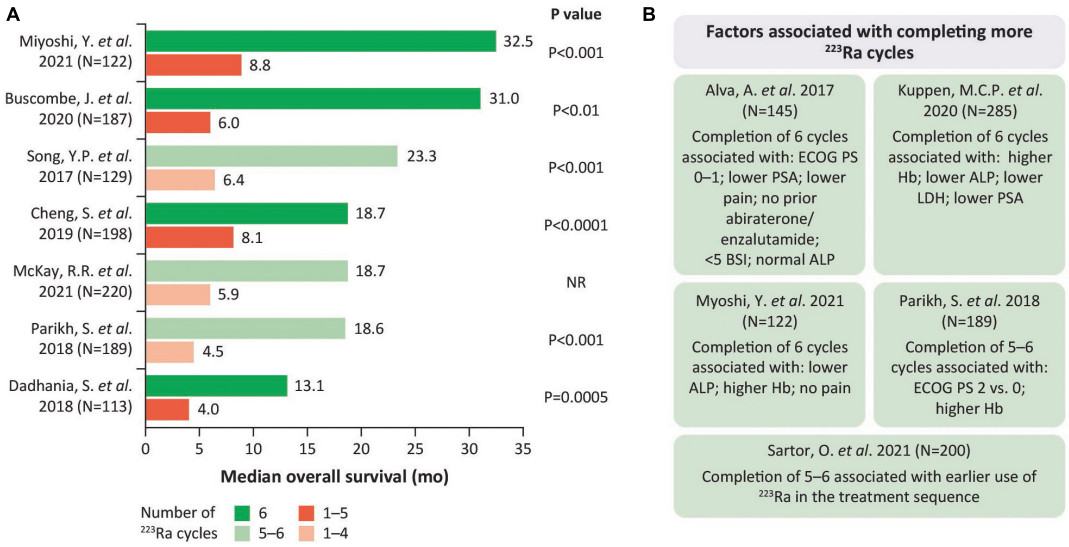


FIGURE 1
Completing more $^{223}$Ra cycles is associated with longer OS. **(A)** Median OS by $^{223}$Ra cycle number. **(B)** Factors associated with completing more $^{223}$Ra cycles. ALP, alkaline phosphatase; BSI, bone scan index; ECOG PS, Eastern Cooperative Oncology Group performance status; Hb, hemoglobin; LDH, lactate dehydrogenase; OS, overall survival; PSA, prostate-specific antigen.

when second line. Later treatment lines had too few fractures for analysis (43).

## 4 $^{223}$Ra therapy/$^{177}$Lu-PSMA treatment sequence and interval duration

$^{177}$Lu-PSMA targets prostate cancer *via* a different mechanism to $^{223}$Ra. $^{177}$Lu-PSMA delivers β-particle radiation to PSMA-expressing tumor cells. In the VISION RCT, $^{177}$Lu-PSMA-617 plus standard-of-care prolonged OS vs. standard-of-care alone (15.3 vs. 11.3 months; HR for death 0.62; $P < 0.001$) (21). Among the 17.4% of patients who had previously received $^{223}$Ra, $^{177}$Lu-PSMA-617 efficacy was not adversely affected (54), although safety has not been reported for these patients.

Although limited by small patient numbers, real-world studies have demonstrated the clinical feasibility of giving $^{177}$Lu-PSMA after $^{223}$Ra and indicate this treatment sequence has an acceptable safety profile (55–58). In a *post hoc* analysis of REASSURE, median OS from start of $^{177}$Lu-PSMA was 13.2 months in patients who had previously received $^{223}$Ra (56). Moreover, in a large retrospective study, median OS was not significantly different in patients who did vs. did not receive prior $^{223}$Ra (10.8 vs. 11.3 months) (55). Furthermore, interim analyses of the RALU study, which investigated $^{177}$Lu-PSMA use in patients previously treated with $^{223}$Ra, found this approach to be clinically feasible (median OS 12.6 months; 95% CI: 8.8–16.1) and well tolerated (58).

Another consideration around treatment sequencing with radionuclide therapies is the treatment interval. Early initiation of $^{177}$Lu-PSMA within 8 weeks of $^{223}$Ra treatment (during which disease progression had occurred) was effective and did not reveal major safety concerns (57).

Thus, sequential treatment with $^{223}$Ra and $^{177}$Lu-PSMA is feasible and can be factored into considerations around optimal sequencing of the LPTs available for patients with mCRPC. However, further studies are warranted.

## 5 Development of response markers

Surrogate markers predicting treatment outcomes with $^{223}$Ra are needed to monitor and achieve optimal treatment duration and to identify patient subpopulations who may benefit most from $^{223}$Ra. Multiple RWE studies have investigated potential markers of survival (**Supplementary Table 3**), with this section focusing on multivariate analyses.

### 5.1 Laboratory parameters

Multivariate analyses have found various factors to be associated with survival outcomes. Baseline Hb was found to be prognostic of OS (59) and elevated baseline Hb (≥ 120 g/L) was associated with increased OS (60), whereas low baseline albumin (< 35 g/L) (61) and elevated PSA (> 80 μg/L) (61) were associated with poor OS. Similarly,

other factors prognostic of OS include baseline neutrophil-to-lymphocyte ratio (28), baseline lactose dehydrogenase (62) [with elevated lactose dehydrogenase associated with shorter OS (41)] and higher baseline ALP (28) [with ALP > 150 U/L associated with poor OS (61)]. Elevated baseline ALP without a subsequent ALP decline of ≥ 10% following the first $^{223}$Ra dose was also prognostic of shorter OS (62).

## 5.2 Clinical parameters

A number of clinical parameters have been associated with patient survival. In terms of patient demographics, age was found to be a predictor of OS (28), with an age of > 75 years being associated with reduced OS (63). Moreover, in an analysis of US electronic heath records of mainly Caucasian patients (73.5%), other race (Asian, Hispanic, Latino, or other) was associated with improved survival (63). With regard to disease characteristics, visceral metastases (63) and prior SSEs (63) reduced OS, whereas bone-only metastases were associated with longer OS (41). Eastern Cooperative Oncology Group performance status (ECOG PS) was also prognostic of OS (59, 62), with ECOG PS 2–3 (61) and ECOG PS 2–4 (63) associated with worse OS and ECOG PS 0–1 associated with increased OS (60). Another clinical parameter prognostic of OS was number of prior systemic therapies (62). Prior chemotherapy use reduced OS (63), whereas no prior use of docetaxel increased OS (60). As discussed in section "2.1 Treatment completion," the number of completed cycles of $^{223}$Ra (5–6 vs. 1–4) was also a predictor of OS (28).

## 5.3 Composite markers

Several studies have reported composite prognostic scoring methods aimed at identifying patients that may benefit most from $^{223}$Ra therapy (59–61, 64). A composite score derived from combining baseline Hb ≥ 120 g/L, total ALP ≤ 110 U/L and ECOG PS 0–1 identified patients with a low-, intermediate- or high-risk of death (composite score 2, 3–4 and 5–6, respectively; median OS 23, 8, and 5 months) (60). A similar 3-variable prognostic score combining baseline ECOG PS, Hb < 12 g/dL and PSA ≥ 20 ng/mL was predictive of OS in an initial cohort (64), with subsequent validation in a larger cohort (59). In the larger cohort, patients in the low (score 0), moderate (score 1–2), or high (score 3–4)-risk groups had a median OS of 33, 16, and 8 months, respectively (59). Likewise, a scoring system that combined albumin < 35 g/L, ALP > 150 U/L, PSA > 80 μg/L, and ECOG PS 2–3 identified three patient groups with different OS outcomes, namely good (score 0–1; median OS 19.4 months), intermediate (score 2; median OS 10.0 months) and poor (score 3–4; median OS 3.1 months) (61).

# 6 Imaging

An expert consensus developed at the European Association of Nuclear Medicine Focus 1 meeting concluded that, for patients with mCRPC who are candidates for $^{223}$Ra, bone scintigraphy is the recommended pre-treatment imaging method. Consensus was not reached as to which imaging method should be used for monitoring treatment response, although bone scintigraphy was favored by most (14/21) panelists (65).

Automated bone scan index (BSI) is useful for assessing skeletal metastases. Baseline BSI was associated with OS in patients who received $^{223}$Ra in two studies (66, 67), with median OS being 8.2 and 15.0 months in patients with BSIs of > 5 or ≤ 5, respectively (HR 2.65; 95% CI: 1.5–4.7; $P$ = 0.001) (67). However, only one of the two studies found a significant association between on-treatment BSI and OS (66). A potential limitation of this approach is the potential uptake of bone scintigraphy agents into healing bone which could confound results (66).

Radionuclide cancer therapies offer considerable potential for personalized treatment as their physical properties enable *in vivo* imaging of their uptake and retention (68). $^{223}$Ra administration is *via* body weight-adjusted standard dosing regimens, although patient-specific dosimetry and treatment optimization may be possible *via* quantitative imaging with $^{223}$Ra (68). Although $^{223}$Ra imaging showed intra- and inter-patient variability for $^{223}$Ra dose absorption in metastases, there was a relationship between lesion-absorbed dose and treatment response (69). $^{18}$F-fluoride, like $^{223}$Ra, localizes primarily to areas of osteoblastic activity in bone and has potential as a surrogate measure of the absorbed $^{223}$Ra dose (69). $^{18}$F-fluoride uptake into bone metastases correlated significantly with that of $^{223}$Ra, as well as the absorbed $^{223}$Ra dose and resultant response (69).

Notably, PSMA-positron emission tomography (PET) has been shown to be more sensitive than bone scintigraphy in detecting bone metastases in patients with prostate cancer (70). High PSMA expression on planar/single-photon emission computed tomography (SPECT) or PET/CT scans following standard therapies for mCRPC, including $^{223}$Ra, was associated with worse OS than low PSMA expression (71).

# 7 Clinical practice recommendations

$^{223}$Ra is recommended for mCRPC in all major treatment guidelines (6–9) and has the highest possible clinical benefit

score for non-curative therapies in mCRPC in the ESMO-Magnitude of Clinical Benefit Scale (indicating a substantial magnitude of clinical benefit) (72). Expert recommendations from 11 nuclear medicine centers across six European countries provide additional insights on how to optimize $^{223}$Ra use (73). These include guidance for center organization/preparation, $^{223}$Ra ordering, preparation and disposal, $^{223}$Ra treatment delivery/administration, and patient referral/experience, and highlight the importance of starting $^{223}$Ra treatment as soon as possible in eligible patients (including those with early symptoms of bone metastases) (73).

However, for $^{223}$Ra to meet the inherent complex needs of patients, communication and coordination within multidisciplinary teams (i.e., nuclear medicine, oncology, and urology services) and centers is advised (73). Communication between the nuclear medicine physician and other specialties is important to maintain awareness for whom and when $^{223}$Ra may be appropriate, and to inform of developments in prostate cancer management (including nuclear medicine options) (73). With regard to such developments, when the Advanced Prostate Cancer Consensus Conference discussed questions relating to $^{223}$Ra and other therapies in 2021, consensus was reached that using $^{223}$Ra after $^{177}$Lu-PSMA is safe (76% consensus), based on outcomes from VISION, in which approximately 2.5% of patients received $^{223}$Ra following $^{177}$Lu-PSMA therapy (74). RWE supporting use of $^{223}$Ra followed by $^{177}$Lu-PSMA are discussed in section "4 $^{223}$Ra therapy/$^{177}$Lu-PSMA treatment sequence and interval duration."

## 8 Discussion

For patients with mCRPC, it is important to offer as many approved LPTs as possible. Real-world studies can help healthcare professionals understand how best to utilize currently available treatment options, such as $^{223}$Ra, and are used by regulatory bodies in decision making (75–78). Although there are well recognized limitations to these studies, including confounding factors, various types of bias (pertaining to selection, patient/caregiver recall, event detection, and data misclassification) and missing data (limiting statistical power), they can complement/supplement clinical trial data and help to determine whether RCT evidence is generalizable to patient populations in clinical practice (79, 80).

The large body of RWE that has emerged for $^{223}$Ra in recent years indicates that $^{223}$Ra is an effective and safe LPT option in mCRPC, supporting RCT findings. Completing 5–6 $^{223}$Ra cycles was associated with better survival outcomes across real-world studies, highlighting the value of being able to identify patients most capable of completing therapy. RWE indicates several potential markers that may help to do this, although these are not yet validated in prospective studies. A potential challenge in optimizing $^{223}$Ra use in clinical practice is how to best integrate it into the mCRPC treatment pathway. However, as current RWE has been variable in this regard, there is a need to further evaluate $^{223}$Ra in the context of other treatments with respect to timing and concurrent, layered, or sequential use, and the effectiveness and safety of such treatment approaches. To this end, several clinical trials (e.g., PEACE-III; AlphaBet; COMRADE; Rad2Nivo; RADIANT; DORA) (22–24, 81–83) and RWE studies (e.g., REASSURE; RaLu) (58, 84) continue to explore $^{223}$Ra use in mCRPC.

## Author contributions

JO'S, RM, KR, KF, DG, BT, AS, PS, FV, and NS contributed to the conception and design, drafting and revising of the work, and approval of the final version. All authors agreed to be accountable for all aspects of the respective work.

## Acknowledgments

Dr. C. Guise, Cancer Communications and Consultancy Ltd., Cheshire, United Kingdom, provided medical writing assistance (funded by Bayer). Dr. Lila Adnane (Bayer) provided editorial assistance.

## Conflict of interest

JO'S reported consulting or advisory role for Bayer, Janssen, Astellas Pharma, Sanofi, and Novartis. Speakers' bureau for Bayer, Janssen, and Novartis. His institution received research funding from Bayer. RM reported consulting or advisory role for AstraZeneca, Aveo, Bayer, Calithera, Caris, Dendreon, Exelixis, Janssen, Merck, Myovant, Novartis, Pfizer, Sanofi, Sorrento Therapeutics, Seagen, Tempus, and Telix. KR reported honoraria from Advanced Accelerator Applications, Bayer Healthcare, SIRTEX, Jahnsen Cielag, and Amgen. Consultancy or advisory role for ABX GmbH, ABX-CRO, Bayer Healthcare, and Advanced Accelerator Applications. KF reported participation in advisory boards and talks for Amgen, Astellas, Astrazeneca, Bayer, Clovis, Daiichi Sankyo, Janssen, MSD, Novartis/AAA, Pfizer, and Sanofi. Participation in advisory boards with personal honorarium for CureVac and Orion. Honoraria from his institution (Gustave Roussy). DG reported grants and/or fees from Acerta Pharma, the American Association for Cancer Research, Astellas, AstraZeneca, Axess Oncology, Bayer, BMS, Calithera, Capio Biosciences, EMD Serono, Exelixis, Flatiron, Ipsen, UroGPO, Janssen, Leidos Biomedical Research, Merck Sharp & Dohme, Michael J. Hennessey Associates, Millennium Med. Publishing, Modra Pharmaceuticals, Myovant Sciences, NCI,

Nektar Therapeutics, Novartis, Pfizer, Physician Education Resource, Sanofi, UroToday, and Vizuri Health Sciences. BT reported Consulting or Advisory Role for Astellas Pharma, Bayer, Ferring, Janssen, Takeda, Steba Biotech, Sanofi, Myovant Sciences, and Pfizer/Astellas. Speakers' Bureau for Amgen, Janssen, and Astellas Pharma. Travel, Accommodations, Expenses for Amgen, Astellas Pharma, Bayer, Ferring, Janssen, and Sanofi. Expert Testimony for Tookad. Honoraria for Amgen, Astellas Pharma, Bayer, Ferring, Sanofi, Janssen, Pfizer, and Myovant Sciences. His institution received research funding from Ferring. AS, PS, and FV were employees of Bayer. NS reported consulting fees from AbbVie, Amgen, Astellas, AstraZeneca, Bayer, BMS, Boston Scientific, Clarity, Clovis Oncology, Cold Genesys, Dendreon, Exact Imaging, Exact Sciences, FerGene, Foundation Medicine, Genesis Care, Invitae, Janssen, Lantheus, Lilly, MDxhealth, Merck, Myovant, Myriad, Nymox, Pacific Edge, Pfizer, Phosphorous, Photocure, Propella, PreView, Sanofi Genzyme, Sema4, Speciality Networks, Sesen Bio, Telix, Tempus, Tolmar, Urogen, and Vaxiion. Payment for expert testimony from Ferring.

## Publisher's note



## Supplementary material

The Supplementary Material for this article can be found online at: https://www.frontiersin.org/articles/10.3389/fmed.2022.1070392/full#supplementary-material

## References

1. Terrisse S, Karamouza E, Parker C, Sartor A, James N, Pirrie S, et al. Overall survival in men with bone metastases from castration-resistant prostate cancer treated with bone-targeting radioisotopes: a meta-analysis of individual patient data from randomized clinical trials. *JAMA Oncol.* (2020) 6:206–16. doi: 10.1001/jamaoncol.2019.4097

2. EMC. *Xofigo Summary of Product Characteristics.* (2022). Available online at: https://www.medicines.org.uk/emc/product/5204/smpc (accessed October 04, 2022).

3. XOFIGO. *Xofigo Prescribing Information.* (2022). Available online at: https://www.accessdata.fda.gov/drugsatfda_docs/label/2013/203971lbl.pdf (accessed October 04, 2022).

4. Bubendorf L, Schopfer A, Wagner U, Sauter G, Moch H, Willi N, et al. Metastatic patterns of prostate cancer: an autopsy study of 1,589 patients. *Hum Pathol.* (2000) 31:578–83. doi: 10.1053/hp.2000.6698

5. Parker C, Nilsson S, Heinrich D, Helle S, O'Sullivan J, Fossa S, et al. Alpha emitter radium-223 and survival in metastatic prostate cancer. *N Engl J Med.* (2013) 369:213–23. doi: 10.1056/NEJMoa1213755

6. Basch E, Loblaw D, Oliver T, Carducci M, Chen R, Frame J, et al. Systemic therapy in men with metastatic castration-resistant prostate cancer: American society of clinical oncology and cancer care ontario clinical practice guideline. *J Clin Oncol.* (2014) 32:3436–48. doi: 10.1200/JCO.2013.54.8404

7. National Comprehensive Cancer Network [NCCN]. *NCCN Clinical Practice Guidelines in Oncology: Prostate Cancer Version 2.* Plymouth Meeting, PA: National Comprehensive Cancer Network (2017).

8. Mottet N, Bellmunt J, Bolla M, Cornford P, De Santis M, Henry A, et al. *Guidelines on Prostate Cancer.* (2016). Available online at: http://uroweb.org/guideline/prostate-cancer (accessed October 4, 2022).

9. Parker C, Castro E, Fizazi K, Heidenreich A, Ost P, Procopio G, et al. Prostate cancer: ESMO clinical practice guidelines for diagnosis, treatment and follow-up. *Ann Oncol.* (2020) 31:1119–34. doi: 10.1016/j.annonc.2020.06.011

10. Caffo O, Wissing M, Bianchini D, Bergman A, Thomsen F, Schmid S, et al. Survival outcomes from a cumulative analysis of worldwide observational studies on sequential use of new agents in metastatic castration-resistant prostate cancer. *Clin Genitourin Cancer.* (2020) 18:69–76e4. doi: 10.1016/j.clgc.2019.09.010

11. Shore N, Laliberte F, Ionescu-Ittu R, Yang L, Mahendran M, Lejeune D, et al. Real-world treatment patterns and overall survival of patients with metastatic castration-resistant prostate cancer in the US prior to PARP inhibitors. *Adv Ther.* (2021) 38:4520–40. doi: 10.1007/s12325-021-01823-6

12. de Bono J, Logothetis C, Molina A, Fizazi K, North S, Chu L, et al. Abiraterone and increased survival in metastatic prostate cancer. *N Engl J Med.* (2011) 364:1995–2005. doi: 10.1056/NEJMoa1014618

13. Ryan C, Molina A, Griffin T. Abiraterone in metastatic prostate cancer. *N Engl J Med.* (2013) 368:1458–9. doi: 10.1056/NEJMc1301594

14. Scher H, Fizazi K, Saad F, Taplin M, Sternberg C, Miller K, et al. Increased survival with enzalutamide in prostate cancer after chemotherapy. *N Engl J Med.* (2012) 367:1187–97. doi: 10.1056/NEJMoa1207506

15. Beer T, Tombal B. Enzalutamide in metastatic prostate cancer before chemotherapy. *N Engl J Med.* (2014) 371:1755–6. doi: 10.1056/NEJMc1410239

16. Chi K, Agarwal N, Bjartell A, Chung B, Pereira de Santana Gomes A, Given R, et al. Apalutamide for metastatic, castration-sensitive prostate cancer. *N Engl J Med.* (2019) 381:13–24. doi: 10.1056/NEJMoa1903307

17. Smith M, Hussain M, Saad F, Fizazi K, Sternberg C, Crawford E, et al. Darolutamide and survival in metastatic, hormone-sensitive prostate cancer. *N Engl J Med.* (2022) 386:1132–42. doi: 10.1056/NEJMoa2119115

18. de Bono J, Mateo J, Fizazi K, Saad F, Shore N, Sandhu S, et al. Olaparib for metastatic castration-resistant prostate cancer. *N Engl J Med.* (2020) 382:2091–102. doi: 10.1056/NEJMoa1911440

19. Hussain M, Mateo J, Fizazi K, Saad F, Shore N, Sandhu S, et al. Survival with olaparib in metastatic castration-resistant prostate cancer. *N Engl J Med.* (2020) 383:2345–57. doi: 10.1056/NEJMoa2022485

20. Kantoff P, Higano C, Shore N, Berger E, Small E, Penson D, et al. Sipuleucel-T immunotherapy for castration-resistant prostate cancer. *N Engl J Med.* (2010) 363:411–22. doi: 10.1056/NEJMoa1001294

21. Sartor O, de Bono J, Chi K, Fizazi K, Herrmann K, Rahbar K, et al. Lutetium-177-PSMA-617 for metastatic castration-resistant prostate cancer. *N Engl J Med.* (2021) 385:1091–103. doi: 10.1056/NEJMoa2107322

22. Fizazi K, Alba A, Mustafa Ö Skoneczna I, Krissel H, Uema D, et al. Radium-223 (Ra-223) versus novel antihormone therapy (NAH) for progressive metastatic castration-resistant prostate cancer (mCRPC) after 1 line of NAH: RADIANT, an international phase 4, randomized, open-label study. *J Clin Oncol.* (2021) 39 (Suppl. 15). doi: 10.1200/JCO.2021.39.15_suppl.TPS5093

23. ClinicalTrials.gov. *Phase I Radium 223 mCRPC-PEACE III (PEACE III). ClinicalTrials.gov Identifier NCT02194842.* (2014). Available online at: https://clinicaltrials.gov/ct2/show/NCT02194842 (accessed October 09, 2022).

24. ClinicalTrials.gov. *A Study to Test Radium-223 with Docetaxel in Patients with Prostate Cancer. Clinicaltrials.gov Identifier NCT03574571*. (2018). Available online at: https://clinicaltrials.gov/ct2/show/NCT03574571 (accessed October 12, 2022).

25. Sherman R, Anderson S, Dal Pan G, Gray G, Gross T, Hunter N, et al. Real-world evidence - what is it and what can it tell us? *N Engl J Med.* (2016) 375:2293–7. doi: 10.1056/NEJMsb1609216

26. Justo N, Schweikert B, Simon A, Reginald Waldeck A, Meinhardt M, Samel Y-R, et al. Insights into treatment patterns in the routine care of patients diagnosed with metastatic castration-resistant prostate cancer in Germany after the introduction of new therapies. *Clin Oncol Res.* (2020) 3:2–8. doi: 10.31487/j.COR.2020.09.04

27. George D, Sartor O, Miller K, Saad F, Tombal B, Kalinovsky J, et al. Treatment patterns and outcomes in patients with metastatic castration-resistant prostate cancer in a real-world clinical practice setting in the United States. *Clin Genitourin Cancer.* (2020) 18:284–94. doi: 10.1016/j.clgc.2019.12.019

28. Parikh S, Murray L, Kenning L, Bottomley D, Din O, Dixit S, et al. Real-world outcomes and factors predicting survival and completion of radium 223 in metastatic castrate-resistant prostate cancer. *Clin Oncol.* (2018) 30:548–55. doi: 10.1016/j.clon.2018.06.004

29. Sartor O, Appukkuttan S, Weiss J, Tsao C. Clinical outcomes, management, and treatment patterns in patients with metastatic castration-resistant prostate cancer treated with radium-223 in community compared to academic settings. *Prostate.* (2021) 81:657–66. doi: 10.1002/pros.24143

30. Cheng S, Arciero V, Goldberg H, Tajzler C, Manganaro A, Kozlowski N, et al. Population-based analysis of the use of radium-223 for bone-metastatic castration-resistant prostate cancer in Ontario, and of factors associated with treatment completion and outcome. *Cancer Manag Res.* (2019) 11:9307–19. doi: 10.2147/CMAR.S213051

31. Buscombe J, Gillett D, Bird N, Powell A, Heard S, Aloj L. Quantifying the survival benefit of completing all the six cycles of radium-223 therapy in patients with castrate-resistant prostate cancer with predominant bone metastases. *World J Nucl Med.* (2021) 20:139–44. doi: 10.4103/wjnm.WJNM_74_20

32. McKay R, Silver R, Bhak R, Korves C, Cheng M, Appukkuttan S, et al. Treatment of metastatic castration resistant prostate cancer with radium-223: a retrospective study at a US tertiary oncology center. *Prostate Cancer Prostatic Dis.* (2021) 24:210–9. doi: 10.1038/s41391-020-00271-7

33. Miyoshi Y, Tsutsumi S, Yasui M, Kawahara T, Uemura K, Hayashi N, et al. A novel prediction model for the completion of six cycles of radium-223 treatment and survival in patients with metastatic castration-resistant prostate cancer. *World J Urol.* (2021) 39:3323–8. doi: 10.1007/s00345-021-03639-z

34. Dadhania S, Alonzi R, Douglas S, Gogbashian A, Hughes R, Dalili D, et al. Single-centre experience of use of radium 223 with clinical outcomes based on number of cycles and bone marrow toxicity. *Anticancer Res.* (2018) 38:5423–7. doi: 10.21873/anticanres.12873

35. Kuppen M, Westgeest H, van der Doelen M, van den Eertwegh A, Coenen J, Aben K, et al. Real-world outcomes of radium-223 dichloride for metastatic castration resistant prostate cancer. *Future Oncol.* (2020) 16:1371–84. doi: 10.2217/fon-2020-0039

36. McKay R, Jacobus S, Fiorillo M, Ledet E, Cotogna P, Steinberger A, et al. Radium-223 use in clinical practice and variables associated with completion of therapy. *Clin Genitourin Cancer.* (2017) 15:e289–98. doi: 10.1016/j.clgc.2016.08.015

37. Jarvis P, Ho A, Sundram F. Radium-223 therapy for metastatic castration-resistant prostate cancer: survival benefit when used earlier in the treatment pathway. *Nucl Med Commun.* (2021) 42:332–6. doi: 10.1097/MNM.0000000000001325

38. Maruzzo M, Basso U, Borsatti E, Evangelista L, Alongi F, Caffo O, et al. Results from a large, multicenter, retrospective analysis on radium223 use in metastatic castration-resistant prostate cancer (mCRPC) in the Triveneto Italian Region. *Clin Genitourin Cancer.* (2019) 17:e187–94. doi: 10.1016/j.clgc.2018.10.013

39. Caffo O, Frantellizzi V, Tucci M, Galli L, Monari F, Baldari S, et al. Fracture risk and survival outcomes in metastatic castration-resistant prostate cancer patients sequentially treated with abiraterone acetate and radium-223. *Eur J Nucl Med Mol Imaging.* (2020) 47:2633–8. doi: 10.1007/s00259-020-04796-w

40. Jiang X, Atkinson S, Pearson R, Leaning D, Cumming S, Burns A, et al. Optimising radium 223 therapy for metastatic castration-resistant prostate cancer - 5-year real-world outcome: focusing on treatment sequence and quality of life. *Clin Oncol.* (2020) 32:e177–87. doi: 10.1016/j.clon.2020.05.002

41. Badrising S, Louhanepessy R, van der Noort V, Coenen J, Hamberg P, Beeker A, et al. A prospective observational registry evaluating clinical outcomes of radium-223 treatment in a nonstudy population. *Int J Cancer.* (2020) 147:1143–51. doi: 10.1002/ijc.32851

42. Parker C, Coleman R, Sartor O, Vogelzang N, Bottomley D, Heinrich D, et al. Three-year safety of radium-223 dichloride in patients with castration-resistant prostate cancer and symptomatic bone metastases from phase 3 randomized alpharadin in symptomatic prostate cancer trial. *Eur Urol.* (2018) 73:427–35. doi: 10.1016/j.eururo.2017.06.021

43. Stattin P, Westerberg M, Lissbrant I, Eriksson M, Kjellman A, Ullen A, et al. Real world outcomes in patients with metastatic, castration-resistant prostate cancer treated with radium-223 in routine clinical practice in Sweden. *Clin Genitourin Cancer.* (2022): doi: 10.1016/j.clgc.2022.09.002 [Epub ahead of print].

44. Zhao H, Howard L, De Hoedt A, Terris M, Amling C, Kane C, et al. Safety of concomitant therapy with radium-223 and abiraterone or enzalutamide in a real-world population. *Prostate.* (2021) 81:390–7. doi: 10.1002/pros.24115

45. Kim S, Szeto A, Morgan K, Brower B, Dunn M, Khandani A, et al. A real-world evaluation of radium-223 in combination with abiraterone or enzalutamide for the treatment of metastatic castration-resistant prostate cancer. *PLoS One.* (2021) 16:e0253021. doi: 10.1371/journal.pone.0253021

46. Ahmed M, Joshi V, Badawy M, Pagliaro L, Karnes R, Lowe V, et al. Radium-223 in the third-line setting in metastatic castration-resistant prostate cancer: impact of concomitant use of enzalutamide on overall survival (OS) and predictors of improved OS. *Clin Genitourin Cancer.* (2021) 19:223–9. doi: 10.1016/j.clgc.2020.12.009

47. Trieu J, Chang M, Rojas V, Varada N, Cao Y, Anderson M, et al. Lower fracture rates in patients treated with radium-223, abiraterone or enzalutamide, when given concurrently with bone health agents: a real-world analysis. *Clin Genitourin Cancer.* (2022) 20:399–403. doi: 10.1016/j.clgc.2022.04.015

48. Shore N, Higano C, George D, Sternberg C, Saad F, Tombal B, et al. Concurrent or layered treatment with radium-223 and enzalutamide or abiraterone/prednisone: real-world clinical outcomes in patients with metastatic castration-resistant prostate cancer. *Prostate Cancer Prostatic Dis.* (2020) 23:680–8. doi: 10.1038/s41391-020-0236-0

49. Smith M, Parker C, Saad F, Miller K, Tombal B, Ng Q, et al. Addition of radium-223 to abiraterone acetate and prednisone or prednisolone in patients with castration-resistant prostate cancer and bone metastases (ERA 223): a randomised, double-blind, placebo-controlled, Phase 3 trial. *Lancet Oncol.* (2019) 20:408–19. doi: 10.1016/S1470-2045(18)30860-X

50. Gillessen S, Choudhury A, Rodriguez-Vida A, Nole F, Diaz E, Roumeguere T, et al. Decreased fracture rate by mandating bone protecting agents in the EORTC 1333/PEACEIII trial combining Ra223 with enzalutamide versus enzalutamide alone: an updated safety analysis. *J Clin Oncol.* (2021) 39 (Suppl. 15):5002. doi: 10.1200/JCO.2021.39.15_suppl.5002

51. O'Sullivan J, Carles J, Cathomas R, Gomez-Iturriaga A, Heinrich D, Kramer G, et al. Radium-223 within the evolving treatment options for metastatic castration-resistant prostate cancer: recommendations from a European Expert Working Group. *Eur Urol Oncol.* (2020) 3:455–63. doi: 10.1016/j.euo.2019.02.007

52. Uemura H, Masumori N, Takahashi S, Hosono M, Kinuya S, Sunaya T, et al. Real-world safety and effectiveness of radium-223 in Japanese patients with castration-resistant prostate cancer (CRPC) and bone metastasis: exploratory analysis, based on the results of post-marketing surveillance, according to prior chemotherapy status and in patients without concomitant use of second-generation androgen-receptor axis-targeted agents. *Int J Clin Oncol.* (2021) 26:753–63. doi: 10.1007/s10147-020-01850-3

53. Dizdarevic S, Petersen P, Essler M, Versari A, Bourre J, la Fougere C, et al. Interim analysis of the REASSURE (Radium-223 alpha emitter agent in non-intervention safety study in mCRPC population for long-term evaluation) study: patient characteristics and safety according to prior use of chemotherapy in routine clinical practice. *Eur J Nucl Med Mol Imaging.* (2019) 46:1102–10. doi: 10.1007/s00259-019-4261-y

54. Vaishampayan N, Morris M, Krause B, Vogelzang N, Kendi A, Nordquist L, et al. [$^{177}$Lu]Lu-PSMA-617 in PSMA-positive metastatic castration-resistant prostate cancer: prior and concomitant treatment subgroup analyses of the VISION trial. *J Clin Oncol.* (2022) 40(16_Suppl.):5001.

55. Ahmadzadehfar H, Zimbelmann S, Yordanova A, Fimmers R, Kurpig S, Eppard E, et al. Radioligand therapy of metastatic prostate cancer using $^{177}$Lu-PSMA-617 after radiation exposure to $^{223}$Ra-dichloride. *Oncotarget.* (2017) 8:55567–74. doi: 10.18632/oncotarget.15698

56. Sartor O, la Fougère C, Essler M, Ezziddin S, Kramer G, Ellinger J, et al. Lutetium-177–prostate-specific membrane antigen ligand following radium-223 treatment in men with bone-metastatic castration-resistant prostate cancer: real-world clinical experience. *J Nucl Med.* (2021) 63:410–4. doi: 10.2967/jnumed.121.262240

57. Baumgarten J, Groener D, Nguyen Ngoc C, Mader N, Chaurasia M, Davis K, et al. Safety and efficacy of $^{177}$Lutetium-PSMA-617 radioligand therapy shortly after failing $^{223}$radium-dichloride. *Cancers.* (2022) 14:557. doi: 10.3390/cancers14030557

58. Rahbar K, Essler M, Eiber M, la Fougère C, Prasad V, Fendler W, et al. Safety and survival outcomes in patients (Pts) with metastatic castration-resistant prostate cancer (mCRPC) treated with lutetium-177–prostate-specific membrane antigen ($^{177}$Lu-PSMA) after radium-223 ($^{223}$Ra): interim analysis of the RALU study. *J Clin Oncol.* (2022) 40:5040.

59. Frantellizzi V, Monari F, Mascia M, Costa R, Rubini G, Spanu A, et al. Validation of the 3-variable prognostic score (3-PS) in mCRPC patients treated with $^{223}$radium-dichloride: a national multicenter study. *Ann Nucl Med.* (2020) 34:772–80. doi: 10.1007/s12149-020-01501-7

60. Charrois-Durand C, Saad F, Barkati M, Lattouf J, Perrotte P, Karakiewicz P, et al. A single-center, multidisciplinary experience with radium-223 dichloride in men with metastatic castrate-resistant prostate cancer. *Can Urol Assoc J.* (2022) 16:199–205. doi: 10.5489/cuaj.7591

61. Al-Ezzi E, Alqaisi H, Iafolla M, Wang L, Sridhar S, Sacher A, et al. Clinicopathologic factors that influence prognosis and survival outcomes in men with metastatic castration-resistant prostate cancer treated with radium-223. *Cancer Med.* (2021) 10:5775–82. doi: 10.1002/cam4.4125

62. van der Doelen M, Stockhaus A, Ma Y, Mehra N, Yachnin J, Gerritsen W, et al. Early alkaline phosphatase dynamics as biomarker of survival in metastatic castration-resistant prostate cancer patients treated with radium-223. *Eur J Nucl Med Mol Imaging.* (2021) 48:3325–34. doi: 10.1007/s00259-021-05283-6

63. George D, Agarwal N, Sartor O, Sternberg C, Tombal B, Saad F, et al. Real-world patient characteristics associated with survival of 2 years or more after radium-223 treatment for metastatic castration-resistant prostate cancer (Epix Study). *Prostate Cancer Prostatic Dis.* (2022) 25:306–13.

64. Frantellizzi V, Farcomeni A, Follacchio G, Pacilio M, Pellegrini R, Pani R, et al. A 3-variable prognostic score (3-PS) for overall survival prediction in metastatic castration-resistant prostate cancer treated with $^{223}$radium-dichloride. *Ann Nucl Med.* (2018) 32:142–8. doi: 10.1007/s12149-017-1228-6

65. Fanti S, Minozzi S, Antoch G, Banks I, Briganti A, Carrio I, et al. Consensus on molecular imaging and theranostics in prostate cancer. *Lancet Oncol.* (2018) 19:e696–708. doi: 10.1016/S1470-2045(18)30604-1

66. Anand A, Tragardh E, Edenbrandt L, Beckman L, Svensson J, Thellenberg C, et al. Assessing radiographic response to $^{223}$Ra with an automated bone scan index in metastatic castration-resistant prostate cancer patients. *J Nucl Med.* (2020) 61:671–5. doi: 10.2967/jnumed.119.231100

67. Fosbol M, Petersen P, Kjaer A, Mortensen J. $^{223}$Ra therapy of advanced metastatic castration-resistant prostate cancer: quantitative assessment of skeletal tumor burden for prognostication of clinical outcome and hematologic toxicity. *J Nucl Med.* (2018) 59:596–602. doi: 10.2967/jnumed.117.195677

68. Flux G. Imaging and dosimetry for radium-223: the potential for personalized treatment. *Br J Radiol.* (2017) 90:20160748. doi: 10.1259/bjr.20160748

69. Murray I, Chittenden S, Denis-Bacelar A, Hindorf C, Parker C, Chua S, et al. The potential of $^{223}$Ra and $^{18}$F-fluoride imaging to predict bone lesion response to treatment with $^{223}$Ra-dichloride in castration-resistant prostate cancer. *Eur J Nucl Med Mol Imaging.* (2017) 44:1832–44. doi: 10.1007/s00259-017-3744-y

70. Dondi F, Albano D, Bertagna F, Treglia G. Bone scintigraphy versus PSMA-targeted PET/CT or PET/MRI in prostate cancer: lessons learned from recent systematic reviews and meta-analyses. *Cancers.* (2022) 14:4470.

71. Vlachostergios P, Niaz M, Sun M, Mosallaie S, Thomas C, Christos P, et al. Prostate-specific membrane antigen uptake and survival in metastatic castration-resistant prostate cancer. *Front Oncol.* (2021) 11:630589.

72. Cherny N, Dafni U, Bogaerts J, Latino N, Pentheroudakis G, Douillard J, et al. ESMO-magnitude of clinical benefit scale version 1.1. *Ann Oncol.* (2017) 28:2340–66. doi: 10.1093/annonc/mdx310

73. Du Y, Carrio I, De Vincentis G, Fanti S, Ilhan H, Mommsen C, et al. Practical recommendations for radium-223 treatment of metastatic castration-resistant prostate cancer. *Eur J Nucl Med Mol Imaging.* (2017) 44:1671–8. doi: 10.1007/s00259-017-3756-7

74. Gillessen S, Armstrong A, Attard G, Beer T, Beltran H, Bjartell A, et al. Management of patients with advanced prostate cancer: report from the advanced prostate cancer consensus conference 2021. *Eur Urol.* (2022) 82:115–41. doi: 10.1016/j.eururo.2022.04.002

75. Arlett P, Kjaer J, Broich K, Cooke E. Real-world evidence in EU medicines regulation: enabling use and establishing value. *Clin Pharmacol Ther.* (2022) 111:21–3. doi: 10.1002/cpt.2479

76. Flynn R, Plueschke K, Quinten C, Strassmann V, Duijnhoven R, Gordillo-Maranon M, et al. Marketing authorization applications made to the European Medicines Agency in 2018-2019: what was the contribution of real-world evidence? *Clin Pharmacol Ther.* (2022) 111:90–7. doi: 10.1002/cpt.2461

77. European Medicines Agency. *A Vision for Use of Real-World Evidence in EU Medicines Regulation.* (2022). Available online at: https://www.ema.europa.eu/en/news/vision-use-real-world-evidence-eu-medicines-regulation (accessed November 22, 2022).

78. US Food and Drug Administration. *Real-World Evidence.* (2022). Available online at: https://www.fda.gov/science-research/science-and-research-special-topics/real-world-evidence (accessed November 22, 2022).

79. Azoulay L. Rationale, strengths, and limitations of real-world evidence in oncology: a Canadian review and perspective. *Oncologist.* (2022) 27:e731–8. doi: 10.1093/oncolo/oyac114

80. Blonde L, Khunti K, Harris S, Meizinger C, Skolnik N. Interpretation and impact of real-world clinical data for the practicing clinician. *Adv Ther.* (2018) 35:1763–74. doi: 10.1007/s12325-018-0805-y

81. ClinicalTrials.gov. *Combination of Radium-223 and Lutetium-177 PSMA-I&T in Men with Metastatic Castration-Resistant Prostate Cancer (AlphaBet). ClinicalTrials.gov Identifier: NCT05383079.* (2022). Available online at: https://clinicaltrials.gov/ct2/show/NCT05383079 (accessed October 09, 2022).

82. ClinicalTrials.gov. *Testing the Safety of Different Doses of Olaparib given Radium-223 for Men with Advanced Prostate Cancer with Bone Metastasis. ClinicalTrials.gov Identifier: NCT03317392.* (2019). Available online at: https://clinicaltrials.gov/ct2/show/NCT03317392 (accessed October 09, 2022).

83. ClinicalTrials.gov. *Study of Nivolumab in Combination with Radium-223 in Men with Metastatic Castration Resistant Prostate Cancer (Rad2Nivo). ClinicalTrials.gov Identifier: NCT04109729.* (2019). Available online at: https://clinicaltrials.gov/ct2/show/NCT04109729 (accessed October 09, 2022).

84. ClinicalTrials.gov. *Observational Study for the Evaluation of Long-Term Safety of Radium-223 used for the Treatment of Metastatic Castration Resistant Prostate Cancer (REASSURE). ClinicalTrials.gov Identifier: NCT02141438.* (2014). Available online at: https://clinicaltrials.gov/ct2/show/NCT02141438 (accessed October 09, 2022).

frontiers | Frontiers in Medicine

TYPE Review
PUBLISHED 04 January 2023
DOI 10.3389/fmed.2022.1057373



OPEN ACCESS

EDITED BY
Roy Larsen,
Sciencons AS, Norway

REVIEWED BY
Johan Blakkisrud,
Oslo University Hospital, Norway
Peter Anderson,
Cleveland Clinic, United States

*CORRESPONDENCE
Michael Lassmann
✉ Lassmann_m@ukw.de

SPECIALTY SECTION
This article was submitted to Nuclear Medicine, a section of the journal Frontiers in Medicine

RECEIVED 29 September 2022
ACCEPTED 05 December 2022
PUBLISHED 04 January 2023

CITATION
Lassmann M and Eberlein U (2023) Comparing absorbed doses and radiation risk of the α-emitting bone-seekers [$^{223}$Ra]$RaCl_2$ and [$^{224}$Ra]$RaCl_2$. *Front. Med.* 9:1057373. doi: 10.3389/fmed.2022.1057373



# Comparing absorbed doses and radiation risk of the α-emitting bone-seekers [$^{223}$Ra]$RaCl_2$ and [$^{224}$Ra]$RaCl_2$

Michael Lassmann* and Uta Eberlein

Department of Nuclear Medicine, University of Würzburg, Würzburg, Germany

[$^{223}$Ra]$RaCl_2$ and [$^{224}$Ra]$RaCl_2$ are bone seekers, emitting high LET, and short range (<100 μm) alpha-particles. Both radionuclides show similar decay properties; the total alpha energies are comparable ($^{223}$Ra: ≈28 MeV, $^{224}$Ra: ≈26 MeV). [$^{224}$Ra]$RaCl_2$ has been used from the mid-1940s until 1990 for treating different bone and joint diseases with activities of up to approximately 50 MBq [$^{224}$Ra]$RaCl_2$. In 2013 [$^{223}$Ra]$RaCl_2$ obtained marketing authorization by the FDA and by the European Union for the treatment of metastatic prostate cancer with an activity to administer of 0.055 MBq per kg body weight for six cycles. For intravenous injections in humans a model calculation using the biokinetic model of ICRP67 shows a ratio of organ absorbed dose coefficients ($^{224}$Ra:$^{223}$Ra) between 0.37 (liver) and 0.97 except for the kidneys (2.27) and blood (1.57). For the red marrow as primary organ-at-risk, the ratio is 0.57. The differences are mainly caused be the differing half-lives of the decay products of both radium isotopes. Both radionuclides show comparable DNA damage patterns in peripheral blood mononuclear cells after internal *ex-vivo* irradiation. Data on the long-term radiation-associated side effects are only available for treatment with [$^{224}$Ra]$RaCl_2$. Two epidemiological studies followed two patient groups treated with [$^{224}$Ra]$RaCl_2$ for more than 25 years. One of them was the "Spiess study", a cohort of 899 juvenile patients who received several injections of [$^{224}$Ra]$RaCl_2$ with a mean specific activity of 0.66 MBq/kg. Another patient group of ankylosing spondylitis patients was treated with 10 repeated intravenous injections of [$^{224}$Ra]$RaCl_2$, 1 MBq each, 1 week apart. In total 1,471 of these patients were followed-up in the "Wick study". In both studies, an increased cancer mortality by leukemia and solid cancers was observed. Similar considerations on long-term effects likely apply to [$^{223}$Ra]$RaCl_2$ as well since the biokinetics are similar and the absorbed doses in the same range. However, this increased risk will most likely not be observed due to the much shorter life expectancy of prostate cancer patients treated with [$^{223}$Ra]$RaCl_2$.

KEYWORDS

**dosimetry, biodosimetry, $^{224}$Ra, $^{223}$Ra, epidemiology**

## Introduction

[$^{223}$Ra]$RaCl_2$ targets bone metastases with high LET and short range (<100 μm) alpha-particles. In 2013, Parker et al. published the results of the phase III, double-blind, randomized, international ALSYMPCA study which compared [$^{223}$Ra]$RaCl_2$ plus best standard of care (BSC) vs. placebo plus BSC in castration resistant prostate cancer (CRPC) patients with bone metastases (1). The authors concluded that the ALSYMPCA study demonstrated significantly improved overall survival and low toxicity, suggesting that [$^{223}$Ra]$RaCl_2$ may provide a new standard of care for patients with CRPC and bone metastases. The results of the ALSYMPCA trial were used to obtain marketing authorization for [$^{223}$Ra]$RaCl_2$ ("XOFIGO"®) in Europe and North America in 2013.

[$^{224}$Ra]$RaCl_2$ has been used from the mid-1940s until 1990 for treating different bone and joint diseases, mainly in Germany (2, 3). After World War II, [$^{224}$Ra]$RaCl_2$ was primarily used for the treatment of children and juveniles suffering from bone tuberculosis, and even for the therapy of Ankylosing Spondylitis (AS) patients. The activities of [$^{224}$Ra]$RaCl_2$ administered at that time were high (approximately 0.66 MBq/kg body weight, corresponding to an activity of 50 MBq), with treatment durations ranging from 1 month to 45 months (median: 4 months). In the "Spiess study" 899 patients who received multiple injections of [$^{224}$Ra]$RaCl_2$ mainly between 1945 and 1955 for the treatment of tuberculosis, AS and some other diseases had been followed (3).

In a second group of patients who were treated with repeated intravenous injections of [$^{224}$Ra]$RaCl_2$ (excluding radiation therapy with X-rays) between 1948 and 1975 an epidemiological study on 1,471 ankylosing spondylitis patients was performed ("Wick study"). The activity was administered as 10 intravenous (IV) injections, 1 MBq each, one a week apart (mean: 0.17 MBq/kg, 10 MBq total). These patients have been followed together with a control group of 1,324 AS patients treated neither with radioactive drugs nor with X-rays (2).

[$^{224}$Ra]$RaCl_2$ has again been made available in Germany between 2000 and 2005 for treating AS. During that period, the German "Bundesinstitut für Arzneimittel und Medizinprodukte (BfArM)" approved an intraveneous injection of [$^{224}$Ra]$RaCl_2$ with total activities of 10 MBq (10 injections per week, 1 MBq each) for AS therapy (4).

[$^{224}$Ra]$RaCl_2$ has only been used in a small patient cohort for the treatment of osteoblastic metastases (5). Groth et al. describe the successful compassionate use treatment of osteoblastic metastases in 10 patients using 12 MBq or 20/30 MBq [$^{224}$Ra]$RaCl_2$. Except these studies, no further publications on patient treatment with [$^{224}$Ra]$RaCl_2$ are available.

The purpose of this work is to compare the dosimetry- and radiation-risk related aspects of treatments with [$^{223}$Ra]$RaCl_2$ and [$^{224}$Ra]$RaCl_2$.

## Radioactive decay and exposure

### Decay chains

#### $^{223}$Ra

$^{223}$Ra is an alpha emitter (half-life = 11.43 d), which decays through a cascade of short-lived alpha- and beta-emitting progeny with the emission of about 20 MeV of energy per starting atom and the first two daughters and about 28 MeV through complete decay of the progeny to stable lead (Figure 1). A listing of the decay chain, branching ratios, half-lives, energies emitted by alpha-, beta, and gamma-transitions is provided e.g., by Schumann et al. (6). The data for the energy per transition in this publication was taken from the MIRD tables by Eckerman and Endo (7).

#### $^{224}$Ra

$^{224}$Ra is also an alpha emitter (half-life = 3.63 d) decaying through a cascade of short-lived alpha- and beta-emitting progeny with the emission of about 19 MeV of energy per starting atom and the first two daughters and about 26 MeV through complete decay of the progeny to stable lead (Figure 2). More details on the decay chain and the energies emitted are provided by Schumann et al. (6) and were also taken from the Eckerman and Endo tables (7).

## Biokinetics and dosimetry

### [$^{224}$Ra]$RaCl_2$

In 2002, Lassmann et al. (8) analyzed the dosimetry after the treatment of ankylosing spondylitis with [$^{224}$Ra]$RaCl_2$ by using model calculations based on ICRP 67 (9). Details on the model are provided in the publication by Lassmann et al. (8). The highest absorbed dose coefficients were found for bone endosteum (443 mGy/MBq), liver (14 mGy/MBq), and red bone marrow (44 mGy/MBq) (8).

### [$^{223}$Ra]$RaCl_2$

For [$^{223}$Ra]$RaCl_2$, Lassmann and Nosske (10) provided a first comprehensive model-based dosimetric calculation of organ doses after intravenous administration of [$^{223}$Ra]$RaCl_2$, in analogy to the previous publication by Lassmann et al. for [$^{224}$Ra]$RaCl_2$ (8). The highest absorbed dose coefficients were also found for bone endosteum (760 mGy/MBq), liver (38 mGy/MBq), and red bone marrow (78 mGy/MBq) (10).

Several clinical studies measured the disappearance of [$^{223}$Ra]$RaCl_2$ from the blood and the excretion pathways (11–14). All studies showed a rapid blood clearance; the major excretion pathway, however, is fecal excretion.

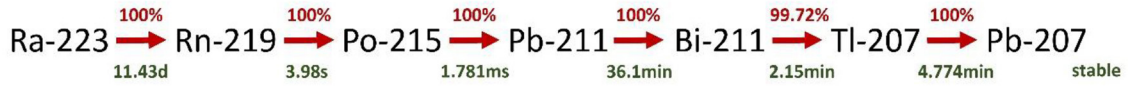


FIGURE 1
Decay chain of $^{223}$Ra. Decay products with branching ratios < 1% are omitted. The decay data were taken from http://www.nucleide.org/Laraweb/index.php.

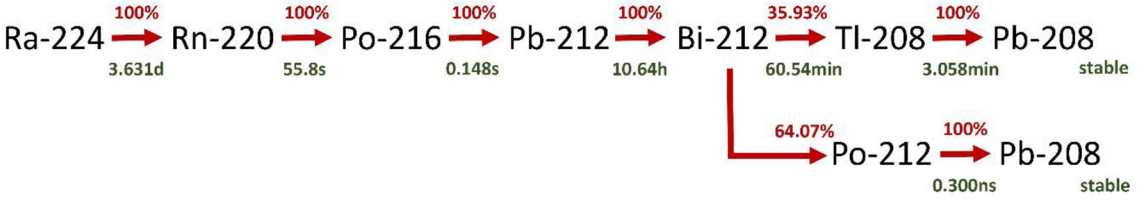


FIGURE 2
Decay chain of $^{224}$Ra. Decay products with branching ratios < 1% are omitted. The decay data were taken from http://www.nucleide.org/Laraweb/index.php.

Chittenden et al. reported a mean absorbed dose coefficient to the bone surfaces of about 5 Gy/MBq and to the red bone marrow of 0.4 Gy/MBq (12).

Yoshida et al. provided mean absorbed doses for six Japanese patients (13). As a result, the authors observed mean absorbed dose coefficients in osteogenic cells of 0.76 Gy/MBq and 0.09 Gy/MBq in the red bone marrow (13).

Pacilio et al. (15) reported, in an Italian multicenter trial in which the dosimetry was based on quantitative imaging, that the mean effective half-life [$^{223}$Ra]$RaCl_2$ in bone lesions is 8.2 d and the absorbed dose after the first injection was 0.7 Gy (range 0.2–1.9 Gy).

Another model-based dosimetry calculation was published by Höllriegl et al. (16) who adopted the newest model of the ICRP [ICRP 137, (17)]. For most organs, their results were in the same range as those reported by Lassmann and Nosske (10), except kidneys and endosteal cells. The absorbed dose coefficient for the liver (alpha contribution) reported by Lassmann and Nosske (10) is almost identical to that of Höllriegl et al. (16) (36 mGy/MBq vs. 34.4 mGy/MBq). However, Höllriegl et al. (16) cited the value by Lassmann and Nosske (10) too low by a factor of ten.

To compare the dosimetry data for both radionuclides the absorbed dose coefficients were taken from the tables provided by Lassmann et al. (8, 10). The data for blood were taken from Schumann et al. (14) and Stephan et al. (18).

## Comparison of absorbed doses to organs or tissues

In Table 1, the ratios of the absorbed dose coefficients ([$^{224}$Ra]$RaCl_2$ vs. [$^{223}$Ra]$RaCl_2$) and, for a comparative analysis, of the absorbed doses of two treatment scenarios (10 MBq [$^{224}$Ra]$RaCl_2$ vs. 25 MBq [$^{223}$Ra]$RaCl_2$, corresponding to 6 cycles of 55 kBq/kg for a 75kg patient) are shown. A direct comparison between the activities administered in the study published by Groth et al. (5) (mean value of the high activities of 25 MBq [$^{224}$Ra]$RaCl_2$) to a standard treatment with [$^{223}$Ra]$RaCl_2$ (25 MBq [$^{223}$Ra]$RaCl_2$) is provided by the direct comparison of the absorbed dose coefficients. The activities for the two treatment scenarios were chosen to reflect the [$^{224}$Ra]$RaCl_2$ administered activities in the "Wick Study" and the activity administered for a standard treatment with [$^{223}$Ra]$RaCl_2$ to a 75 kg patient.

For most organs or tissues all decay products contribute almost equally to the absorbed doses in these organs (14, 16). Experimental data on these effects, however, are sparse and are taken from animal experiments (19). For the red marrow as primary organ-at-risk, the ratio of the absorbed dose coefficients is 0.57. The largest dissimilarities of the absorbed dose coefficient ratios are observed for the kidneys (2.27), blood (1.67), and liver (0.37). The higher values for the kidneys and blood could be attributed to the accumulation of lead and its progeny due to the longer half-life of $^{212}$Pb compared to $^{211}$Pb.

A comparison of the absorbed dose ratios assessed for the two treatment scenarios shows that the absorbed doses are always lower for [$^{224}$Ra]$RaCl_2$. For obtaining equal absorbed doses to the red marrow, the administered activity for [$^{224}$Ra]$RaCl_2$ can be chosen to be approximately 1.8-fold higher than that for [$^{223}$Ra]$RaCl_2$.

This comparison does not include absorbed doses of metastases which take up radium as the underlying ICRP models do not consider this case as they were designed for radiation protection purposes. Therefore, the absorbed doses to organs/tissue could be much lower if a considerable amount of

TABLE 1 Ratio of the absorbed organ dose coefficients (mGy/MBq) and the absorbed doses for typical administrations (10 MBq [$^{224}$Ra]$RaCl_2$ in the "Spiess study", 25 MBq [$^{223}$Ra]$RaCl_2$ for six cycles in a patient of 75 kg).

| Organ | Ratio of absorbed dose coefficients: [$^{224}$Ra]$RaCl_2$/ [$^{223}$Ra]$RaCl_2$ | Ratio of Absorbed doses: 10 MBq [$^{224}$Ra]$RaCl_2$/ 25 MBq [$^{223}$Ra]$RaCl_2$ |
|---|---|---|
| Adrenals | 0.73 | 0.29 |
| Bladder wall | 0.70 | 0.28 |
| Bone endosteum | 0.58 | 0.23 |
| Brain | 0.71 | 0.28 |
| Breast | 0.70 | 0.28 |
| **GI-tract** | | |
| Esophagus | 0.71 | 0.28 |
| St wall | 0.72 | 0.29 |
| SI wall | 0.78 | 0.31 |
| ULI wall | 0.46 | 0.18 |
| LLI wall | 0.57 | 0.23 |
| Colon | 0.54 | 0.22 |
| Kidneys | 2.27 | 0.91 |
| Liver | 0.37 | 0.15 |
| Muscle | 0.72 | 0.29 |
| Ovaries | 0.97 | 0.39 |
| Pancreas | 0.72 | 0.29 |
| Red marrow | 0.57 | 0.23 |
| **Respiratory tract** | | |
| ET airways | 0.67 | 0.27 |
| Lungs | 0.67 | 0.27 |
| Skin | 0.71 | 0.28 |
| Spleen | 0.88 | 0.35 |
| Testes | 0.87 | 0.35 |
| Thymus | 0.71 | 0.28 |
| Thyroid | 0.71 | 0.28 |
| Blood | 1.57 | 0.66 |

The data are taken from Lassmann and Nosske (10) and from Lassmann et al. (8) as the unweighted sum over the alpha and beta radiation contributions for each organ. The data for blood were taken from Schumann et al. (14) and Stephan et al. (18).

the injected activity is taken up by tumors as only a fraction of the remaining activity will be available and taken up by other organs or tissues.

## External exposure

To further elucidate potential differences between $^{224}$Ra and $^{223}$Ra and their respected progenies regarding exposure of staff or persons staying close to patients, the dose rate constants for the ambient dose H* were compared. For the comparison, the newest published values were used for $^{224}$Ra and $^{223}$Ra and the respective progenies (20).

The values for both radionuclides and their decay products are quite similar [45.17 μSv $m^2$/(h GBq), $^{223}$Ra and 49.44 μSv $m^2$/(h GBq), $^{224}$Ra]. The dose rate by a patient after administration of $^{223}$Ra in 1 m distance immediately following administration is 0.05 μSv/(h MBq). This value is in good agreement with the mean values measured by Dauer et al. of 0.02 μSv/(h MBq) (21). Overall, the external exposure of both radionuclides is low compared to other treatments with radiopharmaceuticals.

## Long-term radiation-related effects

### Patient cohorts studying long-term radiation-related effects of [$^{224}$Ra]$RaCl_2$

There are two patient cohorts that were followed for long-term radiation-related effects after the use of [$^{224}$Ra]$RaCl_2$.

In several publications Nekolla et al. (3, 22, 23) followed the health of 899 persons that were included in the "Spiess study". The mostly juvenile patients received, mainly between 1945 and 1955, multiple injections of [$^{224}$Ra]$RaCl_2$ (mean specific activity: 0.66 MBq/kg, corresponding to an injection of 46 MBq to a 70 kg patient) with the aim of treating tuberculosis (TB), AS and some other diseases.

A second patient cohort included 1,471 AS patients treated with repeated intravenous injections of 0.17 MBq/kg [$^{224}$Ra]$RaCl_2$ between 1948 and 1975 (2). These patients have been followed in the "Wick study" together with a control group of 1,324 AS patients treated neither with radioactive drugs nor with X-rays. The mean follow-up time was 26.3 years in the exposed and 24.6 years in the control group.

### Radiation-induced side-effects of [$^{223}$Ra]$RaCl_2$ and [$^{224}$Ra]$RaCl_2$

In the study cohort of the "Spiess study", Nekolla et al. (22) and Nekolla et al. (3) observed shortly after [$^{224}$Ra]$RaCl_2$ injections an increase in bone tumor risk significantly greater for younger ages at exposure. Most of the malignant bone tumors were osteosarcomas and fibrous-histiocytic sarcomas. During the two most recent decades of observation, a significant excess of non-skeletal malignant diseases has also become evident. Until the end of 2007, the total number of observed malignant non-skeletal diseases was 270 compared to 192 expected cases (3).

For [$^{224}$Ra]$RaCl_2$ the most striking observation of the "Wick study" (2) were the 21 cases of leukemia in the exposed group

(vs. 6.8 cases expected, $P < 0.001$) compared to 12 cases of leukemia in the control group (vs. 7.5 cases expected). This increase in total leukemias was significant in direct comparison between the exposed and control groups too ($P < 0.05$). Wick et al. found, besides an increased standardized incidence ratio (= ratio of the number of observed cases vs. the number of expected cases) of leukemias, a significant increase for kidney and thyroid cancer (2).

For [$^{223}$Ra]$RaCl_2$ only mild side and mostly transient effects were observed (1). [$^{223}$Ra]$RaCl_2$ was well tolerated by patients with skeletal metastases. Mild to moderate and transient hematological toxicity was observed at potentially therapeutic doses. Platelets were less affected than neutrophils and white blood cells; toxicity grade I was seen in 5 of the 31 patients (1). Furthermore, only two cases of leukemia have been reported until today (24).

## Discussion

A major drawback for image-based dosimetry of [$^{223}$Ra]$RaCl_2$ is the inherent difficulty to quantify post-therapeutic gamma camera images, although photon emissions suitable for gamma camera imaging are available at ∼82 keV, ∼154 keV, and ∼270 keV. Due to the low photon abundance, the low activities administered to the patients, and the high contribution of down-scatter of higher energy photons leading to severe septal penetration causes large image quantification uncertainties as reported by Hindorf et al. (25). Pacilio et al. (26) and Yoshida et al. (13) provided quantitative results by planar imaging, however, the accuracy of the respective quantification process for *in-vivo* imaging is even more limited due to activity overlay in this type of image. For $^{224}$Ra, data on imaging, though theoretically possible with the 239–241 keV gamma rays for $^{224}$Ra and $^{212}$Pb, and the 73–87 keV gamma rays of $^{212}$Pb and $^{208}$Tl have not been published. A feasibility study on how to quantify the decay product $^{212}$Pb by SPECT/CT imaging was published by Kvassheim et al. (27). However, the direct comparability of the results of this phantom study with activities up to 8 MBq to patient studies with [$^{224}$Ra]$RaCl_2$ is limited. For example, the [$^{224}$Ra]$RaCl_2$ activities administered in the patient study of Groth et al. (5) (maximum 30 MBq over several cycles) were at least one order of magnitude lower as compared to a recent clinical study with $^{212}$Pb-DOTAMTATE (28) (188 MBq per cycle for a 75 kg patient), thus hampering reliable image quantification of [$^{224}$Ra]$RaCl_2$.

A major concern for the application of radium isotopes to patients could be diffusion of the first daughter products $^{219}$Rn (half-life: 4 s) or $^{220}$Rn (half-life: 56 s). This could lead either to an increased diffusion of radon away from the binding site leading to unwanted irradiation of other organs or tissues or to increased emanation of radon, therefore reducing the energy deposited in the tumor/lesion.

Lloyd et al. (29) studied the retention, distribution and dosimetry of injected [$^{224}$Ra]$RaCl_2$ in six young adult beagles which were killed 0.04 to 7 days after [$^{224}$Ra]$RaCl_2$ administration. Their results suggest that, for the beagles, a fraction of roughly 0.08 of $^{220}$Rn or $^{216}$Po is produced *in vivo* and escapes from the skeleton. Increased *in-vivo* emanation of $^{220}$Rn was not observed in a study by Klemm et al. (30) who were looking for increased $^{220}$Rn exhalation in two AS patients after therapy with [$^{224}$Ra]$RaCl_2$.

Why it might be more favorable to use [$^{224}$Ra]$RaCl_2$ as compared to [$^{223}$Ra]$RaCl_2$ to treat solid tumors is shown in two studies by Arazi et al. (31) and Arazi (32). Although a different set-up - diffusing alpha-emitters radiation therapy utilizing implantable sources carrying small activities of $^{224}$Ra - the arguments are applicable also to the case of bone metastases taking up $^{224}$Ra. The released atoms disperse inside the tumor by diffusive and convective processes, creating, through their alpha emissions, a high-dose region measuring several millimeter in diameter about each source. If the decay point of $^{220}$Rn is effectively the starting point for the migration of $^{212}$Pb which may further distribute away from the source, the assessment by Arazi et al. (31) and Arazi (32) demonstrates that the size of the region subject to alpha particle irradiation may be expected to be of the order of millimeters rather than a few dozen micrometers. This might lead to a more homogeneous dose distribution in the tumor as compared to $^{223}$Ra. Similar findings have been reported by Napoli et al. in an experimental study with $^{224}$Ra-labeled $CaCO_3$ microparticles (33). These considerations are not taken into account in any of the absorbed dose calculations until today (8, 10, 16).

Data on the biological effects by [$^{223}$Ra]$RaCl_2$ or [$^{224}$Ra]$RaCl_2$ are sparse. For [$^{224}$Ra]$RaCl_2$, only the publication by Stephan et al. (18) showed radiation dose-related effects on chromosomal aberrations in peripheral lymphocytes after repeated treatments. The frequency of chromosomal aberrations observed during the course of therapy was related to the absorbed dose to the blood. They also observed, that the frequency of dicentric chromosomes induced *in vivo* agreed well with the corresponding value of dicentrics induced *in vitro* (18).

For [$^{223}$Ra]$RaCl_2$ Sciuto et al. showed high dose dependent increase of the number of dicentrics and micronuclei during the course of [$^{223}$Ra]$RaCl_2$ therapy. The authors found a linear correlation between the absorbed dose to the blood and the number of dicentrics after repeated treatments.

Our group could show in several publications in peripheral blood mononuclear cells (PBMCs), by using the γ-H2AX assay as a marker for DNA double strand breaks, that there is, after internal *ex vivo* irradiation, a linear correlation between the number of alpha tracks induced by [$^{223}$Ra]$RaCl_2$ and [$^{224}$Ra]$RaCl_2$ revealing no difference between the radionuclides at the same absorbed dose (6, 34). Furthermore the *ex vivo* repair kinetics of the DNA damage in PBMCs is similar to the repair rate when compared to beta irradiation (35). Schumann

et al. also observed *in vivo* in 9 patients after treatment with [$^{223}$Ra]$RaCl_2$ that the DNA damage is partly repaired (14).

Concerning long-term side effects, Priest et al. (36) compared, in a reanalysis of the AS patient data of the Wick study, the higher incidence of radiation-induced cancer with the fact that the patient treatment resulted decreased pain and increased mobility. Both of which are associated with decreased mortality by non-cancer diseases and from all causes of death. In their analysis they found no excess mortality in the group of AS patients. According to the authors, "the study demonstrates the need to consider all causes of death and longevity when assessing health impacts following irradiation" (36).

With respect to long-term effects of treatment with [$^{223}$Ra]$RaCl_2$, stochastic radiation-induced side-effects, although observed for [$^{224}$Ra]$RaCl_2$, are less relevant in the context of cancer treatment of prostate cancer as the median survival time of patients after treatment is 14 months (1). This is significantly less than 2 years considered to be the latent period for induced leukemia or the 8 year average latent period for induced bone cancer (23, 37, 38). Therefore, presently the benefit of the treatment of prostate cancer patients with [$^{223}$Ra]$RaCl_2$ outweighs the hypothetical risk associated with this treatment.

## Conclusions

When comparing the dosimetry data obtained by model-based calculations on [$^{223}$Ra]$RaCl_2$ and [$^{224}$Ra]$RaCl_2$ or data obtained by bio-dosimetric methods no major differences are observed for most organs. For kidneys, liver and blood the differences, most likely, can be explained by the differing half-lives of the respective progenies. Due to the difficulties associated with quantitative imaging of radium isotopes, absorbed doses derived by imaging procedures are less reliable due to inherent difficulties of image quantification. Furthermore, *in vivo* diffusion by radium progeny particularly in tumors is not well characterized and might need further experimental verification.

Data on long-term radiation-associated side effects are only available for treatment with [$^{224}$Ra]$RaCl_2$. In several studies, an increased cancer mortality by leukemia and solid cancers was observed. Similar considerations likely apply to [$^{223}$Ra]$RaCl_2$ as the biokinetics and the absorbed doses are in the same range, but this increased risk may not be observed due to the much shorter life expectancy of prostate cancer patients treated with [$^{223}$Ra]$RaCl_2$.

## Author contributions

Both authors listed have made a substantial, direct, and intellectual contribution to the work and approved it for publication.

## Funding

This publication was supported by the Open Access Publication Fund of the University of Würzburg.

## Conflict of interest

The authors declare that the research was conducted in the absence of any commercial or financial relationships that could be construed as a potential conflict of interest.

## Publisher's note



## References

1. Parker C, Nilsson S, Heinrich D, Helle SI, O'Sullivan JM, Fossa SD, et al. Alpha emitter radium-223, survival in metastatic prostate cancer. *N Engl J Med.* (2013) 369:213–23. doi: 10.1056/NEJMoa1213755

2. Wick RR, Atkinson MJ, Nekolla EA. Incidence of leukaemia and other malignant diseases following injections of the short-lived alpha-emitter $^{224}$Ra into man. *Radiat Environ Biophys.* (2009) 48:287–94. doi: 10.1007/s00411-009-0227-y

3. Nekolla EA, Walsh L, Spiess H. Incidence of malignant diseases in humans injected with radium-224. *Radiat Res.* (2010) 174:377–86. doi: 10.1667/RR1955.1

4. Alberding A, Stierle H, Brandt J, Braun J. Effectiveness and safety of radium chloride in the treatment of ankylosing spondylitis. Results of an observational study. *Z Rheumatol.* (2006) 65:245–51. doi: 10.1007/s00393-005-0009-0

5. Groth P, Dunkelmann S, Schümichen C. Die Behandlung osteoblastischer Metastasen mit Radium-224-Chlorid. *Nuklearmedizin.* (2008) 47:A106.

6. Schumann S, Eberlein U, Müller J, Scherthan H, Lassmann M. Correlation of the absorbed dose to the blood and DNA damage in leukocytes after internal ex-vivo irradiation of blood samples with $^{224}$Ra. *EJNMMI Res.* (2018) 8:77. doi: 10.1186/s13550-018-0422-4

7. Eckerman KF, Endo A. *MIRD: Radionuclide Data and Decay Schemes.* Reston, Virginia, USA: Society of Nuclear Medicine. (2008).

8. Lassmann M, Nosske D, Reiners C. Therapy of ankylosing spondylitis with $^{224}$Ra-radium chloride: dosimetry and risk considerations. *Radiat Environ Biophys.* (2002) 41:173–8. doi: 10.1007/s00411-002-0164-5

9. ICRP. *Publication 67: Age-dependent doses to members of the public from intake of radionuclides: Part 2 Ingestion dose coefficients.* Ann ICRP 22, 405.

10. Lassmann M, Nosske D. Dosimetry of $^{223}$Ra-chloride: dose to normal organs and tissues. *Eur J Nucl Med Mol Imaging.* (2013) 40:207–12. doi: 10.1007/s00259-012-2265-y

11. Carrasquillo JA, O'Donoghue JA, Pandit-Taskar N, Humm JL, Rathkopf DE, Slovin SF, et al. Phase I pharmacokinetic and biodistribution study with escalating doses of $^{223}$Ra-dichloride in men with castration-resistant metastatic prostate cancer. *Eur J Nucl Med Mol Imaging.* (2013) 40:1384–93. doi: 10.1007/s00259-013-2427-6

12. Chittenden SJ, Hindorf C, Parker CC, Lewington VJ, Pratt BE, Johnson B, et al. A Phase 1, open-label study of the biodistribution, pharmacokinetics, and dosimetry of $^{223}$Ra-Dichloride in patients with hormone-refractory prostate cancer and skeletal metastases. *J Nucl Med.* (2015) 56:1304–9. doi: 10.2967/jnumed.115.157123

13. Yoshida K, Kaneta T, Takano S, Sugiura M, Kawano T, Hino A, et al. Pharmacokinetics of single dose radium-223 dichloride (BAY 88-8223) in Japanese patients with castration-resistant prostate cancer and bone metastases. *Ann Nucl Med.* (2016) 30:453–60. doi: 10.1007/s12149-016-1093-8

14. Schumann S, Eberlein U, Lapa C, Muller J, Serfling S, Lassmann M, et al. alpha-Particle-induced DNA damage tracks in peripheral blood mononuclear cells of [$^{223}$Ra]$RaCl_2$-treated prostate cancer patients. *Eur J Nucl Med Mol Imaging.* (2021) 48:2761–70. doi: 10.1007/s00259-020-05170-6

15. Pacilio M, Ventroni G, De Vincentis G, Cassano B, Pellegrini R, Di Castro E, et al. Dosimetry of bone metastases in targeted radionuclide therapy with alpha-emitting $^{223}$Ra-dichloride. *Eur J Nucl Med Mol Imaging.* (2016) 43:21–33. doi: 10.1007/s00259-015-3150-2

16. Höllriegl V, Petoussi-Henss N, Hurkamp K, Ocampo Ramos JC, Li WB. Radiopharmacokinetic modelling and radiation dose assessment of (223)Ra used for treatment of metastatic castration-resistant prostate cancer. *EJNMMI Phys.* (2021) 8:44. doi: 10.1186/s40658-021-00388-1

17. Paquet F, Bailey MR, Leggett RW, Lipsztein J, Marsh J, Fell TP, et al. ICRP Publication 137: Occupational Intakes of Radionuclides: Part 3. *Ann ICRP.* (2017) 46:1–486. doi: 10.1177/0146645317734963

18. Stephan G, Kampen WU, Nosske D, Roos H. Chromosomal aberrations in peripheral lymphocytes of patients treated with radium-224 for ankylosing spondylitis. *Radiat Environ Biophys.* (2005) 44:23–8. doi: 10.1007/s00411-005-0275-x

19. Lloyd RD, Bruenger FW, Jones CW, Taylor GN, Mays CW. Radium retention in mature beagles injected at 5 years of age. *Radiat Res.* (1983) 94:210–6. doi: 10.2307/3575876

20. Stettner C, Hranitzky C, Poljanc K, Strebl F, Streli C. Catalogue of dose rate constants for more than 400 radionuclides in terms of ambient dose H(*) and comparison of figures to ambient dose equivalent H(*)(10). *Appl Radiat Isot.* (2022) 184:110159. doi: 10.1016/j.apradiso.2022.110159

21. Dauer LT, Williamson MJ, Humm J, O'Donoghue J, Ghani R, Awadallah R, et al. Radiation safety considerations for the use of [$^{223}$Ra]$RaCl_2$ DE in men with castration-resistant prostate cancer. *Health Phys.* (2014) 106:494–504. doi: 10.1097/HP.0b013e3182a82b37

22. Nekolla EA, Kellerer AM, Kuse-Isingschulte M, Eder E, Spiess H. Malignancies in patients treated with high doses of radium-224. *Radiat Res.* (1999) 152:S3–7. doi: 10.2307/3580102

23. Nekolla EA, Kreisheimer M, Kellerer AM, Kuse-Isingschulte M, Gossner W, Spiess H, et al. Induction of malignant bone tumors in radium-224 patients: risk estimates based on the improved dosimetry. *Radiat Res.* (2000) 153:93–103. doi: 10.1667/0033-7587(2000)153[0093:IOMBTI]2.0.CO;2

24. Jacene H, Gomella L, Yu EY, Rohren EM. Hematologic Toxicity From Radium-223 Therapy for Bone Metastases in Castration-Resistant Prostate Cancer: Risk Factors and Practical Considerations. *Clin Genitourin Cancer.* (2018) 16:e919–26. doi: 10.1016/j.clgc.2018.03.007

25. Hindorf C, Chittenden S, Aksnes AK, Parker C, Flux GD. Quantitative imaging of $^{223}$Ra-chloride (Alpharadin) for targeted alpha-emitting radionuclide therapy of bone metastases. *Nucl Med Commun.* (2012) 33:726–32. doi: 10.1097/MNM.0b013e328353bb6e

26. Pacilio M, Cassano B, Chiesa C, Giancola S, Ferrari M, Pettinato C, et al. The Italian multicentre dosimetric study for lesion dosimetry in $^{223}$Ra therapy of bone metastases: Calibration protocol of gamma cameras and patient eligibility criteria. *Phys Med.* (2016) 32:1731–7. doi: 10.1016/j.ejmp.2016.09.013

27. Kvassheim M, Revheim MR, Stokke C. Quantitative SPECT/CT imaging of lead-212: a phantom study. *EJNMMI Phys.* (2022) 9:52. doi: 10.1186/s40658-022-00481-z

28. Delpassand ES, Tworowska I, Esfandiari R, Torgue J, Hurt J, Shafie A, et al. Targeted alpha-emitter therapy with $^{212}$Pb-DOTAMTATE for the treatment of metastatic SSTR-expressing neuroendocrine tumors: first-in-humans dose-escalation clinical trial. *J Nucl Med.* (2022) 63:1326–33. doi: 10.2967/jnumed.121.263230

29. Lloyd RD, Mays CW, Taylor GN, Atherton DR, Bruenger FW, Jones CW, et al. Radium-224 retention, distribution, and dosimetry in beagles. *Radiat Res.* (1982) 92:280–95. doi: 10.2307/3576005

30. Klemm C, Michel K, Rose E, Meringdal J. Storage and excretion of Radium 224 (-thorium X) during treatment of ankylosing spondylitis. *Z Rheumaforsch.* (1970) 29:234–40.

31. Arazi L, Cooks T, Schmidt M, Keisari Y, Kelson I. Treatment of solid tumors by interstitial release of recoiling short-lived alpha emitters. *Phys Med Biol.* (2007) 52:5025–42. doi: 10.1088/0031-9155/52/16/021

32. Arazi L. Diffusing alpha-emitters radiation therapy: approximate modeling of the macroscopic alpha particle dose of a point source. *Phys Med Biol.* (2020) 65:015015. doi: 10.1088/1361-6560/ab5b73

33. Napoli E, Bonsdorff TB, Jorstad IS, Bruland OS, Larsen RH, Westrom S, et al. Radon-220 diffusion from $^{224}$Ra-labeled calcium carbonate microparticles: Some implications for radiotherapeutic use. *PLoS ONE.* (2021) 16:e0248133. doi: 10.1371/journal.pone.0248133

34. Schumann S, Eberlein U, Muhtadi R, Lassmann M, Scherthan H. DNA damage in leukocytes after internal ex-vivo irradiation of blood with the alpha-emitter $^{223}$Ra. *Sci Rep.* (2018) 8:2286. doi: 10.1038/s41598-018-20364-7

35. Göring L, Schumann S, Müller J, Buck AK, Port M, Lassmann M, et al. Repair of alpha-particle-induced DNA damage in peripheral blood mononuclear cells after internal *ex vivo* irradiation with $^{223}$Ra. *Eur J Nucl Med Mol Imaging.* (2022) 49:3981–8. doi: 10.1007/s00259-022-05860-3

36. Priest ND, Dauer LT, Hoel DG. Administration of lower doses of radium-224 to ankylosing spondylitis patients results in no evidence of significant overall detriment. *PLoS ONE.* (2020) 15:e0232597. doi: 10.1371/journal.pone.0232597

37. Rowland RE, Stehney AF, Lucas HF. Dose-response relationships for radium-induced bone sarcomas. *Health Phys.* (1983) 44:15–31. doi: 10.1097/00004032-198306001-00001

38. Gossner W. Target cells in internal dosimetry. *Radiat Prot Dosimetry.* (2003) 105:39–42. doi: 10.1093/oxfordjournals.rpd.a006265

frontiers | Frontiers in Medicine

TYPE Review
PUBLISHED 06 January 2023
DOI 10.3389/fmed.2022.1076210



OPEN ACCESS

EDITED BY
Roy Larsen,
Sciencons AS, Norway

REVIEWED BY
Weijun Wei,
Shanghai Jiao Tong University, China
Sandrine Huclier,
Université de Nantes, France
Kohshin Washiyama,
Fukushima Medical University, Japan

*CORRESPONDENCE
Per Albertsson
✉ per.albertsson@oncology.gu.se

SPECIALTY SECTION
This article was submitted to Nuclear Medicine, a section of the journal Frontiers in Medicine

RECEIVED 21 October 2022
ACCEPTED 06 December 2022
PUBLISHED 06 January 2023

CITATION
Albertsson P, Bäck T, Bergmark K, Hallqvist A, Johansson M, Aneheim E, Lindegren S, Timperanza C, Smerud K and Palm S (2023) Astatine-211 based radionuclide therapy: Current clinical trial landscape. *Front. Med.* 9:1076210. doi: 10.3389/fmed.2022.1076210



# Astatine-211 based radionuclide therapy: Current clinical trial landscape

Per Albertsson[1,2]*, Tom Bäck[3], Karin Bergmark[1,2], Andreas Hallqvist[1,2], Mia Johansson[1,2], Emma Aneheim[1,3], Sture Lindegren[3], Chiara Timperanza[3], Knut Smerud[4] and Stig Palm[3]

[1]Department of Oncology, Sahlgrenska University Hospital, Gothenburg, Sweden, [2]Department of Oncology, Institute of Clinical Sciences, Sahlgrenska Academy, University of Gothenburg, Gothenburg, Sweden, [3]Department of Radiation Physics, Institute of Clinical Sciences, Sahlgrenska Academy, University of Gothenburg, Gothenburg, Sweden, [4]Smerud Medical Research International AS, Oslo, Norway

Astatine-211 ($^{211}$At) has physical properties that make it one of the top candidates for use as a radiation source for alpha particle-based radionuclide therapy, also referred to as targeted alpha therapy (TAT). Here, we summarize the main results of the completed clinical trials, further describe ongoing trials, and discuss future prospects.

KEYWORDS

**targeted alpha therapy, alpha particle, astatine-211, radionuclide, human, clinical trial**

## 1. Introduction

Astatine was first synthesized at the University of California, Berkley in 1940 (1), and the first report of its treatment on humans was published as early as 1954 (2). Because astatine lacks stable or long-lived isotopes, it is named after the ancient Greek word "astatos' meaning "unstable'. Astatine is often referred to as "the rarest element on earth" because only isotopes 214–219 can be found naturally in the earth's crust in equilibrium with uranium. It is estimated that there are only ∼0.07 grams present at any given time. This makes availability an issue. However, substantial amounts of astatine-211 ($^{211}$At) can be produced in cyclotrons. The availability, chemistry, and logistics of handling this rare element have been comprehensively addressed recently (3–6) and will be briefly mentioned here.

$^{211}$At has a 100% alpha emission with only one alpha particle emitted per decay, which prevents unpredictable dose localization caused by the detachment of radioactive daughters from the carrier vector. This is comparable to other alpha emitters such as thorium-227 ($^{227}$Th), radium-223 ($^{223}$Ra), lead-212 ($^{212}$Pb), bismuth-212 ($^{212}$Bi), and actinium-225 ($^{225}$Ac), all of which have a long decay series and may suffer from recoil problems. A half-life (t½) of 7.2 h is also another advantage, with <1% of radioactivity remaining after 2 days, which may decrease normal tissue exposure, while still being long enough to be shipped for up to 3 h to perform chemistry/radiopharmacy with enough remaining activity to use for clinical treatment. This review summarizes the current clinical experiences with $^{211}$At-based treatments, provides an update on ongoing trials,

and provides perspectives on possible paths that may be explored in the near future.

## 2. The past

### 2.1. Summary of the main findings from completed clinical experiences with $^{211}$At

To the best of our knowledge, the first documented use of $^{211}$At in humans was published in 1954, when Hamilton et al. investigated its potential use in the treatment of thyroid disorders (2). Thereafter, a case report was published in 1990 where a patient with an inoperable carcinoma of the tongue received intra-arterially injected $^{211}$At-labeled human serum albumin microspheres as a palliative measure (7). A few conclusions can be drawn from these very early works in humans treated with $^{211}$At, namely, it can accumulate in the thyroid tissue, and alpha-emitting nuclides possess enormous destructive capacity when locally retained. Two published phase I trials used an intra-cavitary route of administration, whereby systemic exposure was minimized and no systemic toxicity could be detected (8, 9). Importantly, both studies calculated locally high absorbed doses in the treated volume that was beneficial to the patients. Signs of this were also found in both studies, with some patients surviving longer than expected, but with a clear risk of biased inclusion. These findings should be explored in correctly designed efficacy-seeking trials. Table 1 summarizes human experiences and the completed clinical trials performed so far.

#### 2.1.1. Berkeley, California, USA 1954

Knowing that the halogen iodine can accumulate in thyroid tissue, the same year that $^{211}$At was discovered in 1940, it was investigated for potential accumulation in thyroid tissues in guinea pigs. Due to other matters, research in this area was halted for several years. In 1954 at the Crocker Laboratory in Berkeley California, Hamilton et al. (2) investigated the thyroid accumulation of $^{211}$At in 7 patients with various thyroid disorders and one papillary adenocarcinoma with cervical lymph node metastases. Here, 1.85 MBq $^{211}$At was dissolved in 25 mL water and given orally to the patients 13–22 h prior to surgery to remove the thyroid gland. From this small data set, it was concluded that the accumulation of $^{211}$At in the thyroid glands was relatively higher than that observed in experiments using rats. Additionally, a correlation was observed between $^{211}$At uptake and stable iodine in the thyroid tissue. There was no discernible accumulation of $^{211}$At in the cervical lymph node metastases present in the patient with papillary adenocarcinoma. No toxicity or adverse events were reported.

#### 2.1.2. Dresden, East Germany 1990

In a case report by Doberenz et al. (7) at the Carl Gustav Carus University Hospital in Dresden, East Germany, a patient with an unresectable recurrent carcinoma of the tongue was treated in 1988 with 200 MBq of $^{211}$At-labeled human serum albumin microspheres that were 15–25 μm in diameter. The radio-conjugate was injected directly into the left lingual artery. Although the tumor tissue supplied by the artery successfully became necrotic within a few days, necrosis eventually spread to the entire tongue. Locally, in the tumor, the dose was calculated to be 302 Gy, and by day 30, no viable tissue was left in the tongue. At 4 and 20 h post injection, 81 and 64% of the radioactivity was found in the tongue, respectively. The thyroid gland was blocked for up-take. In the thyroid, <1 and 3% were found at 4 and 20 h respectively. A slight depression was found in thyroid hormone levels, but within normal range. Using a relative biological effectiveness (RBE) of 7, the lungs were calculated to receive 5.32 Sv. The patient died on day 43 of apparent aspiration pneumonia. The autopsy revealed no signs of pneumonitis in the lungs. Histological examination of the thyroid gland showed atrophy and fibrosis.

#### 2.1.3. Durham, North Carolina, USA, 2008

In 2008, Zalutsky et al. (9) reported the first completed clinical trial using targeted alpha therapy with $^{211}$At at the Duke University Medical Center. $^{211}$At was conjugated to the chimeric (human/mouse) mAb, anti-tenascin, and ch81C6. Tenascin is an extracellular matrix glycoprotein ubiquitously expressed in high-grade gliomas, but not in normal brain tissue. This clinical trial was initiated following a series of well-performed and relevant preclinical investigations with the construct $^{211}$At-ch81C6, demonstrating *in vitro* cytotoxic effects (13), *in vivo* stability (14), tissue distribution after i.v. (intravenous) and intrathecal administration in mice for calculation of human radiation doses (15), and investigations on long-term toxicity and the maximum tolerated activity in mice (16). Considering that the t½ of $^{211}$At is 7.2 h, systemic exposure and product degradation could be minimized by choosing a local administration route. Therefore, $^{211}$At-ch81C6 was administered into a Rickham reservoir and its catheter was placed in the surgically created resection cavity.

This phase I dose escalation study (NCT00003461) was performed between April 1998 and June 2001 to study the feasibility and safety of locally injected $^{211}$At-ch81C6 into the resection cavity of recurrent brain cancer. This study followed as a natural extension after promising results were obtained using beta-particle-emitting constructs with murine-81C6 in similar clinical situations (17, 18). It was argued that the advantages of alpha particle vs. beta particle irradiation could prove to be maximized in this clinical setting, i.e., the risk of small pockets of remaining malignant cells with a low blood supply. Here, the alpha particle has the advantages of a lower sensitivity to tumor

TABLE 1 Completed clinical studies using $^{211}$At. (*NTC number*) is the ClinicalTrials.gov identifier.

| Institution, Reference | Clinical situation | Nb. Pts. | Study Objective | TAT-agent | Target | Adminis-tration | Act-ivity | Toxicity/ effect |
|---|---|---|---|---|---|---|---|---|
| Duke University Medical Center, Durham, USA (9) (*NCT00003461*) | Recurrent surgically resected glioblastoma | 18 | Feasibility and safety | $^{211}$At-ch81C6 | tenascin | Surgically created resection cavity | 71–347 MBq | MTD, Not reached |
| Sahlgrenska University Hospital, Gothenburg, Sweden (8, 10–12) (*NCT04461457*) | Relapsed ovarian cancer | 12 | Safety, Toxicity Pharmacokinetics | $^{211}$At-MX35 F(ab')2 | NaPi2b | Intra peritoneal | 34–355 MBq | MTD, Not reached |
| Carl Gustav Carus University Hospital, Dresden, East Germany (7) | Recurrent carcinoma of the tongue | 1 | Palliation | $^{211}$At-labeled human serum albumin microspheres (15–25μm) | Tumor vasculature | Intra arterially (left lingual artery) | 200 MBq | Tumor necrosis/ tongue necrosis |
| University of California Berkeley and San Francisco, USA (2) | Thyroid gland disorders | 8 | Tracer study | $^{211}$At | $Na^+/I^-$ symporter (NIS) | Per oral in 25ml water | 1.85 MBq | Thyroid uptake was established |

oxygenation and a higher RBE (relative biologic effect) owing to its high linear energy transfer (LET) and shorter path length, which would be beneficial and possibly less toxic.

Nineteen patients were enrolled, 18 of which (nine female) were treated for recurrent brain cancer (glioblastoma multiforme, n = 14; anaplastic oligodendroglioma, $n = 3$; anaplastic astrocytoma, $n = 1$). One patient was excluded because of subgaleal leakage seen in the postoperative flow study with technetium-99 m-labeled albumin. This was performed to verify the Rickham catheter patency, and to ensure that the resection cavity was not communicating with the subarachnoid space (i.e., intrathecal communication). Astatine is a halogen that shares several chemical properties with iodine, whereby uptake in tissues expressing the sodium/iodide symporter (NIS) can be significantly blocked with an excess of iodine. Therefore, all patients received blocking with daily administration of potassium iodine and liothyronine sodium (from 48 h. before initiation to 16 days after the therapy).

Activities of $^{211}$At ranged from 71 to 347 MBq and were conjugated to 10 mg ch81C6 and administered in <6 mL. Four activity levels were identified: 71–104 MBq ($n = 5$), 135–148 MBq ($n = 7$), 215–248 MBq ($n = 5$), and one patient received 347 MBq.

No dose-limiting toxicity was recorded, hence the maximum tolerated dose (MTD) was not identified. Grade 2 headache ($n = 3$), expressive aphasia ($n = 1$), hand numbness ($n = 1$), and quadrant anopsia ($n = 1$) were all possibly attributable to the treatment. All of these resolved within a few weeks, except for the visual deficit. No correlation with administered activity was found. The most common adverse reaction recorded during follow-up was seizures (two with grade 2, three with grade 3 and one with grade 4), but all these occurred during disease progression and therefore were not considered dose-limiting. There was one case of aplastic anemia that occurred 5 weeks after a single dose of chemotherapy (lomustine) was administered, due to recurrent disease 3 months after treatment with 74 MBq $^{211}$*At-ch81C6*. Furthermore, one patient developed a second malignancy, an undifferentiated anaplastic small-cell neoplasm with neuroblastic features in the neck, 8 weeks after treatment with 215 MBq of $^{211}$*At-ch81C6*. None of these events can be considered due to the treatment, but it is important to keep in account while more experience is gathered.

Serial gamma-camera imaging (of the very minute 77 to 92 keV polonium K X-rays emitted during $^{211}$At decay) demonstrated limited catabolism and excellent stability. It was calculated that 96.7% ± 3.6% of all decay occurred within the resection cavity, and correspondingly, the total activity in the blood pool was generally <0.5% ID (injected dose) at all time points up to 24 h. It was concluded that this therapy was feasible and could be delivered safely. Although there were few patients and a risk of biased inclusion, the median overall survival rate of 52 weeks for the glioblastoma patients treated was superior to the literature data.

### 2.1.4. Gothenburg, Sweden, 2009

From February 2005 to March 2011, 12 patients with recurrent ovarian cancer were treated with $^{211}$*At-MX35-F(ab')$_2$*, at the Sahlgrenska University Hospital in Gothenburg Sweden, as first reported by Anderson et al. (8) in 2009. MX35 is a murine IgG mAb targeting the NaPi2b (SLC34A2) cell surface glycoprotein, which is expressed in >90% of human epithelial ovarian cancers.

Radioimmunotherapy based on a beta-emitting radionuclide (yttrium-90) has previously failed to show an effect on overall survival (OS) in a phase 3 randomized trial aimed at preventing local relapse in small-scale disease ovarian carcinoma (19). As shown by biokinetic modeling (20), part of the failure could be because beta-emitting therapy does not reach a sufficiently high dose to eradicate single cells or small cell clusters, which is believed to be the reason for relapse. Numerous preclinical studies have demonstrated dramatic effects using alpha-particle-emitting radionuclides to treat small-scale diseases in mouse models with peritoneal growth of ovarian cancer (21–23). Organ tolerance for the kidney and peritoneal lining, as well as the RBE for bone marrow, were separately investigated in mice using the radiation-sensitive BALB/c strain (24–26).

The aim of this dose-escalation study (NCT04461457) was to investigate the safety and pharmacokinetics of $^{211}$*At-MX35 F(ab')$_2$* using a 3+3 design. To mimic the gross tumor-free adjuvant situation with an undisturbed peritoneal lining, only patients with recurring epithelial ovarian cancer treated with salvage chemotherapy to achieve complete or good partial remission were included. A total of 12 patients were treated with one intraperitoneal (i.p.) infusion of $^{211}$*At-MX35 F(ab')$_2$* in 1–2 L of Extraneal® solution, which was evacuated after 24 h. The treatment was well-tolerated and escalated from 20 to 215 MBq L$^{-1}$ without any dose-limiting toxicities. The most frequent toxicities were low grade, related to the catheter procedure, and generally resolved within a few days; one grade 4 toxicity was due to perforation of the small intestine after catheter insertion (10). No link was found between registered toxicity and radiation exposure. Some patients experience fatigue and nausea, which are known to be frequent radiation-induced side effects. However, these side effects could also be explained by the procedure due to frequent around-the-clock blood sampling, imaging, and the extended abdomen, making low-grade insomnia frequent. No late toxicities were found for thyroid, renal, or bone marrow function. One patient had a new malignancy 2.7 years after treatment, which was later diagnosed as Lynch syndrome (10). Pharmacokinetics with corresponding calculations of normal tissue dose showed low doses (11), which corresponds well with the absence of hematological and biochemical changes (8, 10). By not using thyroid blocking agents in the lowest activity cohort, the thyroid uptake of free $^{211}$At and estimation of the effect of blocking could be performed (8). The following patients received potassium perchlorate 200 mg twice daily from day−1 to day 2.

The absorbed doses for this treatment were calculated (11) and amounted to >2 Sv for 200 MBq L$^{-1}$. However, the term effective dose should not be used for any radiotherapy as stated by the International Commission on Radiological Protection (ICRP) (27) and, for alpha-particle irradiation, a conservative radiation weighting factor of 20 is applied, whereby the risk might be overestimated. To circumvent the problem of an unknown weighting factor, another epidemiologically based approach was used (12). Here, organ-dose data from the same phase I study were used together with published data on cancer development following exposure to alpha-particle-containing medication. Using this epidemiologically based method, the risk of secondary cancers following i.p. therapy with $^{211}$At-mAb was estimated. The resulting estimates varied from 0.11 to 1.84 excess cases per 100 treated (by the i.p. route with 200 MBq L$^{-1}$ of $^{211}$At-mAb), depending on the use of various assumptions made (e.g., age at treatment, low-LET equals high-LET, or competing risk due to stage of disease) (12). Thus, when developing an adjuvant treatment, in the absence of acute toxicity, the presented excessive relative risk per Gray (ERR/Gy), on an organ basis, should be valuable to incorporate in the recommended phase 2 activity, and it may direct the focus of optimization of the therapy to where dose reductions could be most valuable.

# 3. The present

## 3.1. Summary of the ongoing clinical trials with $^{211}$At

Seven ongoing clinical trials with $^{211}$At are summarized in Table 2. Two of these have recently opened in Japan: at Osaka University Hospital *[$^{211}$At] NaAt* is being investigated in patients with differentiated thyroid cancer, and at Fukushima Medical University $^{211}$*At-MABG* (Meta-astatobenzylguanidine) in patients with malignant pheochromocytoma. There are five early phase clinical protocols with $^{211}$At-based radionuclide therapy at the Fred Hutchinson Cancer Center in Seattle, as posted on ClinicalTrials.gov (28). The common theme of the Fred Hutchinson trials is to improve outcomes after hematopoietic cell transplantation (HCT). Two approved constructs are currently under investigation, anti-CD45 ($^{211}$*At-BC8-B10*) and anti-CD38 ($^{211}$*At-OKT10-B10*). The rationale for these clinical trials is logical and relates to the possible ability of alpha particles to eradicate single cells and limit the dose to surrounding healthy tissues. The underlying hypothesis of these clinical trials is that the addition of highly directed cytotoxicity of $^{211}$At to a reduced-intensity conditioning regimen prior to HCT will reduce both late complications and early toxicity, which are frequent following high-dose systemic conditioning (29, 30). In addition to the 7 protocols described here, in Philadelphia, USA, an investigator-initiated dose-escalation trial with $^{211}$*At-MABG* in relapsed or primary refractory neuroblastoma is planned, which is scheduled to use the "rolling six phase I trial design" (31). Also, in Gothenburg, Sweden, we are in the end stages of concluding the necessary workup to continue i.p. treatments in ovarian cancer using a new $^{211}$At-construct.

TABLE 2 Ongoing and planned clinical trials with $^{211}$At. (NTC number) is the ClinicalTrials.gov identifier.

| Institution, reference | Clinical situation | Planned size (nb Pts.) | Study objective(s) | TAT-agent/ Carrier | Target | Primary outcome |
|---|---|---|---|---|---|---|
| Fred Hutchinson Cancer Center, Seattle, USA (*NCT04466475*) | Multiple Myeloma | 24 | Feasibility and safety | $^{211}$At-OKT10-B10 | CD38 | MTD |
| Fred Hutchinson Cancer Center, Seattle, USA (*NCT04579523*) | Multiple Myeloma | 30 | Dose escalation | $^{211}$At-OKT10-B10 | CD38 | MTD |
| Fred Hutchinson Cancer Center, Seattle, USA (*NCT04083183*) | HCT for non-malignant disease | 40 | Dose escalation | $^{211}$At- BC8-B10 | CD45 | Graft rejection |
| Fred Hutchinson Cancer Center, Seattle, USA (*NCT03670966*) | High-risk acute leukemia or MDS | 30 | Dose-escalation | $^{211}$At- BC8-B10 | CD45 | Toxicity |
| Fred Hutchinson Cancer Center, Seattle, USA (*NCT03128034*) | High-risk AML, ALL, MDS or Mixed-phenotype acute leukemia | 50 | Dose-escalation | $^{211}$At- BC8-B10 | CD45 | Toxicity, MTD |
| Osaka University Hospital, Suita, Japan (*NCT05275946*) | Thyroid cancer | 11 | To establish recommended dose for Phase II trial | [$^{211}$At] NaAt | NIS | Treatment-related adverse events |
| Fukushima Medical University, Japan | Malignant pheochromocytoma | Up to 18 | Dose escalation | $^{211}$At-MABG | Norepinephrine transporter | Toxicity, MTD |

HCT, Hematopoietic cell transplantation.

### 3.1.1. Seattle, USA anti-CD45

At the Fred Hutchinson Cancer Center in Seattle, translation of preclinical findings with the anti-CD45 murine $IgG_1$ monoclonal construct $^{211}$*At-BC8-B10* has so far generated three early-phase clinical protocols that are enrolling patients (NCT03128034, NCT03670966, and NCT04083183). CD45 is expressed at high levels on the surface of all nucleated hematopoietic cells and is not internalized when bound to BC8-B10. The preclinical workup could demonstrate promising results using a canine transplantation model (32–34). Additionally, the work and data needed to obtain current good manufacturing practice (cGMP) for this radiopharmaceutical have been published (30). The NCT03128034 trial aims to evaluate escalating doses of $^{211}$At-labeled anti-CD45 mAb BC8 ($^{211}$*At-BC8-B10*) followed by allogeneic HCT for high-risk acute myeloid leukemia (AML), acute lymphocytic leukemia (ALL), or myelodysplastic syndrome (MDS). It is similar in size (n=40) and the outcome measures to the NCT03670966 phase I/II trial using the same construct ($^{211}$*At-BC8-B10*) followed by donor stem cell transplantation in the treatment of patients with relapsed or refractory high-risk acute leukemia or MDS, but differs in patient population, transplantation, and conditioning regimen.

Preliminary results were presented for the first 20 patients in the dose-escalation study with $^{211}$*At-BC8-B10* (NCT03128034) (35). Here, older or medically infirm adult patients with refractory/relapsed leukemia or high-risk MDS received $^{211}$*At-BC8-B10* i.v. for 6–8 h one week before donor HCT. The conditioning treatment included fludarabine and total body irradiation (TBI) at 2–3Gy. The MTD was defined as the primary endpoint toxicity (grade III or IV Bearman regimen-related toxicity) within the first 100 days after transplantation. The secondary endpoints include various measures of efficacy, and 50 patients can be enrolled. A single-patient dose escalation of $^{211}$At in increments at 1.85 MBq kg$^{-1}$ ideal body weight was used until encountering the first dose limiting toxicity (DLT) at 20.35 MBq kg$^{-1}$ (a bilirubin elevation), therefrom a stage 2 escalation commenced starting at 18.5 MBq kg$^{-1}$ in cohorts of 4. The authors concluded that the preliminary efficacy data of a 1-year overall survival of 43% and recurrence-free survival of 35% support further exploration of $^{211}$*At-BC8-B10* in HCT for patients with high-risk AML and MDS.

The NCT04083183 phase I/II trial "Total Body Irradiation and Astatine-$^{211}$-Labeled BC8-B10 Monoclonal Antibody for the Treatment of Non-malignant Diseases" plans to enroll 40 patients to study the best dose of total body irradiation with the $^{211}$*At-BC8-B10* monoclonal antibody as reduced intensity conditioning prior to HCT. This concept was addressed in a canine model of transfusion-induced sensitization and marrow graft rejection, demonstrating that the addition of $^{211}$At-anti-CD45 mAb to conditioning may overcome graft rejection in non-malignant diseases treated with allogeneic

transplantation (36, 37). In this clinical study, $^{211}$*At- BC8-B10* will be administered prior to induction chemotherapy (fludarabine cyclophosphamide and thymoglobulin) + TBI to patients with non-malignant diseases undergoing HCT. The primary endpoint is graft rejection, and secondary endpoints include transplant related mortality, overall survival (OS), donor chimerism, and the rate of acute and chronic graft vs. host disease (GVHD). No results from this study have yet been reported, but the two trials NCT03128034 and NCT04083183 have treated 43 patients as of July 2021 (38).

### 3.1.2. Seattle, USA, anti-CD38

The two trials using the murine $IgG_1$ anti-CD38 mAb OKT10 (NCT04466475 and NCT04579523) have similar treatment settings to the anti-CD45 trials: that is, they are aiming to treat small cell clusters or single cells, but anti-CD38 targets the malignant cells. Thus, the treatment aim is to achieve eradication of multiple myeloma minimal residual disease (MRD). The CD38 antigen is a good target expressed on malignant plasma cells, regardless of mutational status (39, 40). Cell binding and cytotoxicity from *in vitro* studies, favorable biodistribution, and *in vivo* data on efficacy using mouse models of both bulky disease and low disease burdens have been reported (41).

The NCT04466475 trial is active and recruiting. In this trial, escalating doses of $^{211}$*At-OKT10-B10* combined with melphalan as conditioning prior to autologous HCT in patients with multiple myeloma will be tested in 24 patients who have received at least three prior lines of therapy. The primary endpoint, MTD, is defined as a DLT probability of 25% of subjects. The secondary endpoints are response rate, duration of response, overall survival (OS), progression-free survival (PFS), and rates of MRD using flowcytometry, next generation sequencing, and functional imaging with positron emission tomography-computed tomography (PET-CT).

In the NCT04579523 trial, escalating doses of $^{211}$*At-OKT10-B10* followed by HLA-matched or haploidentical donor HCT for high-risk multiple myeloma will be investigated in 30 patients, assigned to one of the two arms, differing in transplant and conditioning matters. The primary endpoint is MTD. It is posted on ClinicalTrials.gov with the status of "Not yet recruiting" as of October 2022.

### 3.1.3. Osaka, Japan, [$^{211}$At] NaAt in thyroid cancer

Iodine is taken up by the thyroid cells by the NIS and so is astatine because of the chemical similarities, both being halogen isotopes. Currently, patients with differentiated thyroid cancer may be treated with radioactive iodine $^{131}$I. Research at Osaka University could demonstrate improved radiochemical purity and increased uptake of astatide in differentiated thyroid cancer cells by adding 1% ascorbic acid to the $^{211}$At solution, thereby stabilizing the oxidative state of $^{211}$At (42). Preclinical toxicity analysis (43) and a formal extended single-dose toxicity study were performed with the aim of initiating a clinical trial (44). In addition, helpful accompanying guidelines focusing on radiation safety have been published (45).

This investigator-initiated clinical trial (NCT05275946) in patients with differentiated thyroid cancer using the targeted alpha therapy drug TAH-1005 (*[$^{211}$At] NaAt*) has opened for inclusion this year and so far, includes three of the 11 planned patients. This dose-escalation phase I study using a single i.v. administration of TAH-1005 is performed in patients with differentiated thyroid cancer (papillary and follicular cancer) that lack response to standard treatment. The escalating starting dose is 1.25 MBq kg$^{-1}$, with an upper limit of 10 MBq kg$^{-1}$. Safety, pharmacokinetics, absorbed dose, and efficacy will be evaluated to determine the recommended dose for a phase II clinical trial.

### 3.1.4. Fukushima, Japan, $^{211}$At-MABG

In the mid-1990s, Meta- [$^{211}$At] astatine-benzylguanidine (*[$^{211}$At] MABG*) was shown to have superior effects to $^{131}$I-MIBG in the treatment of xenografted human neuroblastoma cells (46). Both of these constructs are false analogs of norepinephrine and are taken up by cells that express the norepinephrine transporter, which is also expressed in pheochromocytoma.

At Fukushima Medical University Hospital, a dose escalation phase I trial has started with $^{211}$*At-MABG* in patients with malignant pheochromocytoma or paraganglioma. It is based on preclinical studies, where *[$^{211}$At] MABG* demonstrated therapeutic effects in malignant pheochromocytoma (47), and an investigation of acute toxicity further supported the advancement to a clinical trial (48). Also, a handling guideline for this $^{211}$At construct has been published (49). The study will use the 3 + 3 study design, starting with i.v. 0.65 MBq kg$^{-1}$ and potentially escalate to 1.3 MBq kg$^{-1}$ and 2.6 MBq kg$^{-1}$, depending on toxicity. The primary endpoints are safety, to establish MTD, and to determine the recommended phase II dose. The secondary endpoints include pharmacokinetics, urinary radioactivity efflux rate, and measures of efficacy: urinary catecholamine response rate, overall response rate, and PFS. This study may enroll up to 18 patients.

## 4. The future

### 4.1. Clinical situations regarding the use of $^{211}$At

A selection of preclinical studies where $^{211}$At has been coupled to various vectors and their respective targets is

TABLE 3 A selection of studies with various vectors that have been labeled with $^{211}$At. (IgG, immunoglobulin G).

| Malignancy | Target | TAT-agent (Vector type) | Ref. |
|---|---|---|---|
| Colon cancer | Lewis Y | BR96 (IgG) | (50, 51) |
| Glioma | VEGFR and integrins | iRGD-C6-lys-C6-DA7R (heterodimeric peptide) | (52) |
| | Neurokinin receptors 1–3 | Substance P (peptide) | (53) |
| | LAT1 | Phenylalanine | (54) |
| | Tenascin | ch81C6 (IgG) | (15) |
| Head and neck cancer | CD44vs6 | U36 (IgG) | (55) |
| Leukemia | CD20 | Rituximab (IgG) | (56) |
| | CD45 | 30F11 (IgG) | (34) |
| | CD45 | BC8 (IgG) | (33) |
| | CXCR4 | Anti- CXCR4 (IgG) | (57) |
| Lymphoma | CD20 | 1F5 (IgG) | (58) |
| | CD33 | Gemtuzumab (IgG) | (56) |
| Lung, neuroendocrine | SSTR2 | Octreotide | (59) |
| Melanoma | | Methylene blue | (60) |
| Multiple myeloma | CD38 | OKT10 (IgG) | (41) |
| | CD138 (syndecan-1) | 9E7.4 (IgG) | (61) |
| Neuroblastoma | PARP1 | Parthanatine (1-(4-astatophenyl)-8,9-dihydro-2,7,9a-triazabenzo[cd]azulen-6(7H)-one) | (62) |
| Neuroblastoma, Pheochromocytoma | Norepinephrine transporter | Meta-benzylguanidine (MABG) | (46, 47) |
| Ovarian | FRα | MOv18 (IgG) | (63) |
| | | Farletuzumab (IgG) | (64) |
| | NaPi2b | MX35 (F(ab')$_2$) | (65) |
| | | MX35 (IgG) | (66) |
| Ovarian, gastric, breast cancer | HER2 | Trastuzumab (IgG) | (67, 68) |
| | | 2Rs15d (Nanobody) | (69) |
| | | 5F7 (single-domain antibody) | (70) |
| Various | HER2/CEA | C6.5 & T84.66 (diabodies) | (71) |
| Prostate | PSMA | (2S)-2-(3-(1-carboxy-5-(4-$^{211}$At-astato-benzamido) pentyl)ureido) pentanedioic acid | (72) |
| | PSCA | A11 (Minibody) | (73) |
| | GRPR | Bombesin | (74) |
| Thyroid / NIS expressing tumors | NIS | Astatide | (75–77) |
| Various | - | Gold nanoparticles | (78) |

summarized in Table 3. A few of these $^{211}$At-conjugates have been, or are currently being, tested in early clinical trials, as discussed in Sections 2 and 3. Most of these constructs are potential candidates for translation into clinical trials, and other vectors will surely appear. It is difficult to predict the clinical success using preclinical data. Many drug candidates with high efficacy in small-animal models have failed in humans. Therefore, rather than attempting to predict results, we show possible situations and conditions where alpha-particles and particularly $^{211}$At-based therapies can be of value.

### 4.1.1. Personalized medicine

In recent years, the concept of precision medicine has gained increased attention owing to the development of specific drugs associated with defined genetic alterations in several tumor types. Examples include EGFR, ALK, ROS1 and RET alterations in non-small cell lung cancer, rendering tumors susceptible to tyrosine kinase inhibitors (79), or high microsatellite instability/deficient mismatch repair (MSI-H/dMMR) in gastrointestinal tumors, which is associated with response to PD1 inhibition (80). This has led to an overall belief in precision medicine as a general principle of individual patient management. Precision medicine, sometimes also called personalized medicine, primarily refers to the use of a patient's individual tumor information (e.g., genes or proteins) to guide diagnostic, treatment, or follow-up related decisions.

In radiotheranostics (81, 82), molecular imaging for diagnosis and staging, primarily PET-CT and single-photon emission computed tomography (SPECT), is combined with targeted radionuclide therapy at a later time point. It can use small molecules, peptides, or antibodies as carriers for therapeutic radionuclides, characteristically those emitting α-, β-, or auger-radiation. This radio-pharmacological personalization includes somatostatin receptor positivity in neuroendocrine tumors associated with the efficacy of $^{177}$Lu-DOTATATE/DOTATOC or PSMA-positive prostate cancer treated with the same radionuclide but with a different vector. The individual approach is likely to play an important role in the development of $^{211}$At associated treatment to increase the risk-benefit ratio and expand the treatment strategy to further tumor diagnosis or stages.

### 4.1.2. Adjuvant therapy

Following primary therapy for a malignancy, most often surgery, small-scale disease may go undetected leading to recurrence. The risk of relapse is dependent on the type of malignancy and the disease stage at the time of treatment. This risk can be lowered with adjuvant therapy such as local post-operative external radiation therapy, pharmaceutical therapy, or endocrine therapy. Various adjuvant therapies are used for the most frequent malignancies, such as breast, colorectal, and lung cancers. Although there is a clear effect on survival, in the case of colon cancer, at most, about 30% of patients with micrometastases are cured by the chemotherapy given (83). Comparably low, or even lower, figures apply for breast and other adjuvant therapies regarding the total efficacy of adjuvant chemotherapy. Therefore, adjuvant therapy of small-scale disease using alpha-emitting radionuclides directed to malignant cells offers an appealing treatment approach because of the high LET and short path length of the alpha particles, which may prove more efficient than current standard treatments and with limited toxicity.

### 4.1.3. Adjuvant therapy aimed on single cells

Targeted $^{211}$At might hold great promise as an adjuvant therapy for eradicating single cells or micrometastases remaining following primary therapies. In this setting, a much higher fraction of the radiation energy emitted from $^{211}$At will be deposited in the cancer cells compared to any other beta emitter. Accordingly, the tumor-to-healthy tissue ratio favors $^{211}$At therapy. An even better ratio has been reached for some loco-regional therapies. A good example is intraperitoneal $^{211}$At-radioimmunotherapy, where the calculated absorbed dose to single tumor cells and micrometastases is >20 Gy, while the bone-marrow receives <0.05 Gy (11). The low bone marrow dose was partly due to the addition of an osmotic agent that slows the transport of $^{211}$At-mAb from the peritoneal cavity into the circulation (20).

### 4.1.4. Gross tumor treatment

Gross tumors, that is, macroscopic tumors, are commonly defined as tumor masses that can be detected and measured using imaging techniques, such as CT, MRI, or PET-CT. Treatment can be used for both primary and relapsed diseases. If relapse occurs at a different location from the primary site, it is referred to as metastatic disease. Until recently, metastatic disease had been considered an incurable situation for most epithelial malignancies, but this might be changing with the use of more molecular-based individual treatments. However, non-curability does not mean that a treatment is in vain. The balance between treatment-induced acute side effects and tumor effects should preferably favor low-toxicity treatments. Therapy based on $^{211}$At (short half-life, no serial alpha-daughters in the decay chain) may offer such treatment options.

#### 4.1.4.1. Fractionation

Diffusion and short t½ are arguments often used to suggest that $^{211}$At-based therapy might have a limited potential for success when aiming to treat larger tumor masses. Such limitations might be overcome by introducing a fractionated regime, which allows for lower cumulative bone marrow and kidney doses. This was observed in a preclinical study (84), where fractionated i.v.- radioimmunotherapy (RIT) completely eradicated small solid tumors when the cumulative tumor dose was >10 Gy. Interestingly, small-scale alpha imaging in this study revealed a markedly heterogeneous intratumoral dose-rate distribution even at relatively late time points after the injection. Pre-targeted regimens have been shown to strongly improve intratumoral diffusion and distribution of short-lived alpha-emitters at very short time points (85).

#### 4.1.4.2. PRIT

In contrast to radioimmunotherapy (RIT), pre-targeted radioimmunotherapy (PRIT) combines the ability of antibodies to target specific antigens expressed on tumor cells with

the pharmacokinetic profile of a radiolabeled small molecule (effector molecule). This is used in a multistep delivery system that allows a decrease in the circulation time of radionuclides, which may reduce the dose delivered to healthy tissues. Importantly, this will facilitate the use of short-lived radionuclides that might otherwise be incompatible with antibody-based vectors (86, 87). PRIT presents added complexity in terms of dosing protocol optimization, pre-targeting intervals, and drug manufacturing. At least two products need to be developed, and perhaps a third, a clearing agent, that is needed to remove or at least reduce the unbound blood fraction from the circulation before injecting the therapeutic effector (88). Over the years, several approaches that rely on different *in vivo* ligation mechanisms have emerged. The two most studied are the non-covalent interactions of the streptavidin-biotin system and bispecific antibodies that can bind both to the tumor antigen and to a radiolabeled small molecule. Clinical investigations of both strategies have confirmed the utility of the pre-targeting approach in overcoming the high overall normal tissue radiation doses of conventional RIT (89–93) and that significant tumor doses can be achieved (87).

Other approaches include hybridization of complementary oligonucleotides and the biorthogonal inverse electron demand Diels-Alder (IEDDA) click reaction (87). Preclinical data have shown excellent potential for the clinical translation of PRIT based on the IEDDA approach (94), and clinical studies will soon be attempted (90). Complementary oligonucleotides also demonstrate high potential for application owing to some modifications to the oligomer scaffolds to prevent their *in vivo* degradation (86). Each approach has its own set of advantages and disadvantages, the challenge with PRIT lies in it being a multistep process that is difficult and costly to develop. However, PRIT has demonstrated increased value in permitting optimized reagent dosing, solving the challenge of the relatively high radiation burden on healthy tissue that has repeatedly been associated with the use of beta-emitting radioimmunoconjugates in RIT. In alpha particle-based RIT, the main benefit may lie in better tumor penetration and accompanying higher tumor doses.

## 4.2. Anatomical considerations

### 4.2.1. Systemic treatment

Systemic treatment generally means that the drug reaches the tumor through the blood. This route of radiation delivery is needed if the malignancy initially spreads through the bloodstream. Therefore, malignancies with a high risk of liver, lung, or bone marrow metastasis are likely to be well-suited for systemic delivery. Logistically, it is a good administration route because of the ease of access; however, when the activity is at its highest, all normal organs are exposed to unspecific irradiation in proportion to the organ blood flow. This drawback is more pronounced when radionuclides with shorter t½ values are used.

### 4.2.2. Intra cavitary treatment

The first two clinical studies used an intra cavitary treatment situation (8, 9). By doing so, normal organ exposure can be significantly reduced, which increases the therapeutic window. This is the logical choice if the main clinical problem is local regrowth or relapse.

#### 4.2.2.1. Abdominal cavity – i.p. treatment

Ovarian cancer is an archetypical malignancy with a high rate of intraperitoneally relapses, even after successful surgery and chemotherapy. In fact, ∼70–80% of patients with epithelial ovarian cancer will develop disease relapse (95). However, in gastric, colorectal, and pancreatic cancers, i.p. directed therapy can be useful to reduce local recurrences and associated morbidity. High rates of peritoneal recurrence are for example common following gastric cancer surgery, ranging from 35 to 60% (96). In colon cancer, the incidence of peritoneal metastases during follow-up has been estimated to be 70–80% if positive resection margins or peritoneal nodules are detected during surgery (97, 98). Moreover, pancreatic cancer has a high risk of eventually developing peritoneal metastases, with ∼10% in first recurrences but up to 40–60% in advanced stages (99). Thus, the clinical trial in ovarian cancer with $^{211}$At based radioimmunotherapy (section 2.1.4) may be followed by trials in other clinical malignancies using a similar treatment set-up.

#### 4.2.2.2. Fluid evacuation

Preclinical studies of i.p.-RIT have shown that an improved therapeutic window could be achieved with an accelerated post-administration fluid evacuation and performing peritoneal flushing (100, 101). Using this strategy, the normal tissue organ uptakes was significantly decreased, while the tumor uptakes was preserved (100). This corresponded to an increase in the tumor-to-normal-tissue mean absorbed dose-rate ratio (TND) for blood from 1.7 to 6. This concept was also evaluated in a study using the short-lived alpha-emitter $^{213}$Bi, where the TND for blood increased from 1.3 to 6 (101).

#### 4.2.2.3. Spinal canal, ventricular system -intrathecal treatment

Besides the intra cavitary treatment used in the first $^{211}$At clinical trial (section 2.1.3), other central nervous system (CNS)-located diseases such as neuroblastoma or leptomeningeal metastases have been treated with radioimmunotherapy to achieve better control of minimal residual disease. Intrathecal targeted radiation was introduced at the Memorial Sloan-Kettering Cancer Centre (MSKCC) in New York. Clinical studies have so far involved electron-emitter $^{131}$I conjugated to murine 3F8 (anti-GD2) or 8H9 (anti-B7H3) antibodies (102–104). To this end, the MSKCC team has published several

pharmacokinetic models of intrathecal RIT (105–108). They also modeled alpha-emitter $^{225}$Ac and stated that "as new novel radioisotopes and their microdosimetry become available, further improvement in the pharmacokinetic modeling of CNS-RIT modality should refine this emerging therapy to fit the clinical context" (105). Indeed, recently presented pharmacokinetic models and calculated microdosimetry for intrathecal administered $^{211}$At-labeled 3F8 and 8H9 antibodies are promising (109).

#### 4.2.2.4. Other intra cavitary treatments

Local therapy is, as shown above, an attractive and feasible treatment option. Therefore, in addition to the discussed intraperitoneal and intrathecal body cavities, local treatment may be envisioned in the pleural space following, for example, surgery for mesothelioma, or in palliative care to reduce malignant effusions in the abdomen or pleural cavity by using an appropriate vector with successful stable $^{211}$At chemistry.

## 4.3. Modeling to enhance the therapeutic window

Models of $^{211}$At-radioligand binding and retention to cancer cells (110) combined with microdosimetry (111) and biokinetic models (20) have generated proposals that may optimize radionuclide therapies in the above-mentioned clinical situations. Examples include the use of an osmotic agent in intraperitoneal radioimmunotherapy, mainly to reduce bone marrow absorbed doses (20). Another suggestion from modeling is to add a "cold," i.e., non-radiolabeled, antibody as a post-therapy boost aiming at increasing the absorbed dose to the core of slightly larger microtumors (110).

## 4.4. Vectors and radiolabeling with $^{211}$At

### 4.4.1. The chemistry

Most alpha-emitting radionuclides are radiometals, for which metal chelators can be used for radiolabeling targeting vectors, whereas $^{211}$At is a radio-halogen. Generally, halogen properties can be applied in astatine labeling chemistry, but in contrast to iodine chemistry, they cannot be applied in the direct labeling of proteins (112). It was found very early on that both the chemistry and *in vivo* behavior of astatine were different from those of iodine (113, 114), the closest neighbor in the halogen group. Although astatine is a halogen, it also has metallic properties. However, no efficient chelator has been developed for astatine. The chemistry of astatine has been difficult to fully elucidate, to which its low availability has contributed negatively. However, with the increased interest in its use in TAT, much effort has been made to understand its properties in recent years (5). In principle, two main types of bonds are used for astatine labeling: covalent bonds to aromatic groups and binding to boron cages (115, 116). Several different methods for covalent bonding of astatine have been developed such as the use of boronic acid leaving groups and iodonium salts; however, the most commonly used and well-established method is electrophilic destannylation of an aryl organo-tin group (5, 117). For the radiolabeling of proteins and other vectors, the most common approach is the use of an intermediate bifunctional reagent that includes an amino directing group for conjugation to the vector, for example, an aryl organo-tin group for labeling with $^{211}$At (118). The issue of *in vivo* stability is strongly connected to the radiochemistry methodologies used with astatine. A number of animal studies using $^{211}$At have observed that uptake in normal organs, such as the stomach, spleen, and lungs, was elevated. In most cases, this is likely due to *in vivo* deastatination. Much effort has been put into improving the radiolabeling methods for $^{211}$At (5).

### 4.4.2. Vectors

A wide range of vector types have been radiolabeled with $^{211}$At. Table 3 provides a non-comprehensive summary of these examples. Antibodies have been one of the main vectors for guiding $^{211}$At to the tumor site, and basically all types of antibodies can be astatinated using the intermediate reagents discussed above. However, although alpha-radioimmunotherapy with $^{211}$At is well-suited for local compartment applications such as intracavitary or intraperitoneal treatments, general treatments using a systemic administration route (generally i.v.) are limited by a slow distribution to the tumor tissue and the clearance rate of antibodies, resulting in slow accumulation in the tumor. To circumvent the unfavorable pharmacokinetics of radiolabeled antibodies, pre-targeting techniques (see above section on PRIT) can be employed. In addition, pharmacokinetics can be optimized utilizing smaller protein vectors, such as nanobodies or minibodies, to better match the half-life of $^{211}$At. In addition, small astatinated organic molecules, such as phenylalanine and MABG (Table 3), display a significantly faster distribution pattern than antibodies. With both these types of constructs, one must take clearance through the kidneys into account to avoid nephrotoxicity.

## 4.5. Treatment availability

### 4.5.1. Nuclide production

Astatine is one of the rarest elements on Earth; therefore, $^{211}$At must be artificially produced. The main production route today is to irradiate a bismuth-209 target in a cyclotron capable of producing a 28 MeV alpha beam. The alpha beam transforms the target bismuth into $^{211}$At by the nuclear reaction $^{209}$Bi(α,2n)$^{211}$At (119). Astatine-211 can also be produced by

heavy-ion irradiation of bismuth using the nuclear reaction $^{209}$Bi($^{7}$Li,5n)$^{211}$Rn and subsequently using$^{211}$Rn as a generator of $^{211}$At (3, 120). Isolation of astatine from the spallation reaction is also possible. Comparing the production routes, $^{209}$Bi(α,2n)$^{211}$At is the most straight forward and is likely to be the main route to prevail (3, 4). Currently there are 13 cyclotron facilities that produce $^{211}$At (3). However, several efforts have been made to increase the capacity to meet the demand of $^{211}$At. Approximately 30 production sites are or will shortly be available. Currently, three manufacturers are producing medium-energy cyclotrons with the capacity of an alpha beam. The Ion Beam Applications (IBA) in Belgium, has the multi-particle machine Cyclone 30XP in stock. Sumitomo (Japan) produce the MP-30 cyclotron. Although not yet on the market, Ionetix (USA), is developing new mono-energetic machines for $^{211}$At production. In addition to cyclotron production, linac production has also attracted attention (121). Linac machines can apply a very high current to the target and potentially produce high amounts of $^{211}$At. However, the main hurdles to overcome with linac production are few facilities (i.e., beam time) and targetry.

### 4.5.2. Logistics

The logistics of this type of treatment, utilizing a relatively short-lived nuclide, concern several factors that carry different importance depending on geographical location and national nuclear medicine healthcare traditions. Various local logistical concerns may include the produced nuclide itself, either as a target or a purified fraction, the radiolabeled precursor, the completely synthesized radiopharmaceutical, the patient to be treated, or a combination of these. This creates a complex system where no single solution fits all, as recently reviewed (3, 4). Importantly, the clinical trial performed in Gothenburg, Sweden, received the $^{211}$At from the cyclotron at Rigshospitalet, in Copenhagen, Denmark, proving that a production site can be situated up to approximately 3 h away from the where the radiopharmacy and treatment takes place (8). However, for routine clinical treatment with an astatine-containing radiopharmaceutical, there is a need for automatic recovery of the produced nuclide from the solid target as well as the subsequent radiopharmaceutical synthesis. Several research groups have identified this need, and efforts have been made to automate nuclide recovery with wet extraction (122), solid-phase extraction (123), and dry distillation in combination with radiopharmaceutical synthesis (124).

### 4.5.3. Collaborative initiatives

In Europe, the EU-funded project Network for Optimized Astatine labeled Radiopharmaceuticals (NOAR) was started in 2020, supported by the funding organization of the European Cooperation in Science and Technology (COST). NOAR has addressed the specific question of the future logistics of astatine-based radiopharmaceuticals in terms of production capacity, recovery processes, and transnational movement of patients to specific treatment nodes (125). In the United States, the U.S. Department of Energy (DOE) has a specific isotope program where the National Isotope Development Centre is set out to "support the US Department of Energy Isotope Program as the global leader in the production and distribution of radioactive and enriched stable isotopes that are deemed critical or are in short supply," and where one of the nuclides in focus is $^{211}$At (126). In Japan $^{211}$At based research has been very efficacious, and two clinical trials have been initiated within a short period of time. Part of this success is due to the creation of a nationwide supply chain from five $^{211}$At production facilities to more than 18 end-user facilities.

## 4.6. Summary

Only two clinical trials have been performed to date, but presently, seven different protocols are underway, and two more may be starting within a short period. To date, all performed and scheduled trials are small safety or dose-finding trials, and none have a control population. Hopefully, larger effect-seeking studies, preferably randomized studies, will likely start within a few years once the recommended phase 2 dose has been set. Collaborative initiatives that have started in Europe, Japan, and the USA will facilitate and focus on ongoing research. If joined, these collaborations could clearly aid in the launch of international multicenter controlled clinical trials with $^{211}$At-based radiopharmaceuticals.

# Author contributions

PA, TB, and SP contributed to the design, concept, and completion of this article. All the authors listed contributed with substantial, direct, and intellectual contribution to the work and approved the submitted version for publication.

# Funding

This work was supported by the Swedish Research Council (2020-02204), the Swedish Cancer Society (190523Pj, 190523Fk), the King Gustav V Jubilee Clinic Research Foundation, the Swedish Radiation Protection Authority, the Gösta Miltons Foundation, and grants from the Swedish state under the agreement between the Swedish government and the county councils, the ALF-agreement (ALFGBG-966276, ALFGBG-873621).

## Conflict of interest

PA, TB, KS, SP, EA, and SL are co-founders of Aprit Biotech AB. EA and SL are the co-founders of Atley Solutions AB. KS is the founder of Smerud Medical Research Group.

The remaining authors declare that the research was conducted in the absence of any commercial or financial relationships that could be construed as a potential conflict of interest.

## Publisher's note

All claims expressed in this article are solely those of the authors and do not necessarily represent those of their affiliated organizations, or those of the publisher, the editors and the reviewers. Any product that may be evaluated in this article, or claim that may be made by its manufacturer, is not guaranteed or endorsed by the publisher.

## References


1. Corson DR, MacKenzie KR, Segrè E. Possible production of radioactive isotopes of element 85. *Phys Rev*. (1940) 57:459. doi: 10.1103/PhysRev.57.459

2. Hamilton JG, Durbin PW, Parrott MW. Accumulation of astatine211 by thyroid gland in man. *Proc Soc Exp Biol Med.* (1954) 86:366–9. doi: 10.3181/00379727-86-21100

3. Feng Y, Zalutsky MR. Production, purification and availability of (211)At: near term steps towards global access. *Nucl Med Biol.* (2021) 100:12–23. doi: 10.1016/j.nucmedbio.2021.05.007

4. Lindegren S, Albertsson P, Back T, Jensen H, Palm S, Aneheim E. Realizing clinical trials with astatine-211: the chemistry infrastructure. *Cancer Biother Radiopharm.* (2020) 35:425–36. doi: 10.1089/cbr.2019.3055

5. Guérard F, Maingueneau C, Liu L, Eychenne R, Gestin J-F, Montavon G, et al. Advances in the chemistry of astatine and implications for the development of radiopharmaceuticals. *Acc Chem Res.* (2021) 54:3264–75. doi: 10.1021/acs.accounts.1c00327

6. Yang H, Wilson JJ, Orvig C, Li Y, Wilbur DS, Ramogida CF, et al. Harnessing α-emitting radionuclides for therapy: radiolabeling method review. *J Nucl Med.* (2022) 63:5–13. doi: 10.2967/jnumed.121.262687

7. Doberenz I, Doberenz W, Wunderlich G, Franke W, Heidelbach J, Fischer S, et al. Endoarterielle therapie eines zungenkarzinoms mit 211 at-markierten humanserumalbumin-mikrosphären—erste klinische erfahrungen. *NucCompact.* (1990) 21:124–7.

8. Andersson H, Cederkrantz E, Back T, Divgi C, Elgqvist J, Himmelman J, et al. Intraperitoneal alpha-particle radioimmunotherapy of ovarian cancer patients: pharmacokinetics and dosimetry of (211)At-MX35 F(ab')2–a phase I study. *J Nucl Med.* (2009) 50:1153–60. doi: 10.2967/jnumed.109.062604

9. Zalutsky MR, Reardon DA, Akabani G, Coleman RE, Friedman AH, Friedman HS, et al. Clinical experience with alpha-particle emitting 211At: treatment of recurrent brain tumor patients with 211At-labeled chimeric antitenascin monoclonal antibody 81C6. *J Nucl Med.* (2008) 49:30–8. doi: 10.2967/jnumed.107.046938

10. Hallqvist A, Bergmark K, Back T, Andersson H, Dahm-Kahler P, Johansson M, et al. Intraperitoneal alpha-emitting radioimmunotherapy with (211)At in relapsed ovarian cancer: long-term follow-up with individual absorbed dose estimations. *J Nucl Med.* (2019) 60:1073–9. doi: 10.2967/jnumed.118.220384

11. Cederkrantz E, Andersson H, Bernhardt P, Back T, Hultborn R, Jacobsson L, et al. Absorbed doses and risk estimates of (211)At-MX35 F(ab')2 in intraperitoneal therapy of ovarian cancer patients. *Int J Radiat Oncol Biol Phys.* (2015) 93:569–76. doi: 10.1016/j.ijrobp.2015.07.005

12. Leidermark E, Hallqvist A, Jacobsson L, Karlsson P, Holmberg E, Back T, et al. Estimating the risk for secondary cancer following targeted alpha therapy with astatine-211 intraperitoneal radioimmunotherapy. *J Nucl Med.* (2022). doi: 10.2967/jnumed.121.263349

13. Larsen RH, Akabani G, Welsh P, Zalutsky MR. The cytotoxicity and microdosimetry of astatine-211-labeled chimeric monoclonal antibodies in human glioma and melanoma cells in vitro. *Radiat Res.* (1998) 149:155–62. doi: 10.2307/3579925

14. Reist CJ, Bigner DD, Zalutsky MR. Human IgG2 constant region enhances in vivo stability of anti-tenascin antibody 81C6 compared with its murine parent. *Clin Cancer Res.* (1998) 4:2495–502.

15. Zalutsky MR, Stabin MG, Larsen RH, Bigner DD. Tissue distribution and radiation dosimetry of astatine-211-labeled chimeric 81C6, an alpha-particle-emitting immunoconjugate. *Nucl Med Biol.* (1997) 24:255–61. doi: 10.1016/S0969-8051(97)00060-7

16. McLendon RE, Archer GE, Larsen RH, Akabani G, Bigner DD, Zalutsky MR. Radiotoxicity of systemically administered 211At-labeled human/mouse chimeric monoclonal antibody: a long-term survival study with histologic analysis. *Int J Radiat Oncol Biol Phys.* (1999) 45:491–9. doi: 10.1016/S0360-3016(99)00206-0

17. Bigner DD, Brown MT, Friedman AH, Coleman RE, Akabani G, Friedman HS, et al. Iodine-131-labeled antitenascin monoclonal antibody 81C6 treatment of patients with recurrent malignant gliomas: phase I trial results. *J Clin Oncol.* (1998) 16:2202–12. doi: 10.1200/JCO.1998.16.6.2202

18. Reardon DA, Akabani G, Coleman RE, Friedman AH, Friedman HS, Herndon JE II, et al. Phase II trial of murine (131)I-labeled antitenascin monoclonal antibody 81C6 administered into surgically created resection cavities of patients with newly diagnosed malignant gliomas. *J Clin Oncol.* (2002) 20:1389–97. doi: 10.1200/JCO.2002.20.5.1389

19. Verheijen RH, Massuger LF, Benigno BB, Epenetos AA, Lopes A, Soper JT, et al. Phase III trial of intraperitoneal therapy with yttrium-90-labeled HMFG1 murine monoclonal antibody in patients with epithelial ovarian cancer after a surgically defined complete remission. *J Clin Oncol.* (2006) 24:571–8. doi: 10.1200/JCO.2005.02.5973

20. Palm S, Back T, Haraldsson B, Jacobsson L, Lindegren S, Albertsson P. Biokinetic modeling and dosimetry for optimizing intraperitoneal radioimmunotherapy of ovarian cancer microtumors. *J Nucl Med.* (2016) 57:594–600. doi: 10.2967/jnumed.115.167825

21. Andersson H, Elgqvist J, Horvath G, Hultborn R, Jacobsson L, Jensen H, et al. Astatine-211-labeled antibodies for treatment of disseminated ovarian cancer: an overview of results in an ovarian tumor model. *Clin Cancer Res.* (2003) 9:3914S–21S.

22. Elgqvist J, Andersson H, Back T, Claesson I, Hultborn R, Jensen H, et al. Alpha-radioimmunotherapy of intraperitoneally growing OVCAR-3 tumors of variable dimensions: outcome related to measured tumor size and mean absorbed dose. *J Nucl Med.* (2006) 47:1342–50.

23. Elgqvist J, Andersson H, Back T, Hultborn R, Jensen H, Karlsson B, et al. Therapeutic efficacy and tumor dose estimations in radioimmunotherapy of intraperitoneally growing OVCAR-3 cells in nude mice with (211)At-labeled monoclonal antibody MX35. *J Nucl Med.* (2005) 46:1907–15.

24. Back T, Haraldsson B, Hultborn R, Jensen H, Johansson ME, Lindegren S, et al. Glomerular filtration rate after alpha-radioimmunotherapy with 211At-MX35-F(ab')2: a long-term study of renal function in nude mice. *Cancer Biother Radiopharm.* (2009) 24:649–58. doi: 10.1089/cbr.2009.0628

25. Cederkrantz E, Angenete E, Back T, Falk P, Haraldsson B, Ivarsson ML, et al. Evaluation of effects on the peritoneum after intraperitoneal alpha-radioimmunotherapy with (211)At. *Cancer Biother Radiopharm.* (2012) 27:353–64. doi: 10.1089/cbr.2012.1184

26. Elgqvist J, Bernhardt P, Hultborn R, Jensen H, Karlsson B, Lindegren S, et al. Myelotoxicity and RBE of 211At-conjugated monoclonal antibodies compared with 99mTc-conjugated monoclonal antibodies and 60Co irradiation in nude mice. *J Nucl Med.* (2005) 46:464–71.

27. The 2007 recommendations of the International Commission on Radiological Protection. ICRP publication 103. *Ann ICRP*. (2007) 37:1–332. doi: 10.1016/j.icrp.2007.10.003

28. Home - ClinicalTrials.gov. (2022). Available online at: https://clinicaltrials.gov/ (accessed October 21, 2022).

29. Gyurkocza B, Sandmaier BM. Conditioning regimens for hematopoietic cell transplantation: one size does not fit all. *Blood.* (2014) 124:344–53. doi: 10.1182/blood-2014-02-514778

30. Li Y, Hamlin DK, Chyan MK, Wong R, Dorman EF, Emery RC, et al. cGMP production of astatine-211-labeled anti-CD45 antibodies for use in allogeneic hematopoietic cell transplantation for treatment of advanced hematopoietic malignancies. *PLoS ONE.* (2018) 13:e0205135. doi: 10.1371/journal.pone.0205135

31. Batra V, Samanta M, Makvandi M, Groff D, Martorano P, Elias J, et al. Preclinical Development of [211At]meta- astatobenzylguanidine ([211At]MABG) as an alpha particle radiopharmaceutical therapy for neuroblastoma. *Clin Cancer Res.* (2022) 28:4146–57. doi: 10.1158/1078-0432.CCR-22-0400

32. Chen Y, Kornblit B, Hamlin DK, Sale GE, Santos EB, Wilbur DS, et al. Durable donor engraftment after radioimmunotherapy using alpha-emitter astatine-211-labeled anti-CD45 antibody for conditioning in allogeneic hematopoietic cell transplantation. *Blood.* (2012) 119:1130–8. doi: 10.1182/blood-2011-09-380436

33. Nakamae H, Wilbur DS, Hamlin DK, Thakar MS, Santos EB, Fisher DR, et al. Biodistributions, myelosuppression, and toxicities in mice treated with an anti-CD45 antibody labeled with the alpha-emitting radionuclides bismuth-213 or astatine-211. *Cancer Res.* (2009) 69:2408–15. doi: 10.1158/0008-5472.CAN-08-4363

34. Orozco JJ, Back T, Kenoyer A, Balkin ER, Hamlin DK, Wilbur DS, et al. Anti-CD45 radioimmunotherapy using (211)At with bone marrow transplantation prolongs survival in a disseminated murine leukemia model. *Blood.* (2013) 121:3759–67. doi: 10.1182/blood-2012-11-467035

35. Sandmaier BM, Wilbur DS, Hamlin DK, Vo P, Wong R, Baker K, et al. 57 - a phase I trial of first-in-human alpha-emitter astatine-211-labeled anti-CD45 antibody (211At-BC8-B10) in combination with fludarabine and TBI As conditioning for allogeneic hematopoietic cell transplantation (HCT) for patients with refractory/relapsed leukemia or high-risk myelodysplastic syndrome (MDS): preliminary results of dose escalation. *Transplant Cell Therapy.* (2021) 27:S54. doi: 10.1016/S2666-6367(21)00083-X

36. Frost SH, Miller BW, Back TA, Santos EB, Hamlin DK, Knoblaugh SE, et al. Alpha-imaging confirmed efficient targeting of CD45-positive cells after 211At-radioimmunotherapy for hematopoietic cell transplantation. *J Nucl Med.* (2015) 56:1766–73. doi: 10.2967/jnumed.115.162388

37. Nakaya A, Qiu H, Santos EB, Hamlin DK, Wilbur DS, Storb R, et al. Addition of astatine-211-labeled anti-CD45 antibody to TBI as conditioning for DLA-identical marrow transplantation: a novel strategy to overcome graft rejection in a canine presensitization model: "radioimmunotherapy to overcome transfusion-induced sensitization". *Transplant Cell Ther.* (2021) 27:476–7. doi: 10.1016/j.jtct.2021.02.018

38. Li Y. At-211 user meeting 2021_final_combo_Li & Emory_sm.pdf. (2022). Available online at: https://www.isotopes.gov/sites/default/files/2021-09/At-211%20user%20meeting%202021_final_combo_Li%20%26%20Emory_sm.pdf (accessed October 21, 2022).

39. Green DJ, Orgun NN, Jones JC, Hylarides MD, Pagel JM, Hamlin DK, et al. A preclinical model of CD38-pretargeted radioimmunotherapy for plasma cell malignancies. *Cancer Res.* (2014) 74:1179–89. doi: 10.1158/0008-5472.CAN-13-1589

40. Szlasa W, Czarny J, Sauer N, Rakoczy K, Szymańska N, Stecko J, et al. Targeting CD38 in neoplasms and non-cancer diseases. *Cancer.* (2022) 14:4169. doi: 10.3390/cancers14174169

41. O'Steen S, Comstock ML, Orozco JJ, Hamlin DK, Wilbur DS, Jones JC, et al. The alpha-emitter astatine-211 targeted to CD38 can eradicate multiple myeloma in a disseminated disease model. *Blood.* (2019) 134:1247–56. doi: 10.1182/blood.2019001250

42. Watabe T, Kaneda-Nakashima K, Liu Y, Shirakami Y, Ooe K, Toyoshima A, et al. Enhancement of (211)At uptake via the sodium iodide symporter by the addition of ascorbic acid in targeted alpha-therapy of thyroid cancer. *J Nucl Med.* (2019) 60:1301–7. doi: 10.2967/jnumed.118.222638

43. Liu Y, Watabe T, Kaneda-Nakashima K, Ooe K, Shirakami Y, Toyoshima A, et al. Preclinical evaluation of radiation-induced toxicity in targeted alpha therapy using [(211)At] NaAt in mice: a revisit. *Transl Oncol.* (2020) 13:100757. doi: 10.1016/j.tranon.2020.100757

44. Watabe T, Kaneda-Nakashima K, Ooe K, Liu Y, Kurimoto K, Murai T, et al. Extended single-dose toxicity study of [(211)At]NaAt in mice for the first-in-human clinical trial of targeted alpha therapy for differentiated thyroid cancer. *Ann Nucl Med.* (2021) 35:702–18. doi: 10.1007/s12149-021-01612-9

45. Watabe T, Hosono M, Kinuya S, Yamada T, Yanagida S, Namba M, et al. Manual on the proper use of sodium astatide ([(211)At]NaAt) injections in clinical trials for targeted alpha therapy (1st edition). *Ann Nucl Med.* (2021) 35:753–66. doi: 10.1007/s12149-021-01619-2

46. Vaidyanathan G, Friedman HS, Keir ST, Zalutsky MR. Evaluation of meta-[211At]astatobenzylguanidine in an athymic mouse human neuroblastoma xenograft model. *Nucl Med Biol.* (1996) 23:851–6. doi: 10.1016/0969-8051(96)00115-1

47. Ohshima Y, Sudo H, Watanabe S, Nagatsu K, Tsuji AB, Sakashita T, et al. Antitumor effects of radionuclide treatment using α-emitting meta-211At-astato-benzylguanidine in a PC12 pheochromocytoma model. *Eur J Nucl Med Mol Imaging.* (2018) 45:999–1010. doi: 10.1007/s00259-017-3919-6

48. Sudo H, Tsuji AB, Sugyo A, Nagatsu K, Minegishi K, Ishioka NS, et al. Preclinical evaluation of the acute radiotoxicity of the alpha-emitting molecular-targeted therapeutic agent (211)At-MABG for the treatment of malignant pheochromocytoma in normal mice. *Transl Oncol.* (2019) 12:879–88. doi: 10.1016/j.tranon.2019.04.008

49. Ukon N, Higashi T, Hosono M, Kinuya S, Yamada T, Yanagida S, et al. Manual on the proper use of meta-[211At] astato-benzylguanidine ([211At] MABG) injections in clinical trials for targeted alpha therapy (1st edition). *Ann Nucl Med.* (2022) 36:695–709. doi: 10.1007/s12149-022-01765-1

50. Eriksson SE, Bäck T, Elgstrom E, Jensen H, Nilsson R, Lindegren S, et al. Successful radioimmunotherapy of established syngeneic rat colon carcinoma with 211At-mAb. *EJNMMI Res.* (2013) 3:23. doi: 10.1186/2191-219X-3-23

51. Eriksson SE, Elgstrom E, Bäck T, Ohlsson T, Jensen H, Nilsson R, et al. Sequential radioimmunotherapy with 177Lu- and 211At-labeled monoclonal antibody BR96 in a syngeneic rat colon carcinoma model. *Cancer Biother Radiopharm.* (2014) 29:238–46. doi: 10.1089/cbr.2014.1625

52. Liu W, Ma H, Liang R, Chen X, Li H, Lan T, et al. Targeted alpha therapy of glioma using (211)At-labeled heterodimeric peptide targeting both VEGFR and integrins. *Mol Pharm.* (2022) 19:3206–16. doi: 10.1021/acs.molpharmaceut.2c00349

53. Lyczko M, Pruszynski M, Majkowska-Pilip A, Lyczko K, Was B, Meczynska-Wielgosz S, et al. (211)At labeled substance P (5-11) as potential radiopharmaceutical for glioma treatment. *Nucl Med Biol.* (2017) 53:1–8. doi: 10.1016/j.nucmedbio.2017.05.008

54. Watabe T, Kaneda-Nakashima K, Shirakami Y, Liu Y, Ooe K, Teramoto T, et al. Targeted alpha therapy using astatine ((211)At)-labeled phenylalanine: a preclinical study in glioma bearing mice. *Oncotarget.* (2020) 11:1388–98. doi: 10.18632/oncotarget.27552

55. Cheng J, Ekberg T, Engstrom M, Nestor M, Jensen HJ, Tolmachev V, et al. Radioimmunotherapy with astatine-211 using chimeric monoclonal antibody U36 in head and neck squamous cell carcinoma. *Laryngoscope.* (2007) 117:1013–8. doi: 10.1097/MLG.0b013e31804b1a6d

56. Walte A, Sriyapureddy SS, Korkmaz Z, Krull D, Bolte O, Hofmann M, et al. Preparation and evaluation of 211At labelled antineoplastic antibodies. *J Pharm Pharm Sci.* (2007) 10:277s—85s.

57. Oriuchi N, Aoki M, Ukon N, Washiyama K, Tan C, Shimoyama S, et al. Possibility of cancer-stem-cell-targeted radioimmunotherapy for acute myelogenous leukemia using (211)At-CXCR4 monoclonal antibody. *Sci Rep.* (2020) 10:6810. doi: 10.1038/s41598-020-63557-9

58. Green DJ, Shadman M, Jones JC, Frayo SL, Kenoyer AL, Hylarides MD, et al. Astatine-211 conjugated to an anti-CD20 monoclonal antibody eradicates disseminated B-cell lymphoma in a mouse model. *Blood.* (2015) 125:2111–9. doi: 10.1182/blood-2014-11-612770

59. Zhao B, Qin S, Chai L, Lu G, Yang Y, Cai H, et al. Evaluation of astatine-211-labeled octreotide as a potential radiotherapeutic agent for NSCLC treatment. *Bioorg Med Chem.* (2018) 26:1086–91. doi: 10.1016/j.bmc.2018.01.023

60. Link EM, Michalowski AS, Rosch F. 211At-methylene blue for targeted radiotherapy of disseminated melanoma: microscopic analysis of tumour versus normal tissue damage. *Eur J Cancer.* (1996) 32A:1986–94. doi: 10.1016/0959-8049(96)00236-5

61. Gouard S, Maurel C, Marionneau-Lambot S, Dansette D, Bailly C, Guérard F, et al. Targeted-alpha-therapy combining astatine-211 and anti-CD138 antibody in a preclinical syngeneic mouse model of multiple myeloma. *Min Res Dis.* (2020) 12:2721. doi: 10.3390/cancers12092721

62. Makvandi M, Samanta M, Martorano P, Lee H, Gitto SB, Patel K, et al. Pre-clinical investigation of astatine-211-parthanatine for high-risk neuroblastoma. *Commun Biol.* (2022) 5:1260. doi: 10.1038/s42003-022-04209-8

63. Andersson H, Lindegren S, Bäck T, Jacobsson L, Leser G, Horvath G. Radioimmunotherapy of nude mice with intraperitoneally growing ovarian cancer xenograft utilizing 211At-labelled monoclonal antibody MOv18. *Anticancer Res.* (2000) 20:459–62.

64. Palm S, Bäck T, Aneheim E, Hallqvist A, Hultborn R, Jacobsson L, et al. Evaluation of therapeutic efficacy of (211)At-labeled farletuzumab in an intraperitoneal mouse model of disseminated ovarian cancer. *Transl Oncol.* (2020) 14:100873. doi: 10.1016/j.tranon.2020.100873

65. Elgqvist J, Andersson H, Back T, Claesson I, Hultborn R, Jensen H, et al. Fractionated radioimmunotherapy of intraperitoneally growing ovarian cancer in nude mice with 211At-MX35 F(ab')2: therapeutic efficacy and myelotoxicity. *Nucl Med Biol.* (2006) 33:1065–72. doi: 10.1016/j.nucmedbio.2006.07.009

66. Gustafsson AM, Bäck T, Elgqvist J, Jacobsson L, Hultborn R, Albertsson P, et al. Comparison of therapeutic efficacy and biodistribution of 213Bi- and 211At-labeled monoclonal antibody MX35 in an ovarian cancer model. *Nucl Med Biol.* (2012) 39:15–22. doi: 10.1016/j.nucmedbio.2011.07.003

67. Palm S, Bäck T, Claesson I, Danielsson A, Elgqvist J, Frost S, et al. Therapeutic efficacy of astatine-211-labeled trastuzumab on radioresistant SKOV-3 tumors in nude mice. *Int J Radiat Oncol Biol Phys.* (2007) 69:572–9. doi: 10.1016/j.ijrobp.2007.06.023

68. Li HK, Morokoshi Y, Nagatsu K, Kamada T, Hasegawa S. Locoregional therapy with alpha-emitting trastuzumab against peritoneal metastasis of human epidermal growth factor receptor 2-positive gastric cancer in mice. *Cancer Sci.* (2017) 108:1648–56. doi: 10.1111/cas.13282

69. Dekempeneer Y, Bäck T, Aneheim E, Jensen H, Puttemans J, Xavier C, et al. Labeling of anti-HER2 nanobodies with astatine-211: optimization and the effect of different coupling reagents on their *in vivo* behavior. *Mol Pharm.* (2019) 16:3524–33. doi: 10.1021/acs.molpharmaceut.9b00354

70. Feng Y, Meshaw R, Zhao XG, Jannetti SA III, Vaidyanathan G, Zalutsky MR. Effective treatment of human breast carcinoma xenografts with single-dose (211)At-labeled anti-HER2 single domain antibody fragment. *J Nucl Med.* (2022). doi: 10.2967/jnumed.122.264071. [Epub ahead of print].

71. Robinson MK, Shaller C, Garmestani K, Plascjak PS, Hodge KM, Yuan QA, et al. Effective treatment of established human breast tumor xenografts in immunodeficient mice with a single dose of the alpha-emitting radioisotope astatine-211 conjugated to anti-HER2/neu diabodies. *Clin Cancer Res.* (2008) 14:875–82. doi: 10.1158/1078-0432.CCR-07-1250

72. Kiess AP, Minn I, Vaidyanathan G, Hobbs RF, Josefsson A, Shen C, et al. (2S)-2-(3-(1-Carboxy-5-(4-211At-Astatobenzamido)Pentyl)Ureido)-pentanedioic acid for PSMA-targeted alpha-particle radiopharmaceutical therapy. *J Nucl Med.* (2016) 57:1569–75. doi: 10.2967/jnumed.116.174300

73. Bäck TA, Jennbacken K, Hagberg Thulin M, Lindegren S, Jensen H, Olafsen T, et al. Targeted alpha therapy with astatine-211-labeled anti-PSCA A11 minibody shows antitumor efficacy in prostate cancer xenografts and bone microtumors. *EJNMMI Res.* (2020) 10:10. doi: 10.1186/s13550-020-0600-z

74. Aoki M, Zhao S, Takahashi K, Washiyama K, Ukon N, Tan C, et al. Preliminary Evaluation of Astatine-211-Labeled Bombesin Derivatives for Targeted Alpha Therapy. *Chem Pharm Bull (Tokyo).* (2020) 68:538–45. doi: 10.1248/cpb.c20-00077

75. Carlin S, Mairs RJ, Welsh P, Zalutsky MR. Sodium-iodide symporter (NIS)-mediated accumulation of [(211)At]astatide in NIS-transfected human cancer cells. *Nucl Med Biol.* (2002) 29:729–39. doi: 10.1016/S0969-8051(02)00332-3

76. Petrich T, Helmeke HJ, Meyer GJ, Knapp WH, Potter E. Establishment of radioactive astatine and iodine uptake in cancer cell lines expressing the human sodium/iodide symporter. *Eur J Nucl Med Mol Imaging.* (2002) 29:842–54. doi: 10.1007/s00259-002-0784-7

77. Petrich T, Quintanilla-Martinez L, Korkmaz Z, Samson E, Helmeke HJ, Meyer GJ, et al. Effective cancer therapy with the alpha-particle emitter [211At]astatine in a mouse model of genetically modified sodium/iodide symporter-expressing tumors. *Clin Cancer Res.* (2006) 12:1342–8. doi: 10.1158/1078-0432.CCR-05-1576

78. Sporer E, Poulie C, Lindegren S, Aneheim E, Jensen H, Bäck T, et al. Surface adsorption of the alpha-emitter astatine-211 to gold nanoparticles is stable *in vivo* and potentially useful in radionuclide therapy. *J Nanotheran.* (2021) 2:196–207. doi: 10.3390/jnt2040012

79. Yang SR, Schultheis AM Yu H, Mandelker D, Ladanyi M, Buttner R. Precision medicine in non-small cell lung cancer: current applications and future directions. *Semin Cancer Biol.* (2022) 84:184–98. doi: 10.1016/j.semcancer.2020.07.009

80. Eso Y, Shimizu T, Takeda H, Takai A, Marusawa H. Microsatellite instability and immune checkpoint inhibitors: toward precision medicine against gastrointestinal and hepatobiliary cancers. *J Gastroenterol.* (2020) 55:15–26. doi: 10.1007/s00535-019-01620-7

81. Bodei L, Herrmann K, Schoder H, Scott AM, Lewis JS. Radiotheranostics in oncology: current challenges and emerging opportunities. *Nat Rev Clin Oncol.* (2022) 19:534–50. doi: 10.1038/s41571-022-00652-y

82. Piwowarska-Bilska H, Kurkowska S, Birkenfeld B. Individualization of radionuclide therapies: challenges and prospects. *Cancers.* (2022) 14:3418. doi: 10.3390/cancers14143418

83. Glimelius B, Dahl O, Cedermark B, Jakobsen A, Bentzen SM, Starkhammar H, et al. Adjuvant chemotherapy in colorectal cancer: a joint analysis of randomised trials by the nordic gastrointestinal tumour adjuvant therapy group. *Acta Oncol.* (2005) 44:904–12. doi: 10.1080/02841860500355900a

84. Back T, Chouin N, Lindegren S, Kahu H, Jensen H, Albertsson P, et al. Cure of human ovarian carcinoma solid xenografts by fractionated alpha-radioimmunotherapy with (211)At-MX35-F(ab')2: influence of absorbed tumor dose and effect on long-term survival. *J Nucl Med.* (2017) 58:598–604. doi: 10.2967/jnumed.116.178327

85. Pagel JM, Kenoyer AL, Back T, Hamlin DK, Wilbur DS, Fisher DR, et al. Anti-CD45 pretargeted radioimmunotherapy using bismuth-213: high rates of complete remission and long-term survival in a mouse myeloid leukemia xenograft model. *Blood.* (2011) 118:703–11. doi: 10.1182/blood-2011-04-347039

86. Altai M, Membreno R, Cook B, Tolmachev V, Zeglis BM. Pretargeted imaging and therapy. *J Nucl Med.* (2017) 58:1553–9. doi: 10.2967/jnumed.117.189944

87. Cheal SM, Chung SK, Vaughn BA, Cheung NKV, Larson SM. Pretargeting: a path forward for radioimmunotherapy. *J Nuc Med.* (2022) 63:1302–15. doi: 10.2967/jnumed.121.262186

88. Lindegren S, Frost SH. Pretargeted radioimmunotherapy with alpha-particle emitting radionuclides. *Curr Radiopharm.* (2011) 4:248–60. doi: 10.2174/1874471011104030248

89. Breitz HB, Weiden PL, Beaumier PL, Axworthy DB, Seiler C, Su FM, et al. Clinical optimization of pretargeted radioimmunotherapy with antibody-streptavidin conjugate and 90Y-DOTA-biotin. *J Nucl Med.* (2000) 41:131–40.

90. Jallinoja VIJ, Houghton JL. Current landscape in clinical pretargeted radioimmunoimaging and therapy. *J Nucl Med.* (2021) 62:1200–6. doi: 10.2967/jnumed.120.260687

91. Kraeber-Bodere F, Faivre-Chauvet A, Ferrer L, Vuillez JP, Brard PY, Rousseau C, et al. Pharmacokinetics and dosimetry studies for optimization of anti-carcinoembryonic antigen x anti-hapten bispecific antibody-mediated pretargeting of Iodine-131-labeled hapten in a phase I radioimmunotherapy trial. *Clin Cancer Res.* (2003) 9:3973S—81S.

92. Shen S, Forero A, LoBuglio AF, Breitz H, Khazaeli MB, Fisher DR, et al. Patient-specific dosimetry of pretargeted radioimmunotherapy using CC49 fusion protein in patients with gastrointestinal malignancies. *J Nucl Med.* (2005) 46:642–51.

93. Weiden PL, Breitz HB. Pretargeted radioimmunotherapy (PRIT) for treatment of non-Hodgkin's lymphoma (NHL). *Crit Rev Oncol Hematol.* (2001) 40:37–51. doi: 10.1016/S1040-8428(01)00133-0

94. Houghton JL, Membreno R, Abdel-Atti D, Cunanan KM, Carlin S, Scholz WW, et al. Establishment of the *in vivo* efficacy of pretargeted radioimmunotherapy utilizing inverse electron demand diels-alder click chemistry. *Mol Cancer Ther.* (2017) 16:124–33. doi: 10.1158/1535-7163.MCT-16-0503

95. Pignata S, S CC, Du Bois A, Harter P, Heitz F. Treatment of recurrent ovarian cancer. *Ann Oncol.* (2017) 28(suppl_8):viii51-viii6. doi: 10.1093/annonc/mdx441

96. Deng H, Li B, Qin X. The short- and long-term survival of hyperthermic intraperitoneal chemotherapy (HIPEC) in the advanced gastric cancer with/without peritoneal carcinomatosis: a systematic review and meta-analysis of randomized controlled trials. *Updates Surg.* (2022) 3:5. doi: 10.1007/s13304-022-01376-5

97. Sugarbaker PH, Chang D. Anatomic sites of disease in colorectal cancer patients recorded at the time of cytoreductive surgery for peritoneal metastases. *Eur J Surg Oncol.* (2022) 48:946–55. doi: 10.1016/j.ejso.2022.01.012

98. Honoré C, Goéré D, Souadka A, Dumont F, Elias D. Definition of patients presenting a high risk of developing peritoneal carcinomatosis after curative surgery for colorectal cancer: a systematic review. *Ann Surg Oncol.* (2013) 20:183–92. doi: 10.1245/s10434-012-2473-5

99. Schorn S, Demir IE, Samm N, Scheufele F, Calavrezos L, Sargut M, et al. Meta-analysis of the impact of neoadjuvant therapy on patterns of recurrence in pancreatic ductal adenocarcinoma. *BJS Open.* (2018) 2:52–61. doi: 10.1002/bjs5.46

100. Boudousq V, Ricaud S, Garambois V, Bascoul-Mollevi C, Boutaleb S, Busson M, et al. Brief intraperitoneal radioimmunotherapy of small peritoneal carcinomatosis using high activities of non-internalizing $_{125}$I-Labeled. *Monoclonal Antibodies.* (2010) 51:1748–55. doi: 10.2967/jnumed.110.080226

101. Deshayes E, Ladjohounlou R, Le Fur P, Pichard A, Lozza C, Boudousq V, et al. Radiolabeled antibodies against müllerian-inhibiting substance receptor, type II: new tools for a theranostic approach in

ovarian cancer. *J Nuc Med*. (2018) 59:1234–42. doi: 10.2967/jnumed.118.208611

102. Kramer K, Humm JL, Souweidane MM, Zanzonico PB, Dunkel IJ, Gerald WL, et al. Phase I study of targeted radioimmunotherapy for leptomeningeal cancers using intra-Ommaya 131-I-3F8. *J Clin Oncol*. (2007) 25:5465–70. doi: 10.1200/JCO.2007.11.1807

103. Kramer K, Kushner BH, Modak S, Pandit-Taskar N, Smith-Jones P, Zanzonico P, et al. Compartmental intrathecal radioimmunotherapy: results for treatment for metastatic CNS neuroblastoma. *J Neurooncol*. (2010) 97:409–18. doi: 10.1007/s11060-009-0038-7

104. Kramer K, Pandit-Taskar N, Humm JL, Zanzonico PB, Haque S, Dunkel IJ, et al. A phase II study of radioimmunotherapy with intraventricular (131) I-3F8 for medulloblastoma. *Pediatr Blood Cancer*. (2018) 65:26754 doi: 10.1002/pbc.26754

105. He P, Kramer K, Smith-Jones P, Zanzonico P, Humm J, Larson SM, et al. Two-compartment model of radioimmunotherapy delivered through cerebrospinal fluid. *Eur J Nucl Med Mol Imaging*. (2011) 38:334–42. doi: 10.1007/s00259-010-1633-8

106. Lv Y, Cheung NK, Fu BM, A. pharmacokinetic model for radioimmunotherapy delivered through cerebrospinal fluid for the treatment of leptomeningeal metastases. *J Nucl Med*. (2009) 50:1324–31. doi: 10.2967/jnumed.108.060798

107. Pandit-Taskar N, Zanzonico PB, Kramer K, Grkovski M, Fung EK, Shi W, et al. Biodistribution and dosimetry of intraventricularly administered (124)I-omburtamab in patients with metastatic leptomeningeal tumors. *J Nucl Med*. (2019) 60:1794–801. doi: 10.2967/jnumed.118.219576

108. Yerrabelli RS, He P, Fung EK, Kramer K, Zanzonico PB, Humm JL, et al. IntraOmmaya compartmental radioimmunotherapy using (131)I-omburtamab-pharmacokinetic modeling to optimize therapeutic index. *Eur J Nucl Med Mol Imaging*. (2021) 48:1166–77. doi: 10.1007/s00259-020-05050-z

109. Palm S, Bäck T, Leidermark E, Lindegren S, Aneheim E, Jensen H, et al., editors. Modelling show alpha-emitter astatine-211 is an apposite candidate for intra-thecal radioimmunotherapy of neuroblastoma metastasized to the central nervous system. In *European Association of Nuclear Medicine October 22 – 30, 2020 Virtual 2020 2020/09/01*. *European Journal of Nuclear Medicine and Molecular Imaging*. New York, NY: Springer (2020).

110. Palm S, Back T, Lindegren S, Hultborn R, Jacobsson L, Albertsson P. Model of intraperitoneal targeted alpha-particle therapy shows that posttherapy cold-antibody boost enhances microtumor radiation dose and treatable tumor sizes. *J Nucl Med*. (2018) 59:646–51. doi: 10.2967/jnumed.117.201285

111. Palm S, Humm JL, Rundqvist R, Jacobsson L. Microdosimetry of astatine-211 single-cell irradiation: role of daughter polonium-211 diffusion. *Med Phys*. (2004) 31:218–25. doi: 10.1118/1.1640951

112. Visser GW, Diemer EL, Vos CM, Kaspersen FM. The biological behaviour of some organic astatine compounds in rats. *Int J Appl Radiat Isot*. (1981) 32:913–7. doi: 10.1016/0020-708X(81)90078-8

113. Hamilton JG, Soley MH, A. Comparison of the metabolism of iodine and of element 85 (Eka-Iodine). *Proc Natl Acad Sci U S A*. (1940) 26:483–9. doi: 10.1073/pnas.26.8.483

114. Johnson GL, Leininger RF, Segrè E. Chemical properties of astatine. *J Chem Physics*. (1949) 17:1–10. doi: 10.1063/1.1747034

115. Guerard F, Gestin JF, Brechbiel MW. Production of [(211)At]-astatinated radiopharmaceuticals and applications in targeted alpha-particle therapy. *Cancer Biother Radiopharm*. (2013) 28:1–20. doi: 10.1089/cbr.2012.1292

116. Wilbur DS. Chemical and radiochemical considerations in radiolabeling with alpha-emitting radionuclides. *Curr Radiopharm*. (2011) 4:214–47. doi: 10.2174/1874471011104030214

117. Berdal M, Gouard S, Eychenne R, Marionneau-Lambot S, Croyal M, Faivre-Chauvet A, et al. Investigation on the reactivity of nucleophilic radiohalogens with arylboronic acids in water: access to an efficient single-step method for the radioiodination and astatination of antibodies. *Chemical Science*. (2021) 12:1458–68. doi: 10.1039/D0SC05191H

118. Milius RA, McLaughlin WH, Lambrecht RM, Wolf AP, Carroll JJ, Adelstein SJ, et al. Organoastatine chemistry. Astatination via electrophilic destannylation. *Int J Rad Appl Instrum A*. (1986) 37:799–802. doi: 10.1016/0883-2889(86)90274-1

119. Larsen RH, Wieland BW, Zalutsky MR. Evaluation of an internal cyclotron target for the production of 211At via the 209Bi (alpha,2n)211 at reaction. *Appl Radiat Isot*. (1996) 47:135–43. doi: 10.1016/0969-8043(95)00285-5

120. Crawford JR, Yang H, Kunz P, Wilbur DS, Schaffer P, Ruth TJ. Development of a preclinical (211)Rn/(211)At generator system for targeted alpha therapy research with (211)At. *Nucl Med Biol*. (2017) 48:31–5. doi: 10.1016/j.nucmedbio.2017.01.011

121. Zalutsky MR, Pruszynski M. Astatine-211: production and availability. *Curr Radiopharm*. (2011) 4:177–85. doi: 10.2174/1874471011104030177

122. O'Hara MJ, Krzysko AJ, Hamlin DK Li Y, Dorman EF, Wilbur DS. Development of an autonomous solvent extraction system to isolate astatine-211 from dissolved cyclotron bombarded bismuth targets. *Sci Rep*. (2019) 9:20318. doi: 10.1038/s41598-019-56272-7

123. Tereshatov EE, Burns JD, Schultz SJ, McCann LA, McIntosh LA, Tabacaru GC, et al. Compact automated apparatus for rapid astatine recovery from nitric acid media: design, application, and impurity characterization. *Chem Engin J*. (2022) 442:136176. doi: 10.1016/j.cej.2022.136176

124. Aneheim E, Albertsson P, Back T, Jensen H, Palm S, Lindegren S. Automated astatination of biomolecules–a stepping stone towards multicenter clinical trials. *Sci Rep*. (2015) 5:12025. doi: 10.1038/srep12025

125. Action CA19114 – COST. (2022). Available online at: https://www.cost.eu/actions/CA19114/ (accessed October 21, 2022).

126. Providing the Nation with Critical Isotopes | NIDC: National Isotope Development Center. (2022). Available online at: https://www.isotopes.gov/about-us (accessed October 21, 2022).

frontiers | Frontiers in Medicine

TYPE Mini Review
PUBLISHED 09 January 2023
DOI 10.3389/fmed.2022.1071086



OPEN ACCESS

EDITED BY
Øyvind Bruland,
Oslo University Hospital, Norway

REVIEWED BY
Robert Mairs,
University of Glasgow, United Kingdom
John Humm,
Memorial Sloan Kettering Cancer Center, United States
Oliver Sartor,
Tulane University, United States

*CORRESPONDENCE
Urs B. Hagemann
✉ urs.hagemann@bayer.com

SPECIALTY SECTION
This article was submitted to Nuclear Medicine, a section of the journal Frontiers in Medicine

RECEIVED 15 October 2022
ACCEPTED 15 December 2022
PUBLISHED 09 January 2023

CITATION
Karlsson J, Schatz CA, Wengner AM, Hammer S, Scholz A, Cuthbertson A, Wagner V, Hennekes H, Jardine V and Hagemann UB (2023) Targeted thorium-227 conjugates as treatment options in oncology.
*Front. Med.* 9:1071086.
doi: 10.3389/fmed.2022.1071086



# Targeted thorium-227 conjugates as treatment options in oncology

Jenny Karlsson[1], Christoph A. Schatz[2], Antje M. Wengner[2], Stefanie Hammer[2], Arne Scholz[2], Alan Cuthbertson[1], Volker Wagner[3], Hartwig Hennekes[2], Vicki Jardine[4] and Urs B. Hagemann[2]*

[1]Bayer AS, Oslo, Norway, [2]Bayer AG, Berlin, Germany, [3]Bayer Consumer Care AG, Basel, Switzerland, [4]Bayer PLC, Reading, United Kingdom

Targeted alpha therapy (TAT) is a promising approach for addressing unmet needs in oncology. Inherent properties make α-emitting radionuclides well suited to cancer therapy, including high linear energy transfer (LET), penetration range of 2–10 cell layers, induction of complex double-stranded DNA breaks, and immune-stimulatory effects. Several alpha radionuclides, including radium-223 ($^{223}$Ra), actinium-225 ($^{225}$Ac), and thorium-227 ($^{227}$Th), have been investigated. Conjugation of tumor targeting modalities, such as antibodies and small molecules, with a chelator moiety and subsequent radiolabeling with α-emitters enables specific delivery of cytotoxic payloads to different tumor types. $^{223}$Ra dichloride, approved for the treatment of patients with metastatic castration-resistant prostate cancer (mCRPC) with bone-metastatic disease and no visceral metastasis, is the only approved and commercialized alpha therapy. However, $^{223}$Ra dichloride cannot currently be complexed to targeting moieties. In contrast to $^{223}$Ra, $^{227}$Th may be readily chelated, which allows radiolabeling of tumor targeting moieties to produce targeted thorium conjugates (TTCs), facilitating delivery to a broad range of tumors. TTCs have shown promise in pre-clinical studies across a range of tumor-cell expressing antigens. A clinical study in hematological malignancy targeting CD22 has demonstrated early signs of activity. Furthermore, pre-clinical studies show additive or synergistic effects when TTCs are combined with established anti-cancer therapies, for example androgen receptor inhibitors (ARI), DNA damage response inhibitors such as poly (ADP)-ribose polymerase inhibitors or ataxia telangiectasia and Rad3-related kinase inhibitors, as well as immune checkpoint inhibitors.

KEYWORDS

**alpha-particle emitter, DNA damage response, immune checkpoint inhibitors, anti-androgen therapies, alpha emitter, targeted alpha therapy, targeted thorium conjugates, thorium-227**

# 1. Introduction

Despite drug discovery advances, an unmet clinical need for novel oncology treatment modalities persists. Targeted alpha therapy (TAT) represents one such modality, as α-particles have several properties of potential value in cancer therapy. These include high linear energy transfer (LET), short penetration range, and induction of complex double-stranded DNA breaks (1). High LET means a low number of hits are needed to induce cell death (1), while the short-path length of α-particles (50–100 μm) is expected to minimize damage to surrounding healthy tissue (1). Furthermore, complex double-stranded DNA breaks induced by alpha-radiation are hard to repair, promoting cell cycle arrest and cell death (1, 2). TATs may also promote T-cell infiltration through induction of immunogenic cell death (3–6), or have increased potency against tumor cells with alterations in DNA damage repair genes (cytotoxic radiation-induced DNA damage increases their susceptibility to apoptosis) (7–9).

Selective tumor targeting by TATs can be achieved through two primary mechanisms: inherent radionuclide properties (1) and the ability to chelate the radionuclide to a tumor-targeting molecule (e.g., a monoclonal antibody, peptide or small molecule) (1). Over the last 20 years, several α-particle-emitting radionuclides have been investigated as TATs, including: actinium-225 ($^{225}$Ac, half-life 9.9 days); astatine-211 ($^{211}$At, half-life 7.2 h); bismuth-213 ($^{213}$Bi, half-life 45.6 min); radium-223 ($^{223}$Ra, half-life 11.4 days); and thorium-227 ($^{227}$Th, half-life 18.7 days) (1). Lead-212 ($^{212}$Pb, half-life 10.64 h) is a β-emitter; however, it generates the daughter nuclides bismuth-212 ($^{212}$Bi) and polonium-212 ($^{212}$Po), which are short-lived α-particle emitters (10). $^{223}$Ra dichloride was the first and is still the only approved TAT (11, 12), and is approved for use in metastatic castration-resistant prostate cancer (mCRPC) with bone metastases (13, 14). $^{223}$Ra dichloride acts as a calcium mimetic and is preferentially taken up in osteoblastic bone metastases (15, 16); it cannot currently be complexed to targeting moieties, although recent developments have shown promise (14, 17). Most other TATs, like targeted thorium conjugates (TTCs) or targeted actinium conjugates, use isotopes chelated to various targeting moieties. This enables delivery to a wide range of tumors (14), extending the clinical application of radionuclides.

# 2. Targeted thorium conjugates and their mode of action

$^{227}$Th, the progenitor of $^{223}$Ra, can be used in TTCs, comprised of the $^{227}$Th α-emitting radionuclide, a chelator such as octadentate 3,2-hydroxypyridinone (3,2-HOPO), and a tumor-targeting moiety (13, 14). TTCs enable selective delivery of $^{227}$Th to tumors by targeting antigens expressed in cancer tissues but absent or at low levels in normal tissues (2). For a therapeutic window, TTC characteristics must allow for efficient delivery, accumulation and retention in tumors, while sparing nearby healthy tissue (14). Cytotoxicity results from the induction of clustered double-stranded DNA breaks, followed by subsequent G2/M phase cell cycle arrest and apoptosis (14). Immunogenic cell death has also been demonstrated, occurring *via* increased tumor infiltration by CD8+ T cells (5, 14). The activity of TTCs is not reliant on cellular internalization of $^{227}$Th, given the α-particle path length of 20–100 μM (2–10 cell diameters) in tissue, a property which may overcome heterogeneous antigen expression (14).

The relatively long half-life of $^{227}$Th (18.7 days) compared with other radionuclides in current use for TAT (1) highlights the need to identify appropriate targeting moieties that complement the properties of $^{227}$Th. For example, while typically longer than that of small molecules, the half-lives of antibodies used as therapeutic agents vary considerably (6–32 days) (17–19), suggesting that some may not be suitable for delivery of a radionuclide with a longer half-life. For TTCs, while it may be preferable to select antibodies with comparable half-lives to $^{227}$Th, data are not yet available as to whether this would be necessary for therapeutic efficacy.

When the $^{227}$Th component of a TTC decays, recoil energy releases the daughter radionuclide $^{223}$Ra from the chelator (14). Whilst data on the safety and biodistribution of $^{223}$Ra released from TTCs are not available, $^{223}$Ra is well tolerated when it is used as a treatment (20) and it is rapidly cleared from plasma into the small bowel and excreted (21). Furthermore, the amount of $^{223}$Ra released from a TTC will be much smaller than that of a therapeutic dose of $^{223}$Ra. Daughter radionuclides of $^{227}$Th that lie downstream of $^{223}$Ra in the decay cascade have very short half-lives (14) and have no clinical consequence, as indicated by the good tolerability of $^{223}$Ra as a cancer therapeutic (20).

# 3. TTCs in cancer

Pre-clinical and clinical studies of TTCs have included several tumor types expressing a range of different cancer-related antigens (**Figure 1**).

## 3.1. Hematological cancers

Initial Pre-clinical studies focusing on hematological cancers, targeting CD22 or CD33 in lymphoma and acute myeloid leukemia (AML), respectively, demonstrated promising anti-tumor activity (14, 22). Furthermore, CD22-TTC (BAY 1862864) has been investigated in a Phase 1 study in patients with CD22-positive relapsed/refractory B-cell non-Hodgkin lymphoma (23). In this setting, CD22-TTC was

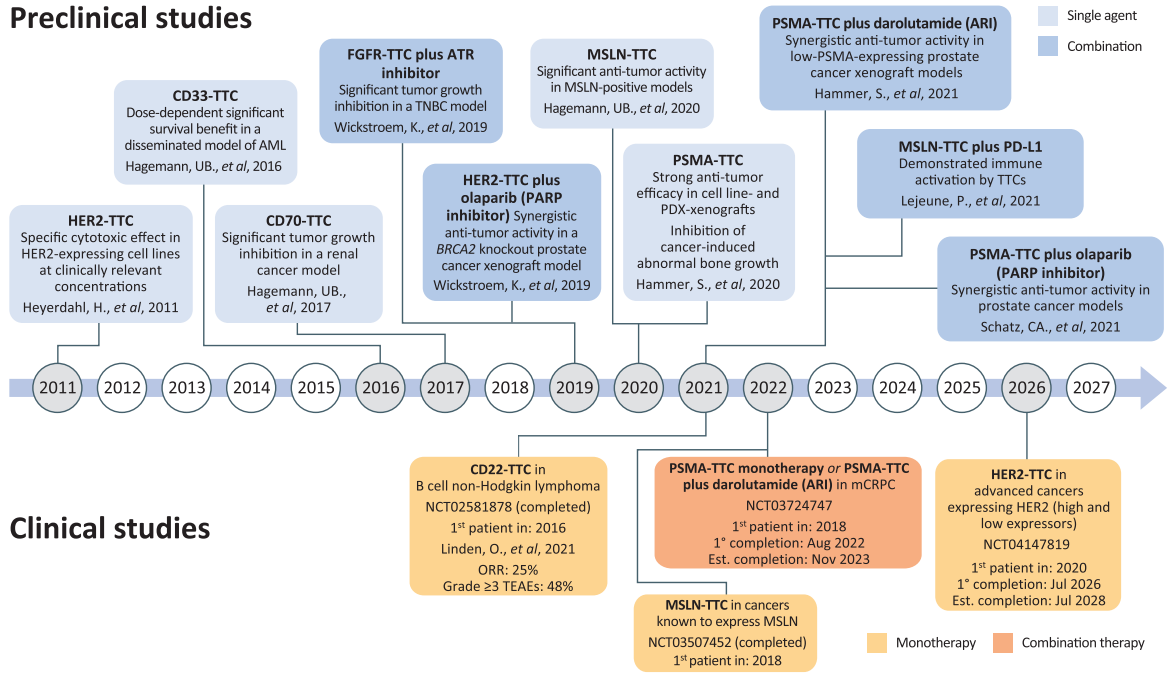


FIGURE 1
Timeline of TTC development. ARI, androgen receptor inhibitor; CD, cluster of differentiation; FGFR, fibroblast growth factor receptor; HER2, human epidermal growth factor receptor-2; MSLN, mesothelin; PARP, poly (ADP)-ribose polymerase; PD-L1, programmed death-ligand 1; PDX, patient-derived xenograft; PSMA, prostate-specific membrane antigen; TTC, targeted thorium conjugate; AML, acute myeloid leukemia; ATR, ataxia telangiectasia and rad3-related protein; mCRPC, metastatic castration-resistant prostate cancer; ORR, overall response rate; TNBC, triple-negative breast cancer; TEAE, treatment-emergent adverse event.

safe, with the most common grade ≥3 adverse events being neutropenia, thrombocytopenia, and leukopenia (23). Maximum $^{227}$Th blood concentrations increased proportionally to the dose administered and stability of CD22-TTC in the blood was demonstrated (23). The overall objective response rate (ORR) was 24% (5/21 patients: 1 complete and 4 partial responses), with the highest ORR seen in patients with relapsed low-grade lymphomas [3/10 patients (30%)] (23).

## 3.2. Renal cell cancer

CD27, part of the tumor necrosis factor receptor superfamily, plays a vital role in T- and B-cell co-stimulation (24). Physiological expression of CD70, the natural ligand of CD27, is transient and restricted to activated immune cells (24). However, CD70 dysregulation and overexpression has been observed in several cancers (25–28), where it may play a role in tumor progression and immunosuppression (29). Therefore, CD70-TTCs have the potential to both eliminate cancer cells and modulate immune responses. A CD70-TTC has been shown to reduce cell viability in renal cancer cell lines and significantly inhibit tumor growth in a renal cancer xenograft model (25).

## 3.3. Breast cancer

Approximately 25–30% of breast cancers overexpress human epidermal growth factor receptor-2 (HER2), which is associated with more aggressive disease (30). Intrinsic and acquired resistance to HER2-targeting antibodies or antibody drug conjugates (ADC) necessitates development of novel therapies (31, 32). A HER2-TTC, utilizing the HER2 antibody trastuzumab ($^{227}$Th-trastuzumab), showed significant dose-dependent anti-tumor effects in HER2-expressing breast cancer xenografts (33, 34). Moreover, when $^{227}$Th-trastuzumab was compared with lutetium-177 ($^{177}$Lu; a β-particle emitter) complexed with trastuzumab, in a similar xenograft study, each radionuclide conjugate had significant anti-tumor effects and increased survival, although efficacy was higher with $^{227}$Th-trastuzumab than with $^{177}$Lu-trastuzumab. However, $^{177}$Lu-trastuzumab had a superior therapeutic index (34). Additionally, clinically relevant concentrations of $^{227}$Th-trastuzumab induced cytotoxic effects in HER2-expressing breast cancer cell lines (35).

Initial HER2-targeted agents were ineffective against HER2-low breast cancer (36). However, the ADC trastuzumab deruxtecan recently demonstrated efficacy in this setting (37). Notably, HER2-TTC has been shown to inhibit tumor growth in

HER2-low colorectal cancer (CRC) xenografts (9), highlighting its potential as an alternative treatment option for HER2-low cancers. Furthermore, a Phase I trial of a HER2-TTC is ongoing in advanced HER2-expressing cancers: HER2-high and low expression in breast, gastric/gastroesophageal and other tumors (38).

Fibroblast growth factor receptor 2 (FGFR2) is also a promising target for TTCs, with amplifications in FGFR2 observed in a subset of triple-negative breast cancers (TNBCs) (39–41). Elevated FGFR2 is associated with an aggressive cancer phenotype and resistance to targeted therapy (39, 42), making FGFR2-TTCs an attractive therapeutic option. Indeed, in a human TNBC xenograft model, single-dose FGFR2-TTC reduced tumor growth and was well tolerated (43).

## 3.4. Gastric cancer

HER2 is overexpressed in over 20% of all gastric cancers and is a valid therapeutic target in this setting (44, 45). HER2-TTC was associated with potent target-mediated cytotoxicity in various cancer cell lines, including gastric cancer cell lines, expressing different levels of HER2 (46).

FGFR2 is also a potential target for TTCs, with some gastric cancers overexpressing the protein (47, 48). In gastric cancer xenograft models, tumor growth was inhibited after a single dose of FGFR2-TTC (48).

## 3.5. Colorectal cancer (CRC)

Next-generation sequencing identified *FGFR2* aberrations in a subset (1.4%) of patients with CRC (49) and FGFR2 expression has been seen in 2.9% of patients with CRC (50), indicating some patients may benefit from therapeutic targeting of this protein. In support of this, single-dose FGFR2-TTC inhibited tumor growth in a xenograft model of CRC (48).

HER2-TTC has also been evaluated in CRC models in combination with a poly (ADP)-ribose polymerase (PARP) inhibitor, which is discussed later in this review (9).

## 3.6. Mesothelioma

Mesothelioma is a rare malignant growth of mesothelial cells, occurring in lining layers of the viscera, e.g., pleura, peritoneum and pericardium (51). Mesothelin (MSLN) mediates cellular adhesion and is normally only expressed in mesothelial cells; however, when dysregulated in cancer, MSLN promotes proliferation, migration and invasion, making it an attractive target for TTC-based therapy (52–55). MSLN-TTC has shown potent cytotoxic effects in MSLN-positive cancer cell lines (including mesothelioma) and, when used in single- or multiple-dose regimens in cell line- and patient-derived xenograft models, the conjugate had significant anti-tumor activity and was well tolerated (56). Furthermore, MSLN-TTC prolonged survival in a disseminated lung cancer model in mice (56).

A first-in-human Phase I study of MSLN-TTC in patients with advanced cancer (mesothelioma, as well as MSLN-positive recurrent serous ovarian cancer and pancreatic adenocarcinoma) was completed in the first half of 2022 (57); results are being analyzed for future publication.

## 3.7. Ovarian cancer

Mesothelin-targeted thorium conjugate has been investigated in MSLN-positive ovarian cancer models, with significant anti-tumor activity seen when MSLN-TTC was used in single-dose regimens in cell line-derived xenografts and single- and multiple-dose regimens in patient-derived xenografts (56). Data from the aforementioned first-in-human study of MSLN-TTC in patients with advanced cancer, including ovarian cancer, are awaited with interest.

Pre-clinical studies have also explored the potential for HER2-TTCs in HER2-positive forms. $^{227}$Th-trastuzumab demonstrated cytotoxic effects in HER2-expressing ovarian cancer cell lines when used at clinically relevant concentrations (35). Furthermore, in HER2-positive ovarian cancer xenograft models, $^{227}$Th-trastuzumab delayed tumor growth and was associated with survival benefit vs. unlabeled trastuzumab (58, 59) or $^{177}$Lu-trastuzumab (at the same absorbed radiation dose to tumor) (59). Notably, fractionation of $^{227}$Th-trastuzumab dosing in xenograft models reduced toxicity while retaining efficacy, showing that administration schedule is an important consideration for TTCs (60).

## 3.8. Prostate cancer

A TTC targeting prostate-specific membrane antigen (PSMA) has been developed. *In vitro*, the antibody-based PSMA-TTC was rapidly internalized in a target-dependent manner, selectively reduced PSMA-expressing cell viability, and induced double-stranded DNA breaks, cell cycle arrest (G2/M phase), and apoptosis in prostate cancer cells (61). Consistent with this, induction of DNA damage markers and apoptosis was observed with PSMA-TTC in patient-derived xenografts in mice (61). Further *in vivo* data showed PSMA-TTC was associated with delayed tumor growth/tumor regression in PSMA-positive patient- and cell line-derived xenograft models mimicking different prostate cancer stages, including models resistant to standard-of-care anti-androgens (including enzalutamide) (61). This effect was seen with single as well as fractionated dosing (61). In a mouse model replicating prostate cancer

bone metastases, PSMA-TTC significantly reduced the growth of tumors in the bone and was associated with changes in tumor-induced bone morphology vs. controls (61).

A Phase I clinical study of PSMA-TTC, either alone or in combination with the novel androgen receptor inhibitor (ARI) darolutamide, in patients with mCRPC is currently ongoing; the primary completion date was August 2022, the estimated completion date is November 2023 (62).

## 4. TTCs in combination with other cancer therapies

Due to the unique mode of action of TTCs, there is a strong rationale for combining these with other cancer therapies, and this has been investigated in several pre-clinical studies.

### 4.1. DNA repair pathway inhibitors

As TTCs induce complex double-stranded DNA breaks (1), it is of interest to combine their use with PARP inhibitors, as PARP-1 and PARP-2 are involved in DNA damage repair (63, 64). *BRCA* mutations have been shown to sensitize cells to PARP inhibition (65, 66), as BRCA proteins are crucial for the repair of double-stranded DNA breaks (63). Indeed, in a *BRCA2*-mutated prostate cancer xenograft model, PSMA-TTC plus the PARP inhibitor olaparib showed more notable anti-tumor activity than PSMA-TTC alone, while olaparib alone showed no activity (67).

Additionally, HER2-TTC has been investigated in parental and *BRCA2* knockout HER2-expressing CRC cell lines and their corresponding xenograft models (9). In cell viability assays, the effect of HER2-TTC plus olaparib was synergistic in *BRCA2* knockout cells vs. additive in parental cells (9). Similarly, when combined with olaparib in *BRCA2*-deficient xenografts, low-dose HER2-TTC resulted in similar tumor growth inhibition to high-dose HER2-TTC alone, with the combination concluded as being synergistic; by contrast, no synergistic effects were seen with the combination in the parental xenograft model (9). These findings support further evaluation of PARP inhibitors in combination with TTCs.

Another protein involved in double-stranded DNA break repair is DNA-dependent protein kinase (DNA-PK), which plays a key role in non-homologous end joining (NHEJ) (68). Loss of DNA-PK makes cells more susceptible to radiation, as NHEJ is important for the repair of DNA double-strand breaks that are induced by ionizing radiation (68). Combining PSMA-TTC with a DNA-PK inhibitor resulted in synergistic anti-proliferative effects in prostate cancer cells (69). The combination was also more effective than PSMA-TCC monotherapy in prostate tumor-bearing mice (69), indicating the clinical potential for this combination.

FGFR2-TTC has been investigated in combination with an inhibitor of the ataxia telangiectasia and rad3-related protein (ATR), an enzyme involved in DNA damage response (43, 70–72). *In vitro*, the combination of FGFR2-TTC plus ATR inhibitor reduced cell viability and increased levels of γH2A.X (an indicator of double-strand DNA breaks) vs. FGFR2-TTC alone, while also reducing FGFR2-TTC-mediated cell cycle arrest (43). *In vivo*, tumor growth was significantly inhibited when the two agents were used in combination at single-agent doses known to have no effect (43). Data from ovarian cancer models studying the MSLN-TTC plus ATR inhibitor combination support these findings (7).

### 4.2. Immune checkpoint inhibitors

Immunostimulatory effects have been shown with radiation, including external beam radiotherapy and α-particle emitters, with the former showing anti-tumor effects when combined with immune checkpoint inhibitors (4, 73–76). These data provide rationale for combining a TTC with an immune checkpoint inhibitor, such as programmed death ligand-1 (PD-L1). MSLN-TTC demonstrated a robust immunostimulatory effect in human cancer cell lines (5). Moreover, in immunocompetent mice bearing implanted murine tumors expressing human MSLN, tumor growth was inhibited by MSLN-TTC and anti-PD-L1 individually, with this benefit enhanced when these agents were used in combination (5). Dendritic cell migration out of tumors and CD8+ T-cell infiltration into tumors was observed when MSLN-TTC was administered as monotherapy, with more extensive T-cell infiltration seen when MSLN-TTC was combined with anti-PD-L1 (5).

### 4.3. ARIs

Although ARIs are a common treatment option for patients with prostate cancer, treatment resistance eventually develops (77). This highlights the need for new therapeutic approaches, such as novel combination treatments or new agents with different mechanisms of action, to overcome this therapeutic barrier.

The ARI darolutamide is approved for non-metastatic CRPC in key markets (78, 79) and more recently for use in combination with docetaxel for metastatic hormone-sensitive prostate cancer in the United States (79). Darolutamide has been shown to induce PSMA expression in prostate cancer cell lines and xenografts (80, 81), providing a rationale for combining the drug with a PSMA-TTC. In prostate cancer xenograft models, darolutamide-mediated increase of PSMA expression

facilitated tumor uptake of PSMA-TTC, and darolutamide also impaired PSMA-TTC-mediated induction of DNA damage repair genes (80). Furthermore, the combination of PSMA-TTC plus darolutamide demonstrated synergistic inhibition of tumor growth in xenograft models (80). The tumor inhibitory activity of the combination was also more notable than either agent alone in xenograft models that were either resistant to the ARI enzalutamide (80) or hormone independent (81). These results support clinical investigation of this combination.

## 5. Discussion

$^{227}$Th is one of a number of α-emitters suitable for chelation and conjugation to tumor-targeting moieties and thus has the potential to cover a broad tumor range. Indeed, pre-clinical studies have shown anti-tumor activity of TTCs as monotherapy across a broad range of tumor types, and TTCs targeting HER2, PSMA, MSLN, and CD22 are under investigation in clinical studies. Furthermore, there is a strong rationale and pre-clinical evidence for combining TTCs with other targeted therapies, supporting their clinical evaluation. However, no additional TTC clinical trials are currently planned.

In addition to $^{227}$Th, various other α-emitters are being explored as conjugates for the treatment of cancer. Those considered to be the most suitable include $^{225}$Ac, $^{211}$At, $^{213}$Bi, and $^{212}$Pb (the latter being a β-emitter that generates daughter α-emitters) (1, 82), with the most clinical experience being available for $^{225}$Ac and $^{213}$Bi (83–90).

The clinical potential of targeted radionuclide therapy is further highlighted by the recent US approval of $^{177}$Lu-PSMA-617 (a β-emitter conjugated to a small molecule PSMA ligand) for the treatment of mCRPC (91–93). Moreover, promising early clinical data has indicated that targeting PSMA with $^{225}$Ac *via* a small molecule (84, 94, 95) or an antibody (96) has substantial potential in advanced prostate cancer, including for patients who have received radiotherapeutics utilizing $^{177}$Lu (97), and suggests feasibility of using different targeted radionuclides sequentially.

In summary, TATs represent an important therapeutic development in oncology and offer promise for addressing unmet medical needs for patients, such as resistance to established therapies.

## Author contributions

VW, HH, VJ, and UBH contributed to the conception and design. JK, CAS, AMW, SH, AS, AC, VW, HH, VJ, and UBH contributed to the drafting and revising of the work, and approval of the final version. All authors agreed to be accountable for all aspects of the respective work.

## Acknowledgments

The authors thank Katrine Wickstroem Biseth, Olav Ryan, Roger M. Bjerke, Ingrid Moen, Veronique Cruciani, Baard Indrevoll, Steinar Uran, Roger Smeets, Thanushan Rajanayagam, Liv-Ingrid Oedegardstuen, Aasmund Larsen, Anne Mobergslien, and Alex Papple (all Bayer AS, Norway) as well as Thorsten Poethko, Sandra Johanssen, Mark Trautwein, Christoph Mahlert, Lars Linden, Sabine Zitzmann-Kolbe, Volker Stickel, Martin Kohs, Melanie Appel, Maria Spelling, Seren Nesan, Meike Fehder, Sarah Boettcher, Lisa Bartnitzky, Kathleen Stadelmann, Stefan Stargard, Jochen Hilbig, Monika Klotz, Claudia Kamfenkel, Stefanie Mai, Tobias Heinrich, and Vu Tung Le (all Bayer AG) for their contributions to data included in this review. Cancer Communications and Consultancy Ltd., Cheshire, United Kingdom, provided medical writing assistance (funded by Bayer). Dr. Lila Adnane (Bayer) provided editorial assistance.

## Conflict of interest

JK, CAS, AMW, SH, AS, AC, VW, HH, VJ, and UBH were employed by Bayer.

## Publisher's note

All claims expressed in this article are solely those of the authors and do not necessarily represent those of their affiliated organizations, or those of the publisher, the editors and the reviewers. Any product that may be evaluated in this article, or claim that may be made by its manufacturer, is not guaranteed or endorsed by the publisher.

## References

1. Parker C, Lewington V, Shore N, Kratochwil C, Levy M, Lindén O, et al. Targeted alpha therapy, an emerging class of cancer agents: a review. *JAMA Oncol.* (2018) 4:1765–72. doi: 10.1001/jamaoncol.2018.4044

2. Tafreshi N, Doligalski M, Tichacek C, Pandya D, Budzevich M, El-Haddad G, et al. Development of targeted alpha particle therapy for solid tumors. *Molecules.* (2019) 24:4314. doi: 10.3390/molecules24234314

3. Ménager J, Gorin J, Maurel C, Drujont L, Gouard S, Louvet C, et al. Combining α-radioimmunotherapy and adoptive T cell therapy to potentiate tumor destruction. *PLoS One.* (2015) 10:e0130249. doi: 10.1371/journal.pone.0130249

4. Malamas A, Gameiro S, Knudson K, Hodge J. Sublethal exposure to alpha radiation (223ra dichloride) enhances various carcinomas' sensitivity to lysis by antigen-specific cytotoxic T lymphocytes through calreticulin-mediated immunogenic modulation. *Oncotarget.* (2016) 7:86937–47. doi: 10.18632/oncotarget.13520

5. Lejeune P, Cruciani V, Berg-Larsen A, Schlicker A, Mobergslien A, Bartnitzky L, et al. Immunostimulatory effects of targeted thorium-227 conjugates as single agent and in combination with anti-Pd-L1 therapy. *J Immunother Cancer.* (2021) 9:e002387. doi: 10.1136/jitc-2021-002387

6. Patel R, Hernandez R, Carlson P, Grudzinski J, Bates A, Jagodinsky J, et al. Low-dose targeted radionuclide therapy renders immunologically cold tumors responsive to immune checkpoint blockade. *Sci Transl Med.* (2021) 13:eabb3631. doi: 10.1126/scitranslmed.abb3631

7. Wickstroem K, Hagemann U, Cruciani V, Wengner A, Kristian A, Ellingsen C, et al. Synergistic effect of a mesothelin-targeted (227)Th conjugate in combination with DNA damage response inhibitors in ovarian cancer xenograft models. *J Nucl Med.* (2019) 60:1293–300. doi: 10.2967/jnumed.118.223701

8. van der Doelen M, Isaacsson Velho P, Slootbeek P, Pamidimarri Naga S, Bormann M, van Helvert S, et al. Impact of DNA damage repair defects on response to radium-223 and overall survival in metastatic castration-resistant prostate cancer. *Eur J Cancer.* (2020) 136:16–24. doi: 10.1016/j.ejca.2020.05.001

9. Wickstroem K, Karlsson J, Ellingsen C, Cruciani V, Kristian A, Hagemann U, et al. Synergistic effect of a HER2 targeted thorium-227 conjugate in combination with olaparib in a BRCA2 deficient xenograft model. *Pharmaceuticals.* (2019) 12:155. doi: 10.3390/ph12040155

10. Kokov K, Egorova B, German M, Klabukov I, Krasheninnikov M, Larkin-Kondrov A, et al. $^{212}$Pb: production approaches and targeted therapy applications. *Pharmaceutics.* (2022) 14:189. doi: 10.3390/pharmaceutics14010189

11. EMC. *Xofigo Summary of Product Characteristics*. (n.d.). Available online at: https://www.medicines.org.uk/emc/product/5204/smpc (Accessed September 20, 2022).

12. Xofigo. *Xofigo Prescribing Information*. (n.d.). Available online at: https://www.Xofigo-us.com/sites/G/files/vrxlpx3306/Files/2020-09/Xofigo_Pi.Pdf (Accessed September 20, 2022).

13. Ramdahl T, Bonge-Hansen H, Ryan O, Larsen S, Herstad G, Sandberg M, et al. An efficient chelator for complexation of thorium-227. *Bioorg Med Chem Lett.* (2016) 26:4318–21. doi: 10.1016/j.bmcl.2016.07.034

14. Hagemann U, Wickstroem K, Hammer S, Bjerke R, Zitzmann-Kolbe S, Ryan O, et al. Advances in precision oncology: targeted thorium-227 conjugates as a new modality in targeted alpha therapy. *Cancer Biother Radiopharm.* (2020) 35:497–510. doi: 10.1089/cbr.2020.3568

15. Suominen M, Wilson T, Käkönen S, Scholz A. The mode-of-action of targeted alpha therapy radium-223 as an enabler for novel combinations to treat patients with bone metastasis. *Int J Mol Sci.* (2019) 20:3899. doi: 10.3390/ijms20163899

16. Suominen M, Fagerlund K, Rissanen J, Konkol Y, Morko J, Peng Z, et al. Radium-223 inhibits osseous prostate cancer growth by dual targeting of cancer cells and bone microenvironment in mouse models. *Clin Cancer Res.* (2017) 23:4335–46. doi: 10.1158/1078-0432.CCR-16-2955

17. Grevys A, Frick R, Mester S, Flem-Karlsen K, Nilsen J, Foss S, et al. Antibody variable sequences have a pronounced effect on cellular transport and plasma half-life. *iScience.* (2022) 25:103746. doi: 10.1016/j.isci.2022.103746

18. Castelli M, McGonigle P, Hornby P. The pharmacology and therapeutic applications of monoclonal antibodies. *Pharmacol Res Perspect.* (2019) 7:e00535. doi: 10.1002/prp2.535

19. Ovacik M, Lin K. Tutorial on monoclonal antibody pharmacokinetics and its considerations in early development. *Clin Transl Sci.* (2018) 11:540–52. doi: 10.1111/cts.12567

20. Parker C, Coleman R, Sartor O, Vogelzang N, Bottomley D, Heinrich D, et al. Three-year safety of radium-223 dichloride in patients with castration-resistant prostate cancer and symptomatic bone metastases from phase 3 randomized alpharadin in symptomatic prostate cancer trial. *Eur Urol.* (2018) 73:427–35. doi: 10.1016/j.eururo.2017.06.021

21. Carrasquillo J, O'Donoghue J, Pandit-Taskar N, Humm J, Rathkopf D, Slovin S, et al. Phase I pharmacokinetic and biodistribution study with escalating doses of $^{223}$Ra-dichloride in men with castration-resistant metastatic prostate cancer. *Eur J Nucl Med Mol Imaging.* (2013) 40:1384–93. doi: 10.1007/s00259-013-2427-6

22. Hagemann U, Wickstroem K, Wang E, Shea A, Sponheim K, Karlsson J, et al. In vitro and in vivo efficacy of a novel CD33-targeted thorium-227 conjugate for the treatment of acute myeloid leukemia. *Mol Cancer Ther.* (2016) 15:2422–31. doi: 10.1158/1535-7163.MCT-16-0251

23. Linden O, Bates A, Cunningham D, Hindorf C, Larsson E, Cleton A, et al. $^{227}$Th-labeled anti-CD22 antibody (BAY 1862864) in relapsed/refractory CD22-positive non-hodgkin lymphoma: a first-in-human, phase I study. *Cancer Biother Radiopharm.* (2021) 36:672–81. doi: 10.1089/cbr.2020.4653

24. Starzer A, Berghoff A. New emerging targets in cancer immunotherapy: CD27 (TNFRSF7). *ESMO Open.* (2020) 4(Suppl. 3):e000629. doi: 10.1136/esmoopen-2019-000629

25. Hagemann U, Mihaylova D, Uran S, Borrebaek J, Grant D, Bjerke R, et al. Targeted alpha therapy using a novel CD70 targeted thorium-227 conjugate in in vitro and in vivo models of renal cell carcinoma. *Oncotarget.* (2017) 8:56311–26. doi: 10.18632/oncotarget.16910

26. Lens S, Drillenburg P, den Drijver B, van Schijndel G, Pals S, van Lier R, et al. Aberrant expression and reverse signalling of CD70 on malignant B cells. *Br J Haematol.* (1999) 106:491–503. doi: 10.1046/j.1365-2141.1999.01573.x

27. Diegmann J, Junker K, Gerstmayer B, Bosio A, Hindermann W, Rosenhahn J, et al. Identification of CD70 as a diagnostic biomarker for clear cell renal cell carcinoma by gene expression profiling, real-time RT-PCR and immunohistochemistry. *Eur J Cancer.* (2005) 41:1794–801. doi: 10.1016/j.ejca.2005.05.005

28. Wischhusen J, Jung G, Radovanovic I, Beier C, Steinbach J, Rimner A, et al. Identification of CD70-mediated apoptosis of immune effector cells as a novel immune escape pathway of human glioblastoma. *Cancer Res.* (2002) 62:2592–9.

29. Flieswasser T, Van den Eynde A, Van Audenaerde J, De Waele J, Lardon F, Riether C, et al. The CD70-CD27 axis in oncology: the new kids on the block. *J Exp Clin Cancer Res.* (2022) 41:12. doi: 10.1186/s13046-021-02215-y

30. Slamon D, Leyland-Jones B, Shak S, Fuchs H, Paton V, Bajamonde A, et al. Use of chemotherapy plus a monoclonal antibody against HER2 for metastatic breast cancer that overexpresses HER2. *N Engl J Med.* (2001) 344:783–92. doi: 10.1056/NEJM200103153441101

31. Pohlmann P, Mayer I, Mernaugh R. Resistance to trastuzumab in breast cancer. *Clin Cancer Res.* (2009) 15:7479–91. doi: 10.1158/1078-0432.Ccr-09-0636

32. Hunter F, Barker H, Lipert B, Rothé F, Gebhart G, Piccart-Gebhart M, et al. Mechanisms of resistance to trastuzumab emtansine (T-DM1) in HER2-positive breast cancer. *Br J Cancer.* (2020) 122:603–12. doi: 10.1038/s41416-019-0635-y

33. Abbas N, Heyerdahl H, Bruland O, Borrebæk J, Nesland J, Dahle J. Experimental α-Particle radioimmunotherapy of breast cancer using 227Th-labeled p-benzyl-DOTA-trastuzumab. *EJNMMI Res.* (2011) 1:18. doi: 10.1186/2191-219x-1-18

34. Abbas N, Heyerdahl H, Bruland ØS, Brevik E, Dahle J. Comparing high LET 227Th- and low LET 177Lu-trastuzumab in mice with HER-2 positive SKBR-3 xenografts. *Curr Radiopharm.* (2013) 6:78–86. doi: 10.2174/18744710113069990017

35. Heyerdahl H, Krogh C, Borrebæk J, Larsen Å, Dahle J. Treatment of HER2-expressing breast cancer and ovarian cancer cells with alpha particle-emitting 227Th-trastuzumab. *Int J Radiat Oncol Biol Phys.* (2011) 79:563–70. doi: 10.1016/j.ijrobp.2010.08.038

36. Lai H, Han J, Fu X, Ren Y, Li Z, You F. Targeted approaches to HER2-low breast cancer: current practice and future directions. *Cancers.* (2022) 14:3774. doi: 10.3390/cancers14153774

37. Modi S, Jacot W, Yamashita T, Sohn J, Vidal M, Tokunaga E, et al. Trastuzumab deruxtecan in previously treated HER2-low advanced breast cancer. *N Engl J Med.* (2022) 387:9–20. doi: 10.1056/NEJMoa2203690

38. Clinicaltrials.Gov. *A first in human study of BAY2701439 to look at safety, how the body absorbs, distributes and excretes the drug, and how well the drug works in participants with advanced cancer expressing the HER2 Protein. ClinicalTrials.gov identifier NCT04147819*. (2019). Available online at: https://clinicaltrials.gov/ct2/show/NCT04147819 (Accessed September 2, 2022).

39. Lei J, Lee M, Miao K, Huang Z, Yao Z, Zhang A, et al. Activation of FGFR2 signaling suppresses BRCA1 and drives triple-negative mammary tumorigenesis that is sensitive to immunotherapy. *Adv Sci.* (2021) 8:e2100974. doi: 10.1002/advs.202100974

40. Du J, Zhao Q, Liu K, Li Z, Fu F, Zhang K, et al. FGFR2/STAT3 signaling pathway involves in the development of MMTV-related spontaneous breast cancer in TA2 mice. *Front Oncol.* (2020) 10:652. doi: 10.3389/fonc.2020.00652

41. Turner N, Lambros M, Horlings H, Pearson A, Sharpe R, Natrajan R, et al. Integrative molecular profiling of triple negative breast cancers identifies amplicon drivers and potential therapeutic targets. *Oncogene.* (2010) 29:2013–23. doi: 10.1038/onc.2009.489

42. Fernández-Nogueira P, Mancino M, Fuster G, López-Plana A, Jauregui P, Almendro V, et al. Tumor-associated fibroblasts promote HER2-targeted therapy

resistance through FGFR2 activation. *Clin Cancer Res.* (2020) 26:1432–48. doi: 10.1158/1078-0432.Ccr-19-0353

43. Wickstroem K, Hagemann U, Kristian A, Ellingsen C, Sommer A, Ellinger-Ziegelbauer H, et al. Preclinical combination studies of an FGFR2 targeted thorium-227 conjugate and the ATR inhibitor BAY 1895344. *Int J Radiat Oncol Biol Phys.* (2019) 105:410–22. doi: 10.1016/j.ijrobp.2019.06.2508

44. Fong C, Chau I. HER2 inhibition in gastric cancer-novel therapeutic approaches for an established target. *Cancers.* (2022) 14:3824. doi: 10.3390/cancers14153824

45. Van Cutsem E, Bang Y, Feng-Yi F, Xu J, Lee K, Jiao S, et al. HER2 screening data from ToGA: targeting HER2 in gastric and gastroesophageal junction cancer. *Gastric Cancer.* (2015) 18:476–84. doi: 10.1007/s10120-014-0402-y

46. Karlsson J, Hagemann U, Schatz C, Grant D, Kristian A, Ellingsen C, et al. Abstract 5859: HER2-targeted thorium-227 conjugate (HER2-TTC): efficacy in preclinical models of trastuzumab and T-DM1 resistance. *Cancer Res.* (2017) 77(Suppl. 13):5859. doi: 10.1158/1538-7445.AM2017-5859

47. Carter J, Cottrell C, McNulty S, Vigh-Conrad K, Lamp S, Heusel J, et al. FGFR2 amplification in colorectal adenocarcinoma. *Cold Spring Harb Mol Case Stud.* (2017) 3:a001495. doi: 10.1101/mcs.a001495

48. Hagemann U, Sommer A, Kristian A, Wang E, Larsen Å, Wirnitzer U, et al. Abstract 5199: preclinical activity of the FGFR2-targeted thorium-227 conjugate in preclinical models of colorectal, gastric and triple-negative breast cancer. *Cancer Res.* (2017) 77(Suppl. 13):5199. doi: 10.1158/1538-7445.AM2017-5199

49. Helsten T, Elkin S, Arthur E, Tomson B, Carter J, Kurzrock R. The FGFR landscape in cancer: analysis of 4,853 tumors by next-generation sequencing. *Clin Cancer Res.* (2016) 22:259–67. doi: 10.1158/1078-0432.CCR-14-3212

50. Yasui H, Takeno A, Hara H, Imamura H, Akamatsu H, Fujitani K, et al. Prospective analysis of the expression status of FGFR2 and HER2 in colorectal and gastric cancer populations: DS-screen study. *Int J Colorectal Dis.* (2022) 37:1393–402. doi: 10.1007/s00384-022-04162-2

51. Jain S, Wallen J. *Malignant mesothelioma*. Treasure Island, FL: Statpearls publishing (2022).

52. Servais E, Colovos C, Rodriguez L, Bograd A, Nitadori J, Sima C, et al. Mesothelin overexpression promotes mesothelioma cell invasion and MMP-9 secretion in an orthotopic mouse model and in epithelioid pleural mesothelioma patients. *Clin Cancer Res.* (2012) 18:2478–89. doi: 10.1158/1078-0432.CCR-11-2614

53. Melaiu O, Stebbing J, Lombardo Y, Bracci E, Uehara N, Bonotti A, et al. MSLN gene silencing has an anti-malignant effect on cell lines overexpressing mesothelin deriving from malignant pleural mesothelioma. *PLoS One.* (2014) 9:e85935. doi: 10.1371/journal.pone.0085935

54. Castelletti L, Yeo D, van Zandwijk N, Rasko J. Anti-mesothelin car T cell therapy for malignant mesothelioma. *Biomark Res.* (2021) 9:11. doi: 10.1186/s40364-021-00264-1

55. Lv J, Li P. Mesothelin as a biomarker for targeted therapy. *Biomark Res.* (2019) 7:18. doi: 10.1186/s40364-019-0169-8

56. Hagemann U, Ellingsen C, Schuhmacher J, Kristian A, Mobergslien A, Cruciani V, et al. Mesothelin-targeted thorium-227 conjugate (MSLN-TTC): preclinical evaluation of a new targeted alpha therapy for mesothelin-positive cancers. *Clin Cancer Res.* (2019) 25:4723–34. doi: 10.1158/1078-0432.CCR-18-347656

57. Clinicaltrials.Gov. *First-in-human study of BAY2287411 injection, a thorium-227 labeled antibody-chelator conjugate, in patients with tumors known to express mesothelin. ClinicalTrials.gov identifier: NCT03507452.* (2018). Available online at: https://clinicaltrials.gov/ct2/show/NCT03507452 (Accessed September 2, 2022).

58. Heyerdahl H, Abbas N, Sponheim K, Mollatt C, Bruland Ø, Dahle J. Targeted alpha therapy with 227Th-trastuzumab of intraperitoneal ovarian cancer in nude mice. *Curr Radiopharm.* (2013) 6:106–16. doi: 10.2174/18744710113069990018

59. Abbas N, Bruland ØS, Brevik E, Dahle J. Preclinical evaluation of $^{227}$Th-labeled and $^{177}$Lu-labeled trastuzumab in mice with HER-2-positive ovarian cancer xenografts. *Nucl Med Commun.* (2012) 33:838–47. doi: 10.1097/MNM.0b013e328354df7c

60. Heyerdahl H, Abbas N, Brevik E, Mollatt C, Dahle J. Fractionated therapy of HER2-expressing breast and ovarian cancer xenografts in mice with targeted alpha emitting $^{227}$Th-DOTA-p-benzyl-trastuzumab. *PLoS One.* (2012) 7:e42345. doi: 10.1371/journal.pone.0042345

61. Hammer S, Hagemann U, Zitzmann-Kolbe S, Larsen A, Ellingsen C, Geraudie S, et al. Preclinical efficacy of a PSMA-targeted thorium-227 conjugate (PSMA-TTC), a targeted alpha therapy for prostate cancer. *Clin Cancer Res.* (2020) 26:1985–96. doi: 10.1158/1078-0432.Ccr-19-2268

62. Clinicaltrials.Gov. *Study to evaluate the safety, tolerability, pharmacokinetics, and antitumor activity of a thorium-227 labeled antibody-chelator conjugate alone and in combination with darolutamide, in patients with metastatic castration resistant prostate cancer. ClinicalTrials.gov identifier: NCT03724747.* (2018). Available online at: https://clinicaltrials.gov/ct2/show/NCT03724747 (Accessed September 2, 2022).

63. Stok C, Kok Y, van den Tempel N, van Vugt M. Shaping the BRCAness mutational landscape by alternative double-strand break repair, replication stress and mitotic aberrancies. *Nucleic Acids Res.* (2021) 49:4239–57. doi: 10.1093/nar/gkab151

64. Morales J, Li L, Fattah F, Dong Y, Bey E, Patel M, et al. Review of poly (ADP-ribose) polymerase (PARP) mechanisms of action and rationale for targeting in cancer and other diseases. *Crit Rev Eukaryot Gene Expr.* (2014) 24:15–28. doi: 10.1615/critreveukaryotgeneexpr.2013006875

65. Rottenberg S, Jaspers J, Kersbergen A, van der Burg E, Nygren A, Zander S, et al. High sensitivity of BRCA1-deficient mammary tumors to the PARP inhibitor AZD2281 alone and in combination with platinum drugs. *Proc Natl Acad Sci USA.* (2008) 105:17079–84. doi: 10.1073/pnas.0806092105

66. Bryant H, Schultz N, Thomas H, Parker K, Flower D, Lopez E, et al. Specific killing of BRCA2-deficient tumours with inhibitors of poly(ADP-ribose) polymerase. *Nature.* (2005) 434:913–7. doi: 10.1038/nature03443

67. Schatz C, Hammer S, Wengner A, Hagemann U, Mumberg D, Scholz A. Abstract 1393: PSMA-targeted thorium conjugate (BAY 2315497) and olaparib combination show synergistic anti-tumor activity in prostate cancer models. *Cancer Res.* (2021) 81(Suppl. 13):1393. doi: 10.1158/1538-7445.Am2021-1393

68. Chen S, Lees-Miller J, He Y, Lees-Miller S. Structural insights into the role of DNA-PK as a master regulator in NHEJ. *Genome Instab Dis.* (2021) 2:195–210. doi: 10.1007/s42764-021-00047-w

69. Berger M, Wortmann L, Buchgraber P, Lucking U, Zitzmann-Kolbe S, Wengner A, et al. BAY-8400: a novel potent and selective DNA-PK inhibitor which shows synergistic efficacy in combination with targeted alpha therapies. *J Med Chem.* (2021) 64:12723–37. doi: 10.1021/acs.jmedchem.1c00762

70. Wengner A, Siemeister G, Lücking U, Lefranc J, Wortmann L, Lienau P, et al. The novel ATR inhibitor BAY 1895344 is efficacious as monotherapy and combined with DNA damage-inducing or repair-compromising therapies in preclinical cancer models. *Mol Cancer Ther.* (2020) 19:26–38. doi: 10.1158/1535-7163.Mct-19-0019

71. Yap T, Tan D, Terbuch A, Caldwell R, Guo C, Goh B, et al. First-in-human trial of the oral ataxia telangiectasia and RAD3-Related (ATR) inhibitor BAY 1895344 in patients with advanced solid tumors. *Cancer Discov.* (2021) 11:80–91. doi: 10.1158/2159-8290.Cd-20-0868

72. Marechal A, Zou L. DNA damage sensing by the ATM and ATR kinases. *Cold Spring Harb Perspect Biol.* (2013) 5:a012716. doi: 10.1101/cshperspect.a012716

73. Gameiro S, Jammeh M, Wattenberg M, Tsang K, Ferrone S, Hodge J. Radiation-induced immunogenic modulation of tumor enhances antigen processing and calreticulin exposure, resulting in enhanced T-cell killing. *Oncotarget.* (2014) 5:403–16. doi: 10.18632/oncotarget.1719

74. Vanpouille-Box C, Alard A, Aryankalayil M, Sarfraz Y, Diamond J, Schneider R, et al. DNA exonuclease Trex1 regulates radiotherapy-induced tumour immunogenicity. *Nat Commun.* (2017) 8:15618. doi: 10.1038/ncomms15618

75. Ko E, Formenti S. Radiation therapy to enhance tumor immunotherapy: a novel application for an established modality. *Int J Radiat Biol.* (2019) 95:936–9. doi: 10.1080/09553002.2019.1623429

76. Gorin J, Ménager J, Gouard S, Maurel C, Guilloux Y, Faivre-Chauvet A, et al. Antitumor immunity induced after α irradiation. *Neoplasia.* (2014) 16:319–28. doi: 10.1016/j.neo.2014.04.002

77. Simon I, Perales S, Casado-Medina L, Rodríguez-Martínez A, Garrido-Navas M, Puche-Sanz I, et al. Cross-resistance to abiraterone and enzalutamide in castration resistance prostate cancer cellular models is mediated by AR transcriptional reactivation. *Cancers.* (2021) 13:1483. doi: 10.3390/cancers13061483

78. European Medicines Agency. *Nubeqa Summary of Product Characteristics.* (n.d.). Available online at: https://www.ema.europa.eu/en/medicines/human/epar/nubeqa (Accessed October 3, 2022).

79. Food and Drug Administration. *Nubeqa Prescribing Information.* (n.d.). Available online at: https://www.accessdata.fda.gov/drugsatfda_docs/label/2022/212099s002lbl.Pdf (Accessed October 3, 2022).

80. Hammer S, Schlicker A, Zitzmann-Kolbe S, Baumgart S, Hagemann U, Scholz A, et al. Darolutamide potentiates the antitumor efficacy of a PSMA-targeted thorium-227 conjugate by a dual mode of action in prostate cancer models. *Clin Cancer Res.* (2021) 27:4367–78. doi: 10.1158/1078-0432.Ccr-21-0342

81. Schatz C, Zitzmann-Kolbe S, Haendler B, Hennekes H, Hammer S, Scholz A editors. Abstract 3311: darolutamide potentiates the antitumor efficacy of a PSMA-targeted thorium-227 conjugate (PSMA-TTC) in a hormone-independent prostate cancer model. *Cancer Res.* (2022) 82:3311. doi: 10.1158/1538-7445.AM2022-3311

82. Eychenne R, Cherel M, Haddad F, Guerard F, Gestin J. Overview of the most promising radionuclides for targeted alpha therapy: the "hopeful eight". *Pharmaceutics.* (2021) 13:906. doi: 10.3390/pharmaceutics13060906

83. Sathekge M, Bruchertseifer F, Knoesen O, Reyneke F, Lawal I, Lengana T, et al. $^{225}$Ac-PSMA-617 in chemotherapy-naive patients with advanced prostate cancer: a pilot study. *Eur J Nucl Med Mol Imaging.* (2019) 46:129–38. doi: 10.1007/s00259-018-4167-0

84. Sathekge M, Bruchertseifer F, Vorster M, Lawal I, Knoesen O, Mahapane J, et al. Predictors of overall and disease-free survival in metastatic castration-resistant prostate cancer patients receiving $^{225}$Ac-PSMA-617 radioligand therapy. *J Nucl Med.* (2020) 61:62–9. doi: 10.2967/jnumed.119.229229

85. Sathekge M, Bruchertseifer F, Vorster M, Lawal I, Knoesen O, Mahapane J, et al. mCRPC patients receiving $^{225}$Ac-PSMA-617 therapy in post androgen deprivation therapy setting: response to treatment and survival analysis. *J Nucl Med.* (2022) 63:1496–502. doi: 10.2967/jnumed.121.263618

86. Juneau D, Saad F, Berlin A, Metser U, Puzanov I, Lamonica D, et al. Preliminary dosimetry results from a first-in-human phase I study evaluating the efficacy and safety of [$^{225}$Ac]-FPI-1434 in patients with IGF-1R expressing solid tumors. *J Nucl Med.* (2021) 62(Suppl. 1):74.

87. Atallah E, Berger M, Jurcic J, Roboz G, Tse W, Mawad R, et al. A phase 2 study of actinium-225 ($^{225}$Ac)-lintuzumab in older patients with untreated acute myeloid leukemia (AML). *J Med Imaging Radiat Sci.* (2019) 50(Suppl. 1):S37.

88. Abedin S, Murthy G, Hamadani M, Michaelis L, Runaas L, Carlson K, et al. Lintuzumab-Ac225 in combination with CLAG-M yields high MRD (-) responses in R/R AML with adverse features: interim results of a phase I study. *Blood.* (2021) 138(Suppl. 1):3414. doi: 10.1182/blood-2021-148746

89. Rosenblat T, McDevitt M, Carrasquillo J, Pandit-Taskar N, Frattini M, Maslak P, et al. Treatment of patients with acute myeloid leukemia with the targeted alpha-particle nanogenerator actinium-225-lintuzumab. *Clin Cancer Res.* (2022) 28:2030–7. doi: 10.1158/1078-0432.CCR-21-3712

90. Morgenstern A, Apostolidis C, Kratochwil C, Sathekge M, Krolicki L, Bruchertseifer F. An overview of targeted alpha therapy with $^{225}$Actinium and $^{213}$Bismuth. *Curr Radiopharm.* (2018) 11:200–8. doi: 10.2174/1874471011666180502104524

91. Sartor O, de Bono J, Chi K, Fizazi K, Herrmann K, Rahbar K, et al. Lutetium-177–PSMA-617 for metastatic castration-resistant prostate cancer. *N Engl J Med.* (2021) 385:1091–103. doi: 10.1056/NEJMoa2107322

92. Hofman M, Emmett L, Violet J, Y Zhang A, Lawrence N, Stockler M, et al. Therap: a randomized phase 2 trial of $^{177}$Lu-PSMA-617 theranostic treatment vs cabazitaxel in progressive metastatic castration-resistant prostate cancer (clinical trial protocol ANZUP 1603). *BJU Int.* (2019) 124:5–13. doi: 10.1111/bju.14876

93. Kratochwil C, Fendler W, Eiber M, Baum R, Bozkurt M, Czernin J, et al. EANM procedure guidelines for radionuclide therapy with $^{177}$Lu-labelled PSMA-ligands ($^{177}$Lu-PSMA-RLT). *Eur J Nucl Med Mol Imaging.* (2019) 46:2536–44. doi: 10.1007/s00259-019-04485-3

94. Ballal S, Yadav M, Sahoo R, Tripathi M, Dwivedi S, Bal C. $^{225}$ Ac-PSMA-617-targeted alpha therapy for the treatment of metastatic castration-resistant prostate cancer: a systematic review and meta-analysis. *Prostate.* (2021) 81:580–91. doi: 10.1002/pros.24137

95. Sen I, Thakral P, Tiwari P, Pant V, Das S, Manda D, et al. Therapeutic efficacy of $^{225}$Ac-PSMA-617 targeted alpha therapy in patients of metastatic castrate resistant prostate cancer after taxane-based chemotherapy. *Ann Nucl Med.* (2021) 35:794–810. doi: 10.1007/s12149-021-01617-4

96. Tagawa S, Osborne J, Fernandez E, Thomas C, Niaz M, Ciriaco A, et al. Phase I dose-escalation study of PSMA-targeted alpha emitter $^{225}$Ac-J591 in men with metastatic castration-resistant prostate cancer (mCRPC). *J Clin Oncol.* (2020) 38:5560. doi: 10.1200/JCO.2020.38

97. Feuerecker B, Tauber R, Knorr K, Heck M, Beheshti A, Seidl C, et al. Activity and adverse events of actinium-225-PSMA-617 in advanced metastatic castration-resistant prostate cancer after failure of lutetium-177-PSMA. *Eur Urol.* (2021) 79:343–50. doi: 10.1016/j.eururo.2020.11.013

frontiers | Frontiers in Medicine

TYPE Hypothesis and Theory
PUBLISHED 17 January 2023
DOI 10.3389/fmed.2022.1051825



OPEN ACCESS

EDITED BY
Dawei Jiang,
Huazhong University of Science and Technology, China

REVIEWED BY
Tom A. Bäck,
University of Gothenburg, Sweden
Reinier Hernandez,
University of Wisconsin-Madison, United States
Hanyi Fang,
Huazhong University of Science and Technology, China

*CORRESPONDENCE
Asta Juzeniene
✉ astaj@rr-research.no

SPECIALTY SECTION
This article was submitted to Nuclear Medicine, a section of the journal Frontiers in Medicine

RECEIVED 23 September 2022
ACCEPTED 05 December 2022
PUBLISHED 17 January 2023

CITATION
Juzeniene A, Stenberg VY, Bruland ØS, Revheim M-E and Larsen RH (2023) Dual targeting with $^{224}$Ra/$^{212}$Pb-conjugates for targeted alpha therapy of disseminated cancers: A conceptual approach. *Front. Med.* 9:1051825. doi: 10.3389/fmed.2022.1051825



# Dual targeting with $^{224}$Ra/$^{212}$Pb-conjugates for targeted alpha therapy of disseminated cancers: A conceptual approach

Asta Juzeniene[1,2]*, Vilde Yuli Stenberg[1,3,4], Øyvind Sverre Bruland[3,5], Mona-Elisabeth Revheim[3,6] and Roy Hartvig Larsen[4]

[1]Department of Radiation Biology, Institute for Cancer Research, The Norwegian Radium Hospital, Oslo University Hospital, Oslo, Norway, [2]Department of Physics, University of Oslo, Oslo, Norway, [3]Institute for Clinical Medicine, University of Oslo, Oslo, Norway, [4]ARTBIO AS, Oslo, Norway, [5]Department of Oncology, The Norwegian Radium Hospital, Oslo University Hospital, Oslo, Norway, [6]Division of Radiology and Nuclear Medicine, Oslo University Hospital, Oslo, Norway

Metastases are the primary cause of death among cancer patients and efficacious new treatments are sorely needed. Targeted alpha-emitting radiopharmaceuticals that are highly cytotoxic may fulfill this critical need. The focus of this paper is to describe and explore a novel technology that may improve the therapeutic effect of targeted alpha therapy by combining two radionuclides from the same decay chain in the same solution. We hypothesize that the dual targeting solution containing bone-seeking $^{224}$Ra and cell-directed complexes of progeny $^{212}$Pb is a promising approach to treat metastatic cancers with bone and soft tissue lesions as well as skeletal metastases of mixed lytic/osteoblastic nature. A novel liquid $^{224}$Ra/$^{212}$Pb-generator for rapid preparation of a dual targeting solution is described. Cancer cell targeting monoclonal antibodies, their fragments, synthetic proteins or peptides can all be radiolabeled with $^{212}$Pb in the $^{224}$Ra-solution in transient equilibrium with daughter nuclides. Thus, $^{224}$Ra targets stromal elements in sclerotic bone metastases and $^{212}$Pb-chelated-conjugate targets tumor cells of metastatic prostate cancer or osteosarcoma. The dual targeting solution may also be explored to treat metastatic breast cancer or multiple myeloma after manipulation of bone metastases to a more osteoblastic phenotype by the use of bisphosphonates, denosumab, bortezomib or hormone therapy prior to treatment. This may improve targeting of bone-seeking $^{224}$Ra and render an augmented radiation dose deposited within metastases. Our preliminary preclinical studies provide conceptual evidence that the dual $^{224}$Ra-solution with bone or tumor-targeted delivery of $^{212}$Pb has potential to inhibit cancer metastases without significant toxicity. In some

settings, the use of a booster dose of purified $^{212}$Pb-conjugate alone could be required to elevate the effect of this tumor cell directed component, if needed, e.g., in a fractionated treatment regimen, where the dual targeting solution will act as maintenance treatment.

KEYWORDS

cancer, lead-212, radiopharmaceutical, radium-224, radium-223, targeted radionuclide therapy (TRT), targeted alpha particle therapy (TAT)

## Introduction

Wide-spread (skeletal, lymph and/or visceral) metastases are responsible for ∼70% of cancer mortality worldwide (1, 2). Understanding and developing targeted therapies for metastatic cancers remain a large unmet medical need. Therapeutic nuclear medicine is emerging rapidly as an additional treatment modality in oncology (3–5). Recently approved beta-emitting $^{177}$Lu-DOTATATE (Lutathera®, 2018) targeting somatostatin-2 receptors in patients with metastatic neuroendocrine tumors and $^{177}$Lu-PSMA-617 (Pluvicto®, 2022) targeting prostate-specific membrane antigen (PSMA) in patients with metastatic castration-resistant prostate cancer (mCRPC) will clearly shift targeted radionuclide therapy (TRT) into the mainstream of cancer treatment. Nevertheless, some patients either do not respond or following initially good response develop resistance to $^{177}$Lu-based therapies, despite sufficient expression of target proteins (6, 7). These patients may, however, respond to targeted alpha therapy (TAT) with $^{225}$Ac (6, 7). Both preclinical and clinical studies have clearly demonstrated that alpha-emitting radiopharmaceuticals are more efficient in tumor cell killing and less damaging to the surrounding normal tissue than beta-emitting radiopharmaceuticals (5, 8–11). Alpha particles deliver a high amount of ionization over a short range (< 100 μm in water/tissue, < 40 μm in bone), inducing more complex double-strand DNA breaks that are harder to repair than single-strand breaks induced by beta particles (10, 11). Alpha-emitting radionuclides are particularly suited for the elimination of single cells and cancer micrometastases (10). TRT with beta- or alpha- emitting radionuclides improve the quality of life and delay disease progression (12, 13), but they are most likely not curative. Further improvements are warranted to enhance the therapeutic benefit. Combining TRT with potentially synergistic agents (chemotherapy, immune checkpoint inhibitors, PARP inhibitors, etc.) or with other radiopharmaceuticals is being evaluated in ongoing clinical trials (14–17). The focus of this paper is to describe and explore a novel technology platform that may improve the therapeutic effect of TRT by combining two radionuclides from the same decay chain; one TAT component targeting the stromal elements of osteoblastic skeletal metastases and the other by selective cell-surface binding to cancer cells in extraskeletal and skeletal metastases.

## Dual targeting strategies: Alpha and beta radiopharmaceuticals

It has been demonstrated that tandem therapy with beta-emitting $^{177}$Lu-PSMA-617 and alpha-emitting $^{225}$Ac-PSMA-617 is an effective treatment approach for mCRPC patients (18–20). In addition, the combination of $^{177}$Lu-PSMA-I&T and $^{225}$Ac-J591 for progressive mCRPC (33 patients) is being evaluated in an ongoing phase I/II clinical study in the United States (ClinicalTrials.gov Identifier: NCT04886986). It has been hypothesized that additive radiation to PSMA-positive cells should occur when administering the radiopharmaceuticals concurrently since the monoclonal antibody (mAb) J591 and the small molecule ligand PSMA-I&T have different PSMA binding sites (21). Additionally, the team hypothesized that $^{225}$Ac-J591 could deliver antitumor activity without xerostomia (21, 22), that is the most common side effect of PSMA-TAT with small molecule ligands (13). However, at the present time, the insufficient availability and radiopharmaceutical aspects of $^{225}$Ac limit the wide clinical applications of $^{225}$Ac (23–25).

The first, and so far, only approved alpha-emitting radiopharmaceutical $^{223}RaCl_2$ (Xofigo®, 2013) is used to treat mCRPC that has spread only to the bone (3, 26). Ra-223 binds to osteoblastic stromal elements of bone metastases during mineralization since $^{223}$Ra is a calcium mimetic that binds to hydroxyapatite in the bone matrix in areas of high bone turnover. Such osteoblastic bone metastases are predominant in patients with mCRPC (27–29). The spatial distribution of the hydroxyapatite within an osteoblastic tumor facilitates a volume distribution of $^{223}$Ra (30). Due to the bone-seeking characteristics of $^{223}$Ra, its clinical use is limited to patients with osteoblastic bone (sclerotic, new bone deposition, or formation) metastases (31). Biologically stable complex between a bifunctional chelator with $^{223}$Ra and a tumor-targeting vector (small molecule, peptide, mAb, or its fragment) is essential to treat extraskeletal metastases (lymph nodes and visceral).

Unfortunately, $^{223}$Ra, like other alkaline earth metals, does not form stable complexes *in vivo* (32–34). A phase I/II study, the AlphaBet trial, evaluating the combination of $^{177}$Lu-PSMA-I&T and $^{223}$Ra to target PSMA-expressing cancer cells and bone metastasis in 36 mCRPC patients has recently been started in Australia (NCT05383079).

## Dual targeting strategy: A cancer cell-surface seeker targeted $^{227}$Th and stromal bone-seeker $^{223}$Ra

Another radionuclide that attracts interest is $^{227}$Th that can be linked to a variety of mAbs. These $^{227}$Th-immunoconjugates have shown promising preclinical results (30, 35, 36). Furthermore, $^{227}$Th acts as an *in vivo* generator of bone-seeking $^{223}$Ra (**Figure 1**) that can be additionally exploited to improve therapeutic effects in sclerotic bone metastases (30, 37). Dual bone-targeting strategy by bone-targeted $^{227}$Th and $^{223}$Ra was introduced in 2004 (38, 39). Radium-223 produced from $^{227}$Th decay is a cation that can easily penetrate into sclerotic metastasis. Henriksen et al. suggested to use $^{227}$Th-polyphosphonate compounds, DOTMP [1,4,7,10 tetraazacyclododecane N, N′, N″, N‴ 1,4,7,10-tetra(methylene) phosphonic acid] or DTMP [diethylene triamine N, N′, N″ penta(methylene) phosphonic acid] to deliver alpha particle radiation to primary bone cancer or skeletal metastases from solid cancers (38). They proposed that the total radioactivity in bone should increase as $^{227}$Th decays and $^{223}$Ra appears, if the $^{227}$Th–labeled bone-seeker solution was free from $^{223}$Ra at the time of administration (38). Washiyama et al. studied the biodistribution of bone-seeking $^{227}$Th-EDTMP (ethylenediamine-tetramethylenephosphonic acid) and its daughter $^{223}$Ra in mice and found high uptake of $^{227}$Th-EDTMP and long retention of $^{223}$Ra in bones (39). They concluded that even if $^{223}$Ra escapes from the bone after $^{227}$Th decay, it redistributes to bone, as there are no physical or biological differences between $^{223}$Ra injected intravenously and that generated *in vivo* after $^{227}$Th injection (39). In 2008, a dual targeting approach was introduced for the treatment of soft tissue and bone metastases: $^{227}$Th-chelator-mAb targeting cancer cell surface antigens and $^{223}$Ra targeting osteoblastic stroma (30, 37). The main advantage of $^{227}$Th is high availability from beta decay of $^{227}$Ac (36). The 18.7 day half-life of $^{227}$Th is long enough for proper radiopharmaceutical preparation, transportation and administration. However, a therapeutic window allowing treatment with $^{227}$Th-conjugates with acceptable toxicity may exist due to $^{223}$Ra ingrowth. A few clinical trials evaluating $^{227}$Th-conjugates targeting CD22, mesothelin, PSMA and human epidermal growth factor 2 (HER-2) are registered at clinicaltrials.gov (NCT02581878, NCT03507452, NCT03724747, NCT04147819), but the results are not yet available.

## Dual targeting strategy: A bone-seeker $^{224}$Ra and a cancer cell-seeker targeted $^{212}$Pb in one solution

Two radionuclides from the same decay chain, $^{224}$Ra and $^{212}$Pb, with its alpha emitting daughter $^{212}$Bi (**Figure 1**), are attractive for cancer therapy due to availability and physical half-lives. These radionuclides can be produced by the end user in clinically relevant amounts from $^{228}$Th generators (40–42). The 1.9 year half-life of $^{228}$Th allows long-term use of the generator. Similarly to $^{223}$Ra, the lack of suitable chelators has limited $^{224}$Ra to bone-targeting applications. Both radium isotopes have similar chemical and decay properties, total energies, and biodistribution (41, 43–45). Importantly, $^{224}$Ra was widely used decades ago as a pain-relieving treatment of the chronic inflammatory rheumatic disease ankylosing spondylitis (46–49). Administration of total activities of 5.6–11.1 MBq $^{224}$Ra (1 MBq of $^{224}$Ra chloride solution per weekly injection) to these patients between 1945 and 1975 had neither negative impact on the survival, nor increased significantly the overall rate of second malignancies, as compared to the control population after a mean follow-up time of 24 years (46). The incidence rates of leukemias were 0.014 and 0.009 [hazard ratio 2.56 (95% confidence interval (CI) 0.89–7.54)] in in patients treated and non-treated with $^{224}$Ra, respectively (46, 48, 50). Such long-term follow up of a large non-cancer patient population seems very relevant from a radiation safety perspective. The life expectancies in patients with metastatic cancer are significantly shorter.

The daughter nuclides of $^{224}$Ra, namely $^{220}$Rn ($t_{1/2} \approx$ 56 s), $^{212}$Pb ($t_{1/2} \approx$ 10.6 h), and $^{212}$Bi ($t_{1/2} \approx$ 1 h), have longer half-lives than those of $^{223}$Ra (**Figure 1**). Lead-212 is suitable for radiolabeling of mAbs, peptides, or other targeting vectors conjugated with appropriate bifunctional chelators. Conjugates of $^{212}$Pb/$^{212}$Bi have already been tested in clinical trials for cancer treatment (51–53). Moreover, these daughter nuclides can be conjugated to chelated targeting agents in the radiopharmaceutical solution of $^{224}$Ra in equilibrium with progeny (**Figure 2**), such as EDTMP for retention of progeny in bone, or a cancer-specific ligand/mAb with a bifunctional chelator TCMC (S-2-(4-isothiocyanatobenzyl)-1,4,7,10-tetraaza-1,4,7,10-tetra(2-carbamoylmethyl)cyclododecane) for cancer cell targeting (41, 54, 55). We hypothesize that the resulting solution will have dual TAT properties: (1) Unbound bone-seeking $^{224}$Ra will target metastatic cells on the endosteal surface of bone as well as the stromal elements of osteoblastic skeletal metastases killing these cells; and (2) tumor cell-surface seeking $^{212}$Pb-TCMC-targeting agent that will kill the circulating cancer cells and micrometastases by selective binding and deposition of DNA breaking alpha radiation to the cancer cells. The aim of the dual targeting approach is to direct

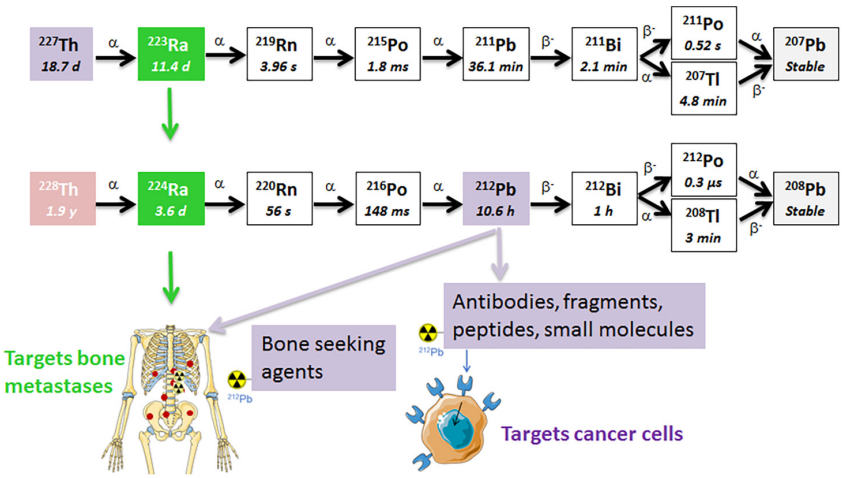


FIGURE 1
The decay chains of $^{227}$Th and $^{228}$Th. The radium isotopes are chemically similar to calcium and are natural bone-seekers, and thus, will target osteoblastic bone metastases. The progeny $^{212}$Pb in the $^{224}$Ra decay chain has a suitable half-life for chelation by a tumor-specific ligand/mAb that targets cancer cells (41, 54, 55). The short half-life of progeny $^{211}$Pb in the $^{223}$Ra decay chain is not practical for conjugation to a targeting ligand since the majority of the decay will occur before the ligand reaches the tumor sites. α, alpha particle; β, beta particle.

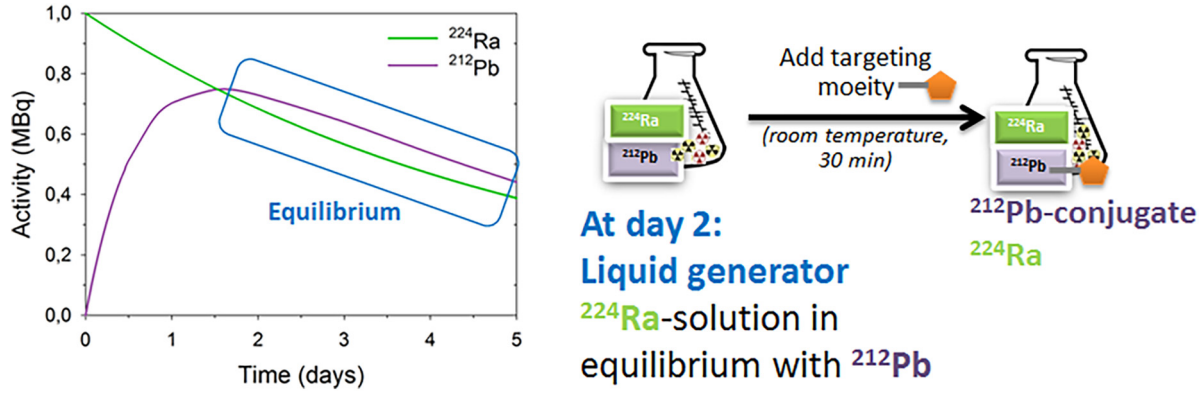


FIGURE 2
The $^{224}$Ra-liquid generator for preparation of dual alpha targeting solution. For details see references (41, 54, 55).

as much as possible of the ionizing radiation of the $^{224}$Ra decay chain to the entire spectrum of metastases.

## Dual targeting technology: The $^{224}$Ra/$^{212}$Pb liquid generator

A $^{224}$Ra-liquid generator for the preparation of dual targeting solution (Figure 2) was developed and patented by Larsen (54). Targeting moieties can be rapidly (≤ 1 h) and efficiently labeled with $^{212}$Pb in the $^{224}$Ra-solution in transient equilibrium with progenies (41, 55). Additionally, up to 80% free $^{212}$Bi can also be conjugated (41). Similar binding and uptake abilities of the $^{212}$Pb-labeled PSMA-targeting ligand NG001 in $^{224}$Ra-solution or in $^{212}$Pb-solution were observed *in vitro* and *in vivo* (41, 56, 57). Biodistribution studies of $^{224}$Ra with free $^{212}$Pb, $^{212}$Pb-NG001, and $^{212}$Pb-PSMA-617 were tested in athymic nude mice with C4-2 xenografts (41). Importantly, a high uptake of $^{224}$Ra in the femur and skull in all groups was shown, demonstrating that $^{212}$Pb can be chelated to ligands without compromising the bone-seeking properties of radium in the radiopharmaceutical solution containing the radionuclides (41).

## Diffusion of $^{224}$Ra progenies and "dose-smoothening effect"

As mentioned above, $^{224}$Ra has longer lived progenies, $^{220}$Rn and $^{212}$Pb, than the isotopes of the same elements in the

$^{223}$Ra series (Figure 1). Theoretically, these daughter nuclides, especially noble gas $^{220}$Rn, will diffuse from the target, because of differing physical half-lives and biological affinities. The first $^{220}$Rn progeny, $^{216}$Po, has a half-life of 148 ms and decays within very close vicinity to the creation site (58). The mean diffusion length of $^{216}$Po in water (soft tissue) is only around 4 μm (58). Lloyd et al. studied retention and distribution of $^{224}$Ra and its daughters in beagle dogs, and concluded that the majority of $^{220}$Rn produced in bone by $^{224}$Ra decay stays in bone (59). It has been demonstrated that $^{220}$Rn redistribution leads to toxicity to non-targeted tissues only when extremely high activities of $^{224}$Ra were given to patients or animals (47, 59–61). Napoli et al. studied the diffusion and re-adsorption of $^{224}$Ra progenies from $^{224}$Ra-labeled calcium carbonate microparticles (61). These particles were chosen since radium's calcium-mimetic properties allow the adsorption of $^{224}$Ra onto their surface. It has been demonstrated that $^{220}$Rn can escape from the particles, however, it can diffuse from $^{224}$Ra-labeled calcium carbonate microparticles only around 300–400 μm in water. It was also documented that the microparticles have the ability to re-adsorb almost all $^{212}$Pb generated in the liquid phase from escaped $^{220}$Rn (61). If we assume that these particles resemble bone or an osteoblastic bone metastasis, the obtained results may explain the low leakage of $^{212}$Pb from bone into systemic circulation, thereby reducing the risk of unwanted radiation exposure of distant tissues. The diffusion of $^{220}$Rn up to a few hundred micrometers can extend the effective range of the shorter-range alpha particles from $^{224}$Ra itself and may cause a "dose-smoothening" effect in the metastases. Ra-223 is initially shown to be deposited on bone surface and with time is incorporated into the volume of the bone (59). However, areas with "uncalcifying" stroma containing cancer cells in bone metastases (29) will most likely not be eradicated. This contribution from $^{220}$Rn may overcome one major limitation of the approved bone-seeking radiopharmaceutical Xofigo when it comes to the short range (only up to 40 μm in bone) of alpha particles in skeletal metastases.

Diffusing alpha-emitters radiation therapy (DaRT) is a novel brachytherapy employing implantable $^{224}$Ra enriched seeds for the treatment of solid tumors (58, 62, 63). The $^{224}$Ra progenies are shown to diffuse 5–7 mm from the seed and are reported as responsible for the therapeutic effect (63). The efficacy and safety of DaRT have been found to be promising in preclinical and clinical studies (62, 63). DaRT is now in clinical trials for many different cancer types (Table 1).

As mentioned above three of the four alpha particles in the decay chain of $^{224}$Ra will decay within a radius of about 400 μm from the $^{224}$Ra atom in tissues, while the $^{212}$Pb due to the long half-life can potentially diffuse up to several mm in tissues as indicated by the DART technology. If decay takes place in the skeleton, association of $^{212}$Pb to hydroxyapatite may considerably limit diffusion range.

## Dual targeting alpha therapy and cancers with bone metastases

Bone is the third most frequent site of cancer metastases and the organ-system involved in multiple myeloma (64–66). Bone metastases are especially common in prostate and breast cancer (Table 2). These metastases frequently result in skeletal-related events such as increased pain, hypercalcemia, bone fractures and spinal cord compression, which cause considerable morbidity and reduced quality of life (1, 66, 67). Bone metastases occur as osteolytic lesions, characterized by destruction of normal bone, or as osteoblastic metastases, characterized by formation of new bone matrix (Table 2). The majority of patients with advanced prostate cancer have osteoblastic bone metastases (29). However, some of these patients may have a mixed phenotype or even osteolytic lesions (29).

Dual targeting alpha therapy seems the most suitable for prostate cancer and osteosarcoma since radium localizes in osteoblastic active zones, including on skeletal surfaces and in osteoblastic metastases (77, 78). For cancers without extraskeletal metastases, $^{212}$Pb can be chelated to organic phosphates, e.g., EDTMP, which are incorporated into the bone matrix (79), whereas for cancers with extraskeletal metastases, $^{212}$Pb can be chelated to small molecules or mAbs targeting cancer cells.

## Stromal manipulations: From osteolytic to osteoblastic

The skeletal lesions in multiple myeloma, breast, renal, and lung cancer patients are most commonly osteolytic (Table 2). Additionally, patients with these cancers may have extraskeletal metastases. A few clinical trials are registered to explore the potential of $^{223}$Ra, mainly in combination with other drugs (Table 3). However, bisphosphonates, denosumab, bortezomib, and antihormonal therapies may alter the bone matrix of the disease and lead to a more avid target for radium (80, 81).

TABLE 1 List of ongoing clinical trials with diffusing alpha-emitters radiation therapy (DaRT).

| Cancer | Clinical study identifier |
|---|---|
| Squamous cell carcinoma (SCC) | NCT03353077, NCT05065346, NCT05047094, NCT04068155 |
| Cutaneous, Mucosal, Superficial Soft Tissue Neoplasia | NCT03737734, NCT03886181, NCT03889899, NCT04534127, NCT04540588 |
| Prostate | NCT04543903 |
| Breast | NCT03970967, NCT04906070 |
| Pancreatic | NCT04002479 |
| Vulva | NCT04761146 |

TABLE 2 Incidence of bone metastases in advanced cancer.

| Primary cancer | Incidence of bone metastases (%) | Dominant type of bone metastases | Frequency of skeletal-related events (%) | References |
|---|---|---|---|---|
| Prostate | 65–85 | Osteoblastic | 49 | (64, 66, 68) |
| Breast | 65–75 | Mixed osteolytic/osteoblastic | 64–68 | (64, 66, 68) |
| Multiple myeloma | 80–90 | Osteolytic | 51 | (68–70) |
| Renal | 20–40 | Osteolytic | 34 | (64, 67, 68) |
| Lung (non-small cell) | 30–60 | Osteolytic | 60 | (64, 71, 72) |
| Lung (small cell) | 34–50 | Osteoblastic | 9–63 | (64, 66, 73, 74) |
| Neuroendocrine tumors | 15–21 | Mixed osteoblastic/osteolytic | 26 | (75) |
| Bone cancers (osteosarcoma) | Bone cancer | Osteoblastic | 100% | (76) |

It is documented that the administration of bisphosphonates alters the lytic/blastic ratio in bone lesions toward a more blastic phenotype, and increase uptake of bone-seeking beta-emitting radiopharmaceuticals, such as $^{89}$Sr and $^{153}$Sm-EDTMP (81). Bortezomib and other proteasome inhibitors can also restore the impaired osteoblast activity (81–83). Denosumab is a mAb that binds the cytokine receptor activator of NFκB ligand (RANKL) that is an essential factor initiating bone turnover (84). RANKL inhibition blocks osteoclast maturation, function and survival, thus reducing bone resorption (84). It has been demonstrated that breast cancer patients after chronic bisphosphonate therapy and multiple myeloma patients after bortezomib treatment had increased $^{99}$Tm-labeled methylene diphosphonate (MTD) uptake in osseous bone metastases (81).

Ra-223 has been used for breast cancer patients with bone-dominant disease with osteoblastic and osteolytic lesions (85–87). Coleman et al. have demonstrated that $^{223}$Ra targeted osteoblastic, but not osteolytic lesions, in breast cancer patients with bone-dominant disease (85). The results are not surprising because the balance between osteoblastic and osteolytic lesions have not been taken into account (87). However, these studies have demonstrated that $^{223}$Ra is safe (85–87), with the potential to be combined with other therapies after pretreatment with bisphosphonates and denosumab.

Suominen et al. investigated the effect of $^{223}$Ra, bortezomib and their combination in the syngeneic 5TGM1 mouse multiple myeloma model *in vivo* (82). The combination of bortezomib and $^{223}$Ra improved the incorporation of $^{223}$Ra into multiple myeloma bone lesions, decreased synergistically the area of osteolytic lesions and decreased tumor burden and restored body weights in mice (82).

TABLE 3 List of clinical trials with Xofigo alone or in combination with other drugs in cancers with dominant osteolytic lesions.

| Cancer | Drugs | Clinical study identifier |
|---|---|---|
| Relapsed multiple myeloma | Bortezomib, dexamethasone | NCT02605356, NCT02928029 |
| Renal cell carcinoma | Pazopanib, sorafenib | NCT02406521 |
| | Cabozantinib S-malate | NCT04071223 |
| Breast | – | NCT01070485 |
| | Exemestane, everolimus | NCT02258451 |
| | – | NCT02258464 |
| | Denosumab | NCT02366130 |
| | Paclitaxel | NCT04090398 |
| Lung | Pembrolizumab | NCT03996473 |
| | – | NCT02283749 |

## Preclinical studies of dual targeting alpha therapy

Dual targeting alpha therapy seems more suitable for breast cancer patients than $^{223}$Ra alone because a $^{212}$Pb-conjugate potentially can target breast cancer cells all over the body or alternatively be made bone directed (i.e., dual bone targeting). Preclinical results demonstrated that a single dose of dual bone $^{224}$Ra-solution with EDTMP prolonged survival time and lowered incidence of paralysis and bone metastases in nude mice with breast cancer micrometastases (55). Epidermal growth-factor receptor (EGFR) is overexpressed in 15–70% of breast cancer (88, 89), and thus, is an attractive candidate for dual targeting alpha therapy.

Example 1

To test the proof of concept of our dual targeting approach the EGFR-targeting mAb cetuximab (CTX) and bone-targeting EDTMP were chosen for our pilot studies (unpublished results). The mAb or EDTMP were labeled with $^{212}$Pb in $^{224}$Ra solutions in equilibrium with progenies (pH adjusted to 5–6 by 0.5 M $C_2H_7NO_2$ or $C_2H_3NaO_2$). TCMC-mAb was added to a final concentration of 0.1–1 mg/ml. The solutions

were mixed on a Thermomixer (Eppendorf, Hamburg) for 30 min at 37°C. Radiochemical purity of the samples was determined by instant thin layer chromatography (Tec-control, Biodex, Medical Systems, Shirley, NY), and only products with purities ≥ 95% were used in the experiments.

The anti-cancer effects of $^{224}$Ra-solutions with TCMC-CTX or EDTMP were investigated in 6 weeks old female athymic Nude-Foxn1nu mice (bred at the Comparative Medicine Department, Oslo University Hospital) with breast cancer metastasis. MDA-MB-231-luciferase (Luc) expressing breast cancer cells ($2 \times 10^5$ cells/100 μl PBS per mouse) were injected into the left ventricle of mouse heart (intracardiac injection). Sodium chloride (0.9% NaCl, control), 300 kBq/kg $^{224}$Ra & $^{212}$Pb-EDTMP, or 300 kBq/kg $^{224}$Ra&$^{212}$Pb-TCMC-CTX were intravenously administered to mice 2 days after cell injection. Tumor metastases were monitored by bioluminescence imaging in an IVIS Spectrum *in vivo* imaging system (PerkinElmer, Waltham, MA) 24, 31, and 38 days after intravenous injection of compounds. Each mouse was injected intraperitoneally with 0.2 ml D-luciferin (Biosynth AG, Staad, Switzerland) dissolved in Dulbecco's PBS (20 mg/ml) 10 min prior to imaging. During imaging, mice were under gas anesthesia (~3.5% Sevoflurane in oxygen at 0.5 L/min; Baxter, IL, USA). All bioluminescence data are displayed in radiance (photons/s/cm$^2$/str) under identical acquisition conditions. Mice were euthanized by cervical dislocation when cachexia, paraplegia or any signs of severe sickness or discomfort was observed. The studies were approved by the Institutional Committee on Research Animal Care (Department of Comparative Medicine, Oslo University Hospital) and the Norwegian Food Safety Authority (Brumunddal, Norway, approval: FOTS ID 22197).

Dual targeting alpha therapy extended survival in EDTMP and cetuximab group compared to the control [0.9% sodium chloride (NaCl)] group, and lowered the incidence of bone and extraskeletal metastases (Figure 3). The preliminary studies provide conceptual and strong evidence that dual targeting $^{224}$Ra-solution with bone or tumor-targeted delivery of $^{212}$Pb has potential to inhibit cancer metastases without significant toxicity. Several molecular targets are being explored to target HER2, estrogen receptor and progesterone receptor for nuclear medicine imaging (90, 91), and they can be suitable for dual targeting alpha therapy of breast cancer after stromal manipulation.

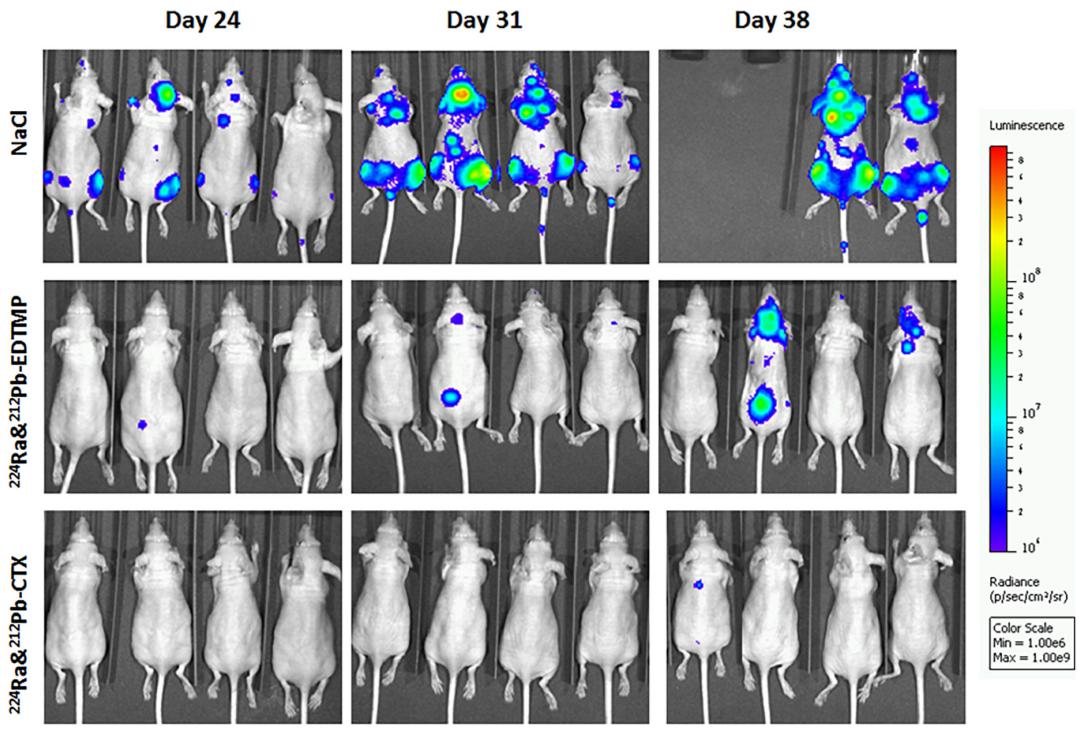


FIGURE 3
The influence of dual targeting alpha solution on breast cancer metastases growth in mice. Tumor metastases were monitored by bioluminescence imaging in the different therapy groups 24, 31, and 38 days after intravenous injection of 0.9% sodium chloride (NaCl, control), 300 kBq/kg $^{224}$Ra&$^{212}$Pb-EDTMP, or 300 kBq/kg $^{224}$Ra&$^{212}$Pb-TCMC-cetuximab (CTX). MDA-MB-231-Luc breast cancer cells ($2 \times 10^5$ cells/mouse) were injected intracardially into athymic Nude-Foxn1nu mice 2 days before the treatment. The mice are positioned in the same order at all-time points. The studies were approved by the Institutional Committee on Research Animal Care (Department of Comparative Medicine, Oslo University Hospital) and the Norwegian Food Safety Authority (Brumunddal, Norway, approval: FOTS ID 22197).

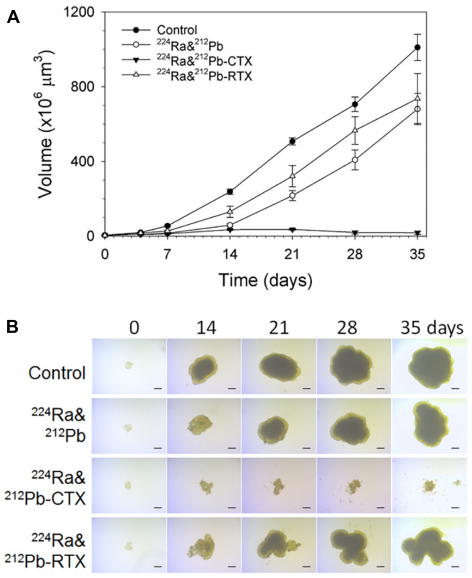


FIGURE 4
The influence of dual targeting alpha solution on prostate cancer multicellular LNCaP spheroid growth after incubation for 4 h. **(A)** Growth of spheroids treated with 1 kBq/ml $^{224}$Ra&$^{212}$Pb, $^{224}$Ra&$^{212}$Pb-TCMC-cetuximab (CTX), and $^{224}$Ra&$^{212}$Pb-TCMC-rituximab (RTX, negative control) groups was measured for up to 35 days and is presented as volume ($\times 10^6$ µm$^3$) ± *SD*. The images of LNCaP spheroids were measured for up to 35 days. **(B)** Representative microscope images (×4 magnification) were taken at the predefined study end point of 35 days using a bright-field microscope with AxioVision Rel. 4.8 software. LNCaP spheroids were generated by cultivation of cells in liquid overlay in 1.5% agarose-coated flat bottom 96-well plates (94). Cell suspensions of 500 cells in 100 µL medium were added to each well, followed by centrifugation of the plates at 470 × g for 15 min. After an initial incubation time of 3 days, spheroids with diameter of ~229 µm were formed.

Example 2

In prostate cancers, EGFR is weakly expressed in neoplastic cells while it is highly expressed in metastatic lesions (92, 93). The effectiveness of $^{224}$Ra-solution with $^{212}$Pb-TCMC-CTX directed against EGFR-positive multicellular LNCaP spheroids, an *in vitro* model for micrometastatic cancer, was investigated (unpublished data).

Ra-224-solution with CTX effectively stopped the growth of LNCaP spheroids relative to the equivalent dose of $^{224}$Ra-solution alone or RTX (unpublished data, Figure 4).

## Transferring dual targeting solution into clinic

Several combination treatments with TAT have been proposed (95–98). Their goal is to increase efficacy by using therapies with different action mechanisms together with TAT keeping toxic effects to a minimum. Dual targeting solution may allow increasing therapeutic efficacy and reducing toxicities of $^{224}$Ra and its progenies to normal organs. Transferring dual targeting solution into clinic will be more complicated due to the complexity of the product ($^{224}$Ra, its progenies, targeting agent, and chelator). A few therapy cycles of dual targeting alpha therapy, similarly to single alpha therapies, will be needed. In some cases, a booster dose of cancer cell-seeker targeted $^{212}$Pb alone will be required. At the same time, the non-toxic administered activity of $^{224}$Ra and/or $^{212}$Pb may be chosen based on earlier or ongoing clinical studies. As was mentioned earlier, $^{224}$Ra was used in the treatment of ankylosing spondylitis, and long-term toxicity and carcinogenicity data in humans exist (46–48). Additionally, the seeds with $^{224}$Ra (Table 1) and bio-degradable calcium carbonate microparticles with $^{224}$Ra (NCT03732768) are under clinical investigations for cancer treatment. A few clinical trials investigating $^{212}$Pb-conjugates are registered on Clinicaltrials.gov (Table 4). Phase I studies of $^{212}$Pb-TCMC-trastuzumab and $^{212}$Pb-DOTAMTATE demonstrated safety and feasibility in patients with HER-2 expressing malignancies (99) and somatostatin receptor (SSTR) expressing neuroendocrine tumors (52).

## Summary of dual targeting technology

The dual targeting solutions taking advantage of both the bone seeking $^{224}$Ra and cell directed complexes of $^{212}$Pb seems a promising approach to treat metastatic cancers presenting

TABLE 4 List of clinical trials with $^{212}$Pb-conjugates.

| Phase | Disease | Target | $^{212}$Pb-conjugate | Clinical study identifier |
|---|---|---|---|---|
| 1 | Breast, peritoneal, ovarian, pancreatic and stomach neoplasms | Human epidermal growth factor 2 receptor (HER-2) | TCMC-trastuzumab | NCT01384253 |
| 1 | Neuroendocrine tumor | Somatostatin receptor (SSTR) | DOTAMTATE | NCT03466216 |
| 2 | Neuroendocrine tumor | Somatostatin receptor (SSTR) | DOTAMTATE | NCT05153772 |
| 1 | Cutaneous melanoma, cervical, prostate, breast and colon cancers | Gastrin-releasing peptide receptor (GRPR) | DOTAM-GRPR1 | NCT05283330 |

with bone and soft tissue lesions and also of skeletal metastases of mixed lytic/osteogenic nature. The radioactivity of the solutions will probably be dictated by the tolerability to the longer lived $^{224}$Ra. In this regard, the knowledge of long-term and short-term toxicity of $^{224}$Ra in the previous mentioned ankylosing spondylitis series may be important in determining the suitable activity levels. In some settings the use of a booster dose of purified $^{212}$Pb-radioligand alone could be a possible tactic to elevate the effect of this component, if needed, e.g., in fractionated scheduled treatment regimen, where the dual targeting solution then will act as maintenance treatment. It could be a regulatory challenge to develop such a combined product. Anyhow, some clinical data of the purified $^{212}$Pb-ligand alone would be required.

## Cell lines

The cell lines present in this study were obtained from ATCC (LNCaP cell line) and Cell Biolabs Inc. (MDA-MB-231-Luc cell line).

## Data availability statement

The raw data supporting the conclusions of this article will be made available by the authors, without undue reservation.

## Ethics statement

The animal study was reviewed and approved by the Norwegian Food Safety Authority (Brumunddal, Norway, approval: FOTS ID 22197).

## Author contributions

AJ, ØB, and RL: conceptualization. AJ, VS, ØB, and RL: designing the work and interpretation of results. AJ and RL: *in vitro, in vivo* experiments, and analyzing data. AJ, VS, ØB, M-ER, and RL: drafting the manuscript and revising it critically for important intellectual content. All authors have read and agreed to the published version of the manuscript.

## Funding

This research was funded by the Norwegian Research Council and Artbio AS [Industrial Ph.D. project number 260639 (Vilde Stenberg), Oslo, Norway], and the South-Eastern Norway Regional Health Authority (project number 2020028, Oslo, Norway).

## Acknowledgments

We would like to thank Li-Wei Ma for his support in the execution and follow-up of the multicellular tumor spheroid and animal experiments described in this manuscript.

## Conflict of interest

ØB and RL hold ownership interest in ARTBIO AS.

The remaining authors declare that the research was conducted in the absence of any commercial or financial relationships that could be construed as a potential conflict of interest.

## Publisher's note



## References

1. Coleman R, Hadji P, Body J, Santini D, Chow E, Terpos E, et al. Bone health in cancer: ESMO Clinical Practice Guidelines. *Ann Oncol.* (2020) 31:1650–63. doi: 10.1016/j.annonc.2020.07.019

2. Dillekås H, Rogers M, Straume O. Are 90% of deaths from cancer caused by metastases? *Cancer Med.* (2019) 8:5574–6. doi: 10.1002/cam4.2474

3. Herrmann K, Schwaiger M, Lewis J, Solomon S, McNeil B, Baumann M, et al. Radiotheranostics: a roadmap for future development. *Lancet Oncol.* (2020) 21:e146–56. doi: 10.1016/s1470-204530821-6

4. Solnes L, Shokeen M, Pandit-Taskar N. Novel agents and future perspectives on theranostics. *Semin Radiat Oncol.* (2021) 31:83–92. doi: 10.1016/j.semradonc.2020.07.010

5. Jadvar H, Colletti P. Targeted α-therapy in non-prostate malignancies. *Eur J Nucl Med Mol Imaging.* (2021) 49:47–53. doi: 10.1007/s00259-021-05405-0

6. Zhang J, Kulkarni H, Baum R. 225Ac-DOTATOC-targeted somatostatin receptor α-therapy in a patient with metastatic neuroendocrine tumor of the thymus, refractory to β-radiation. *Clin Nucl Med.* (2021) 46:1030–1. doi: 10.1097/rlu.0000000000003792

7. Kratochwil C, Bruchertseifer F, Giesel F, Weis M, Verburg F, Mottaghy F, et al. 225Ac-PSMA-617 for PSMA-targeted α-radiation therapy of metastatic castration-resistant prostate cancer. *J Nucl Med.* (2016) 57:1941–4. doi: 10.2967/jnumed.116.178673

8. Marcu L, Bezak E, Allen B. Global comparison of targeted alpha vs targeted beta therapy for cancer: in vitro, in vivo and clinical trials. *Crit Rev Oncol Hematol.* (2018) 123:7–20. doi: 10.1016/j.critrevonc.2018.01.001

9. Brechbiel M. Targeted alpha-therapy: past, present, future? *Dalton Trans.* (2007) 43:4918–28. doi: 10.1039/b704726f

10. Pouget J, Constanzo J. Revisiting the radiobiology of targeted alpha therapy. *Front Med.* (2021) 8:692436. doi: 10.3389/fmed.2021.692436

11. Ruigrok E, Tamborino G, de Blois E, Roobol S, Verkaik N, De Saint-Hubert M, et al. In vitro dose effect relationships of actinium-225- and lutetium-177-labeled PSMA-I&T. *Eur J Nucl Med Mol Imaging.* (2022) 49:3627–38. doi: 10.1007/s00259-022-05821-w

12. Sartor O, de Bono J, Chi K, Fizazi K, Herrmann K, Rahbar K, et al. Lutetium-177-PSMA-617 for metastatic castration-resistant prostate cancer. *N Engl J Med.* (2021) 385:1091–103. doi: 10.1056/NEJMoa2107322

13. Ma J, Li L, Liao T, Gong W, Zhang C. Efficacy and safety of 225Ac-PSMA-617-targeted alpha therapy in metastatic castration-resistant prostate cancer: a systematic review and meta-analysis. *Front Oncol.* (2022) 12:796657. doi: 10.3389/fonc.2022.796657

14. Gafita A, Marcus C, Kostos L, Schuster D, Calais J, Hofman M. Predictors and real-world use of prostate-specific radioligand therapy: PSMA and beyond. *Am Soc Clin Oncol Educ Book.* (2022) 42:1–17. doi: 10.1200/edbk_350946

15. Yordanova A, Ahmadzadehfar H. Combination therapies with PRRT. *Pharmaceuticals.* (2021) 14:1005. doi: 10.3390/ph14101005

16. Aicher A, Sindrilaru A, Crisan D, Thaiss W, Steinacker J, Beer M, et al. Short-interval, low-dose peptide receptor radionuclide therapy in combination with PD-1 checkpoint immunotherapy induces remission in immunocompromised patients with metastatic merkel cell carcinoma. *Pharmaceutics.* (2022) 14:1466. doi: 10.3390/pharmaceutics14071466

17. Hallqvist A, Svensson J, Hagmarker L, Marin I, Rydén T, Beauregard J, et al. Optimizing the schedule of PARP inhibitors in combination with 177Lu-DOTATATE: a dosimetry rationale. *Biomedicines.* (2021) 9:1570. doi: 10.3390/biomedicines9111570

18. Khreish F, Ebert N, Ries M, Maus S, Rosar F, Bohnenberger H, et al. (225)Ac-PSMA-617/(177)Lu-PSMA-617 tandem therapy of metastatic castration-resistant prostate cancer: pilot experience. *Eur J Nucl Med Mol Imaging.* (2020) 47:721–8. doi: 10.1007/s00259-019-04612-0

19. Rosar F, Hau F, Bartholomä M, Maus S, Stemler T, Linxweiler J, et al. Molecular imaging and biochemical response assessment after a single cycle of [225Ac]Ac-PSMA-617/[177Lu]Lu-PSMA-617 tandem therapy in mCRPC patients who have progressed on [177Lu]Lu-PSMA-617 monotherapy. *Theranostics.* (2021) 11:4050–60. doi: 10.7150/thno.56211

20. Rosar F, Krause J, Bartholomä M, Maus S, Stemler T, Hierlmeier I, et al. Efficacy and safety of [225Ac]Ac-PSMA-617 Augmented [177Lu]Lu-PSMA-617 radioligand therapy in patients with highly advanced mCRPC with poor prognosis. *Pharmaceutics.* (2021) 13:722. doi: 10.3390/pharmaceutics13050722

21. Miyahira A, Soule H. The history of prostate-specific membrane antigen as a theranostic target in prostate cancer: the cornerstone role of the prostate cancer foundation. *J Nucl Med.* (2022) 63:331–8. doi: 10.2967/jnumed.121.262997

22. Tagawa S, Sun M, Sartor O, Thomas C, Singh S, Bissassar M, et al. editors. Phase I study of 225Ac-J591 for men with metastatic castration-resistant prostate cancer (mCRPC). *J Clin Oncol.* (2021) 39:5015.

23. Robertson A, Ramogida C, Schaffer P, Radchenko V. Development of 225Ac radiopharmaceuticals: TRIUMF perspectives and experiences. *Curr Radiopharm.* (2018) 11:156–72. doi: 10.2174/1874471011666180416161908

24. Morgenstern A, Apostolidis C, Bruchertseifer F. Supply and clinical application of actinium-225 and bismuth-213. *Semin Nucl Med.* (2020) 50:119–23. doi: 10.1053/j.semnuclmed.2020.02.003

25. Thiele N, Wilson J. Actinium-225 for targeted α therapy: coordination chemistry and current chelation approaches. *Cancer Biother Radiopharm.* (2018) 33:336–48. doi: 10.1089/cbr.2018.2494

26. Parker C, Nilsson S, Heinrich D, Helle S, O'Sullivan J, Fosså S, et al. Alpha emitter radium-223 and survival in metastatic prostate cancer. *N Engl J Med.* (2013) 369:213–23. doi: 10.1056/NEJMoa1213755

27. Suominen M, Rissanen J, Käkönen R, Fagerlund K, Alhoniemi E, Mumberg D, et al. Survival benefit with radium-223 dichloride in a mouse model of breast cancer bone metastasis. *J Natl Cancer Inst.* (2013) 105:908–16. doi: 10.1093/jnci/djt116

28. Suominen M, Wilson T, Käkönen S, Scholz A. The mode-of-action of targeted alpha therapy radium-223 as an enabler for novel combinations to treat patients with bone metastasis. *Int J Mol Sci.* (2019) 20:3899. doi: 10.3390/ijms20163899

29. Roudier M, Morrissey C, True L, Higano C, Vessella R, Ott S. Histopathological assessment of prostate cancer bone osteoblastic metastases. *J Urol.* (2008) 180:1154–60. doi: 10.1016/j.juro.2008.04.140

30. Bruland ØS, Dahle J, Olsen D, Larsen R. Targeted high-LET therapy of bone metastases. In: Stigbrand T, Carlsson J, Adams G, editors. *Targeted Radionuclide Tumor Therapy Biological Aspects*. Dordrecht: Springer (2008). p. 181–94.

31. Bruland ØS, Nilsson S, Fisher D, Larsen R. High-linear energy transfer irradiation targeted to skeletal metastases by the alpha-emitter 223Ra: adjuvant or alternative to conventional modalities? *Clin Cancer Res.* (2006) 12(20 Pt 2):6250s–7s. doi: 10.1158/1078-0432.Ccr-06-0841

32. Henriksen G, Hoff P, Larsen R. Evaluation of potential chelating agents for radium. *Appl Radiat Isot.* (2002) 56:667–71. doi: 10.1016/s0969-804300282-2

33. Abou D, Thiele N, Gutsche N, Villmer A, Zhang H, Woods J, et al. Towards the stable chelation of radium for biomedical applications with an 18-membered macrocyclic ligand. *Chem Sci.* (2021) 12:3733–42. doi: 10.1039/d0sc06867e

34. Gott M, Yang P, Kortz U, Stephan H, Pietzsch H, Mamat C. A 224Ra-labeled polyoxopalladate as a putative radiopharmaceutical. *Chem Commun.* (2019) 55:7631–4. doi: 10.1039/c9cc02587a

35. Hagemann U, Wickstroem K, Hammer S, Bjerke R, Zitzmann-Kolbe S, Ryan O, et al. Advances in precision oncology: targeted thorium-227 conjugates as a new modality in targeted alpha therapy. *Cancer Biother Radiopharm.* (2020) 35:497–510. doi: 10.1089/cbr.2020.3568

36. Frantellizzi V, Cosma L, Brunotti G, Pani A, Spanu A, Nuvoli S, et al. Targeted alpha therapy with thorium-227. *Cancer Biother Radiopharm.* (2020) 35:437–45. doi: 10.1089/cbr.2019.3105

37. Dahle J, Larsen R. Targeted alpha-particle therapy with 227Th-labeled antibodies. *Curr Radiopharm.* (2008) 1:209–14. doi: 10.1097/MNM.0b013e328354df7c

38. Henriksen G, Bruland O, Larsen R. Thorium and actinium polyphosphonate compounds as bone-seeking alpha particle-emitting agents. *Anticancer Res.* (2004) 24:101–5.

39. Washiyama K, Amano R, Sasaki J, Kinuya S, Tonami N, Shiokawa Y, et al. 227Th-EDTMP: a potential therapeutic agent for bone metastasis. *Nucl Med Biol.* (2004) 31:901–8. doi: 10.1016/j.nucmedbio.2004.05.001

40. Westrøm S, Generalov R, Bønsdorff T, Larsen R. Preparation of 212Pb-labeled monoclonal antibody using a novel 224Ra-based generator solution. *Nucl Med Biol.* (2017) 51:1–9. doi: 10.1016/j.nucmedbio.2017.04.005

41. Stenberg V, Juzeniene A, Bruland ØS, Larsen R. In situ generated 212Pb-PSMA ligand in a 224Ra-solution for dual targeting of prostate cancer sclerotic stroma and PSMA-positive cells. *Curr Radiopharm.* (2020) 13:130–41. doi: 10.2174/1874471013666200511000532

42. Li R, Stenberg V, Larsen R. A novel experimental generator for production of high purity lead-212 for use in radiopharmaceuticals. *J Nucl Med.* (2022). doi: 10.2967/jnumed.122.264009

43. Jiang W, Ulmert D, Simons B, Abou D, Thorek D. The impact of age on radium-223 distribution and an evaluation of molecular imaging surrogates. *Nucl Med Biol.* (2018) 62–3:1–8. doi: 10.1016/j.nucmedbio.2018.05.003

44. Henriksen G, Breistøl K, Bruland ØS, Fodstad Ø, Larsen R. Significant antitumor effect from bone-seeking, alpha-particle-emitting 223Ra demonstrated in an experimental skeletal metastases model. *Cancer Res.* (2002) 62:3120–5.

45. Schumann S, Eberlein U, Müller J, Scherthan H, Lassmann M. Correlation of the absorbed dose to the blood and DNA damage in leukocytes after internal ex-vivo irradiation of blood samples with Ra-224. *EJNMMI Res.* (2018) 8:77. doi: 10.1186/s13550-018-0422-4

46. Priest N, Dauer L, Hoel D. Administration of lower doses of radium-224 to ankylosing spondylitis patients results in no evidence of significant overall detriment. *PLoS One.* (2020) 15:e0232597. doi: 10.1371/journal.pone.0232597

47. Lassmann M, Nosske D, Reiners C. Therapy of ankylosing spondylitis with 224Ra-radium chloride: dosimetry and risk considerations. *Radiat Environ Biophys.* (2002) 41:173–8. doi: 10.1007/s00411-002-0164-5

48. Wick R, Nekolla E, Gaubitz M, Schulte T. Increased risk of myeloid leukaemia in patients with ankylosing spondylitis following treatment with radium-224. *Rheumatology.* (2008) 47:855–9. doi: 10.1093/rheumatology/ken060

49. Nekolla E, Kreisheimer M, Kellerer A, Kuse-Isingschulte M, Gössner W, Spiess H. Induction of malignant bone tumors in radium-224 patients: risk

estimates based on the improved dosimetry. *Radiat Res.* (2000) 153:93–103. doi: 10.1667/0033-7587(2000)153[0093:iombti]2.0.co;2

50. Wick R, Nekolla E, Gössner W, Kellerer A. Late effects in ankylosing spondylitis patients treated with 224Ra. *Radiat Res.* (1999) 152(6 Suppl.):S8–11.

51. Meredith R, Torgue J, Azure M, Shen S, Saddekni S, Banaga E, et al. Pharmacokinetics and imaging of 212Pb-TCMC-trastuzumab after intraperitoneal administration in ovarian cancer patients. *Cancer Biother Radiopharm.* (2014) 29:12–7. doi: 10.1089/cbr.2013.1531

52. Delpassand E, Tworowska I, Esfandiari R, Torgue J, Hurt J, Shafie A, et al. Targeted alpha-emitter therapy with 212Pb-DOTAMTATE for the treatment of metastatic SSTR-expressing neuroendocrine tumors: first-in-human, dose-escalation clinical trial. *J Nucl Med.* (2022) 63:1326–33. doi: 10.2967/jnumed.121.263230

53. Kokov K, Egorova B, German M, Klabukov I, Krasheninnikov M, Larkin-Kondrov A, et al. 212Pb: production approaches and targeted therapy applications. *Pharmaceutics.* (2022) 14:189. doi: 10.3390/pharmaceutics14010189

54. Larsen R. *Radiopharmaceutical Solutions with Advantageous Properties. US10434198B2US10434198B2.* (2019). Available online at: https://patents.google.com/patent/US10434198B2/en

55. Juzeniene A, Bernoulli J, Suominen M, Halleen J, Larsen R. Antitumor activity of novel bone-seeking, α-emitting 224Ra-solution in a breast cancer skeletal metastases model. *Anticancer Res.* (2018) 38:1947–55. doi: 10.21873/anticanres.12432

56. Stenberg V, Juzeniene A, Chen Q, Yang X, Bruland ØS, Larsen R. Preparation of the alpha-emitting prostate-specific membrane antigen targeted radioligand [212Pb]Pb-NG001 for prostate cancer. *J Labelled Comp Radiopharm.* (2020) 63:129–43. doi: 10.1002/jlcr.3825

57. Stenberg V, Tornes A, Nilsen H, Revheim M, Bruland ØS, Larsen R, et al. Factors influencing the therapeutic efficacy of the PSMA targeting radioligand 212Pb-NG001. *Cancers.* (2022) 14:2784. doi: 10.3390/cancers14112784

58. Arazi L. Diffusing alpha-emitters radiation therapy: approximate modeling of the macroscopic alpha particle dose of a point source. *Phys Med Biol.* (2020) 65:015015. doi: 10.1088/1361-6560/ab5b73

59. Lloyd R, Mays C, Taylor G, Atherton D, Bruenger F, Jones C. Radium-224 retention, distribution, and dosimetry in beagles. *Radiat Res.* (1982) 92:280–95.

60. Muggenburg B, Hahn F, Griffith W Jr, Lloyd R, Boecker B. The biological effects of radium-224 injected into dogs. *Radiat Res.* (1996) 146:171–86.

61. Napoli E, Bønsdorff T, Jorstad I, Bruland ØS, Larsen R, Westrøm S. Radon-220 diffusion from 224Ra-labeled calcium carbonate microparticles: some implications for radiotherapeutic use. *PLoS One.* (2021) 16:e0248133. doi: 10.1371/journal.pone.0248133

62. Bellia S, Feliciani G, Duca M, Monti M, Turri V, Sarnelli A, et al. Clinical evidence of abscopal effect in cutaneous squamous cell carcinoma treated with diffusing alpha emitters radiation therapy: a case report. *J Contemp Brachytherapy.* (2019) 11:449–57. doi: 10.5114/jcb.2019.88138

63. Feliciani G, Bellia S, Del Duca M, Mazzotti G, Monti M, Stanganelli I, et al. A new approach for a safe and reproducible seeds positioning for diffusing alpha-emitters radiation therapy of squamous cell skin cancer: a feasibility study. *Cancers.* (2022) 14:240. doi: 10.3390/cancers14010240

64. Huang J, Shen J, Li X, Rengan R, Silvestris N, Wang M, et al. Incidence of patients with bone metastases at diagnosis of solid tumors in adults: a large population-based study. *Ann Transl Med.* (2020) 8:482. doi: 10.21037/atm.2020.03.55

65. Bădilă A, Rădulescu D, Niculescu A, Grumezescu A, Rădulescu M, Rădulescu A. Recent advances in the treatment of bone metastases and primary bone tumors: an up-to-date review. *Cancers.* (2021) 13:4229. doi: 10.3390/cancers13164229

66. Macedo F, Ladeira K, Pinho F, Saraiva N, Bonito N, Pinto L, et al. Bone metastases: an overview. *Oncol Rev.* (2017) 11:321. doi: 10.4081/oncol.2017.321

67. Woodward E, Jagdev S, McParland L, Clark K, Gregory W, Newsham A, et al. Skeletal complications and survival in renal cancer patients with bone metastases. *Bone.* (2011) 48:160–6. doi: 10.1016/j.bone.2010.09.008

68. Brozovich A, Garmezy B, Pan T, Wang L, Farach-Carson M, Satcher R. All bone metastases are not created equal: revisiting treatment resistance in renal cell carcinoma. *J Bone Oncol.* (2021) 31:100399. doi: 10.1016/j.jbo.2021.100399

69. Hameed A, Brady J, Dowling P, Clynes M, O'Gorman P. Bone disease in multiple myeloma: pathophysiology and management. *Cancer Growth Metastasis.* (2014) 7:33–42. doi: 10.4137/cgm.S16817

70. Eda H, Santo L, David Roodman G, Raje N. Bone disease in multiple myeloma. *Cancer Treat Res.* (2016) 169:251–70. doi: 10.1007/978-3-319-40320-5_14

71. Knapp B, Devarakonda S, Govindan R. Bone metastases in non-small cell lung cancer: a narrative review. *J Thorac Dis.* (2022) 14:1696–712. doi: 10.21037/jtd-21-1502

72. Hendriks L, Hermans B, van den Beuken-van Everdingen M, Hochstenbag M, Dingemans A. Effect of bisphosphonates, denosumab, and radioisotopes on bone pain and quality of life in patients with non-small cell lung cancer and bone metastases: a systematic review. *J Thorac Oncol.* (2016) 11:155–73. doi: 10.1016/j.jtho.2015.10.001

73. Gong L, Xu L, Yuan Z, Wang Z, Zhao L, Wang P. Clinical outcome for small cell lung cancer patients with bone metastases at the time of diagnosis. *J Bone Oncol.* (2019) 19:100265. doi: 10.1016/j.jbo.2019.100265

74. Megyesfalvi Z, Tallosy B, Pipek O, Fillinger J, Lang C, Klikovits T, et al. The landscape of small cell lung cancer metastases: organ specificity and timing. *Thorac Cancer.* (2021) 12:914–23. doi: 10.1111/1759-7714.13854

75. Garcia-Torralba E, Spada F, Lim K, Jacobs T, Barriuso J, Mansoor W, et al. Knowns and unknowns of bone metastases in patients with neuroendocrine neoplasms: a systematic review and meta-analysis. *Cancer Treat Rev.* (2021) 94:102168. doi: 10.1016/j.ctrv.2021.102168

76. Sheng G, Gao Y, Yang Y, Wu H. Osteosarcoma and metastasis. *Front Oncol.* (2021) 11:780264. doi: 10.3389/fonc.2021.780264

77. Larsen R, Saxtorph H, Skydsgaard M, Borrebaek J, Jonasdottir T, Bruland O, et al. Radiotoxicity of the alpha-emitting bone-seeker 223Ra injected intravenously into mice: histology, clinical chemistry and hematology. *In Vivo.* (2006) 20:325–31.

78. Pandit-Taskar N, Larson S, Carrasquillo J. Bone-seeking radiopharmaceuticals for treatment of osseous metastases, part 1: α therapy with 223Ra-dichloride. *J Nucl Med.* (2014) 55:268–74. doi: 10.2967/jnumed.112.112482

79. Tomblyn M. The role of bone-seeking radionuclides in the palliative treatment of patients with painful osteoblastic skeletal metastases. *Cancer Control.* (2012) 19:137–44. doi: 10.1177/107327481201900208

80. Humm J, Sartor O, Parker C, Bruland O, Macklis R. Radium-223 in the treatment of osteoblastic metastases: a critical clinical review. *Int J Radiat Oncol Biol Phys.* (2015) 91:898–906. doi: 10.1016/j.ijrobp.2014.12.061

81. Sartor O, Hoskin P, Bruland O. Targeted radio-nuclide therapy of skeletal metastases. *Cancer Treat Rev.* (2013) 39:18–26. doi: 10.1016/j.ctrv.2012.03.006

82. Suominen M, Mäki-Jouppila J, Huhtinen A, Sjöholm B, Rissanen J, Luostarinen A, et al. Additive benefits of radium-223 dichloride and bortezomib combination in a systemic multiple myeloma mouse model. *Int J Mol Sci.* (2021) 22:5570. doi: 10.3390/ijms22115570

83. Heider U, Kaiser M, Müller C, Jakob C, Zavrski I, Schulz C, et al. Bortezomib increases osteoblast activity in myeloma patients irrespective of response to treatment. *Eur J Haematol.* (2006) 77:233–8. doi: 10.1111/j.1600-0609.2006.00692.x

84. Hanley D, Adachi J, Bell A, Brown V. Denosumab: mechanism of action and clinical outcomes. *Int J Clin Pract.* (2012) 66:1139–46. doi: 10.1111/ijcp.12022

85. Coleman R, Aksnes A, Naume B, Garcia C, Jerusalem G, Piccart M, et al. A phase IIa, nonrandomized study of radium-223 dichloride in advanced breast cancer patients with bone-dominant disease. *Breast Cancer Res Treat.* (2014) 145:411–8. doi: 10.1007/s10549-014-2939-1

86. Takalkar A, Adams S, Subbiah V. Radium-223 dichloride bone-targeted alpha particle therapy for hormone-refractory breast cancer metastatic to bone. *Exp Hematol Oncol.* (2014) 3:23. doi: 10.1186/2162-3619-3-23

87. Winter M, Coleman R, Kendall J, Palmieri C, Twelves C, Howell S, et al. A phase IB and randomised phase IIA trial of CApecitabine plus radium-223 (Xofigo$^{TM}$) in breast cancer patients with BONe metastases: CARBON trial results. *J Bone Oncol.* (2022) 35:100442. doi: 10.1016/j.jbo.2022.100442

88. Maennling A, Tur M, Niebert M, Klockenbring T, Zeppernick F, Gattenlöhner S, et al. Molecular targeting therapy against EGFR family in breast cancer: progress and future potentials. *Cancers.* (2019) 11:1826. doi: 10.3390/cancers11121826

89. Lorusso V, Forcignano R, Cinieri S, Tinelli A, Porcelli L, Quatrale A, et al. Which role for EGFR therapy in breast cancer? *Front Biosci.* (2012) 4:31–42. doi: 10.2741/s249

90. Altunay B, Morgenroth A, Mottaghy F. Use of radionuclide-based imaging methods in breast cancer. *Semin Nucl Med.* (2022) 52:561–73. doi: 10.1053/j.semnuclmed.2022.04.003

91. Sharma R, Mukherjee A, Mitra J, Sarma H. Unravelling the potential of lutetium-177 labeled pertuzumab targeting HER 2 receptors for theranostic applications. *Int J Radiat Oncol Biol Phys.* (2022). doi: 10.1016/j.ijrobp.2022.07.029

92. Carlsson J, Shen L, Xiang J, Xu J, Wei Q. Tendencies for higher co-expression of EGFR and HER2 and downregulation of HER3 in prostate cancer lymph node metastases compared with corresponding primary tumors. *Oncol Lett.* (2013) 5:208–14. doi: 10.3892/ol.2012.996

93. Day K, Lorenzatti Hiles G, Kozminsky M, Dawsey S, Paul A, Broses L, et al. HER2 and EGFR overexpression support metastatic progression of prostate cancer to bone. *Cancer Res.* (2017) 77:74–85. doi: 10.1158/0008-5472.Can-16-1656

94. Stenberg V, Larsen R, Ma L, Peng Q, Juzenas P, Bruland ØS, et al. Evaluation of the PSMA-binding ligand 212Pb-NG001 in multicellular tumour spheroid and mouse models of prostate cancer. *Int J Mol Sci.* (2021) 22:4815. doi: 10.3390/ijms22094815

95. Damiana T, Dalm S. Combination therapy, a promising approach to enhance the efficacy of radionuclide and targeted radionuclide therapy of prostate and breast cancer. *Pharmaceutics.* (2021) 13:674. doi: 10.3390/pharmaceutics13050674

96. Abou D, Fears A, Summer L, Longtine M, Benabdallah N, Riddle R, et al. Improved radium-223 therapy with combination epithelial sodium channel blockade. *J Nucl Med.* (2021) 62:1751–8. doi: 10.2967/jnumed.121.261977

97. Reissig F, Runge R, Naumann A, Kotzerke J. Cisplatin – A more efficient drug in combination with radionuclides? *Nuklearmedizin.* (2022) 61:325–32. doi: 10.1055/a-1759-1749

98. Milenic D, Baidoo K, Shih J, Wong K, Brechbiel M. Evaluation of platinum chemotherapy in combination with HER2-targeted α-particle radiation. *Cancer Biother Radiopharm.* (2013) 28:441–9. doi: 10.1089/cbr.2012.1423

99. Meredith R, Torgue J, Shen S, Fisher D, Banaga E, Bunch P, et al. Dose escalation and dosimetry of first-in-human α radioimmunotherapy with 212Pb-TCMC-trastuzumab. *J Nucl Med.* (2014) 55:1636–42. doi: 10.2967/jnumed.114.143842

frontiers | Frontiers in Medicine

TYPE Review
PUBLISHED 02 February 2023
DOI 10.3389/fmed.2022.1070497



OPEN ACCESS

EDITED BY
Egesta Lopci,
University of Milan, Italy

REVIEWED BY
Christian Goetz,
University Medical Center Freiburg, Germany
Christof Seidl,
Technical University of Munich, Germany

*CORRESPONDENCE
Emanuele Ostuni
✉ emanuele.ostuni@artbiotx.com

SPECIALTY SECTION
This article was submitted to Nuclear Medicine, a section of the journal Frontiers in Medicine

RECEIVED 14 October 2022
ACCEPTED 29 December 2022
PUBLISHED 02 February 2023

CITATION
Ostuni E and Taylor MRG (2023) Commercial and business aspects of alpha radioligand therapeutics.
*Front. Med.* 9:1070497.
doi: 10.3389/fmed.2022.1070497



# Commercial and business aspects of alpha radioligand therapeutics

Emanuele Ostuni[1]* and Martin R. G. Taylor[2]

[1]ARTbio Inc., Cambridge, MA, United States, [2]F-Prime Capital, London, United Kingdom

Radioligand therapy (RLT) is gaining traction as a safe and effective targeted approach for the treatment of many cancer types, reflected by a substantial and growing commercial market (valued at $7.78 billion in 2021, with a projected value of $13.07 billion by 2030). Beta-emitting RLTs have a long history of clinical success dating back to the approval of Zevalin and Bexxar in the early 2000s, later followed by Lutathera and Pluvicto. Alpha radioligand therapeutics (ARTs) offer the potential for even greater success. Driven by ground-breaking clinical results in early trials, improved isotope availability, and better understanding of isotope and disease characteristics, the global market for alpha emitters was estimated at $672.3 million for the year 2020, with projected growth to $5.2 billion by 2027. New company formations, promising clinical trial data, and progression for many radioligand therapy products, as well as an inflow of investor capital, are contributing to this expanding field. Future growth will be fueled by further efficacy and safety data from ART clinical trials and real-world results, but challenges remain. Radionuclide supply, manufacturing, and distribution are key obstacles for growth of the field. New models of delivery are needed, along with cross-disciplinary training of specialized practitioners, to ensure patient access and avoid challenges faced by early RLT candidates such as Zevalin and Bexxar. Understanding of the history of radiation medicine is critical to inform what may be important to the success of ART—most past projections were inaccurate and it is important to analyze the reasons for this. Practical considerations in how radiation medicine is delivered and administered are important to understand in order to inform future approaches.

KEYWORDS

**ART, distributed manufacturing, capacity, logistics, isotopes**

## Introduction

Alpha radioligand therapeutics (ARTs) have been gaining increasing attention as a rapidly advancing experimental modality that holds promise for delivering high doses of lethal radioactivity specifically to cancer cells. The combination of the high energy and short tissue range typical of alpha-emitting isotopes enables effective killing of the targeted tumor while sparing the surrounding normal tissue. ARTs offer the potential to overcome resistance to beta-emitting radioligand therapies, which have already entered the market, or chemotherapy drugs. The promise of alpha has led to growth in new clinical trials and new company formations fueled by risk-tolerant investors.

In this chapter, we explore the history of the targeted radioligand therapy commercial landscape, including the approval and performance of key drug candidates that have shaped the current and future directions of the field. We provide an overview of the current market and

its potential, as well as challenges faced in therapeutic and isotope availabilities and barriers for the delivery of ARTs at commercial scale.

# Section 1: Historical context

## The foundations of nuclear medicine and targeted therapies

The origins of radiotherapy start with the discovery of X-rays as the first radiative source by Wilhelm Conrad Röntgen in 1895, who realized their ability to penetrate human flesh to allow photography of higher-density substances such as bone. As diagnostics applications flourished, the ability of X-rays to selectively kill rapidly dividing cells did not go unnoticed. The clinical usefulness of radiation to treat cancer was observed in 1896, when Grubbe used X-rays from an improvised X-ray tube to treat patients with breast cancer and later lymphoma (1, 2).

However, it was Marie Skłodowska Curie who laid the real foundations for ART, and nuclear medicine in general, with the discovery of polonium and radium in 1898. Later, in 1902, Marie and Pierre Curie identified and purified radium-226 in the form of radioactive mineral salts isolated from radioactive pitchblende in their laboratory in Paris. In the following year, they shared the 1903 Nobel Prize in Chemistry with fellow scientist A. Henri Becquerel for their ground-breaking investigations of radioactivity, following the first observations that tumor-forming cells were destroyed faster than healthy cells when exposed to alpha-emitting radium-226 (3).

Early in its development, X-ray based radiation medicine struggled against its limits: directionality and localization, collateral damage. Therefore, many cancer physicians instead turned their attention to surgical techniques and other approaches (4). Nevertheless, ongoing innovation in external beam radiation and brachytherapy has been a hugely important development in cancer treatment, discussed in detail below.

While the physics and applications of radiation were being investigated, researchers remained intrigued by the concept of a molecular "magic bullet"–a term coined by Paul Erlich–to selectively deplete cancer cells while sparing healthy tissue. An array of approaches to achieve this effect has since been deployed in oncology, building on huge advances in cell and molecular biology over the past 50 years. This culminated many years later with the exciting possibility of being able to selectively direct a radioactive warhead to a target highly expressed uniquely on a cancer cell to engender selective cell killing.

## Modern day applications

Great progress has been achieved through radiation-centric approaches in the fields of diagnostics, nuclear medicine, and targeted therapies. Millions of lives have been saved as a result of faster and accurate diagnosis and treatment of injuries and diseases that would not have been possible without nuclear medicine, with significantly improved delivery of care. The medical X-ray market was estimated to be worth $12.4 billion in 2020 (5), while the global radiology market was valued at $26.6 billion in 2021 and is expected to reach $43.0 billion by 2029 (6).

The targeted therapeutics market has also grown substantially, valued at $67.7 billion in 2020 and projected to reach $87 billion by 2030 (7), with multiple targeted agents now approved for diseases such as cancer.

The use of nuclear medicine in oncology has also grown significantly: approximately 50% of all cancer patients receive radiation therapy during their course of illness, with two modern day applications of radiotherapy–external beam radiation therapy (EBRT) and brachytherapy–making up the bulk (8). One analysis of the US Surveillance, Epidemiology, and End Results (SEER) database estimated that 3.05 million cancer survivors were treated with either brachytherapy or EBRT in a single year, accounting for 29% of all cancer survivors that year–with breast (40%) and prostate cancer (23%) patients comprising the majority of radiation-treated survivors (9).

## External beam radiation therapy and brachytherapy–Lessons learned

EBRT used to deliver high-energy X-ray or electron beams to a patient's tumor.

Modern-day EBRT has proven to be hugely successful for its target indications. Men with high-risk localized prostate cancer treated with EBRT have a cure rate of around 91% (10): 10-years overall survival is above 80% (11), leading to commercial success (12). The global radiation oncology market is valued at $6.8 billion in 2020: EBRT dominated the field with a 79.3% revenue share in 2020, with expectations that it will continue to expand to reach revenue of $11.6 billion by 2030 (13).

Brachytherapy comes in the form of seeds, ribbons or wires placed within the body, in or near the tumor site. High-dose-rate brachytherapy temporarily introduces iridium isotopes close to the tumor site to deliver a higher dose of radiation over a shorter period of time and overcomes limitations of early brachytherapy approaches (14). Evidence-based medicine indicates that brachytherapy may be superior to EBRT in terms of efficacy and safety in several patient groups (15, 16). Survival rates are remarkable: 17-years survival of 97% in prostate cancer (17); 79.4% 3-years survival in cervical cancer patients (18).

These results supported the global brachytherapy market valuation of $788.5 million in 2020 with an expected compounded annual growth rate (CAGR) of 7.1% from 2021 to 2028 (13).

Despite the evidence supporting brachytherapy as an effective treatment modality for a wide range of malignancies, its use to treat patients with localized prostate cancer in the US and Europe saw a steady decline in recent years (19); the percentage of prostate cancer patients receiving brachytherapy dropped from 17% in 2002 to 8% in 2010 (20, 21).

A significant reason for this decline is the development of more technologically sophisticated treatments, including robot-assisted surgery and proton therapy, as well as more advanced forms of non-invasive EBRT such as IMRT and SBRT (20–26; **Figure 1**). Falling rates of brachytherapy administration in the US in favor of EBRT have also been attributed in part to financial considerations–a shift partly facilitated by hospital reimbursement policies that favor newer approaches. Brachytherapy is more labor- and cost-intensive for hospitals–some studies have shown that the total cost and staff time

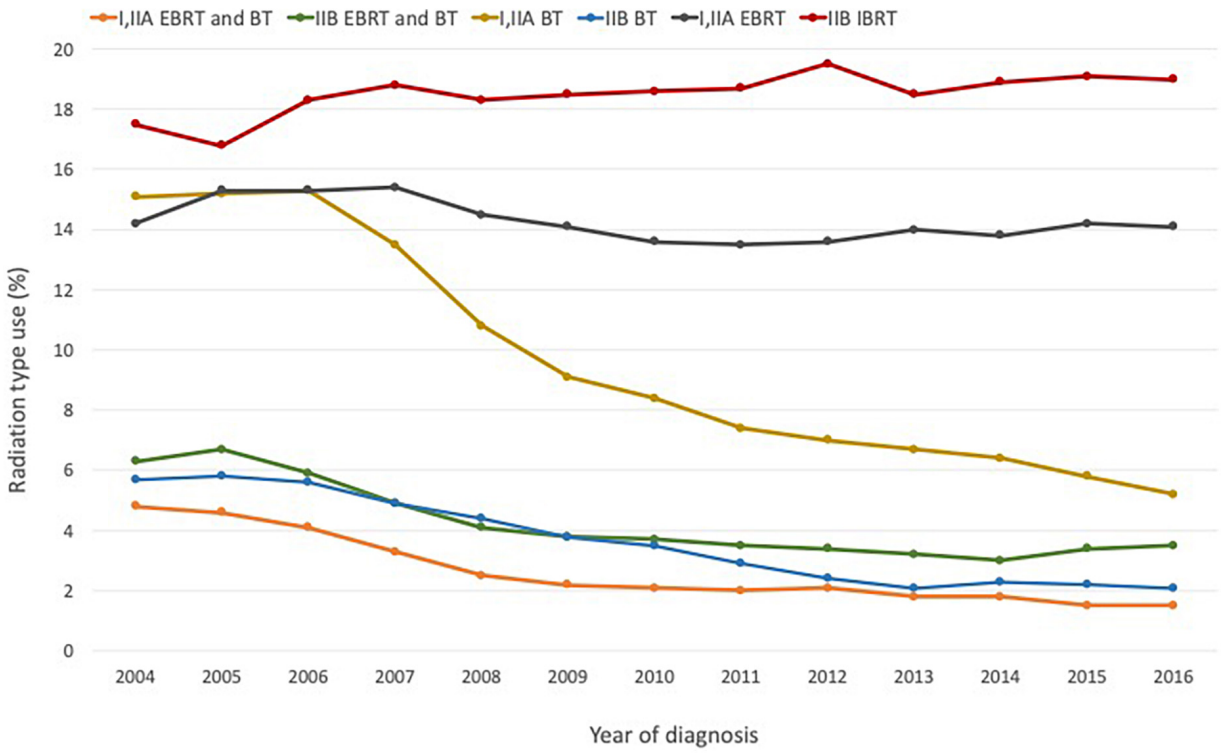


FIGURE 1
Radiation modality by stage and diagnosis year for prostate cancer based on NCDB data for the period 2004–2016. Figure adapted with permission from (23), ACS.

devoted to brachytherapy are double those of EBRT (27). In addition, the reimbursement levels set for EBRT are nearly double those for brachytherapy (22, 23).

## The first targeted radio-immunotherapies

Although EBRT and brachytherapy remain two of the most efficient tools for eliminating isolated and discrete cancer, their application in treatment of more advanced and systemic disease is limited. In parallel to their development, nuclear medicine pioneers such as Saul Hertz experimented with the therapeutic applications of metabolically targeted radionuclides, such as iodine-131 in thyroid cancer. Further major advances in this area occurred after the development of peptide receptor radionuclide therapy (PRRT) in the late 1980s by Mark Kaminski, Richard Wahl and colleagues at the University of Michigan (28, 29). In this approach, an engineered peptide (or antibody) aimed at a specific marker found in abundance on cancer cells would carry a radioactive atom capable of delivering a lethal dose of radiation to the tumor–creating a magic bullet against cancer.

Further developments in antibody conjugate technologies led to the launch of monocloncal antibody (mAb)-targeted radiotherapeutics in the early 2000s. Zevalin (yttrium-90-labeled anti-CD20 mAb) and its competitor Bexxar (iodine-131-labeled anti-CD20 mAb) were the first pioneers to appear on the market within this new class, approved for treatment-resistant slow-growing lymphoma.

## Zevalin

$^{90}$Y-ibritumomab tiuxetan (later marketed as Zevalin) is a radioactive drug product comprised of the beta-emitting isotope yttrium-90 linked to the mAb ibritumomab in conjunction with the chelator tiuxetan, and was designed to target the already validated cancer protein marker CD20 (30).

Developed by IDEC Pharmaceuticals, now part of Biogen Idec, $^{90}$Y-ibritumomab tiuxetan was the first radioimmunotherapy drug approved by the FDA to treat cancer. The drug had a superior response rate in patients who did not respond to rituximab (marketed as Rituxan by Genentech/Biogen Idec) (31–33).

$^{90}$Y-ibritumomab tiuxetan was approved by the FDA (2002) and EMA (2004) for treatment of patients with relapsed or refractory low-grade, follicular non-Hodgkin's lymphoma, including patients who were refractory to rituximab, and as consolidation therapy in follicular non-Hodgkin's lymphoma in patients who achieved a partial or complete response to first-line chemotherapy.

When Zevalin first came onto the market, Wall Street analysts had projected that sales would reach $100 million in 2003 (34). Merrill Lynch predicted it could eventually hit $500 million in sales, equivalent to approximately 20,000 doses a year (34). Despite the efficacy, better response rate compared to Rituxan, and an acceptable safety profile, Zevalin failed to meet forecasts (**Figure 2**). The launch was slow and it reached $15–30 million annually in the first decade, before undergoing a steady decline in sales from 2013 (Biogen and Spectrum financial reports). Issues cited with the slow uptake include high price, complicated prescribing, administration and monitoring

TABLE 1 Reasons cited for the commercial challenges of Zevalin and Bexxar, highlighting market-driven forces that contributed to declining sales and discontinuation of the drugs.

| | Zevalin | Bexxar |
|---|---|---|
| Preference for familiar tools and processes amongst physicians | X | X |
| Complicated prescribing, administration, and monitoring process | X | X |
| Complicated referral/referral outside of doctors' offices | X | X |
| Complex dosimetry requirements | X | X |
| Unclear data around long-term benefit/outcomes | X | X |
| Potential toxicities | X | X |
| High price/costs | X | X |
| Reimbursement challenges | X | X |
| Clinical trial strategy challenges/delays with FDA | | X |
| Manufacturing and supply-chain challenges | X | X |
| Public fears about radiation risks | X | X |

Note that Zevalin is still marketed for use in Europe.

process, and preference for familiar tools and processes and non-radioactive competitors amongst physicians (Table 1). The drug was divested by Spectrum Pharmaceuticals but is currently marked by Aurobindo Pharma Ltd., to treat non-Hodgkin's lymphoma in Europe, and by its subsidiary Acrotech Biopharma L.L.C. in the US (35).

## Bexxar

$^{131}$I-tositumomab (later marketed as Bexxar) was a radio-immunotherapeutic composed of the mAb tositumomab covalently bound to the radioisotope iodine-131. The compound was also targeted at the CD20 antigen and delivered a powerful local dose of gamma and beta radiation.

The drug was developed in the late 1990s by Coulter Pharmaceutical and acquired in 2000 by Corixa (36), who attracted significant investment for the manufacturing and marketing of the drug. Along with support from big pharma partner Glaxo Smith Kline (GSK), $^{131}$I-tositumomab had promising clinical trial data–its pivotal study enrolled 40 patients with non-Hodgkin's lymphoma with no treatment options following failed attempts with rituximab and several rounds of chemotherapy. Sixty-three percent of patients experienced significant tumor shrinkage with $^{131}$I-tositumomab and the benefit lasted more than 2 years (median 25 months), with 29% percent of patients entering complete remission. These results were supported by four additional single-arm studies in which overall response rates ranged from 47 to 64% with median response durations of 13–16 months (37).

The drug was granted orphan drug designation in 1994, and fast-track designation was added in 1998. $^{131}$I-tositumomab was first approved by the FDA and EMA in 2003 for patients refractory to rituximab or that had relapsed following chemotherapy; in 2004, the indication was expanded to include patients who had not been treated with rituximab. Approval was delayed in the US, however, by a series of FDA requests for information, and was granted 4 years after the new drug application was filed in June 1999. During those 4 years, the competing combination of Rituxan and chemotherapy established itself as the standard of care in non-Hodgkin's lymphoma.

Forecasts of Bexxar's market potential were high on the basis of an earlier US launch. In the year 2000, Data monitor estimated that Bexxar sales would reach $350 million by 2005; in February 2001, ABN Amro Predicted launch in 2001 and sales of $25 million, rising to $70 million in 2003. Bexxar sales failed to meet expectations following the delay by the FDA. First-quarter 2004 sales were $1.3 million, rising to just $2.2 million in the second quarter of 2004 (36).

Corixa, despite having remarkable clinical trial data, struggled to turn Bexxar into a commercial success, and was acquired by GSK in 2005 for $300 million. Bexxar usage peaked in 2006, and sales decreased by 30% annually thereafter. In 2012, only 75 patients received Bexxar (38). On 20 February 2014, GSK announced that the manufacture of Bexxar would be voluntarily discontinued, due a projected decline in sales and the availability of alternative treatments. Issues cited more widely included clinical trial strategy and issues with the FDA, complicated patient referral process, supply chain issues, reimbursement, and emergence of non-radioactive competitors. Safety concerns may also have contributed to the drug's dwindling use, following a 2011 trial suspension for a study comparing the use of $^{131}$I-tositumomab and rituximab in addition to chemotherapy among patients with newly diagnosed follicular lymphoma, an indication for which Bexxar had not received approval. Survival was worse in $^{131}$I-tositumomab arms of the study, and although not statistically significant, the results highlighted potential harms such as severe allergic reactions at the time of infusion and cytopenia (38).

## Market-driven challenges of Zevalin and Bexxar

Zevalin and Bexxar, as first-in-class targeted radiotherapeutics, shared some common commercial penetration issues (Table 1). Both drugs faced competition from Genentech and Biogen Idec's blockbuster drug Rituxan, which was the leading treatment at the time, and were considered expensive at around $25,000 per treatment. However, as one dose is usually enough, the cost of the drugs was actually similar to a full 4-months regimen of chemotherapy and Rituxan.

The radioactivity of the treatments made some oncologists worry that it might prevent them from giving other treatments later. Prescribing the drugs also requires oncologists to coordinate care with the hospitals that administer it–to get either drug, patients first receive a low-radiation diagnostic dose, then imaging scans, then a high-radiation therapeutic dose, which comes a week after the first dose. Other more familiar and thoroughly tested drugs were also preferred as first-line treatment, leading physicians to prescribe such drugs even when Zevalin and Bexxar might have worked better. Financial incentives were also at play–as Zevalin and Bexxar were radioactive, they were administered in hospitals by nuclear medicine experts following a referral by hematologists, who were likely to lose revenue in some markets. As a result, referral rates were lower than they could have been based on the product labels.

This led to the use of Zevalin and Bexxar as last resort treatments only. In 2007, it was estimated that fewer than 10% of lymphoma patients who were candidates for Zevalin and Bexxar ever received the therapies (39). Despite the potential and clinical data of the two

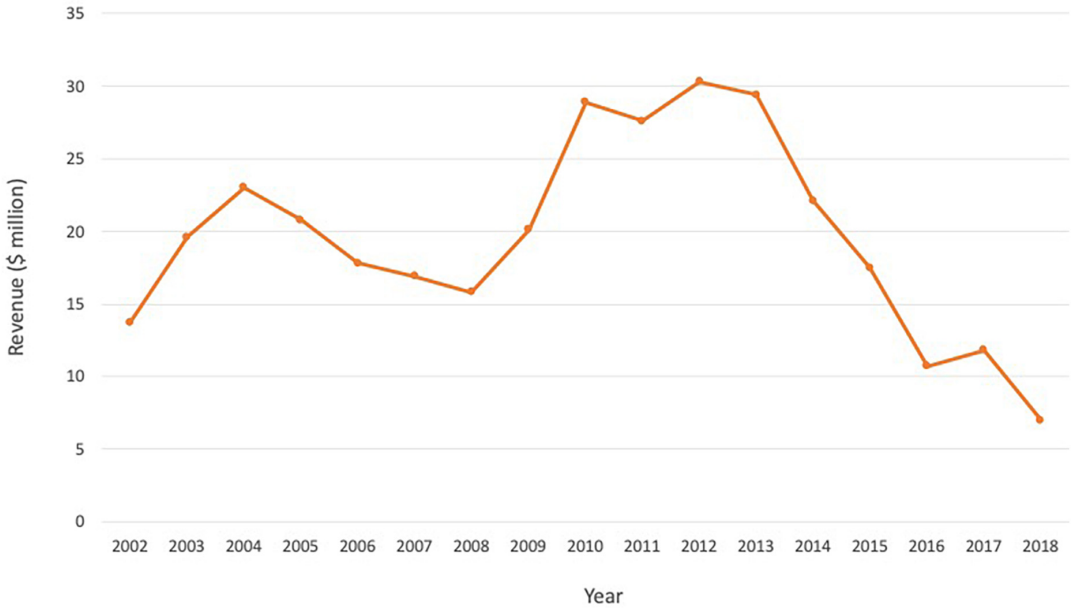


FIGURE 2
Annual revenue for Zevalin over the period 2002–2018, reflecting a steady decline and failure to meet forecasts. Source: Biogen and Spectrum financial reports.

drugs, the positive sales forecasts, and non-Hodgkin's lymphoma being a common cancer in Europe and the US that accounts for around 4% of all cases (40), the commercial challenges reflect the market-driven forces and the lack of coordination among physicians that can distort medical decisions.

## The arrival of alpha

While beta-emitters Zevalin and Bexxar traversed along their respective journeys, the development of targeted radionuclide therapies using different alpha-emitters was also in progress. The first alpha emitter to appear on the market was metabolically targeted, analogous to $^{131}$I for thyroid cancer.

## Xofigo

$^{223}$Ra-dichloride (later marketed as Xofigo) was the first alpha-emitter to enter the market. Once injected into the blood, its active moiety radium-223 mimics calcium and selectively targets bone due to natural tropism, with high specificity for areas of bone metastases.

First developed by Algeta and later by Bayer following a $2.9 billion acquisition, $^{223}$Ra-dichloride was designed to treat metastatic castration-resistant prostate cancer (mCRPC). In its pivotal ALSYMPCA Phase III trial, the compound resulted in a 30% reduction in the risk of death compared with placebo, and extended patient lives by a median of 14 months compared to 11.2 months (41, 42).

Use of $^{223}$Ra-dichloride was approved by the FDA in 2013 for mCRPC patients with symptomatic bone metastases. This was more than 3 months ahead of schedule due to the FDA's priority review program, with the trial ending early due to the drug's strong performance–reasons cited included the drug's precise targeting and strong risk–benefit profile. Approval was also received from the EMA in 2018.

Xofigo had very high commercial promise due to its high efficacy and targeting specificity, and its potential to treat late-stage prostate cancer patients with few other options. It was heralded as one of Bayer's "Big Five" crucial new drugs, and analysts estimated that annual sales could peak at around $1.5 billion by 2020 (43). However, although Xofigo fared significantly better than Zevalin and Bexxar, with sales reaching $300–400 million annually at its peak (**Figure 3**), it also faced challenges. Firstly, the prostate cancer market evolved rapidly with many non-radioactive competitors. Secondly, in 2017, safety concerns arose when the Phase III Era-223 clinical trial for use of $^{223}$Ra-dichloride in combination with abiraterone acetate (Johnson and Johnson's Zytiga) in mCRPC patients pre-chemo was terminated early. In the trial, the combination caused more fractures and deaths than abiraterone acetate alone (44). The resulting negative perceptions of the drug, the challenges to extend its use to earlier stages of prostate cancer, and the difficulties in combining with other emerging important prostate cancer medicines, made Xofigo subject to the increasing competition provided by new therapies. Xofigo may face additional commercial threats from the recently approved targeted radioligand therapy Lu-177-PSMA-617 (Pluvicto), which has the potential for utility in a broader population of metastatic prostate cancer patients; unlike Xofigo, Lu-177-PSMA-617 use is not restricted to patients with metastases predominantly in bone.

Following the failed trial and fast-changing nature of the prostate cancer market, analyst sales estimates fell. Xofigo revenues were no longer expected to breach $500 million in 2017, more than 4 years from launch (43). In 2018, Xofigo suffered a double-digit sales decline that continued for several years (**Figure 3**), exacerbated by COVID-19 restrictions (45). Despite the challenges, Xofigo remains an approved therapy for the treatment of prostate cancer and $^{223}$Ra-chloride is undergoing further evaluation in several ongoing trials;

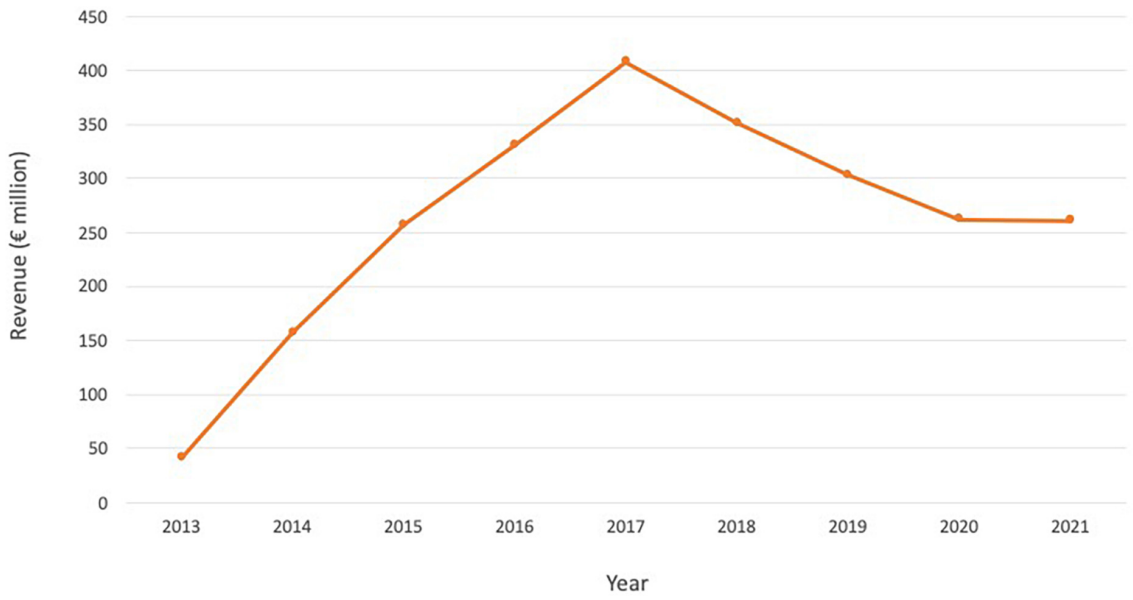


FIGURE 3
Annual revenue for Xofigo over the period 2013–2021. Source: Bayer annual reports.

the commercial performance of Xofigo has far exceeded those of the beta-emitters Zevalin and Bexxar (42).

# Section 2: Present

## Radioligand therapeutics come to life

Since the approvals of Zevalin, Bexxar and Xofigo, momentum has continued in the field. Promising proof-of-concept signals from small compassionate-use case series, investigator-led clinical trials, and improvements in tumor-targeting technologies resulted in more refined and optimized targeted RLTs. The next pivotal step in the evolution of the field came in the form of two major commercial transactions, Novartis' acquisitions of Advanced Accelerator Applications (AAA) and Endocyte in 2018.

## Movement in the RLT field: Novartis acquisitions of advanced accelerator applications and endocyte

In January 2018, Novartis announced the completion of its $3.9 billion ($41 per share) acquisition of radiopharmaceutical specialist AAA and its RLT candidate $^{177}$Lu-DOTATATE (later named Lutathera).

$^{177}$Lu-DOTATATE, which combines the beta-emitting radionuclide lutetium-177 with the somatostatin analogue DOTATATE to target somatostatin receptors (SSTRs) on tumor cells, was the first radiopharmaceutical on the market for PRRT (46). The drug gained rapid approval for clinical use following ground-breaking clinical data–in the NETTER-1 Phase III study of 229 patients with inoperable SSTR-positive advanced midgut neuroendocrine tumors, $^{177}$Lu-DOTATATE increased progression-free survival (65% versus 11% survival at 20 months) and response rate (18% versus 3%) compared with high-dose octreotide LAR (Sandostatin LAR Depot) (46–48). These results led to authorization by the EMA (2017) and the FDA (2018) for the treatment of SSTR-positive gastroenteropancreatic neuroendocrine tumors. The drug has also show potential in off-label use in other neuroendocrine tumors (e.g., bronchial) in both the US and Europe.

In December of the same year, Novartis announced completion of its $2.1 billion takeover of Endocyte and its lead asset $^{177}$Lu-PSMA-617 (later named Pluvicto). $^{177}$Lu-PSMA-617 was a RLT candidate in development against prostate-specific membrane antigen (PSMA)-positive mCRPC. Upon completion of the Phase III VISION trial, it was shown that $^{177}$Lu-PSMA-617 with standard of care reduced risk of death by 38% compared to standard of care alone and increased progression-free survival (8.7 months versus 3.4 months in the control group) and overall survival (15.3 versus 11.3 months) (49, 50). $^{177}$Lu-PSMA-617 became the first RLT to be approved by the FDA and EMA for mCRPC, receiving authorization from both agencies in 2022 alongside $^{68}$Ga gozetotid (Locametz)–a PSMA-targeted positron emission tomography imaging tracer that is used to identify patients suitable for treatment with the radioligand.

Novartis have initiated additional early stage development programs for $^{177}$Lu-PSMA-617 in earlier lines of prostate cancer therapy, with two other Phase III studies for mCRPC now ongoing. If successful, these trials could significantly increase the patient pool eligible for $^{177}$Lu-PSMA-617.

## A commercial success story, so far

Following the ground-breaking clinical data and approvals in US and Europe, and despite its indication for a rare cancer type, Lutathera brought in sales of $445 million in 2020, reaching over 5,000 patients (**Table 2**). Sales rose to $475 million in 2021 and continued to grow in all regions with approximately 450 centers now actively treating patients globally. As Lutathera becomes accessible

to more hospitals and clinics, the number of patients qualifying for the treatment is projected to increase. Analysts predict peak sales of Lutathera could exceed $800 million (**Figure 4**; 51).

Although too early to review longer-term revenue data for Pluvicto, Novartis reported initial sales of $10 million for Q2 2022 (52). Evaluate Vantage recently projected Pluvicto's 2026 sales of $851 million, while analysts at Jefferies have previously predicted that sales could reach $600 million in the current indication, with additional upside from further approvals (including the pre-chemotherapy setting in mCRPC and treatment-naive metastatic hormone-sensitive prostate cancer patients). The two additional trials in progress are expected to drive a 2–3x increase in currently modeled sales if successful, indicating the blockbuster potential of Pluvicto (**Figure 5**; 51).

In 2022, Novartis forecast annual sales up to or exceeding $1 billion for both Pluvicto and Lutathera, which together represent a major opportunity for Novartis in nuclear medicine (53). The company has also continued to increase its exposure to radiopharmaceuticals–for example by participation in the Series A financing of Aktis Oncology and the in-licensing of a other targeting agents from SOFIE Biosciences.

## Growth of new candidates and companies for RLT

The acquisition of AAA and Endocyte by Novartis triggered significant and growing interest and expectations for RLTs. The subsequent approvals and early robust market uptakes of the two lutetium-based drugs coupled with lofty future projections suggest better market readiness for RLTs than at the time of the launches of Zevalin and Bexxar two decades ago. This commercial success has in turn sparked the interest of investors and other large pharmaceutical companies looking to address unmet needs in cancer.

Several developments facilitated further expansion of the RLT concept for oncology. These included improved drug targeting; the increased availability of $^{177}$Lu and growing investment in production of alpha emitters; advances in new processes for efficient manufacturing of RLTs and increasing production capacity; and compelling clinical data. This progress transformed the dynamic, fueling a new flow of investor capital into these technologies and increasing mergers and acquisition (M&A) activity (28). As a result, momentum has continued to build in the nuclear medicine field, with the potential to elevate the profile of the entire sector. If the industry is able to effectively manage historical challenges, there is significant opportunity for a new and promising wave of RLTs to significantly change oncology treatment paradigms–particularly if alpha emitters are effectively utilized.

## Market reception for public and private companies

With this momentum, new company formation has grown since 2018, and pharma giants such as Bayer and Novartis continue to build early stage pipelines that expand into other targets and radioisotopes–with increasing focus on alpha-emitters.

Hard data and future potential attracted significant capital. For instance, prior to the Novartis acquisition, after the disclosure of the 79% reduction in the risk of disease progression or death for patients with SSRT-positive neuroendocrine tumors following treatment with $^{177}$Lu-DOTATATE in the NETTER-1 Phase III trial, AAA raised more than $75 million in an oversubscribed IPO in 2015. Investors again showed their support in October 2016, when AAA raised more than $150 million in a follow-on offering (28).

Private companies have also experienced positive market reception. Analysis indicates that at least 11 companies working in the ART space have raised significant amounts of capital during the period 2019–2022. We estimate the amount raised by those companies totalling close to $1.2 billion, although this estimate is not exhaustive given the private nature of some of this information. Much of the focus of this new investment has been on targeted alpha approaches as investors seek out opportunities with differentiated clinical efficacy potential. Investment has also continued into companies pursuing beta-based approaches which have a different risk profile given the existence of two approved products and a more established supply chain.

## Current state of the market

Promising clinical trial data, the inflow of investor capital, and M&A activity are contributing to an expanding radionucleotide field.

The overall global nuclear medicine market size expected to reach $24.4 billion by 2030 at a CAGR of 13.0% from 2022 to 2030 (54). Meanwhile, the global market for radioligand therapy is projected to reach $13.07 billion by 2030 (55). This is a reflection of increased public and private funding and clinical progression for many RLT products between 2018 and 2022, as well as increasing cancer prevalence. Other opportunities and drivers for further growth in the RLT market include the aging population, increased awareness and understanding of radiotherapy isotopes, product innovation and development, and improvements to isotope production and infrastructure for clinical use. Increasing use of radiopharmaceuticals by physicians and rising per capita health care expenditure will also boost the market's growth.

Beta-emitting isotopes currently dominate research efforts, as they have done since the inception of RLT (56). In September 2021, of 161 ongoing registered radionuclide therapy clinical trials, 133 were focused on beta-emitters and 28 on alpha-emitters (57). This has been driven mostly by the availability of isotopes such as lutetium and the market is expected to evolve to reflect a shift to alpha emitter therapeutics. The global market for alpha emitters was estimated at $672.3 million for the year 2020, with projections of $5.2 billion by 2027, indicating a CAGR of 34.1% over the period 2020–2027 (58). In comparison, beta emitters were projected to exhibit a CAGR of only 13.7% (56).

Despite the advances in RLT and the positive outlook of the projected commercial landscape, challenges in the commercial penetration and uptake remain. Primarily, radionuclide supply, manufacturing and distribution, in particular for alpha-emitting radionuclides, are key obstacles for growth of the field. Effective delivery of RLT requires carefully orchestrated manufacturing, transport and preparation of radiopharmaceuticals, and necessitates dedicated infrastructure and mechanisms for waste disposal. The existing model for manufacturing, transporting and preparing radioligand therapy is suitable for administering the therapy to a

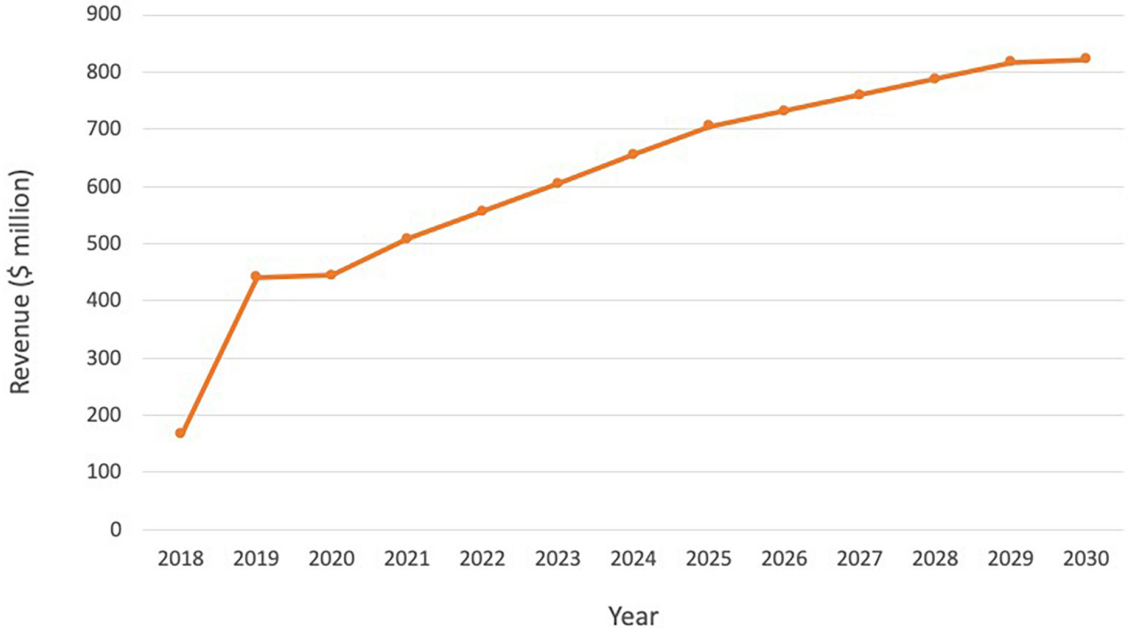


FIGURE 4
Lutathera sales and projected sales for the period 2018–2030. Source: (51).

**TABLE 2** Lutathera revenue and estimated number of doses and treatments for the period 2018–2021.

| Years | Lutathera revenue ($ million) | ASP per dose ($) | Implied number of Lutathera doses | Implied number of treatments (4 doses per treatment) |
|---|---|---|---|---|
| 2018 | 167 | 20,000 | 8,350 | 2,088 |
| 2019 | 441 | 20,000 | 22,050 | 5,513 |
| 2020 | 445 | 20,000 | 22,250 | 5,563 |
| 2021 | 475 | 20,000 | 23,750 | 5,938 |

Source: (93), Novartis annual report 2021.

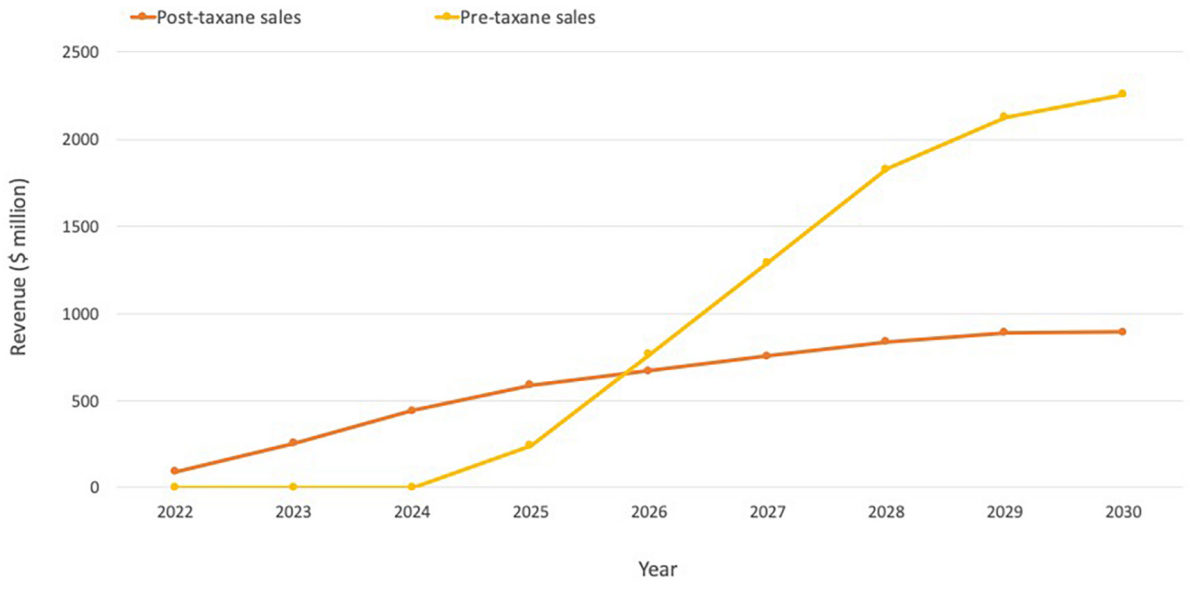


FIGURE 5
Pluvicto sales projections. Projections include estimates for both pre- and post-taxane markets assuming ~20% penetration in the US and ~15% elsewhere. If Pluvicto is approved for the pre-taxane market, it is estimated that this would lead to an additional ~$2 billion on top of current projections for the post-taxane market. Based on estimates from (51).

limited number of people per week, and so there is a need to develop different models for larger patient populations. These models of delivery will need to account for differences in radiopharmaceuticals, eligibility assessment techniques and number of treatment cycles (to be explored further in Section "Exploring models for the delivery of ART") (59, 60).

Additional challenges include the failure by physicians to adopt and rigorously evaluate this treatment modality, which may be explained in part by the multidisciplinary nature of the treatment and financial incentive challenges, as experienced by Zevalin and Bexxar (59). Public perception and fear of radioactivity, as well as the perceived complexity of the treatment, may also be a difficulty, but one that can be overcome with better communication of risk–benefit profiles and increasing positive data around side effects and effectiveness.

## Section 3: The future is alpha

Radioligand therapy (RLT) is a growing market despite the challenges faced. Assuming that the early ground-breaking results obtained with ART continue to be borne out in rigorous clinical trials, the growth of ART is also likely to accelerate over the use of EBRT.

### Benefits of alpha

Alpha particles are helium nuclei that are emitted from the nucleus of a radioactive atom. The amount of energy deposited per path length traveled (linear energy transfer or LET) is approximately 1,500 times greater than beta particles, leading to substantially more damage along the path of travel (59, 61, 62).

Depending on their emission energy, alpha particles can travel 50–100 μm in tissue. The combination of high energy and a short tissue range ensures the deposition of a large amount of energy within a short radius, leading to the effective killing of the targeted tumor with sparing of the surrounding normal tissue. This occurs due to direct DNA damage from alpha particle collisions with DNA, leading to severe DNA double-strand breaks, which are difficult to repair and trigger cell death. This is a key advantage of alpha-emitters as double-strand breaks are harder for a cell to survive than the single-stranded breaks induced by beta radiation (59, 61, 62).

### Differences among alphas

For radionuclides to be used effectively over time, commensurable with their half-life period, it is necessary to produce and isolate them, perform synthesis with the targeting molecule, and execute control of key parameters such as the absence of long-lived and/or toxic daughters (63–67). Each of these requirements is explored in more detail below.

#### Half-life

A shorter half-life means the radioisotopes must be isolated closer to the time and site of treatment, whereas a longer half-life means the radioisotope can be produced in a specialized, central location and subsequently delivered to hospitals and clinics, provided that the daughters can be stable in the complexes during delivery. The 9.92-day half-life of actinium-225 ($^{225}$Ac) is suitable from this perspective, but the poses potential toxicity risks stemming from mother radionuclide recoil caused by the energy from four successive alpha emissions in its decay cascade. In addition, care must be taken to ensure the quality of the product is not compromised by prolonged storage periods, which can occur due to radiolysis from the targeting ligand–these characteristics may limit the deployment of $^{225}$Ac therapeutics. Lead-212 ($^{212}$Pb), with a shorter but still manageable half-life of 10.64 h, decays to bismuth-212 ($^{212}$Bi) ($T_{1/2}$ = 1 h) and is used as a means to deliver $^{212}$Bi without being constrained by its shorter half-life. This allows for delivery of up to 10 times more dose per unit of administered activity and provides the possibility for the synthesis of complex radiopharmaceuticals with minimum loss of radioactivity during preparation (66).

#### Ability to complex

For a radiopharmaceutical to be used successfully, it must manifest sufficient stability *in vivo* to retain its targeting properties, and in the case of metal isotopes an appropriate chelator needs to be identified that matches the physical properties of the isotope to link the isotopes to targeting ligands (68, 69). With target in mind, the half-life of the isotope should also be compatible with the characteristics and half-life of the vector molecule (64, 65). Astatine-211 ($^{211}$At) ($T_{1/2}$ = 7.2 h) and $^{212}$Pb ($T_{1/2}$ = 10.64 h) exhibit favorable characteristics in this regard, with half-lives that are suitable to the kinetics of small peptides and small molecules that require short periods to reach an optimal tumor-to-blood dose ratio, as well as high decay efficiencies and stability to reduce toxicity (61, 64). Isotopes with longer half-lives are often complexed with long-lived antibodies: while the targeting is adequate, the long circulation times of antibodies may increase the risk of non-specific toxicity and off-target effects, e.g., toxicity to the bone marrow.

#### Toxicity

Many isotopes emit alpha particles but some leave behind toxic by-products or decay before they reach a cell. Issues arising when using $^{225}$Ac for therapy, for example, as mentioned above, include unwanted toxicity from recoiled daughter radionuclides without a targeting ligand (70). Upon the emission of an alpha particle, the radioactive daughter nuclides experience a recoil energy of about 100–200 keV, which is sufficient to allow the daughter nuclide to break free from the targeting agent. Further, the different chemical properties of the daughter radionuclide can make re-association with the chelator unlikely. These "free," untargeted daughter nuclides could be a source of dose-limiting toxicity.

When these factors are taken into account, despite that many different alpha-emitting radionuclides have been identified, only a few have desirable characteristics that render them suitable for clinical application (66, 67). Of the alpha-emitting radionuclides that have been identified as suitable for therapeutic use, several candidates have now been complexed to ligands such as PSMA inhibitors for evaluation in preclinical and clinical studies for cancer such as mCRPC (71). Following these early evaluations, four of the most promising isotopes emerging within the ART field are $^{225}$Ac, $^{211}$At, $^{212}$Pb, and thorium-227 ($^{227}$Th)–although $^{213}$Bi has been used with positive results in select malignancies, we are not aware of large scale commercial efforts with this isotope.

## Isotope availabilities

Medical isotope shortages are a concern globally due to limited source material and challenging production processes. Although many isotopes are produced in nature, extracting a significant amount of purified material demands an accelerator or nuclear reactor and the facilities and expertise to chemically separate out the desired isotope from many others created during production. Other strategies include generators, where a parent isotope decays to the desired radionuclide that is then extracted, and cyclotrons that accelerate and bombard a target using variety of particles, including protons, alpha particles, lithium, and carbon ions.

For the four isotopes identified as most suitable for therapeutic use, the availability and ease of production are therefore a key factor to consider for their use. Below is a state-of-play for each, including current and potential future availability and production methods.

### Astatine-211

$^{211}$At can be produced at reasonable yield and high radionucleic purity using an alpha-particle beam to bombard natural and widely available bismuth at ∼28 MeV *via* cyclotron irradiation. Despite being a straightforward method of production, the number of accelerators capable of a 28 MeV alpha-beam limits the availability of $^{211}$At, and current quantities are inadequate for widespread clinical use (72).

### Lead-212

The main production route of $^{212}$Pb is through the use of radium-224 ($^{224}$Ra)-based generators from which $^{212}$Pb is obtained by elution. This does not come without challenges–the generator must be replaced after 1–2 weeks due to the short half-life of $^{224}$Ra–but it can produce high yields of $^{212}$Pb (> 90% of expected activity per daily elution) and its daughter $^{212}$Bi at quantities sufficient for preclinical and clinical use. The US Department of Energy's Oak Ridge National Laboratory (ORNL) currently produces $^{212}$Pb using this approach, and some biotechnology companies are also developing their own facilities and methods to produce high-purity $^{212}$Pb (61). The short half-life of $^{212}$Pb and the relatively long separation times of the methods above reduced its applicability to date. However, several companies such as ARTBIO recently started to innovate such production processes and made significant process toward scaling up the supply of $^{212}$Pb through sustainable methods (73). While the specific production and purification methods of $^{212}$Pb are under development, there is good availability of the potential parent radionuclide $^{228}$Th, which provides good confidence in the ability of these approaches to ultimately scale to accommodate commercial therapeutic volumes.

### Actinium-225

$^{225}$Ac has limited availability as it can currently only be extracted by separation from the natural decay of $^{229}$Th that is obtained from waste stockpiles containing $^{233}$U (from past reactions for nuclear energy or nuclear weapons purposes). At present, there are two sources of $^{225}$Ac that have been used in clinical trials, held at ORNL in the US and the Institute for Transuranium Elements (ITU) in Karlsruhe, Germany. Additional sources are also available at the Leypunsky Institute for Physics and Power Engineer (IPPE) in the Russian Federation, South Africa's iThemba Laboratory for Accelerator Based Sciences and Canada's TRI-University Meson Facility (TRIUMF)" (74–77, 78, 79) **Table 4** lists the overall available capacities of current and future methods (75). Future production methods in development for the production of $^{225}$Ac include neutron, proton and deuteron irradiation of $^{226}$Ra targets, and high-energy proton irradiation of $^{232}$Th targets. Large-scale production of $^{225}$Ac by cyclotron proton irradiation of $^{226}$Ra has also shown promise (75).

### Thorium 227

$^{227}$Th has been commercially available for many years as it can be obtained in clinically meaningful quantities *via* beta-particle decay of $^{227}$Ac ($T_{1/2}$ = 21.8 years). Since it can be produced in virtually unlimited amounts with current technology, $^{227}$Th has attracted attention as a viable radionuclide for several forms of systemic radionuclide therapy (80, 81). $^{227}$Th is currently available from ORNL and the Pacific Northwest National Laboratory in the US, the Rosatom State Nuclear Energy Corporation in Russia, and from the pharmaceutical company Bayer (74).

Although production of most alpha-emitting isotopes remains limited, many industry experts assume that capacity will increase as clinical evidence supporting the benefits of ARTs grows over time. In addition, technology development continues in the public and private sectors (59). For example, **Table 3** shows current and anticipated production methods for therapeutic alpha-emitter systems. Location of the different facilities will also be important for the scale-up of isotope production for clinical and commercial use, as ART is delivered as a just-in-time therapy. For the widespread treatment of patients in the future, facilities will be needed in each continent to ensure broad access. Growing radioisotopes demand will require sustained efforts from the health and energy sectors to ensure consistent supply and delivery (particularly as there can be additional logistical difficulties in post-production processing and distribution to hospitals) (82).

## The rush to $^{225}$Ac

$^{225}$Ac has gained much attention as a promising isotope for use in ART, due to its 9.92-day half-life; high LET; manageable chelation and conjugation to targeting molecules such as antibodies and peptides; four net alpha particles emitted per decay for high lethality to target cells; and existing body of early clinical experience (83).

The efficacy of $^{225}$Ac was demonstrated in early first-in-human patient studies for mCRPC–one of which was conducted under a collaboration between the Joint Research Center in Karlsruhe and University Hospital Heidelberg in 2016 (84). Two patients in highly challenging clinical situations showed a positive response to $^{225}$Ac-PSMA-617 therapy–both experienced a complete response with prostate-specific antigen decline and no hematologic toxicity, with manageable xerostomia as the only notable side effect (85). While the clinical application of $^{225}$Ac-PSMA-617 was further developed with the collaboration of JRC and hospitals in Heidelberg, Pretoria and Munich, the remarkable potential of $^{225}$Ac also gained worldwide interest due to its use in a growing number of studies for patients with late mCRPC (86, 87). Consequently, an increasing number of novel $^{225}$Ac-labeled compounds are currently under development. We last counted 16 active clinical programs in clinicaltrials.gov

TABLE 3 Overview of current and potential production methods for four key alpha-emitting isotopes.

| Isotope | Half-life | Isotope availability | Main production approach | Current and potential production methods | |
|---|---|---|---|---|---|
| | | | | Method | Status |
| $^{211}$At | 7.21 h | Very low | Cyclotron | $^{209}$Bi(α,2n)$^{211}$At | Production |
| | | | | $^{232}$Th(p,x)$^{211}$Rn | Research |
| | | | | $^{238}$U(p,x)$^{211}$Rn | Research |
| | | | | $^{209}$Bi(7Li,5n)$^{211}$Rn | Research |
| | | | | $^{209}$Bi(6Li,4n)$^{211}$Rn | Research |
| $^{212}$Pb/$^{212}$Bi | 10.64/1 h | Scaling | Generator decay | $^{224}$Ra/$^{212}$Pb generator | Production |
| $^{225}$Ac | 9.92 days | Low–growing | Generator decay | $^{229}$Th/$^{225}$Ac generator | Production |
| | | | | $^{226}$Ra(p,2n)$^{225}$Ac | Research |
| | | | | $^{226}$Ra(γ,n)$^{225}$Ra | Potential |
| | | | | $^{226}$Ra(n,2n)$^{225}$Ra | Potential |
| | | | | $^{226}$Ra(d,3n)$^{225}$Ac | Potential |
| | | | | $^{232}$Th(p,x)$^{225}$Ac | Research |
| $^{227}$Th | 18.7 days | High | Generator decay | $^{227}$Ac decay | Production |
| | | | | $^{235}$U decay | Production |

Potential routes to increase production for each isotope include: $^{211}$At: explore production at existing and upcoming facilities and $^{221}$Rn generator routes; $^{212}$Pb/$^{212}$Bi: increase production of $^{228}$Th; $^{225}$Ac: provide additional stock of $^{229}$Th, scale up spallation on $^{232}$Th production and new cyclotron methods; $^{227}$Th: produce $^{227}$Ac *via* neutron irradiation of $^{226}$Ra. Source: (74, 94, 95).

TABLE 4 Summary of current and potential future capacity for key $^{225}$Ac production facilities.

| | Production method | Facility | Capabilities | Monthly $^{225}$Ac production (GBq) |
|---|---|---|---|---|
| Current sources | $^{226}$Th generator | ORNL | 0.704 g of $^{229}$Th | 2.2 |
| | | ITU | 0.215 g of $^{229}$Th | 1.1 |
| | | IPPE | 0.704 g of $^{229}$Th | 2.2 |
| Potential sources | $^{232}$Th(p, x)$^{225}$Ac | TRIUMF | 500 MeV, 120 μA | 11266.5 |
| | | BNL | 200 MeV, 173 μA | 2675.84 |
| | | INR | 160 MeV, 120 μA | 1002.0 |
| | | Arronax | 70 MeV, 2 × 375 μA | 462.1 |
| | | LANL | 100 MeV, 250 μA | 444.0 |
| | | iThemba LABS | 66 MeV, 250 μA | 127.7 |
| Future sources | $^{226}$Ra(p, 2n)$^{225}$Ac | 20 MeV, 500 μA cyclotron | | 3983.1 |
| | | 15 MeV, 500 μA cyclotron | | 1157.4 |
| | ISOL | TRIUMF (existing) | | 0.37 |
| | | TRIUMF (potential upgrades) | | 190.6 |
| | $^{226}$Ra(γ, n)$^{225}$Ra | Medical linac | 18 MeV, 26 μA | 48.1 |
| | | ALTO | 50 MeV, 10 μA | 55.5 |
| | $^{226}$Ra(n, 2n)$^{225}$Ra | Fast breeder reactor | | ∼37 |

Current production levels are listed for current sources, while values for potential sources list estimates of maximum possible production at sample of existing and operational facilities that have dedicated stations for large-scale medical isotope production. This list includes key facilities but is not exhaustive and does not include potential yet currently impractical methods that may be established in the future. However, without knowing details of each institution's target irradiation facilities, estimates have been based on maximal yield estimates with optimal site assumptions. As a result, practical yields will be lower. For example, while TRIUMF could theoretically produce 11.2 TBq of $^{225}$Ac per month, 3 TBq of monthly $^{225}$Ac production is a more practical estimate given the existing target station's size and cooling capacity. Reproduced from (75).

and we estimate double that number in pre-clinical stage as many companies do not publish their programs until start of clinical trials.

However, as noted above, $^{225}$Ac faces major production challenges due to scarce availability of source material and the infancy of alternative production methods. The total global annual $^{225}$Ac production volume is approximately 66 GBq, which is inadequate for current and future demand from researchers and for the development of new agents (75; **Figure 6**). Estimates of current demand for $^{225}$Ac are less than 185 GBq per year and it is estimated to grow by about 200–400 GBq per year for each $^{225}$Ac-based therapy that is approved for clinical use. Should efforts to develop $^{213}$Bi-based therapies also increase, $^{225}$Ac demand may be even higher (75).

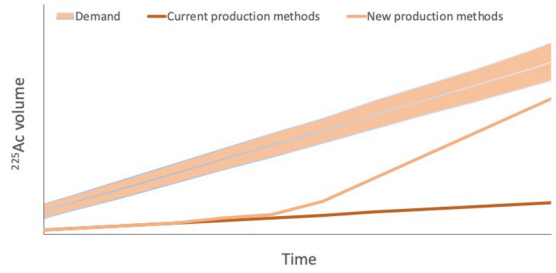


FIGURE 6
Projected $^{225}$Ac demand versus current $^{225}$Ac production *via* $^{229}$Th production from $^{223}$U legacy waste and potential future production. Current $^{225}$Ac production is estimated to be 55–65 GBq per year, which is inadequate even for current demand from researchers. Demand is projected to increase by 200–400 GBq per year for each $^{225}$Ac-based therapy that is approved for clinical use. Should efforts to develop $^{213}$Bi-based therapies also increase, $^{225}$Ac demand may be even higher, highlighting the importance of new production methods to increase $^{225}$Ac supply to meet increasing demand. However, it should be noted that estimates of both demand and future production capacity vary widely.

Private and public efforts to increase $^{225}$Ac supply for medical research and clinical use are ongoing. For example, in 2018, the International Atomic Energy Agency convened a meeting to discuss a global strategy to meet the rising demand for $^{225}$Ac. The resulting report described potential production routes *via* multiple sources, including proton cyclotrons, linear accelerators, and nuclear waste. The US Department of Energy is also supporting many initiatives to increase production quantities to meet market demand for trials and experimental drugs and is currently leading the Tri-Lab Research Effort to Provide Accelerator-Produced Actinium-225 for Radioimmunotherapy. Private companies such as TerraPower, a leading nuclear innovation company founded by Bill Gates and like-minded visionaries, are also contributing to efforts to increase production. While others are working to ramp up production of $^{225}$Ac by using a linear accelerator or cyclotron, TerraPower has been working since 2018 to increase the global supply of $^{225}$Ac from $^{229}$Th decay, and hopes to harvest the equivalent of 200,000 to 600,000 doses a year (100 times the number of doses currently available globally) from US Department of Energy $^{233}$U legacy wastes (88).

A delay is expected before production capacity can meet demand. Table 4 provides examples of current and potential sources of $^{225}$Ac production going forward. Although new production facilities have been set up or are under construction through efforts such as those of the US Department of Energy, new processes for supply expansion have not been fully developed, have only been demonstrated at small scale, or do not currently produce any commercially available quantities. It appears that the shift and rush to $^{225}$Ac has happened more quickly than with the beta emitter $^{177}$Lu: in that case, the supply has grown at a rate commensurate with the demand without creating long-term major shortages (89).

There is also significant concern in the sector that the rush to use $^{225}$Ac before full investigation of the stability of its chelated state and how its long-half life may result in potential toxicity was premature. In addition, the disconnect between supply and demand of $^{225}$Ac is slowing down academic research and is driving academic and industrial stakeholders to consider alternative isotopes such as $^{212}$Pb, which has a more favorable decay profile.

# Section 4: Delivery and optimization of ART

## Exploring models for the delivery of ART

There are a number of considerations when selecting an appropriate isotope for use in ART. Once an isotope–molecule combination has been matched to the target disease and its clinical profile, logistics and supply chains must also be built to match. Currently, it appears that several companies may have chosen the isotope first, based on logistics, rather than the approach proposed here. Developers face additional challenges in this space as guidelines and protocols vary between countries, adding complexity to an international delivery solution (82). The scale at which models are implemented may vary, with certain benefits and challenges associated with implementation at a localized or centralized level.

## Localized versus centralized models

A localized model, where manufacturing and administration facilities are co-located, could be beneficial for many reasons. Such a structure may reduce geographical access challenges compared to a centralized model where people are required to travel significant distances, or where isotope choice is limited due to the need to transport therapeutic doses over long distances, even across countries, for treatment. In the early days of RLT, physicians experimented locally in these ways.

A localized model may garner support by physicians as it could provide facilities with their own generators and production stations, improving treatment autonomy and the ease of referrals. Localized models of delivery and care may also alleviate the challenges posed by financial incentives and reimbursement that contributed to the issues experienced by Zevalin and Bexxar.

The regulatory framework for such a model is not well-developed for pharmaceuticals while there is significant experience in radioactive diagnostics: current frameworks would have to be adjusted while the purveyors of such models may also have to develop processes with different requirements and features to enable such models. Quality assurance and quality controls are fundamental parts of the currently accepted GMP standards: manufacturers are expected to adhere to such standards and ensure them in every country where they supply therapies. Regulators such as FDA and EMA routinely inspect manufacturers' facilities and quality management systems to ensure that patient safety is maintained in every batch that is released in markets. A localized model creates challenges to such approaches as each individual hospital could be considered a manufacturing site, each with their own approaches and facilities out of the management of the originator companies. Regulators may have to inspect hundreds or thousands of individual sites, raising fears that patients may receive therapeutic doses with varying characteristics across different hospitals.

In addition, several post-launch processes may become increasingly difficult: data collection pertaining to real-world use of the therapies; pharmacovigilance processes; product liability assignments; and others. In spite of this, it is worth remembering that distributed manufacturing models are routinely used in the nuclear medicine industry for diagnostic radionuclides such as $^{68}$Ga and $^{99m}$Tc, which have even shorter half -lives than $^{212}$Pb and can be produced with generators close to the point of use. It is therefore likely that a regulatory framework can be achieved for an analogous concept in the ART setting.

A centralized model fits within the existing regulatory framework, enabling consistent quality controls across manufacturing sites of a given manufacturer. Such facilities could offer advantages such as improved manufacturing infrastructure for high-volume production, streamlined influx of source material, more uniform rules for developers and better regulatory and quality control. In a centralized model, it should also be easier to assemble and train teams with the relevant manufacturing expertise in this budding new area.

Centralized models do, however, create supply chain risk. A manufacturing network with few facilities and low supply chain redundancy may lead to radionuclide shortages and disrupt patient treatment. For example, in May 2022, Novartis was forced to halt production of both Lutathera and Pluvicto at facilities in Italy, the US and Canada due to quality issues. Delivery of Lutathera was suspended in the US and Canada as a result, and delivery of Pluvicto was also suspended in the US. The disruption led to shortages in Europe and Asia, but these areas were also supplied from another facility in Zaragoza, Spain. Enrolment for clinical trials of Pluvicto stopped globally, as did Lutathera's clinical studies in the US and Canada (90, 91).

## A way forward: Distributed model

Looking to the future, a middle ground may be the best option in the form of a distributed model, with a moderate number of manufacturing facilities supported by an integrated supply network. This may overcome challenges that prevent rapid scale up on a local level, while addressing challenges such as long patient travel, isotope transport times, supply chain security, and regulatory consistency.

In this model, although not every country (or state in the US) may have its own production and manufacturing facility, multiple sites could ensure that therapies are more accessible, reducing patient travel and therapy transport times. Such a network may also be more resilient to supply chain shocks, and render regulatory compliance more manageable than in the localized model. A network of 10–15 sites per region may be sufficiently redundant for a resilient supply chain and it should be manageable from a regulatory perspective.

Distributed networks are known to be far more stable and productive than centralized alternatives, and the redundancy that would be introduced will be essential for effective and stable therapeutic supply in the future. Taking the internet as example, network redundancy provides multiple paths for traffic, so that data can keep flowing even in the event of a failure. Put simply, more redundancy equals more reliability. The redundancy created by distributed networks can be considered necessary complexity to reduce the probability of failures that could impact the entire network and, ultimately, patients' lives.

Currently, the unexpected closing of one reactor or one specialized laboratory could already lead to worldwide problems in the supply of medical radionuclides and therapeutics. Other reactors or manufacturing sites may not always absorb the increased demand. This phenomenon was eminently on display during the productions issues of Novartis described above (90, 92).

# Conclusion and future outlook

Alpha radioligand therapeutics (ARTs) offer great promise for the treatment of cancer that is reflected in high expectations for patient impact and financial returns. It is encouraging to see this reflected by the rapid growth of ART-focused companies and expanding clinical pipelines within the field. Future growth will be fueled by further efficacy and safety data from ART clinical trials and real-world results–with expanded investigations of earlier stages of cancer. Thorough investigations of the fundamentals of ART coupled with combination therapies with other modalities, particularly immunotherapeutics, provide fertile ground for academic and industrial researchers alike. Sustained efforts to increase the availability of isotopes by establishing more manufacturing facilities and new methods of production are key to successful growth of the field. Such advances will need to keep pace with each other to avoid situations such as the current expected imbalance between supply and demand of $^{225}$Ac. Cross-disciplinary training of specialized practitioners to overcome the referral challenges to adoption will also need to be supplemented with an adjustment of financial incentives that puts patients first. New delivery models must also be developed and implemented to provide equal and resilient patient access. This innovation will require that regulatory frameworks evolve at the speed of the rest of the field in order to balance the needs of all stakeholders.

# Author contributions

Both authors listed have made a substantial, direct, and intellectual contribution to the work, and approved it for publication.

# Funding

This manuscript was partially supported by ARTbio Inc.

# Conflict of interest

EO was employed by ARTbio Inc. MT was employed by F-Prime Capital.

# Publisher's note

# References


1. British Medicine Journal. Obituary: E. H. GRUBBE, M.D., F.A.C.P. *Br Med J.* (1960) 2:609. doi: 10.1136/bmj.2.5198.609-a

2. Vujošević B, Bokorov B. Radiotherapy: past and present. *Arch Oncol.* (2010) 18:140–2.

3. Zustovich F, Barsanti R. Targeted α therapies for the treatment of bone metastases. *Int J Mol Sci.* (2018) 19:74. doi: 10.3390/ijms19010074

4. Timins JK. Communication of benefits and risks of medical radiation: paper communication of benefits and risks of medical radiation: a historical perspective. *Health Phys.* (2011) 101:562–5. doi: 10.1097/HP.0b013e3182259a71

5. Fortune Business Insights. *Medical X-ray Market Size, Share & Growth Report [2021-2028]*. Baner Gaon: Fortune Business Insights (2021).

6. Data Bridge Market Research. *Global Radiology Market – Industry Trends and Forecast to 2029*. Hadapsar: Data Bridge Market Research (2022).

7. Vision Research. *Targeted Therapeutics Market Size, Growth, Trends, Revenue, Forecast 2021-2030*. Wayne, NY: Vision Research (2022).

8. Baskar R, Lee KA, Yeo R, Yeoh K. Cancer and radiation therapy: current advances and future directions. *Int J Med Sci.* (2012) 9:193–9.

9. Bryant AK, Banegas MP, Martinez ME, Mell LK, Murphy JD. Trends in radiation therapy among cancer survivors in the United States, 2000–2030. *Cancer Epidmiol Biomark Prev.* (2017) 26:963–70. doi: 10.1158/1055-9965.EPI-16-1023

10. Targeting Cancer. *Radiation Therapy: Effective for Prostate Cancer Accessed*. (2022). Available online at: https://www.targetingcancer.com.au/2015/02/radiation-therapy-95-effective-prostate-cancer/ (Accessed October 27, 2022).

11. Boladeras A, Martinez E, Ferrer F, Gutierrez C, Villa S, Pera J, et al. Localized prostate cancer treated with external beam radiation therapy: long-term outcomes at a European comprehensive cancer centre. *Rep Pract Oncol Radiother.* (2016) 21:181–7. doi: 10.1016/j.rpor.2015.12.002

12. Transparency Market Research. *External Beam Radiation Therapy Market - Global Industry Analysis, Size, Share, Growth, Trends, and Forecast, 2020 - 2030*. Baner: Transparency Market Research (2021).

13. Grandview Research. *Radiation Oncology Market Size, Share & Trends Report 2021 - 2028*. Baner: Grandview Research (2022).

14. Lim YK, Dohyeon K. Brachytherapy: a comprehensive review. *Prog Med Phys.* (2021) 32:25–39.

15. Kee DLC, Peiffert D, Hannoun-Lévi J. Brachytherapy boost for prostate cancer: a national survey from groupe curiethérapie – société française de radiothérapie oncologique. *Cancer Radiother.* (2019) 23:847–52. doi: 10.1016/j.canrad.2019.06.003

16. Xie X, Zhang Y, Ge C, Liang P. Effect of brachytherapy vs. external beam radiotherapy on sexual function in patients with clinically localized prostate cancer: a meta-analysis. *Front Cell Dev Biol.* (2022) 9:792597. doi: 10.3389/fcell.2021.792597

17. Lazarev S, Thompson MR, Stone NN, Stock RG. Low-dose-rate brachytherapy for prostate cancer: outcomes at >10 years of follow-up. *BJU Int.* (2018) 121:781–90.

18. Li R, Shinde A, Chen Y, Amini A, Lee S, Dellinger T, et al. Survival benefit of adjuvant brachytherapy after hysterectomy with positive surgical margins in cervical cancer. *Int J Radiat Oncol Biol Phys.* (2018) 102:373–82.

19. The Lancet Oncology. Brachytherapy—a dose of pragmatism needed. *Lancet Oncol.* (2021) 22:737. doi: 10.1016/S1470-2045(21)00299-0

20. Eisenstein M. The declining art of brachytherapy. *Nature.* (2019) 574:S81.

21. Zaorsky NG, Davis BJ, Nguyen PL, Showalter TN, Hoskin PJ, Yoshioka Y, et al. Evolution of brachytherapy for prostate cancer. *Nat Rev Urol.* (2017) 14:415–39.

22. Petereit DG, Frank S, Viswanathan A, Erickson B, Eifel P, Nguyen P, et al. Brachytherapy: where has it gone? *J Clin Oncol.* (2015) 33:980–2. doi: 10.1200/JCO.2014.59.8128

23. Brookland RK, Mallin K. *Current Trends in Prostate Cancer: The Role of Brachytherapy. Bull*. New York, NY: ACS (2019).

24. Nguyen KA, Lee A, Patel SA, Chakravorty A, Yu JB, Kishan AU, et al. Trends in use and comparison of stereotactic body radiation therapy, brachytherapy, and dose-escalated external beam radiation therapy for the management of localized, intermediate-risk prostate cancer. *JAMA Netw Open.* (2020) 3:e2017144. doi: 10.1001/jamanetworkopen.2020.17144

25. Gill BS, Lin JF, Krivak TC, Sukumvanich P, Laskey RA, Ross MS, et al. National cancer data base analysis of radiation therapy consolidation modality for cervical cancer: the impact of new technological advancements. *Int J Radiat Oncol Biol Phys.* (2014) 90:1083–90. doi: 10.1016/j.ijrobp.2014.07.017

26. Roberts KB, Soulos PR, Herrin J, Yu JB, Long JB, Dostaler E, et al. The adoption of new adjuvant radiation therapy modalities among medicare beneficiaries with breast cancer: clinical correlates and cost implications. *Int J Rad Oncol Biol Phys.* (2013) 85:1186–92. doi: 10.1016/j.ijrobp.2012.10.009

27. Bauer-Nilson K, Hill C, Trifiletti D, Libby B, Lash D, Lain M, et al. Evaluation of delivery costs for external beam radiation therapy and brachytherapy for locally advanced cervical cancer using time-driven activity-based costing. *Int J Radiat Oncol Biol Phys.* (2018) 100:88–94. doi: 10.1016/j.ijrobp.2017.09.004

28. Sherman M, Levine R. Nuclear medicine and wall street: an evolving relationship. *J Nucl Med.* (2019) 60:9. doi: 10.2967/jnumed.118.220798

29. Faijtel D, de Jong M, Nonnekens J. Peptide receptor radionuclide therapy: looking back, looking forward. *Curr Top Med Chem.* (2020) 20:2959–69. doi: 10.2174/1568026620666200226104652

30. Hernandez MC, Knox SJ. Radiobiology of radioimmunotherapy with 90Y ibritumomab tiuxetan (Zevalin). *Semin Oncol.* (2003) 30:6–10. doi: 10.1053/j.seminoncol.2003.10.005

31. Knox SJ, Goris ML, Trisler K, Negrin R, Davis T, Liles TM, et al. Yttrium-90-labeled anti-CD20 monoclonal antibody therapy of recurrent B-cell lymphoma. *Clin Cancer Res.* (1996) 2:457–70.

32. Witzig TE. The use of ibritumomab tiuxetan radioimmunotherapy for patients with relapsed B-cell non-Hodgkin's lymphoma. *Semin Oncol.* (2000) 27:74–8.

33. Marcus R. Use of 90Y-ibritumomab tiuxetan in non-Hodgkin's lymphoma. *Semin Oncol.* (2005) 32(Suppl. 1):S36–43.

34. Berenson A. *Market Forces Cited in Lymphoma Drugs' Disuse*. New York, NY: New York Times (2007).

35. Business Wire. *Spectrum Pharmaceuticals Sells Marketed Portfolio to Acrotech Biopharma L.L.C. to Focus on New and Innovative Therapies for Cancer Patients*. San Francisco, CA: Business Wire (2019).

36. Corixa. *Corixa Corp: 8-K - Current Report*. Corixa: Washington, DC (2004).

37. Pharmacyce,. *BEXXAR§ Tositumomab and Iodine I 131 Tositumomab*. Albuquerque, NM: Pharmacyce (2022).

38. Prasad V. The withdrawal of drugs for commercial reasons the incomplete story of tositumomab. *JAMA Intern Med*. (2014) 174:1887–8. doi: 10.1001/jamainternmed.2014.5756

39. NBC News. *Smart-Bomb' Drugs for Lymphoma Underused*. New York, NY: NBC News (2007).

40. Cai W. Trends analysis of non-hodgkin lymphoma at the national, regional, and global level, 1990–2019: results from the global burden of disease study 2019. *Front Med.* (2021) 8:738693. doi: 10.3389/fmed.2021.738693

41. Parker C, Nilsson S, Heinrich D, Helle SI, O'Sullivan JM, Foss SDÅ, et al. Alpha emitter radium-223 and survival in metastatic prostate cancer. *N Engl J Med.* (2013) 369:213–23.

42. Skelton WP, Dibenedetto SW, Pang SS, Pan K, Barish JL, Nwosu-Iheme A, et al. A single-center retrospective analysis of the effect of radium-223 (Xofigo) on pancytopenia in patients with metastatic castration-resistant prostate cancer. *Cureus.* (2020) 12:e6806. doi: 10.7759/cureus.6806

43. Plieth J. *Bayer's Pharma day Turns into a Pharma Nightmare*. London: Evaluate Vantage (2017).

44. Smith M, Parker C, Saad F, Miller K, Tombal B, Ng QS, et al. Addition of radium-223 to abiraterone acetate and prednisone or prednisolone in patients with castration-resistant prostate cancer and bone metastases (ERA 223): a randomised, double-blind, placebo-controlled, phase 3 trial. *Lancet.* (2019) 20:408–19.

45. Liu A. *Bayer's Growth-Driving Quintet? Better Make it a Trio, Thanks to Stivarga and Xofigo Stall*. Washington, DC: Fierce Pharma (2018).

46. Hennrich U, Kopka J. Lutathera§: the first FDA- and EMA-approved radiopharmaceutical for peptide receptor radionuclide therapy. *Pharmaceuticals.* (2019) 12:114. doi: 10.3390/ph12030114

47. NIH. *New Therapy Benefits Patients with Neuroendocrine Tumors*. Bethesda, MA: NIH (2017).

48. Strosberg J, El-Haddad G, Wolin E, Hendifar A, Yao J, Chasen B, et al. Phase 3 trial of 177Lu-dotatate for midgut neuroendocrine tumors. *N Engl J Med.* (2017) 376:125–35.

49. Sartor O, Bono J d, Chi KN, Fizazi K, Herrmann K, Rahbar K, et al. Lutetium-177–PSMA-617 for metastatic castration-resistant prostate cancer. *N Engl J Med.* (2021) 385:1091–103.

50. Novartis. *Novartis Pluvicto™ Approved by FDA as first Targeted Radioligand Therapy for Treatment of Progressive, PSMA Positive Metastatic Castration-Resistant Prostate Cancer*. Basel: Novartis (2022).

51. Bernstein. *Novartis: First PSMA-617 Headlines Positive - Initial Thoughts and Deep Dive*. Nashville, TE: Bernstein (2021).

52. Novartis. *Novartis Financial Results – Q2 2022*. Basel: Novartis (2022).

53. Pagliarulo N. *Novartis Suspends Production of two Radiopharmaceutical Drugs Over Quality Concerns*. Washington, DC: BioPharma Dive (2022).

54. ITN. *Global Nuclear Medicine Market Analysis Report*. London: ITN (2022).

55. P&S Intelligence. *Global Radioligand Therapy Market Size, Share, Growth Drivers, Regional Forecast Analysis 2030*. Noida: P&S Intelligence (2022).

56. Research and Markets. *Global Radiopharmaceuticals Market – Products and Applications*. Dublin: Research and Markets (2019).

57. Point BioPharma. *The First Principles of Radiopharmaceuticals*. Indianapolis, IA: Point BioPharma (2021).

58. Research and Markets. *Alpha Emitters - Global Market Trajectory & Analytics*. Dublin: Research and Markets (2021).

59. Sgouros G. Radiopharmaceutical therapy in cancer: clinical advances and challenges. *Nat Rev Drug Discov.* (2020) 19:589–608.

60. Health Policy Partnership. *Health System Readiness for Radioligand Therapy in the UK*. London: Health Policy Partnership (2021).

61. Kokov KV, Egorova BV, German MN, Klabukov ID, Krasheninnikov ME, Larkin-Kondrov AA, et al. 212Pb: production approaches and targeted therapy applications. *Pharmaceutics.* (2022) 14:189. doi: 10.3390/pharmaceutics14010189

62. Scheinberg D. *Actinium-225 and Bismuth-213 alpha Particle Immunotherapy of Cancer. In "Alpha Emitting Radionuclides and Radiopharmaceuticals for Therapy*. Vienna: IAEA (2013).

63. Huclier-Markai S, Alliot C, Varmenot N, Cutler C, Barbet J. Alpha-emitters for immuno-therapy: a review of recent developments from chemistry to clinics. *Curr Top Med Chem.* (2012) 12:2642–54. doi: 10.2174/1568026611212230002

64. Hatcher-Lamarre JL, Sanders VA, Rahman M, Cutler CS, Francesconi LC. Alpha emitting nuclides for targeted therapy. *Nucl Med Biol.* (2021) 92:228–40.

65. Poty S, Francesconi L, McDevitt M, Morris M, Lewis J. α-Emitters for radiotherapy: from basic radiochemistry to clinical studies-Part 1. *J Nucl Med.* (2018) 59:878–84. doi: 10.2967/jnumed.116.186338

66. Poty S, Francesconi LC, McDevitt MR, Morris MJ, Lewis JS. α-Emitters for radiotherapy: from basic radiochemistry to clinical studies—Part 2. *J Nucl Med.* (2018) 59:1020–7. doi: 10.2967/jnumed.117.204651

67. Lindegren S, Albertsson P, Bäck T, Jensen H, Palm S, Aneheim E. Realizing clinical trials with astatine-211: the chemistry infrastructure. *Cancer Biother Radiopharm.* (2020) 35:425–36. doi: 10.1089/cbr.2019.3055

68. Vincentis GD, Gerritsen W, Gschwend JE, Hacker M, Lewington V, O'Sullivan JM, et al. Advances in targeted alpha therapy for prostate cancer. *Ann Oncol.* (2019) 30:1728–39.

69. Yang H, Wilson J, Orvig C, Li Y, Wilbur D, Ramogida C, et al. Harnessing α-emitting radionuclides for therapy: radiolabeling method review. *J Nucl Med.* (2022) 63:5–13. doi: 10.2967/jnumed.121.262687

70. Kruijff Robin MD, Wolterbeek Hubert T, Denkova Antonia G. A critical review of alpha radionuclide therapy—how to deal with recoiling daughters? *Pharmaceuticals.* (2015) 8:321–36. doi: 10.3390/ph8020321

71. Sathekge MM, Bruchertseifer F, Vorster M, Morgenstern A, Lawal IO. Global experience with PSMA-based alpha therapy in prostate cancer. *Eur J Nucl Med Mol Imaging.* (2021) 49:30–46.

72. Feng Y, Zalutsky MR. Production, purification and availability of 211At: near term steps towards global access. *Nucl Med Biol.* (2021) 100-101:12–23. doi: 10.1016/j.nucmedbio.2021.05.007

73. Li, RG, Stenberg V, Larsen R. A novel experimental generator for production of high purity lead-212 for use in radiopharmaceuticals. *J Nucl Med.* (2022). doi: 10.2967/jnumed.122.264009

74. Radchenko V, Morgenstern A, Jalilian A, Ramogida C, Cutler C, Duchemin C, et al. Production and supply of α-particle–emitting radionuclides for targeted α-therapy. *J Nucl Med.* (2021) 62:1495–503. doi: 10.2967/jnumed.120.261016

75. Robertson AK, Ramogida CF, Schaffer P, Radchenko V. Development of 225Ac radiopharmaceuticals: TRIUMF perspectives and experiences. *Curr Radiopharm.* (2018) 11:156–72. doi: 10.2174/1874471011666180416161908

76. Actinide Research Quarterly. *4th Quarter 2009/1st Quarter 2010*. Los Alamos, NM: Los Almos National Laboratory (2010).

77. Nuclear Engineering International. *IBA and SCK CEN to Collaborate in Production of Actinium-225*. London: Nuclear Engineering International (2021).

78. Ahenkorah S, Cassells I, Deroose CM, Cardinaels T, Burgoyne AR, Bormans G, et al. Bismuth-213 for targeted radionuclide therapy: from atom to bedside. *Pharmaceutics.* (2021) 13:599. doi: 10.3390/pharmaceutics13050599

79. Lederman M. The early history of radiotherapy: 1895–1939. *Int J Radiat Oncol Biol Phys.* (1981) 7:639–48. doi: 10.1016/0360-3016(81)90379-5

80. Hagemann UB, Wickstroem K, Hammer S, Bjerke RM, Zitzmann-Kolbe S, Ryan OB, et al. Advances in precision oncology: targeted thorium-227 conjugates as a new modality in targeted alpha therapy. *Cancer Biother Radiopharm.* (2020) 35:497–510. doi: 10.1089/cbr.2020.3568

81. Elgqvist J, Frost S, Pouget J, Albertsson P. The potential hurdles of targeted alpha therapy– clinical trials and beyond. *Front Oncol.* (2014) 3:324. doi: 10.3389/fonc.2013.00324

82. Merkel C, Whicher CH, Bomanji J, Herrmann K, Ækwikła J, Jervis N, et al. Realising the potential of radioligand therapy: policy solutions for the barriers to implementation across Europe. *Eur J Nucl Med.* (2020) 47:1335–9. doi: 10.1007/s00259-020-04745-7

83. Thiele NA, Brown V, Kelly J, Amor-Coarasa A, Jermilova U, MacMillan S, et al. An eighteen-membered macrocyclic ligand for actinium-225 targeted alpha therapy. *Angwe Chem.* (2017) 56:14712–7. doi: 10.1002/anie.201709532

84. Kratochwil C, Bruchertseifer F, Giesel FL, Weis M, Verburg FA, Mottaghy F, et al. 225Ac-PSMA-617 for PSMA-targeted α-radiation therapy of metastatic castration-resistant prostate cancer. *J Nucl Med.* (2016) 57:1941–4. doi: 10.2967/jnumed.116.178673

85. Satapathy S, Sood A, Das CK, Mittal BR. Evolving role of 225Ac-PSMA radioligand therapy in metastatic castration-resistant prostate cancer—a systematic review and meta-analysis. *Nature.* (2021) 24:880–90. doi: 10.1038/s41391-021-00349-w

86. Morgenstern A, Apostolidis C, Bruchertseifer F. Supply and clinical application of actinium-225 and bismuth-213. *Semin Nucl Med.* (2020) 50:119–23.

87. Feuerecker B, Tauber R, Knorr K, Heck M, Beheshti A, Seidl C, et al. Activity and adverse events of actinium-225-PSMA-617 in Advanced Metastatic Castration-resistant Prostate Cancer After Failure of Lutetium-177-PSMA. *Eur Urol.* (2021) 79:343–50. doi: 10.1016/j.eururo.2020.11.013

88. Yan W. *Mining Medical Isotopes from Nuclear Waste*. C&EN: Washington, D.C (2020).

89. Vogel WV, van der Marck SC, Versleijen MWJ. Challenges and future options for the production of lutetium-177. *Eur J Nucl Med Mol Imaging.* (2021) 48:2329–35. doi: 10.1007/s00259-021-05392-2

90. Liu A. *Novartis Halts US Production of Cancer Radiotherapies, Citing Potential Quality Issues*. Washington, DC: Fierce Pharma (2022).

91. Novartis. *Novartis Annual Report 2021*. Basel: Novartis (2022).

92. Novartis. *Novartis Provides Update on Production of Radioligand Therapy Medicines*. Basel: Novartis (2022).

93. Eckert Ziegler, GA. 2021. Available online at: https://www.ezag.com/fileadmin/user_upload/ezag/investors-analysen/englisch/Hauck_und_Aufhaeuser_2021_03_10_englisch.pdf (accessed September 1, 2022).

94. Juzeniene A, Stenberg VY, Bruland ØS, Larsen RH. Preclinical and clinical status of PSMA-targeted alpha therapy for metastatic castration-resistant prostate cancer. *Cancers.* (2021) 13:779. doi: 10.3390/cancers13040779

95. Nelson BJ, Andersson JD, Wuest F. Targeted alpha therapy: progress in radionuclide production, radiochemistry and applications. *Pharmaceutics.* (2021) 13:49. doi: 10.3390/pharmaceutics13010049

frontiers | Frontiers in Medicine

TYPE Original Research
PUBLISHED 08 February 2023
DOI 10.3389/fmed.2023.1058914



OPEN ACCESS

EDITED BY
Francesco Cicone,
Magna Græcia University,
Italy

REVIEWED BY
Cinzia Pettinato,
IRCCS Ca 'Granda Foundation Maggiore Policlinico Hospital,
Italy
Hugo Levillain,
Université libre de Bruxelles, Belgium

*CORRESPONDENCE
Simen Rykkje Grønningsæter
✉ sirygr@ous-hf.no

SPECIALTY SECTION
This article was submitted to Nuclear Medicine, a section of the journal Frontiers in Medicine

RECEIVED 30 September 2022
ACCEPTED 18 January 2023
PUBLISHED 08 February 2023

CITATION
Grønningsæter SR, Blakkisrud J, Selboe S, Revheim M-E, Bruland ØS, Bønsdorff TB, Larsen SG and Stokke C (2023) Radiation safety considerations for the use of radium-224-calciumcarbonate-microparticles in patients with peritoneal metastasis.
*Front. Med.* 10:1058914.
doi: 10.3389/fmed.2023.1058914



# Radiation safety considerations for the use of radium-224-calciumcarbonate-microparticles in patients with peritoneal metastasis

Simen Rykkje Grønningsæter[1]*, Johan Blakkisrud[1], Silje Selboe[1], Mona-Elisabeth Revheim[1,2], Øyvind Sverre Bruland[3,4], Tina Bjørnlund Bønsdorff[5], Stein Gunnar Larsen[6] and Caroline Stokke[1,7]

[1]Division of Radiology and Nuclear Medicine, Oslo University Hospital, Oslo, Norway, [2]Faculty of Medicine, University of Oslo, Oslo, Norway, [3]Department of Oncology, Oslo University Hospital, Oslo, Norway, [4]Institute of Clinical Medicine, University of Oslo, Oslo, Norway, [5]Oncoinvent AS, Oslo, Norway, [6]Department of Gastroenterological Surgery, Oslo University Hospital, Oslo, Norway, [7]Department of Physics, University of Oslo, Oslo, Norway

**Aim:** Two ongoing phase I studies are investigating the use of radium-224 adsorbed to calcium carbonate micro particles ($^{224}$Ra-$CaCO_3$-MP) to treat peritoneal metastasis originating from colorectal or ovarian cancer. The aim of this work was to study the level of radiation exposure from the patients to workers at the hospital, carers and members of the public.

**Method:** Six patients from the phase 1 trial in patients with colorectal cancer were included in this study. Two days after cytoreductive surgery, they were injected with 7MBq of $^{224}$Ra-$CaCO_3$-MP. At approximately 3, 24 and 120h after injection, the patients underwent measurements with an ionization chamber and a scintillator-based iodide detector, and whole body gamma camera imaging. The patient was modelled as a planar source to calculate dose rate as a function of distance. Scenarios varying in duration and distance from the patient were created to estimate the potential effective doses from external exposure. Urine and blood samples were collected at approximately 3, 6, 24, 48 and 120h after injection of $^{224}$Ra-$CaCO_3$-MP, to estimate the activity concentration of $^{224}$Ra and $^{212}$Pb.

**Results:** The patients' median effective whole-body half-life of $^{224}$Ra-$CaCO_3$-MP ranged from 2.6 to 3.5days, with a mean value of 3.0days. In the scenarios with exposure at the hospital (first 8days), sporadic patient contact resulted in a range of 3.9–6.8μSv per patient, and daily contact resulted in 4.3–31.3μSv depending on the scenario. After discharge from the hospital, at day 8, the highest effective dose was received by those with close daily contact; 18.7–83.0μSv. The highest activity concentrations of $^{224}$Ra and $^{212}$Pb in urine and blood were found within 6h, with maximum values of 70Bq/g for $^{224}$Ra and 628Bq/g for $^{212}$Pb.

**Conclusion:** The number of patients treated with $^{224}$Ra-$CaCO_3$-MP that a single hospital worker - involved in extensive care - can receive per year, before effective doses of 6mSv from external exposure is exceeded, is in the order of 200–400. Members of the public and family members are expected to receive well below 0.25mSv, and therefore, no restrictions to reduce external exposure should be required.

KEYWORDS

**radium-224, radiation safety, alpha emitter, targeted alpha particle therapy, peritoneal metastasis**

# 1. Introduction

Peritoneal metastasis (PM) is most frequently caused by gastrointestinal and gynecological malignancies disseminating, and growing in serosa linings the abdominal cavity (1). The main treatment is cytoreductive surgery (CRS), often combined with hyperthermic intraperitoneal chemotherapy (HIPEC). Still there is a risk of recurrence of the disease.

Two ongoing phase I studies, RAD-18-001 (NCT03732768) and RAD-18-002 (NCT03732781), are investigating the use of radium-224 ($^{224}$Ra) adsorbed in calcium carbonate microparticles ($^{224}$Ra-$CaCO_3$-MP) to treat peritoneal metastasis originating from colorectal and ovarian cancer. Patients at the highest planned activity level receive an injection of approx. 7 MBq of $^{224}$Ra intraperitoneally through a catheter, 2 days after CRS. Patients with PM with origin from colorectal cancer included in the RAD-18-002 trial also receive treatment with HIPEC after CRS.

The decay chain of $^{224}$Ra consists of radon-220 ($^{220}$Rn), polonium-216 ($^{216}$Po), lead-212 ($^{212}$Pb), bismuth-212 ($^{212}$Bi), polonium-212 ($^{212}$Po, 64%), thallium-208 ($^{208}$Tl, 36%) and stable lead-208 ($^{208}$Pb; Figure 1; 2). $^{212}$Pb and $^{208}$Tl are the main photon emitters. $^{212}$Pb emits 77.4 keV x-ray photons (17.5%) and 239 keV γ-photons (43.6%), amongst others (2). The γ-photons of highest intensities with origin from $^{208}$Tl is 2,615 keV photons (99.8%) and 583 keV photons (85.0%). However, as $^{212}$Bi is branched, and 36% decays to $^{208}$Tl, the overall intensities of these photons are lower. $^{224}$Ra has a half-life ($t_{1/2}$) of 3.6 days, while the daughters have shorter half-lives varying from

$3{\cdot}10^{-7}$ s to 10.6 h.

From the 1910's, $^{224}$Ra has sporadically been used to treat ankylosing spondylitis (3), but to the best of the authors' knowledge, no publications on the subject of radiation safety protection for $^{224}$Ra exist. Although not completely comparable, more research has been done in recent years on another isotope of radium; radium-223 ($Ra^{223}$). Treatment fractions of 55 kBq/kg radium-223-dichloride $^{223}RaCl_2$ is used for treating bone metastases with origin from metastatic castration resistant prostate cancer. Two publications have concluded that the product could be given on an outpatient basis, without restrictions on normal interactions and that patients do not need to follow specific restrictions related to radiation safety, as long as they attain to a set of hygienic precautions related to bodily fluids (4, 15).

For the treatment of peritoneal metastases, $^{224}$Ra is thought to be more suitable than $^{223}$Ra due to its shorter half-life, as it is expected that some of the injected radionuclide could be transported out of the peritoneal cavity (5). Hence, with a longer half-life more of the absorbed dose could potentially be deposited outside the peritoneal cavity.

The Council of the European Union sets in its Council Directive 2013/59/EURATOM effective dose limits for different categories of personnel, carers and the public (6). For example, the effective dose limit for occupational exposure is 20 mSv per year (the average over 5 years may be considered), while the limit for the public is 1 mSv per year.

The aim of the current study was to estimate radiation doses to hospital workers, carers and the public from patients receiving $^{224}$Ra-$CaCO_3$-MP in a dosimetry cohort of six patients with peritoneal metastasis from colorectal cancer, undergoing measurements of external dose rates and radioactivity in urine and blood at several time points post treatment.

# 2. Methods

## 2.1. Patient population and $^{224}$Ra-$CaCO_3$-MP treatment

Subjects with histologically confirmed colorectal carcinoma and peritoneal metastases eligible for CRS and HIPEC treatment were enrolled in a phase 1 trial to evaluate the dose, safety and tolerability of $^{224}$Ra-$CaCO_3$-MP. For the current study, six patients from an expansion cohort at Oslo University Hospital were included. $^{224}$Ra was extracted from a generator consisting of thorium-228, which has a half-life of 1.9 years (7). $^{224}$Ra-$CaCO_3$-MP was produced by Oncoinvent AS. A peritoneal catheter was inserted after surgery (day −2). $^{224}$Ra-$CaCO_3$-MP, containing 0.7–1 g microparticles with nominally 7 MBq of $^{224}$Ra in equilibrium with daughters, was administered to the patients *via* the catheter at day 1 (Figure 2). Before injection, $^{224}$Ra-$CaCO_3$-MP was diluted to 50 ml with Plasmalyte® (Baxter) isotonic solution. The suspension was injected intraperitoneally, and the injection was followed by a flushing with 200 ml of Plasmalyte®.

The study was approved by the Regional Committee for Medical and Health Research Ethics (REK). A written informed consent was given by all patients.

## 2.2. Dose rate measurements

Dose rate measurements were performed at day 1, 3 h after injection of $^{224}$Ra-$CaCO_3$-MP, day 2 (24 h after injection) and day 6 (120 h after injection) with a hand held ionization chamber, a SmartION 2120S (Thermo Fisher Scientific, Waltham, Massachusetts, United States) with shielding cover. Dose rates were measured at a distance of 10 cm and 20 cm from the upper abdomen of the patients. Based on these measurements, mono-exponential curve fits were made in Matlab R2020b (MathWorks, Natic, Massachusetts, United States) to extra- and interpolate the dose rate of a patient as a function of time. Additionally, the curves were used to calculate the minimum, maximum and mean dose rates at each day.

To calculate the dose rate at other distances, the radiation source was assumed to be a flat finite plane with a radius $r$ (8). A distance dependent ratio, $R$, for finding the dose rate at a distance $x_2$ is then given by

$$R = \frac{\ln\left(\frac{r^2}{{x_2}^2}+1\right)}{\ln\left(\frac{r^2}{{x_1}^2}+1\right)} \qquad \text{(Equation 1)}$$

## 2.3. Whole body measurements and effective half-life

Imaging was performed at day 1, day 2 and day 6 using a Siemens Symbia Intevo Bold gamma camera. A planar scan of 100 cm was acquired starting from the base of the skull, using medium energy collimators and a 240 keV energy window, and a 5% upper and lower scatter window. Automatic body contouring was

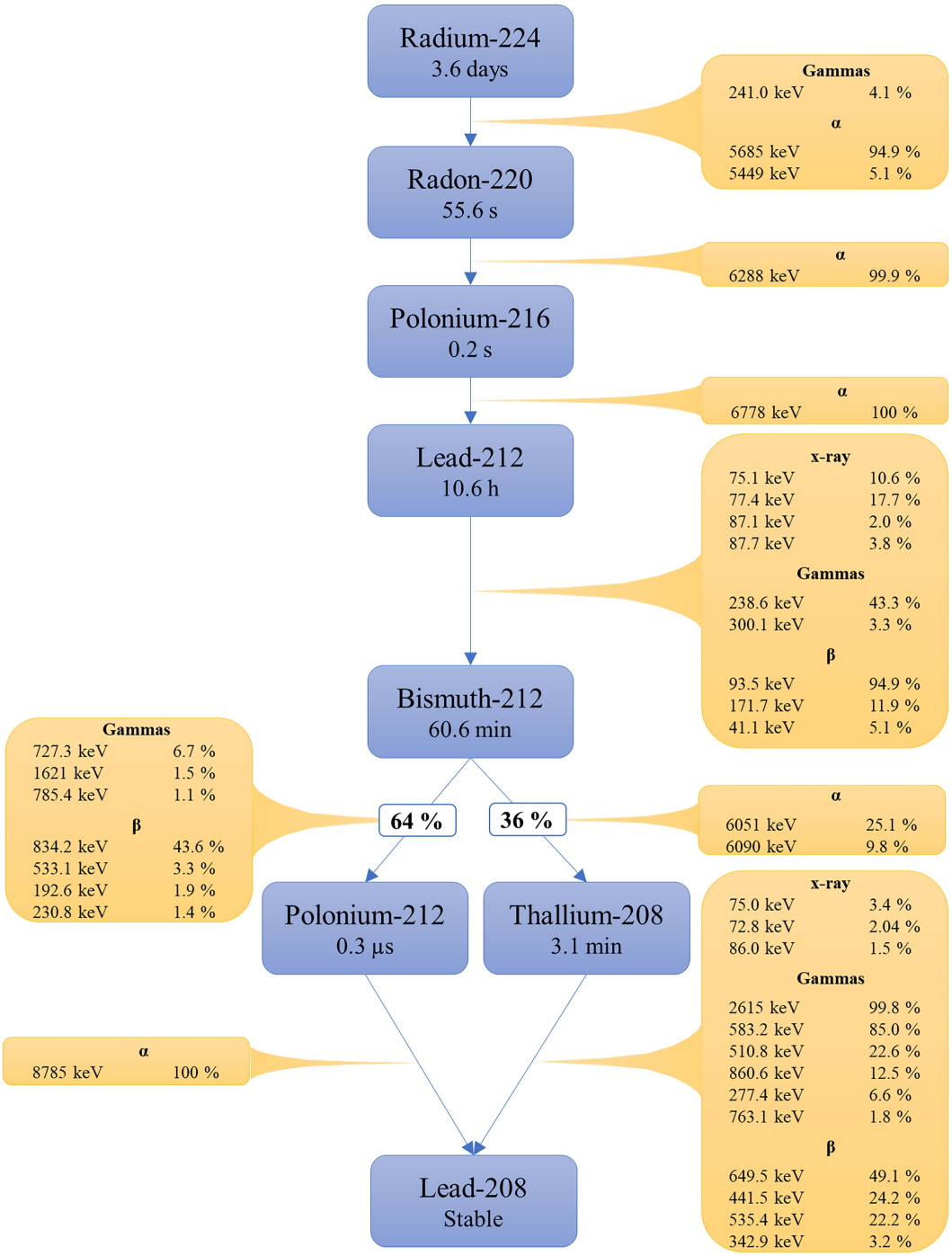


FIGURE 1
Overview of the $^{224}$Ra decay chain. Radiations with intensity <1% and photons with energy <70keV are excluded. Data from the supplementary material of ICRP 107.

used, and the scan had a 20 min acquisition time. Large regions of interest (ROIs) were drawn with margins around the patient on both the anterior and posterior images, using 3D Slicer version 4.8.1, revision 26,813 (The Slicer Community). The geometric mean of the counts found in the anterior and posterior ROIs were then calculated.

During the gamma camera imaging sessions, a measurement using a scintillator probe, RadEye SX with an FHZ 514A scintillation probe (Thermo Fisher Scientific, Waltham, Massachusetts, United States) was taken 50 cm from the upper abdomen, on the right side of the patient. Background measurements were also performed, and subtracted from the patient measurement to obtain the number of counts at each time point.

To estimate the whole body effective half-life of $^{224}$Ra-$CaCO_3$-MP, three separate approaches were used. The gamma camera (the geometric means), SmartIon (the dose rates at 10 cm) and the RadEye (the number of counts). Separate mono-exponential curve fits and effective half-lives were calculated.

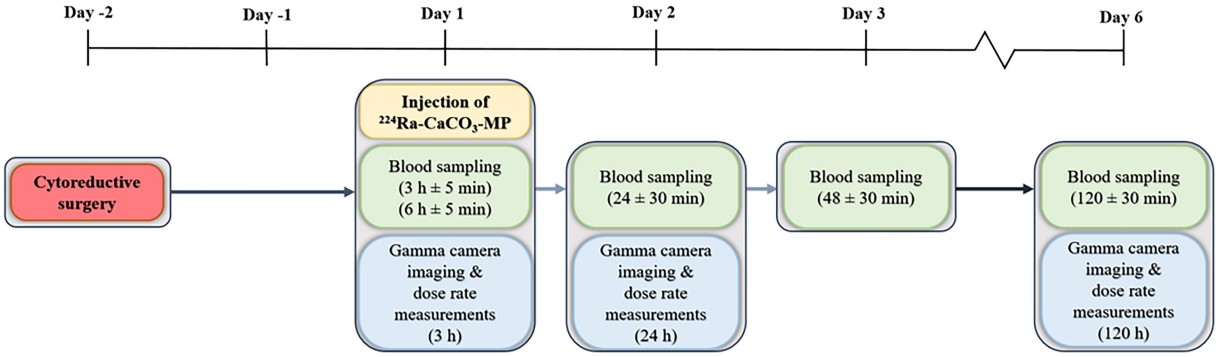


FIGURE 2
An overview of the treatment and measurement schemes for patients treated with $^{224}$Ra-CaCO$_3$-MP.

## 2.4. Scenarios

The mean, minimum and maximum dose rate measurements were used to evaluate radiation doses received by workers at the hospital, members of the family and the public from external exposure. Different scenarios were created, based on various assumptions regarding distance from and time spent with a patient. The day of discharge from the hospital varied for scenario 4.b, ranging from day 4 to day 12 (i.e., 6–14 days after surgery), with day 8 being the default for other scenarios.

1. Sporadic contact at the hospital: Assumes contact with patient on day 1, 2 and 6, with 10 min duration at 0.1 m and 15 min at 1 m. This could for instance reflect employees performing imaging or collecting patient samples, clinicians or nurses not involved in daily care, or employees involved in cleaning, transport of patients, etc. This scenario can also be relevant for family and friends visiting.
2. Daily contact at the hospital: Assumes daily contact with patient each day during day 1 to the day of discharge (day 8 as default). The subcategories a-c further divide the exposure according to the extent of daily contact. This may be relevant for employees at the hospital ward, involved in daily care, and possibly also visiting family members.

a. Low degree: 5 min at 0.1 m and 10 min at 0.5 m.
b. Moderate degree: 10 min at 0.1 m and 30 min at 0.5 m.
c. Extensive degree: 20 min at 0.1 m and 60 min at 0.5 m.

3. Sporadic contact after leaving the hospital: Separated in two scenarios, where the first assumes contact every third day, and the second one time encounters. The second may reflect prolonged transportation settings or similar occupations for members of the public.

a. Regular contact: 60 min of contact at 0.5 m every third day starting the day after discharge (day 9 as default).
b. Singular close contact: 3 h at 0.1 m at day 8.

4. Daily contact after leaving the hospital: Assumes frequent or prolonged contact starting at the day after discharge (day 9 as default). This may reflect family, or in some situations members of the public. The subcategories further divide the exposure according to the extent of contact.

a. Daily contact: 8 h at 1 m.
b. Close daily contact: 4 h at 0.1 m and 4 h at 1 m per day.

### 2.4.1. Effective dose estimation equation

To estimate the effective dose, $H$, in these scenarios, the following equation has been used

$$H = \sum_{t_d} \dot{H}_{t_d} \sum_{x} t_x \, R_x \qquad \text{(Equation 2)}$$

where $\dot{H}_{t_d}$ is the dose rate of a given day (assumed constant each day for simplicity), $t_d$ is the number of days since the injection of $^{224}$Ra-CaCO$_3$-MP included in the scenario, $t_x$ is the time (in hours) spent at a distance $x$ from a patient, and $R_x$ is a distance dependent ratio for the distance x. The function $\dot{H}(t_d)$ is given by

$$\dot{H}_{t_d} = \dot{H}_0 \cdot e^{-\lambda_e t_d} \qquad \text{(Equation 3)}$$

where $\dot{H}_0$ is the dose rate measured at 10 cm on day 1 and $\lambda_e$ is the effective decay constant. $\dot{H}_0$ and $\lambda_e$ varies for mean, minimum or maximum measurements. The distance dependent ratio, $R_x$, is given by

$$R_x = \frac{\ln\left(\frac{2025\,cm^2}{x^2} + 1\right)}{3.056} \qquad \text{(Equation 4)}$$

where $x$ is the distance between the patient and the person in question. Equation 4 is found by using equation 1 and assuming a radius of 45 cm ($r^2 = 2025\,cm^2$). The denominator of equation 1 thereby equals 3.056 for $x_1 = 10$ cm.

## 2.5. Fluid samples

Samples of fluids were collected approximately 3, 6, 24, 48 and 120 h after injection of $^{224}$Ra-CaCO$_3$-MP. A minimum of 3 ml of urine and blood was collected, where the urine samples were collected from a urine

TABLE 1 Characteristics of the patients included in the study.

| Patient number | Gender | Age | Weight [kg] | Height [cm] | Injected $^{224}$Ra [MBq] |
|---|---|---|---|---|---|
| 21-017 | Female | 68 | 65 | 158 | 7.23 |
| 21-020 | Female | 56 | 92 | 177 | 6.99 |
| 21-021 | Male | 66 | 82 | 178 | 7.07 |
| 21-023 | Female | 43 | 59 | 164 | 7.23 |
| 21-024 | Female | 28 | 67 | 164 | 7.38 |
| 21-025 | Female | 68 | 80 | 150 | 7.08 |

TABLE 2 Effective half-life for the six patients included in the study, based on measurements with whole body gamma camera (WB), scintillator counter (RadEye) and ionization chamber (SmartION).

| | $t_{effective}$ [d] | | |
|---|---|---|---|
| Patient number | WB | Radeye | Smartion |
| 21-017 | 2.8 | 3.1 | 3.2 |
| 21-020 | 3.8 | 2.8 | 3.2 |
| 21-021 | 3.6 | 3.1 | 2.3 |
| 21-023 | 3.4 | 4.2 | 3.5 |
| 21-024 | 2.6 | 2.2 | 2.4 |
| 21-025 | 3.2 | 2.6 | 2.4 |

collector bag. Each sample was measured at two different time points (time point 1 and 2) at least 48 h apart, with a Hidex Automatic Gamma Counter (Hidex, Turku, Finland), qualified for GxP analysis. The samples were weighted during analysis and consist of approximately 2.5 g for urine and blood, resulting in activity measurements given in Bq/g. The measurements at time point 1 were scheduled within 4 h of sampling from the patient, and time point 2 within 48–72 h after time point 1, when equilibrium between radium-224 and the progeny lead-212 has been established. The energy window was 60–110 keV with 10 min measurement time. Two measuring time points was used to estimate the amount of $^{224}$Ra.

The activity of $^{224}$Ra, $A_{Ra,t_s}$, in fluids was estimated using

$$A_{Ra,t_s} = \frac{A_{Pb,t_{m2}} - A_{Pb,t_s} \cdot e^{-\lambda_{Pb}(t_{m2}-t_s)}}{\frac{\lambda_{Pb}}{\lambda_{Pb}-\lambda_{Ra}}\left(e^{-\lambda_{Ra}(t_{m2}-t_s)} - e^{-\lambda_{Pb}(t_{m2}-t_s)}\right)}, \text{ (Equation 5)}$$

where $A_{Pb,t_s}$ is the activity of $^{212}$Pb at sampling, $A_{Pb,t_{m2}}$ is the activity of $^{212}$Pb at time point 2, $(t_{m2}\text{-}t_s)$ is the time between sampling and measurement number 2, and $\lambda_{Pb}$ and $\lambda_{Ra}$ are the decay constants of $^{212}$Pb and $^{224}$Ra, respectively. The decay constant is $\lambda = ln(2)/t_{1/2}$, where $t_{1/2}$ is the physical half-life of the nuclide.

Bi-exponential curve fits were created for the measurements of $^{224}$Ra and $^{212}$Pb in blood and urine. Using the wash-out phase of the curves, the effective half-lives of $^{224}$Ra and $^{212}$Pb in urine and blood for this phase was calculated for each patient.

## 2.6. Hand exposure

Radiation doses to the hands of hospital workers receiving, preparing and injecting 7 MBq of $^{224}$Ra was measured at two occasions early in the study, using ring thermos-luminescence dosimeters (TLDs). Additionally, electronic personal dosimeters placed 5 cm from the glass containing $^{224}$Ra during vortexing, were used to record doses on three occasions.

# 3. Results

## 3.1. Patient group and protocol deviations

Of the six included patients, the median age was 61 years, and the average weight and height was 74 kg and 165 cm (Table 1).

The 6 h blood measurement was not attainable for patient 21-017, and the 48 h gamma camera scan was not collected for patient 21-024. The procedures scheduled for day 2 and 6 was for patient 21-021 collected at day 3 and 7. However, the collection of fluid samples at 24 h after injection, was performed as planned.

## 3.2. Effective half-life

The effective half-life estimated from whole body planar acquisitions (WB), scintillator probe (RadEye) and ionisation chamber (SmartION) measurements are shown in Table 2. There was overall a fair agreement between the three measurement techniques. The effective half-life for the whole body planar acquisitions, the RadEye and SmartION measurements was estimated to 3.2 d, 3.0 d and 2.8 d, respectively. Anterior whole body measurements acquired at day 1, 2 and 6 are shown in Figure 3.

## 3.3. Dose rate measurements

The dose rate measurements of the individual patients, and their fitted curves, are shown in Figure 4. The mean, minimum and maximum measurements at 3, 24 and 120 h after injection are summarized in Table 3.

### 3.3.1. Estimated effective doses

The coefficients used in equation 2, for the estimations of effective dose, are shown in Table 4. The effective doses for different scenarios are shown in Table 5. While the patient was at the hospital, the highest effective doses were not surprisingly found for scenarios involving extensive daily contact, with an average effective dose of 22.7 µSv. The number of patients needed for a hospital worker to reach various effective doses were also calculated (Table 6), and, e.g., a moderate degree of daily contact would allow for approx. 350–700 patients per year before 6 mSv were reached. After leaving the hospital at day 8, close daily contact resulted in an average effective dose of 46.6 µSv, which would increase to 125 µSv if the patient left the hospital 4 days earlier, and decrease to 17.2 µSv if the patient left the hospital 4 days later. If someone would visit the hospital for all 4 days with extensive patient contact and have close daily contact after this, it would result in an average effective dose of 148 µSv. Transport, for 3 h at day 8 (scenario 3b), resulted in 7.3 µSv.

## 3.4. Urine and blood samples

For urine, the highest measurements of $^{224}$Ra were commonly found at the first two time points, 3 h and 6 h, and ranged from approximately

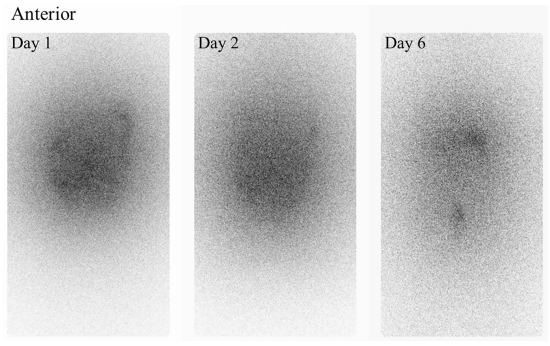


FIGURE 3
Anterior whole body images collected at day 1, 2 and 6.

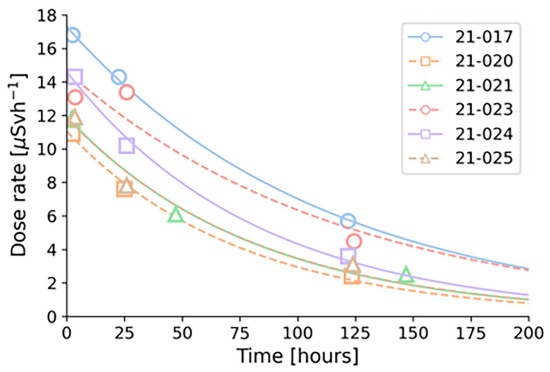


FIGURE 4
Dose rate measurements at 10cm with corresponding curve fits. Each patient is indicated by a different colour, dots showing measurements and lines the fitted curves.

TABLE 3 Mean, min, and max dose rate measurements at 10 and 20cm for patients administered approx.

| | 10cm | | | 20cm | | |
|---|---|---|---|---|---|---|
| | Day 1 | Day 2 | Day 6 | Day 1 | Day 2 | Day 6 |
| Mean | 13.1 uSv/h | 10.4 uSv/h | 3.7 uSv/h | 7.9 uSv/h | 6.4 uSv/h | 2.6 uSv/h |
| Min | 10.6 uSv/h | 8.0 uSv/h | 2.3 uSv/h | 6.5 uSv/h | 4.8 uSv/h | 0.8 uSv/h |
| Max | 16.8 uSv/h | 13.9 uSv/h | 5.9 uSv/h | 9.8 uSv/h | 8.2 uSv/h | 3.7 uSv/h |
| CoV | 18% | 22% | 41% | 16% | 20% | 43% |

7 MBq 224Ra. Based on the values of the fitted curves at 3, 24 and 120 h after injection, shown in Figure 2 for measurements at 10 cm.

TABLE 4 Coefficients for use in equation 3 when estimating daily dose rate based on mean, min or max measurements.

| | Mean | Min | Max |
|---|---|---|---|
| $\dot{H}_0$ [μSvh$^{-1}$] | 13.8 | 11.0 | 17.3 |
| $\lambda_e$ [d$^{-1}$] | 0.249 | 0.3172 | 0.2163 |

30 to 70 Bq/g (Figure 5). For $^{212}$Pb, the peak values were usually found at the same time points, and ranged from 41 to 150 Bq/g, with one patient showing a higher value of over 600 Bq/g at 3 h. Urine samples showed an average (min-max) effective half-life during the wash-out phase of 0.7 d (0.3–1.3 d) for $^{224}$Ra. Due to high influx of $^{212}$Pb to urine, the effective half-life for the wash-out phase of the curve was 1.0 d in average (0.1–2.8 d).

Similarly for blood, the highest measurements of $^{224}$Ra was found at 3 to 6 h, and ranged from 22 to 40 Bq/g. For $^{212}$Pb in blood, the highest measurements was found at 6 h and ranged from 114 to 234 Bq/g. The effective half-life for the wash-out phase in blood was 0.6 d (0.4–0.8 d) for $^{224}$Ra and 2.1 d (1.3–2.9 d) for $^{212}$Pb.

## 3.5. Hand exposure

The doses from the TLDs were found to be lower than the limit of registration for the detectors (0.1 mSv). From the electronic personal dosimeters, doses of 1.3 μSv (0.41–2.05 μSv) were measured for vortexing and preparing the product.

# 4. Discussion

In this study, dose rate measurements of patients treated with $^{224}$Ra-$CaCO_3$-MP gave an average dose rate of 13.1 μSvh$^{-1}$ (10.6–16.8 μSvh$^{-1}$) at 10 cm, approximately 3 h after injection. Since both alpha and beta particles will primarily stop in the tissue, this is mainly due to photons. Of the scenarios created, the highest effective dose, with a mean value of 46.6 μSv, were found for carers having close daily contact with a patient that was discharged at day 8 from the hospital, or a value of 124.9 μSv if the patient was released day 4. The number of patients treated with $^{224}$Ra-$CaCO_3$-MP that a hospital worker - involved in extensive care - can receive per year, before effective doses of 1 mSv is exceeded, is in the order of 32–63, and is in the order of 639–1,257 before effective doses of 20 mSv is reached.

The Council of the European Union states, in its Council Directive 2013/59/EURATOM, an effective dose limit for occupational exposure in planned exposure situations of 20 mSv per year (6). This may for certain circumstances be extended to 50 mSv as long as the yearly exposure averaged over a period of 5 years do not exceed 20 mSv. The directive also states that personnel who are liable to receive more than 6 mSv per year should be individually monitored. For pregnant personnel, the radiation dose should not exceed 1 mSv from the pregnancy is discovered. The limit for the public is 1 mSv per year (6). Beyond this, there are also some national differences in dose constraints for hospital workers, carers, and members of the public. The European Council Directive requires that "Member States shall ensure that dose constraints are established for the exposure of carers and comforters, where appropriate." For example in Norway, this has been implemented as that close family members may receive an effective dose of 1 mSv (children), 3 mSv (adults under 60 years of age), and 15 mSv (older adults) per treatment (9). In addition to Table 5 showing the effective doses received from exposure from a single patient, Table 6 shows the number of patients treated with $^{224}$Ra-$CaCO_3$-MP that can be handled by employees in various scenarios, and different limits are hence included. Adaptations to other scenarios and limits can be done using equation 2 and Table 4.

The estimated effective dose for different scenarios allows an assessment for hospital workers, carers, and the public. The scenarios for sporadic and daily contact at the hospital were based on our experience during the trials. Only scenarios 1 and 2, involving sporadic and daily contact, are relevant for hospitals workers. As the overall clinical status and needs for support of individual patients vary, the category of daily

TABLE 5 Mean, min, and max effective doses received from one single patient for nine different scenarios.

| | Effective dose (μSv/patient) | | |
|---|---|---|---|
| Scenario | Mean | Min | Max |
| Sporadic contact at hospital (1) | 5.0 | 3.9 | 6.8 |
| Some daily contact at hospital (2.a) | 6.1 | 4.3 | 8.4 |
| Moderate degree of daily contact at hospital (2.b) | 12.2 | 8.6 | 16.8 |
| Extensive daily contact at hospital (2.c) | 22.7 | 15.9 | 31.3 |
| Sporadic contact after hospital, regular (3.a) | 0.7 | 0.4 | 1.3 |
| Sporadic contact after hospital, singular (3.b) | 7.3 | 3.6 | 11.4 |
| Daily contact after hospital (4.a) | 8.6 | 4.0 | 14.6 |
| Close daily contact; discharged at day 12 (4.b) | 17.2 | 5.3 | 34.9 |
| Close daily contact; discharged at day 8 (4.b) | 46.6 | 18.7 | 83.0 |
| Close daily contact; discharged at day 4 (4.b) | 124.9 | 66.7 | 197.2 |

When not otherwise indicated, hospital discharge was assumed day 8.

contact was divided into three subgroups, ranging from some degree of contact (2a) to extensive degree of contact (2c). Highly conservative scenarios, including such as occupancy at 10 cm distance and prolonged contact, were also included as the patients may be in need of close clinical care. Table 6 show the number of patients that can be treated yearly in different scenarios before reaching dose limits of 0.25, 1, 6 and 20 mSv. It has been estimated that between 40 and 45 patients with colorectal cancer is a realistic number of patients treated yearly with $^{224}$Ra-$CaCO_3$-MP at the Norwegian Radium Hospital. Hence, for most scenarios, the number of patients that can be treated before surpassing limits significantly outweighs the number of patients that are expected. Adding to this is that patient care of course is divided between several hospital workers, which will lower the individual exposure. However, with a limit of 1 mSv yearly, pregnant workers may theoretically surpass this limit if they were to single-handed treat more than 32 patients with need for extensive daily contact. Generally, in regard of the limits, it should be noted that all potential sources of exposure (numbers and types of other patients the employees are also treating) should be considered as a whole.

The patients undergo comprehensive surgery and can be expected to stay at the hospital for up to 2 weeks after surgery (day 12 after injection of $^{224}$Ra-$CaCO_3$-MP). Day 12 was then investigated as a potentially time point of discharge, together with day 8 and day 4 Day 8 was here primarily used as the time of departure from the hospital based on our experience in the trial so far. Those with daily contact and close daily contact after discharge (scenario 4a and 4b) received effective doses up to 14.6 μSv and 83 μSv, respectively. If daily visits to the hospital are included (scenario 2c), they may receive up to 45.9 μSv and 110 μSv. If patients were to be discharged earlier, it would increase the effective dose to carers, and members of the public. In a setting where the patient leaves the hospital at day 4, instead of at day 8, the effective dose to those with close daily contact would increase to a maximum effective dose of 197 μSv, compared to 83.0 μSv for those discharged at day 8. This is still far below the dose limits, and do not generate any need for precautions.

In Norway, members of the public should not be exposed to more than 0.25 mSv from a single source of exposure (9). Members of the public may in contact with patients through several settings, and colleagues are typically often the most exposed. However, due to the strain the patients go through in relation to the treatment, they are not expected to go back to work for some time. If they were, the effective doses could be estimated through scenario 4a (daily contact) and would still be well below 0.25 mSv. Transportation, or other sporadic settings with contact, will only result in negligible contributions. E.g. after 3 h contact at 10 cm (scenario 3b), a member of the public will receive <4.6% of their yearly limit of 0.25 mSv. Even a continuous exposure at 20 cm for 4 weeks after the patient leaves the hospital at day 8, which is not a realistic scenario even for family members, would only result in up to 0.28 mSv and it is therefore no need for any restrictions for patients regarding the public.

Different approaches can be used to estimate the dose rate as a function of distance. A common method, the inverse square law, assumes a point source, which is not realistic for patients with activity distributed throughout the peritoneal cavity, as seen in Figure 3. Hence, it was assumed that a finite plane source would be more appropriate in the case of $^{224}$Ra-$CaCO_3$-MP. The distance dependent ratio, *R*, was then given by equation 1. Although a source with a diameter of 90 cm will not truly represent the typical patient size, the agreement between the model and the measurements at 20 cm were very good, we therefore chose this diameter to avoid an underestimation of the dose rate for larger distances. Ideally, measurements at increased distances should have been included as well, to validate the model further. However, in this study, it was challenging to measure dose rates at more then 10 and 20 cm from the patients, since dose rates at larger distances would approach the background level.

Except for the use of $^{223}RaCl_2$ to treat bone metastasis with origin from castration resistant prostate cancer (10), radionuclide therapy using alpha emitters is still mostly in its research stage. A higher number of radiation safety studies have therefore been published for radionuclide therapies using beta-emitters or for diagnostic tracers. While other radionuclides have been studied for treating peritoneal metastasis with origin from ovarian cancer, such as $^{90}$Y-HMFG1 and $^{211}$At-MX35-F(ab')$_2$ being two of the candidates (11, 12), we have not been able to find radiation protection publications related to these treatments. Stefanoyiannis et al. (13) compared studies examining radiation exposure to caregivers from patients for different common radionuclide therapies. These included radiopharmaceuticals with iodine-131 ($^{131}$I), yttrium-90 ($^{90}$Y) and lutetium-177 ($^{177}$Lu). The different studies varied in injected activity, number of patients, types of dosimeters used, disease treated and the duration of the study. For thyroid cancer (all studies used $^{131}$I), activities ranging from 1,004–11,100 MBq was given, but did not result in effective doses to caregivers higher than 1.1 mSv. For B-cell lymphoma and neuroblastoma, activities up to 23,310 MBq of $^{131}$I were used, up to 7,400 MBq of $^{177}$Lu was used, and up to 1,200 MBq of $^{90}$Y was

TABLE 6 The number of patients that can be treated by a single individual before reaching 0.25, 1, 6 and 20mSv, for the four different scenarios relevant for hospital workers.

| | Number of patients before reaching limit | | | | | | | |
|---|---|---|---|---|---|---|---|---|
| | 0.25mSv | | 1mSv | | 6mSv | | 20mSv | |
| Scenario | Min | Max | Min | Max | Min | Max | Min | Max |
| Sporadic contact at hospital (1) | 65 | 37 | 259 | 148 | 1,551 | 886 | 5,170 | 2,952 |
| Some daily contact at hospital (2.a) | 58 | 30 | 234 | 119 | 1,403 | 714 | 4,675 | 2,379 |
| Moderate degree of daily contact at hospital (2.b) | 29 | 15 | 117 | 59 | 701 | 357 | 2,338 | 1,189 |
| Extensive daily contact at hospital (2.c) | 16 | 8 | 63 | 32 | 377 | 192 | 1,257 | 639 |

Patients are here assumed to leave the hospital at day 8.

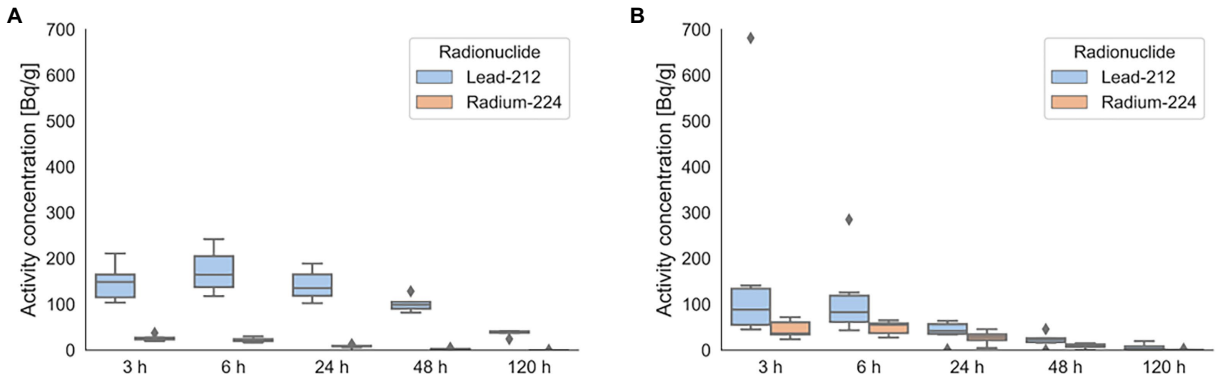


FIGURE 5
Activity concentration of $^{224}$Ra and $^{212}$Pb found in blood **(A)** and urine **(B)** for the six patients included. Dots indicate measurements that lies outside 1.5 of the interquartile range.

used. This resulted in effective doses to caregivers of up to 3.81 mSv, with the mean effective dose being considerably lower. Although amounts of activity should not be directly compared in most circumstances, it is worth mentioning that in the case of $^{224}$Ra-$CaCO_3$-MP, an activity of three or four orders of magnitude lower (7 MBq) is used. In summary, Stefanoyiannis et al. found that the doses was within the dose constraints of 5 mSv to home caregivers, recommended by the International Commission of Radiological Protection (ICRP) (13). They also highlighted the importance of giving specific instructions to caregivers, as the highest dose values were found when no instructions were given.

The standard activity dosage of $^{223}RaCl_2$ is 55 MBq/kg body weight given intravenously in six administrations 4 weeks apart (14). In contrast, for $^{224}$Ra-$CaCO_3$-MP, one administration of 7 MBq is given intraperitoneally. Dauer et al. published in 2014 a study on radiation safety considerations for $^{223}RaCl_2$ (15). They reported a dose rate immediately after injection being 0.02 $\mu Svh^{-1}$/MBq at 1 m distance from the patient, and concluded that $^{223}RaCl_2$ could be given on an outpatient basis, without restrictions on normal interactions with friends, relations, or co-workers. The dose rates measured for $^{224}$Ra-$CaCO_3$-MP was equivalent to 0.11 $\mu Svh^{-1}$/MBq at 1 meter distance, at the day of administration, found by dividing the average measured dose rate by the injected activity. The difference between dose rates may be caused by highly different distribution between the radiotherapeuticals (primarily blood pool versus only peritoneal cavity), resulting in a higher amount of radioactivity closer to the dose rate meter for $^{224}$Ra-$CaCO_3$-MP, and the different radiations emitted. Furthermore, the kinetics of $^{224}$Ra-$CaCO_3$-MP and $^{223}RaCl_2$ may change the dose rates differently over time. While the majority of $^{224}$Ra-$CaCO_3$-MP is expected trapped in the peritoneal cavity, some is transferred into the blood stream (Figure 5A). The two isotopes of radium is expected to chemically behave the same way and should follow the same biodistribution pathways after entering the blood stream (16). Differences lie in nuclear properties, like radiation energies and the physical half-life; which is 11.4 days for $^{223}$Ra and 3.6 days for $^{224}$Ra. Dauer et al. (15) found that for $^{223}RaCl_2$ up to 60% of the injected activity was bound in the skeleton within 4 h after injection. While this is probably somewhat less than the percentage of $^{224}$Ra-$CaCO_3$-MP remaining in the peritoneal cavity, the main factor contributing to different dose rates over time is most likely the different physical half-life of the two isotopes.

Findings reported by Serencsits et al. (4) support those of Dauer for $^{223}RaCl_2$, but also stresses the importance of proper equipment for radiation protection and detection, as well as training of hospital workers to avoid contamination. They also conclude that patients do not need to follow specific restrictions related to radiation safety, as long as they attain to a set of hygienic precautions related to bodily fluids. An example of hygienic precautions would for instance be to flush twice after using the toilet. For both isotopes of radium, urine and fecal excretion are the two main excretion routes. Studies of $^{223}RaCl_2$ showed that the cumulative excretion of urine was about 2% 48 h after injection, while the cumulative fecal excretion was 13% (1–25%) after 48 h and 64% (29–95%) after 72 h (17, 18). Dauer et al. (15) suggested that personnel involved in surgery, up to 2 m after injection of $^{223}RaCl_2$, to take no extra precautions other than to be aware to reduce contamination. For $^{224}$Ra-$CaCO_3$-MP,

measurements of $^{224}$Ra and $^{212}$Pb in urine (Figure 5) show amounts below 40 Bq/g of $^{224}$Ra in blood and 90 Bq/g in urine. Higher activity concentrations are found for $^{212}$Pb, with up to 250 Bq/g found in blood and 140 Bq/g in urine (measurement for one patient up to 700 Bq/g). Still, while these are low amounts, both patients, carers and hospital workers potentially involved in handling fluids should be informed and instructed in best practice.

Radon gas may potentially be emitted from the patient through exhalation or from excreted fluids (16). Yamamoto et al. (19) found in a study investigating the detection of alpha emitting daughters of $^{223}$Ra, that the increase of alpha emitters in air were lower than the daily variation and therefore not an important source of radiation exposure. However, the gaseous daughter of $^{223}$Ra, $^{219}$Rn, has a half-life of 3.96 s, while $^{220}$Rn have half-life of 55.6 s. This may lead to a higher exposure from $^{220}$Rn. Since the amount $^{224}$Ra activity in urine was here found below the limit of what is considered radioactive (10 Bq/g) (6) already after 48 h, release from urine is most likely a minor issue. Exposure to radon gas is also relevant if re-surgery of the peritoneal cavity is required. While this has not been measured in this study, previous investigations of $^{224}$Ra in liquid volumes indicate that the mean diffusion length of $^{220}$Rn is limited to 300–400 µm, and hence only a small amount of $^{220}$Rn will have the potential to evaporate (20).

Radiation dose from photon contributions to hands is not considered an issue for $^{224}$Ra-$CaCO_3$-MP, as the yearly dose limit to hands is set to 500 mSv (21). However, one should follow standard precautions for handling alpha-emitters to avoid contamination of the skin.

In summary, due to the low dose rates from the patients and low amount of activity found in blood and urine, no precautions related to external exposure should be required for patients treated with $^{224}$Ra-$CaCO_3$-MP. The number of patients hospital workers can treat before exceeding an effective dose of for instance 6 mSv is 200–400 for patients with the need for extensive care. This is considered a worst-case scenario and significantly outweighs realistic number of patients.

## Data availability statement

The raw data supporting the conclusions of this article will be made available by the authors, without undue reservation.

## Ethics statement

The studies involving human participants were reviewed and approved by Regional Committee for Medical and Health Research Ethics (REK). The patients/participants provided their written informed consent to participate in this study.

## Author contributions

SG and CS conceived and developed most of the experiments. SG and SS performed or supervised the measurements by probes and gamma camera. TB planned and supervised the bioanalysis. SL was responsible for the patient inclusion and treatment. M-ER for administration of the radiotherapeutical. CS, M-ER, TB, and ØB supervised the project. SG and JB performed the data analysis and calculations. SG, JB, and CS wrote the first draft of the manuscript, including tables and figures. All authors contributed to the article and approved the submitted version.

## Funding

The clinical study is sponsored by Oncoinvent.

## Acknowledgments

The authors would like to acknowledge the R&D department of Oncoinvent AS for the development of the analytical method used to measure radioactivity in blood and urine, as well as for performing the measurements.

## Conflict of interest

ØB - Clinical consultant and shareholder - Oncoinvent AS. TB - Chief Scientific Officer and shareholder - Oncoinvent AS. JB has participated in a scientific advisory board of GE Healthcare.

The remaining authors declare that the research was conducted in the absence of any commercial or financial relationships that could be construed as a potential conflict of interest.

## Publisher's note



## References

1. Coccolini, F, Gheza, F, Lotti, M, Virzi, S, Iusco, D, Ghermandi, C, et al. Peritoneal carcinomatosis. *World J Gastroenterol.* (2013) 19:6979–94. doi: 10.3748/wjg.v19.i41.6979
2. ICRP. ICRP publication 107: nuclear decay data for dosimetric calculations. *Ann ICRP.* (2008) 38:7–96. doi: 10.1016/j.icrp.2008.10.004
3. Priest, ND, Dauer, LT, and Hoel, DG. Administration of lower doses of radium-224 to ankylosing spondylitis patients results in no evidence of significant overall detriment. *PLoS One.* (2020) 15:e0232597. doi: 10.1371/journal.pone.0232597
4. Serencsits, B, Chu, BP, Pandit-Taskar, N, McDevitt, MR, and Dauer, LT. Radiation safety considerations and clinical advantages of alpha-emitting therapy radionuclides. *J Nucl Med Technol.* (2022) 50:10–6. doi: 10.2967/jnmt.121.262294
5. Westrom, S, Malenge, M, Jorstad, IS, Napoli, E, Bruland, OS, Bonsdorff, TB, et al. Ra-224 labeling of calcium carbonate microparticles for internal alpha-therapy: preparation, stability, and biodistribution in mice. *J Labelled Comp Radiopharm.* (2018) 61:472–86. doi: 10.1002/jlcr.3610
6. Council Directive 2013/59/Euratom. *Off J Eur Union.* (2014) 57:13–14, 50–53. doi: 10.3000/19770677.L_2014.013.eng

7. Li, RG, Lindland, K, Tonstad, SK, Bonsdorff, TB, Juzeniene, A, Westrom, S, et al. Improved formulation of (224) Ra-labeled calcium carbonate microparticles by surface layer encapsulation and addition of EDTMP. *Pharmaceutics*. (2021) 13:634. doi: 10.3390/pharmaceutics13050634

8. Johnson, HCT. *Introduction to Health Physics*. *4th* ed New York, USA: The McGraw-Hill Companies, Inc. (2009).

9. Norwegian Radiation and Nuclear Safety Authority, Østerås, Norway. Guidance for nuclear medicine. Guidance to "Regulations on Radiation Protection and Use of Radiation and regulations on radioactive waste and pollution". Guidance no. 10. (2020).

10. King, AP, Lin, FI, and Escorcia, FE. Why bother with alpha particles? *Eur J Nucl Med Mol Imaging*. (2021) 49:7–17. doi: 10.1007/s00259-021-05431-y

11. Hallqvist, A, Bergmark, K, Back, T, Andersson, H, Dahm-Kahler, P, Johansson, M, et al. Intraperitoneal alpha-emitting radioimmunotherapy with (211) at in relapsed ovarian cancer: long-term follow-up with individual absorbed dose estimations. *J Nucl Med*. (2019) 60:1073–9. doi: 10.2967/jnumed.118.220384

12. Seidl, C, and Essler, M. Radioimmunotherapy for peritoneal cancers. *Immunotherapy*. (2013) 5:395–405. doi: 10.2217/imt.13.20

13. Stefanoyiannis, AP, Ioannidou, SP, Round, WH, Carinou, E, Mavros, MN, Liotsou, T, et al. Radiation exposure to caregivers from patients undergoing common radionuclide therapies: a review. *Radiat Prot Dosim*. (2015) 167:542–51. doi: 10.1093/rpd/ncu338

14. Agency EM ed. *Annex I-Summary of Product Characteristics*. Amsterdam, Noord-Holland, Netherlands: European Medicines Agency; (2013).

15. Dauer, LT, Williamson, MJ, Humm, J, O'Donoghue, J, Ghani, R, Awadallah, R, et al. Radiation safety considerations for the use of 223RaCl2 DE in men with castration-resistant prostate cancer. *Health Phys*. (2014) 106:494–504. doi: 10.1097/HP.0b013e3182a82b37

16. ICRP. ICRP Publication 137: Occupational Intakes of Radionuclides: Part 3. Ottawa, Ontario, Canada: SAGE, International Comission on Radiological Protection; (2017).

17. Yoshida, K, Kaneta, T, Takano, S, Sugiura, M, Kawano, T, Hino, A, et al. Pharmacokinetics of single dose radium-223 dichloride (BAY 88-8223) in Japanese patients with castration-resistant prostate cancer and bone metastases. *Ann Nucl Med*. (2016) 30:453–60. doi: 10.1007/s12149-016-1093-8

18. Chittenden, SJ, Hindorf, C, Parker, CC, Lewington, VJ, Pratt, BE, Johnson, B, et al. A phase 1, open-label study of the biodistribution, pharmacokinetics, and dosimetry of 223Ra-dichloride in patients with hormone-refractory prostate cancer and skeletal metastases. *J Nucl Med*. (2015) 56:1304–9. doi: 10.2967/jnumed.115.157123

19. Yamamoto, S, Kato, K, Fujita, N, Yamashita, M, Nishimoto, T, Kameyama, H, et al. Detection of alpha radionuclides in air from patients during Ra-223 alpha radionuclide therapy. *Sci Rep*. (2018) 8:10976. doi: 10.1038/s41598-018-29449-9

20. Napoli, E, Bonsdorff, TB, Jorstad, IS, Bruland, OS, Larsen, RH, and Westrom, S. Radon-220 diffusion from 224Ra-labeled calcium carbonate microparticles: some implications for radiotherapeutic use. *PLoS One*. (2021) 16:e0248133. doi: 10.1371/journal.pone.0248133

21. ICRP. ICRP Publication 103: The 2007 Recommendations of the International Comission on Radiological Protection. Ottawa, Ontario, Canada: Elsevier, International Comission on Radiological Protection; (2007).

frontiers | Frontiers in Medicine

TYPE Clinical Trial
PUBLISHED 01 March 2023
DOI 10.3389/fmed.2023.1070362



OPEN ACCESS

EDITED BY
Aditi Bhatt,
Zydus Hospitals,
India

REVIEWED BY
Vikas Prasad,
Washington University,
United States
Chukwuemeka Ihemelandu,
MedStar Washington Hospital Center,
United States
Ignace Vergote,
University Hospitals Leuven,
Belgium

*CORRESPONDENCE
Stein Gunnar Larsen
✉ stl@ous-hf.no

SPECIALTY SECTION
This article was submitted to Nuclear Medicine, a section of the journal Frontiers in Medicine

RECEIVED 14 October 2022
ACCEPTED 23 January 2023
PUBLISHED 01 March 2023

CITATION
Larsen SG, Graf W, Mariathasan AB, Sørensen O, Spasojevic M, Goscinski MA, Selboe S, Lundstrøm N, Holtermann A, Revheim M-E and Bruland ØS (2023) First experience with $^{224}$Radium-labeled microparticles (Radspherin®) after CRS-HIPEC for peritoneal metastasis in colorectal cancer (a phase 1 study).
*Front. Med.* 10:1070362.
doi: 10.3389/fmed.2023.1070362



# First experience with $^{224}$Radium-labeled microparticles (Radspherin®) after CRS-HIPEC for peritoneal metastasis in colorectal cancer (a phase 1 study)

Stein Gunnar Larsen[1]*, Wilhelm Graf[2,3], Anthony Burton Mariathasan[1], Olaf Sørensen[1], Milan Spasojevic[1], Mariusz Adam Goscinski[1], Silje Selboe[4], Nadja Lundstrøm[3,5], Anne Holtermann[1], Mona-Elisabeth Revheim[4,6] and Øyvind Sverre Bruland[6,7,8]

[1]Department of Gastroenterological Surgery, Section for Surgical Oncology, Norwegian Radium Hospital, Oslo University Hospital, Oslo, Norway, [2]Department of Surgical Sciences, Uppsala University, Uppsala, Sweden, [3]Uppsala Academic Hospital, Uppsala, Sweden, [4]Division of Radiology and Nuclear Medicine, Oslo University Hospital, Oslo, Norway, [5]Department of Nuclear Medicine, Uppsala, Sweden, [6]Institute for Clinical Medicine, Faculty of Medicine, University of Oslo, Oslo, Norway, [7]Department of Oncology, Oslo University Hospital, Oslo, Norway, [8]Oncoinvent AS, Oslo, Norway

**Background:** Peritoneal metastasis (PM) from colorectal cancer carries a dismal prognosis despite extensive cytoreductive surgery and hyperthermic intraperitoneal chemotherapy (CRS-HIPEC). With a median time to recurrence of 11–12 months, there is a need for novel therapies. Radspherin® consists of the α-emitting radionuclide radium-224 ($^{224}$Ra), which has a half-life of 3.6 days and is adsorbed to a suspension of biodegradable calcium carbonate microparticles that are designed to give short-range radiation to the serosal peritoneal surface linings, killing free-floating and/or tumor cell clusters that remain after CRS-HIPEC.

**Methods:** A first-in-human phase 1 study (EudraCT 2018–002803-33) was conducted at two specialized CRS-HIPEC centers. Radspherin® was administered intraperitoneally 2 days after CRS-HIPEC. Dose escalation at increasing activity dose levels of 1-2-4-7-MBq, a split-dose repeated injection, and expansion cohorts were used to evaluate the safety and tolerability of Radspherin®. The aim was to explore the recommended dose and biodistribution using gamma-camera imaging. The results from the planned safety interim analysis after the completion of the dose-limiting toxicity (DLT) period of 30 days are presented.

**Results:** Twenty-three patients were enrolled: 14 in the dose escalation cohort, three in the repeated cohort, and six in the expansion cohort. Of the 23 enrolled patients, seven were men and 16 were women with a median age of 64 years (28–78). Twelve patients had synchronous PM stage IV and 11 patients had metachronous PM [primary stage II; (6) and stage III; (5)], with a disease-free interval of 15 months (3–30). The peritoneal cancer index was median 7 (3–19), operation time was 395 min (194–515), and hospital stay was 12 days (7–37). A total of 68 grade 2 adverse events were reported for 17 patients during the first 30 days; most were considered related to CRS and/or HIPEC. Only six of the TEAEs were evaluated as related to Radspherin®. One TEAE, anastomotic leakage, was reported as grade 3. Accordion ≥3 grade events occurred in a total of four of the 23 patients: reoperation due to anastomotic leaks (two) and drained abscesses (two). No DLT was documented at the 7MBq dose level that was then defined as

the recommended dose. The biodistribution of Radspherin® showed a relatively even peritoneal distribution.

**Conclusion:** All dose levels of Radspherin® were well tolerated, and DLT was not reached. No deaths occurred, and no serious adverse events were considered related to Radspherin®.

**Clinical Trial Registration:** Clinicaltrials.gov, NCT 03732781.

KEYWORDS

metastatic colorectal cancer, peritoneal metastasis, cytoreductive surgery, hyperthermic intraperitoneal chemotherapy, $^{224}$Ra, alpha emitter, targeted alpha particle therapy

# Introduction

Peritoneal metastasis from colorectal cancer (CRC) carries a worse prognosis than hepatic and lung metastases (1). Most patients with metastatic CRC (mCRC) cannot be cured, illustrated by a 5-year survival of 10–20% in study patients (2, 3), and with an even more grim prognosis in population-based registries reporting a median survival of 5–12 months and 5-year survival of 5–10% (4, 5). The incidence of peritoneal metastasis (PM) is approximately 4–10% at the time of diagnosis and 4–12% in patients with recurrence after primary curative resection (6–8).

In cases with limited peritoneal tumor load, improved and even long-term survival can be achieved by combining complete cytoreductive surgery (CRS) and hyperthermic intraperitoneal chemotherapy (HIPEC) as shown in a randomized controlled trial (9), case–control studies (10–12), meta-analysis (13), and several cohort studies (14, 15). Systemic chemotherapy alone has a limited effect on localized PM-CRC with a median survival of 13–16 months (1, 16). CRS-HIPEC aims to remove all macroscopic tumors and achieve high intraperitoneal concentrations of hyperthermic cytotoxic drugs (17).

The outcome of CRS-HIPEC is, however, highly variable, and most patients will experience disease recurrence with a 5-year overall survival (OS) reported in about 40% of CRS-HIPEC cases (13, 15). However, the 5-year disease-free survival (DFS) is only 18% with a median time to relapse between 11 and 12 months. At the moment of recurrence, two-thirds of patients suffer either from peritoneal relapse or peritoneal relapse and distant metastases together (18).

If PM recurrence after CRS-HIPEC occurs, the prognosis is dismal. Hence, there is a definite unmet medical need for novel treatments against abdominal cancer dissemination and novel therapeutic strategies that may help preserve the surgical complete response after CRS-HIPEC.

Intraperitoneal (IP) therapy with α-emitters may be beneficial for patients with PM-CRC since hallmarks of the disease include dissemination within the abdominal cavity and residual micrometastases in a substantial number of patients. Preclinical studies have tested α-emitting radioimmunoconjugates as IP treatment of ovarian cancer, and $^{211}$At and $^{212}$Pb conjugated to antibodies are in clinical development (19–22). Preclinical and clinical data indicate that α-emitters are well tolerated without dose-limiting toxicity (23, 24).

Radspherin® is a novel treatment principle especially designed to give local radiation to the surface of the abdominal cavity based on biodegradable microparticles with $^{224}$Ra adsorbed to the particle. By injection into the peritoneal cavity, the particles are distributed and emit internal α-particle radiation to the tissue of the peritoneal lining and potentially kill remaining free cancer cells and small cell clusters and hopefully will prevent the further spread of disease.

In this study, we report our first experience from a phase 1 study in patients with PM-CRC to evaluate the safety and toxicity of Radspherin®, determine the recommended, and/or establish a recommended dose for Radspherin® as a single IP or two repeated doses following CRS-HIPEC.

# Materials and methods

## Approval

The study was approved by the National Ethics Committees in Norway and Sweden, the Norwegian Medicines Agency, and the Swedish Medical Products Agency. Data were registered in the Sponsors database (Viedoc eCRF).

## Patients and surgical treatment

A first-in-human, phase 1 study (EudraCT 2018–002803-33) was conducted at two specialized CRS-HIPEC centers in Oslo, Norway, and Uppsala, Sweden. Twenty-three patients were included between 11 May 2020 and 16 August 2021. Twenty-nine patients were screened. CRS was performed to remove all macroscopically visible tumors, involving peritonectomy procedures and organ resections as necessary. Peritoneal tumor distribution was classified using the peritoneal cancer index (PCI) (25), and the completeness of cytoreduction (CC) score (25) was used to evaluate residual tumor after CRS. All CC-0 cases were given HIPEC. All anastomoses were completed before the HIPEC procedure.

The synchronous PM was defined as a diagnosis at or within 6 months of primary surgery, and disease-free interval (DFI) was the time from primary surgery to diagnosis of PM. Postoperative complications (30-day morbidity and mortality) were classified according to Accordion (26).

## Hyperthermic intraperitoneal chemotherapy

Hyperthermic intraperitoneal chemotherapy was administrated using a closed technique with an open abdomen in Norway (27), whereas the closed abdomen technique was used in Sweden (28). In Norway, the HIPEC regimen contained mitomycin, 35 mg/m$^2$ (maximum 70 mg), given in three fractions for 90 min (50% initially, 25%/30 min, and 25%/60 min), whereas in Sweden, oxaliplatin 460 mg/m$^2$ or irinotecan 460 mg/m$^2$ were both given in 30 min.

### Catheter insertion

Following the CRS-HIPEC, an in-dwelling peritoneal Blake catheter was placed anteriorly in the upper abdominal cavity. The catheter was obliquely tunneled, clamped, and fixed to the abdominal wall to reduce the risk of leakage or displacement.

### Study design and administration of Radspherin®

The dose escalation was performed as a 3 + 3 design (Figure 1), increasing dose levels starting at 1 MBq followed by 2, 4, and 7 MBq or until eventual dose-limiting toxicity (DLT) was observed. The repeated injection cohort included three subjects for the highest dose level that has been declared safe (explored as a split dose of two separate injections given 1 week apart). The study also involved an expansion cohort with six subjects at the highest safe activity dose safe. Radspherin® was injected in the abdominal cavity through a catheter 2 days after CRS-HIPEC for patients to have stabilized after the complex surgery. Each subject was followed until disease progression in the abdominal cavity or for 12 months (18 months after the highest dose level) after the administration of Radspherin®. The results from the safety interim analysis after the completion of the pre-defined DLT period of 30 days are presented.

Dose-calibrated Radspherin® (up to 10 mL containing 0.7–1 g of particles) was prepared at the nuclear medicine department at the site and administered as a single bolus injection *via* a three-way Luer lock connected to the inserted peritoneal catheter. After the injection, the catheter was flushed with about 250 ml of isotonic solution, and in all instances, all drains were kept clamped for a minimum of 72 h, except in one patient where a laparotomy was performed after 65 h. The patient moved from side to side in the bed regularly for the first 2 h after installation. For repeated injections, the same in-dwelling peritoneal catheter was used and then removed 3–4 days later.

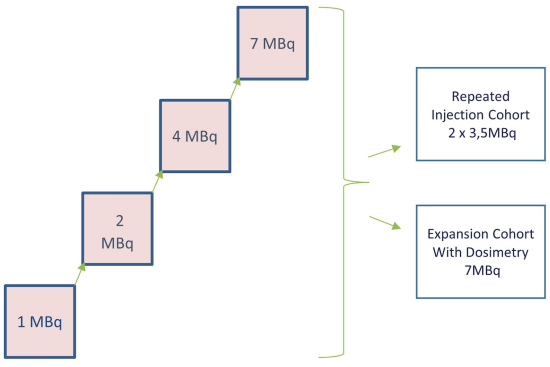


FIGURE 1
Dose escalation aimed to define the recommended dose on 3+3 subjects (12). Thereafter, a repeated injection cohort (3) and an expansion cohort were performed (6).

The peritoneal distribution of Radspherin® particles was examined by single-photon emission computed tomography/computed tomography (SPECT/CT) gamma-camera imaging performed on days 1, 2, and 3 (Day 6 for the dosimetry cohort). The patients were followed closely during the hospital stay and later at pre-scheduled intervals to discover complications such as suspected unexpected serious adverse reactions (SUSARs), serious adverse effects (SAEs), and adverse effects (AEs). The EMA "Guideline on strategies to identify and mitigate risks for first-in-human and early clinical trials with investigational medicinal products" (EMEA/CHMP/SWP/28367/07 Rev. 1) has been considered for the assessment of factors of risk.

## Study objectives

The primary objectives of the study were to investigate the safety and toxicity of Radspherin® and to determine the recommended dose of Radspherin®, among the four suggested doses of 1, 2, 4, and 7 MBq following CRS and HIPEC (Figure 1).

The secondary objectives of the study were to establish a recommended dose of Radspherin® as a single IP injection or two repeated IP injections following CRS and HIPEC and to describe the biodistribution of Radspherin®.

## Additional systemic chemotherapy

According to national guidelines, adjuvant chemotherapy was not routinely given. In the case of synchronous PM with locoregional lymph node metastasis, adjuvant chemotherapy was recommended after CRS-HIPEC/Radspherin®, otherwise not.

## Data analysis

All data were recorded in the eCRF, and external study monitoring and source data verification were performed. The study was reviewed by an Independent Data Monitoring Committee. Categorical variables were described using frequencies/percentages, and continuous variables were described with median/range. Safety evaluations were based on the incidence, intensity, and type of AEs, and clinically significant changes in the subjects' vital signs and clinical laboratory results.

# Results

Twenty-nine patients were screened for the study (Figure 2). Totally, there were six screening failures due to the extent of metastasis (PCI > 20; 3), other previous malignant diseases (2), or peroperative bleeding (1) leading to exclusion from the study before the decision on giving Radspherin®. Accordingly, 23 patients were given Radspherin®. Of the 23 patients, 19 patients were treated at Oslo University Hospital and four at Uppsala Academic Hospital in

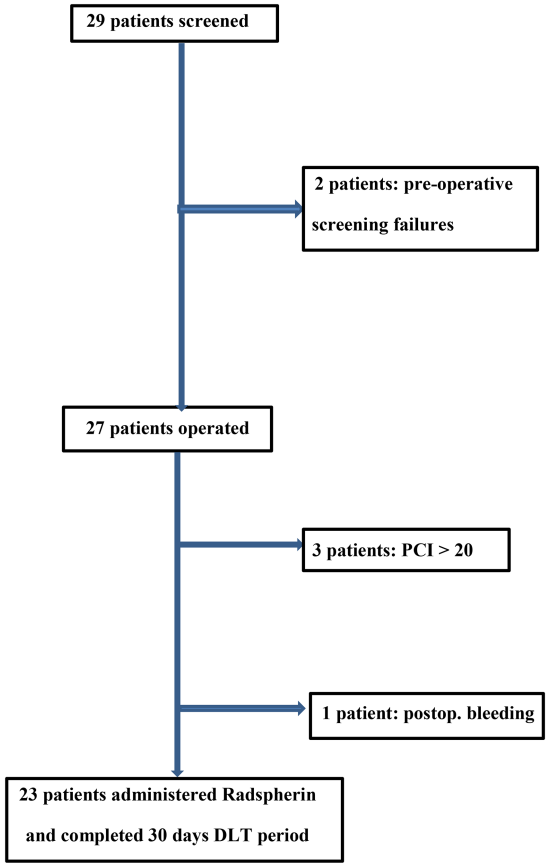


FIGURE 2
Consort flow diagram of the study patients ($n$=23).

Sweden. The study had a dose escalation cohort (14 pts.) with increasing doses from 1 MBq (4 pts.) to 2 MBq (3 pts.), 4 MBq (4 pts.), and 7 MBq (3 pts.), a repeated cohort (3 pts.) with 3.5 MBq given two times with 1-week interval, and an expansion cohort on highest dose level 7 MBq with additional six patients (Figure 1).

Table 1 summarizes the clinicopathological characteristics of the study cohort, which comprised 16 women (70%) and seven men (30%) with a median age of 64 years (28–78). Twelve patients were diagnosed with IUCC stage IV disease after primary surgery. Metachronous metastasis occurred after a disease-free interval (DFI) of median of 11 months (range 3–30). Approximately 43% had received chemotherapy at some point before CRS-HIPEC. Performance status was in most cases ECOG 0, while only one patient was in ECOG 1. One patient in the 7 MBq cohort received neoadjuvant irradiation therapy. Lymph node metastasis was present in 15 patients (65%) of the primary cases.

The median PCI at the time of CRS-HIPEC was 7 (3–19; Table 2). The median duration of surgery was 374 min (266–508). The median peroperative bleeding was 300 mL (50–1,000 mL). In-hospital time was 11 days (7–37). At Norwegian Radium Hospital, HIPEC is performed with mitomycin C, 35 mg/m$^2$ up to 70 mg, median 63 mg (57–70), and given in a closed perfusion circuit with open abdomen; duration 90 min; and intra-abdominal temperature median 42.0°C. In Uppsala, oxaliplatin 460 mg/m$^2$ or irinotecan 460 mg/m$^2$ was perfused for 30 min. Accordingly, the total operation time was reduced by 60 min compared to the Norwegian site. The knife time is then median more than 4 h before HIPEC in this study with complex surgery for PM.

The highest dose escalation level 4, the 7 MBq dose, was selected as recommended dose, as no DLT was observed. The incidence of DLTs, TEAEs, and SAEs is summarized in Table 3. The actual amount of Radspherin® administered is shown in Table 4. All 23 patients were included in the safety population. A total of 68 TEAEs were reported for 17 patients (74%) during the first 30 days. Of these, 23 of grade 2 before Radspherin® installation and 45 of grade 2 in the time period after Radspherin® installation (Days 1–30) were reported in 16 patients. There was one grade 3 TEAE which was reported as SAE but unrelated to Radspherin®. The most frequently reported AEs were vomiting, pyrexia, nausea, and decreased appetite, and the majority were considered related to CRS and/or HIPEC. Only six of the TEAEs were evaluated as related to Radspherin® and laboratory test abnormalities [platelet count increased, blood alkaline phosphatase increased, hemoglobin decreased ($n$=2), monocyte count increased, and hepatic enzyme abnormal]. All these TEAEs were resolved with no actions taken and no need for additional treatment.

Four SAEs within 30 days were reported for three patients, and all were considered unrelated to Radspherin®. These SAEs included one anastomotic leak (grade 3), which was reoperated on Day 2, two abdominal infections (grade 2) that required a drain on Day 10, and an anastomotic leak that required reoperation on Day 10 and a drain on Day 15 (see the section "Discussion"). During reoperations, abdominal fluid was drained before opening the abdomen, washed out with physiological saline solution liquid, and removed as irradiation waste. No patients in the repeat injection cohort had any SAE. No deaths or study discontinuations due to TEAEs or SAEs were reported during the 30 days.

Corresponding Accordion grade 3 events occurred in two of the 23 patients (draining of abscesses) and Accordion grade 4 events in two (reoperation due to anastomotic leaks; Table 3). There were no deaths within 100 days. The biodistribution of Radspherin® showed a relatively even peritoneal distribution, and an example is shown in Figure 3.

## Discussion

The CRS-HIPEC procedure is well known to be associated with postoperative complications (29), and significantly higher incidences of severe postoperative complications (i.e., fistulas and anastomotic leaks) have been observed in patients treated with HIPEC than in patients treated without HIPEC (30).

In the current study, there was no 30-day mortality. The incidence of severe postoperative complications (Accordion 3), the need for drainage or parenteral nutrition occurring in five of the 23 patients (22%), and the reoperation rate of 9% (two of 23 patients) were all as expected and suggest that the treatment with Radspherin® is well tolerated and safe. The first patient with anastomotic leakage in the study experienced an increase in white blood cells to 18.7 × 10$^9$/L and a moderate elevation of C-reactive protein (CRP) to 61 the day after surgery and the day before Radspherin® installation, followed by antibiotics the next day and reoperation with the verification of anastomotic leakage 2 days after Radspherin®. The other patient also experienced an increase in white blood cells to 16.7 × 10$^9$/L and a moderate CRP increase to 58 the day after surgery and received

10.3389/fmed.2023.1070362

TABLE 1 Clinicopathological characteristics after CRS-HIPEC (*n*=23).

| | Dose escalation and expansion cohorts | | | | Repeat injection cohort | |
|---|---|---|---|---|---|---|
| | 1MBq | 2MBq | 4MBq | 7MBq | 2×3.5MBq | Total |
| | *N*=4 | *N*=3 | *N*=4 | *N*=9 | *N*=3 | *N*=23 |
| Age, years | | | | | | |
| Median | 58.0 | 72.0 | 68.0 | 61.0 | 71.0 | 64.0 |
| Min, Max | 44, 71 | 69, 74 | 56, 78 | 28, 68 | 42, 78 | 28, 78 |
| Sex, *n* (%) | | | | | | |
| Male | 2 (50%) | 0 | 1 (25%) | 2 (22%) | 2 (67%) | 7 (30%) |
| Female | 2 (50%) | 3 (100%) | 3 (75%) | 7 (78%) | 1 (33%) | 16 (70%) |
| Stage, *n* (%) | | | | | | |
| Stage II | 0 | 2 (67%) | 1 (25%) | 1 (11%) | 2 (67%) | 6 (26%) |
| Stage III | 1 (25%) | 1 (33%) | 0 | 3 (33%) | 0 | 5 (22%) |
| Stage IV | 3 (75%) | 0 | 3 (75%) | 5 (56%) | 1 (33%) | 12 (52%) |
| Metachr mets | 1 | 3 | 1 | 4 | 2 | 11 |
| DFI | | | | | | |
| Median (mnt) | 10 | 19 | 13 | 11 | 11 | 15 |
| Min, Max | 10 | 11,25 | 13 | 3,17 | 6,16 | 3,30 |
| ECOG performance status | | | | | | |
| Grade 0 | 4 (100%) | 3 (100%) | 4 (100%) | 8 (89%) | 3 (100%) | 22 (96%) |
| Grade 1 | 0 | 0 | 0 | 1 (11%) | 0 | 1 (4%) |
| Prior chemotherapy, n (%) | | | | | | |
| Yes | 2 (50%) | 1 (33%) | 1 (25%) | 4 (44%) | 2 (67%) | 10 (43%) |
| No | 2 (50%) | 2 (67%) | 3 (75%) | 5 (56%) | 1 (33%) | 13 (57%) |
| | | | | | | |
| LN + | 3 (75%) | 1 (33%) | 3 (100%) | 7 (78%) | 1 (33%) | 15(65%) |
| Median | 2 | 0 | 3 | 1 | ** | 4 |
| Min,Max | 2,11 | 0,14 | 0,13 | 0,19 | ** | 1, 19 |

*N*, number of patients in the analysis set; *n*, number of patients meeting the criterion; Max, maximum; Min, minimum; DFI, disease-free interval from surgery for a metachronous primary tumor; LN+, number of lymph node metastases; **N1c.

Radspherin® the following day. Five days later, intravenous antibiotics were started due to an infection. Anastomotic leakage was diagnosed on Day 10, and a laparotomy with resection and stoma was performed. Both cases were considered caused by infection before Radspherin® and to be related to the CRS and HIPEC procedures.

In other larger patient series, postoperative mortality between 0.7 and 7.7% has been reported (29, 31, 32) with reoperation rates varying between 4 and 20.8% (13). Oslo University Hospital has previously reported corresponding numbers of 0% (mortality), 15% (Accordion ≥3), and 8% (reoperation rate) (14) with CRS-HIPEC and without Radspherin®.

Norwegian Radium Hospital recently performed a dose-escalating phase I trial with intraperitoneal (IP) MOC31PE immunotoxin in PM-CRC after CRS-HIPEC (33) showing promising results for better control of PM. The hospital has used radium and α-emitters for the treatment of metastatic cancer with Xofigo®, a $^{223}$Ra radiopharmaceutical. Xofigo® was approved by the FDA and EMEA in 2013 for the treatment of symptomatic bone metastasis from prostate cancer.

Because of the short range and high linear energy transfer of α-particle emitters, there is a much higher relative biological effectiveness of the radiation from Radspherin® than from β-particle emitting radiopharmaceuticals previously used. Thereby, α-particle emitters are theoretically more efficient in treating micrometastases and killing chemotherapy-resistant tumor cells. The much shorter radiation range prevents the radiation of tissue in deeper regions of sensitive abdominal organs (i.e., small intestine), which was the prime reason for abandoning the β-particle emitting radiopharmaceuticals, giving a discrete surface irradiation of just the serosal lining of the peritoneal cavity.

This favorable safety profile in the current study is in line with documentation from other preclinical and clinical studies with other related alpha-emitting compounds administered intraperitoneally. Safety and effect of IP administration have been demonstrated in animal models both with colloids/particles and antibodies as carriers of a range of radionuclides: $^{211}$At polymers (34, 35), bismuth-213 ($^{213}$Bi) antibodies (36), $^{211}$At antibodies (37, 38), $^{212}$Pb antibodies (21, 39, 40), thorium-227 ($^{227}$)Th antibodies (41), and actinium-225 ($^{225}$Ac) antibodies (42).

TABLE 2 Characteristics after CRS-HIPEC ($n$=23).

| | Dose escalation and expansion cohorts | | | | Repeat injection cohort | |
|---|---|---|---|---|---|---|
| | 1MBq | 2MBq | 4MBq | 7MBq | 2×3.5MBq | Total |
| | *N*=4 | *N*=3 | *N*=4 | *N*=9 | *N*=3 | *N*=23 |
| PCI | | | | | | |
| Median | 10.5 | 7 | 11.5 | 8 | 6 | 7 |
| Min Max | 6,19 | 6,14 | 4,19 | 3,17 | 5,16 | 3,19 |
| Blood loss (mL) | | | | | | |
| Median | 550 | 500 | 250 | 300 | 200 | 300 |
| Min,Max | 200,1,000 | 100,500 | 50,500 | 50,500 | 75,300 | 50,1,000 |
| Duration of surgery | | | | | | |
| Median | 426 | 380 | 410 | 410 | 280 | 374 |
| Min Max | 374–485 | 372–480 | 330–500 | 301–508 | 266–288 | 266–508 |
| HIPEC with Mitomycin C | | | | | - | |
| Median (mg) | 70 | 61 | 64 | 62 | - | 63 |
| Min,Max | 70.70 | 60,63 | 59,70 | 57,70 | - | 57,70 |
| HIPEC in Sweden* | | | | | | |
| Median (mg) | - | - | Comment* | - | Comment* | - |
| Min,Max | - | - | - | - | - | - |
| Hospital stay | | | | | | |
| Median | 9.5 | 7 | 16 | 11 | 16 | 12 |
| Min,Max | 8,16 | 7,21 | 9,37 | 8,16 | 15,16 | 7,37 |
| Accordion | | | | | | |
| Median | 1.5 | 1 | 2.5 | 1 | 2 | 2 |
| Min,Max | 1,4 | 1,3 | 1,4 | 1,2 | 2,2 | 1,4 |

*N*, number of patients in the analysis set; Max, maximum; Min, minimum; PCI, peritoneal cancer index; and duration of surgery, knife time.*HIPEC in Sweden: Patient 4 MBq oxaliplatin 620 mg/30 min. Patients repeat injection cohort; irinotecan 960 mg/90 min or oxaliplatin 920 or 760 mg/30 min.

TABLE 3 Number of treatment-emergent adverse events in the time period of 1–30 days.

| | Dose escalation and expansion cohorts | | | | Repeat injection cohort | |
|---|---|---|---|---|---|---|
| | 1MBq | 2 MBq | 4MBq | 7MBq | 2×2.5MBq | Total |
| | *N*=4 | *N*=3 | *N*=4 | *N*=9 | *N*=3 | *N*=23 |
| | E, n (%) | E, n (%) | E, n (%) | E, n (%) | E, n (%) | E, n (%) |
| TEAE of CTCAE Grade 2 | 4, 2 (50%) | 3, 1 (33%) | 17, 4 (100%) | 18, 8 (89%) | 3, 1 (33%) | 45, 16 (70%) |
| TEAE of CTCAE Grade ≥ 3 | 0, 0 | 0, 0 | 1, 1 (25%) | 0, 0 | 0, 0 | 1, 1 (4%) |
| SAE | 1, 1 (25%) | 1, 1 (33%) | 2, 1 (25%) | 0, 0 | 0, 0 | 4, 3 (13%) |
| DLT | 0, 0 | 0, 0 | 0, 0 | 0, 0 | 0, 0 | 0, 0 |

E, number of adverse events after the administration of Radspherin; *N*, number of patients in the analysis set; *n*, number of patients meeting the criterion; TEAE, treatment-emergent adverse event, SAE, serious adverse event; DLT, dose-limiting toxicity.

TABLE 4 Administered dose and compliance.

| | Dose escalation and expansion cohorts | | | | Repeat injection cohort |
|---|---|---|---|---|---|
| | 1MBq | 2MBq | 4MBq | 7MBq | 2×2.5MBq |
| | *N*=4 | *N*=3 | *N*=4 | *N*=9 | *N*=3 |
| Administered Dose, Radspherin® MBq | | | | | |
| Median | 1.01 | 2.05 | 3.92 | 7.15 | 7.06 |
| Min, Max | 0.98, 1.07 | 1.98, 2.09 | 3.74, 4.05 | 6.99, 7.36 | 7.05, 7.20 |

*N*, number of patients in the analysis set; Max, maximum; and Min, minimum.

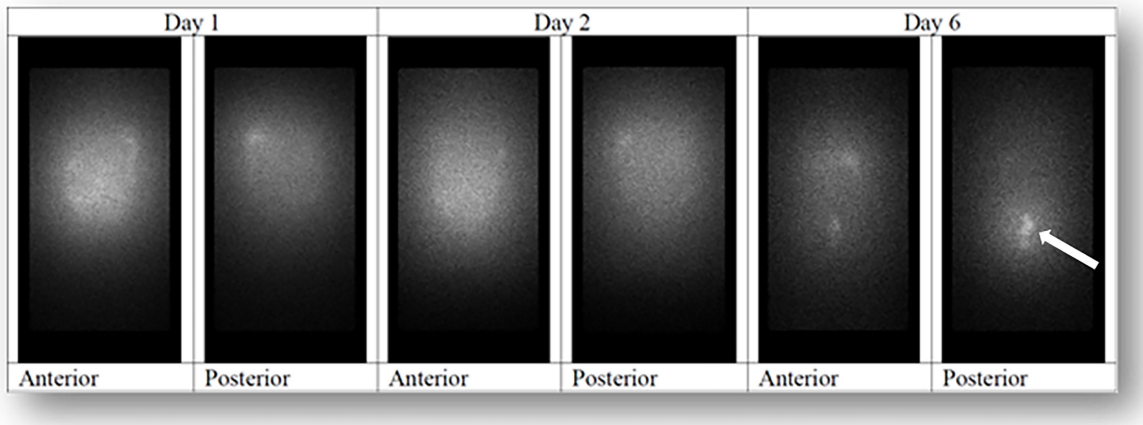


FIGURE 3
$^{224}$Ra-labeled microparticles for patient at 7 MBq were evenly distributed in the abdominal cavity both in the anterior and posterior images. In this subject, an area with a slightly higher activity was observed in the left upper region. No areas with low levels of activity were observed. At a late time point, uptake was observed in the distal large intestine (arrow).

All dose levels of Radspherin® were well tolerated with DLT not reached. No deaths occurred, and no SAEs were considered related to Radspherin®. The biodistribution of Radspherin® showed a good peritoneal distribution of the radiolabeled microparticles. Long-term safety, dosimetry, and first efficacy results of Radspherin® will be reported after 18 months of the follow-up period.

## Conclusion

All dose levels of Radspherin® were well tolerated with DLT not reached. No deaths occurred, and no SAEs were considered related to Radspherin®. The biodistribution of Radspherin® showed a good peritoneal distribution of the radiolabeled microparticles.

## Data availability statement

The raw data supporting the conclusions of this article will be made available by the authors, without undue reservation.

## Ethics statement

The studies involving human participants were reviewed and approved by National Ethics Committees in Norway and Sweden. The patients/participants provided their written informed consent to participate in this study.

## Author contributions

SL, M-ER, and ØB: conceptualization. SL, WG, M-ER, and ØB: study design and drafting the manuscript and revising it critically for important intellectual content. SL, WG, and ØB: data analysis. SL, WG, SS, NL, AH, M-ER, and ØB: interpretation of results. All authors contributed to the article and approved the submitted version.

## Funding

This study was funded by Oncoinvent AS and Innovation Norway.

## Acknowledgments

The authors thank the sponsor Oncoinvent AS for their teams involved in Radspherin® production and clinical trial support. We also thank the other members on the delegation log for their collaboration (Lars Tore Gyland Michalsen, Benedicte Haug Olsen, Ayca Muftuler Løndalen, Gasha Rashid, Anders Tulipan, Ebbe Billmann Thorgersen, Simen Grønningsæter, and Ingrid Vedaa Skåla) and the nurse staffs in both hospitals.

## Conflict of interest

ØB is a clinical consultant to and holds ownership in Oncoinvent AS.

The remaining authors declare that the research was conducted in the absence of any commercial or financial relationships that could be construed as a potential conflict of interest.

The authors declare that this study received funding from Oncoinvent AS. Oncoinvent AS was involved in the study design, collection, analysis, interpretation of data and the decision to submit this article for publication.

## Publisher's note

# References


1. Franko, J, Shi, Q, Meyers, JP, Maughan, TS, Adams, RA, Seymour, MT, et al. Prognosis of patients with peritoneal metastatic colorectal cancer given systemic therapy: an analysis of individual patient data from prospective randomised trials from the analysis and research in cancers of the digestive system (ARCAD) database. *Lancet Oncol*. (2016) 17:1709–19. doi: 10.1016/S1470-2045(16)30500-9

2. Kopetz, S, Chang, GJ, Overman, MJ, Eng, C, Sargent, DJ, Larson, DW, et al. Improved survival in metastatic colorectal cancer is associated with adoption of hepatic resection and improved chemotherapy. *J Clin Oncol*. (2009) 27:3677–83. doi: 10.1200/JCO.2008.20.5278

3. Tveit, KM, Guren, T, Glimelius, B, Pfeiffer, P, Sorbye, H, Pyrhonen, S, et al. Phase III trial of cetuximab with continuous or intermittent fluorouracil, leucovorin, and oxaliplatin (Nordic FLOX) versus FLOX alone in first-line treatment of metastatic colorectal cancer: the NORDIC-VII study. *J Clin Oncol*. (2012) 30:1755–62. doi: 10.1200/JCO.2011.38.0915

4. Sorbye, H, Cvancarova, M, Qvortrup, C, Pfeiffer, P, and Glimelius, B. Age-dependent improvement in median and long-term survival in unselected population-based Nordic registries of patients with synchronous metastatic colorectal cancer. *Ann Oncol*. (2013) 24:2354–60. doi: 10.1093/annonc/mdt197

5. Abdel-Rahman, O. A real-world, population-based study of the outcomes of patients with metastatic colorectal cancer to the peritoneum treated with or without cytoreductive surgery. *Int J Color Dis*. (2020) 35:719–25. doi: 10.1007/s00384-020-03525-x

6. Segelman, J, Granath, F, Holm, T, Machado, M, Mahteme, H, and Martling, A. Incidence, prevalence and risk factors for peritoneal carcinomatosis from colorectal cancer. *Br J Surg*. (2012) 99:699–705. doi: 10.1002/bjs.8679

7. Koppe, MJ, Nagtegaal, ID, de Wilt, JH, and Ceelen, WP. Recent insights into the pathophysiology of omental metastases. *J Surg Oncol*. (2014) 110:670–5. doi: 10.1002/jso.23681

8. Confuorto, G, Giuliano, ME, Grimaldi, A, and Viviano, C. Peritoneal carcinomatosis from colorectal cancer: HIPEC? *Surg Oncol*. (2007) 16:S149–52. doi: 10.1016/j.suronc.2007.10.026

9. Verwaal, VJ, Bruin, S, Boot, H, van Slooten, G, and van Tinteren, H. 8-year follow-up of randomized trial: cytoreduction and hyperthermic intraperitoneal chemotherapy versus systemic chemotherapy in patients with peritoneal carcinomatosis of colorectal cancer. *Ann Surg Oncol*. (2008) 15:2426–32. doi: 10.1245/s10434-008-9966-2

10. Elias, D, Lefevre, JH, Chevalier, J, Brouquet, A, Marchal, F, Classe, JM, et al. Complete cytoreductive surgery plus intraperitoneal chemohyperthermia with oxaliplatin for peritoneal carcinomatosis of colorectal origin. *J Clin Oncol*. (2009) 27:681–5. doi: 10.1200/JCO.2008.19.7160

11. Franko, J, Ibrahim, Z, Gusani, NJ, Holtzman, MP, Bartlett, DL, and Zeh, HJ 3rd. Cytoreductive surgery and hyperthermic intraperitoneal chemoperfusion versus systemic chemotherapy alone for colorectal peritoneal carcinomatosis. *Cancer*. (2010) 116:3756–62. doi: 10.1002/cncr.25116

12. Mahteme, H, Hansson, J, Berglund, A, Pahlman, L, Glimelius, B, Nygren, P, et al. Improved survival in patients with peritoneal metastases from colorectal cancer: a preliminary study. *Br J Cancer*. (2004) 90:403–7. doi: 10.1038/sj.bjc.6601586

13. Mirnezami, R, Mehta, AM, Chandrakumaran, K, Cecil, T, Moran, BJ, Carr, N, et al. Cytoreductive surgery in combination with hyperthermic intraperitoneal chemotherapy improves survival in patients with colorectal peritoneal metastases compared with systemic chemotherapy alone. *Br J Cancer*. (2014) 111:1500–8. doi: 10.1038/bjc.2014.419

14. Froysnes, IS, Larsen, SG, Spasojevic, M, Dueland, S, and Flatmark, K. Complete cytoreductive surgery and hyperthermic intraperitoneal chemotherapy for colorectal peritoneal metastasis in Norway: prognostic factors and oncologic outcome in a national patient cohort. *J Surg Oncol*. (2016) 114:222–7. doi: 10.1002/jso.24290

15. Larsen, SG, Goscinski, MA, Dueland, S, Steigen, SE, Hofsli, E, Torgunrud, A, et al. Impact of KRAS, BRAF and microsatellite instability status after cytoreductive surgery and HIPEC in a national cohort of colorectal peritoneal metastasis patients. *Br J Cancer*. (2022) 126:726–35. doi: 10.1038/s41416-021-01620-6

16. Franko, J, Shi, Q, Goldman, CD, Pockaj, BA, Nelson, GD, Goldberg, RM, et al. Treatment of colorectal peritoneal carcinomatosis with systemic chemotherapy: a pooled analysis of north central cancer treatment group phase III trials N9741 and N9841. *J Clin Oncol*. (2012) 30:263–7. doi: 10.1200/JCO.2011.37.1039

17. Brucher, BL, Piso, P, Verwaal, V, Esquivel, J, Derraco, M, Yonemura, Y, et al. Peritoneal carcinomatosis: cytoreductive surgery and HIPEC--overview and basics. *Cancer Investig*. (2012) 30:209–24. doi: 10.3109/07357907.2012.654871

18. Elias, D, Gilly, F, Boutitie, F, Quenet, F, Bereder, JM, Mansvelt, B, et al. Peritoneal colorectal carcinomatosis treated with surgery and perioperative intraperitoneal chemotherapy: retrospective analysis of 523 patients from a multicentric French study. *J Clin Oncol*. (2010) 28:63–8. doi: 10.1200/JCO.2009.23.9285

19. Andersson, H, Cederkrantz, E, Back, T, Divgi, C, Elgqvist, J, Himmelman, J, et al. Intraperitoneal alpha-particle radioimmunotherapy of ovarian cancer patients: pharmacokinetics and dosimetry of (211)at-MX35 F(ab')2--a phase I study. *J Nucl Med*. (2009) 50:1153–60. doi: 10.2967/jnumed.109.062604

20. Milenic, DE, Molinolo, AA, Solivella, MS, Banaga, E, Torgue, J, Besnainou, S, et al. Toxicological studies of 212Pb intravenously or intraperitoneally injected into mice for a phase 1 trial. *Pharmaceuticals (Basel)*. (2015) 8:416–34. doi: 10.3390/ph8030416

21. Kasten, BB, Azure, MT, Schoeb, TR, Fisher, DR, and Zinn, KR. Imaging, biodistribution, and toxicology evaluation of $^{212}$Pb-TCMC-trastuzumab in nonhuman primates. *Nucl Med Biol*. (2016) 43:391–6. doi: 10.1016/j.nucmedbio.2016.04.001

22. Meredith, R, Torgue, J, Shen, S, Fisher, DR, Banaga, E, Bunch, P, et al. Dose escalation and dosimetry of first-in-human alpha radioimmunotherapy with 212Pb-TCMC-trastuzumab. *J Nucl Med*. (2014) 55:1636–42. doi: 10.2967/jnumed.114.143842

23. Cederkrantz, E, Andersson, H, Bernhardt, P, Back, T, Hultborn, R, Jacobsson, L, et al. Absorbed doses and risk estimates of (211)at-MX35 F(ab')2 in intraperitoneal therapy of ovarian cancer patients. *Int J Radiat Oncol Biol Phys*. (2015) 93:569–76. doi: 10.1016/j.ijrobp.2015.07.005

24. Meredith, S, Hilliard, J, and Vaillancourt, R. Evaluation of a rapid hydration protocol: safety and effectiveness. *J Oncol Pharm Pract*. (2017) 23:249–54. doi: 10.1177/1078155216631406

25. Jacquet, P, and Sugarbaker, PH. Clinical research methodologies in diagnosis and staging of patients with peritoneal carcinomatosis. *Cancer Treat Res*. (1996) 82:359–74. doi: 10.1007/978-1-4613-1247-5_23

26. Strasberg, SM, Linehan, DC, and Hawkins, WG. The accordion severity grading system of surgical complications. *Ann Surg*. (2009) 250:177–86. doi: 10.1097/SLA.0b013e3181afde41

27. Benoit, L, Cheynel, N, Ortega-Deballon, P, Giacomo, GD, Chauffert, B, and Rat, P. Closed hyperthermic intraperitoneal chemotherapy with open abdomen: a novel technique to reduce exposure of the surgical team to chemotherapy drugs. *Ann Surg Oncol*. (2008) 15:542–6. doi: 10.1245/s10434-007-9635-x

28. Goldenshluger, M, Zippel, D, Ben-Yaacov, A, Dux, J, Yalon, T, Zendel, A, et al. Core body temperature but not intraabdominal pressure predicts postoperative complications following closed-system Hyperthermic intraperitoneal chemotherapy (HIPEC) administration. *Ann Surg Oncol*. (2018) 25:660–6. doi: 10.1245/s10434-017-6279-3

29. Cashin, PH, Graf, W, Nygren, P, and Mahteme, H. Cytoreductive surgery and intraperitoneal chemotherapy for colorectal peritoneal carcinomatosis: prognosis and treatment of recurrences in a cohort study. *Eur J Surg Oncol*. (2012) 38:509–15. doi: 10.1016/j.ejso.2012.03.001

30. Baratti, D, Kusamura, S, Laterza, B, Balestra, MR, and Deraco, M. Early and long-term postoperative management following cytoreductive surgery and hyperthermic intraperitoneal chemotherapy. *World J Gastrointest Oncol*. (2010) 2:36–43. doi: 10.4251/wjgo.v2.i1.36

31. Simkens, GA, van Oudheusden, TR, Braam, HJ, Luyer, MD, Wiezer, MJ, van Ramshorst, B, et al. Treatment-related mortality after Cytoreductive surgery and HIPEC in patients with colorectal peritoneal Carcinomatosis is underestimated by conventional parameters. *Ann Surg Oncol*. (2016) 23:99–105. doi: 10.1245/s10434-015-4699-5

32. Yonemura, Y, Canbay, E, and Ishibashi, H. Prognostic factors of peritoneal metastases from colorectal cancer following cytoreductive surgery and perioperative chemotherapy. *ScientificWorldJournal*. (2013) 2013:978394. doi: 10.1155/2013/978394

33. Froysnes, IS, Andersson, Y, Larsen, SG, Davidson, B, Oien, JT, Olsen, KH, et al. Novel treatment with intraperitoneal MOC31PE immunotoxin in colorectal peritoneal metastasis: results from the ImmunoPeCa phase 1 trial. *Ann Surg Oncol*. (2017) 24:1916–22. doi: 10.1245/s10434-017-5814-6

34. Larsen, RH, Hoff, P, Vergote, IB, Bruland, OS, Aas, M, De Vos, L, et al. Alpha-particle radiotherapy with 211At-labeled monodisperse polymer particles, 211At-labeled IgG proteins, and free 211At in a murine intraperitoneal tumor model. *Gynecol Oncol*. (1995) 57:9–15. doi: 10.1006/gyno.1995.1093

35. Vergote, I, Larsen, RH, de Vos, L, Nesland, JM, Bruland, O, Bjorgum, J, et al. Therapeutic efficacy of the alpha-emitter 211At bound on microspheres compared with $^{90}$Y and $^{32}$P colloids in a murine intraperitoneal tumor model. *Gynecol Oncol*. (1992) 47:366–72. doi: 10.1016/0090-8258(92)90141-5

36. Milenic, D, Garmestani, K, Dadachova, E, Chappell, L, Albert, P, Hill, D, et al. Radioimmunotherapy of human colon carcinoma xenografts using a $^{213}$Bi-labeled domain-deleted humanized monoclonal antibody. *Cancer Biother Radiopharm*. (2004) 19:135–47. doi: 10.1089/108497804323071904

37. Elgqvist, J, Andersson, H, Back, T, Hultborn, R, Jensen, H, Karlsson, B, et al. Therapeutic efficacy and tumor dose estimations in radioimmunotherapy of intraperitoneally growing OVCAR-3 cells in nude mice with $^{211}$At-labeled monoclonal antibody MX35. *J Nucl Med*. (2005) 46:1907–15. PMID: 16269606

38. Palm, S, Back, T, Claesson, I, Danielsson, A, Elgqvist, J, Frost, S, et al. Therapeutic efficacy of astatine-211-labeled trastuzumab on radioresistant SKOV-3 tumors in nude mice. *Int J Radiat Oncol Biol Phys*. (2007) 69:572–9. doi: 10.1016/j.ijrobp.2007.06.023

39. Milenic, DE, Garmestani, K, Brady, ED, Albert, PS, Ma, D, Abdulla, A, et al. Alpha-particle radioimmunotherapy of disseminated peritoneal disease using a $^{212}$Pb-labeled

radioimmunoconjugate targeting HER2. *Cancer Biother Radiopharm*. (2005) 20:557–68. doi: 10.1089/cbr.2005.20.557

40. Boudousq, V, Bobyk, L, Busson, M, Garambois, V, Jarlier, M, Charalambatou, P, et al. Comparison between internalizing anti-HER2 mAbs and non-internalizing anti-CEA mAbs in alpha-radioimmunotherapy of small volume peritoneal carcinomatosis using $^{212}$Pb. *PLoS One*. (2013) 8:e69613. doi: 10.1371/journal.pone.0069613

41. Heyerdahl, H, Abbas, N, Sponheim, K, Mollatt, C, Bruland, O, and Dahle, J. Targeted alpha therapy with 227Th-trastuzumab of intraperitoneal ovarian cancer in nude mice. *Curr Radiopharm*. (2013) 6:106–16. doi: 10.2174/18744710113069990018

42. Essler, M, Gartner, FC, Neff, F, Blechert, B, Senekowitsch-Schmidtke, R, Bruchertseifer, F, et al. Therapeutic efficacy and toxicity of 225Ac-labelled vs. 213Bi-labelled tumour-homing peptides in a preclinical mouse model of peritoneal carcinomatosis. *Eur J Nucl Med Mol Imaging*. (2012) 39:602–12. doi: 10.1007/s00259-011-2023-6

# Frontiers in Medicine

**Translating medical research and innovation into improved patient care**

A multidisciplinary journal which advances our medical knowledge. It supports the translation of scientific advances into new therapies and diagnostic tools that will improve patient care.

## Discover the latest Research Topics

See more →


**Frontiers**

Avenue du Tribunal-Fédéral 34
1005 Lausanne, Switzerland
frontiersin.org

**Contact us**

+41 (0)21 510 17 00
frontiersin.org/about/contact